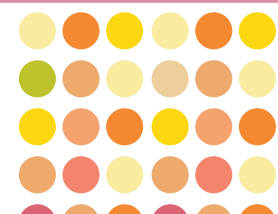# RICTA Tarragona '14

2nd Iberian Meeting on Aerosol Science and Technology

7-9 July 2014

PROCEEDINGS BOOK

Edited by
Joan Rosell-Llompart and Jordi Grifoll

[publicacions] urv

2nd Iberian Meeting
on
Aerosol Science and Technology

RICTA 2014

Tarragona, Catalunya, Spain, July 7-9, 2014

Edited by

Joan Rosell-Llompart
and
Jordi Grifoll

Universitat Rovira i Virgili

Tarragona

Preface

This Proceedings Book collects the conference articles and abstracts presented at *RICTA 2014*, the 2nd Iberian Meeting on Aerosol Science and Technology (also named Reunión Ibérica de Ciencia y Tecnología de los Aerosoles), held during July 7-9, 2014, in Tarragona, Spain.

RICTA 2014 is the second Portuguese-Spanish meeting on Aerosol Science and Technology. Like the previous RICTA congress held in 2013 in Évora, Portugal, *RICTA 2014* is the continuation of the successful RECTA, Reunión Española de Ciencia y Tecnología de Aerosoles, conferences, which have been held in Spain since 2007.

RICTA 2014 has been organized by the *Droplets, intErfaces, and floWs (DEW) Research Laboratory* of the Universitat Rovira i Virgili, with the collaboration of the *Asociación Española de Ciencia y Tecnología de los Aerosoles* (AECyTA). The congress was held at the Campus Catalunya of the Universitat Rovira i Virgili.

As in previous editions of RICTA and RECTA, the participation of young researchers has been encouraged, with the organization of the 5th Summer School on Aerosol Science and Technology, as well as awards for the best poster and PhD thesis.

This book comprises three parts: the Conference Program, the Conference Articles, and the Conference Abstracts.

We would like to express our gratitude to all participants, especially those who have contributed conference articles. We would also like to thank the Scientific Committee members for invaluable help in reviewing the conference abstracts, and most especially the voluntary speakers of the Summer School. We also would like to thank the help and advice received from the President of AECyTA, Dr. José Luis Castillo Gimeno, and from Scientific Committee co-chair Dr. Maria João Tavares da Costa. Last but not least, we acknowledge the competent assistance in the organization by the *Centre Internacional de Congressos Catalunya Sud* (Fundació Universitat Rovira i Virgili) directed by Ms. Charo Romano, most especially Ms. Raquel Rabassa, Ms. Gemma Sánchez, and Ms. Montse Torrents.

Sadly, while organizing this congress, we have been shocked by the sudden decease of Dr. Rui Manuel Almeida Brandão. He diligently served as a member of the Scientific Committee of this congress. We mourn his passing, which is a loss to the aerosol scientific community.

Joan Rosell-Llompart and *Jordi Grifoll*
Conference organizers

July 2014

Scientific Committee

<u>Chairs</u>

Joan Rosell-Llompart
Universitat Rovira i Virgili

Maria João Tavares da Costa
Universidade de Évora

<u>Members</u>

Lucas Alados Arboledas
Universidad de Granada

Ana Maria Almeida e Silva
Universidade de Évora

Célia Alves
Universidade de Aveiro

Rui Brandão
Universidade de Évora

Victoria Cachorro Revilla
Universidad de Valladolid

Maria Filomena Camões
Universidade de Lisboa

José Luis Castillo Gimeno
Universidad Nacional de Educación a Distancia

Juan Fernández de la Mora
Yale University

Pedro García Ybarra
Universidad Nacional de Educación a Distancia

Ignacio González Loscertales
Universidad de Málaga

Jordi Grifoll Taverna
Universitat Rovira i Virgili

Cristina Gutiérrez-Cañas Mateo
Euskal Herriko Unibertsitatea

Francisco José Olmo Reyes
Universidad de Granada

Xavier Querol Carceller
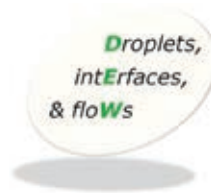*Institut de Diagnosi Ambiental i Estudis de l'Aigua – CSIC*
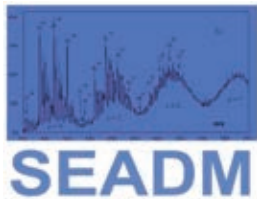
Organizing Committee

<u>Chair</u>

Joan Rosell-Llompart

<u>Co-Chair</u>

Jordi Grifoll Taverna

This congress was organized with the collaboration of

Sponsors

Program

Monday – Summer School July 7, 2014	
8:30 **9:15**	**Registration**
9:15 10:30	Francisco Gómez Moreno, *CIEMAT* *The measurement of atmospheric aerosol size distribution and other properties by means of DMAs*
10:30 **11:00**	**Coffee break**
11:00 12:15	Xavier Querol, *IDAEA-CSIC* *Research on atmospheric aerosols and air quality*
12:15 13:30	Cristina Gutiérrez-Cañas, *UPV-EHU* *The measurement and characterization of aerosols in industrial and work environments*
13:30 **15:00**	**Lunch**
15:00 16:15	Luís Tarelho, *Universidade de Aveiro* *Research on particulate matter formation and emission during biomass combustion*
16:30 **18:30**	**Visit to Tarragona**
18:30 **19:30**	**Welcome cocktail**

Tuesday July 8, 2014	
8:30 **9:00**	**Registration**
9:00 **9:30**	**Opening session**
	ORAL SESSION I - *Atmospheric Aerosols*
9:30 9:50	Aplicación del sistema tandem DMA-MS al análisis atmosférico *A. Álvarez Carballido, D. Zamora Pérez, G. Fernández de la Mora*
9:50 10:10	Longwave radiative forcing of mineral dust: Improvement of its estimation with tools recently developed by the EARLINET community *M. Sicard, S. Bertolín, C. Muñoz, A. Comerón, A. Rodríguez*
10:10 10:30	Trends in air pollution between 2000 and 2012 in the Western Mediterranean: A zoom over regional, suburban and urban environments in Mallorca (Balearic Islands) *J. C. Cerro, V. Cerdà, J. Pey*
10:30 10:50	Gas and particle phase chemical composition of marine emissions from Mediterranean seawaters: Results from a mesocosm study *J. Pey, H. L. Dewitt, B. Temime-Roussel, A. Même, B. Charriere, R. Sempere, A. Delmont, S. Mas, D. Parin, C. Rose, A. Schwier, B. Rmili, K. Sellegri, B. D'Anna, N. Marchand*
10:50 11:10	Instrumento de análisis y clasificación de especies en suspensión mediante ionización secundaria por electrospray, análisis de movilidad y masa *Company: SEADM*
11:10 **11:40**	**Coffee break**
11:40 **13:00**	**POSTER SESSION I**
13:00 **14:30**	**Lunch**

Tuesday July 8, 2014	
	ORAL SESSION II - *Aerosols and Health*
14:30 14:50	Microbial indicators of biological contamination at indoor workplaces *M. Gołofit-Szymczak, R. L. Górny, A. Ławniczek-Wałczyk*
14:50 15:10	Microorganisms on fibers as indoor air pollutants *R. L. Górny, A. Ławniczek-Wałczyk*
15:10 15:30	Sensitivity of the airborne pollen to the climate variability in the North East of the Iberian Peninsula *M. Alarcón, J. Belmonte; H. T. Maheed; C. Periago*
15:30 15:50	Airborne Phl p 5 in different fractions of ambient air and grass pollen counts in 10 countries across Europe *J.T.M. Buters, C. Antunes, R. Brandao, HIALINE working group*
15:50 16:10	Assessment of the human health risks and toxicity associated to particles (PM10, 2.5 and 1), organic pollutants and metals around cement plants *F. Sánchez, N. Roig, J. Sierra, M. Schuhmacher*
16:10 16:40	**Coffee break**
16:40 18:00	**POSTER SESSION II**

Wednesday July 9, 2014	
8:30 9:00	**Registration**
	ORAL SESSION III - *Atmospheric Aerosols*
9:00 9:20	Ground-based atmospheric monitoring in Mallorca and Corsica in summer 2013 in the context of ChArMEx: Results on number-size distributions, on-line and off-line aerosol chemistry, and volatile organic compounds *J. Pey, J. C. Cerro, S. Hellebust, H. L. Dewitt, B. Temime-Roussel, M. Elser, N. Pérez, A. Sylvestre, D. Salameh, G. Močnik, A. S. H. Prévôt, Y. L. Zhang, S. Szidat, N. Marchand*
9:20 9:40	Annual behavior of black carbon aerosols at Varanasi, India *M. K. Srivastava, R. S. Singh, B. P. Singh, R. K. Singh, B. N. Rai, S. Tiwari, A. K. Srivastava*
9:40 10:00	Atmospheric air quality assessment in an industrial area in Gijón, North of Spain *J. Lage, S.M. Almeida, M. A. Reis, P. C. Chaves, M. C. Freitas, S. Garcia, J. P. Faria, B. G. Fernández, H. TH. Wolterbeek*
10:00 10:20	First moon photometric aerosol measurements at Arctic stations *M. Mazzola, V. Vitale, A. Lupi, R. S. Stone, T. A. Berkoff, T. C. Stone, J. Wendell, D. Longenecker, C. Wehrli, N. Kouremeti, K. Stebel*
10:20 10:40	Rapid measurement of the size distribution with a SMPS using a new classifier *Company: Alava Ingenieros*
10:40 11:10	**Coffee break**

Wednesday July 9, 2014	
	ORAL SESSION IV - *Aerosol Fundamentals (Physics, Chemistry) & Aerosol Technology*
11:10 11:30	Characterization of carbonaceous particulate matter and factors affecting its variations in the Veneto region, Italy *MD. B. Khan, M. M. G. Formenton, A. di Gioli, G. de Gennaro, B. Pavoni*
11:30 11:50	Simulación de un electrospray cerca del caudal mínimo *S. E. Ibáñez, F. J. Higuera*
11:50 12:10	Ligament characterization in microdripping droplet emission mode *A. J. Hijano, S. E. Ibáñez, F. Higuera, I. G. Loscertales*
12:10 12:30	Electrohydrodynamic atomization of liquid suspensions for preparation of catalytic materials *P. L. Garcia-Ybarra, S. Martin, B. Martinez-Vazquez, J. L. Castillo*
12:30 13:00	**CLOSING**
13:00	**Lunch**

Contents

ARTICLES

Aerosols and Health

Atmospheric Aerosols

ABSTRACTS – ORAL PRESENTATIONS

Aerosol Fundamentals (Physics, Chemistry)

Aerosol Technology

Aerosols and Health

ABSTRACTS – POSTERS

Aerosol Fundamentals (Physics, Chemistry)

Aerosol Instrumentation

Aerosol Technology

Aerosols and Health

Articles

Characteristics of indoor aerosol size distribution in a gymnasium

Amaya Castro[1], Ana Calvo[2], Célia Alves[3], Liliana Marques[4], Teresa Nunes[5], Elisabeth Alonso-Blanco[6], Roberto Fraile[7]

Abstract — In this study, an indoor/outdoor monitoring programme was carried out in a gymnasium belonging to the University of Leon (Spain). The aerosol particles were measured in 31 discrete channels (size ranges) using a laser spectrometer probe (Passive Cavity Aerosol Spectrometer Probe, PMS Model PCASP-X). The air quality of the gymnasium was strongly influenced by the use of magnesia alba ($MgCO_3$) and the number of gymnasts who were training. For this reason, aerosol size distributions under several conditions were studied: i) before sports activities, ii) activities without using magnesia alba, iii) activities using magnesia alba, iv) cleaning activities and v) outdoors. From the aerosol size composition, the aerosol refractive index and density indoors were estimated: 1.577-0.003i and 2.055 g/cm^3, respectively. Using the estimated density, the mass concentration was calculated, and the evolution, for different activities, of PM_1, $PM_{2.5}$ and PM_{10} was assessed. Due to the climbing chalk and the constant process of resuspension, average PM_{10} concentrations above 440 $\mu g\ m^{-3}$ are achieved. Daily maximum concentrations ranging from 500 to 900 $\mu g\ m^{-3}$ were registered in the gymnasium. As particle size determines its deposition site, according to the Spanish standard UNE 77213, equivalent to the ISO 7708:199, the inhalable and thoracic fractions were assessed and, then, the tracheobronchial and respirable fractions for healthy adults and high risk people (children, frail or sick people). The different physical activities and attendance to the sport facility have a significant influence on the concentration and size distributions observed.

Keywords — aerosol size distribution, alveolar fraction, tracheobronquial fraction, fine mode, coarse mode, PM_{10}

1 INTRODUCTION

Indoor air quality (IAQ) has a significant impact on public health, because people nowadays spend about 90% of their time indoors. Hence, several IAQ monitoring programmes have been carried out in schools [e.g. 1], homes [2] and offices [3]. Comparatively, almost nothing is known about IAQ in recreation facilities [4]. Particulate matter is one of the most important pollutants in indoor air. Gymnasts and other sports practitioners can be at risk when they are training or exercising because the amounts of pollutants drawn into the lungs increase proportionally with increasing ventilation rates and the air is inhaled through the mouth, bypassing the normal nasal mechanisms for filtration of particles [5]. Particle size determines its deposition site and fraction in human lungs and its potential translocation to other target organs [6]. In studies of alveolar fraction of deposited particles (metals) in an urban city, air monitoring programmes, at least of the size ranges under 2.5 μm, have been recommended [7]. On the other hand, the particle size distribution is also one of the key characteristics as a basis for developing air quality regulations [8].

Very few studies have addressed the levels of this pollutant in gyms or similar facilities. Branis et al. [9] reported a direct relationship between the indoor levels of coarse particles and the number of children attending a school gym. Buonanno et al. established a connection between the high levels of coarse particles in an identical indoor space and the pupils' activities [4]. The chemical/mineral composition of particles resuspended by children during physical activities [10] and the particle size distribution [4] have been characterised in a very few investigations.

The study of the particle size distribution will allow a better understanding of the effects of aerosols on health and to take preventive actions [11,12].

In this study, in a gymnasium with different sports activities, using magnesium alba for drying the hands, the particle size distributions, the fine and coarse modes, and the different depositions of particles in the respiratory tract were analysed as a basis for developing indoor air quality regulations.

1. *Amaya Castro is with Department of Physics (IMARENAB), University of León, León 24071, Spain. E-mail: amaya.castro@unileon.es*
2. *Ana Calvo is with Department of Physics (IMARENAB), University of León, León 24071, Spain.. E-mail: aicalg@ unileon.es*
3. *Célia Alves is with the Centre for Environment and Marine Studies, Department of Environment, University of Aveiro, 3810-193 Aveiro, Portugal. E-mail: celia.alves@ ua..pt*
4. *Liliana Marques is with the Centre for Environment and Marine Studies, Department of Environment, University of Aveiro, 3810-193 Aveiro, Portugal. E-mail: lrmarques@ ua..pt*
5. *Teresa Nunes is with the Centre for Environment and Marine Studies, Department of Environment, University of Aveiro, 3810-193 Aveiro, Portugal. E-mail: tnunes@ ua..pt*
6. *Elisabeth Alonso Blanco is with Centre for Energy, Environment and Technology Research (CIEMAT) Madrid. E-mail: elisabeth.alonso@ciemat.es*
7. *Roberto Fraile is with Department of Physics (IMARENAB), University of León, León 24071, Spain. E-mail: roberto.fraile@unileon.es*

2 METHODOLOGIES

2.1 Description of sports facilities

A gymnasium was the sport facility belonging to the University of Léon, Spain, chosen to carry out the monitoring programme. The gymnasium is 15 m wide, 27 m long and has a height of 10.6 m. It has no windows and a half-cylinder skylight (5 m diameter and 20.3 m length) centred on the roof. The vinyl flooring is practically coated with gym mats and safety mattresses. The sports equipments included asymmetric bars/high bar, rings, parallel bars, beams, pummel horse, tumble track, trampolines, wall bars, and dug pit with foam cubes. Due to the high temperatures reached after the late morning hours, a side gate was frequently open when the gymnasium was busy. The gym does not have any mechanical ventilation system. Further details have been described in [13]. During the sampling campaign, it was occupied by college gymnasts between 7:00 and 12:00 (UTC) and between 15:00 and 17:00 (UTC).

2.2 Sampling and measurement equipments

The monitoring campaign was carried out between 15 and 21 July, 2012. During the week, measurements took place in the gymnasium, one sport facility belonging to the University of León, Spain. Continuous measurements of temperature, relative humidity (RH), CO_2, CO and total volatile organic compounds (TVOCs) were performed with an Indoor Air IQ-610 Quality Probe (Gray Wolf® monitor). The same measurements, excepting TVOCs, were continuously carried out outside using an IAQ-CALC monitor (model 7545) from TSI. From Monday to Friday, VOCs and carbonyls were sampled in parallel, both indoors and outdoors, using Radiello® diffusive passive tubes (cartridge codes 130 and 165, respectively). NO_2 was monitored, also from Monday to Friday, using diffusion tubes supplied by Gradko. On working days, during the occupancy periods, simultaneous indoor and outdoor sampling of particulate matter with equivalent aerodynamic diameter less than 10 μm (PM_{10}) was performed. At weekends, a 24-h sampling schedule was adopted. The PM_{10} samples were collected onto pre-baked (6 h at 500°C) 47 mm diameter quartz filters using Echo TCR Tecora samplers, following the EN 12341 norm. The gaseous pollutant and PM_{10} concentrations, together with the chemical composition of the latter, have already been published [13,14]. In addition, the particle size spectra were measured in 31 discrete channels (size ranges) using a laser spectrometer probe (Passive Cavity Aerosol Spectrometer Probe, PMS Model PCASP-X).

During the sampling campaign, the sports facility was occupied daily in the morning (between 7:00 and 12:00 UTC) by college gymnasts (16 to 29 gymnasts, and among them 8 to 16 used magnesium alba, and in the afternoon (between 15:00 and 17:00 UTC) there were only 4 to 8 gymnasts. The much higher attendance observed until mid-morning was due to a summer academy for kids sponsored by the university.

2.3 Methodology

The measures are grouped into fourteen categories: activities in the gym (I to XII), weekend (XIII) and outdoor (XIV) (Table 1). The use of magnesia alba as drying agent for hands is considered as a differentiating element in sports activities.

From the aerosol size composition, the aerosol refractive index and density, outdoors and indoors, were estimated. The values obtained were: 1.549-0.025i and 1.577-0.003i, and 1.940 and 2.055 g/cm³ for outdoors and indoors of gymnasium, respectively [14]. The diameters corresponding to the different channels (particle bin sizes) were corrected using these indices of refraction in a model based on the Mie Theory [15]. Using the calculated density, the mass concentration was estimated, and the evolution of PM_1, $PM_{2.5}$ and PM_{10} was assessed.

Table 1. Code and activities in the gymnasium (occupancy periods and weekend) and outdoors for different sampling periods.

CODE	ACTIVITIES	Time interval (UTC)
I	before sports activities	4:00 -7:00
II	sports activities without using magnesia alba in the morning (tatamis)	
III	sports activities without using magnesia alba in the morning (pit and tatamis)	Total 7:00 – 12:00
IV	sports activities using magnesia alba in the morning (pit and tatamis)	
V	vacant period	12:00 – 15:00
VI	sports activities without using magnesia alba in the afternoon (tatamis)	
VII	sports activities without using magnesia alba in the afternoon (pit and tatamis)	Total 15:00 – 17:00
VIII	sports activities without using magnesia alba in the afternoon (pirouettes)	
IX	cleaning activities	17:00 – 18:00
X	after sport activities (0h-2h)	18:30 – 20:30
XI	after sport activities (2h-4h)	20:30 – 22:30
XII	maximum of magnesia alba concentration	
XIII	weekend	24 hours
XIV	outdoors	30 min

3 RESULTS AND DISCUSION

3.1 Aerosol Number, Surface and Volume distributions

During nocturnal periods, the number of particles increased significantly, reaching values as high as 620 particles cm^{-3} before sports activities. This increase is experienced in the fine mode (fig. 1). Formation of new aerosol particles by nucleation and growth has been recently observed at night in chamber experiments [16].

Table 2. Total Number of Particles, Total Surface, Total Volume, Geometric Mean Diameter (CMD), Surface Mean Diameter (SMD), Volume Mean Diameter (VMD) and Geometric Standard Deviation (σ_g) of the number, surface and volume distributions obtained for different activities in the gymnasium, weekend and outdoors.

CODE	Number Size Distribution		
	N_T (cm^{-3})	CMD (μm)	σ_g
I	620±180	0.16±0.02	1.41±0.03
II	590±170	0.16±0.01	1.50±0.16
III	490±150	0.16±0.02	1.67±0.13
IV	520±160	0.17±0.01	1.77±0.16
V	440±150	0.17±0.01	1.64±0.17
VI	420±150	0.16±0.01	1.55±0.08
VII	300±100	0.17±0.00	1.61±0.06
VIII	379	0.17	1.60
IX	450±190	0.16±0.00	1.48±0.05
X	460±170	0.16±0.00	1.45±0.03
XI	530±170	0.15±0.01	1.40±0.02
XII	600±160	0.19±0.00	1.96±0.11
XIII	318	0.17	1.37
XIV	228	0.17	1.37
CODE	Surface Size Distribution		
	S_T (μm^{2}cm^{-3})	SMD (μm)	σ_g
I	79±19	1±1	5±2
II	400±400	4±3	6±2
III	1200±600	8±1	3±0
IV	1400±400	8±1	3±0
V	600±300	7±2	3±1
VI	400±300	6±2	4±1
VII	540±120	8±1	3±0
VIII	659	8	3
IX	160±16	4±1	6±1
X	98±8	2±1	6±1
XI	80±11	1±1	6±1
XII	2200±600	8±1	3±0
XIII	40	0.4	4
XIV	27	0.3	3
CODE	Volume Size Distribution		
	V_T (μm^{3}cm^{-3})	VMD (μm)	σ_g
I	100±40	1±1	8±3
II	700±800	13±0	2±0
III	2200±1100	13±0	2±0
IV	2600±700	13±0	2±0
V	1100±700	13±1	2±0
VI	700±500	13±1	2±0
VII	1000±300	14±1	2±0
VIII	1233	13	2
IX	210±50	12±1	2±0
X	90±40	10±1	2±0
XI	50±20	8±1	2±1
XII	3900±1200	13±1	2±0
XIII (*)	12	7	4
XIV (*)	3	1	5

(*) Sampling in just one day

The nocturnal events have been explained by the oxidation of volatile organic compounds (VOCs). Thus, VOCs emitted during the cleaning activities in the late afternoon may have contributed to nocturnal nucleation events [13].

In the morning, there were between 16 to 29 gymnasts, 11 of them using magnesia. During the periods of sports activities without using magnesia alba (table 2) the number of particles was high, but in the course of activities with the use of this drying agent (IV) the number of particles was 520±160 particles cm^{-3} with a Geometric Mean Diameter (CMD) of 0.17 µm, and the mean of maximum values observed (XII) was 600±160 particles cm^{-3} with a CMD of 0.19 µm. A decrease in the number of particles was registered during vacant periods. In the afternoon, the number of particles during the periods of sports activities without using magnesia decreased with respect to the morning, because the number of gymnasts in the sports arena was lower (between 4 and 8).

A limited number of measurements was performed outdoors. The availability of only a single aerosol spectrometer, associated with its high fragility, have restricted the number of displacements of this unit to the outside.

3.2 Fine and coarse modes

The size distributions are highly variable when the activities in the gymnasium are changing throughout the day (table 3). Thus, the fine and coarse modes are also very different depending on the type of activity within the enclosure.

Table 3. Number of particles, Geometric Mean Diameter (CMD) and Geometric Standard Deviation (σ_g) of the number distributions obtained for different activities in the gymnasium (occupancy periods and weekend) and outdoors for the fine and coarse modes.

CODE	Fine Mode			Coarse Mode		
	N (cm^{-3})	CMD (μm)	σ_g	N (cm^{-3})	CMD (μm)	σ_g
I	768	0.13	1.57	-	-	-
II	608	0.13	1.60	30	1.27	4.04
III	616	0.13	1.61	19	0.99	2.67
IV	622	0.13	1.58	32	0.64	3.17
V	551	0.13	1.55	15	0.55	3.80
VI	517	0.13	1.52	10	0.50	3.85
VII	336	0.14	1.53	8	0.93	2.63
VIII	402	0.15	1.50	11	0.88	2.71
IX	553	0.13	1.53	-	-	-
X	565	0.13	1.53	-	-	-
XI	608	0.13	1.50	-	-	-
XII	648	0.13	1.60	150	0.16	6.00
XIII	418	0.14	1.55	-	-	-
XIV	235	1.16	1.40	-	-	-

It was observed that:
- The distributions are lognormal, only for the fine mode, before sports activities (code I), when cleaning is taking place (IX), four hours after cleaning the enclosure (X and XI), at the weekend (XIII) and outdoors (XIV).
- In the morning, with the simultaneous presence in the sports facility of about 20 gymnasts, the

activities started without using magnesia (II). A large number of particles were recorded in the coarse mode (around 30 particles cm^{-3}). These particles were previously deposited on the surfaces and were resuspended to the surrounding environment due to complex effects. The dry deposition takes place from since the end of the previous day's activities (for about 14 hours). Subsequently (activity III), gymnasts use the pit and the tatamis, at the same time. The pit contains large foam cubes, which accumulate a lot of dust and magnesia. Later, gymnasts began to perform exercises using magnesia alba (IV). In all three cases, the distributions are bimodal with fine and coarse modes (Fig. 1). For each day, measurements of maximum concentrations of magnesia (XII) indicate a very large number of particles (150 particles cm^{-3}) in the coarse mode. This suggests that the use of magnesia alba causes, in the sports facility, a significant change in air quality due to the gradual emergence of many particles larger than one micron.

- During 3 hours, in the vacant period (V), processes for dry deposition of the particles were initiated. Later, a small group of gymnasts (between 4 and 8) for two hours in the afternoon, started to use the tatami mats for physical activities (VI), then the pit and tatamis simultaneously (VII) and finally performed pirouettes on the floor (VIII). During these three activities, a decrease in the number of particles has been recorded in relation to the morning, both in fine and coarse modes. Comparing the activity of the morning with the afternoon it can be concluded that the number of gymnasts in the room is a very important factor affecting the indoor air quality.

- Subsequently, the cleaning activities of the enclosure (code IX) has started. This alters the characteristics of the size distributions. That change is still observed four hours after the gym has been cleaned (codes X and XI). The mode fine fits a lognormal distribution, but the small number of particles in the coarse mode does not.

- On weekends (XIII) the number of particles in the fine mode decreased, the coarse mode is not observed and the size distribution is similar to that detected daily before the sports activities in the gym start.

3.3 Mass concentration

From the estimated particle density (2.055 g/cm^3) it was possible to also estimate the mass concentration of TSP, PM$_1$, PM$_{2.5}$, PM$_{10}$ and particles larger than PM$_{10}$ (Table 4). As soon as sports activities began in the morning (code II), significant increases in concentration of PM$_{10}$ were
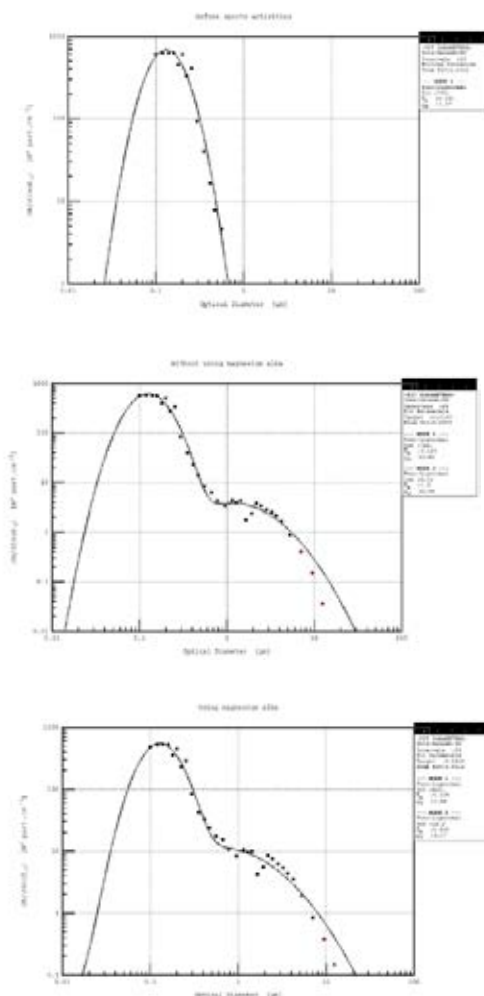
Fig.1. Experimental and theoretical aerosol size bimodal number distribution before sports activities (I), for sports activities without using magnesia in the morning (II and III) and using magnesia (IV).

observed. The main cause is the resuspension of dust deposited on the gym equipments, on the pit and on the tatamis. Subsequently, with the use of magnesia by gymnasts (phase IV), average PM$_{10}$ concentrations of 440 µg m^{-3} were achieved. Daily maximum concentrations, ranging from 500 to 900 µg m^{-3}, were measured. This indicates that there was a strong environmental contamination inside the gym while gymnasts were training with magnesia. During the vacant period (3 hours), the concentration decreased to an average value of 190 µg m^{-3} and increased again with sports activities in the afternoon. As the number of gymnasts was much lower and with a decreased usage of magnesia in the afternoon, the mass concentration was not greater than 220 µg m^{-3}. It is a value well below the 380 µg m^{-3} observed in the morning, when occupancy was higher. The cleaning activities caused a drastic decrease (40 µg m^{-3}), which is progressive in the next four hours (up to 13 µg m^{-3}). These values are maintained until the next morning, before the sports

activities started again. The use of liquid chalk, instead of the common magnesia alba, has been recently proven to be an effective and inexpensive measure to reduce particle levels in gymnasiums [17].

Table 4. Mass concentration: TSP, PM_1, $PM_{2.5}$, PM_{10} and larger than PM_{10} ($\mu g\ m^{-3}$).

CODE	TSP	PM_1	$PM_{2.5}$	PM_{10}	$> PM_{10}$
I	12±6	5±2	6±2	10±3	2±4
II	140±160	5±1	16±14	120±150	15±15
III	400±200	7±3	44±20	380±190	60±20
IV	520±140	8±1	51±11	440±130	80±20
V	210±130	5±1	23±9	190±110	21±16
VI	130±100	4±1	14±8	120±90	13±14
VII	210±60	4±1	19±1	180±50	32±9
VIII	250±90	5±1	24±8	220±70	30±40
IX	45±8	3±1	9±1	40±9	5±2
X	21±6	3±1	6±1	20±5	2±1
XI	13±3	4±1	6±1	13±3	0±0
XII	800±200	14±4	90±20	700±200	100±90
XIII	3.2	2.1	2.7	3.2	0
XIV	20±20	2±0	8±1	20±20	0±0

3.4 Inhalable, Thoracic, Tracheobronquial and Respirable Fractions

In Table 5 the percentages corresponding to the different aerosol fractions in the gymnasium for different activities (I to XII), weekend (code XIII) and outdoors (code XIV) are shown. The number of particles per unit volume retained in the regions of the human respiratory tract according to the experimental size distributions has been indicated.

Before the different sports activities (code I) and in the interval from 2h to 4h after the sports activities (code XI), the percentage of the number of particles inhaled in every fraction and the deposition of the particles in the different parts of the respiratory tract had a similar behaviour. For high risk population, around 35% of the particles reached the alveolar region (bronchioles and alveoli), whilst a percentage of around 45% was estimated for a healthy adult. These percentages applied to the total number of particles.cm^{-3}, showed that, in the case of a healthy adult, around 160 particles cm^{-3} cannot cross the nonciliated airways and are retained by the trachea and bronchia (tracheobronchial region). As regards to high risk population around 220 particles cm^{-3} were obtained. As a consequence, 240 and 280 particles cm^{-3}, respectively, reach the alveolar region (bronchioles and alveoli).

Concurrently with physical activities, a significant number of large particles were detected. Therefore, the deposition rates in the alveolar region will be smaller (around 12 to 16%).

On the weekend, inside the gymnasium (code XIII), for each fraction, similar percentages of deposition were observed, but as the total number particle per cm^3 is lower, the number of particles retained in the human respiratory tract is also lower.

A very different behaviour is observed when sports activities are initiated with or without using magnesia alba in the morning or afternoon. For a healthy adult or for high risk population, as children, frail or sick people, the percentages of deposition in the tracheobronquial area (about 40%-50%, for codes II to VIII) increased or decreased the percentages in the respirable fraction (about 6%-13%). These results are due to the dissimilar particle size distributions when different sports activities are taking place in the gym. The large particles present in the air do not reach the alveoli, being retained in the tracheobronchial region by the trachea and bronchies. From the particle size distribution, for a healthy adult, in the tracheobronchial region, it is possible to observe that 120-210 particles cm^{-3} cannot cross the nonciliated airways and are retained by the trachea and bronchi. The remaining particles, i.e. between 38-90 particles cm^{-3}, reach the alveolar region (bronchioles and alveoli)..

Table 5. Tracheobronquial and respirable fractions for a healthy adult and high risk groups (children, frail or sick people) and Nº particles/cm^3 for different activities in the gymnasium (occupancy periods and weekend) and outdoors.

	Tracheob. Fraction-Healthy adult	Tracheob. Fraction-High risk	Respirable Fraction-Healthy adult	Respirable Fraction-High risk
CODE	%	%	%	%
I	26±8	34±9	45±24	40±30
II	35±11	43±13	16±4	8±3
III	40±4	49±5	13±2	5±1
IV	40±0	49±1	10±2	5±1
V	41±1	50±2	15±3	6±2
VI	40±1	49±2	15±2	7±2
VII	39±3	47±5	13±3	5±1
VIII	39±0	47±0	12 ±0	5±0
IX	39±2	50±3	23±5	12±4
X	36±5	46±7	30±15	20±12
XI	32±8	44±9	45±12	33±13
XII	41±1	52±3	16±4	6±2
XIII (*)	21	30	60	52
XIV (*)	29	35	14	8
	Nº part./cm^3	Nº part./cm^3	Nº part./cm^3	Nº part./cm^3
I	160±90	210±100	280±130	240±140
II	210±40	250±50	90±30	47±19
III	190±60	240±70	70±30	22±9
IV	210±60	260±80	70±30	26±10
V	180±60	220±80	70±30	26±14
VI	170±60	210±70	70±30	27±15
VII	120±30	140±30	38±3	14±1
VIII	150±40	180±50	47±16	18±8
IX	180±70	220±90	100±60	60±40
X	170±50	210±80	140±120	90±90
XI	170±30	230±60	240±140	180±120
XII	247±70	310±90	100±40	35±16
XIII(*)	68	94	192	165
XIV(*)	124	150	60	34

(*)Sampling just in one day

During the vacant period, which lasted

approximately 3 hours, between the morning and afternoon activities, , the dry deposition was slow and did not cause appreciable changes in the size distributions. Their behaviour was similar to those registered during the periods with sport activities.

However, in the afternoon, after the cleaning activities, the percentages for the different fractions approached the values of deposition observed before sports activities. This means that particles originated from magnesia alba are more efficiently eliminated by cleaning activities than by dry deposition phenomena.

CONCLUSIONS

In the indoor environment of a gymnasium the PM_{10} concentrations are highly variable, depending on the activities of practitioners, occupancy rates, cleaning, etc. Some activities, such as gymnastics, lead to a constant resuspension process of particles from the surfaces of tatamis and foam cubes. The use of magnesia alba as drying agent for hands contributes to a dusty indoor air due to the gradual emergence of many particles larger than one micron.

The particle size distributions are different when different gymnastic activities are practiced in the gym. The presence of substantial amounts of large particles has been observed in the air. Many of them do not reach the alveolar region, because they are retained in the tracheobronchial region by the trachea and bronchia.Particles originated from magnesia alba**,** and especially those from resuspension of dust settled when sports activities take place, are eliminated more efficiently by cleaning activities than by dry deposition phenomena.

In view of the results, in a gymnasium, the daily use of powerful vacuum cleaners using multi-stage HEPA filtration systems with graduated filters are highly recommended. A regular renewal of tatami and foam cubes is also advised.

Given that the health effects of these particles are not well established, the precautionary principle should be applied in conjunction with other preventive and remedial measures to reduce indoor levels.

REFERENCES

[1] P.N. Pegas, T. Nunes, C.A. Alves, J.R. Silva, S.L.A. Vieira, A. Caseiro, C. Pio, "Indoor and outdoor characterisation of organic and inorganic compounds in city centre and suburban elementary schools of Aveiro, Portugal," *Atmos. Environ.*, vol. 55, pp. 80-89, 2012.

[2] S. Semple, C. Garden, M. Coggins, K.S. Galea, P. Whelan, H. Cowie, A. Sánchez-Jiménez, P.S. Thorne, J.F. Hurley , J.G. Ayres, "Contribution of solid fuel, gas combustion, or tobacco smoke to indoor air pollutant concentrations in Irish and Scottish homes," *Indoor Air*, vol. 22, pp. 212-223, 2012.

[3] G. Sangiorgi, L. Ferrero, B.S. Ferrini, C. Lo Porto, M.G. Perrone, R. Zangrando, A. Gambaro, Z. Lazzati, E. Bolzacchini, "Indoor airborne particle sources and semi-volatile partitioning effect of outdoor fine PM in offices", *Atmos. Environ.*, vol. 65, pp. 205-214, 2013.

[4] G. Buonanno, F.C. Fuoco, S. Marini, L. Stabile, "Particle resuspension in school gyms during physical activities," *Aerosol Air Qual. Res.*, vol. 12, pp. 803-813, 2012.

[5] A. Carlisle, N. Sharp "Exercise and outdoor ambient air pollution," *Br. J. Sports Med.*, vol. 35, pp. 214-222, 2001.

[6] W.G. Kreyling, M. Semmler-Behnke, W. Moller, "Ultrafine particle-lung interactions: Does size matter?," *J. Aerosol Med.*, vol. 19, pp. 74-83, 2006.

[7] A.J. Fernández, M.Ternero, F.J. Barragán, J.C. Jiménez, "Size distribution of metals in urban aerosols in Seville (Spain)", *Atmos. Environ.*, vol. 35, pp. 2595–2601, 2001.

[8] L. Morawska, D. U. Keogh, S.B. Thomas, K.L. Mengersen, "Modality in ambient particle size distributions and its potential as a basis for developing air quality regulation," *Atmos. Environ.*, vol. 42, pp. 1617-1628, 2008.

[9] M. Braniš, J.Šafránek, A. Hytychová, "Indoor and Outdoor Sources of Size-Resolved Mass Concentration of Particulate Matter in A School Gym-Implications for Exposure of Exercising Children". *Environ. Sci. Pollut. Res. Int.* vol. 18, pp. 598-609, 2011.

[10] M. Braniš, J. Šafránek, "Characterization of Coarse Particulate Matter in School Gyms". *Environ. Res.* vol. 111, pp. 485-491, 2011.

[11] M. Cambra-López, A.J.A.Aarnink, Y.Zhao, S. Calvet, A.G. Torres, "Airborne particulate matter from livestock production systems: A review of an air pollution problem", *Environ Pollut*, vol. 158, pp.1-17, 2010.

[12] D.L. Bartley, J.H. Vicent, "Sampling conventions for estimating ultrafine and fine aerosol particle deposition in the human respiratory tract", *Ann Occup Hyg* , vol. 55, pp. 696-709, 2011.

[13] C.A. Alves, A.I. Calvo, A. Castro, R. Fraile, M. Evtyugina, E.F. Bate-Epey, "Indoor Air Quality in Two University Sports Facilities".*Aerosol Air Qual. Res.*, vol.13, pp. 1723–1730, 2013.

[14] C.A. .Alves, A. I. Calvo, L. Marques, A. Castro, E. Coz, R. Fraile, "Particulate matter in the indoor and outdoor air of a gymnasium and a frontón". *Environ. Sci. Poll. Res., (in press)*.

[15] C.F. Bohren, D.R. Huffman, Absorption and Scattering of Light by Small Particles,Willey, New York, 1983.

[16] I.K. Ortega, T. Suni, M. Boy, T. Grönholm, H.E. Manninen, T. Nieminen, M. Ehn, H. Junninen, H. Hakola, H. Hellén, T. Valmari, H. Arvela, S. Zegelin, D. Hughes, M. Kitchen, H. Cleugh, D.R. Worsnop, M. Kulmala, V.-M. Kerminen, "New insights into nocturnal nucleation", *Atmos. Chem. Phys.*, vol. 12, pp. 4297-4312, 2012.

[17] S. Weinbruch, T. Dirsch, K. Kandler, M. Ebert, G. Heimburger, F. Hohenwarter, "Reducing dust exposure in indoor climbing gyms," *J. Environ. Monit.*, vol. 14, pp. 2114-2120, 2012.

Fly-ash emissions control efficiency and heavy metals particle size distribution in an application of a hybrid filter to biomass-waste co-firing flue gas

Gaizka Aragón[2], David Sanz[1], Enrique Rojas[1], Jesús Rodríguez-Maroto[1], Raquel Ramos[3], Ricardo Escalada[3], Elena Borjabad[3], Miren Larrión[2], Iñaki Mujica[2], Cristina Gutiérrez-Cañas[2]

[1]*Grupo de Emisiones Industriales Contaminantes, CIEMAT, Avda. Complutense 40*
28040 Madrid, España, david.sanz@ciemat.es

[2]*Dpto. De Ing. Quim. y del Medio Ambiente, Universidad del País Vasco, Alda. de Urquijo s/n*
48013 Bilbao, España, garagon001@ikasle.ehu.es

[3]*Unidad de Procesos de Conversión Térmica, CEDER-CIEMAT, Autovía A-15, salida 56*
42290 Cubo de la Solana, España, raquel.ramos@ciemat.es

Abstract — Control of emissions of heavy metals is a necessary requirement for waste-to-energy combustion applications. Even in biomass combustion, emissions of certain heavy metals may pose a so far unnoticed or underestimated risk.

Hybrid filters (HF) (combination of electrostatic precipitator and fabric filter) applied to the control of emissions of particulate matter (PM) present more robust performance under varying operating conditions, and increased efficiency in the control of PM emissions in the particle size range where a greater enrichment in heavy metals is expected.

This paper investigates the fractional penetration and enrichment in fly-ash of different metals of interest, under different operating conditions, through a semi-industrial scale HF applied to the control of emissions from co-combustion of biomass and wastes. Heavy metals size distribution in fly-ash was determined.

Depending on operating conditions, an average efficiency of 96.85 to 99.41% in terms of total mass concentration of PM was found. Some of the corresponding values for heavy metals were 79.17-98.57%, in the case of Pb, and 93.63-99.27% , in the case of Cu, in the solid phase; note that some elements may be also present in vapor phase depending on volatility.

A preferential enrichment in Cl, Na, K, Cd, and Pb was found in the fly-ash collected in the fabric filter module. Copper was found preferably in the submicron fraction of the raw fly-ash, being able the HF to produce a depurated emission without preferential size enrichment in Cu.

The HF ability to efficiently control emissions of both overall PM, and heavy metals fraction in particular was demonstrated within a wide range of load and different fuels. The preferential occurrence of some heavy metals in the ultrafine fraction of fly-ash has been detected, which makes clear the need of effective control systems for PM in that size range.

    Keywords — Abatement strategies, biomass combustion, emissions, Particulate Matter, filtration, fabric filter, electrostatic precipitators, hybrid filter, heavy metals.

1 INTRODUCTION

Hybrid filters are a combination of electrostatic precipitator and fabric filter. These elements can be coupled in series or in parallel (Miller, 2003; Gebert, 2002). Special textile materials have been developed and applied, with the inclusion of catalysts, for the simultaneous control of persistent organic pollutants in gaseous phase and particulate matter. In the FHIBCAT project ("Catalytic hybrid

filter for control of gaseous emissions of PM10 toxic pollutants POPs and heavy metals: design, parametric study, construction, commissioning and validation"), a semi-industrial hybrid filter pilot equipped with catalytic textile has been developed. The filter was installed in a line of validation where different techniques were used for the characterization of emissions. The objective of the project was the construction and commissioning of a facility for demonstration and evaluation of trace toxic pollutants control techniques, a semi-industrial scale.

2 EXPERIMENTAL

2.1 Experimental facility

The experimental facility consisted in a validation process line (Fig. 1) (Sanz, 2009; Sanz, 2010)., treating 1000 Nm^3/h of flue gases from a 1 MW_{th} bubbling fluidized bed combustor. The main piece of equipment in this validation process line is the hybrid filter. The hybrid filter is made up of an electrostatic precipitation module (ESP) and a bag filter module (BF) connected in series.

The ESP module had a plate-wire configuration in 2 fields divided in 4 longitudinal channels 200mm wide, there are six discharge electrodes per channel in each field. Collected fly ash is dislodged from the electrodes into four hoppers at the bottom of ESP module by periodical mechanical rapping. ESP module body and hoppers are electrically traced for heating up and to minimize heat loss. Regulation and control of the potential applied between the electrodes is achieved using a controller with microprocessor which allows selecting the energization mode (continuous or pulse) and to adjust different parameters (maximum secondary voltage, frequency of electrodes rapping, etc...).

The filter media installed in BF is chemically active, combining surface filtration together with catalytic activity, and thus selective abatement of certain pollutants. Filter bags contain a catalyst designed for organic gaseous pollutants destruction (Fritsky, 2001). Filter media consist of an ePTFE membrane laminated over a catalytic felt substrate. Prescribed operation temperature for acceptable chemical conversion was 190 C. The relatively small size of the bag module as well as the ease for loaded media replacement determine that the arrangement follow a "pocket" rather a right bag pattern. BF module had its own ash hopper, ash discharge valve and collecting bin, thus allowing separate ESP and BF ash collection and sampling. BF module was also electrically traced. Cleaning of the filter is made by pulses of compressed air.

The bubbling fluidized bed boiler (1 m diameter and 4 m height) is equipped with a complete set of sensors for temperature, differential pressure and flows. Feed, in the range from 150 to 350 kg/h

should be pelletized. Burnout quality has been ensured through temperature (>850 C) and residence time (>0.5 s). The bed material was silica, which was entirely replaced every time fuel formulation was changed.
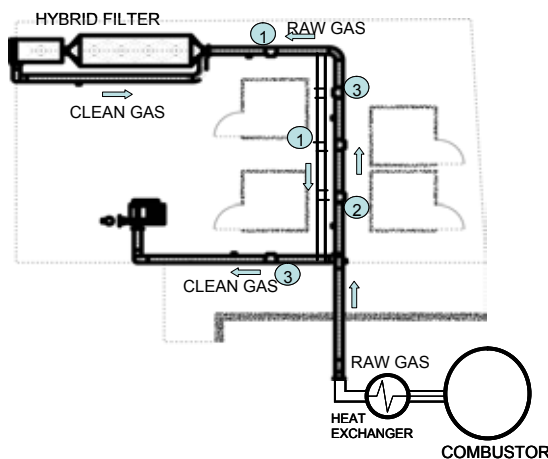
Fig. 1 Experimental validation line lay-out

2.2 Method

Every test day the hybrid filter and connecting pipes were electrically preheated before boiler start-up. Any ash in hybrid filter hoppers from preceding tests was removed before the test begun. Then the boiler was started. Once stable boiler operation was reached, aerosol sampling was undertaken. The operating temperature of the hybrid filter was controlled regulating the flue gas condenser cooling air flow. Flue gas flow rate through the hybrid filter was also controlled using an induced draft variable speed blower. The ESP module of the hybrid filter was operated with continuous energization, an electronic automatic controller kept the selected applied voltage value. The groups of bags in BF module were sequentially back pulsed. An automatic timer controlled the process, back pulsing interval was adjusted to keep filter pressure drop under control.

Three different material were used for the formulation of the fuel blends: olive tree pruning (C), compost (A) and a refuse derived fuel, RDF (B) . The olive pruning pellets employed, were commercial pellets from Granada (Spain). Pelletized compost was provided by the same company, which had experimentally produced them. RDF consisted of a mixture of two fractions of municipal solid

waste (MSW) from a waste treatment plant in Tudela (Navarra, Spain). A 90% of RDF came from the organic fraction refuse and a 10% from the packaging refuse line. RDF was pelletized in CEDER. Three different fuel blends were used during the experiments: blends AC and BC (50/50 by weight) and C fuel alone. A complete characterization of the fuels can be found elsewhere (Sanz, 2011; Sanz, 2010).

Samples were taken upstream and downstream the filter to determine the removal efficiency of particulate matter and heavy metals. An aerosol sampling and measuring station was assembled close to two adjoining fly-ash aerosol sampling ports (one upstream and one downstream of the hybrid filter).

In each port an aerosol sampling probe was mounted on a hermetically closed flange. The probes were provided with thin wall nozzles facing the gas stream on the pipe axis line. Pitot tubes and thermocouples were also provided for measurement of gas velocity and temperature at the sampling point. Sampling could be switched between upstream and downstream ports using valves.

In the upstream port the aerosol was conducted to a cyclone and an Optical Particle Counter-sizer (OPC).

Pseudo-isokynetic sampling of flue gas was conducted for particulate matter characterisation. Flue gas aerosol was sampled on 47mm glass fiber filters for determination of total mass concentration, and Berner low pressure impactor, BLPI (Hauke) and 8-stage Andersen (MARK III) type cascade impactor for mass size distribution. Also, size distribution measurements were made using light scattering optical particle counter (OPC) (Palas PCS 2000), differential electrical mobility analyser (TSI SMPS) and real time Electrical low pressure impactor (ELPI). Aerosol sampling devices (filter holders and impactors) were placed into an electrically heated box to avoid condensation. OPC was used only when sampling upstream fly-ash.

Samples of ashes recovered from ESP and BF were taken on a daily basis for further analysis by Inductively Coupled Plasma Mass Spectrometry (ICP/MS), and Inductively Coupled Plasma Atomic Emission Spectroscopy (ICP/AES) (metal elements), flame photometry (alkali metals), and specific technique for chlorine (extraction with Eschka mixture and titration).

For the determination of heavy metals concentration, sample loaded filters and impactor substrates were subjected to acid digestion. The resulting solutions were analysed by ICP/AES and ICP/MS thus allowing determination of high and low concentration elements. Blank samples of filters and impactor substrates were also analysed. Net content of each element in fly-ash was computed by difference between sample loaded and blank results.

2.3 Test Matrix

A test matrix was planned (Table 1), focusing on the more relevant operating conditions: gas flow rate, operating temperature and applied voltage to the ESP.

Due to the requirements of catalytic activity of the filter media for the claimed conversion of PCDD/Fs, the temperature through the hybrid filter must be over 190 C. This raises the question of the role of potentially condensable matter and the interpretation of size distribution of emitted particles. Thus, a set of experiments (B160-12, B190-09 and C170-14) was specifically conducted to ascertain the effect of the filter temperature on the size distribution of emitted aerosol.

Table 1 Test Matrix

Test code	Fuel (olive:other w/w ratio)	Air to cloth ratio (m3/m2/min)	Operating temperature (°C)	Applied voltage (kV)
A190-12	AC (57:43)	1.32	185	20 - 15
A190-09	AC (48:52)	1.15	190	20 - 15
A190Dx	AC (51:49)	1.06	197	15
A210Dx	AC (51:49)	1.27	213	15
B190-12	BC (67:33)- (49:51)	1.3 - 1.24	194 - 195	20 - 15
B160-12	BC (52:48)	1.29 - 1.27	198 - 163	20 - 15
B190Dx	BC (52:48)	1.23	193	15
B190-09	BC (58:42)	1.22 - 1.3	168 - 192	20
C170-14	C	1.42	168	20
C190Dx	C	1.26	196	15
C170-12	C	1.25	170	20

3 RESULTS

3.1 Overall total mass and solid phase heavy metals concentration reduction

Mass concentration of fly-ash aerosol in raw and treated flue gas, i.e. upstream and downstream of hybrid filter, was gravimetrically assessed from 47mm glass fiber filter samples. The net weight of collected fly-ash was divided by total accumulated flue gas sample volume.

Table 2 shows the results regarding total fly-ash mass concentration, classified by fuel/blend. Table 3 shows results for removal efficiency of heavy metals. For obtaining the figures in the table the concentration of each element in fly-ash was multiplied by fly-ash mass concentration in flue gas.

mass size distributions are monomodal upstream the filter, with 0.25 micrometers median. Downstream the filter Pb, Cd and Cu mass are evenly distributed over the size range covered by the cascade impactor.

Table 2. Overall filtration efficiency (total mass basis)

Fuel/Blend	% reduction
AC	99.01 - 99.41
BC	96.85 - 98.08
C	99.40

Fig. 2 Cd and Pb cumulative size distributions upstream and downstream the hybrid filter for fuel blend AC

Table 3. Percentual removal of solid phase heavy metals load in the hybrid filter

	Blend AC	Blend BC	Fuel C
Pb	98.16	98.57	79.17
Cd	97.18	97.23	75.00
As	90.59	49.69	75.00
Sb	97.23	93.62	35.00
Cr	93.91	66.46	47.50
Mn	91.90	61.12	95.80
Mo	97.79	77.36	50.00
V	90.59	49.69	75.00
Cu	99.27	98.78	93.63
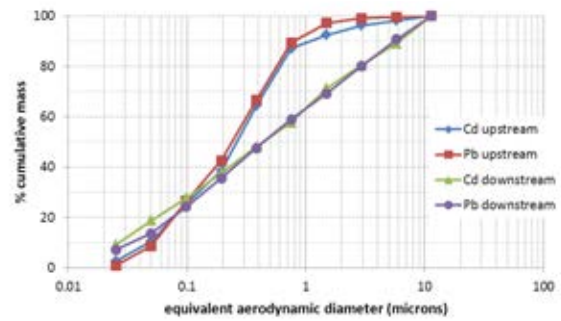
Fig. 3 Cd and Pb cumulative size distributions upstream and downstream the hybrid filter for fuel blend BC

3.2 Heavy metals reduction by particle size

The most outstanding findings from data obtained with the low pressure cascade impactor are as follows:

Fuel AC produces extremely fine fly-ash, on average over 30% of mass falls in the ultrafine size range upstream the filter. Aerodynamic size distribution is skewed monomodal both upstream and downtream of the filter.

Fuel BC fly-ash size distribution is bimodal upstream the filter, but monomodal downstream. The filter seems to remove completely the finer mode.

Fuel C fly-ash size distribution is bimodal upstream the filter, but monomodal downstream. The filter seems to remove completely the finer mode.

Regarding specifically heavy metals, Cu, Cd an Pb size distributions are not affected by the filter for fuel C (figure 4). The size distribution is not affected or only slighly affected in the case of fuel AC (figure 2). But it is significantly affected in the case of fuel BC (figure 3). In this case Pb, Cd and Cu

Fig. 4 Cd and Pb cumulative size distributions upstream and downstream the hybrid filter for fuel C

4   CONCLUSIONS

The HF is able to efficiently control emissions of both overall PM, and heavy metals fraction in particular was demonstrated within a wide range of load and different fuels. The preferential occurrence of some heavy metals in the ultrafine fraction of fly-ash has been detected, which makes clear the need of effective control systems for PM in that size range.

The fine fraction of fly ash is enriched in some heavy metals. Volatile elements in fly ash, in particular some heavy metals originating from co-fired residue such as Cd and Pb, condensate on fine biomass-produced fly-ash. Not particularly volatile Cu follows similar trends because it is present in a significant amount in the olive tree biomass selected for this work.

REFERENCES

[1] Miller, S.J. et al (1999) "Advanced Hybrid Particulate Collector and Method of Operation" United States Patent 5,938,818

[2] Gebert, R. et al (2002). "Commercialization of the advance hybrid filter technology"*Air quality III Conference.* Arlington 9 nov 2002

[3] Fritsky, K.J., Kumm, J.H. and Wilken, M., "Combined PCDD/PCDF Destruction and Particulate Control in a Baghouse: Experience with a Catalytic Filter System at a Medical Waste Incineration Plant" *J. Air Waste Management Association*, Dec 2001, 1642-1649

[4] D. Sanz, J. J. Rodríguez, J. L. Dorronsoro, E. Rojas, P. Galán, R. Ramos, R. Escalda, E. Ruiz, M. A. Martínez, A. Bahillo, S. Astarloa, W. Hagemann, C. Gutierrez-Cañas (2010) "Proyecto FHIBCAT, control simultáneo de PM y PCDD/Fs en combustión de biomasa y residuos biomásicos. Determinación del rango de admisión de combustibles." IV Reunión Española de Ciencia y Tecnología de Aerosoles, Granada, 28-30 June.

[5] Sanz D., Rodríguez J.J., Dorronsoro J.L., Rojas, E., Bahillo A., Ramos R., Ruiz E., Gutierrez-Cañas C., and Hagemann W. (2009). "Actividades en el marco del proyecto FHIBCAT, filtro híbrido catalítico" *3a Reunión Española de Ciencia y Tecnología de Aerosoles*. Bilbao, 24-26 June.

[6] Sanz D., Rodríguez-Maroto J.J., Dorronsoro J.L., Rojas E., Bahillo A., Ramos R., Ruiz E., Galán P., Martínez M.A., Gutierrez-Cañas C., Larrion M., Peña E., Hagemann W., Astarloa S., (2011) "Hybrid filtration and catalytic control of toxic pollutants from a 1.2 MW waste biomass cofiring boiler", European Aerosol Conference, Manchester, September, 2011

Aerosol Deposition in Balearic Islands as Overview of the deposition in the Western Mediterranean

J. C. Cerro[1], S. Caballero[2], C. Bujosa[3], A. Alastuey[4], X. Querol[4], J. Pey[4,5]

Abstract — Atmospheric deposition, as the last stage of the aerosol cycle, brings nutrients and pollutants to earth and sea surfaces. The quantification of deposition fluxes, their chemical characterization and the knowledge about the sources becomes necessary when analysing different ecosystem responses.

In the context of the ChArMEx (The Chemistry-Aerosol Mediterranean Experiment, https://charmex.lsce.ipsl.fr) initiative, a 2-year study on wet and dry deposition of atmospheric aerosols has been conducted at a regional background environment in Mallorca (Balearic Islands, western Mediterranean). From September 2010 to August 2012 weekly dry and wet deposition samples were collected. In addition, atmospheric particulate matter was regularly sampled in both PM10 and PM1 fractions, as well as gaseous pollutants and meteorological parameters were continuously registered.

Deposition samples were subjected to different analytical procedures including quantification of deposition volumes and subsequent filtration on quartz fibre filters, determination of pH, and complete acidic digestion of filters. Solutions obtained were analysed by a number of techniques determining the concentrations of soluble and insoluble fractions of a number of species including typical mineral elements (Al, Ba, Ca, Mg, Mn, Sr, Ti), major marine components (Cl, Na, Mg), anthropogenic tracers (Cu, K, Mn, Ni, NO_3^-, NH_4^+, Pb, V, Zn), and some multiple-origin components such as SO_4^{2-}. Episodic and seasonal patterns were assessed, and differences between wet and dry deposition, and their relation with specific scenarios were established.

Special attention has been paid to the deposition of phosphorous, nitrogen (as NH_4^+ and NO_3^-) and iron and their possible influence on the sea Chlorophyll concentration, detected by different satellites (www.globcolour.info).

A preliminary source exploration by means of Principal Component Analysis has been done. Wet deposition samples exhibit three sources: crustal, marine and mixed-anthropogenic, whereas dry deposition samples split the anthropogenic source in three different components: a Cu-Zn-Fe, a K-Ni-Pb and a NO_3^--NH_4^+.

Keywords — Air Pollution, Atmospheric Dust, Aerosol Deposition, Particulate Matter, Dry Deposition, Wet Deposition.

1 INTRODUCTION

Both the magnitude and the mineralogical composition of atmospheric dust inputs to the Mediterranean indicate that eolian deposition is an important (50%) or even dominant (80%) contribution to sediments in the offshore waters of the entire Mediterranean basin [1].

The atmospheric dynamics provides the main route for dispersion and transport of pollutants in gaseous and aerosol forms among different environmental systems.

The trajectories followed by the pollutants in the atmosphere and the distance they travel depend on different factors, such as meteorological conditions. Finally, most of the pollutants return to the surface of the earth trough wet or dry deposition, or through direct sorption of gaseous compounds by surface water, plants or soil.

Therefore, the deposition of particulate matter might have a direct effect on the ecosystems by harming (pollutant deposition) or benefiting (nutrients deposition).

Mallorca is located in the middle of the Western Mediterranean, a location that might be regarded as representative of the Western Mediterranean. The Balearic Islands are regularly affected by Northern African dust incursions, occasionally bringing large loads of particulate matter [2].

Wet deposition is defined as the flux of a chemical compound to the earth's surface by precipitation (in whatever form falls into the collector), dry deposition as the flux of trace gases and particles via turbulent exchange and gravitational settling followed by interaction with exposed surfaces [3], and 'total' deposition as the sum of both.

In our latitudes, most of the atmospheric deposition occurs in the form of wet deposition. However, in southern European regions such as the western Mediterranean, the role of dry deposition is essential [4].

Factors upon which the dry deposition are mainly the level of turbulence in the atmosphere, the chemical properties of the deposited species, their solubility, particle size, and the nature of the surface [3].

The flow of dry deposition is directly proportional to the concentration of the species being deposited by one of

1. *Laboratory of Environmental Analytical Chemistry, Illes Balears University, Ctra. Palma-Valldemossa, Km 7.2, 07008, Palma de Mallorca, Spain, jccerro@dgqal.caib.es*
2. *Atmospheric Pollution Laboratory, Miguel Hernández University, Av.de la Universidad s/n, 03202 Elche, Spain, san.cab@umh.es*
3. *ENDESA c/ Sant Joan de Déu 1, 07007, Palma de Mallorca, Spain, carles.bujosa@endesa.es*
4. *Institute of Environmental Assessment and Water Research, IDÆA-CSIC, C/ Jordi Girona 18-26, 08034, Barcelona, Spain, andres.alastuey@idaea.csic.es , xavier.querol@idaea.csic.es*
5. *Laboratory of Environmental Chemistry LCE-IRA, Aix Marseille University, 3 Place Victor Hugo,13001 Marseille, France, jorge.pey@univ-amu.fr*

the lower height area of 10 m:

$$F = -V_d\, C \qquad (1)$$

F, vertical flux of dry deposition ($\mu g\ m^{-2}\ day^{-1}$)

V_d, speed deposition factor ($m\ day^{-1}$)

C, concentration as mass in a volum ($\mu g\ m^{-3}$)

The European Directives (2008/50/CE) indicate the necessary study of atmospheric deposition.

There are some CEN Standards for the determination of pollutants in deposition samples that have been taken in account, like EN 15853 for mercury and EN 15980 for Polycyclic Aromatic Hydrocarbons.

The main objective of this research work is to study Particulate Matter Deposition in a regional background environment in Mallorca, where the influence of local anthropogenic contributions is minimal.

Another objective is to evaluate the influence on the levels and chemical composition of PM Deposition of long-range air mass transport, with special interest in air masses of African origin.

This study has been carried out for the same period as the ChArMEx (The Chemistry-Aerosol Mediterranean Experiment, https://charmex.lsce.ipsl.fr) initiative, so a 2-year campaign of wet and dry deposition has been conducted (Balearic Islands, western Mediterranean). From September 2010 to August 2012 weekly dry and wet deposition samples were collected.

In addition, atmospheric particulate matter was regularly sampled in both PM10 and PM1 fractions, as well as gaseous pollutants and meteorological parameters were continuously registered.

2 METHODOLOGY

ESM Andersen wet and dry deposition sampler were used to collect de particulate matter deposition (Fig. 2).

This device holds two plastic containers of 40 cm of height and 29 cm of diameter. The collector was located on the roof (to minimize deposition processes from local soil resuspension) of an air quality measurement station sited in a place called Can Llompart, in the North of the Island. The collector is equipped by a rainfall sensor which activates a mechanism in case of rain, covering the dry container and leaving open the wet one.

The samples obtained were weekly brought to the laboratory and the containers were cleaned with distilled water. Wet deposition volumes were quantified. Dry and wet deposition aliquots were filtered on 47 mm quartz fibre filters, and the pH was determined.

Consequently, a maximum of 4 fractions were obtained for each sampling interval: non-soluble dry deposition fraction (dry deposition filter), soluble dry deposition fraction, non-soluble wet deposition fraction (wet deposition filter), and soluble wet deposition fraction. Filters were treated using different analytical procedures to determine the concentrations of a range of elements and components, as described in [5]. Each filter was acidic digested ($HF:HNO_3:HClO_4$) to subsequently determine the amount of major and trace elements (Al, Ba, Ca, Cu, Fe, K, Mg, Mn, Na, Ni, P, Pb, Sr, Ti, V, Zn) by using Inductively Coupled Plasma Atomic Emission Spectroscopy (ICP-AES).

The aliquots were analysed by Ion Chromatography to quantify water soluble ions such as SO_4^{2-}, NO_3^-, NO_2^-, Cl^-, Na^+, K^+, Mg^{2+}, Ca^{2+} and NH_4^+.

The Can Llompart site was also equipped with automatic monitors for the measurement of the levels of the size-resolved (PST, PM_{10}, $PM_{2.5}$ and PM_1) aerosol, on hourly basis. Furthermore, two with high-volume samplers of PM_{10} and PM_1 collected 24-hour filters for similar chemical analyses as described before.

In order to interpret our database, we have made use of different meteorological tools such as the analysis of air mass back-trajectories and meteorological maps, and the consultation of aerosol concentration maps and satellite imagery. A special focus was paid to the occurrence of African dust outbreaks, taking into consideration that they are the episodes with the largest influence on PM levels and therefore in the chemical composition of the particulates in the Iberian Peninsula and the Balearic Islands.

Finally, a Principal Component Analysis was executed individually for wet and dry deposition, in order to identify some of their potential sources.

3 RESULTS

3.1 Seasonal differences between Wet and Dry Deposition

Mean daily mass flux of deposition aerosol in this regional background environment has been 17 mg m^{-2} day^{-1} for dry deposition with a range of 3-232 mg m^{-2} day^{-1}, and a mean value of 51 with a range of 1-406 mg m^{-2} day^{-1} for wet deposition.

These results are higher than others obtained in similar studies that were focused only in mineral factor [1].

Our results reveal that almost 70% of the atmospheric deposition occurs as wet deposition, being around 30% dry deposition. Dry and wet deposition loads display different seasonal patterns (Fig. 1). Whereas wet deposition is extraordinarily abundant during fall and winter seasons, dry deposition shows a slight increase in summer and fall seasons. In the Balearic Islands, suspended Particulate Matter maximize in summer-early autumn, which is connected to the higher dry deposition rate. On the other hand, precipitation events occur mostly during fall and winter seasons, therefore explaining the elevated wet deposition rates.

Some windy periods may occur in fall and spring, and they can provoke some peaks of deposition, both wet and dry (Fig. 2). Moreover, the phenomenology of African dust incursions along the year presents some differences. Spring and fall episodes give rise to frequent red-rains, whereas summer dust events are mostly dry episodes.
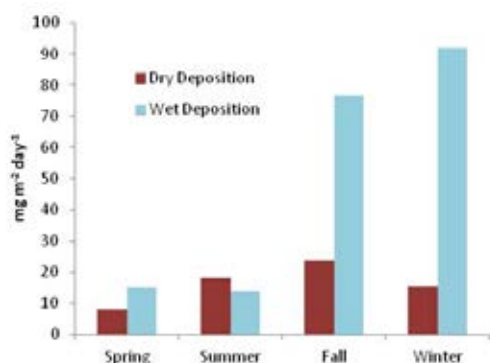
Fig. 1. Seasonal Dry and Wet Deposition bar charts
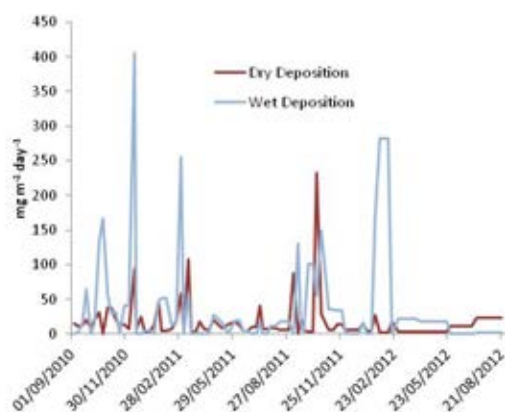
Fig. 2. Time variation of dry and wet deposition at Can Llompart.

Some seasonal patterns are patent in the different major and trace elements. Table 1 shows seasonal deposition rates of selected compounds and elements clearly related with marine (Cl, Na), mineral (Ca, Al) and anthropogenic (Cu, Pb, NH_4) emission sources.

Cl and Na are perfectly correlated, and their seasonal behaviour indicates that fall is the most important period for dry deposition, and also winter for wet deposition.

Al and Ca have different seasonal pattern for dry and wet deposition. Additionally, those elements are not directly correlated. Thus could put forward that different types of outbreaks of crustal sources take place throughout the year, with diverse origins. But also the contribution of local and regional dust sources may partially the moderate Ca-Al correlation.

Some anthropogenic source indicators like Cu, Pb and NH_4 have dissimilar seasonal pattern. This could suggest different types of emissions sources that achieve its maximum in different periods.

Ca soluble and insoluble ratio depends on the dry or wet deposition. In dry deposition both, soluble and insoluble, are similar. In wet deposition soluble and insoluble deposition are noticeably different.

3.2 Source Contributions

The Principal Component Analysis have extracted three common sources both for dry and wet deposition: 1) a mixed-marine factor defined by Na, Cl, and partly by Mg, NO_3^- and SO_4^{2-}; 2) a mineral factor composed mainly of

elements derived from silicate and carbonate minerals such as Al, Ba, Ca, Ti, Sr, Fe, Ca, Mg, and relatively associated to K, Mn and V; 3) an anthropogenic source characterized by Ni, Pb, Cu, Zn, NH_4^+ and moderately by SO_4^{2-}, NO_3^-.

Table 1. Seasonal depositions in ($\mu gm^{-2}day^{-1}$) for all the compounds analyzed

Dry Deposition ($\mu gm^{-2}day^{-1}$)				
analyte	Spring	Summer	Fall	Winter
Cl^-	1760	4796	9835	4659
Na^+	825	2225	4899	2223
NH_4^+	40	20	73	67
Ca^{2+}	820	1389	1602	984
Ca_insol	1468	2638	1398	1766
Al_insol	598	1642	423	1154
Cu_insol	1.3	1.4	3.2	2.0
Pb_insol	0.4	0.6	0.7	0.4
Wet Deposition ($\mu gm^{-2}day^{-1}$)				
analyte	Spring	Summer	Fall	Winter
Cl^-	4083	6291	37264	32054
Na^+	2141	2714	18584	16732
Ca^{2+}	508	150	627	1502
Na^+	1934	763	2799	3171
Ca_insol	105	174	64	63
Al_insol	721	256	281	471
Cu_insol	1.0	0.7	1.3	1.0
Pb_insol	0.6	0.4	0.7	0.6

In the case of dry deposition, the anthropogenic source was split in three different components: a Cu-Zn-Fe factor, a K-Ni-Pb profile and a NO_3^--NH_4^+ association.

After the identification of the factors, a multilinear regression analysis was done. The contribution of the different factors has been integrated in Fig. 3. From this figure it becomes obvious that the marine component dominates both dry (56%) and wet deposition (75%). However, a clear difference between dry and wet deposition is apparent. The anthropogenic factor is clearly enhanced during wet deposition periods, and the mineral factor is more important during dry deposition intervals.

3.3 Temporal variation of dry and wet deposition sources

The temporal variation of dry and wet deposition sources has been represented in Fig. 4.

Dry deposition was observed all over the year, with some peak episodes (between 50 and 200 mg/m^2 day) in January, March and October 2011. Some of these dry deposition episodes were driven by marine inputs, whereas the rest were linked to mineral sources. On the other hand, wet deposition occurred more sporadically and always out

of the summer season. In some cases, deposition loadings increased up to 250-400 mg/m^2 day. Most of these events were linked to intense marine-source deposition, and occasionally mineral dust or anthropogenic inputs were important.
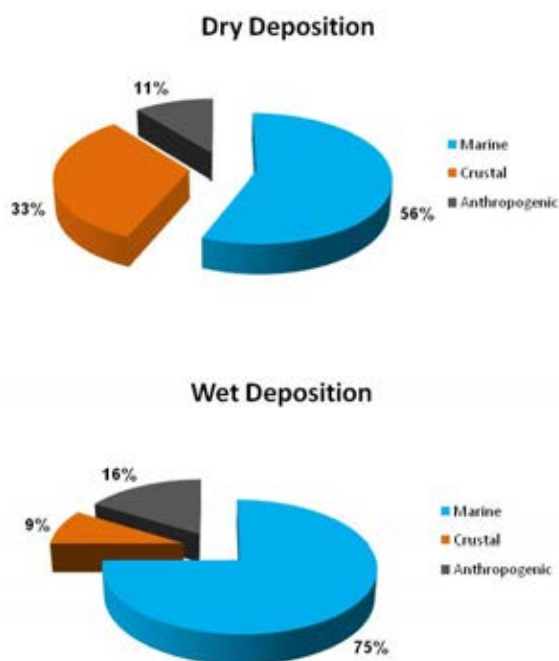
Fig. 3. Partitioning of marine, crustal and anthropogenic contributions for dry (top) and wet (bottom) deposition samples.

Certain windy events (with no rain associated), such as one occurred in November 2011, were characterized by an increase in marine factor, probably reflecting intense bubble bursting processes in the surrounding Mediterranean waters.
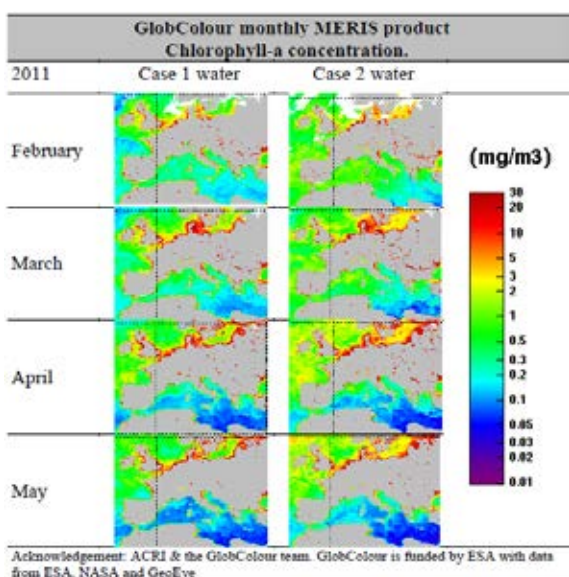
Fig. 4. Chlorophyll-a concentration since February to May 2011. Calculate with Hermes tool (globcolour.info)

The most important anthropogenic deposition input was observed in February 2012, simultaneous with crustal and marine contributions. This episode occurred during a period in between the entrance of diverse European pollution plumes over the western Mediterranean, and the development of stagnant pollution episodes.

On the other hand the growth of phytoplankton has been investigated by consulting chlorophylls with the Hermes tool (www.globcolour.info) [5]. Deposition during February and March 2011 is greater than the following months, April and May (Fig. 4).

The photosynthesis activity is more important during the first two months, when the contrary effect would be expect in function of the temperature. This evidences the important affection of the deposition, which can be more important than the temperature in some cases.

3.4 Dry and wet deposition sources: seasonal patterns

When regarding the seasonal variations of the deposition sources, and considering wet and dry deposition, interesting features are observed. The marine factor is more important in wet deposition, especially in fall and winter. In spring and summer, wet and dry deposition of marine aerosols are comparable. The crustal factor is clearly enhanced in the dry deposition part, especially in summer, when around 80% of the crustal contribution took places via dry deposition. The partitioning wet and dry deposition for this source during the other seasons is around 40 and 60%, respectively.
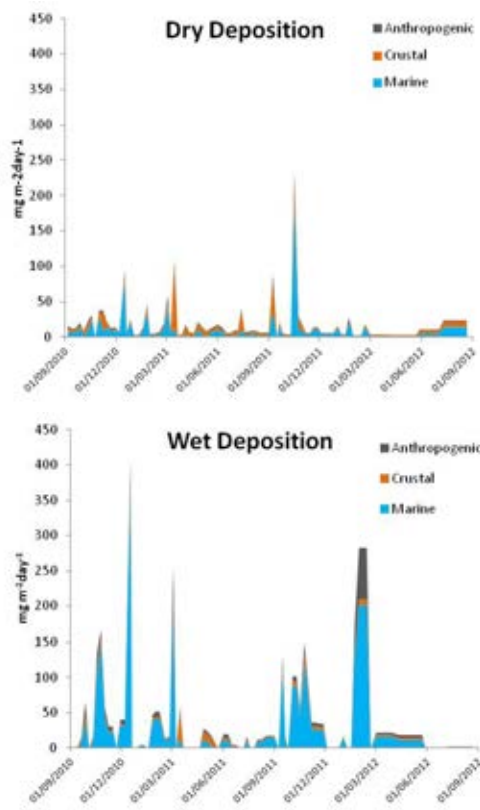
Fig. 5. Time variation (in mg/m^2 day) of anthropogenic, crustal and marine inputs in dry (top) and wet (bottom) deposition samples.

Finally, anthropogenic contributions were mostly observed as wet deposition, especially during fall and winter. In summer, dry anthropogenic inputs prevailed over the wet ones, most probably because of the lack of rainy events.
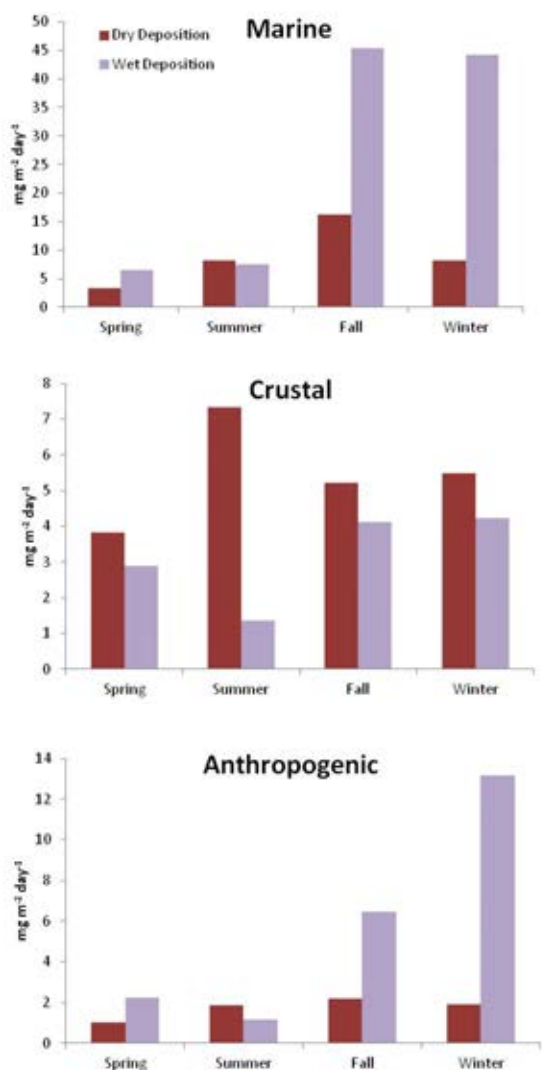
Fig. 6. Seasonal variation (in mg/m^2 day) of marine, crustal and anthropogenic factors in dry and wet deposition.

4   CONCLUSIONS

Two years sampling campaign shows a wide range of dry and wet deposition.

Different seasonal patterns for crustal elements in both dry and wet deposition, suggest diverse origins of North African outbreaks and/or the contribution of different dust types (with respect to Saharan dust) from local and regional origins.

A Principal Component Analysis has been done and three clear contribution sources were detected: marine, mineral and anthropogenic.

Marine factor is the most important for both wet and dry samples. Dissimilar results were obtained for mineral and anthropogenic factors for wet and dry deposition.

Whilst mineral is the second in importance in dry deposition, anthropogenic factor is more important in wet. Some of these dust outbreaks are related with an increase of the chlorophyll activity in the Western Mediterranean basin, which corroborates the importance of certain atmospheric deposition in specific marine ecosystems.

Crustal and anthropogenic dry deposition is similar throughout the year, while marine has more remarkable seasonal behavior. Wet deposition is directly related to the precipitation periods of the year, achieving its maximum in fall and winter for all the factors, marine, crustal and anthropogenic.

REFERENCES

[1] Stefano Guerzoni, Roy Chester, François Dulac, Barak Herut, Marie-Dominique Loÿe-Pilot, Chris Measures, Christophe Migon, Emanuela Molinaroli, Cyril Moulinc, Paolo Rossinia, Cemal Saydami, Alexandre Soudinej and Patrizia ZiverikGuerzoni "The role of atmospheric deposition in the biogeochemistry in the Mediterranean Sea" *Progress in Oceanography* Volume 44, Issues 1–3, Pages 147–190, August 1999

[2] Rafael Morales-Baquero, Elvira Pulido-Villena and Isabel Reche "Chemical signature of Saharan dust on dry and wet atmospheric deposition in the south-western Mediterranean region" *Tellus B*, 65, 18720, 2013

[3] Mészáros, E., *Fundamentals of Atmospheric Aerosol Chemistry*, Akadémiai KiadoMészáros, 1999

[4] Antoni Jordi, Gotzon Basterretxea, Antonio Tovar-Sanchez, Andrés Alastuey and Xavier Querol, "Copper aerosols inhibit phytoplankton growth in the Mediterranean Sea" *PNAS* ; December 10, 2012.

[5] Querol, X., Pey, J., Minguillón, MC., Pérez, N., Alastuey, A., and Viana, M. "PM speciation and sources in Mexico during the MILAGRO-2006 Campaign" *Atmospheric Chemistry and Physics*, 8, 111–128, 2008.

Ammonia Levels In Different Kinds Of Sampling Sites In The Central Iberian Peninsula

M.A. Revuelta[1,2]*, B. Artíñano[1], F. J. Gómez-Moreno[1], M. Viana[3], C. Reche[3], X. Querol[3], A.J. Fernández[1], J.L. Mosquera[1], L. Núñez[1], M. Pujadas[1], A. Herranz[1], B. López[1], F. Molero[1], J.C. Bezares[1], E. Coz[1], M. Palacios[1], M. Sastre[1], J. M. Fernández[1], P. Salvador[1], B. Aceña[1]

Abstract — Ammonia is the Secondary Inorganic Aerosol (SIC) gaseous precursor which has been studied to a lesser extent in the Madrid Metropolitan Area up to date. A study conducted in the city of Madrid with the aim of characterizing levels of ammonia took place in 2011. These campaigns formed part of a larger study conducted in 6 Spanish cities. A time series of weekly integrated ammonia measurements available at an EMEP rural site (Campisábalos) has been used to obtain information on the ammonia rural background in the region. The results point to traffic and waste treatment plants as the main ammonia sources in Madrid. Relevant seasonal differences have not been observed in the Metropolitan Area. The explanation can be related to the fall in the rural background levels during July 2011, which might conceal urban summer emission increases observed in other cities.

Keywords — ammonia, traffic, urban waste, rural background

1 INTRODUCTION

Ammonia is the SIC gaseous precursor which has been studied to a lesser extent in the Madrid Metropolitan Area up to date. Air Quality objectives have not been established yet in Spain, but the main role of this gas in the formation of secondary particles raises the interest in its study. In general terms, it is recognised that the main source of ambient ammonia is livestock waste, followed by vegetation and agriculture. However, the source contribution to ammonia in urban areas is not yet fully characterised. These sources would include traffic, human and pets´ excretions, landfill, garbage, household products and sewage treatment plants.

In 2002, Perrino et al studied the relationship between gaseous ammonia and traffic in the urban area of Rome. The authors found at traffic sampling sites a high correspondence between the hourly time evolution of a primary gas emitted by traffic, carbon monoxide, and NH_3. This study also corroborated results from other researchers who found that in the USA the petrol-engine vehicles equipped with three-way catalytic converters generated gaseous ammonia [1]. Most recent observations also suggest that the NH_3 emissions from the traffic exhaust could be a major source of the ambient NH_3 in other urban areas such as New York [2] Manchester [8] or Beijing [3].

1. *Department of Environment, CIEMAT, Avda. Complutense 40, 28040, Madrid, Spain .* E-mail: arevueltame@cofis.es*
2. *Currently at AEMET,C/Leonardo Prieto Castro 8, 28071 Madrid, Spain*
3. *Institute for Environmental Assessment and Water Research (IDÆA-CSIC), Barcelona, Spain*

2 METHODOLOGY

A study conducted in the city of Madrid with the aim of characterizing levels of ammonia in the urban ambient air took place in 2011 [6]. Two 10-11 days sampling campaigs were performed in two periods - winter and summer, and allowed to make a first estimation of the spatial distribution pointing at the main contributing sources. Passive samplers were used, obtaining a measurement integrated over the exposure time period. Madrid campaigns formed part of a larger study conducted in 6 Spanish cities: Barcelona, A Coruña, Valencia, Huelva and Santa Cruz de Tenerife. The results obtained in Barcelona were presented by Reche et al [5].

High sensitivity passive samplers (CEH ALPHA: Adapted Low-cost High Absorption) designed at the Centre for Ecology and Hydrology of Edinburgh [7]. were used. Samplers are made up of a polyethylene vial with one open end. An internal ridge supports a filter, which is coated with a solution of phosphorous acid in methanol, which serves to capture the ammonium ion. The ambient air ammonia concentrations were calculated according to the principle of diffusion of gases from the atmosphere along a sampler of defined dimensions onto an absorbing medium, governed by Fick's law.

In the winter period, 64 passive samplers were deployed all over the Metropolitan Area of Madrid with the objective of identifying ammonia sources and also obtaining the highest possible spatial coverage. 29 samplers were placed in traffic sites, 28 in urban background sites, 6 close to sewage treatment plants and 1 close to a solid waste treatment plant. Some of the samplers had a

duplicate separated around 10m to study the reproducibility of the procedure, taking into account shielding effects and the proximity to point sources (sewers). In the summer campaign the number of sites was smaller due to sampler availability. (See Appendix I)

Ancillary data were used to obtain information on the ammonia rural background in the region. A time series of weekly integrated ammonia measurements is available at a rural site in the Central Iberian Peninsula (Campisábalos, 41.27° N, 3.14° W, 1360 m asl.) provided by the EMEP network. These samples are analysed using visible spectrophotometry.

3 RESULTS

3.1 Madrid Metropolitan Area

Two sampling campaigns covering more than 50 sites in the Metropolitan Area of Madrid were performed with the objective of estimating the levels of this pollutant and its seasonal variability, and at the same time identifying the sources which contribute most to ammonia concentrations in the city. The results obtained in the campaigns are presented below according to the type of site.

Sites close to sewage and solid waste treatment plants registered the highest concentrations. The traffic sites showed significantly higher than the urban background sites in both seasons. No significant differences between winter and summer were registered for any kind of sampling site in the Madrid Metropolitan Area.

Figure 1 shows the mean NH_3 concentrations calculated for the traffic sites in the winter and summer campaigns. The mean values were very similar in both seasons (2.7 ± 0.5 µg·m^{-3} in winter and 2.6 ± 0.4 µg·m^{-3} in summer). In winter, three of the four samplers placed very close to bus stops registered concentrations above the mean. In P15 and E16 very high concentrations were measured in both seasons. These sites were nearby the very busy streets Alcalá and Arturo Soria (yearly average 47812 and 29087 vehicles·day^{-1})
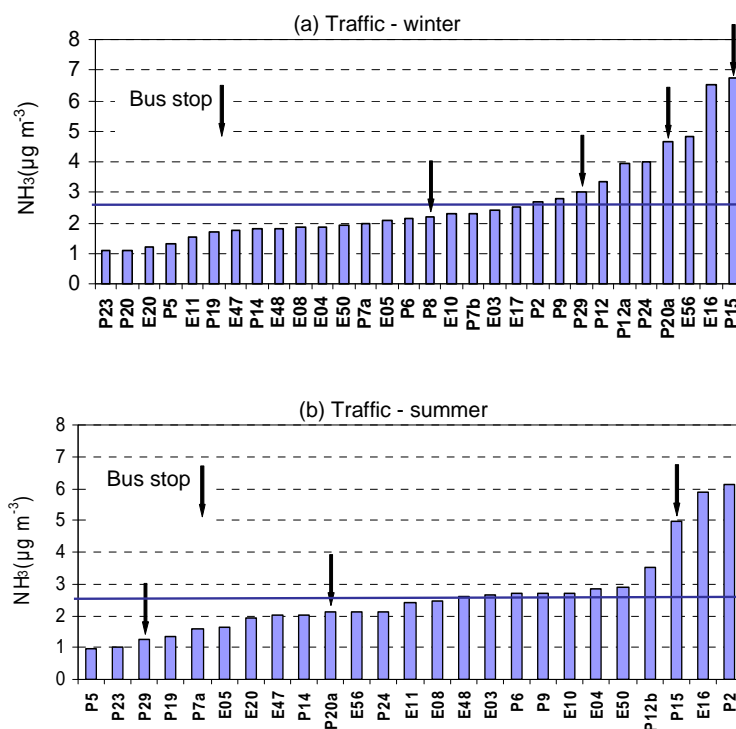
Figure 1. Mean NH3 concentrations in the traffic sites in (a) winter and (b) summer. Horizontal lines represent the average of all measurements. Black arrows indicate bus stops.

Urban background sites also registered very similar mean NH_3 concentrations in both seasons (1.6 ± 0.3 µg·m^{-3} and 1.5 ± 0.3 µg·m^{-3}). RV (Retiro Viveros) showed very high concentrations both in winter and summer. The sampler was placed in a big urban park, close to the park's nursery. The lowest values were registered at Casa de Campo (E24), a big forested area located on the western part of the city.

Figure 2 shows the mean NH_3 concentrations calculated for the sewage treatment plants and the solid waste treatment plant (so-called

"Valdemingómez incinerator") sites in winter and summer. The Rejas sewage treatment plant registered concentrations more than two times higher in summer, being the highest value

obtained (~4 µg·m^{-3} winter; ~10 µg·m^{-3} summer) in the study. The rest of the plants showed values in the range 2-5 µg·m^{-3} in both seasons.
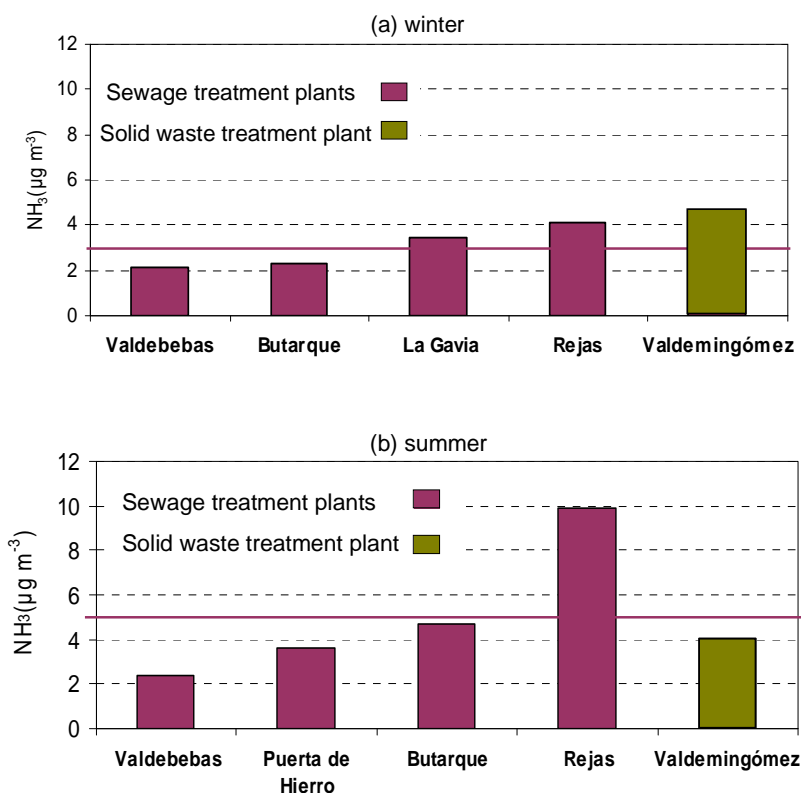
Figure 2. Mean NH3 concentrations in the sewage treatment plants and the incinerator in (a) winter and (b) summer. Horizontal lines represent the average of the sewage treatment plants.

Table 1 shows the results obtained in the sites adjacent to sewers and the duplicates, separated >10 m. The sampler closer to the sewer showed slightly higher ammonia concentrations at P7 and P12 (traffic sites) and P21 (urban background). However, P20a, located on a bus stop, showed a much higher ammonia concentration than P20b. Thus, the proximity to sewers might influence ambient ammonia levels locally, but the results obtained are not conclusive.

Table 1. Mean NH$_3$ concentrations (µg·m^{-3}) in sites adjacent to sewers and duplicates. *bus stop

Site	Sewer adjacent	NH$_3$	Sewer >10m	NH$_3$
Traffic	P7b	2.3	P7a	2.0
	P20b	1.1	P20a*	4.7
	P12a	4.0	P12b	3.4
Urban bg	P21a	1.1	P21b	1.0

Comparing the mean values calculated in

traffic and urban background sites we can see there is a statistically significant difference in both seasons, with higher mean concentrations in the traffic sites. In contrast, the sewage treatment plants and incinerator showed the highest NH$_3$ levels, but the difference with the mean ammonia levels registered in the traffic sites was not significant. This result is in agreement with the studies in other cities which had pointed to traffic emissions as a major source of ammonia in urban areas. No significant differences between winter and summer were registered for any kind of sampling site.

3.2 Rural background: Campisábalos

Weekly integrated ammonia measurements have been obtained at Campisábalos since August 2004 (see Figure 3). Monthly mean concentrations are in the range 0-2.5 µg·m^{-3} and a seasonal pattern with summer maxima is observed most of the years being less pronounced in 2007 and 2011. Nevertheless, a drop in the middle of the summer is clearly observed in 4 out of the 8 years

sampled, very pronounced in 2011. The explanation may be due to the extreme dryness of the countryside during the summer months, which inhibits the decomposition of soil organic matter, responsible for a large part of the emissions of NH_3 at rural areas.

Trend analysis has been performed by the Theil-Sen method using deseasonalised data. The analysis does not show any tendency (see upper-right corner of Figure 3), i.e., annual mean concentrations remained constant at this site in the period Aug-2004 to Dec-2012.

In winter the mean concentrations registered at the urban background sites in the Madrid Metropolitan Area were slightly higher than the monthly mean in March 2011 at Campisábalos (~1 $\mu g \cdot m^{-3}$). However, in July 2011 mean NH_3 at Campisábalos were extremely low. This fall in summer ammonia rural background can be related to the constant ammonia concentrations observed in the urban area of Madrid, inhibiting possible summer increases observed in other cities such as Barcelona [5].
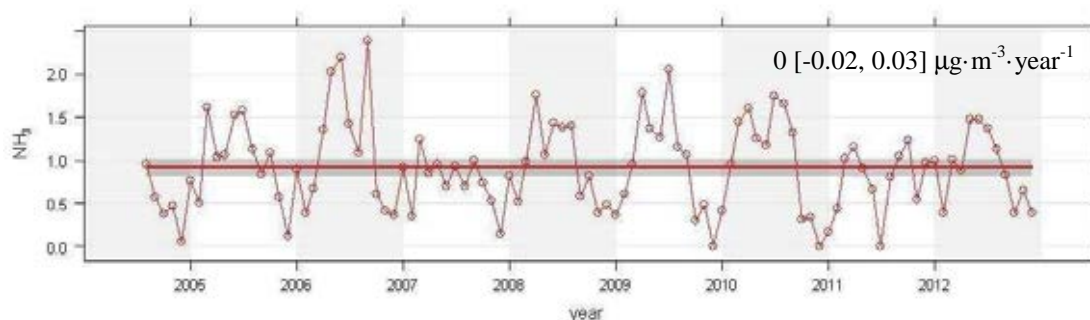
Figure 3. Ammonia monthly evolution at Campisábalos

4 CONCLUSIONS

Ammonia measurement campaigns were performed in 2011 in the Metropolitan Area of Madrid. More than 50 passive samplers were deployed in two seasons: winter and summer.

Sites close to sewage and solid waste treatment plants registered the highest concentrations, followed by the traffic sites. The latter showed significant higher values than the urban background sites in both seasons.

In winter, three of the four samplers placed very close to bus stops registered concentrations above the mean. Sites nearby the very busy streets Alcalá and Arturo Soria registered very high concentrations in both seasons. Traffic emissions could be related to catalytic converters, which have been proved to lead to outstanding reductions in NOx emissions, but also to generate gaseous ammonia, raising controversy on the use of these devices.

The samplers close to sewers showed slightly higher ammonia concentrations than duplicates separated a distance > 10 m. The proximity to sewers might influence ambient ammonia levels locally, but the results obtained are not conclusive.

No significant differences between winter and summer were registered for any kind of sampling site in the Madrid Township, in contrast with the summer maxima observed at the rural EMEP site Campisábalos most of the years. Nevertheless, a drop in the middle of the summer is clearly observed in 4 out of the 8 years sampled, very pronounced in 2011. In winter the mean concentrations registered at the urban background sites were consistent with the monthly mean in March 2011 at Campisábalos, but in summer 2011 the mean NH_3 registered at the rural site was extremely low. This fall in summer ammonia rural background can be related to the constant ammonia concentrations observed in the urban area of Madrid, inhibiting possible summer increases observed in other cities.

5 APPENDIX I

Table A.1 shows the sampling sites selected in the winter NH_3 campaign in Madrid. EXX correspond to stations belonging to the city hall air quality network (Red de Calidad de Aire del Ayuntamiento de Madrid). Sites marked with I and II (samplers D14-D15; D25-D26; D30-D31; D59-D60) were separated a few meters. One of them was adjacent to a sewer. The sampler at Rejas was replicated (D17, D28) to check the reproducibility of the procedure.

The following samplers were not deployed in the summer campaign: D7, D11, D13, D15, D26, D29, D31, D39, D42, D47, D56, D58 and D59. This was due to a lesser availability of samplers.

Table A.1. Sampling sites in the winter NH$_3$ campaign in Madrid. STP=sewage treatment plant. Urban bg=urban background.

Sampler	Site name	Latitude	Longitude	Type
D1	Puerta de Hierro	40°27'3"N	3°44'36"W	STP
D2	E05-B° del Pilar	40°28'40"N	3°42'43"W	Traffic
D3	E10-Cuatro Caminos	40°26'43"N	3°42'26"W	Traffic
D4	E11-Ramón y Cajal	40°27'4"N	3°40'39"W	Traffic
D5	E48-Castellana	40°26'22"N	3°41'25"W	Traffic
D6	E50-Plaza de Castilla	40°27'56"N	3°41'20"W	Traffic
D7	E57-San Chinarro	40°29'43"N	3°39'33"W	Urban bg
D8	E58-El Pardo	40°31'6"N	3°46'31"W	Urban bg
D9	E86-Tres Olivos	40°30'1"N	3°41'22"W	Urban bg
D10	P2-Plaza 2 de Mayo	40°25'40"N	3°42'13"W	Traffic
D11	P4-Tetuán	40°27'40"N	3°41'51"W	Traffic
D12	P10-Molins de Rey	40°29'39"N	3°41'34"W	Urban bg
D13	P16-Pinar de Chamartín	40°28'35"N	3°40'22"W	Urban bg
D14	P21a-Antonio Machado I	40°27'55"N	3°43'17"W	Urban bg
D15	P21b-Antonio Machado II	40°27'55"N	3°43'17"W	Urban bg
D16	P22-CIEMAT	40°27'23.25"N	3°43'31.87"W	Urban bg
D17	Rejas	40°27'4.46"N	3°32'7.16"W	STP
D18	Valdebebas	40°29'39.31"N	3°32'54.86"W	STP
D19	E16-Arturo Soria	40°26'24.17"N	3°38'21.24"W	Traffic
D20	E27-Barajas Pueblo	40°28'36.93"N	3°34'48.11"W	Urban bg
D21	E55-Urb. Embajada	40°27'41.02"N	3°34'55.21"W	Urban bg
D22	E59-Juan Carlos I	40°27'54.80"N	3°36'32.70"W	Urban bg
D23	P1-Gran Vía de Hortaleza	40°28'2.21"N	3°39'8.61"W	Urban bg
D24	P3-Silvano	40°27'28.60"N	3°38'38.28"W	Urban bg
D25	P7a-Arcentales I	40°26'4.24"N	3°36'28.70"W	Traffic
D26	P7b-Arcentales II	40°25'59.61"N	3°36'27.94"W	Traffic
D27	P15-Alcalá	40°25'46.26"N	3°39'55.16"W	Traffic
D28	Rejas	40°27'4.46"N	3°32'7.16"W	STP
D29	P18-Sorzano	40°27'7.68"N	3°39'24.61"W	Urban bg
D30	P20a-G. Noblejas I	40°25'55.80"N	3°38'2.40"W	Traffic
D31	P20b-G. Noblejas II	40°25'55.80"N	3°38'2.40"W	Traffic
D32	P26-El Capricho	40°27'16.04"N	3°35'56.22"W	Urban bg
D33	Butarque	40°19'59.5"N	3°39'40.2"W	STP
D34	La Gavia	40°21'8.9"N	3°39'31.7"W	STP
D35	E08-Escuelas Aguirre	40°25'22.1"N	3°40'51.9"W	Traffic
D36	E13-Pte. De Vallecas	40°23'22"N	3°39'1"W	Urban bg
D37	E20-Moratalaz	40°24'32.7"N	3°38'38.4"W	Traffic
D38	E47-Plaza del Amanecer	40°24'0.8"N	3°41'1.7"W	Traffic
D39	E49-Retiro	4025'15.5"N	3°40'44.9"W	Urban bg
D40	Retiro viveros	40°24'40"N	3°41'4.2"W	Urban bg
D41	E54-Pau de Vallecas	40°22'27.0"N	3°36'39.4"W	Urban bg
D42	SODAR-RASS	40°25'22.1"N	3°38'7.1"W	Urban bg
D43	P6-Vicálvaro	40°24'26.2"N	3°36'15.5"W	Traffic
D44	P14-Valdebernardo	40°24'13.8"N	3°37'8.8"W	Traffic
D45	P24-P. Cotos	40°24'6.8"N	3°39'26.6"W	Traffic
D46	P25-G. Dávila	40°22'41.0"N	3°38'17.3"W	Urban bg
D47	P27-S. Alcaraz	40°23'29"N	3°40'0.9"W	Urban bg
D48	P28-Valdemingómez	40°20'10.4"N	3°35'38.3"W	Incinerator
D49	E03-Plaza del Carmen	40°25'07.67"N	3°42'12.91"W	Traffic
D50	E04-Plaza de España	40°25'25.89"N	3°42'45.10"W	Traffic
D51	E17-Villaverde	40°20'51.15"N	3°42'47.95"W	Urban bg
D52	E18-Farolillo	40°23'41.38"N	3°43'55.25"W	Urban bg
D53	E24-Casa de Campo	40°25'06.07"N	3°44'14.19"W	Urban bg
D54	E56-Pza. Fdez. Ladreda	40°23'07.10"N	3°42'59.83"W	Traffic

D55	P5-Aluche A5	40°23'40.58"N	3°46'06.22"W	Traffic
D56	P8-Valle del Oro	40°23'18.58"N	3°43'52.14"W	Traffic
D57	P9-Cava Baja	40°24'43.80"N	3°42'35.00"W	Traffic
D58	P11-Zoo	40°24'28.54"N	3°45'44.54"W	Urban bg
D59	P12a-Lavapies I	40°24'32.64"N	3°42'04.92"W	Traffic
D60	P12b-Lavapies II	40°24'33.26"N	3°42'05.09"W	Traffic
D61	P13-Templo de Debod	40°25'26.59"N	3°43'07.40"W	Urban bg
D62	P19-Carabanchel Alto	40°22'25.92"N	3°45'02.82"W	Traffic
D63	P23-R. Ybarra	40°22'07.86"N	3°42'44.15"W	Traffic
D64	P29-Cuatro Vientos	40°22'39.88"N	3°46'49.59"W	Traffic

REFERENCES

[1] A.J. Kean, Harley,R.A., Littlejohn,D., Kendall,G.R. (2000). On-road measurement of ammonia and other motor vehicle exhaust emissions. Environmental Science and Technology. 34,3535–35 39.

[2] Y. Li, James J. Schwab, and Kenneth L. Demerjian (2006). Measurements of Ambient Ammonia Using a Tunable Diode Laser Absorption Spectrometer: Characteristics of Ambient Ammonia Emissions in an Urban Area of New York City. J. Geophys. Res. 111, no. D10: D10S02.

[3] Z. Meng, Y., Lin, W. L., Jiang, X. M., Yan, P., Wang, Y., Zhang, Y. M., Jia, X. F., Yu, X. L. (2011). Characteristics of atmospheric ammonia over Beijing, China, Atmos. Chem. Phys., 11, 6139-6151.

[4] C. Perrino, M. Catrambone, A. Di Menno Di Bucchianico, I. Allegrini (2002). Gaseous Ammonia in the Urban Area of Rome, Italy and Its Relationship with Traffic Emissions. Atmospheric Environment 36, no. 34: 5385-94.

[5] C. Reche, M. Viana, M. Pandolfi, A. Alastuey, T. Moreno, F. Amato, A. Ripoll, X. Querol (2012). Urban NH3 Levels and Sources in a Mediterranean Environment. Atmospheric Environment 57, no. 0: 153-64.

[6] M.A. Revuelta (2013). Study of secondary inorganic aerosol compounds in the urban atmosphere: temporal evolution and characterisation of episodes. PhD Thesis. *http://eprints.ucm.es/21553/*

[7] Y.S. Tang, Cape, J.N., Sutton, M.A. (2001). Development and types of passive samplers for monitoring atmospheric NO2 and NH3 concentrations. In Proceedings of the International Symposium on Passive Sampling of Gaseous Air Pollutants in Ecological Effects Research. TheScientificWorld 1, 513–529.

[8] J. Whitehead, I. Longley, M. Gallagher (2007). Seasonal and Diurnal Variation in Atmospheric Ammonia in an Urban Environment Measured Using a Quantum Cascade Laser Absorption Spectrometer. Water, Air, & Soil Pollution 183, no. 1: 317-29.

Analysis of the aerosol optical properties at a continental background site in the southern Pyrenees (El Montsec, 1574 m a.s.l.)

Yolanda Sola[1], Alba Lorente[1], Jerónimo Lorente[1]

Abstract — Aerosol optical properties from one year of AERONET Cimel sunphotometer measurements in a continental background site have been analyzed. The instrument was installed in El Montsec in the Southern Pyrenees at 1574 m a.s.l. The AOD shows a seasonal pattern with minimum values in winter when the stations is over the planetary boundary layer (PBL) and can be considered representative of the free troposphere, whereas maximum values of the AOD are detected in summer due to the long range transport of Saharan dust as well as regional recirculation. The annual average of the AOD at 0.08, although in winter is only 0.03. The Angstrom exponent is also similar to other continental background sites although it is lower, probably due to more frequent Saharan dust episodes as well as to a mixture of local coarse aerosols from regional recirculation. The volume size distribution also varies depending on the season, even on the considered month. In winter, the coarse mode is almost inexistent; whereas in summer fine and coarse mode are remarkable, especially the medium-size particles.

Keywords — AERONET Cimel; Angstrom exponent; aerosol optical properties; continental background station

1 INTRODUCTION

Atmospheric aerosols play an important role in the radiative budget in the earth-atmosphere system. Moreover, as condensation nuclei, they contribute to the cloud formation. For these reasons, aerosols contribute to the radiative forcing, either positive or negative in a complicate way. Indeed, the aerosol radiative forcing is one of the main uncertainties in the climate change assessments [1]. The interest in the spatial and temporal distribution of the aerosols, as well as the concern about the effect on health has increased the number of measurement stations, especially in densely populated regions and in highly polluted areas. However, the study of the aerosol properties and their influence on the radiative balance requires a wide variety of measurement scenarios. Of special interest are high altitude stations, located in the free troposphere, because they are more representative of the global atmosphere [2], whereas measurements in the planetary boundary layer describe local conditions that cannot be extrapolated to other regions. For this reason, during the last decades some measurement networks have been developed, such as, among others, Aerosol Robotic Network (AERONET) and SKYNET- AERONET includes a great number of stations worldwide with the Cimel CE-318 as a standard [3]. SKYNET developed a network mainly in Eastern Asia [4] with the PREDE sunphotometer but and a European branch has grown up from 2010 [5] that joins user with both instruments.

This paper describes the aerosol optical properties determined from an AERONET Cimel sunphotometer located in El Montsec, a high-altitude site in the Western Mediterranean basin. The location of this remote site confers it the category of continental background station [6]

2 SITE DESCRIPTION AND DATA

2.1 Site description

The station of El Montsec is located in the Pyrenees Mountain region (42° 3' 5.10" N, 0° 43' 46.88" E) at 1574 m a.s.l. The distance from urban areas and other anthropogenic sources confer continental background properties to the station. Changes in the aerosol concentrations in these sites are mainly related to long-range transport as well as regional re-circulation. Moreover, in some cases the station, due to its altitude, is over the boundary layer; therefore, it is characterized as free-troposphere station. This situation is more common in summer months than in winter months [6].

The lower surrounding mountains and the free-horizon with no wind obstruction was an advantage for remote-sensing instrumentation. For this reason a Cimel CE-318 sunphotometer was installed, taking advantage that the Institute of Environmental Assessment and Water Research (IDAEA-CSIC) was monitoring real time concentrations of particulate matter (PM_{10}), black carbon (BC) and

---

1. *Department of Astronomy and Meteorology, University of Barcelona. Martí i Franquès 1, E-08028 Barcelona, Spain. E-mail: ysola@am.ub.es*

particle number, as well as, chemical characterization at the same place. A deep analysis of the variation of these parameters is presented by Ripoll et al. [6], in which the instruments are also described.

Additionally, a complete automatic meteorological station of the Meteorological Service of Catalonia is installed at the same facilities. It includes real-time measurements of temperature, humidity, and solar total radiation and wind components.

2.2 Data

A Cimel CE-318 sunphotometer was installed in El Montsec in 2011 and has been running at this site continuously. The AERONET Cimel #416 was monitoring up to 8 March 2012 when it was replaced by the Cimel #411 more than one year (10 May 2013). Until now Cimel #416 has been measuring again continuously. Both instruments were calibrated in the facilities of the Atmospheric Optics Group of the University of Valladolid (GOA-UVA) in the framework of the Red Ibérica de Medida de Aerosoles (RIMA), under the Aerosols, Clouds, ad Trace gases Research Infrastructure network (ACTRIS) project.

The two photometers installed in El Montsec was seven common filters for aerosol characterization at 340, 380, 440, 500, 675, 870, and 1020 nm and an additional channel at 935 nm for water vapour retrievals.

The AERONET level 1.5 aerosol optical depth (AOD) data, in which automatic cloud screening (ref) is applied, are available for all the data series. However, the quality assured level 2.0 data is only available from October 2011 to May 2013 when post field calibration has been performed. The use of data series from different instruments needs to introduce corrections in the AOD to assure the consistency of the data series [7]. The KCICLO method [8] to the AOD results in corrections in the multi-annual monthly means from 2% to 12% depending on the channel and the month [7]. To avoid differences from instrument changes, we have analyzed aerosol properties determined from photometer #411 for one year measurements, from May 2012 to April 2013, using the AERONET methodology. In our case, we have not considered possible fictitious diurnal cycles described by other authors [7,8].

2.3 Analysis of the air masses

Continental background sites are characterized by long-term transport of aerosols, therefore the analysis of the air masses affecting the measurement site can help to classify the aerosol properties. The Hybrid Single-Particle Lagrangian Integrated Trajectory (HYSPLIT, [9]) is commonly used to derive the backward trajectories, although the air mass types and the classification methodology differ depending on the study [6,10]. We have computed

120 h backward trajectories at three altitude above the model ground, 750, 1500 and 2500 m a.g.l., according to (ref). The trajectories end at the station coordinates at 12 UTC. The meteorological database is the Global Data Assimilation System (GDAS) with a 1° x 1° grid resolution and the trajectories are modelled using vertical velocity hypothesis.

3 RESULTS

3.1 Aerosol optical depth

Fig. 1 shows the variation of the monthly mean total AOD at 500 nm, as well as the fine and coarse mode contributions. The total AOD ranges from 0.02 to 0.14 in a clear seasonal pattern with minimum values in December and maximum values in April (see also Table 1 for mean values). During the winter months, the station is frequently over the PBL reducing the aerosol concentrations, both the fine and the coarse mode. In these cases the values are comparable with other free-troposphere stations [11]. According to the analysis of the HYSPLIT backward trajectories, there is a prevalence of the Atlantic advections that contribute to a larger fine mode fraction, although it is also important during summer months. In summer, there is an increase of the AOD, especially of the fine mode. According to [6], a variety of factors cause this increase including summer recirculation of air masses over the western Mediterranean that accumulates aerosols and the increase of the PBL, which favour the mixing of atmospheric pollutants at a regional scale. It is worthy to note the increase in the coarse AOD in August 2012 due to different tropical and African air masses transporting mineral aerosols.
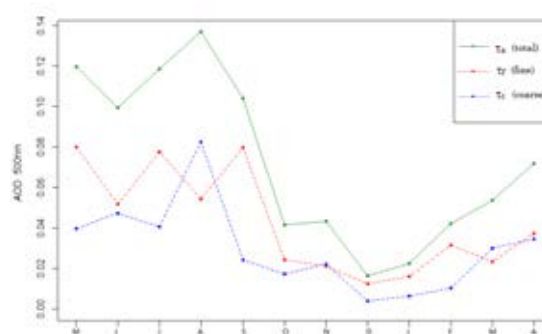
Fig. 1. Variation of the total AOD and the fine and coarse mode contributions at 500 nm from May 2012 to April 2013.

The analysis of the fine mode fraction (not shown here) shows an important decrease during March and April; indeed their value is lower than in summer. In spring, there is a peak in the African dust transport as well as a higher frequency of polluting episodes mainly as a consequence the advection of polluted

air masses from Europe [6,12]

High daily variability is observed from May to September (Fig. 2), especially for high AOD whereas winter months only present small variations. In some case, in December and January, the AOD at 550 nm is about 0.01. AOD lower than 0.05 are measured throughout the year mainly associated with Atlantic air masses.
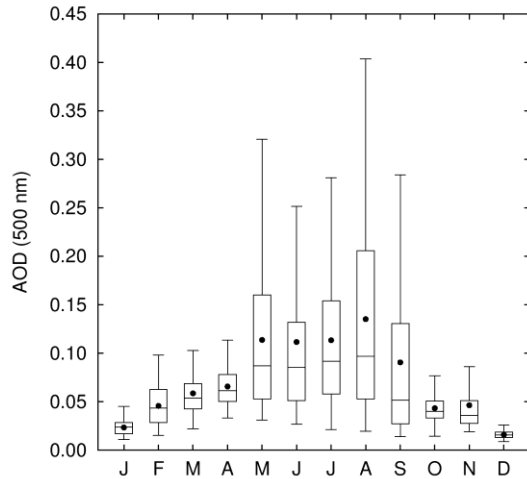
Fig. 2. Monthly box and whisker plot of AOD at 500 nm for the period May 2012 to April 2013. From each box, whiskers extend to 1.5 times the inter-quartile range. Black circles represent monthly means.

Table 1. Seasonal mean values of the AOD, fine mode fraction at 500 nm, Angstrom exponent, and asymmetry parameter at 441 nm. Summer for JJA, autumn for SON, winter for DEF and spring for MAM. Means have been calculated from consecutive months, excepting for spring

	AOD 500 nm	η 500 nm	α 440–870	g 441 nm
Summer	0.12	0.61	1.140	0.669
Autumn	0.07	0.64	1.179	0.677
Winter	0.03	0.74	1.284	0.688
Spring	0.09	0.56	1.033	0.682

3.2 Angstrom exponent

In our study we have considered the Angstrom exponent determined with AOD wavelengths from 440 to 870 nm.
The Angstrom exponent has a strong variability with values higher than 2 in some cases and also negatives in others. The winter months show the lowest daily variability with mean values higher than 1.2. The highest values are also detected in winter associated with smaller particles. This fact coincides with low

AOD periods. During summer, there is a wider range of values representing different cases: African air masses transporting bigger particles and therefore, a lower Angstrom exponent. However, simultaneously larger Angstrom exponents associated with fine particles are also associated with summer period. The lowest seasonal mean values is detected in spring (Table 1) coinciding with a peak in the Saharan dust outbreaks.
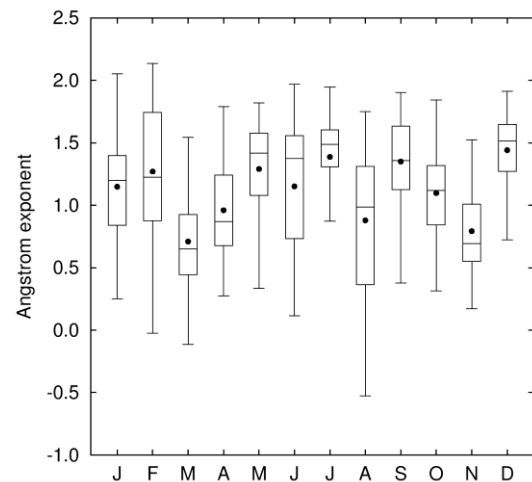
Fig. 3. Monthly box and whisker plot of Angstrom exponent for the period May 2012 to April 2013. From each box, whiskers extend to 1.5 times the inter-quartile range. Black circles represent monthly means.

The annual mean values of the Angstrom exponent is 1.16 that is lower than others reported in the literature for clean continental background sites [13]. Differences can be associated with a major frequency of Saharan dust outbreaks. In any case our study is based in only one year that cannot be representative of the long-term conditions. Other studies are based on longest databases [13].

3.3 Asymmetry parameter

Fig. 4 shows the seasonal evolution of the asymmetry parameter, g, that is indicative of the particle size. There are only slightly differences in the asymmetry parameter throughout the year. Although the lowest value is detected in October, it coincides with a small number of measurements in the AERONET AOD level 2.0 during this month. The annual mean values is about 0.67 in agreement with other studies [14]

3.5 Volume size distribution

Fig. 5 shows the volume size distribution averaged according to the season. It is observed a prevalence of small particles in summer months with an almost non-existent contribution of medium-size particles.
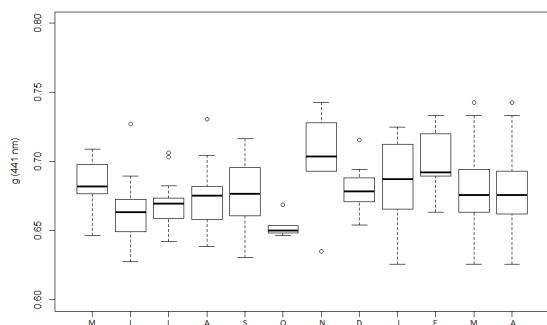
Fig. 4. Monthly box and whisker plot of asymmetry parameter, g, at 441 nm for the period May 2012 to April 2013. Outliers are represented with circles.

The fine-mode aerosols increase during the other seasons. The coarse-mode shows the largest value in summer months; indeed it is larger than the fine-mode. The effective radius in the coarse-mode is smaller during spring than during the other seasons. In a similar way, the radius of the fine-mode in summer is smaller than in the other seasons.
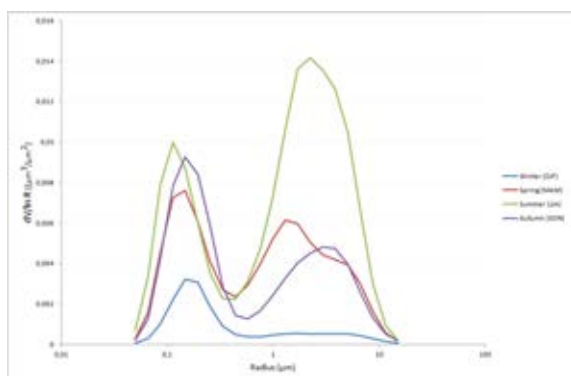
Fig. 5. Volume size distribution averaged for the four seasons. Seasonal means have been determined from consecutive months, with the exception of spring for which May 2012, and March and April 2013 have been considered.

8 CONCLUSIONS

One year of AERONET AOD level 2.0 data in El Montsec has been analyzed. The station is located at high altitude and far away from urban areas or anthropogenic sources; therefore it is considered a continental background station, as it is shown by other previous studies based on PM analyses [6]. Moreover, especially during winter months, the station is over the PBL, as it is determined using the HYSPLIT model, and it can be considered representative of the free-troposphere.

The aerosol optical properties analyzed are in agreement with the station definition. The annual mean AOD at 500 nm is 0.08 although considering only from autumn to spring, it reduces up to 0.06.

The lowest AOD is monitored in winter when the station is over the PBL, whereas the maximum values are associated with summer months when African air masses are more frequent and also a recirculation of air masses over the Mediterranean favor the accumulation of aerosols [6]. In August 2012 the coarse AOD was high due to the occurrence of various Saharan dust episodes.

The seasonal pattern of the Angstrom exponent is not so clear but the variation range in summer is higher than in other months due to the different air masses affecting the station. Nevertheless, it is worthy to note that the smallest values are detected in spring coinciding with a peak in the African dust outbreaks [15] and more polluted air masses from Europe [12].

The volume size distribution shows great differences depending on the season, indeed on the month. In winter, the fine fraction dominates the distribution over an almost non-existent coarse fraction. On the other hand, in summer both peaks are important, although the coarse particles are more important. The radii of the coarse particles are smaller in spring than in the other months.

Although results are in agreement with other studies of continental background sites, the limited number of data prevents from definite conclusions about the seasonal pattern of the aerosols properties determined from columnar measurements. Nevertheless, the wide variety of instruments will allow us to confirm the results comparing with particulate matter. In a future work, we analyze the aerosol optical properties according to an air mass classification comparing them with other studies performed at the same location [6].

REFERENCES

[1] IPCC, "Climate change 2007: The physical science basis". Contribution of Working Group, S. Solomon, D. Qin, M. Manning, Z. Chen, M. Marquis, K.B. Averyt, M. Tignor, and H.L. Miller (Eds.), Cambridge University Press, Cambridge, UK and New York, USA, 996 pp., 2007.

[2] P. Laj, J. Klausen, M. Bilde, C. Plab-Duelmer, G. Pappalardo, C. Clerbaux, U. Baltensperger, J. Hjorth, D. Simpson, S. Reimann, P.-F. Coheur, A. Richter, M. De Mazière, Y. Rudich, G. McFiggans, K. Torseth, A. Wiedensohler, S. Morin, M. Schulz, J.D. Allan, J.-L. Attié, I. Barnes, W. Birmili, J.P. Cammas, J. Dommen, H.-P. Dorn, D. Fowler, S. Fuzzi, M. Glasius, C. Granier, M. Hermann, I.S.A. Isaksen, S. Kinne, I. Koren, F. Madonna, M. Maione, A. Massling, O. Moehler, L. Mona, P.S. Monks, D. Müller, T. Müller, J. Orphal, V.-H. Peuch, F. Stratmann,

D. Tanré, G. Tyndall, A. Abo Riziq, M. Van Roozendael, P. Villani, B. Wehner, H. Wex, and Z. Zardini, "Measuring atmospheric composition change," *Atmos. Environ.*, vol. 43, pp. 5351-5414, doi:10.1016/j.atmosenv.2009.08.020, 2009.

[3] B.N. Holben, T.F. Eck, I. Slutsker, D. Tanré, J.P. Buis, A. Setzer, E.F. Vermote, J.A. Reagan, Y.J. Kaufman, T. Nakajima, F. Lavenu, I. Jankowiak, and A. Smirnov, "AERONET – A federated instrument network and data archive for aerosol characterization," *Remote Sensing Environ.*, vol. 66, pp. 1-16, 1998.

[4] T. Takamura, and T. Nakajima, and SKYNET community group, "Overview of SKYNET and its activities," *Optica Pura y Aplicada*, vol. 37, pp. 3303-3303, 2004.

[5] V. Estellés, M. Campanelli, T.J. Smyth, M.P. Utrillas, and J.A. Martínez-Lozano, "Evaluation of the new ESR network software for the retrieval of direct sun products from CIMEL CE318 and PREDE POM01 sun-sky radiometers," *Atmos. Chem. Phys.*, vol. 12, pp. 11619-11630, 2012.

[6] A. Ripoll, J. Pey, M.C. Minguillón, N. Pérez, M. Pandolfi, X. Querol, and A. Alastuey, "Three years of aerosol mass, black carbon and particle number concentrations at Montsec (southern Pyrenees, 1570 m a.s.l.)," *Atmos. Chem. Phys.*, vol. 14, pp. 4279-4295, 2014.

[7] C. Toledano, V.E. Cachorro, A. Berjón, A.M. de Frutos, M. Sorribas, B.A. de la Morena, and P. Goloub, "Aerosol optical depth and Angstrom exponent climatology at El Arenosillo AERONET site (Huelva, Spain), *Q. J. R. Meteorol. Soc.*, vol. 133, pp. 795-807, 2007.

[8] V.E. Cachorro, P.M. Romero, C. Toledano, E. Cuevas, and A.M. de Frutos, "The fictitious diurnal cycle of aerosol optical depth: A new approach for in situ calibration and correction of AOD data series," *Geophys. Res. Lett.*, vol. 31, L12106, doi:10.1029/2004GL019651, 2004.

[9] R.R. Draxler and G.D. Hess, "An overview of the HYSPLIT_4 modeling system for trajectories, dispersion, and deposition," *Aust. Meteor. Mag.,* vol. 47, pp. 295-308, 1998.

[10] C. Toledano, V.E. Cachorro, A.M. de Frutos, B. Torres, A. Berjón, M. Sorribas, and R.S. Stone, "Airmass classification and analysis of aerosol types at El Arenosillo (Spain)," *J. App. Meteorol. Climatol.*, vol. 48, pp. 962-981, 2009.

[11] O.E. García, "Estudio de las propiedades radiativas de los aerosols atmosféricos mediante técnicas de teledetección. Forzamiento radiativo," *PhD Thesis*, 2008.

[12] J. Pey, X. Querol, and A. Alastuey, "Discriminating the regional and urban contributions in the North-Western Mediterranean: PM levels and composition," *Atmos. Environ.*, vol. 44, pp. 1587-1596, 2010.

[13] Y.S. Bennouna, V.E. Cachorro, B. Torres, C. Toledano, A. Berjón, A.M. de Frutos, I. Alonso Fernández Copel, "Atmospheric turbidity determined by the annual cycle of the aerosol optical depth over north-center Spain from ground (AERONET) and satellite (MODIS)," *Atmos. Env.*, vol. 67, pp. 352-364, doi:10.1016/j.atmosenv.2012.10.065, 2012.

[14] V.E. Cachorro, P. Durán, R. Vergaz, and A.M. de Frutos, "Columnar physical and radiative properties of atmospheric aerosols in north central Spain," *J. Geophys. Res.*, vol. 105, pp. 7161-7175, 2000.

[15] J. Pey, X. Querol, A. Alastuey, F. Forastiere, and M. Stafoggia, "African dust outbreaks over the Mediterranean basin during 2001-2011: PM_{10} concentrations, phenomenology and trends, and its relation with synoptic and mesoscale meteorology," *Atmos. Chem. Phys.*, vol. 13, pp. 1395-1410, 2013.

Building and Tuning-up of an HTDMA and its First Measurements in an Urban Background Area

E. Alonso-Blanco[1], F.J. Gómez-Moreno[1], S. Sjogren[2] and B. Artíñano[1]

Abstract — In this work the building and tuning-up of a custom-built HTDMA is described. This equipment has been built at CIEMAT, based on EUSAAR HTDMA standards, allowing us to measure a maximum growth factor of 2.2 for particle sizes up to 265 nm, between 10 to 98% RH. The accuracy and quality of the measurements have been validated by pure ammonium sulphate aerosol. The first measurements have been carried out at an urban background station located in the CIEMAT facilities in Madrid during October 2013. A remarkable dependence between particle size and the growth factor is observed. The largest particle sizes have a greater growth factor possibly as a result of aging of aerosols, which determines their chemical composition. This agrees with the observed daily pattern of the growth factor associated with emissions from anthropogenic combustion processes.

Keywords — Custom-Built HTDMA, Growth Factor, Hygroscopicity

1 INTRODUCTION

The study of hygroscopic properties involves a notable complexity as it encompasses the analysis of three main aspects: the aerosol composition, the aerosol size, and the humidity/temperature ambient conditions [1].

Changes associated with aerosol water absorption capacity alter their incidence/impact on air quality, human health and direct effects (scattering and absorption of radiation that reaches and leaves the Earth´s surface) and indirect effects (associated with the modification of clouds' properties and coverage) on climate [2].

Reduced visibility is one of the most direct air quality indicators. Visibility degradation is attributed primarily to the scattering and absorption of visible light. Some studies indicate that the size increase undergone by the particles as a result of water absorption triggers an increased extinction coefficient [3].

In relation to human health, the potential damage caused by the particles is mainly associated with their ability to penetrate/deposited into the respiratory system and consequently their ability to incorporate into the bloodstream [4].

_____

1. *E. Alonso-Blanco, F.J. Gómez-Moreno, and B. Artíñano belong to the Department of Environment, Research Center for Energy, Environment and Technology (CIEMAT), Avda. Complutense 40, 28040, Madrid, Spain. E-mail: elisabeth.alonso@ciemat.es; fj.gomez@ciemat.es; b.artinano@ciemat.es.*
2. *S. Sjogren is with the University of Applied Sciences Northwestern Switzerland, Brugg-Windisch, Switzerland, E-mail: staffan.sjogren@nuclear.lu.se.*

Changes occurring in the aerosol size, associated to hygroscopic properties, imply variations in the aerosol deposition pattern within the respiratory tract [5], [6].

Aerosol hygroscopicity determines its ability to become **C**loud **C**ondensation **N**uclei (**CCN**) for the formation of water droplets or **I**ce **N**uclei (**IN**) for the formation of ice crystals. Besides aerosol size distribution [7], [8] the ratio of soluble/insoluble fraction of the aerosol and its mixing state determine whether it will act as a CCN or not [9], [10].

The Hygroscopic Tandem Differential Mobility Analyzer (HTDMA) is the most commonly used technique for performing real-time measurements about the relationship between particle size and hygroscopic growth, by providing information on its mixing state and solubility [11], [12], [13].

Under subsaturation conditions, the water absorption of a dried particle is defined by the concept of hygroscopic growth factor diameter:

$$GF = \frac{D_w(RH)}{D_p} \quad (1)$$

Where D_w is the wet particle diameter at a given RH and D_p is the dry diameter of the particle.

Since the development of the first HTDMA [14] until present, the evolution of these equipments has focused on improving the accuracy and quality of measures and increase operation time by reducing the frequency of maintenance. Most of these equipments are custom-built [15], [16], [17], [18], [19], [20]. Some companies have recently developed commercial HTDMA: MSP Corporation the

HTDMA Model 1040XP and BRECHTEL company the HTDMA Model 3002, however the presence of published works collecting measurements using these HTDMA models is scarce [21], [22].

This work presents the tuning up and quality assurance procedures of an HTDMA and the first measurements made in a suburban area of Madrid.

2 HYGROSCOPIC TANDEM DIFFERENTIAL MOBILITY ANALYZER (HTDMA): DESCRIPTION

The HTDMA built at CIEMAT was designed to allow us to know the size changes of the submicrometer aerosol in relation to the relative humidity (RH). Its construction was carried out based on the HTDMA developed by [15] following EUSAAR HTDMA standards [23], [24].

The HTDMA is formed by two custom-made Vienna-type Differential Mobility Analyzers (DMAs) [25] connected in tandem by a humidifying system (Fig. 1).
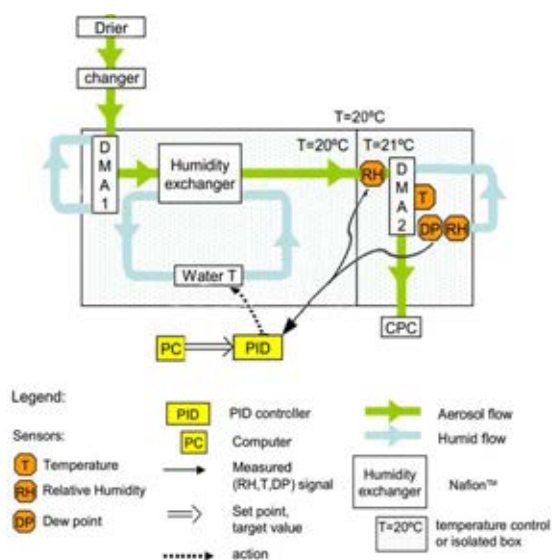
Fig. 1. Schematic of the H-TDMA system illustrating the humidification and inputs systems and control system of the relative humidity following the scheme developed by [23].

The HTDMA built at CIEMAT works with aerosol flow of 0.95 l/min. The atmospheric particles sample is conditioned by a nafion dryer (Perma Pure Inc., MD-070-24E-S 467 1110), reducing the relative humidity below 40% prior to enter the neutralizer, a Kr-85 source.

Once the particles have been charged, they pass through the first DMA (DMA1). The DMA1 is insulated by an aluminum box (box 1) with outer dimensions 640×500×1000 mm and covered inside with expanded polystyrene (EPS). Environmental conditions in the DMA1 are stable thanks to a Peltier element (Supercool AA-040-12-22-00-00) with an external control unit (Supercool TC-XX-PR-59) allowing the air circulation inside the box 1. The temperature in the box 1 is kept constant around 20ºC approximately.

In the DMA1 (inner and outer working section radii R1 = 2.5 cm; R2 = 3.35 cm; length 28 cm), the electric potential corresponding to the particle size to be measured is fixed. Thus, the particles that leaves the DMA1, corresponds to a monodisperse population. El DMA1 works with a closed loop system for excess-sheath flows of 6.2±0.01 l/min regulated by a critical orifice (CO). This system allows greater autonomy of work to the HTDMA. Additionally the pressure in the DMA1 sheath flow is measured by a pressure sensor MPX4115AP. The sheath flow is controlled by a mass flow sensor (MFS). Sample conditions of RH/T in the DMA1 are monitored by two Rotronic sensors, the first located in the aerosol flow, at the exit of the neutralizer, and the second located at the exit of the sheath flow. The Rotronic sensors have an accuracy of ±0.8% for RH and ±0.1K for temperature.

The aerosol sample passes through the humidifier where the aerosol absorbs water vapor. The humidification system consists of a membrane of Gore-Tex® of 5 cm length located in the aerosol flow between the two DMAs. The water vapor is produced by temperature control of the Milli-Q liquid water through a 25×25 mm Peltier cell which heats or cools the water according to the needs of the aerosol sample. The humidification system is regulated by a PID control programmed in LabView from the combination of two output signals, the RH Rotronic sensor signal located at the entrance of DMA2, and the RH calculated by a Mirror Dew Point Hygrometer located at the exit of the DMA2 sheath flow. Both sensors will be described in detail later.

Subsequently the aerosol sample enters the DMA2 where relative humidity conditions are kept constant. Just like the DMA1, the DMA2 is isolated by an aluminum box (box 2) with outer dimensions of 435×440×620 mm and coated inside with EPS. One of the most important sources of uncertainty in the hygroscopicity measurements is the variability of RH inside DMA2 [20], therefore ambient conditions in the box 2 remain stable thanks to two Peltier elements (Supercool AA-040-12-22-00-00) with an external control unit (Supercool TC-XX-PR-59), which allows maintaining a constant temperature around 21°C.

The outer vertical temperature gradient of the DMA2 is monitored by three Pt100-elements located at different heights (lower, mid and upper). These sensors have been calibrated by a thermometer with an accuracy of ±0.03ºC. In addition, the RH/T in this DMA is monitored by three sensors. Two Rotronic sensors located one at the entrance of the aerosol flow and the other at the exit of the sheath flow

subsequently to a third sensor, a Chilled Mirror Dew Point Hygrometer (EdgeTech, Dewmaster, MA, USA). The latter sensor measures the dew point temperature and calculates the relative humidity according to the mean temperature the Pt100-elements following the methodology developed by [26]. The accuracy of the dew-point hygrometer is ±0.2ºC. An appropriate accuracy of the Rotronic sensor, located in the aerosol flow of DMA2, together with a low uncertainty in the hygrometer measures, assure a good functioning of the humidification system.

The DMA2 has the same radius as the DMA1 but a greater length, L=50 cm, which allows measuring higher particle sizes, i.e. GF of 2.2 for a maximum particle size selected in the DMA1 of 265 nm. The DMA2 has the same closed loop system for excess-sheath flow rates as the DMA1, but works at a lower flow rate of 4.4±0.01 l/min. In this flow, the pressure is measured by a pressure sensor MPXV7002DP. The DMA2 is connected to a Condensation Particle Counter (CPC) and works as a Scanning Mobility Particle Size (SMPS) which allows measuring the growth factor distribution of the aerosol selected in the DMA1. The counter used is TSI CPC 3772, which have a counting range between 10^{-3} and 10^4 cm^{-3} and size range from 0.01 to 1.0 μm.

The laboratory temperature has remained constant at 20°C in order to maintain the equipment in a stable environment thereby facilitating an adequate aerosol humidification.

The HTDMA system described allows measuring the growth factor between 10-98% RH with a temporal resolution of about 3 min for each scan. The time required by the equipment to achieve a relative humidity of 90% (set point at which the equipment works) from a RH of 10% is approximately 15 hours.

Both the instrument regulation and the data acquisition software were developed in LabVIEW code.

Although the equipment is working properly under the conditions described above, in order to improve the system we will continue making improvements in equipment addressed to:

1. Increase flow ratio; 10:1 and 6:1 for DMA1 and DMA2 respectively.
2. Improve insulation of equipment to mitigate the potential environmental temperature variations.

Furthermore, with the goal of improving the data quality, as many HTDMA modifications as necessary will be undertaken, and those elements that have lowered their efficiency will be replaced.

3 CALIBRATION, VALIDATION AND DATA ANALYSIS

3.1 Calibration

The different components of the HTDMA have been calibrated independently. First, the pressure sensors were calibrated in relation to atmospheric pressure values. Subsequently, mass flow sensors which measure sheath flows have been calibrated by Sensidyne™ Gilian™ Gilibrator-2™ Calibrator Kits (with a reading accuracy of ±1%) with a calibration error less than 1%.

The high voltage sources (HVS) have been calibrated with a high voltage probe (accuracy ±2% for 0 kV to 40 kV at 10ºC to 45ºC) with a calibration error less than 1%. Later, the aerosol particle sizing has been checked independently for each of the DMAs and for the equipment as a whole. For this purpose, PSL spheres of 80 (C.V. of 18%) and 190 nm (C.V. of 5%) from Microgenics Corporation have been used. The PSL spheres suspension was performed using a Collison atomizer [27]. The size error for DMA1 in relation to PSL spheres of 80 y 190 nm was 1.44±1.0 and -0.5±1.0 nm respectively and for DMA2 is -2.2±0.5 and -3.1±0.6 nm respectively. These data are in line with findings from [23] and [24]. Once calibrated the particle size in the DMA2, the plumbing time between DMA2 and the CPC was estimated through up-scanning and down-scanning measurements for different particle sizes obtaining an optimal value of 2.6 s. Subsequently, PSL spheres measurements have also been conducted for the whole system, avoiding their passage through the humidifier, observing errors of 4.4±1.0 nm and 0.3±1.1 nm for PSL of 80 and 190 nm respectively.

Finally the four Rotronic sensors that monitor the RH/T throughout the whole equipment have been calibrated. For this purpose it has been used saline suspensions saturated of 10% RH (uncertainty ±0.3%) and 95% (uncertainty ±1.2%).

The main basis of the quality of the growth factor data provided by the HTDMA is an adequate and careful control of the relative humidity at which the equipment works [12] [16], [20].

3.2 Data Validation with Pure Ammonium Sulphate

The accuracy and quality of the equipment as a whole have been tested through some laboratory tests performed with polydisperse aerosol suspensions of pure ammonium sulphate (AS) ((NH_4)$_2SO_4$ purity>99.5%). With its known efflorescence-deliquescence hysteresis cycle it allows us to ensure the reliability of the measured hygroscopicity [28], [29].

A pneumatic nebulizer has been used to generate

a polydisperse aerosol of AS in the submicrometer range (TSI 3076 model). The two particle sizes selected in the DMA1 has been 80 and 110 nm.

The RH is reduced from 90% down to 0% a 1% every 3600 s, time required to perform two scans (upstream and downstream). This allows properly observing changes in the GF for the AS particles

The results are consistent with those found by other authors as [18], [31] and [32] (Fig. 2).
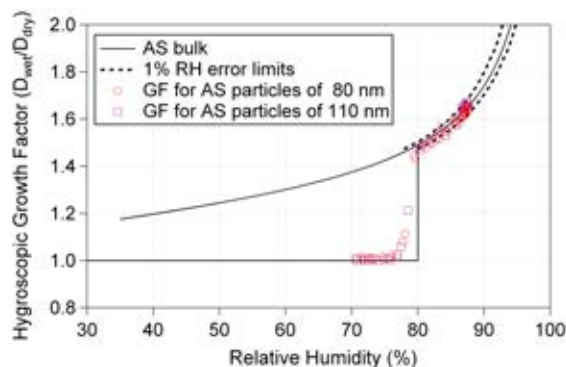
Fig. 2. Humidogram of ammonium sulphate particles for 80 and 110 nm. The modeled curve is calculated based on [28] without regard to Kelvin effect.

3.3 Retrieval and Standard Data Analysis

The TDMAinv (Inversion of Tandem Differential Mobility Analyser) method developed by [30] was used to invert the HTDMA data. Measurement errors in dry conditions associated with the equipment characteristics and inaccuracy errors of the different components have been corrected on the basis of dry scans (under RH<20%) of ammonium sulphate particles for five different sizes; 50, 80, 110, 190 and 265 nm. The dry scans allow calibrating the growth factor and width of the HTDMA's transfer function [30].

4 THE FIRST MEASUREMENTS OF THE HYGROSCOPIC GROWTH FACTOR

4.1 Measurement Area and Meteorological Conditions of the Study Period

From 11 to 22 October 2013 the first measurements with a HTDMA have been conducted in an urban background area located at CIEMAT facilities (40° 27 '23.2 "N, 03 °43 '32.3 "E) in the north-northwest of Madrid.

Madrid city is characterized by a high population density and the absence of industrial activity within the urban area determines that the primary sources of gaseous and particulate pollutants are emissions from traffic and domestic activity.

The study period was characterized by atmospheric stable conditions favoured by the presence of a high pressure system inhibiting the dispersion of pollutants. The average temperature for

the period is 15.7±3.5ºC, with the presence of thermal inversions during night time. The average RH is 67±18%. The accumulated precipitation in the study period is 2.9 mm, registered between 19 and 22 October 2013.

The average wind speed is 2.9±1.6 m/s and the wind direction follows the usual directional pattern of the study area with a NE-SW steering axle conditioned by the orography of the area [31].

4.2 Methodology

The first measures with the HTDMA for atmospheric particles sizes of 50, 80, 110, 190 and 265 nm were obtained for a relative humidity of 90%. To obtain comparable data, these have been corrected for RH variations of ±2% about target value, RH of 90% (88% ≤ RH set point ≤ 92%) from TDMA$_{inv}$ according to [30]. After correcting the RH, a coverage data of 85 % scans for the study period was reached. Lost scans were due to noise in the measurements or variations in RH greater than ±2% from the set point. Errors in the scans are higher the greater the particle size selected.

The Growth Factor (GF) has been classified in three groups based on GF (90%) of measurements particles with respect to GF of ammonium sulphate particles of 100 nm [12]: nearly hydrophobic particles (GF=1.0-1.11), less-hygroscopic particles (GF=1.11-1.33) and more-hygroscopic particles (GF>1.33).

4.3 Results and Discussion

The average growth factor (GF$_{avg}$) for the five particle sizes (50, 80, 110, 190 and 265 nm) comprising submicron fraction of atmospheric aerosol has been analyzed for the 12-day study.

During this study period it has been observed a clear dependence between growth factor and particle size, i.e. a larger growth factor for larger particles (Fig. 3). While for the particle sizes of 50, 80 y 110 nm, almost every day atmospheric particles were nearly hydrophobic (GF=1.0-1.11) and less-hygroscopic (GF=1.11-1.33), for particle sizes of 190 and 265 nm were less-hygroscopic (GF=1.11-1.33) and more-hygroscopic (GF>1.33). This is because the larger particles have been subjected for a longer period to physical-chemical atmospheric processes and consequently the degree of aging is greater.

Furthermore, normally particle sizes of 50, 80 and 110 nm had a growth factor unimodal distribution versus particle sizes of 190 and 265 nm that had a growth factor bimodal distribution. This indicated that the external mixture state of the larger particles was greater than that for the smaller particles. This result has been found by other authors as [11] and [32].
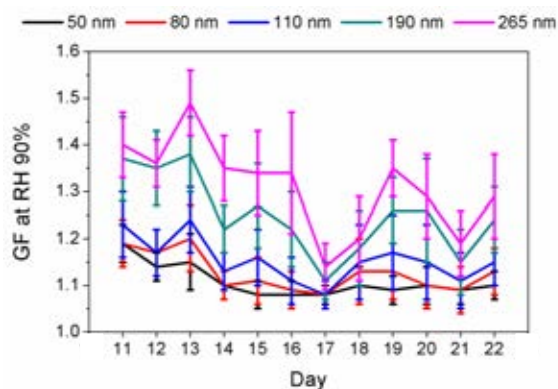
Fig. 3. Evolution of the daily average GF_{avg} and its standard deviations for each dry particle size of the 12-day study.

A daily pattern of GF_{avg} has been observed in relation to emission sources in the study area. An example of this situation was observed on October 17, 2013 (Fig. 4). Two peaks in the particle concentration were seen this day, the first between 06:00 to 09:00 UTC (local time = UTC time+1) on October 17 and the second between 18:00 to 00:00 UTC on October 18. These were associated with emissions from anthropogenic combustion processes. In both periods were exceeded the 4000 counts·cm^{-3}. The peak observed at early hours of the morning is higher than that observed late in the afternoon. This behavior in the particle concentration is characteristic of the measurement station during the autumn and winter season [33]. These two peaks coincide with two minimums of growth factor, with a GF_{avg} value between 1.0 to 1.1 (nearly hydrophobic particles) for the five particle sizes. However, for the rest of the day and linked to particle aging in the atmosphere, for particle sizes of 50, 80 and 110 nm the GF_{avg} was found between 1.05 and 1.15 (nearly hydrophobic particles) and for particle sizes of 190 and 265 nm, between 1.1 and 1.25 (less-hygroscopic particles).
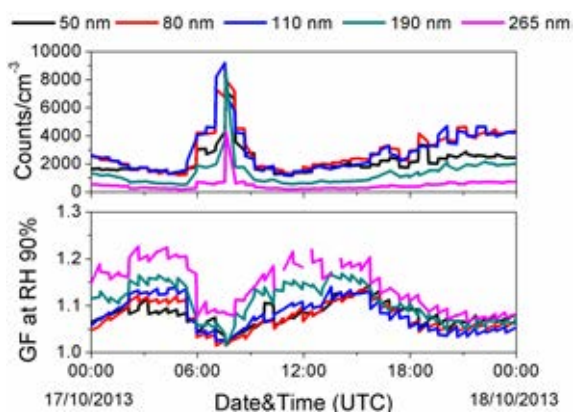
Fig. 4. Typical example of number of counts and GF_{avg} for the five dry particle sizes on 17 October 2013.

5 CONCLUSIONS

The present work describes a HTDMA custom-built based on EUSAAR HTDMA standards, developing the different procedures for its calibration and validation. As well as presenting the first results obtained.

Validation samples with AS particles have allowed confirming that HTDMA built at CIEMAT provides good quality measurements.

The first measurements at an urban background station show dependence between particle size and the GF, a larger particle size implies a higher degree of aging and consequently a higher GF. Furthermore a marked diurnal pattern in the GF is observed in relation to emission sources, with two minimum peaks corresponding to the two periods of higher particulate emissions from anthropogenic combustion processes.

These results are a first approximation to the hygroscopic properties characterization in relation to the growth factor of the atmospheric aerosol present in this study area. This aerosol property will be the subject of future research.

REFERENCES

[1] V.M. Kerminen, "The effects of particle chemical character and atmospheric processes on particle hygroscopic properties," *J. Aerosol Sci.*, vol. 28, pp. 121-132, 1997.

[2] IPCC. Climate Change 2013: *The Physical Science Basis*, 2013.

[3] Y.L. Lee, R. Sequeira, "Water-soluble aerosol and visibility degradation in Hong Kong during autumn and early winter, 1998," *Environ. Poll.*, vol. 116, pp. 225-233, 2002.

[4] G. Oberdärster, E. Oberdärster, J. Oberdärster, "Nanotoxicology: an emerging discipline evolving from

studies of ultrafine particles," *Environ. Health Perspect.*, vol. 113, 2005.

[5] K.W. Tu, E.O. Knutson, "Total deposition of ultrafine hydrophobic and hygroscopic aerosols in the human respiratory system," *Aerosol Sci. Tech.*, vol. 3, pp. 453-465, 1984.

[6] S.K. Varghese, S. Gangamma, "Particle deposition in human respiratory tract: effect of water-soluble fraction," *Aerosol Air Qual. Res.*, vol. 6, pp. 360-379, 2006.

[7] U. Dusek, G.P. Frank, L. Hildebrandt, J. Curtius, J. Schneider, S. Walter, D. Chand, F. Drewnick, S. Hings, D. Jung, "Size matters more than chemistry for cloud-nucleating ability of aerosol particles," *Science*, vol. 312, pp. 1375-1378, 2006.

[8] H.W. Gaggeler, "Size dependent aerosol activation at the high-alpine site Jungfraujoch (3580 m ASL)," *Volume V General Energy*, pp. 115, 2001.

[9] J.W. Fitzgerald, "Dependence of the supersaturation spectrum of CCN on aerosol size distribution and composition," *J. Atmos. Sci.*, vol. 30, pp. 628-634, 1973.

[10] M.O. Andreae, D. Rosenfeld, "Aerosol-cloud-precipitation interactions. Part 1. The nature and sources of cloud-active aerosols," *Earth Sci. Rev.*, vol. 89, pp. 13-41, 2008.

[11] S. Sjogren, M. Gysel, E. Weingartner, M.R. Alfarra, J. Duplissy, J. Cozic, J. Crosier, H. Coe, U. Baltensperger, "Hygroscopicity of the submicrometer aerosol at the high-alpine site Jungfraujoch, 3580 m asl, Switzerland," *Atmos. Chem. Phys.*, vol. 8, pp. 5715-5729, 2008.

[12] E. Swietlicki, H.C. Hansson, K. Hämeri, B. Svenningsson, A. Massling, G. McFiggans, P.H. McMurry, T. Petäjä, P. Tunved, M. Gysel, "Hygroscopic properties of submicrometer atmospheric aerosol particles measured with H-TDMA instruments in various environments: A review," *Tellus*, vol. B 60, pp. 432-469, 2008.

[13] E.O. Fors, E. Swietlicki, B. Svenningsson, A. Kristensson, G.P. Frank, M. Sporre, "Hygroscopic properties of the ambient aerosol in southern Sweden-a two year study," *Atmos. Chem. Phys.*, vol. 11, pp. 8343-8361, 2011.

[14] P.H. McMurry, M.R. Stolzenburg, "On the sensitivity of particle size to relative humidity for Los Angeles aerosols," *Atmos. Environ. (1967)*, vol. 23, pp. 497-507, 1989.

[15] E. Nilsson, E. Swietlicki, S. Sjogren, J. Löndahl, M. Nyman, B. Svenningsson, "Development of an H-TDMA for long-term unattended measurement of the hygroscopic properties of atmospheric aerosol particles," *Atmos. Meas. Tech.*, vol. 2, pp. 313-318, 2009.

[16] J. Duplissy, M. Gysel, M.R. Alfarra, J. Dommen, A. Metzger, A.S.H. Prevot, E. Weingartner, A. Laaksonen, T. Raatikainen, N. Good, "Cloud forming potential of secondary organic aerosol under near atmospheric conditions," *Geophys. Res. Lett.*, vol. 35, 2008.

[17] M.J. Cubison, H. Coe, M. Gysel, "A modified hygroscopic tandem DMA and a data retrieval method based on optimal estimation," *J. Aerosol Sci.*, vol. 36, pp. 846-865, 2005.

[18] E. Weingartner, M. Gysel, U. Baltensperger, "Hygroscopicity of aerosol particles at low temperatures. 1. New low-temperature H-TDMA instrument: Setup and first applications," *Environ. Sci. Technol.*, vol. 36, pp. 55-62, 2002.

[19] K. Hämeri, M. Väkevä, H.C., Hansson, A. Laaksonen, Hygroscopic growth of ultrafine ammonium sulphate aerosol measured using an ultrafine tandem differential mobility analyser," *J. Geoph. Res.: Atmospheres (1984-2012)*, vol. 105, pp. 22231-22242, 2000.

[20] T. Hennig, A. Massling, F.J. Brechtel, A. Wiedensohler, "A Tandem DMA for highly temperature-stabilized hygroscopic particle growth measurements between 90% and 98% relative humidity," *J. Aerosol Sci.*, vol. 36, pp. 1210-1223, 2005.

[21] A. Wonaschütz, M. Coggon, A. Sorooshian, R. Modini, A.A. Frossard, L. Ahlm, J. Mülmenstädt, G.C. Roberts, L.M. Russell, S. Dey, "Hygroscopic properties of smoke-generated organic aerosol particles emitted in the marine atmosphere," *Atmos. Chem. Phys.*, vol. 13, pp. 9819-9835, 2013.

[22] A. Sorooshian, J. Csavina, T. Shingler, S. Dey, F.J. Brechtel, A.E. Sáez, E.A. Betterton, "Hygroscopic and chemical properties of aerosols collected near a copper smelter: Implications for public and environmental health," *Environ. Sci. Technol.*, vol. 46, pp. 9473-9480, 2012.

[23] J. Duplissy, M. Gysel, S. Sjogren, N. Meyer, N. Good, L. Kammermann, V. Michaud, R. Weigel, S.M. dos Santos, C. Gruening, "Intercomparison study of six HTDMAs: results and recommendations," *Atmos. Meas. Tech.*, vol. 2, pp. 363–378, 2009.

[24] A. Massling, N. Niedermaier, T. Hennig, E. Fors, E. Swietlicki, M. Ehn, K. Hämeri, P. Villani, P. Laj, N. Good, "Results and recommendations from an intercomparison of six Hygroscopicity-TDMA systems," *Atmos. Meas. Tech.*, vol. 3, pp. 637-674, 2010.

[25] W. Winklmayr, G.P. Reischl, A.O. Lindner, A. Berner, "A new electromobility spectrometer for the measurement of aerosol size distributions in the size range from 1 to 1000 nm," *J. Aerosol Sci.*, vol. 22, pp. 289-296, 1991.

[26] A.L. Buck, "New Equations for Computing Vapour Pressure and Enhancement Factor," *J. Appl. Meteorol.*, vol. 20, pp. 1527–1532, 1981.

[27] K.R. May, "The Collison nebulizer: description, performance and application," *J. Aerosol Sci.*, vol. 4, pp. 235-243, 1973.

[28] D.O. Topping, G.B. McFiggans, H. Coe, "A curved multi-component aerosol hygroscopicity model framework: Part 1: Inorganic compounds," *Atmos. Chem. Phys.*, vol. 5, pp. 1205-1222, 2005.

[29] I.N. Tang, H.R. Munkelwitz, "Composition and temperature dependence of the deliquescence properties of hygroscopic aerosols," *Atmos. Environ. Part A. General Topics*, vol. 27, pp. 467-473, 1993.

[30] M. Gysel, G.B. McFiggans, H. Coe, "Inversion of tandem differential mobility analyser (TDMA) measurements," *J Aerosol Sci.*, vol. 40, pp. 134-151, 2009.

[31] P. Salvador, "Characterization of air pollution produced by particles in suspension in Madrid". Doctoral Thesis. Faculty of Physics, University Complutense of Madrid, Madrid (Spain), 2004.

[32] S. Bezantakos, S. Vratolis, L. Diapouli, K. Eleftheriadis, G. Biskos, "Hygroscopic Properties of Fine and Ultrafine Aerosol Particles over an Urban Background Site in Athens", in European Aerosol Conference, 2012.

[33] F.J. Gómez-Moreno, M. Pujadas, J. Plaza, J.J. Rodríguez-Maroto, P. Martínez-Lozano, B. Artiñano, "Influence of seasonal factors on the atmospheric particle number concentration and size distribution in Madrid," *Atmos. Environ.*, vol. 45, pp. 3169-3180, 2011.

Characterization of African Dust source areas contributing to ambient aerosol levels across the Western Mediterranean Basin

Pedro Salvador[1], Begoña Artíñano[1], Francisco Javier Gómez-Moreno[1], Silvia Alonso-Pérez[2,3], Jorge Pey[2,4], Andrés Alastuey[2], Xavier Querol[2],

Abstract — The occurrence of African dust outbreaks over the western Mediterranean basin were identified on an 11-year period (2001-2011). PM10 daily data from nine regional background air quality monitoring sites across the study area were compiled and the net dust load transported during each event was estimated. Then, the potential source areas of mineral dust were identified by trajectory statistical methods for any year of the period of study. Our results indicate that the sources areas of African mineral dust strongly depended on the atmospheric circulation patterns prevailing during each of the years, which condition the intensity of the dust outbreaks and the areas affected by the transport and deposition of the mineral.

Keywords — PM10, mineral dust contribution, long-range transport, source areas

1 INTRODUCTION

It is well known that significant amounts of African dust are transported westward, towards the Caribbean, the eastern coasts of North America and South America [1]. Large quantities of mineral dust are also carried across the Mediterranean basin to Europe and the Middle East as in [2]. During such African Dust Outbreaks (ADO) mineral dust represents a significant contribution to daily PM10 levels registered at rural and urban monitoring sites in the Mediterranean Basin "[3], [4], [5], [6], [7]". Some recent studies demonstrated that a relevant percentage of the exceedances of the PM10 daily limit value (50 µg/m^3 after the 2008/50/EC European Directive) registered at these sites, can be exclusively attributed to the net African dust load (ADL) transported during ADO "[8], [9], [10]".

With the aim to document the occurrence of ADO over different areas of the western Mediterranean basin all the ADO occurring in this region from 2001 to 2011 were analyzed.

_____

1. *P. Salvador, B. Artíñano and F.J. Gómez-Moreno are with the Environmental Department of the Research Center for Energy, Environment and Technology (CIEMAT). Avenida Complutense 40, 28040 Madrid. Spain. E-mails:* pedro.salvador@ciemat.es; b.artinano@ciemat.es; fj.gomez@ciemat.es
2. *S. Alonso-Pérez, J. Pey, A. Alastuey and X. Querol are with the Institute of Environmental Assessment and Water Research (IDÆA-CSIC). Provisional address: c) Lluis Solé i Sabarís S/N, 08028 Barcelona. Spain. E-mails:* salonsop@aemet.es;jorge.pey@univ-amu.fr; andres.alastuey@idaea.csic.es;xavier.querol@idaea.csic.es
3. *S. Alonso-Pérez is also with the Center of Atmospheric Research, AEMET, C) La Marina 20,38071 Santa Cruz de Tenerife, Spain*
4. *J. Pey are also with the Aix-Marseille Université, CNRS, LCE FRE 3416, Marseille, 13331, France.*

Additionally, an estimation of the ADL contributing to the PM10 daily mean levels during each event was obtained for each region of study. In this study the main atmospheric processes which give rise to the ADO are characterized and the source areas of dust are identified using different objective statistical procedures. The seasonality and the geographical differences within the areas of study, of the occurrence of the ADO are described.

2 METHODOLOGY

Firstly, daily patterns of geopotential height at the 850 hpa topography corresponding to episodic days were grouped into homogeneous groups by non-hierarchical k-means cluster analysis, each one representing a characteristic atmospheric circulation type. Synoptic situations which give rise to these circulation types, were characterized by composite synoptic maps of geopotential height at the 850 hPa level. The seasonal occurrence of ADO during each circulation type, was analyzed. Finally, the potential source areas of the mineral dust transported during the different circulation types were estimated by trajectory statistical methods.

During the 2001-2011 period, the occurrence of ADO over different regions of the western Mediterranean basin was identified using a robust methodology, which consists in the daily interpretation of meteorological products and air masses back-trajectories. The procedure can be found elsewhere [8] and consequently will not be described here in detail.

Then, daily data from nine regional background air quality monitoring sites were obtained during this 11-year period, to evaluate the African dust contributions and to assess their impact on PM10

levels. Fig. 1 shows the various stations used in this study. Seven out of the nine stations are members of EMEP (Co-operative Programme for Monitoring and Evaluation of the Long-Range Transmission of Air Pollutants in Europe). Of the remaining sites, Bellver belongs to the Balearic Islands Regional Air Quality Network whereas Monagrega is part of the ENDESA (Empresa Nacional de Electricidad S.A.) Air Quality Network. 2 different techniques have been used to determine PM10 concentrations: gravimetric determinations at the EMEP sites and real time monitors based on Beta gauge attenuation at Monagrega and Bellver. In these two monitoring sites the real time concentrations were corrected against the gravimetric ones. Since only the official data reported to the European Commission are used in this work, their quality is guaranteed.

These monitoring sites were selected according to data coverage and geographical location criteria. They were the regional background sites with the best data coverage of PM10 daily mean values in the period of study (PM10 daily data coverage ranging from 84% to 99%). Besides, they were distributed throughout the Iberian Peninsula and the Balearic Islands, covering southeastern, southwestern, central, eastern, northeastern, northern and northwestern regions (Fig. 1). It should be noted that until the year 2004, no rural background station was recording PM10 concentration levels on a regular basis in Portugal. For this reason Portugal was not considered in this work.

A procedure for the quantification of the net African dust load transported during each ADO was applied to estimate the impact of the African dust contributions on the PM10 daily records. Such methodology is based on the identification of days under the influence of African dust and a statistical analysis based on the calculation of the 30 days moving 40th percentile for the different regional background PM10 time series (not containing the PM10 values when African dust was detected). This percentile is an indicator of the non-African regional background to be subtracted from the daily PM10 levels during African dust outbreaks and thus allows calculating the daily values of ADL. The feasibility of this method was demonstrated by different approaches "[8], [9]".

This methodology became the Spanish and Portuguese reference method to identify and quantify African dust contributions to PM10 levels since 2004. The method is also applicable across the whole Southern Europe, as demonstrated by [4] and more recently by [7]. Currently, this is one of the official methods recommended by the European Commission for evaluating the occurrence of ADO and quantifying its contributions [11].

As a consequence of this preliminary analysis, days contributing with a positive value of ADL in at least, one of the 9 regional background monitoring sites during the 2001-2011 period, were identified.

Henceforth they will be referred to as "episodic days".

In this study daily fields of geopotential height at the 850 hpa level, were obtained from the ERA-Interim Archive at ECMWF (European Centre for Medium-Range Weather Forecasts) for the period 2001-2011. The ERA-Interim atmospheric model and reanalysis system uses the cycle 31r2 version of the ECMWF's Integrated Forecast System, which was configured for the following spatial resolution: 60 levels in the vertical, with the top level at 0.1 hPa; T255 spherical-harmonic representation for the basic dynamical fields; a reduced Gaussian grid with approximately uniform 79 km spacing for surface and other grid-point fields.
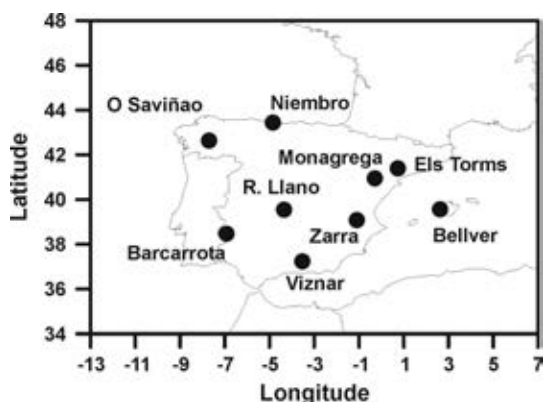
Fig. 1. Location of regional background air quality monitoring sites used in this study.

Next, a nonhierarchical k-means cluster analysis method was applied for classifying time series of daily fields of geopotential height at the 850 hPa topography, into similar groups or "circulation types" as in [12].

Finally, the Redistributed Concentration Field (RCF) method [13] was used to identify potential source areas of the mineral dust transported during ADO towards Spanish regions. 5-day backward 3-D air trajectories arriving at all of the 9 sampling sites at 00:00, 06:00, 12:00 and 18:00 UTC were computed for each day of the 2001-2011 period, using the HYSPLIT model [14]. Fixed height of 1500 m ASL was chosen as the air masses arrival height, because this altitude approximately coincides with the 850 hPa geopotential height topography. In all, more than 22,000 trajectories corresponding to episodic days were available for analysis, each with 120 endpoints.

A RCF was thus computed for each circulation type, over the region defined by $12^{0}N-60^{0}N$ and $28^{0}W-24^{0}E$. For each 2^{0} longitude x 2^{0} latitude grid cell, a weighted concentration of ADL was computed using the procedure defined in [13].

To provide detailed information on the source areas of dust contributing to the different regions of

the WMB, RCF maps were obtained using African dust contribution values and back-trajectories from western (Barcarrota and O Saviñao), central (Viznar, Risco Llano and Niembro) and eastern (Zarra, Bellver, Monagrega and Els Torms) regions of the WMB during each season (spring, summer, autumn and winter) and each circulation type.

3 RESULTS

3.1 Circulation classifications

During the period 2001-2011, 1592 episodic days were identified (on average 145 episodic days per year) increasing the daily concentration levels of PM10 recorded in regional background air quality monitoring stations, due to African mineral dust. The highest number of episodic days was recorded in 2007 (187 days) and the lowest in 2005 (125 days).

The occurrence of episodic days showed an increasing gradient from the N (21% at O Saviñao and Niembro) to the S (65% at Viznar). At most southern locations it is evident a higher frequency of episodic days, due to the higher proximity to the African mainland.

26% of the episodic days (409 days) were detected only at one of the sampling sites. Some of these episodic days corresponded to ADO with short duration, which only transported dust to one of the regions. Otherwise during ADO with duration of several days, mineral dust could be transported to further areas, being firstly detected at borderline sites such as Barcarrota (18% of the episodic days detected only in this site), Viznar (22%) and Bellver (46%). Otherwise, 3% of the episodic days (41 days) were registered simultaneously in all of the stations, during the most intense ADO.

On average the highest number of episodic days was recorded, in summer (June-August) followed by those registered in the spring (March-May) and the autumn (September-November) months. The lowest number of episodic days was recorded from December to February.

The application of the methodology exposed in section 2 showed that for the period 2001-2011 ADO were preferentially generated by 4 circulation types.

Fig. 2 shows the 4 final cluster centroids of the geopotential height at the 850 hPa level, after the last iteration in the clustering procedure. From now on, the four circulation types resulting from the circulation classification will be referred to as CT-1, CT-2, CT-3 and CT-4.

CT-1 centroid illustrated a synoptic meteorological scenario, characterized by a relative low pressure system observed at the 850 hPa levels west or southwest of the Iberian Peninsula coast and by an upper level high, located over northern Algeria (Fig. 2a). The so called North African high is a common synoptic feature in all the circulation types giving rise to ADO over the western Mediterranean basin. It is produced by the intense heating of the North African surface which generates the development of thermal lows. As a consequence, a compensatory high pressure system is formed at higher altitudes over different geographical locations, depending on the circulation pattern. CT-1 favored the advection of African air masses towards the Iberian Peninsula by south and southwestern winds in the upper atmospheric levels.
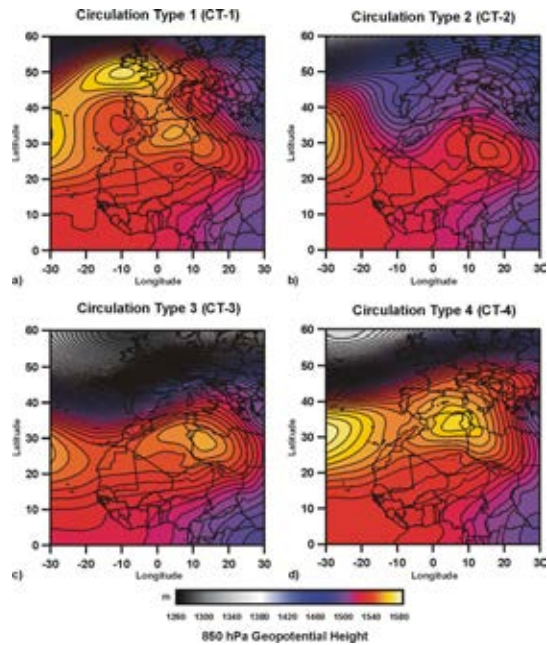
Fig. 2. Composite 850 hPa geopotential height (m) representing Circulation Types 1-4 leading to ADO over the western Mediterranean basin.

The CT-2 composite 850 hPa geopotential height field was characterized by a shift of the North African high to the west and a trough placed over the western Iberian Peninsula coast. A small low pressure system, centered over Morocco, was also noticeable (Fig. 2b). This synoptic meteorological situation generated southwestern winds over the Iberian Peninsula.

It should be noted that other authors identified meteorological scenarios dominated by Atlantic depressions between January and June, inducing transport of African dust towards southern and eastern Spain "[15], [16]". Clusters 1 and 2 gathered these scenarios, discriminating between those in which the North African was located over northeastern Algeria and Tunisia (CT-1) or at more eastern locations (CT-2).

The CT-3 centroid showed a strong high pressure system extended over eastern Argelia and Libya in the map of geopotential height at the 850 hPa level. Besides, a strong longitudinal baric gradient

produced by a strong Icelandic low and weak Azores high, which is displaced towards the southwest, caused a clear zonal circulation over the Iberian Peninsula (Fig. 2c). This circulation type was not associated in previous studies with dust transport over the western Mediterranean basin.

The most remarkable feature of the synoptic situation described by the CT-4 centroid, was the development of an intense North African high over northeastern Algeria and Tunisia, advecting warm African air masses onto the Iberian Peninsula from southern and southeastern areas (Fig. 2d). This was the most frequent synoptic meteorological situation causing ADO over eastern and central Spain "[15], [16], [10]".

The most frequent circulation types were CT-4 and CT-2, representing 33% and 31% of the episodic days, respectively. CT-1 accounted for 24% of the episodic days whereas CT-3 grouped the transport regimes less frequently observed. It represented only 12% of the episodic days.

3.2 Identification of potential source areas of dust

CT-1 transported dust from different source areas. On the one hand the low pressure system located southwest of the Iberian Peninsula coast leaded the transport of dust from Western Sahara and southern Morocco towards the western and the central sides of the Iberian Peninsula (Fig. 3a-b). On the other hand, the upper-level high over Northern Algeria promoted the transport of dust from Northeastern Algeria and Tunisia towards the eastern side of the Iberian Peninsula and the Balearic Islands (Fig. 3c-d). This type of transport was predominantly produced in summer and autumn.
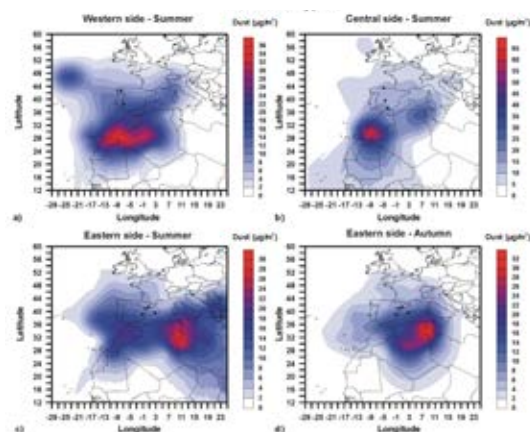
Fig. 3. Redistributed concentration fields (RCF) for African dust contributions ($\mu g/m^3$) during ADO generated by CT-1 over the western, central and eastern sides of the area of study in summer and autumn.

CT-2 transported dust mainly from northern Algeria in spring and summer, towards each of the three zones of study (Fig. 4a-c).
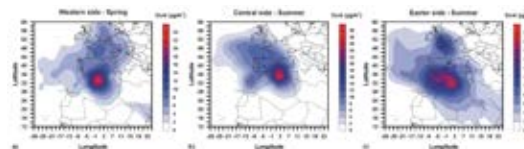
Fig. 4. Redistributed concentration fields (RCF) for African dust contributions ($\mu g/m^3$) during ADO generated by CT-2 over the western, central and eastern sides of the area of study in spring and summer.

The longitudinal baric gradient which characterized CT-3 (Fig. 2-c) promoted an effective transport of dust in spring, from Western Sahara and southern Morocco towards the eastern side of the Iberian Peninsula and the Balearic Islands (Fig. 5a). During winter, the transport of lower concentrations of African dust from regions of northern Morocco, was also detected associated to this circulation type (Fig.5b).
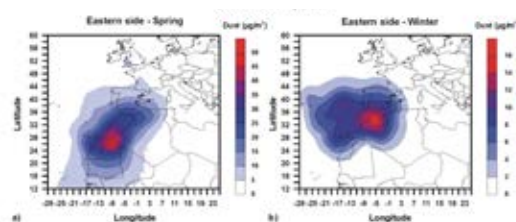
Fig. 5. Redistributed concentration fields (RCF) for African dust contributions ($\mu g/m^3$) during ADO generated by CT-3 over the eastern side of the area of study in spring and winter.
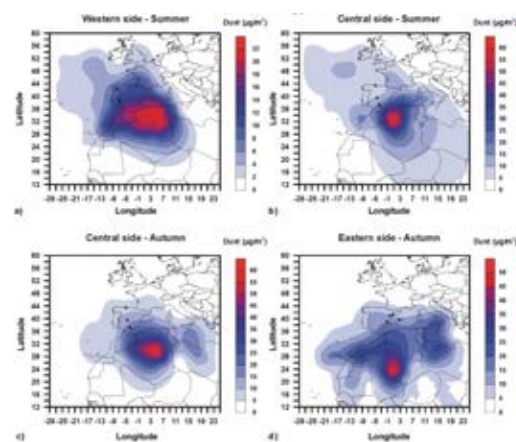
Fig. 6. Redistributed concentration fields (RCF) for African dust contributions ($\mu g/m^3$) during ADO generated by CT-4 over the western, central and eastern sides of the area of study in summer and autumn.

CT-4 generated the transport of dust essentially from Algeria. In summer (Fig. 6a-b) the main sources areas of dust were located over northern Algeria. Finally in autumn, the North African high was displaced on the way to lower latitudes. Consequently the main sources of dust were identified over more southern regions of Algeria. The transport of dust from these source areas was preferably achieved towards the central and the eastern sides of the Iberian Peninsula and the Balearic Islands (Fig. 6c-d).

8 CONCLUSIONS

In this work the occurrence of African Dust Outbreaks (ADO) over the western Mediterranean basin were analyzed on an 11-years period (2001-2011) with the aim to characterize the prevailing atmospheric circulation patterns and the associated dust source areas. Estimations of the values of African Dust contribution in PM_{10} during each event were obtained at 9 regional background sites across the western Mediterranean basin and analyzed together with daily fields of meteorological variables and daily air mass back-trajectories arriving at these sites.

The summer months dominated ADO occurrence (40% of the total number of episodic days produced during the 2001-2011 period), under two prevailing circulation types (CT-1 and CT-4). Their transport mechanisms were composed of two stages. In the first stage, convective injection of dust from source areas was produced by the intense surface heating. In the second stage, transport towards the Iberian Peninsula and the Balearic Islands was produced at the upper levels, being driven by the North African high, alone in the case of the CT-4 or in combination with a relative low pressure system placed west of the Iberian Peninsula coast in the case of the CT-1. ADO produced during the circulation type IV generated the highest impact at southern, eastern and central areas of the Iberian Peninsula and the Balearic Islands. The transport of dust was predominantly produced from northern and southern areas of Algeria in summer and autumn, respectively.

Events generated by CT-1 produced a higher impact at western than eastern areas of the Iberian Peninsula. The transport of dust was produced from Western Sahara and Southern Morocco towards the western and the central sides of the Iberian Peninsula and from northeastern Algeria and Tunisia towards the eastern side of the Iberian Peninsula and the Balearic Islands.

CT-2 and CT-3 were more frequently produced during the spring season. They were characterized by a displacement of the North African high to the east and by a stronger baric gradient than the one obtained in CT-1 and CT-4. South to southwestern winds were the prevailing flows generated by these synoptic situations, transporting dust mainly from northern Algeria in the case of CT-2 and from Western Sahara and Morocco in the case of CT-3. Our results indicated a progressive higher influence of the ADO originated during these circulation types towards the eastern areas of the Iberian Peninsula and the Balearic Islands.

The results obtained in this study demonstrate that the ADO across the western Mediterranean basin were caused by different atmospheric circulation patterns, which condition their intensity and the areas affected by mineral dust. The four main synoptic meteorological situations that generate this type of events were described in this work and the highest potential source areas of mineral dust, associated to each of them, were also characterized. This information can be used as a complementary tool for forecast and analysis of aerosol properties.

REFERENCES

[1] J.M. Prospero, "Long-term measurements of the transport of African mineral dust to the southeastern United States: Implications for regional air quality", *J. Geophys. Res.*, 104(D13), pp. 15917–15927, 1999.

[2] D. Moulin, C.E. Lambert, U. Dayan, V. Masson, M. Ramonet, P. Bousquet, M. Legrand, Y.J. Balkanski, W. Guelle, B. Marticorena, G. Bergametti, and F. Dulac, "Satellite climatology of African dust transport in the Mediterranean atmosphere", *J. Geophys. Res.*, 103(D11), pp. 13137-13144, 1998.

[3] X. Querol, A. Alastuey, J.A. Puicercus, E. Mantilla, J.V. Miró, A. López-Soler, F. Plana, and B. Artíñano, „Seasonal evolution of suspended particles around a large coal-fired power station: particles levels and sources", *Atmos. Environ.*, 32, pp. 1963-1978, 1998.

[4] X. Querol, J. Pey, M. Pandolfi, A. Alastuey, M. Cusack, N. Pérez, N. Moreno, V. Viana, N. Mihalopoulos, G. Kallos, G. and S. Kleanthous, "African dust contributions to mean

ambient PM10 mass-levels across the Mediterranean basin", *Atmos. Environ.*, 43, 4266-4277, 2009.

[5] M. Escudero, X. Querol, A. Ávila and E. Cuevas, "Origin of the exceedances of the European daily PM limit value in regional background áreas of Spain", *Atmos. Environ.* 41, pp. 730-744, 2007.

[6] E. Gerasopoulos, G. Kouvarakis, P. Babasakalis, M. Vrekoussis, J.P. Putaud, and N. Mihalopoulos, "Origin and variability of particulate matter (PM10) mass concentrations over the Eastern Mediterranean", *Atmos. Environ.*, 40, pp. 4679-4690, 2006.

[7] J. Pey, X. Querol, A. Alastuey, F. Forastiere, and M. Stafoggia, "African dust outbreaks over the Mediterranean Basin during 2001-2011: PM10 concentrations, phenomenology and trends, and its relation with synoptic and mesoscale meteorology", *Atmos. Chem. Phys.*, 13, pp. 1395-1410, 2013.

[8] M. Escudero, X. Querol, J. Pey, A. Alastuey, N. Pérez, F. Ferreira, S. Alonso, S. Rodríguez, and E. Cuevas, "A methodology for the quantification of the net African dust load in air quality monitoring networks", *Atmos. Environ.* 41, pp. 5516-5524, 2007.

[9] M. Viana, P. Salvador, B. Artíñano, X. Querol, A. Alastuey, J. Pey, A.J. Latz, M. Cabañas, T. Moreno, S. García, M. Herce, P. Diez, D. Romero, and R. Fernández, "Assessing the performance of methods to detect and quantify African dust in airborne particulates", *Environ. Sci. Technol.*, 44, pp. 8814-8820, 2010.

[10] P. Salvador, B. Artíñano, F. Molero, M. Viana, J. Pey, A. Alastuey, and X. Querol, "African dust contribution to ambient aerosol levels across central Spain: Characterization of long-range transport episodes of desert dust", *Atmos. Res.*, 127, pp. 117-129, 2013.

[11] Commission staff working paper, establishing guidelines for demonstration and subtraction of exceedances attributable to natural sources under the Directive 2008/50/EC on ambient air quality and cleaner air for Europe, Brussels, 15.02.2011. SEC(2011) 208 final, 37 pp: http://ec.europa.eu/environment/air/quality/legislation/pdf/sec_2011_0208.pdf. (last access: 2014), 2011.

[12] R. Huth, "An intercomparison of computer-assisted circulation classification methods", *Int. J. Climatol.* 16, pp. 893–922. 1996.

[13] A. Stohl, "Trajectory statistics-a new method to establish source-receptor relationships of air pollutants and its application to the transport of particulate sulfate in Europe", *Atmos. Environ.*, 30, pp. 579-587, 1996.

[14] R.R. Draxler, and G.D. Rolph, HYSPLIT (HYbrid Single-Particle Lagrangian Integrated Trajectory), [Online]. Silver Spring. MD. Model access via NOAA ARL READY Website: http://www.arl.noaa.gov/ready/hysplit4.html, (last access: 2014), 2003.

[15] M. Escudero, S. Castillo, X. Querol, A. Avila, M. Alarcón, M.M. Viana, A. Alastuey, E. Cuevas, and S. Rodríguez, "Wet and dry African dust episodes over eastern Spain", *J. Geophys. Res.* 110, D18S08. http://dx.doi.org/10.1029/2004JD004731, 2005

[16] S. Rodríguez, X. Querol, A. Alastuey, G. Kallos, and O. Kakaliagou, "Saharan dust contributions to PM10 and TSP levels in Southern and Eastern Spain", *Atmos. Environ.*, 35, pp. 2433-2447, 2001.

Characterization of PMx Data Belonging to the Desert-Dust-Inventory Based on AOD-Alpha RIMA-AERONET Data at Palencia-Autilla Stations

V.E. Cachorro[1], M.A. Burgos[1], Y. Bennouna[1], C. Toledano[1], B. Torres[1], D. Mateos[1], A. Marcos[1], A.M. de Frutos[1]

Abstract — This work analyses PMx data recorded as part of the inventory of desert dust intrusions over north-central Spain during the period 2003-2012, [3]. The inventory is based on the values of the aerosol optical depth (AOD), the alpha Ångström parameter and PM_{10} together with supplementary information, as air masses retro-trajectories, etc…. With the aim of characterising the PMx values for these days, the analysis of the monthly climatology and the interannual variability have been established. The most relevant aspect of this work is the evaluation of desert dust contribution of PMx data to the monthly climatology and the mean annual values for the whole period. The annual cycle of PMx desert contribution shows a clear bimodality (peaked in March and August) giving the characteristic shape for this region. This bimodality of desert contribution is already found for the parameter AOD (440 nm) as demonstrated in the previous work. Regarding the tendency of PMx, it shows the decreasing contribution along the decade with a pronounced minimum in 2009 but a new increase in 2011-2012.

Keywords — Aerosol Optical Depth, Desert Aerosol, EMEP, Particulate Matter

1 INTRODUCCIÓN

Numerosos estudios ponen de manifiesto la influencia sobre el clima que tienen las altas concentraciones de materia particulada (PM) suspendida en el aire así como su relación con diversos efectos nocivos para la salud humana, [1]. La concentración de la materia particulada suspendida en la atmósfera, que viene dada en unidades de masa por unidad de volumen de aire, se utiliza para evaluar los niveles de polución y para establecer los valores umbrales máximos de contaminación impuestos por la Comisión Europea a través de la Directiva 1990/30/EC para la calidad del aire. La concentración de PMx es una de las principales variables a la hora de proponer las políticas medio ambientales en la EU o bien en cada país desde el organismo estatal correspondiente. La caracterización general de los aerosoles atmosféricos como su composición química, la microfísica, la evaluación de los niveles de carga y su evolución espacio-temporal son elementos básicos en la evaluación del impacto de los aerosoles en el cambio climático tal como muestran los informes del IPCC, [2].

Su toxicidad se relaciona con la capacidad de penetración en el sistema respiratorio, ligada al diámetro aerodinámico de las partículas. Distinguimos pues, aquellas partículas que tienen un diámetro inferior a 10 μm, representadas por su concentración másica PM_{10} y aquellas con diámetro menor a 2.5 μm, conocidas como partículas finas y caracterizadas por el $PM_{2.5}$. Podemos evaluar el denominado modo grueso o "coarse" como la diferencia entre las concentraciones másicas anteriores, $PM_{10-2.5}$.

Con el fin de proporcionar información acerca de la concentración, depósito y transporte transfronterizo de los contaminantes atmosféricos, se creó el programa EMEP (European Monitoring and Evaluation Programme), que con la colaboración de científicos y expertos, contribuye a la recolección sistemática de datos así como a su análisis y evaluación.

De entre los tipos de aerosoles atmosféricos, es el aerosol desértico compuesto por partículas de polvo gruesas, el que juega un papel muy importante en el balance radiativo a nivel de atmósfera y de superficie y por tanto su impacto sobre el clima es objeto de un amplio estudio en las últimas décadas. La Península Ibérica debido a la proximidad geográfica con África, está sujeta a frecuentes intrusiones desérticas, donde los desiertos del Sahara y Sahel son las fuentes principales de este aerosol mineral, y por tanto el peso o influencia de los mismos sobre la climatología global de los aerosoles es de la mayor relevancia.

Es por ello que el estudio de los aerosoles sobre la Península Ibérica conlleva la evaluación y caracterización de los aerosoles desérticos. En un trabajo anterior se ha realizado un inventario de las intrusiones desérticas sobre la región de Castilla y León [3], y en el presente estudio se propone la

---

evaluación o influencia de estas intrusiones sobre los niveles de PMx.

Utilizando como base las medidas del radiómetro Cimel de la estación de Palencia (dentro de la red RIMA-AERONET), y los datos de PM_{10}, $PM_{2.5}$ de la estación de Peñausende (Zamora) de la red EMEP, así como información complementaria compuesta por datos de retrotrayectorias, imágenes satelitales, mapas sinópticos y modelos de predicción de aerosoles, se crea el inventario de intrusiones desérticas sobre la región de Castilla y León durante el periodo comprendido entre 2003 y 2012, [3].

En relación a este inventario, se pretende caracterizar de manera detallada el comportamiento de los valores de PMx durante los días con intrusión desértica previamente establecidos, analizando su variabilidad interanual, su climatología y la contribución del aerosol desértico al valor total del PMx.

2 ESTACIÓN DE MEDIDA E INSTRUMENTACIÓN

Los valores de PMx que utilizamos son los que proporciona la estación de EMEP situada en Peñausende (41.24º N, 5.90º O, 985 m.s.n.m.), perteneciente a la provincia de Zamora y dentro de la meseta castellana al noroeste de la Península Ibérica. Aunque dista unos 150 km de Palencia, donde se encuentra la estación de medida de RIMA-AERONET de la que se obtuvieron los datos de AOD-Alfa, ambas estaciones están aisladas de núcleos urbanos o industriales grandes, recogiendo así los valores característicos de fondo regional rural. Para tener mayor precisión a la hora de evaluar un episodios desértico, y saber si entró por el este o por el oeste de la Península, se comprueban los datos de PMx proporcionados por las estaciones de EMEP de Campisábalos (Guadalajara) y Barcarrota (Badajoz),

Los datos de las tres estaciones de EMEP se recogen a través de métodos gravimétricos de medida que siguen los procedimientos establecidos por la DIRECTIVA 2008/50/CE del parlamento europeo y del consejo del 21 de Mayo de 2008 relativa a la calidad del aire ambiente y a una atmósfera más limpia en Europa, desde la cual se establecen tanto los puntos de muestreo como los niveles críticos o los métodos de medición de referencia. La recolección de datos en las estaciones EMEP se realiza con frecuencia diaria.

En relación a las estadísticas anuales de toda la base de datos del periodo 2003-2012 de PMx, que se pueden consultar en [5], destacamos que en promedio para un año, se obtienen datos el 88% de los días, que representan 321 días con datos disponibles por año.

3 METODOLOGÍA

Hemos de recalcar que dicho inventario se ha realizado de forma manual, supervisando visualmente los datos de AOD-alpha y PMx, día a día, así como otros datos suplementarios como retrotrayectorias, datos satelitales, mapas sinópticos, y modelos de predicción de aerosoles. Todo ello nos permitía considerar que un día presentaba intrusión desértica, basado en la definición de unos niveles umbrales de estos 3 parámetros AOD-alpha-PM10 y considerando el origen de las masas de aire. Así por ejemplo si un día (o días) no había datos fotométricos de AOD-alpha pero sí de PMx y estos valores junto con la información complementaria de masas de aire, condiciones sinópticas, etc., indicaban la existencia de una intrusión, este día entraba a formar parte del inventario. Lo mismo ocurría si no había dato de PMx. El valor umbral de PM_{10} considerado es el valor medio de la serie. Ciertamente esta evaluación conlleva una incertidumbre, marcada básicamente por la falta de datos o información, así como por el hecho de contabilizar días completos como pertenecientes o no al inventario.

Para considerar que un día tiene una carga de aerosol en la columna atmosférica correspondiente a un evento desértico, debe presentar valores de AOD superiores a 0.18 y a su vez, los valores de α deben ser menores a 1.0. Los días que cumplen este criterio, presentan una carga de aerosol desértico puro, siendo generalmente los más intensos del episodio o los días centrales del mismo. Sin embargo, podemos encontrar otros días (generalmente al final a al comienzo del episodio) en que los valores de AOD siguen siendo igualmente elevados pero en los que el parámetro α toma valores entre 1.0 y 1.5. En estos casos se considera que el aerosol desértico ha podido sufrir una mezcla con el aerosol local, de tipo continental, o bien el aerosol que llega a la zona de detección, llega ya envejecido y mezclado con otros tipos que ha encontrado a su paso, como ocurre en las típicas recirculaciones de las masas de aire que se dan en verano sobre la Península. En tal caso, se decide clasificar estos días como DC o desértico mezcla, donde se indica que la carga de aerosol desértico no es tan pura como la que aparece en los clasificados como D. Sin embargo aquí se va a considerar el total de días considerados como desérticos, tanto los denominados "puros" como "mezcla" para evaluar y caracterizar los valores de PMx.

Para obtener la contribución del aerosol desértico al valor total de PMx que conforma el ciclo anual o el interanual, será necesario calcular los promedios (mensuales o anuales) de todos los días del periodo de estudio, así como los de todos los días excepto los desérticos. La contribución será, por tanto, la diferencia entre ambas.

4 RESULTADOS Y DISCUSIÓN

4.1 Inventario

Mostramos en la Tabla 1, a modo de resumen, los datos más relevantes del inventario de intrusiones desérticas [3]. Se ha cuantificado para cada año el número de eventos que tuvieron lugar y el número de días que los conforman, el porcentaje que representan respecto al total de días del año y la duración promedio que tuvieron dichas intrusiones. Además, en la Tabla 2 se recogen los valores medios junto con sus desviaciones estándar para los parámetros AOD (440 nm), Alfa (440-870 nm), PM_{10}, $PM_{2.5}$ y Ratio, $PM_{2.5}/PM_{10}$.

El valor medio de PM_{10} de este inventario es de 23.0 $\mu g/m^3$ con una desviación estándar de 11.5 $\mu g/m^3$, mientras que para el $PM_{2.5}$ tenemos 16.5 ± 5.9, lo cual señala una muy alta variabilidad, pues estas desviaciones representan un 50% y un 35.8% respectivamente. Vemos que la variabilidad relativa del $PM_{2.5}$ es mucho menor que la de PM_{10}. La ratio ($PM_{2.5}/PM_{10}$) presenta un valor medio de 0.55, con una desviación estándar de 0.14. Este valor, junto con el del parámetro alfa (0.91), caracteriza el tamaño medio de las partículas de tipo desértico en esta área de estudio.

4.2 Ciclo anual

Se estudia el ciclo anual para cada unas de las concentraciones, PM_{10}, $PM_{2.5}$ y PMcoarse, evaluándose para todos los días del periodo 2003-2012 (ciclo que da la climatología) y para todos los días excepto aquellos considerados como desérticos. A continuación se calculan las diferencias absolutas y relativas entre ambos ciclos anuales para obtener la contribución neta del aerosol desértico. Los resultados se muestran en la Fig. 1., para cada una de las fracciones: PM_{10}, $PM_{2.5}$ y PMcoarse.

En primer lugar, notamos que la curva correspondiente al ciclo anual de PM_{10} donde consideramos todos los días del periodo (barras negras), presenta en una clara bimodalidad con un máximo al final de invierno-principio de primavera (el máximo aparece en Marzo) y en verano (con el máximo en Agosto en el PM_{10}) y mínimos en los meses noviembre-diciembre de forma general. Ello conlleva la aparición de un mínimo local en el mes de Abril. Este mismo comportamiento muestra el $PM_{2.5}$ pero más suavizado, pues Febrero y Marzo presentan valores similares y lo mismo Julio y Agosto, aunque el mínimo de esa bimodalidad sigue apareciendo en Abril. Vemos que para la fracción gruesa se reproduce la misma forma del ciclo anual del PM_{10} pero aún más acentuada.

Todo estos comportamiento se repiten para el ciclo anual de los datos donde se han eliminado los días de desérticos (barras grises). Así pues, este comportamiento bimodal es subyacente o intrínseco a la climatología de esta zona, pero se ve reforzado con el aporte de los aerosoles desérticos, como se pone de manifiesto al observar tanto las diferencias absolutas como las relativas. Este comportamiento general se repite para las otras dos fracciones, $PM_{2.5}$ y $PM_{10-2.5}$, pero con ligeras diferencias porcentuales, como es lógico esperar debido al diferente aporte que los aerosoles desérticos hacen a cada modo o fracción.

La evaluación de estas diferencias absolutas y relativas nos permite por tanto cuantificar la contribución de cada fracción al total de masa.

Estos resultados son análogos a los obtenidos en otros estudios, como el mostrado recientemente en [4], aunque no enfatizan tan claramente esta bimodalidad estacional del aporte de los datos desérticos ni su influencia o modulación en el ciclo anual de la climatología.

Resultados aquí no mostrados sobre estaciones del sur de España, manifiestan una mayor acentuación de esta bimodalidad en el ciclo anual o climatología de los datos totales de la concentración másica, por el mayor aporte de los desérticos en la zona sur de la Península, con un claro gradiente de aumento de norte a sur.

Este patrón de aporte de desérticos ya se encuentra en el estudio anterior [3], donde se evaluaba el ciclo anual de los eventos desérticos pero a partir de los datos de AOD. No queremos hacer aquí una comparativa con el ciclo anual del AOD, [5],[6], que presenta ciertas diferencias con respecto al PM_{10} pues esto queda fuera del objetivo de este artículo.

Tabla 1: Resumen de las principales características del Inventario de intrusiones desérticas

	2003	**2004**	**2005**	**2006**	**2007**	**2008**	**2009**	**2010**	**2011**	**2012**	**Por año**
N. Episodios	19	17	21	20	16	16	14	12	16	16	16.7
N. Días	49	47	46	61	52	35	30	20	32	33	40.5
Porcentaje días, (%)	13.4	12.9	12.6	16.7	14.2	9.6	8.2	5.5	8.8	9.0	11.09
Duración Media (días)	2.6	2.8	2.2	2.8	3.3	2.2	2.1	1.7	2.0	2.1	2.43

Tabla 2: Resumen de los valores medios y las desviaciones estándar de los principales parámetros a estudiar.

	2003	2004	2005	2006	2007	2008	2009	2010	2011	2012	Por año
AOD (440 nm)Medio	**0.32**	**0.34**	0.27	0.26	0.31	0.27	**0.19**	0.32	0.27	0.30	0.29
Sigma AOD (440 nm)	0.11	0.15	0.16	0.10	0.14	0.10	0.05	0.13	0.09	0.10	0.13
Alfa (440–870 nm) Medio	0.96	0.93	0.93	0.80	1.05	0.99	0.84	0.81	0.91	0.77	0.91
Sigma Alfa (440–870 nm)	0.37	0.37	0.41	0.32	0.36	0.46	0.33	0.50	0.37	0.47	0.40
PM_{10} Medio	**27.7**	**28.7**	**28.9**	21.6	18.4	21.9	**16.0**	24.7	20.5	21.6	23.0
Sigma PM_{10}	12.5	31.6	27.6	8.1	11.1	8.9	6.0	25.2	10.6	19.7	11.5
$PM_{2.5}$ Medio	**14.8**	13.9	**14.9**	11.9	9.8	**14.8**	8.3	10.6	8.7	**7.7**	16.1
Sigma $PM_{2.5}$	6.0	8.6	11.1	3.5	4.1	5.5	4.5	9.2	3.1	3.3	5.9
Ratio Medio	0.57	0.58	0.58	0.58	0.59	**0.70**	0.51	0.48	0.47	**0.45**	0.55
Sigma Ratio	0.14	0.16	0.15	0.14	0.13	0.15	0.11	0.09	0.14	0.17	0.14

4.3 Variabilidad interanual

Mostramos en la Fig. 2 la variabilidad interanual para el PM_{10}, $PM_{2.5}$ y PMcoarse. De nuevo indicamos en cada gráfica el valor promedio para todos los días y para todos los días exceptuando los desérticos. Como muestra la Fig 2., el año con valores más altos de concentración de PM_{10} y $PM_{2.5}$ fue el 2004, seguido de 2003 y 2005, y con los mínimos valores promedio de éste parámetro el 2010 (2012 para el $PM_{2.5}$).

Los años con mayor aporte de desérticos al valor absoluto de PM_{10} se reparten casi por igual en los años 2003 al 2006 según la Fig. 2 aunque la tabla 2 nos dice que este es 2006. Por otro lado, la ratio de la tabla 2 nos indica que el año que presenta aerosoles desérticos de mayor tamaño medio fue 2012 y el que menor 2008. Vemos que este año 2012 que presenta un aerosol desértico más puro (las partículas prevalentes son mas gruesas y su ratio es menor), no necesariamente corresponde con el año de intrusiones más intensas o de mayor número. Vemos que tenemos muchos elementos a cuantificar en un inventario de este tipo.

Sin embargo, la contribución relativa del mayor aporte del desértico al total la presentan los años 2006 para el PM_{10} y $PM_{2.5}$. La contribución porcentual del modo grueso es algo diferente, ya que es el año 2004 el que presenta el máximo, seguido por 2003 y después ya aparece 2006.

En cuanto a las tendencias que se observan en estos 10 años, tenemos un decrecimiento de los valores totales de las concentraciones de estas dos fracciones, PM_{10} y $PM_{2.5}$, pero el modo grueso no da un decrecimiento significativo con un claro mínimo en 2008. Su contribución relativa de desérticos al aporte total es minima en 2009 y máxima en 2004.
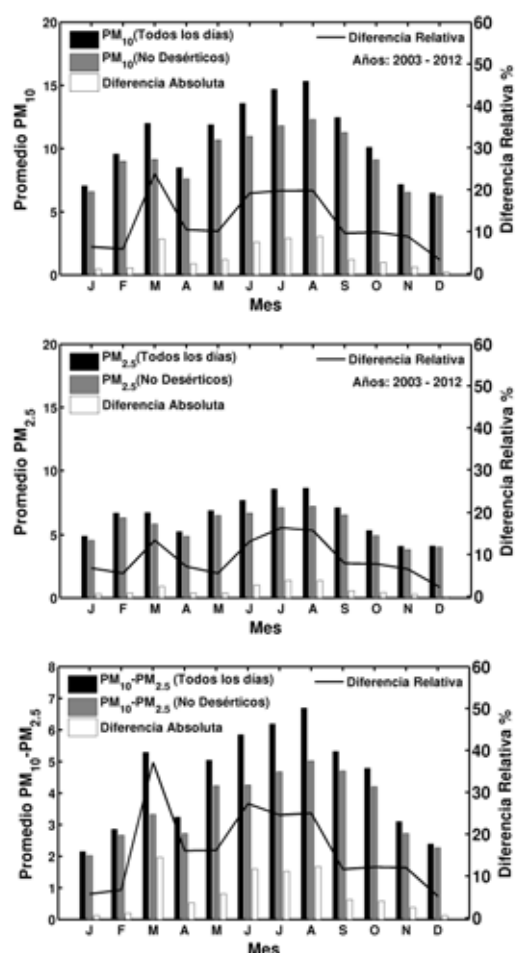
Fig.1: Ciclo anual del peso o contribución del PMx desértico sobre el PMx total.

5 CONCLUSIONES

En este estudio, se han analizado los datos de PMx de los días con intrusión desértica en el centro norte de la Península correspondientes al periodo 2003-2012. Se encuentra que en el ciclo anual durante este periodo de estudio, el aporte de
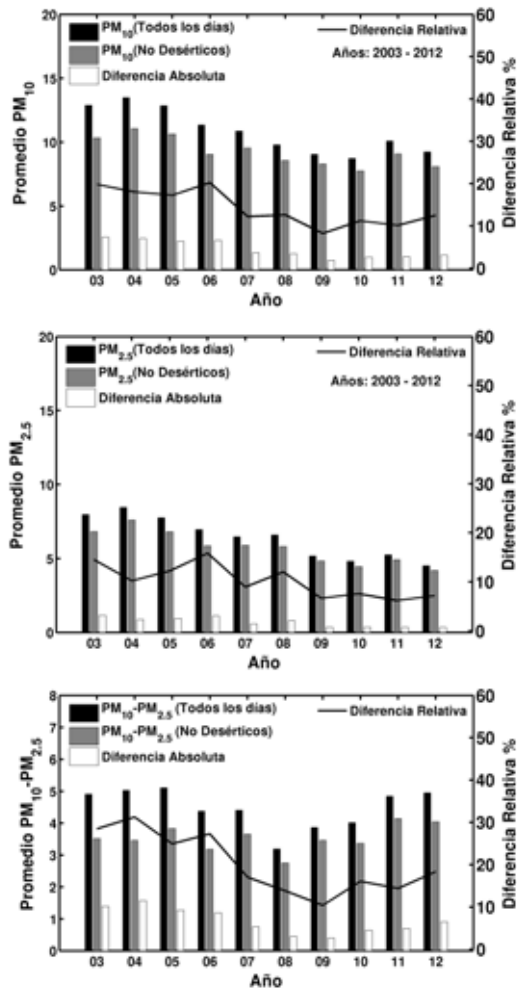
Fig.2: Variación interanual del peso o contribución del PMx desértico sobre el PMx total.

los aerosoles desérticos presenta una bimodalidad con un máximo en Marzo y otro Agosto y un mínimo en Abril. Esta aportación modula el ciclo anual de la climatología general, reforzándola, ya que el ciclo subyacente (climatología descontando desérticos) ya presenta esta bimodalidad. Dada la variabilidad interanual en cuanto a los valores medios de PMx de este aporte de desérticos, los máximos en la climatología pueden aparecer en otros meses diferentes del año, es decir, el máximo de agosto puede aparecer en julio o en septiembre.

Es evidente que una climatología de los aerosoles atmosféricos, en este caso a través de los valores PMx, precisa un mayor número de años para su establecimiento, pero los datos existentes parecen ya mostrar una forma del ciclo anual bien definida, corroborada por la cantidad y calidad de estos datos.

Finalmente, en relación a las medias anuales de los valores de PMx, la tendencia muestra un decrecimiento a lo largo de este periodo de estudio para los valores medios de PM_{10} y $PM_{2.5}$. En cuanto a los aportes o contribución de los aerosoles desérticos, se muestra también una tendencia decreciente en las fracciones fina y total, pero no en la fracción gruesa.

AGRADECIMIENTOS

REFERENCIAS

[1] Pope, C.A., Dockery D.W., 2006. "Health effects of fine particulate air pollution: lines that connect". A journal of the Air & Waste Management Association 56, 709-742.

[2] IPCC, 2007: Cambio climático 2007: Informe de síntesis. Contribución de los Grupos de trabajo I, II y III al Cuarto Informe de evaluación del Grupo Intergubernamental de Expertos sobre el Cambio Climático [Equipo de redacción principal: Pachauri, R.K. y Reisinger, A. (directores de la publicación)]. IPCC, Ginebra, Suiza, 104 págs.

[3] Cachorro, V.E., Burgos, M.A., Bennouna, Y., Toledano, C., Torres, B., Herguedas, A., González Orcajo, J., de Frutos, A.M., "Inventory of desert dust aerosols in the región of Castilla y León (2003-2012)" 1st Iberian Meeting on Aerosol Science and Technology (RICTA 2013), Evora, Portugal, 1-3 July 2013.

[4] Pey, J., Querol, X., Alastuey, A., Forastiere, F., Stafoggia, M. 2013. "African dust outbreaks over the Mediterranean Basin during 2001-2011: PM_{10} concentrations, phenomenology and trends, and its relation with synoptic and mesoscale meteorology" Atmospheric Chemistry and Physics, 13, 1395-1410.

[5] Bennouna, Y.S., Cachorro, V.E., Burgos, M.A., Toledano, C., Herguedas, A., González Orcajo, J., de Frutos, A.M., "The relations between AOD and PMx from long-term data for north-central Spain". 1st Iberian Meeting on Aerosol Science and Technology (RICTA 2013), Evora, Portugal, 1-3 July 2013.

[6] Bennouna, Y.S., Cachorro, V.E., Burgos, M.A., Toledano, C., Torres, B., de Frutos, A.M., "Relationships between columnar aerosol optical properties and Surface Particulate Matter observations in north-central Spain from long-term records (2003-2011)". AMTD

Comparison between simulated and measured solar irradiance during a desert dust episode

M.A. Obregón[1], V. Salgueiro[2], M.J. Costa[3], S. Pereira[4], A. Serrano[5], A.M. Silva[6]

Abstract — The aim of this study is to analyze the reliability of the libRadtran v. 1.7model in the estimation of irradiance in the shortwave spectral range (285-2800 nm) during a desert dust episode. For that purpose downward irradiance measurements at the surface and corresponding model simulations have been compared during the three days of a desert dust event (9-11 August 2012) observed over Évora, Portugal. The comparison between measured and simulated values shows a highly significant correlation, with a correlation coefficient of 0.999 and a slope very close to unity (0.998±0.006), supporting the validity of the model in the estimation of global irradiance in the shortwave spectral range. Relative differences between the simulated and measured irradiances have also been calculated and indicated that the libRadtran model slightly underestimates the experimental global irradiance, with a mean relative difference equal to 1.28 %. These small differences could be associated with the experimental errors of the measurements, as well as with uncertainties in the input values given to the model, namely those related with the actual aerosol properties. The notably good agreement between simulated and measured irradiances guarantees that the libRadtran model can be used to estimate clear sky irradiance when no radiation measurements are available during desert dust events. In order to obtain accurate estimations of the irradiance, the model must be fed with reliable values of the aerosol properties.

Keywords — libRadtran model, AERONET, desert dust, Évora

1 INTRODUCTION

It is well known the interest for accurately quantifying the effects of atmospheric aerosols on the energy balance of the Earth-atmosphere system. Their role involves the attenuation of solar radiation through scattering and absorption processes, and also the modulation of terrestrial radiation by scattering, absorbing and emitting such radiation. Atmospheric aerosols also indirectly affect the radiation balance by influencing the cloud formation and the modification of their properties. According to the Intergovernmental Panel on Climate Change

————————————————

1. M.A. Obregón is with the *Geophysics Centre of Évora, University of Évora. Rua Romao Ramalho, 59, 7000 Évora. Portugal* E-mail: nines@unex.es
2. V. Salgueiro is with the *Geophysics Centre of Évora, University of Évora. Rua Romao Ramalho, 59, 7000 Évora. Portugal* E-mail: vsalgueiro@uevora.pt
3. M.J. Costa is with the *Geophysics Centre of Évora and Physics Dep., University of Évora. Rua Romao Ramalho, 59, 7000 Évora. Portugal* E-mail: mjcosta@uevora.pt
4. S. Pereira is with the *Geophysics Centre of Évora, University of Évora. Rua Romao Ramalho, 59, 7000 Évora. Portuga.l* E-mail: sergiopereira@uevora.pt
5. *A.Serrano is with the Department of Physics, University of Extremadura. Avda. De Elvas, s/n, 06006 Badajoz. Spain.* E-mail: asp@unex.es
6. A.M.Silva is with the *Geophysics Centre of Évora, University of Évora. Rua Romao Ramalho, 59, 7000 Évora. Portugall* E-mail: asilva@uevora.pt

2013, the total aerosol radiative forcing is estimated to be -0.9 [-1.9 to -0.1] W m^{-2} [1]. Although the global cooling effect due to the aerosols is now relatively well established, some uncertainties still remain. Accurate and reliable measurements and analyses are demanded to reduce those uncertainties.

Due to the uncertainties that exist about the aerosol effects, it is of great interest to identify different aerosol types and analyze their effects in the radiative balance of the Climate System. An aerosol type which plays an important role in this radiation balance is the desert dust [2]. The study of the effects of this aerosol type in the Iberian Peninsula has a great interest due to its proximity to the Sahara Desert. Desert dust events in the Iberian Peninsula are associated to certain synoptic situations [3, 4, 5] and show a typical seasonal pattern [6, 7] due to the annual latitudinal displacement of the general atmospheric circulation.

Estimations of irradiance provided by reliable radiative transfer codes are of great interest in order to analyze the aerosol effects in the radiative balance of the Climate System. Therefore, the aim of this work is to validate the libRadtran model [8] by simulating the global irradiance in the shortwave spectral range during a desert dust event over Évora station, Portugal. This work is organized as follows:

a brief description of the study region and instrumentation is presented in section 2; data set and methodology are provided in section 3; results are discussed in section 4. Finally, conclusions are given in section 5.

2 STUDY REGION AND INSTRUMENTATION

The location of Évora radiometric station is shown in Figure 1. It is installed in the Geophysics Center Observatory in Évora, whose geographical coordinates are: 38.6º N, 7.9º W, 293.0 m.a.s.l. This station is located near the center of a small town with about 60000 inhabitants, about 100 km eastward from the Atlantic west coast. Évora is influenced by different aerosol types, namely urban as well as mineral and forest fire aerosol particles [9 - 14].

Figure 1. Iberian Peninsula showing the location of Évora station.

Évora station is managed by the Geophysics Centre of Évora, at the University of Évora (Portugal). This station is equipped with an Eppley Black & White pyranometer and CIMEL CE-318 sunphotometers, among several other radiometric instruments. An Eppley Black & White pyranometer measures the global shortwave irradiance (285-2800nm), providing 10 minutes averages of 10 seconds sampling time. The uncertainty associated with this instrument is estimated to be about 5% encompassing calibration, temperature and cosine characteristics of the radiometer. The CIMEL CE-318 sunphotometer is integrated in the NASA AERONET (Aerosol Robotic NETwork) network [15], make direct sun measurements with a 1.2º full field of view at 340, 380, 440, 500, 675, 870, 940 and 1020 nm. In addition, measurements of sky radiances in the almucantar and principal planes geometries, at 440, 675, 870 and 1020 nm, are also performed by this instrument. More details about this instrument are given by Holben et al. [15]. The parameters obtained from Cimel sunphotomers and used in this

study are aerosol optical depths (τ), Ångström α exponent (440-870) (α), single scattering albedo (ω), asymmetry factor (g) and precipitable water vapor column (PWC). These parameters have been used as input to the radiative transfer model for simulating the irradiance in the shortwave spectral range and to identify the desert dust event.

3 DATASET AND METHODOLOGY

In this study the reliability of the libRadtran model [8] for simulating the irradiance in the shortwave spectral range during a desert dust event has been analysed. This was done through the comparison between hourly averaged values of the measured downward irradiance at the surface and the corresponding model simulations. Previously, the desert dust episode over Évora station has been identified. For this purpose, we have analyzed two aerosol quantities: aerosol optical depth at 500 nm (τ_{500}) and Ångström α exponent (440-870) (α).

Version 1.7 of the libRadtran is used in this study with inputs of aerosol, total ozone, and precipitable water vapor columns and surface albedo data. Hourly average values of the aerosol properties obtained from AERONET measurements were used as input to the simulations. Total ozone column was provided by the Ozone Monitoring Instrument (OMI). Daily values were used which were downloaded from http://avdc.gsfc.nasa.gov/index.php?site=83016510 9. The surface albedo data have been obtained from the Surface and Atmospheric Radiation Budget (SARB) working group, part of NASA Langley Research Center's Clouds and the Earth's Radiant Energy System (CERES) mission (http://snowdog.larc.nasa.gov/surf/pages/lat_lon.ht ml). Other variables taken into account in setting up the model are the following: extraterrestrial irradiance values (obtained from Gueymard [16]), profiles of temperature, air density, ozone and other atmospheric gases (taken from the midlatitude summer/winter standard atmospheres) and the radiative equation solver (the discrete ordinate method of Stamnes et al. [17], DISORT2 calculated with 16 streams, was used). Hourly simulations of shortwave global irradiance at the surface level (285-2800 nm) were then performed during this event.

In addition, radiation was measured by an Eppley pyranometer installed at the Évora Geophysics Center Observatory in Évora. Only cloud-free measurements corresponding to solar zenith angle lower than 80º have been considered in this study.

4 RESULTS AND DISCUSSION

The aim of this section is to analyze the reliability of the libRadtran model [8] in the simulation of irradiances in the shortwave spectral range (285-2800 nm) during a desert dust event. Figure 2 shows the time evolution of $\tau 500$ and α during the Saharan dust episode which was detected between 9 and 11 August 2012. From 8 to 9 August an increase in τ from about 0.10 to 0.45 was observed and maximum turbidity was further observed in the day after with τ close to 0.45. A simultaneous decrease in α down to about 0.2 indicates the coarse mode predominance in the aerosol population that perturbed the atmospheric aerosol at Évora.

Figure 3 shows the comparison between hourly-averaged downward irradiance measurements and simulated values. Measured and simulated values show a highly significant correlation; with a correlation coefficient of 0.999 and a slope very close to unity (0.998±0.006). These values clearly support the validity of the model in the simulation of irradiances in the shortwave spectral range. This behaviour is also seen in Figure 4, where the temporal evolution of the hourly averaged measurements and corresponding model simulations are shown.
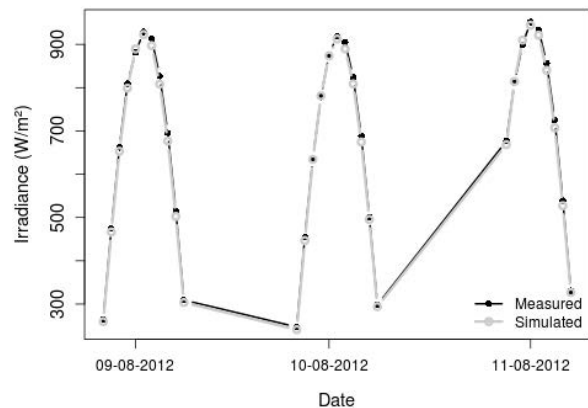
Figure 4. Evolution of hourly averaged measurements of downward irradiance at the surface and corresponding model simulations during the desert dust event (9-11/08/2012).

Figure 2. Evolution of $\tau 500$ nm and α during the time period 8-12/08/2012 which includes the desert dust event (9-11/08).

Figure 5 shows relative differences between the hourly-averaged downward irradiance measurements and simulated values for the desert dust episode. The libRadtran model slightly underestimates the experimental global irradiance with most of the differences between 0 and 3 %, indicating the reliability of the radiative transfer model used in this work. The mean value of these relative differences is 1.28%. These small differences could be associated with experimental errors in the measurements as well as with uncertainties in the input values given to the model, namely those related with the actual aerosol properties.

Figure 3. Comparison of simulated SW irradiances with the corresponding measurements. The thin dashed line represents the zero bias line (1:1 slope) and the solid line represents the regression line. The regression equation and correlation coefficient are also included.
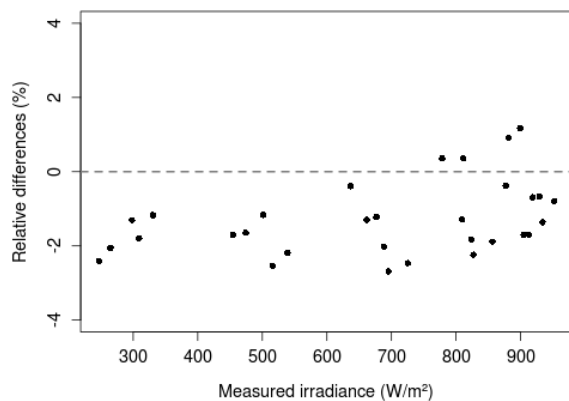
Figure 5. Relative differences between hourly averaged measurements of downward irradiance at the surface and corresponding model simulations.

The notably good agreement between simulated and measured irradiances guarantees that the libRadtran model can be used to estimate irradiance when no radiation measurements are available during desert dust outbreaks. In order to obtain accurate estimations of the irradiance, the model must be fed with reliable values of the aerosol properties.

5 CONCLUSIONS

This study contributes to the analysis of aerosol effects in the radiative balance of the Climate System through the estimation of downward irradiance, at the surface, in the shortwave spectral range, with libRadtran model. The reliability of this model has been validated by the comparison between simulated and measured values observed over Évora during a desert dust event. A correlation coefficient of 0.999 and a slope very close to unity (0.998±0.006) were obtained. Relative differences between the simulated and measured irradiances, with respect to the measured values, also confirm the reliability of the model, with most of the differences between 0 and 3 % (mean relative difference equal to 1.28 %). Therefore, the libRadtran model can be used to estimate the irradiance when no radiation measurements are available during desert dust events. For that purpose, the model must be fed with reliable values of the aerosol properties. These estimations may be used in future works to calculate aerosol radiative forcing values of this aerosol type and analyze their effects in the radiative balance of the Climate System.

REFERENCES

[1] O. Boucher, D. Randall, P. Artaxo, C. Bretherton, G. Feingold, P. Forster, V.-M. Kerminen, Y. Kondo, H. Liao, U. Lohmann, P. Rasch, S.K. Satheesh, S. Sherwood, B. Stevens and X.Y. Zhang, " Clouds and Aerosols. In: Climate Change 2013: The Physical Science Basis. Contribution of Working Group I to the Fifth Assessment Report of the Intergovernmental Panel on Climate Change [Stocker, T.F., D. Qin, G.-K. Plattner, M. Tignor, S.K. Allen, J. Boschung, A. Nauels, Y. Xia, V. Bex and P.M. Midgley (eds.)]". Cambridge University Press, Cambridge, United Kingdom and New York, NY, USA, 2013.

[2] R. Arimoto, "Eolian dust and climate: relationship to sources, tropospheric chemistry, transport and deposition", Earth Sci. Rev., vol.54, pp.29-42, 2001.

[3] S. Rodriguez, X. Querol, A. Alastuey, G. Kallos, and O. Kakaliagou, "Saharan dust contributions to PM10 and TSP levels in Southern and Eastern Spain", Atmos. Environ., vol.35, pp.2433–2447, 2001.

[4] X. Querol, S. Rodriguez, E. Cuevas, M.M. Viana, and A Alastuey, "Intrusiones de masas de aire africano sobre la Península Ibérica y Canarias: mecanismos de transporte y variación estacional", 3rd Asamblea Hispano portuguesa de Geodesia y Geofísica, Inst. Nac. de Meteorol. Esp., Valencia, 2002.

[5] M. Escudero, S. Castillo, X. Querol, A. Avila, M. Alarcón, M.M. Viana, A. Alastuey, E. Cuevas, and S. Rodríguez, "Wet and dry African dust episodes over eastern Spain", J. Geophys. Res., vol.110, D18S08, doi:1029/2004JD004731, 2005.

[6] V.E. Cachorro, C. Toledano, A.M. de Frutos, M. Sorribas, J.M. Vilaplana, and B. de la Morena, "Aerosol characterization at El Arenosillo (Huelva, Spain) with an AERONET/PHOTONS CIMEL sunphotometer", Geophys. Res. Abstract, vol. 7(08559), 2005.

[7]   C. Toledano, "Climatología de los aerosoles mediante la caracterización de propiedades ópticas y masas de aire en la estación El Arenosillo de la red AERONET". PhD thesis, Universidad de Valladolid, Spain, 2005.

[8]   B. Mayer, and A. Kylling, "Technical note: The libRadtran software package for radiative transfer calculations – description and examples of use", Atmos. Chem.Phys., vol.5, pp. 1855–1877, 2005.

[9]   S. Pereira, A.M. Silva, T. Elias, and F. Wagner, "Aerosol monitoring at Cabo da Roca site", paper presented at 4º Simpósio de Meteorologia e Geofísica da APMG/6º Encontro Luso-Espanhol de Meteorologia, Sesimbra, Portugal, 2005.

[10] S. Pereira, F. Wagner, and A.M. Silva, "Scattering properties and mass concentration of local and long-range transported aerosols over the South Western Iberia Peninsula". Atmos. Environ., vol. 42 (33), pp. 7623-7631, 2008, http://dx.doi.org/10.1016/j.atmosenv.2008.06.008.

[11] S. Pereira, F. Wagner, and A.M. Silva, "Seven years of measurements of aerosol scattering properties, near the surface, in the south-western Iberia Peninsula". Atmos. Chem. Phys., vol.11, pp.17-29, 2011. http://dx.doi.org/10.5194/acp-11-17-2011.

[12] T. Elias, A.M. Silva, N. Belo, S. Pereira, P. Formenti, G. Helas, and F. Wagner, "Aerosol extinction in a remote continental region of the Iberian Peninsula during summer". J. Geophys. Res. 111 (D14204), 1-20, 2006. http://dx.doi.org/10.1029/2005JD006610.

[13] A.M. Silva, F. Wagner, S. Pereira, and T. Elias, "Aerosol properties at the most western point of continental Europe", paper presented at International Aerosol Conference, Minnesota, USA, 2006.

[14] M.A. Obregón, S. Pereira, F. Wagner, A. Serrano, M.L. Cancillo, and A.M. Silva, "Regional differences of column aerosol parameters in western Iberian Peninsula" , Atmos. Environ., vol 12, pp.1–10, 2012, doi:10.1016/j.atmosenv.2012.08.016.

[15] B. Holben, T.F. Eck, I. Slutsker, D. Tanre, J. Buis, K. Setzer, E. Vermote, J. Reagan, Y. Kaufman, T. Nakajima, F. Lavenu, I. Jankowiak, and A. Smirnov, "AERONET-A Federated Instrument Network and Data Archive for Aerosol Characterization". Remote Sens. Environ.,vol. 66, pp.1–16,1998.

[16] C. Gueymard, "The sun's total and spectral irradiance for solar energy applications and solar radiation models", Sol. Energy, vol.76, pp.423-453, 2004.

[17] K. Stamnes, S.C. Tsay, W. Wiscombe, and I. Laszlo, "DISORT, a General-Purpose Fortran Program for Discrete-Ordinate-Method Radiative Transfer in Scattering and Emitting Layered Media: Documentation of Methodology", Tech. rep. Dept. of Physics and Engineering Physics, Stevens Institute of Technology, Hoboken, NJ 07030, 2000.

Discrimination between Aerosol and Cloud Contributions to Global Solar Radiation Trends between 2003 and 2010 in North-Central Spain

D. Mateos[1], A.Sanchez-Lorenzo[2], V.E. Cachorro[1], M. Antón[3], C. Toledano[1], J. Calbó[2]

Abstract — Aerosols and clouds are the main factors involved in the determination of the energy balance of the planetary system. Surface solar radiation trends observed during the last decades have evidenced a progressive increase, i.e., a substantial reduction in the radiative effects at the surface of the cloud-aerosol system. However the separate contributions of aerosols and clouds to these trends are not well analyzed yet. The main aim of this study is to evaluate the radiative effects of three systems separately: cloud and aerosols (CARE), clouds (CRE), and aerosols (ARE). Specifically, the temporal trends are determined by using monthly measurements of global solar radiation at Valladolid (Spain) site together with simulations from a radiative transfer code. Surface solar irradiance in Valladolid has increased +1.4 W m-2 per year (period 2003-2010). CARE, CRE, and ARE trends have shown the following rates (with a significance level over 95%): +1.3, +0.8, and +0.4 W m^{-2} per year, respectively. Overall, clouds and aerosols have contributed around 2/3 and 1/3 to the solar radiation increase at the study site between 2003 and 2010, respectively. CERES-EBAF-Surface collection corroborates the SW radiation trend and the CRE estimations obatined at Valladolid site.

Keywords — shortwave radiation trend; brightening period; cloud and aerosol radiative effects

1 INTRODUCTION

The temporal trends of surface solar radiation in the shortwave range (SW) have been investigated in the last years since their key role played on the Earth's radiative budget [1]. This latter variable is modulated by the radiative effects of atmospheric components like clouds and aerosols [2].

The separate contribution of clouds and aerosols to the SW trends is a topic of controversy. Some studies reported that aerosols seem to play a major role on the SW trends, while other stated that aerosols alone cannot explain all the SW changes [3],[4]. Hence, the main aim of this study is to provide separately the radiative effects of cloud, aerosol, and cloud-aerosol systems. In a recent article, Mateos et al. [5] described a methodology to obtain the radiative effects for the cloud-aerosol system as a whole. This methodology is expanded in the current study including experimental data of SW radiation, aerosol observations, and simulations from a radiative transfer code. In this way, it can be applied at a large number of stations worldwide.

_____

1. Grupo de Óptica Atmosférica, Facultad de Ciencias, Universidad de Valladolid, Paseo Belén 7, 47011, Valladolid, Spain. E-mail: mateos@goa.uva.es
2. Group of Environmental Physics, University of Girona, Girona, Spain
3. AIRE Research Group, Department of Physics, University of Extremadura, Badajoz, Spain

A period with a notable increase in the SW radiation levels was observed in the Iberian Peninsula since the early 2000s [6],[7]. We applied our method to discriminate between clouds and aerosols effect in this recent brightening period.

2 DATABASE AND METHODS

2.1 Database

The SW radiation measurements at the Valladolid (41.65ºN, 4.77ºW, 735 m a.s.l.) site were provided by the Spanish Meteorological Agency (AEMET). All the procedures about the calibration, quality control, and homogenization of the data series were published in detail by Sanchez-Lorenzo et al. [6]. The monthly aerosol properties are obtained from the close Palencia-AERONET (Aerosol Robotic Network) station. To obtain reliable data of the aerosol optical depth (AOD) and Ångström coefficient α, level 2.0 is only used in this study [8].

In addition to the ground-based data, the Clouds and the Earth's Radiant Energy System (CERES) EBAF-Surface data set (Ed2.7) was downloaded at the CERES ordering tool (http://ceres.larc.nasa.gov/) [9]. Two products of this collection are used in 1º x 1º grid resolution: surface SW radiation (SW_{CERES}), and surface shortwave cloud radiative effect (CRE_{CERES}).

Other required data, such as total ozone column, water vapor, and surface albedo (alb_{sur}) are considered (from ERA-Interim and MERRA reanalysis collections) with the same procedures described by Mateos et al. [5].

2.2 Methods

All the data mentioned above are used as input for the libRadtran radiative transfer model v1.7. We performed simulations of the monthly SW in the period 2003-2010 under two different conditions: clear atmosphere (cloud-free + aerosol-free), SW_{clear}; and cloud-free atmosphere, SW_{CF}.

The experimental radiative effects of the cloud-aerosol, cloud, and aerosol systems are obtained following Ramanathan et al. [10], using the experimental ground-based data, SW_{exp}:

$$CARE_{exp} = (1 - alb_{sur}) (SW_{exp} - SW_{clear}) \quad (1)$$

$$CRE_{exp} = (1 - alb_{sur}) (SW_{exp} - SW_{CF}) \quad (2)$$

$$ARE_{exp} = (1 - alb_{sur}) (SW_{CF} - SW_{clear}) \quad (3)$$

Thus, the experimental CRE (CRE_{exp}) can be compared against CERES CRE data (CRE_{CERES}).

The temporal trend of SW_{exp}, $CARE_{exp}$, CRE_{exp}, and ARE_{exp} are evaluated with the Sen's slope method, evaluating their significance with the Mann-Kendall test. The monthly anomalies are also evaluated to minimize the impact of the annual cycle from these calculations. The anomaly is the difference between the monthly data and the evaluated monthly mean for the whole time period (2003-2010).

3 BRIGHTENING PERIOD IN VALLADOLID (2003-2010)

Fig.1 shows the monthly evolution of global SW irradiance between 2003 and 2010 in Valladolid site using ground-based and CERES data. There is a high agreement between both time series. Additionally, the temporal trend rates are also in agreement. Specifically, the SW_{exp} exhibits a temporal trend rate of +1.4 Wm^{-2} per year (p value = 0.01, 95% confidence interval [4.4, 26.3]), while SW_{CERES} presents a rate of +1.2 Wm^{-2} per year (p value = 0.06, 95% confidence interval [1.3, 21.4]). These rates imply a notable increase over 12 W m^{-2} during the last decade. This strong brightening was already reported by, e.g., Bilbao et al. [7] in the period 2001-2010 with an increase of 0.75% per year. In relative changes, our trends are about 0.8% per year, which is in line with the previous study in the same station but with different time period and methodology.
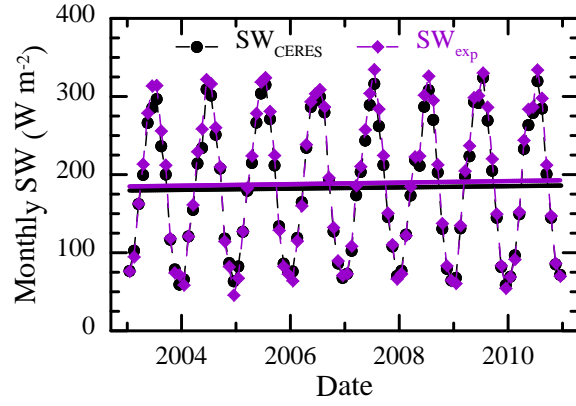
Fig 1. Monthly SW evolution using ground-based (SW_{exp}, diamonds) and CERES (SW_{CERES}, circles) data. Solid thick lines show the Sen's slope estimates.

4 RADIATIVE EFFECTS OF CLOUD, AEROSOL, AND CLOUD-AEROSOL SYSTEMS

Fig. 2 shows the monthly $CARE_{exp}$, CRE_{exp}, and ARE_{exp} in Valladolid for the period 2003-2010. The largest absolute value for the radiative effects of the cloud-aerosol system is achieved in May-2008 with a value around -100 Wm^{-2}. In this month, the contribution of ARE is small, and this large reduction of the SW radiation levels is due to clouds. Values of $CARE_{exp}$ over -70 Wm^{-2} are also observed in April-2007, and for this particular month the contribution of ARE_{exp} to the total $CARE_{exp}$ is around 20%.
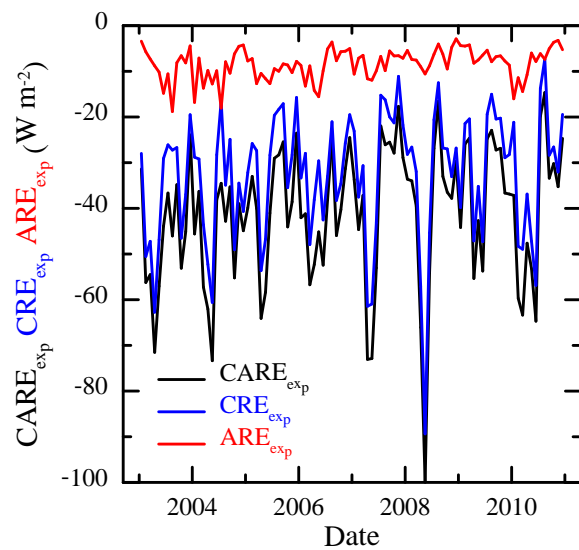
Fig 2. Monthly $CARE_{exp}$, CRE_{exp}, and ARE_{exp} values in Valladolid between 2003 and 2010.

The largest ARE_{exp} occur in August-2003 explaining more than 40% of the all effect caused by the cloud-aerosol system. Overall, CRE_{exp} values are higher than ARE_{exp}, presenting the former variable values between -10 and -50 Wm^{-2}, while the latter has a range between 0 and -20 Wm^{-2}.

Table 1 presents the temporal trends for the three variables in Valladolid between 2003 and 2010. Overall, the reduction of the cloud-aerosol radiative effects is in line with the previous brightening observed in Fig. 1.

Table 1. Summary of the temporal trends (Wm^{-2} per year) obtained in this study.

	$CARE_{exp}$	CRE_{exp}	ARE_{exp}
Trend rate	+1.3	+0.8	+0.4
p value	0.006	0.07	0.01
confidence interval	[4.0,21.1]	[-0.1,16.3]	[1.3,6.1]

The contribution of clouds can explain around 2/3 of the total trend, while aerosols explain the other 1/3. The trend for the ARE_{exp} shown in Table 1 (+0.4 Wm^{-2} per year) is in line with the cloud-free radiation increase obtained by previous studies [1],[3]. Therefore, the decreases of the cloud and aerosol radiative effects lead to the strong brightening period observed in the central area of the Iberian Peninsula in the 2000s.

5   COMPARISON BETWEEN CRE_{EXP} AND CRE_{CERES}

The good agreement observed in Sect. 3 between SW_{exp} and SW_{CERES} is also tested for the CRE values derived from experimental and CERES data. Table 2 summarizes the results of this comparison. There is a high correlation between both data series with a correlation coefficient over 0.9. Although some differences occur in the CRE values (e.g., root-mean-square-error of 9.2 Wm^{-2}), the linear fit points out a notable agreement. Nevertheless, the simulations of radiative fluxes under cloud-free sky in the CERES EBAF-Surface-Ed2.7 collection can have caused some problems due to a change in the aerosol data used [9]. Overall, the obtained results confirm the high agreement between CRE_{CERES} and CRE_{exp}.

Table 2. Statistics of the comparison CRE_{exp} vs CRE_{CERES}. Methods following Willmott [11].

	Value
Number of data	120
Mean CRE_{exp}	-32.2 Wm^{-2}
Mean CRE_{CERES}	-38.8 Wm^{-2}
mean-bias-error	6.6 Wm^{-2}
mean-bias-absolute-error	7.6 Wm^{-2}
root-mean-square-error	9.2 Wm^{-2}
index of agreement	0.91
correlation coefficient	0.91
slope (linear fit)	0.87
intercept (linear fit)	1.57

6   CONCLUSIONS

Monthly values of SW radiation in Valladolid (Central Spain) in the period 2003-2010 and simulations from a radiative transfer code are employed to evaluate the radiative effects of the cloud, aerosol, and cloud-aerosol systems. The experimental findings are corroborated against CERES EBAF-Surface-Ed2.7 collection. SW radiation exhibits an increase trend of +1.4 (SW_{exp}) and +1.2 (SW_{CERES}) Wm^{-2} per year. This increase is in line with the obtained temporal trend for $CARE_{exp}$ (+1.3 Wm-2 per year). The contributions to this trend can be defined as 2/3 due to clouds and the other 1/3 is explained by aerosols. In general, CRE_{exp} is larger than ARE_{exp}. The largest values of these two variables are -90 (May 2008) and -19 Wm^{-2} (August 2003), respectively. There is a good agreement between CERES-EBAF-Surface-Ed2.7 and the experimental results for both the SW radiation (values and trends) and the CRE estimations.

REFERENCES

[1] Wild, M. (2009), Global dimming and brightening: a review, J. Geophys. Res. 114, D00D16. http://dx.doi.org/10.1029/2008JD011470.

[2] Kim, D., and V. Ramanathan (2008), Solar radiation budget and radiative forcing due to aerosols and clouds, J. Geophys. Res., 113, D02203, doi:10.1029/2007JD008434.

[3] Ruckstuhl, C., et al. (2008), Aerosol and cloud effects on solar brightening and the recent rapid warming, Geophys. Res. Lett., 35, L12708, doi:10.1029/2008GL034228.

[4] Long, C. N., E. G. Dutton, J. A. Augustine, W. Wiscombe, M. Wild, S. A. McFarlane, and C. J. Flynn (2009), Significant decadal brightening of downwelling shortwave in the continental United States, J. Geophys. Res., 114, D00D06, doi:10.1029/2008JD011263

[5] Mateos, D., M. Antón, A. Sanchez-Lorenzo, J. Calbó, and M. Wild (2013), Long-term changes in the radiative effects of aerosols and clouds in a mid-latitude region (1985–2010), Global Planet. Change, 111, 288-295, http://dx.doi.org/10.1016/j.gloplacha.2013.10.004.

[6] Sanchez-Lorenzo, A., J. Calbó, and M. Wild (2013), Global and diffuse solar radiation in Spain: Building a homogeneous dataset and assessing trends, Global Planet. Change, 100, 343-352, http://dx.doi.org/10.1016/j.gloplacha.2012.11.010.

[7] Bilbao, J., R. Roman, A. de Miguel, and D. Mateos (2011), Long-term solar erythemal UV irradiance data reconstruction in Spain using a semiempirical method, J. Geophys. Res., 116, D22211, doi:10.1029/2011JD015836.

[8] Toledano, C., V.E. Cachorro, A. Berjon, A.M. de Frutos, M. Sorribas, B. de la Morena, and P. Goloub (2007), Aerosol optical depth and Ångström exponent climatology at El Arenosillo AERONET site (Huelva, Spain), Q. J. R. Meterol. Soc., 133, 795-807.

[9] Kato S, Loeb NG, Rose FG, Doelling DR, Rutan DA, Caldwell TE, Yu LS, Weller RA (2013) Surface irradiances consistent with CERES-derived top-of-atmosphere shortwave and longwave irradiances. J. Clim., 26(9), 2719-2740. doi: 10.1175/Jcli-D-12-00436.

[10] Ramanathan, V., R.D. Cess, E.F. Harrison, P. Minnis, B.R. Barkstrom, E. Ahmad, D. Hartmann (1989), Cloud-Radiative Forcing and Climate: Results from the Earth Radiation Budget Experiment, Science, 243(4887), 57–63.

[11] Willmott, C. J. (1982), Some Comments on the Evaluation of Model Performance, Bull. Am. Meteorol. Soc., 63, 1309–1313.

Gas and particle phase chemical composition of marine emissions from Mediterranean seawaters: results from a mesocosm study

Pey J.[1], DeWitt H.L.[1], Temime-Roussel B.[1], Même A.[2], Charriere B.[3,4], Sempere R.[3], Delmont A.[3], Mas S.[5], Parin D.[6], Rose C.[6], Schwier A.[6], R'mili B.[2], Sellegri K.[6], D'Anna B.[2], Marchand N.[1]

Abstract — Marine emissions are among the largest sources of secondary organic aerosols (SOA) globally. Whereas physical processes control the primary production of marine aerosols, biological activity is responsible for most of the organic components, both aerosol and gas-phase, released from marine sources and potentially transformed into SOA when exposed to atmospheric oxidants.

As part of the Source of marine Aerosol particles in the Mediterranean atmosphere (SAM) project, a mesocosm study was conducted at the Oceanographic and Marine Station STARESO (Corsica) in May 2013. During these experiments, 3 mesocosms were deployed, filled with 2260 L of bay water and covered with a transparent Teflon dome. To observe the effect of biological activity on volatile organic compounds (VOCs) and aerosol emissions, two of the mesocosms were enriched with different levels of nitrate and phosphate respecting Redfield ratio (N:P = 16) and one was left unchanged to be used as a control. Physical and chemical properties of mesocosms and ambient atmospheres were followed during 20 days by using a high resolution real-time instruments. Aerosol size and concentration were measured by a Scanning Mobility Particle Sizer; gas-phase composition of VOCs was determined by using Proton Transfer Reaction Time-of-Flight Mass Spectrometer; and aerosol chemical composition was obtained from High Resolution Time-of-Flight Aerosol Mass Spectrometer. In parallel, numerous additional measurements were conducted to fully characterize the water within each of the enclosed mesocosms, including water temperature, pH, conductivity, chemical and biological analyses, fluorescence of chlorophyll-a, and dissolved oxygen concentration. Incident light within the mesocosms was also measured.

Preliminary results suggest new particle formation processes linked to iodine chemistry. Aerosol composition inside the mesocosms was slightly enriched in organic aerosols with respect to the outside atmosphere. Oxygenated organic compounds were the most important species in terms of mass concentration, but amine-related aerosol mass peaks varied the greatest in concentration between the mesocosms. Finally, a clear enhancement of VOCs occurred in the enriched mesocosms.

Keywords — Atmosphere; on-line chemical characterization; semi-controlled environment; organic compounds

1 INTRODUCTION

Oceans cover approximately 70% of the Earth surface and are in permanent interaction with the atmosphere via heat and momentum exchange, as part of the water cycle, and by a variety of physical and chemical processes in which gases and particles play a role.

Marine aerosols are the largest natural source of atmospheric particles at the global scale, contributing to the Earth's radiative budget. The composition of marine aerosol may influence cooling or warming at the top of the atmosphere, depending on the optical properties of these compounds, which remains so far uncertain [1]. The knowledge of the particle composition, as function of size, is necessary for understanding and predicting the marine aerosol properties relevant to climate, for example, their ability to act as cloud condensation nuclei (CCN) and to influence cloud droplet concentration [2]. In addition, marine aerosols take part of several biogeochemical cycles [3], and of course they have to be considered from air quality perspectives [4, 5].

Despite the importance of marine aerosols, our ability to correctly describe and simulate their phenomenology is still limited, and the mechanisms yielding marine aerosol formation and/or air-sea exchanges are still unclear. This lack of knowledge is even more accentuated in the Mediterranean region.

1. *Aix Marseille Université, CNRS, LCE FRE 3416, 13331 Marseille, France (jorge.pey@univ-amu.fr)*
2. *Université Lyon 1, CNRS, UMR5256, IRCELYON, Institut de Recherches sur la Catalyse et l'Environnement de Lyon, 69626 Villeurbanne, France*
3. *Aix Marseille Université, Université du Sud Toulon-Var, CNRS/INSU, UMR7294, IRD, MIO, UM110, 13288, Marseille, Cedex 09, France*
4. *University Perpignan Via Domitia, CEntre de Formation et de Recherche sur les Environnements Méditerranéens, UMR5110, 66860, Perpignan, France*
5. *Université de Montpellier 2 CC 093, UMR 5119, CNRS-UM2-IRD-IFREMER-UM1 ECOSYM, 34095 Montpellier, France*
6. *Laboratoire de Météorologie Physique, CNRS-Université Blaise Pascal, Observatoire de Physique du Globe, Aubière, France*

Up to date, detailed size segregated chemical characterization of North Atlantic Ocean [6, 7] and Artic Sea and Southeast Pacific Ocean [8] marine aerosols have been performed. However, marine aerosols over the Mediterranean Sea might be significantly different to those from cleaner oceans. It is well known that the phytoplankton activity over the Mediterranean Sea is lower than over cooler oceans. In addition, the Mediterranean Sea is a semi-closed environment subjected to a deep anthropogenic pressure in terms of water and atmospheric pollution.

Primary marine aerosol production results from wind stress at the ocean surface which gives rise to the mechanical production of sea-spray aerosol, which is traditionally assumed to be mainly composed by sea salt and water. Secondary marine aerosol production occurs via condensation of gas phase species onto themselves (nucleation) or onto pre-existing particles. Among secondary marine aerosols, sulphate species are considered as dominant. However, a number of relatively recent investigations point out to other species, such as iodine and organic compounds, as possible aerosol precursors over certain regions and/or environments [7, 9, 10].

Different observations in clean marine environments suggest a direct link between the concentration of primary and secondary aerosol components and the oceanic biological activity, with marked seasonal differences. It seems that the organic fraction of such marine aerosols may be linked to phytoplankton activity.

Since sea-surface water composition is expected to highly influence the formation of both marine primary organic aerosol (POA) and secondary organic aerosol (SOA), recent findings on marine aerosol relative to a cleaner and cooler regions as North Atlantic or Artic cannot directly be applied to a more polluted, salty and warm Sea. There is therefore an urgent need to better characterize organic primary and secondary marine aerosols in the Mediterranean Sea, characterized by a lower biological activity.

The SAM project (Sources of marine Aerosol particles in the Mediterranean atmosphere), funded by the Research French Agency (ANR, *Agence Nationale de la Recherche*) aims at addressing the issue of primary and secondary marine aerosol in the Western Mediterranean Sea, as a function of the biochemical composition of the sea water. The project combines laboratory and mesocosm studies using real sea-water samples. In this work we focus on the results obtained in the mesocosm study.

2 METHODS

2.1 The field campaign: a mesocosm study

In May 2013, an intensive field campaign was conducted at the Oceanographic and Marine Station STARESO (Corsica).

During the experiment, three mesocosms were deployed in the bay-water, filled with 2260 L of autochthon water and covered with a transparent Teflon dome (Fig. 1). Two of the mesocosms (B and C) were enriched with different levels of nitrate and phosphate respecting Redfield ratio (N:P = 16) and one was left unchanged to be used as a control (A).

Water and air characteristics of the mesocosms were followed during 15 consecutive days. The emerged part of the mesocosms (the atmosphere, around 1 m^3) received a constant flow of filtered natural air (16 l/min), and was equipped with a single inlet for atmospheric sampling. The immerged part of the mesocosms were equipped with a pack of optical and physicochemical sensors: water temperature, conductivity, pH, incident light, fluorescence of chlorophyll a, and dissolved oxygen concentration.
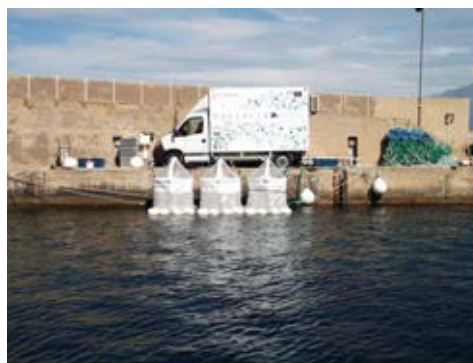
Fig. 1. View of the mesocosms and the mobile van (MASSALYA, http://lce.univ-amu.fr/massalya.html) in which the instruments were placed.

2.2 The instrumental set-up for atmospheric monitoring

During the campaign were used a set of high-resolution instruments for gas and particle physic-chemical characterization (Fig. 2). Every day, the following routine was repeated a couple of times from around 09:00h to 20:00h local time: the first 20 minutes of sampling in the ambient atmosphere, the next 20 minutes in mesocosm-A (the control one), and the subsequent 60 minutes in mesocosm-B or C (one of each was controlled every day).

SMPS (Scanning Mobility Particle Sizer). Particle number and size distribution of fine and ultrafine particles were determined by using this instrument, constituted by a condensation particle counter coupled to a differential mobility analyser. The SMPS allowed the measurement of aerosols between 10 and 600 nm, every 2.5 minutes.

HR-ToF-AMS (High Resolution Time-of-Flight Aerosol Mass Spectrometer). It allowed us to measure the real-time non-refractory chemical composition and mass loading of aerosols with aerodynamic diameters between 70 and 1000 nm as a function of particle size. In practice, organic species, NO_3^-, SO_4^{2-}, NH_4^+ and chloride are detected, but mineral matter, and black carbon are not [11]. This instrument provided us data every 3 minutes.

PTR-ToF-MS (Proton Transfer Reaction Time-of-Flight Mass Spectrometer). This instrument is devoted to the quantification of a wide spectra of volatile organic compounds (VOCs), both primary compounds (such as isoprene, monoterpenes, benzene, xylenes, DMS) and secondary gaseous products such as methacrolein, glyoxal, methylvinylketone. The detection limit reaches few parts per trillion, with a mass resolution of more than 4000 (m/Δm). The time resolution fixed for this instrument was 2 minutes. During the campaign, H_3O^+ and O_2^+ ionization modes were automatically alternated every 10 minutes.
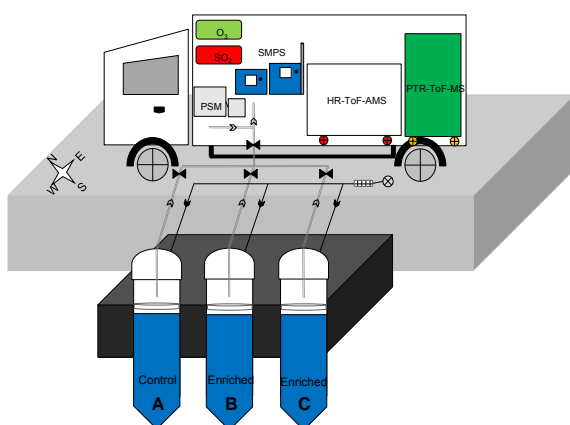
Fig. 2. Schematic view of the experimental design.

In parallel, water samples were taken every day in order to perform detailed laboratory analyses (through bubble bursting experiments) on POA characterization and CCN properties of marine aerosols. Furthermore, different aliquots were taken every day from each mesocosm to characterize the amount and type of different biological populations.

3 RESULTS

3.1 Particle number concentration and size distribution

The atmosphere inside the mesocosms, even somewhat isolated from the ambient atmosphere, displayed strong similarities in terms of particle concentrations and size with respect to that (Fig. 3). However, some interesting events were observed in the control mesocosm (A), and more sporadically in the enriched mesocosms (B and C). In mesocosm-A, the concentrations of ultrafine particles exceeded those measured outside during five consecutive days as a results of new-particle formation processes. Two of these events were high-intensity episodes, with daily average concentrations 10 to 20 times higher than in the natural atmosphere. This phenomenon was also observed in the enriched mesocosms, although the intensity was substantially lower.
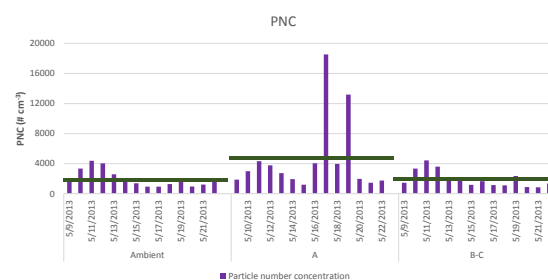
Fig. 3. Daily averages of particle number concentration (PNC, in #/cm^3) in the ambient air, in mesocosm-A, and in mesocosm B/C. Green lines denote the average concentration at each environment during the campaign.

3.2 Drivers of new-particle formation processes

The use of HR-ToF-AMS and PTR-ToF-MS instruments during the campaign has allowed us to explore the chemical drivers of these nucleation processes. Thus, we have found that iodine species are clearly the compounds leading for such phenomenon (Fig. 4). As seen in these figure, iodine species were significantly enhanced in the mesocosms with respect to their abundance in the surrounding atmosphere, and they were much more abundant in mesocosm-A than in B-C. As seen in Fig. 4, the correlation between particle number concentration and iodine species (especially I$^+$) is fairly good. However, there was found another factor to fully explain the occurrence of this phenomenon. Such new-particle formation processes were clearly induced by photochemical reactions, as they occurred essentially during sunny days.

Obviously, the HR-ToF-AMS is unable to analyse the composition of nucleation mode particles. Thus, such iodine germens are thought to coagulate with pre-existing particles.
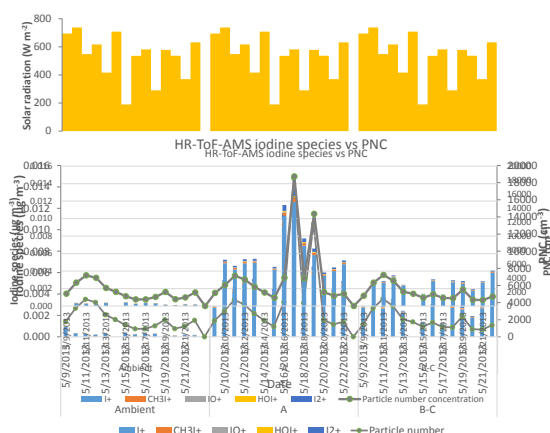
Fig. 4. Daily averages of iodine species (in µg/m^3), particle number concentration (PNC, in #/cm^3), and solar radiation (in W/m^2).

The occurrence of new particle formation processes driven by iodine chemistry was previously documented over certain coastal areas in Atlantic and Pacific regions [9, 10]. In such previous studies the iodine abundance in the atmosphere was linked to the presence of macro algae. In our case, the observation of this singularity was unexpected, being the iodine sources unclear up to date.

3.3 Biological bloom: atmospheric signatures

One of the objectives of our experiment was to study the chemical signatures of oceanic blooms in Mediterranean environments.

It was expected that the enrichment of two of the mesocosms with nitrogen and phosphate would create a bloom. This point was corroborated in situ as progressively the water and the mesocosm walls turned to greener colours. In addition, the concentrations of Chlorophyll-a confirmed the occurrence of the biological blooms in mesocosm B and C (Fig. 5).
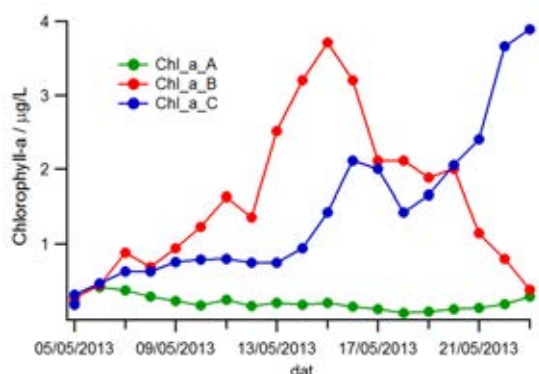
Fig. 5. Evolution of Chlorophyll-a (in µg/l) in mesocosms A, B, and C

A complementary proxy to evaluate the biological activity in the mesocosms was the quantification of the dissolved organic carbon (DOC). Whereas

bloom impacts in Chlorophyll-a concentrations were evident during a relatively short period, DOC concentrations continuously augmented during and after the blooms (Fig. 6).
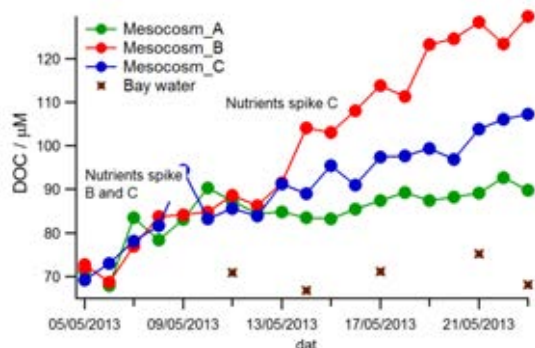
Fig. 6. Evolution of dissolved organic carbon (in µM) in mesocosms A, B, and C, and in bay-water.

It is expected that biological activity might affect the composition of the organic fraction of the gas and the aerosol phase. In Fig. 7 it has been plotted the daily concentration of HR-organics in ambient, and mesocosms A, B and C. It is evident that the concentration of organic species found at all the environments is governed by ambient concentrations. However, organic compounds (as bulk) appeared always enhanced in the mesocosms, with no significant differences between the different mesocosms. Our results indicate that there is not a direct connection between Chlorophyll-a concentrations in the seawater and the organic aerosol observed in the sea-air interface.
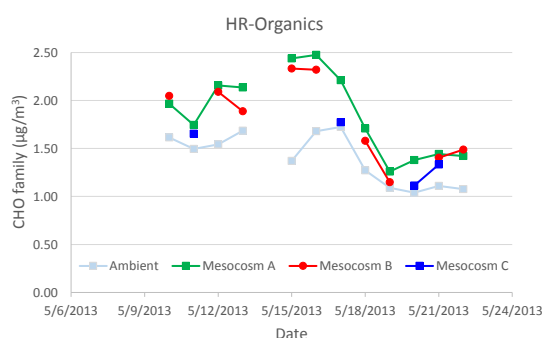
Fig. 7. Evolution of organic aerosols (µg/m3) in ambient air and in mesocosms A, B, C.

When investigating the specific evolution over time of certain organic aerosol families, it becomes clear that CH and CHO families were always higher in the mesocosms than in the ambient atmosphere (Fig. 8). However, it was not obvious a clear enhancement during the blooms nor in the course of the campaign as was evident in the concentration of DOC.
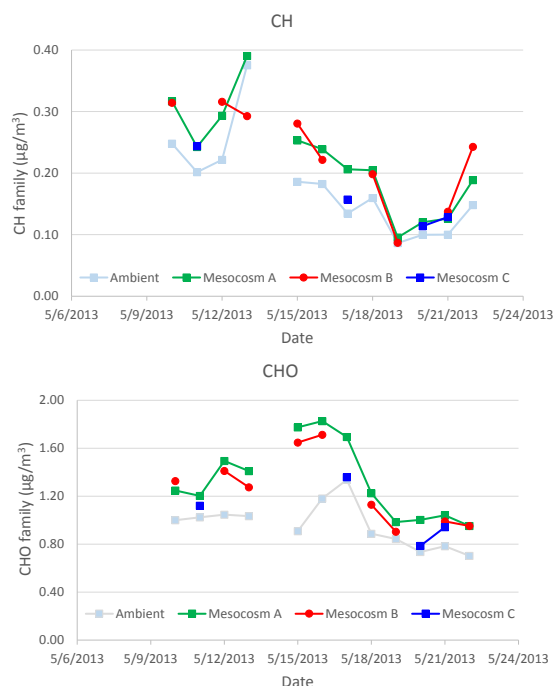
Fig. 8. Evolution of CH (top) and CHO (bottom) aerosol families (µg/m^3) in ambient air and in mesocosms A, B, C.

The only organic aerosol family clearly enhanced inside the enriched mesocosms was the CHN (Fig. 9). This group of organic compounds are essentially amines that could be directly related with different biological processes occurring in the mesocosms.
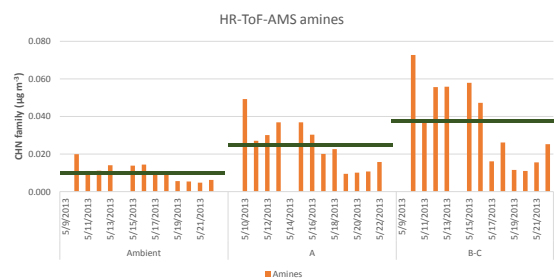
Fig. 9. Daily averages of CHN species (in µg/m^3) in ambient air and in mesocosms A, B, C. Green lines denote the average concentration at each environment during the campaign.

During the campaign we used a PTR-ToF-MS to determine the concentrations of VOCs. In order to simplify the presentation of the results we have grouped the VOCs in different families, as seen in in Fig. 10. Among these main families, ethanol and methanol were the main alcohols; acetic and formic acids were the most abundant acids; the alkane/alkene group was mainly driven by m/z 55.039; formaldehyde, acetaldehyde and acetone dominated the carbonyls group. Other groups of VOCs such as N containing, S containing, highly reactive unsaturated hydrocarbons and aromatics were found in very low abundances.
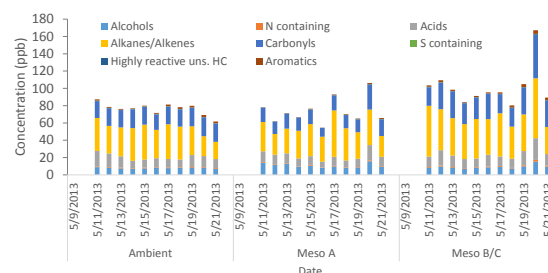
Fig. 10. Daily averages of VOCs (in ppbv) in ambient air and in mesocosms A, B, C.

In this Fig. 10 it becomes patent that VOC concentrations were higher in mesocosms B and C than in mesocosm-A, or in the ambient atmosphere. In order to visualize better this issue, we have subtracted the ambient VOC concentrations to those determined in mesocosm B/C (Fig. 11). In this plot it is patent that three periods of enhanced VOC concentrations were observed during the campaign, being the most intense at the end. Two of these peak periods were recorded under the maximum of the biological blooms around the 15th and 21st May 2013. The other VOCs episode was recorded on 11-13th May, during a severe windy period. It has been noted that windy conditions may facilitate the release of VOC species as two of the three VOC peak periods were observed under windy (and sea-altered) conditions.
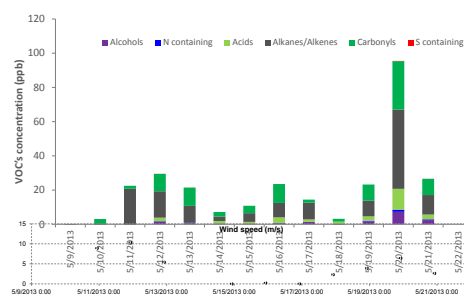
Fig. 11. Daily averages (ambient subtracted) of VOC families (in ppbv) in mesocosms B/C in relation with wind speed (m/s).

4 CONCLUSIONS

-Our preliminary results reveal that at the sea-air interface (inside the mesocosms dome), new particle formation is observed and seems to occur in the presence of iodine species (AMS analysis) in the presence of sunlight.

-There is not a direct connection between the concentration of Chlorophyll-a and the amount of organic aerosols. However, amine species were clearly enhanced in the mesocosms, especially in the enriched ones.

-VOCs emissions increased inside the enriched

mesocosms, most probably linked to biologic activity. Windy periods, which favour water mixing, may enhance the emission of VOCs stored in the water column.

REFERENCES

[1] Randles C.A., Russell L.M., Ramaswamy V. (2004). Hygroscopic and optical properties of organic sea salt aerosol and consequences for climate forcing. *Geophys. Res. Lett.*, *31*(16).

[2] Rinaldi M., Decesari S., Finessi E., Giulianelli L., Carbone C., Fuzzi S., O'Dowd C.D., Ceburnis D., Facchini M. C. (2010). Primary and Secondary Organic Marine Aerosol and Oceanic Biological Activity: Recent Results and New Perspectives for Future Studies. Advances in Meteorology Volume 2010, Article ID 310682, 10 pages.

[3] O'Dowd C.D., De Leeuw G. (2007). Marine aerosol production: a review of the current knowledge. Philos. Trans. R. Soc. London, A, 365(1856), 1753-1774.

[4] Knipping E.M., Dabdub D. (2003). Impact of chlorine emissions from sea-salt aerosol on coastal urban ozone. Environmental Science & Technology, 37(2), 275-284.

[5] Viana M., Pey J., Querol X., Alastuey A., de Leeuw F., Lükewille A. (2014). Natural sources of atmospheric aerosols influencing air quality across Europe. Science of the Total Environment 472, 825-833.

[6] Cavalli F., Facchini M.C., Decesari S., Mircea M., Emblico L., Fuzzi S., Ceburnis D., Yoon Y.J., O'Dowd C.D., Putaud J.P., Dell'Acqua A. (2004). Advances in characterization of size-resolved organic matter in marine aerosol over the North Atlantic, J. Geo. Res. Atmos., 109(D24).

[7] O'Dowd C.D., Facchini M.C., Cavalli F., Ceburnis D., Mircea M., Decesari S., Fuzzi S., Yoon Y.J., Putaud J.P. (2004). Biogenically driven organic contribution to marine aerosol. Nature, 431(7009), 676-680.

[8] Russell L.M., Hawkins L.N., Frossard A.A., Quinn P.K., Bates T.S. (2010). Carbohydrate-like composition of submicron atmospheric particles and their production from ocean bubble bursting. Proc. Natl. Acad. Sci. U. S. A., 107(15), 6652-6657.

[9] Jimenez J.L., Bahreini R., Cocker D.R., Zhuang H., Varutbangkul V., Flagan R.C., Seinfeld J.H., O'Dowd C.D., Hoffmann T. (2003). New particle formation from photooxidation of diiodomethane (CH2I2). J. Geo. Res. Atmos., 108(D10), 25.

[10] O'Dowd C.D., Jimenez J.L., Bahreini R., Flagan R.C., Seinfeld J.H., Hameri K., Pirjola L., Kulmala M., Jennings S.G., Hoffmann T. (2002). Marine aerosol formation from biogenic iodine emissions. Nature, 417(6889), 632-636.

[11] DeCarlo P.F., Kimmel J.R., Trimborn A., Northway M.J., Jayne J.T., Aiken A.C., Gonin M., Fuhrer K., Horvath T., Docherty K.S., Worsnop D.R., Jimenez J.L. (2006). Field-deployable, high-resolution, time-of-flight aerosol mass spectrometer. Analytical Chemistry, 78, 8281-8289.

Ground-based atmospheric monitoring in Mallorca and Corsica in summer 2013 in the context of ChArMEx: results on number-size distributions, on-line and off-line aerosol chemistry, and volatile organic compounds

Pey J.[1], Cerro J.C.[2,3], Hellebust S.[1], DeWitt H.L.[1], Temime-Roussel B.[1], Elser M.[4], Pérez N.[5], Sylvestre A.[1], Salameh D.[1], Mocnik G.[6], Prévôt A.S.H.[4], Zhang Y.L.[7], Szidat S.[7], Marchand N.[1]

Abstract — As part of the Chemistry-Aerosol Mediterranean Experiment (ChArMEx), simultaneous field campaigns were conducted in the summer of 2013 in several Mediterranean observatories. Among these observatories, Ersa-Corsica site had the most complete set of instrumentation and was where most of the scientific effort was concentrated. In addition to participating in the Ersa supersite, the Laboratoire the Chimie de L'Environnement, in collaboration with the University of the Balearic Islands, installed a complementary observatory in Mallorca (Spain) in the Spanish Ministry of Defense facilities "Cap Es Pinar". A number of European institutions were involved in the campaign. Overall, a complete instrumentation set-up to measure the aerosol and gas-phase chemical and physical properties and concentrations in Mallorca was deployed: a HR-ToF-AMS to measure the real-time non-refractory chemical composition and mass loading of aerosols with aerodynamic diameters between 70 and 1000 nm (e.g., sulfate, nitrate, ammonium, chloride and organic compounds); a PTR-ToF-MS to quantify a wide spectral range of volatile organic compounds (VOCs), including primary species such as isoprene, monoterpenes, benzene, xylene and DMS, and secondary products such as methacrolein, glyoxal, methylvinylketone; a SMPS to obtain particle number and size distribution of aerosols in the range 14-650 nm; a LAAPTOF to characterize in real time individual particles in terms of size and chemical composition; a 7 length-wave aethalometer to monitor the absorption coefficients of < 1000nm aerosols; two high-volume samplers for subsequent chemical determinations, including off-line 14C analysis, of the PM_{10} and PM_1 fractions; a mobile van with air quality surveillance instruments (e.g., CO, CO_2, NO_x); and a meteorological tower.

During the campaign, wide-scale atmospheric episodes were observed at both Mallorca and Corsica, including Saharan dust outbreaks, new-particle formation events and regional accumulation of pollutants. Different air mass sources and meteorology were found to influence Mallorca and Corsica. In particular, more Saharan dust episodes and persistent accumulation processes were observed in Mallorca, while outflows from the Po valley were observed at times in Corsica. Thus, the general atmospheric characteristics of the Mediterranean basin as well as region-specific aerosol episodes were able to be differentiated and characterized by the comparison of these two sampling sites and conclusions about factors influencing anthropogenic aerosol concentrations in the Mediterranean can be drawn.

Keywords — Western Mediterranean; on-line monitoring; regional conditions; nucleation; accumulation

1. *Aix-Marseille Université, CNRS, LCE FRE 3416, 13331 Marseille, France (jorge.pey@univ-amu.fr).*
2. *University of the Balearic Islands, 07122 Palma de Mallorca, Spain*
3. *Department of Agriculture, Environment and Territory, Balearic Islands Government, 07009 Palma de Mallorca, Spain*
4. *Laboratory of Atmospheric Chemistry, Paul Scherrer Institute, 5232 Villigen, Switzerland*
5. *Institute of Environmental Assessment and Water Research CSIC, 08034 Barcelona, Spain*
6. *Aerosol d.o.o., 100 Ljubljana, Slovenia*
7. *Department of Chemistry and Biochemistry, University of Bern, 3012 Bern, Switzerland*

1 Introduction

Despite vast efforts in recent years to understand the origin, formation mechanisms and effects of atmospheric aerosols (on health, ecosystems and climate, among others), and regardless of new strategies developed to reduce their concentration in the atmosphere, the Mediterranean atmosphere still contains high loadings of atmospheric aerosols

during the warm season. Such elevated concentrations of atmospheric aerosols are mostly driven by mineral dust (in part from natural sources), sulphate (mostly anthropogenic) and organic compounds (with multi-source origin). While the sources of mineral dust and sulphate are fairly well-characterized [1, 2], the origin of the organic aerosol is not fully understood, although it has been found that the organic carbon is mostly from contemporary (non-fossil) sources. Such gaps of knowledge are partially linked to the aerosol phenomenology complexity. Specifically, 1/ several aerosol sources release constantly or sporadically particles and/or their precursors to the atmosphere; 2/ these inputs may enclose hundreds of chemicals, most of them extremely reactive in the atmosphere; 3/ the emitted and/or the new-formed particles display various sizes, and they evolve during their lifetime; 4/ the meteorology play a key role in the atmospheric physic and chemical processes, to such an extent that the emissions from a single source may result in dissimilar particle compositions under contrasted meteorological conditions.

With respect to other European regions, Mediterranean countries are exposed to higher emissions from road dust and construction activities [3], they suffer regularly the incursion of Saharan dusty air masses [4], they receive higher loadings of shipping-related emissions [5], and punctually they may be affected by biomass burning and industrial aerosols [6, 7]. Indeed, over the western part of the Mediterranean, such aerosol complexity is incremented during the warm season as the recirculation of air masses at a regional scale becomes recurrent [8], creating multi-layers of pollution [9] and enhancing the magnitude of aging processes [10].

With this in mind, a vast atmospheric monitoring mission was developed in summer 2013, mostly in the western part of the Mediterranean. As part of ChArMEx, simultaneous field campaigns were conducted in the summer of 2013 in different Mediterranean observatories. Among these observatories, the Ersa-Corsica site had the most complete set of instrumentation and was where most of the scientific effort was concentrated. In addition to participating in the Ersa supersite, the Laboratoire the Chimie de L'Environnement (LCE), in collaboration with the University of the Balearic Islands, installed a complementary observatory in Mallorca (Spain) in the Spanish Ministry of Defense facilities "Cap Es Pinar".

2   METHODS

2.1   The sites: Es Pinar (Mallorca) and Ersa (Corsica)

In summer 2013 different field campaigns to study the Mediterranean atmosphere took place. In this

work, some of the measurements carried out in Es Pinar-Mallorca (EPM) and Ersa-Corsica (ErC) are presented (Fig. 1). Both observatories were installed in the northern side of each island.

Fig. 1. Location of Mallorca and Corsica, with indication of the position of EPM and ErC sites (orange points). Image elaborated with Google maps.

The EPM site was set-up at the beginning of July 2013, exclusively for this summer campaign. The site was built in the "Es Pinar" military facilities, a forested and isolated area in between the Alcudia and Pollença bays (Fig. 2). The exact location of the site is 39.885°N, 3.195°E, at around 20 m a.s.l.

Fig. 2. View from the North-East of the EPM site (orange point). Image elaborated with Google maps.

The ErC supersite is in operation since 2011 (Fig. 3), and it was elongated in summer 2013 in order to hold numerous scientific platforms. The exact location of the site is 42.969°N, 9.380°E, at around 400 m a.s.l.

Fig. 3. View from the North-West of the ErC site (orange point). Image elaborated with Google maps.

2.2   Instrumental deployment and dates

The summer campaign started during the first week of July in Mallorca and during the second week of July in Corsica, and finished on 5 August 2013 in Corsica and on 12 August 2013 In Mallorca. A summary of instrumental deployment as well as the involved institutions is presented in Table 1.

Table 1. Summary of instrument deployment at each site, their operation period and the involved institution.

		Jul (w. 1)	Jul (w. 2)	Jul (w. 3)	Jul (w. 4)	Aug (w. 1)	Aug (w. 2)	Institutions
SMPS	Mallorca							LCE-Marseille (FR)
	Corsica							LCE-Marseille (FR)
HR-ToF-AMS	Mallorca							PSI-Villigen (CH)
	Corsica							LCE-Marseille (FR)
Aethalometer	Mallorca							Aerosol doo-Ljubljana (SI)
MAAP	Corsica							LCE-Marseille (FR)
PM10 off-line	Mallorca							IDAEA (CSIC)-Barcelona (ES)
	Corsica							
PM2.5 off-line	Mallorca							
	Corsica							LCE-Marseille (FR)
PM1 off-line	Mallorca							IDAEA (CSIC)-Barcelona (ES)
	Corsica							LGGE-Grenoble (FR)
PTR-ToF-MS	Mallorca							LCE-Marseille (FR)
	Corsica							
LAAPTOF	Mallorca							LCE-Marseille (FR)
	Corsica							
Meteo	Mallorca							CAIB-Balearic Islands (ES)
	Corsica							Qualitair Corse (FR)
Gas/PM10 on-line	Mallorca							CAIB-Balearic Islands (ES)
	Corsica							Qualitair Corse (FR)

SMPS (Scanning Mobility Particle Sizer). To determine particle number and size distribution of fine and ultrafine particles. The SMPS was set-up to measure in the range 14-650 nm, every 5 min.

HR-ToF-AMS (High Resolution Time-of-Flight Aerosol Mass Spectrometer). It allowed the measurement in real-time of non-refractory chemical components and their mass loadings, in the range 70-1000 nm, as a function of particle size. Organic species, NO_3^-, SO_4^{2-}, NH_4^+ and chloride are detected, but mineral matter and black carbon are not [11]. This instrument provided us data every 3 min.

MAAP (Multi-Angle Absorption Photometer). The instrument provides equivalent BC concentrations. The time resolution fixed was 5 min.

Aethalometer. It measured light absorption by suspended aerosol particles at seven wavelengths, from 370 nm (UV) to 950 nm (IR) every 5 min. The interpretation of optical differences across the wavelength spectrum may reveal information regarding aerosol size distribution and physical properties, and may help in identifying certain primary emission sources.

PM-offline. Daily sampling on filters was performed in order to quantify and characterize aerosol chemical composition in different PM fractions. Amongst various species, special care was paid in the characterisation of trace elements [5], organic species [7], and radiocarbon analysis [12].

PTR-ToF-MS (Proton Transfer Reaction Time-of-Flight Mass Spectrometer). This instrument is devoted to the quantification of a wide spectra of volatile organic compounds (VOCs), both primary compounds and secondary gaseous products such as methacrolein, glyoxal, methylvinylketone. The detection limit reaches few parts per trillion, with a mass resolution of more than 4000 (m/Δm). The time resolution fixed for this instrument was 2 min.

LAAPTOF (Laser Ablation of Aerosol Particles Time Of Flight Mass Spectrometer). It is a single particle aerosol mass spectrometer capable of analysing aerosol particles in the range of 70 nm to 2500 nm. It provides with combined information on the size of the particles and their chemical signature. *Gaseous pollutant concentrations* (NO, NO_2, SO_2, CO, O_3), *PM_{10}* and *meteorological parameters* were obtained in situ at both sites in real time.

2.3 Air mass origins and aerosol incursions

In order to interpret our results we have computed daily back-trajectories (120 h) of air masses at 500 and 1500 m a.s.l. by using the HYSPLIT model (http://ready.arl.noaa.gov/HYSPLIT.php). Moreover, we have consulted different aerosol maps to corroborate the impact of Saharan dust incursions (http://www.bsc.es/projects/earthscience/visor/dust/med8/sfc/archive/) and anthropogenic pollution plumes (http://www.nrlmry.navy.mil/).

3 RESULTS

3.1 Meteorological conditions

Aerosol phenomenology in Mallorca and Corsica was in connection to the concatenation of diverse meteorological situations. Regional conditions (lack of intense advection) prevailed during the campaigns at both sites, sometimes interrupted by the incursion of some Saharan dust plumes over Mallorca, by the cleaning effect of westerly winds, or by the arrival of anthropogenic pollution plumes from the European continent. Overall, regional conditions were observed during 67% of time in Mallorca, and during 85% of the time in Corsica (Fig. 4).
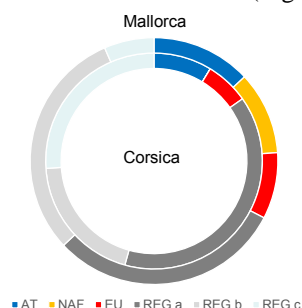
Fig. 4. Average air mass origin at Mallorca and Corsica in the period 01/07-15/08/2013. AT: Atlantic; NAF: Saharan dust; EU: European pollution; REG: regional conditions (a: from NE; b: from NW; c: rest).

3.2 Aerosol and gas characteristics at EPM-Mallorca

During the campaign at Mallorca, three vast periods under regional conditions were observed (Fig. 5). At the beginning of each period under regional conditions, intense new particle formation (NPF) events were observed. After one or two days dominated by NPF, regional conditions were extended over time. Such regional episodes finished in all cases with moderate incursions of dust particles from North Africa. Two of these REG-NAF

Accumulation of atmospheric pollutants → Ageing

Clean conditions → NPF
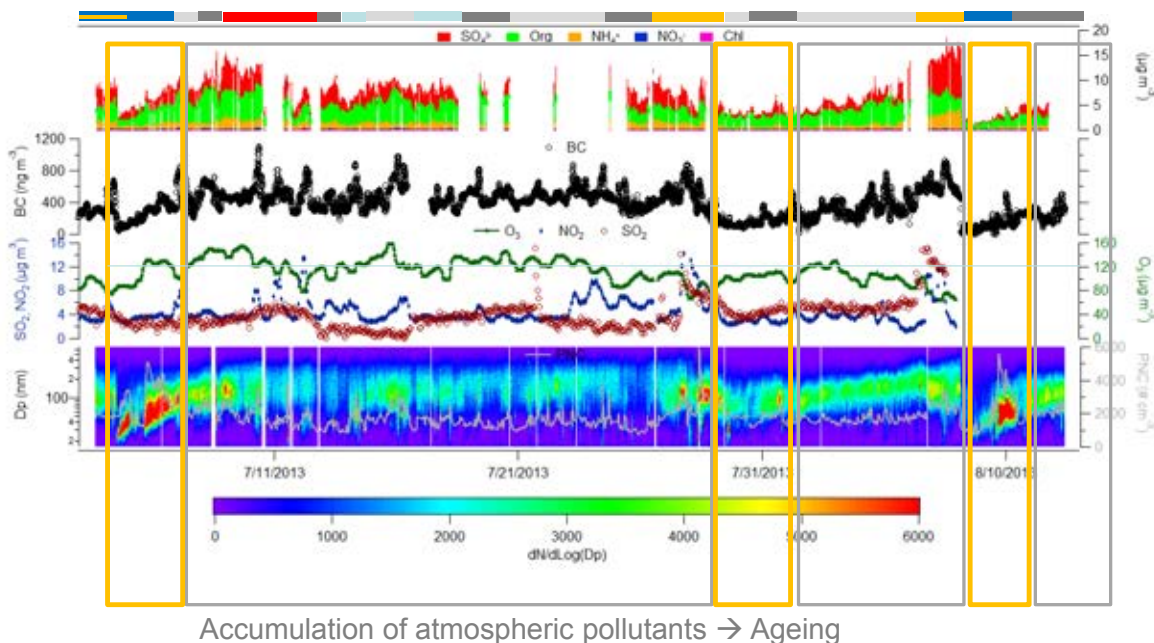
Fig. 5. Mallorca overview data from July 3 to August 12. SMPS data (bottom figure); O_3, NO_2 and SO_2 (center-bottom); black carbon (center-top); and SO_4^{2-}, organics, NO_3^-, NH_4^+ and Cl^- (top). Air mass origins are shown in the upper side.

periods were followed by AT advections, being the other one continued by regional conditions. During regional episodes, mineral dust increased slightly (Fig. 6), O_3 concentrations raised considerably, clear accumulation mode particles prevailed (SMPS data), and ammonium sulphate, organic aerosols (AMS measurements) as well as black carbon aerosols (Aethalometer data) dominated the aerosol composition.
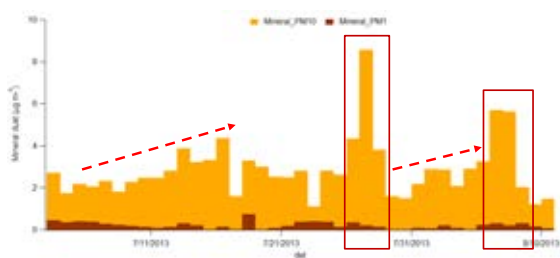
Fig. 6. Partitioning of mineral dust in between PM_{10} and PM_1 fractions at EPM. Saharan dust episodes are marked.

The two Saharan dust episodes observed during the campaign brought moderate amounts of mineral dust (Fig. 6) and provoked an enhancement of sulphate concentrations in both fine (AMS results; Fig. 5) and coarse fractions. After such dust outbreaks, westerly winds cleaned the atmosphere sharply or moderately, creating conditions for new particle formation. During the second week of July, an air mass from the European continent carried significant amounts of specific anthropogenic pollutants, especially sulphate, organics, O_3 and certain trace elements.

3.3 Aerosol characteristics at ErC-Corsica

In Corsica, an extended period of regional conditions occurred from the beginning of the campaign to end July, when some westerly winds renovated the atmosphere (Fig. 7). During the stagnant period, atmospheric particles were observed in the accumulation mode (SMPS data), essentially made up of sulphate and organics (AMS results), with moderate amounts of black carbon (MAAP results). Such episode finished abruptly after a heavy rainy event, and was followed by three days of consecutive NPF episodes. The last part of the campaign registered somewhat regional conditions, although the relatively high concentrations of aerosols and their chemical constituents observed during the first part of the campaign were not achieved again. In Corsica, some short ammonium nitrate episodes were observed under cloudy conditions. During these episodes, the observatory was located inside the clouds.
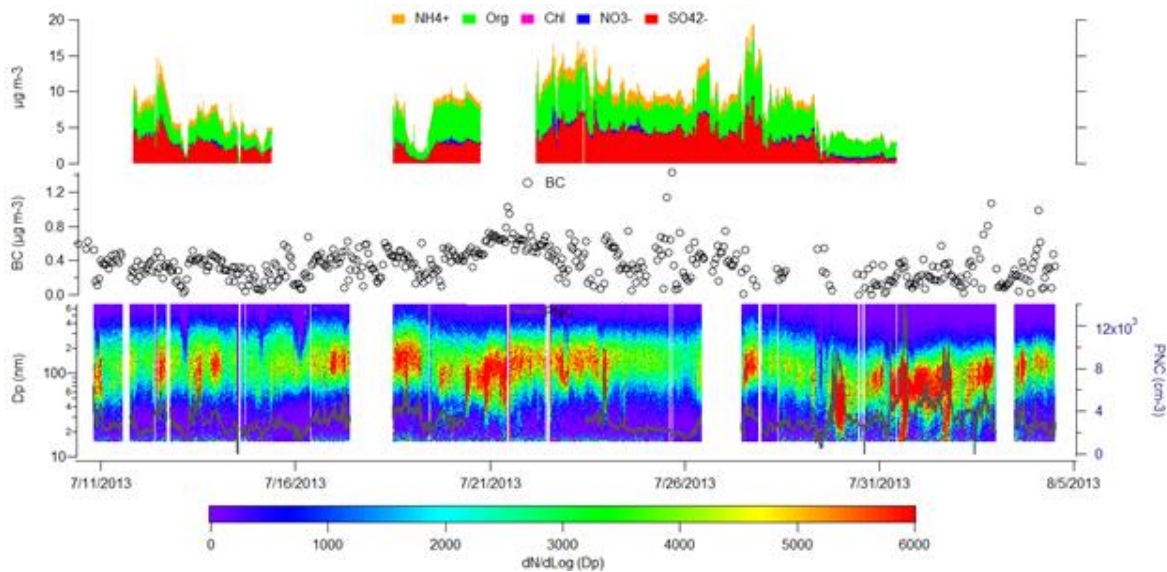
Fig. 7. Corsica overview data from July 10 to August 5. SMPS data (bottom figure); black carbon (center); and SO_4^{2-}, organics, NO_3^-, NH_4^+ and Cl^- (top).

3.3 Common overview

A number of simultaneously recorded episodes occurred at both sites. This is the case of certain NPF events after Saharan dust and/or during AT conditions. They will be object of dedicated research. In addition, a quite intense pollution event from Eastern Europe was recorded at both sites, increasing O_3 concentrations, BC and sulphate-organic aerosols. From the SMPS results (Fig. 8), it is obvious that aerosol characteristics varied in parallel at both sites during most of the time, but especially the second half of the campaign.
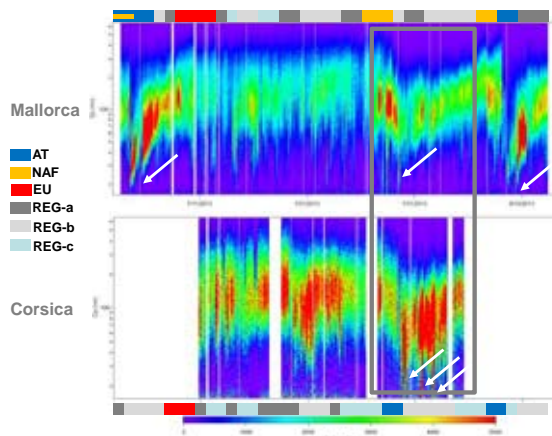
Fig. 8. SMPS data at EPM and ErC, with indication of average concentrations, aerosol mode and the common period under similar conditions.

When regarding the BC diurnal profile at both sites (almost flat at both locations) in becomes obvious that local fresh emissions are absent as no traffic peaks are observed. Moreover, BC concentrations were comparable (Fig. 9).
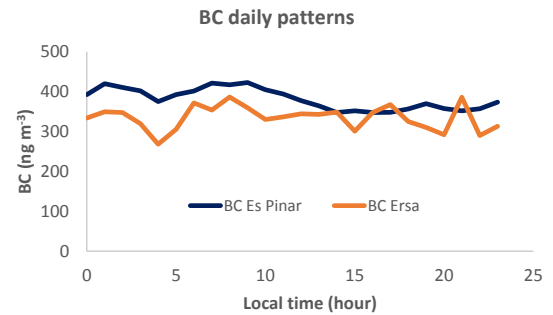
Fig. 9. BC diurnal pattern at EPM and ErC.

An evaluation of the average chemical composition at both sites may be useful to identify individual particularities. At both sites, PM was strongly driven by sulphate and ammonium (Fig. 10). In ErC, organic aerosols were almost equally abundant as sulphate, whereas they were not so important at EPM. On the contrary, sea-spray and nitrate were clearly enhanced at EPM. Thus, there are key compositional differences between EPM (PM_{10}) and ErC ($PM_{2.5}$). In part these differences may be explained because two different fractions are considered (sea-spray and nitrate). However, the difference in the organic aerosol content might be connected to particularities of each region.
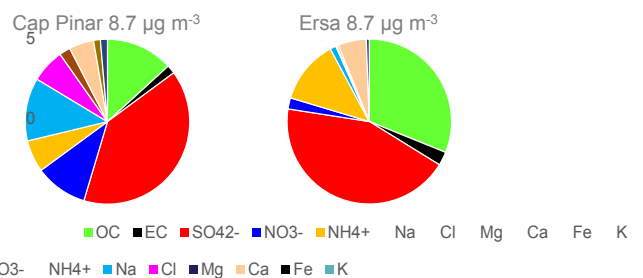
Fig. 10. Average chemical composition at EPM (PM_{10}) and ErC ($PM_{2.5}$).

In line with the previous discussion, the preliminary radiocarbon analyses (performed in PM_1) have revealed exciting differences between organic aerosol origins at EPM and ErC. In Mallorca, around 35% of the organic aerosol came from fossil sources, whereas in Corsica the fossil origin was only 19% (Fig. 11). Thus, when normalizing these percentages according to the OC content it becames apparent that the abundance of fossil carbon is comparable at both sites, but the non-fossil organic aerosol is two times higher at ErC than at EPM. These differences will deserve a particular focus in the next future.
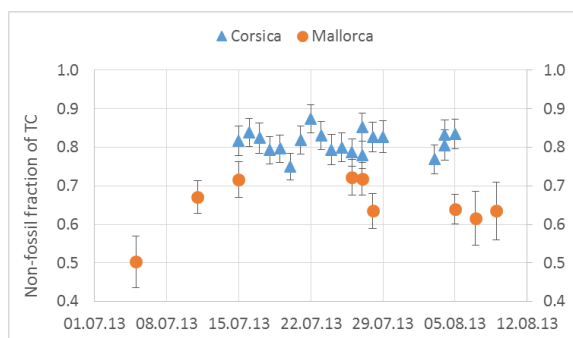
Fig. 11. Fossil vs non-fossil total carbon (TC) at EPM and ErC. Note that more than 95% of TC is organic aerosol.

4 CONCLUSIONS

During the campaign, wide-scale atmospheric episodes were observed at both Mallorca and Corsica, including Saharan dust outbreaks, new-particle formation events and regional accumulation of pollutants. Different air masses and sources were found to influence Mallorca and Corsica in different ways. In particular, more Saharan dust episodes and persistent accumulation processes were observed in Mallorca, while some outflows from the Po valley were observed at times in Corsica. Although some aerosol physical properties varied in parallel at both sites, compositional differences are patent, especially concerning the organic fraction. The first results suggest a more biogenic load at Corsica, whilst the anthropogenic component remains comparable. This work can be seen as a very preliminary step in the data analysis and data assimilation from different instruments.

REFERENCES

[1] Querol X., Alastuey A., Pey J., Cusack M., Pérez N., Mihalopoulos N., Theodosi C., Gerasopoulos E., Kubilay N., Koçak M. (2009). Variability in regional background aerosols within the Mediterranean. Atmospheric Chemistry and Physics 9, 4575-4591.

[2] Putaud J.P., Van Dingenen R., Alastuey A., Bauer H., Birmili W., Cyrys J., Flentje H., Fuzzi S., Gehrig R., Hansson H.C., Harrison R.M., Herrmann H., *et al.* (2010). A European aerosol phenomenology-3: Physical and chemical characteristics of particulate matter from 60 rural, urban, and kerbside sites across Europe. Atmospheric Environment 44, 1308-1320.

[3] Amato F., Pandolfi M., Moreno T., Furger M., Pey J., Alastuey A., Bukowiecki N., Prevot A.S.H., Baltensperger U., Querol X. (2011). Sources and variability of inhalable road dust particles in three European cities. Atmospheric Environment 45, 6777-6787.

[4] Pey J., Querol X., Alastuey A., Forastiere F., Stafoggia M. (2013). African dust outbreaks over the Mediterranean Basin during 2001–2011: PM10 concentrations, phenomenology and trends, and its relation with synoptic and mesoscale meteorology. Atmospheric Chemistry and Physics 13, 1395-1410.

[5] Pey J., Pérez N., Cortés J., Alastuey A., Querol X. (2013). Chemical fingerprint and impact of shipping emissions over a western Mediterranean metropolis: primary and aged contributions. Science of the Total Environment 463-464, 497-507.

[6] Sciare J., Oikonomou K., Favez O., Liakakou E., Markaki Z., Cachier H., Mihalopoulos N. (2008). Long-term measurements of carbonaceous aerosols in the Eastern Mediterranean: evidence of long-range transport of biomass burning. Atmospheric Chemistry and Physics 8, 5551-5563.

[7] El Haddad I., Marchand N., Wortham H., Piot C., Besombes J.L., Cozic J., Chauvel C., Armengaud A., Robin D., Jaffrezo J.L. (2011). Primary sources of PM2.5 organic aerosol in an industrial Mediterranean city, Marseille. Atmospheric Chemistry and Physics 11, 2039-2058.

[8] Millan M.M., Salvador R. Mantilla E., Kallos G. (1997). Photooxidant Dynamics in the Mediterrannean Basin in Summer: Results from European Research Projects. Journal of Geophysical Research – Atmospheres 102, D7, 8811-8823.

[9] Pérez C., Sicard M., Jorba O., Comerón A., Baldasano J.M. (2004). Summertime recirculations of air pollutants over the north-eastern Iberian coast observed from systematic EARLINET lidar measurements in Barcelona. Atmospheric Environment 38, 3983-4000.

[10] Pandolfi M., Cusack M., Alastuey A., Querol X. (2011). Variability of aerosol optical properties in the Western Mediterranean Basin. Atmospheric Chemistry and Physics 11, 8189-8203.

[11] DeCarlo P.F., Kimmel J.R., Trimborn A., Northway M.J., Jayne J.T., Aiken A.C., Gonin M., Fuhrer K., Horvath T., Docherty K.S., Worsnop D.R., Jimenez J.L. (2006). Field-deployable, high-resolution, time-of-flight aerosol mass spectrometer. Analytical Chemistry, 78, 8281-8289.

[12] Zhang Y.L., Perron N., Ciobanu V.G., Zotter P., Minguillón M.C., Wacker L., Prévôt A.S.H., Baltensperger U., Szidat S. (2012). On the isolation of OC and EC and the optimal strategy of radiocarbon-based source apportionment of carbonaceous aerosols, Atmos. Chem. Phys., 12, 10841-10856, doi:10.5194/acp-12-10841-2012.

Influence of Air Masses Origin on Radioactivity in Aerosols

Francisco Piñero-García[1], Mª Ángeles Ferro-García[2]

Abstract — the aim of this research is to study the influence of the air masses origin on radioactivity in aerosols at surface air, (Gross α, Gross β and [7]Be activity concentration). A total of 148 samples were weekly collected from January 4th, 2011 to December 31st, 2013. The specific activity (Bq/m^3) of gross alpha and gross beta was measured by α/β Low-Level counter, whereas [7]Be was detected by gamma spectrometry (Eγ = 477.6 KeV, Yield = 10.42 %). Evolution of Gross α and Gross β have showed a Log-Normal distribution, while [7]Be fits better a Normal distribution according to Kolmogorov Simirnov test. The air mass origings have been set using k-means clustering analysis of daily 72-h kinematic 3D backward trajectories was at altitudes of: mean altitude of Spain (500 m; 950 hPa), planetary boundary layer (1500 m; 850 hPa) and free atmosphere (3000 m; 700 hPa). Finally, Multiple Regression Analysis (MRA) have been applied to determine the influence of the air mass origin (Backward trajectory), and local meteorology on Gross α, Gross β and [7]Be activity concentration.. In brief, the MRA results show that the re-suspended continental particles from northern Africa and the southern part of western and central Europe transported by Mediterranean air masses at low altitude (500 m) and African air masses at high altitude (3000 m) increase the radioactivity concentration in aerosols at surface atmosphere.

Keywords — Aerosols, Backwards Trajectories, Radioactivity, Saharan Intrusions.

1 INTRODUCTION

The measurements of radioactivity in aerosols are crucial to control and avoid radiological risk for the environment and human health. Furthermore, these measurements are useful to study several atmospheric processes since the radionuclides realised into the atmosphere take part in the formation and growth of aerosols. In order to study the influence of air masses origin on radioactivity in aerosols, Gross α, Gross β and [7]Be have been used as radiotracers.

[7]Be is a natural cosmogenic radionuclide, it is produced by spallation reactions of primary components of cosmic rays (protons and neutrons) with light atmospheric nuclei (C, O, N) [1]. Its production rate depends on the solar cycle, cosmic ray rate and decreases exponential with altitude [2], [3]. Therefore, the highest concentrations of [7]Be are mainly generated in the stratosphere. The stratosphere is characterized by the lack of convection currents, for that reason [7]Be-aerosols only reach the ground level of troposphere via vertical transport [4], [5].

The European Commission assesses that atmospheric radioactivity is mainly controlled by natural sources, in particular radioactive decay products of gas [222]Rn. [222]Rn is mainly produced by decay of the [238]U series and is an unreactive noble gas with a long half-life, 3.8 days. It diffuses rapidly when it is released into the atmosphere and it can be transported widely over the surface of the earth by natural air movement. [222]Rn has several daughters but from the radiological point of view the most important ones are: [210]Pb (22.3 y, β⁻); [210]Bi (5 d, β⁻); [210]Po (138 d, α) since they are α and β emitters and have a high potential risk of internal contamination. In this sense, the measurements of Gross α and Gross β radioactivity in airborne particulates can be a useful tool to study Radon exhalation from Earth's upper crust through their daughter [6]; without forgetting the effects of secondary sources such as: re-suspension of soil dust, volcanic eruption, forest fire or anthropogenic activities [7].

Therefore, the aim of this research is to determine the influence of the air masses on the aerosols radioactive content. This study focuses on the effects of re-suspended mineral particles on atmospheric radioactivity, especially during the Saharan intrusions.

2 MATERIAL AND METHODS

2.1 Sampling

Granada (Spain) is placed in a natural basin at the southeast of Iberian Peninsula. Granada Basin is surrounded by mountains, especially at the east where Sierra Nevada is located. Sierra Nevada is the major mountain range of the basin with 20 peaks higher than 3,000 m of altitude and contains the

1. *Radiochemistry and Environmental Radiology Laboratory (LABRADIQ), Department of Inorganic Chemistry, University of Granada, Granada, 18071, E-mail: franciscopigar@ugr.es*
2. *Radiochemistry and Environmental Radiology Laboratory (LABRADIQ), Department of Inorganic Chemistry, University of Granada, Granada, 18071, E-mail: ferro@ugr.es*

highest peak in the Iberian Peninsula, Mulhacen 3,478.6 m.

Therefore, the orography of the basin influences the Continental Mediterranean Climate of Granada. The main seasons are cold winter and hot summer. However, spring and autumn are only a short transition between the summer and the winter.

Aerosols were sampled in the roof of the Faculty of Sciences at the University of Granada (37°10′50″N, 3°35′44″W, 702 a.s.l), from January of 2011 to December of 2013. The atmospheric dust was weekly collected on a cellulose filter of 4.2 cm of effective diameter and 0.8 μm of pore size, using an air sampler, Radeco AVS-60A. Once the samples were collected, they were stored in desiccators until the measurement in order to avoid contamination or alteration of the samples.

2.2 Radiometric Analyses

In the current research, the radioactivity in aerosols has been characterized by ^7Be, Gross α activity and Gross β activity. ^7Be has been identified and quantified in the samples by gamma spectrometry, using the photopeak generated at 477.6 keV (Yield 10.42%). Otherwise, background contribution was removal and decay correction was carried out considering the mid-point of the collection period and the half-life of ^7Be (53.3 days).

Gross α and Gross β activities were simultaneously measured using a low background proportional counter, Berthold LB 770-2/5. The mean efficiency was 17.8% and 42.8% for α and β, respectively. The samples were measured after ten days from end-point of collection in order to ^{210}Po represents the main contribution of gross α activity and ^{210}Pb and ^{210}Bi control Gross β activity [8]. Furthermore, background and mass thickness correction were applied to calculate the specific activity (Bq/m^3) of Gross α and Gross β activities.

2.3 Backward Trajectories

To study the influence of the air masses on radioactivity in aerosols is necessary to identify the origin of the air masses. For that purpose, the model developed by Draxler and Rolph Hysplit [9] (Hybrid Single Particle Lagrangian Integrated Trajectory) has been used. 72-h kinematic 3D back-trajectories each day from January-11 to December-13 at three different altitudes (500 m, 1500 m and 3000 m) have been computed. Then the trajectories were clustered by k-means method in order to identify the main air mass origins.

To complete the study of the influence of air masses origin on radioactive aerosols, other local atmospheric parameters like: Temperature (ºC), rainfall (mm) and wind direction (tenth of an hour) were used. These parameters were provided by Spanish National Institute of Meteorology, AEMET.

3 RESULTS

3.1 Radioactivity Evolution

A total of 148 samples were weekly collected from January 4th, 2011 to December 31st, 2013. In all samples, the activity concentration of ^7Be, Gross α activity and Gross β activity were higher than the Minimum Detectable Activity (MDA).

Gross α activity varied from 0.02 to 0.82 mBq/m^3, in addition its average activity was 0.19 mBq/m^3. Gross β activity ranged between 0.07 mBq/m^3 and 1.57 mBq/m^3, its mean activity was 0.50 mBq/m^3. Similar behaviour was detected for both indices. On the one hand, the maximum activities were measured during the summer months. On the other hand, the minimum activities were found during the winter. Therefore, the Gross α and Gross β activities could have a similar main source, Radon exhalation from Earth's crust [8].

The activity concentration of ^7Be varied from 0.99 to 12.19 mBq/m^3; its mean activity was 5.61 mBq/m^3. The behaviour of ^7Be showed a typical trend of middle latitudes, that is, maximum activities in summer and the minimums in winter [10], [11], [12].

The radiotracers evolution were fitted to the best theoretical distribution (like: Normal, Normal-log, Uniform and Exponential) using Kolmogorov Smirnov test. The Table 1 shows the result of the test. It confirm that Normal-log distribution is the best fitting for Gross α and Gross β, however ^7Be evolution fits better to Normal distribution.

Table 1. Kolmogorov Smirnov Test, Z_{K-S} (p-Value)

	Normal	Normal-Log	Uniform	Exponential
Gross α	2.16 (0.00)	0.69 (0.74)	6.34 (0.00)	2.49 (0.00)
Gross β	1.44 (0.03)	0.85 (0.47)	5.31 (0.00)	3.57 (0.00)
^7Be	0.71 (0.69)	0.78 (0.57)	2.93 (0.00)	3.82 (0.00)

3.2 Wind Direction and Air Mass Origin
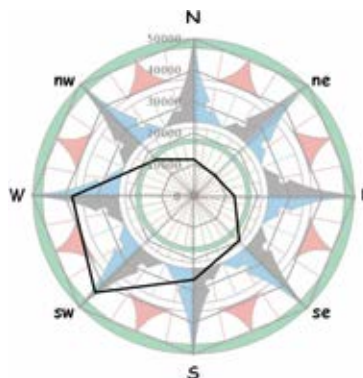
Fig. 1. Total weekly wind rose (tenths of an hour).

Wind direction is related to the pathway of dispersion of aerosols in the atmosphere. The Fig. 1 illustrates the total weekly wind rose during the current research. The figure shows that wind usually blew form the South, Southwest and West. These results are in agreement with the orography of basin of Granada since the unusual directions were the North and the East where the highest mountain range of Granada are located.

In addition, Fig. 2, Fig. 3 and Fig. 4 show the clustering analyses of the back-trajectories at altitude of 500 m, 1500 m and 3000 m, respectively. These analyses had allowed determining the main air masses origin and the pathway followed by them before arriving at Granada during the research period. The most important results of the k-means clustering analysis are:
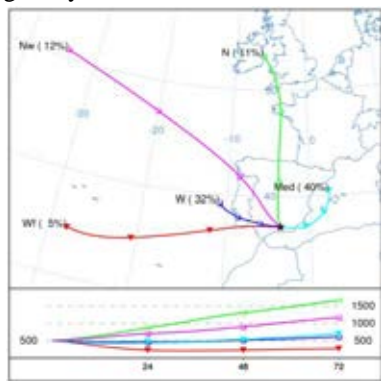
Fig. 2. Cluster Centroids at altitude of 500 m.

- **500 m:** 5 clusters classify the backward trajectories at 500 m of altitude (Fig. 2). The usual air mass origins were West and Mediterranean that represent 32% and 40% of all them, respectively. Mediterranean air mass collects warm polar continental air masses over Mediterranean Sea. They are influenced by slow tropical continental air masses from Africa and therefore they could transport some mineral dust [13].
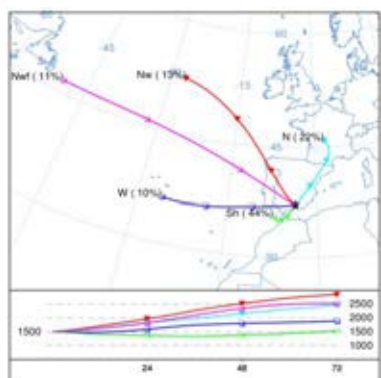
Fig. 3. Cluster Centroids at altitude of 1500 m.

- **1500 m:** 5 clusters group the backward trajectories at 1500 m of altitude (Fig. 3). Saharan and North cluster were the most important with a frequency of 44% and 22%, respectively. The African air masses

get mixed with the tropical maritime and continental air masses that cross the northern of Africa. As a result of the pass over African dessert; they could transport a high concentration of mineral dust.
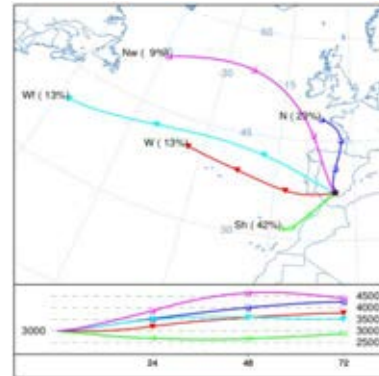
Fig. 4. Cluster Centroids at altitude of 3000 m.

- **3000 m:** 5 clusters represent the typical air masses origin at 3000 m of altitude over Granada (Fig. 4). As altitude of 1500 m, Saharan and North clusters controlled the origin of the air masses at 3000 m; 42% and 23%, respectively.

3.3 Multiple Regression Analyses

The influence of air mass and local climate on radioactivity in aerosols was determined by Multiple Regression Analysis (MRA). Table 2 summarizes the results of MRA. In addition, Table 3 shows the standardized beta coefficient of MRA besides the acronym of the chosen independent variables.

Table 2. Summary of the Multiple Regression Analysis (MRA).

	R	R^2	R^2_c
Gross α	0.79	0.62	0.60
Gross β	0.81	0.65	0.64
^{7}Be	0.72	0.51	0.49

The three models of MRA are statically significant; moreover they have a strong correlation (R > 0.70, Table 2). The models explain the 60%, 64% and 49% of the behaviour of Gross α activity, Gross β activity, and ^{7}Be activity concentration, respectively. The MRA results highlight:

- **Gross α activity:** On the one hand, its evolution is influence in positive by T and Med-500. On the other, the mm, Se, W, Nw-3000 and Wf-500 decreased Gross α activity, Table 3. The raise of temperature favour Radon exhalation from ground to atmosphere increasing the concentration of alpha descendent of Radon in the surface atmosphere [14]. Furthermore, Mediterranean air masses at low altitude (Med-500) could transport alpha radionuclides attached into the re-suspended

continental particles from northern Africa and the southern part of western and central Europe [15] increasing the activity concentration of Gross α. However, the entrance of clean and maritime air masses (like: Nw-3000 and W-500) reduced the concentration of alpha radionuclides [15]. Also, rainfalls wash the lower troposphere sweeping out α-aerosol toward the ground.

Table 3. Standardized beta coefficients of MRA model.

		Gross α	Gross β	^{7}Be
Temperature	T	0.50	n/i	0.32
Rainfall	mm	-0.27	-0.38	-0.34
Saharan air masses at 3000m	Sh-3000	n/i	0.19	0.46
North West air masses at 3000m	Nw-3000	-0.15	-0.18	n/i
Saharan air masses at 1500m	Sh-1500	n/i	n/i	-0.27
Mediterranean air masses at 500m	Med-500	0.18	0.23	n/i
North West air masses at 500m	Nw-500	n/i	-0.14	n/i
Fast West air masses at 500m	Wf-500	-0.12	-0.19	n/i
South Wind Direction	S	n/i	0.11	0.17
Southeast Wind Direction	Se	-0.25	n/i	n/i
West Wind Direction	W	-0.27	n/i	n/i

n/i: not included in the MRA model

- **Gross β activity:** the MRA results show that the re-suspended dust transported by Saharan intrusions (Sh-3000) and Mediterranean air masses (Med-500) together with south wind increased the concentration of Gross β activity, Table 3. However, maritime air masses (Nw-500, Nw-3000 and Wf-500) and rainfalls favour the scavenging of radioactive aerosols from the troposphere to ground decreasing the Gross β activity.

- **^{7}Be activity:** On the one hand, MRA results show that Sh-3000, Temperature and South wind increase the activity concentration of ^{7}Be-aerosols; however the Sh-1500 and precipitations decrease their concentrations (Table 3). Several authors have studied the effects of temperature on the behaviour of ^{7}Be aerosols. On the one hand, the raise of temperatures increases the rate of exchange of air masses rich in ^{7}Be from high levels to low levels into troposphere. On the other, higher temperatures favour the entrance of stratospheric air masses with high concentration of ^{7}Be-aerosols [16].

Table 3 shows an important influence of African air masses at 3000 m of altitude (Sh-3000) on ^{7}Be aerosols, together with the wind direction of the south. Therefore, the high concentration of mineral dust of Saharan and Sahel intrusions at high altitudes (> 3000 m) increase the activity of ^{7}Be measured in the samples, since the mineral dust stick on ^{7}Be-aerosols of the free troposphere sweeping them from the upper layer to ground levels [15]. However, when the African intrusions are near to planetary boundary layer (Sh-1500), the mineral dust could reduce the residence time of ^{7}Be-aerosol in the surface atmosphere decreasing the ^{7}Be activity concentration detected in the samples [17], [18]. In addition, the scavenging of the ^{7}Be aerosols increased when the precipitations occur.

4 CONCLUSIONS

In conclusion, the current research demonstrates that the radioactivity in aerosols depends on the origin of air masses and the trajectory followed by them. On the one hand, the clean maritime air masses reduce the radioactivity in aerosols. On the other hand, the mineral dust transported by African air masses could be an important source of radioactive aerosols, since they introduce re-suspended β radionuclides transported by continental particles which favour the scavenging of ^{7}Be-aerosols from upper heights to surface levels of the troposphere. Although, it should be noted that sometimes when Saharan intrusions arrive near the boundary layer with high levels of mineral dust, they could remove the ^{7}Be-aerosols from the surface level of the troposphere scavenge them to ground via dry deposition.

REFERENCES

[1] C. Papastefanou. "Beryllium-7 aerosols in ambient air". *Aerosol and Air Quality Research* 9, 187–197, 2009.

[2] M. Azahra, A. Camacho García, C. González Gómez, J. López Peñalver, T. El Bardouni. "Seasonal 7Be concentrations in near-surface air of Granada (Spain) in the period 1993–2001". *Applied Radiation and Isotopes* 59, 159–164, 2003.

[3] C. Papastefanou, A. Ioannidou. "Beryllium-7 and solar activity". *Applied Radiation and Isotopes* 61, 1493–1495, 2004.

[4] C. Papastefanou, A. Ioannidou. "Aerodynamic size association of 7Be in ambient aerosols". *Journal of Environmental Radioactivity* 26, 273–282, 1995.

[5] R. Winkler, F. Dietl, G. Franck, J. Tschierch. "Temporal variation of 7Be and 210Pb size distribution in ambient aerosol". *Atmos Environ* 32(6), 983–991, 1998.

[6] A. Camacho, I. Valles, A. Vargas, M. Gonzalez-Perosanz, X. Ortega X. "Activity size distributions for long-lived radón decay products in aerosols collected in Barcelona (Spain)". *Applied Radiation and Isotopes* 67, 872–875, 2009.

[7] C.A. Rahim Mohamed, A. Azrin Sabuti, A., N. Affizah Saili. "Atmospheric deposition of 210Po and 210Pb in Malaysian waters during haze events". *Journal of Radioanalytical and Nuclear Chemistry* 297, 257–263, 2013.

[8] C. Dueñas, M.C. Fernández, J. Carretero, E. Liger, S. Cañete. "Long-term variation of the concentrations of long-lived Rn descendants and cosmogenic 7Be and determination of the MRT of aerosols". *Atmospheric Environment* 38, 1291–1301, 2004.

[9] R.R. Draxler, G.D. Rolph. "HYSPLIT (Hybrid Single-Particle Lagrangian Integrated Trajectory)" Model. access *via NOAA ARL READY Website. NOAA Air Resources Laboratory, Silver Spring, MD*. http://www.arl.noaa.gov/ready/hysplit4.html , 2003.

[10] F. Cannizzaro, G. Greco, M. Raneli, M.C. Spitale, E. Tomarchio. "Concentration measurements of 7Be at ground level air at Palermo, Italy comparison with solar activity over a period of 21 years". *Journal of Environmental Radioactivity* 72, 259–271, 2004.

[11] C. Doering, R. Akber. "Describing the annual cyclic behaviour of 7Be concentrations in surface air in Oceania". *Journal of Environmental Radioactivity* 99, 1703–1707, 2008.

[12] I. Valles, A. Camacho, X. Ortega, I. Serrano, S. Blázquez, S. Peréz. "Natural and anthropogenic radionuclides in airborne particulate samples collected in Barcelona (Spain)". *Journal of Environmental Radioactivity* 100, 102–107, 2009.

[13] J.L. Guerrero-Rascado, F.J. Olmo, I. Avilés-Rodríguez, F. Navas-Guzmán, D. Pérez-Ramírez, H. Lyamani, L. Alados-Arboledas. "Extreme Saharan dust event over the southern Iberian Peninsula in september 2007: active and passive remote sensing from surface and satellite". *Atmospheric Chemistry and Physics* 9, 8453–8469, 2009.

[14] I. Dadong, Y. Hiromi, I. Takao. "Quantification of the dependency of Radon emanation power on soil temperature". *Applied Radiation and Isotopes* 60(6), 971–973, 2004.

[15] C. Dueñas, J.A.G. Orza, M. Cabello, M.C. Fernández, S. Cañete, M. Pérez, E. Gordo. "Air mass origin and its influence on radionuclide activities (7Be and 210Pb) in aerosol particles at a coastal site in the western Mediterranean". *Atmospheric Research* 101, 205–214, 2011.

[16] H.W. Feely, R.J. Larsen, C.G. Sanderson. "Factors that cause seasonal variations in Beryllium-7 concentrations in surface air". *Journal of Environmental Radioactivity* 9, 223–249, 1989.

[17] F. Hernández, J. Hernández-Armas, A. Catalán, J.C. Fernández-Aldecoa, L. Karlsson. "Gross alpha, gross beta activities and gamma emitting radionuclides composition of airborne particulate samples in an oceanic island". *Atmospheric Environment* 39, 4057–4066. , 2005.

[18] F. Hernández, S. Rodríguez, L. Karlsson, S. Alonso-Pérez, M. López-Pérez, J. Hernández-Armas, E. Cuevas. "Origin of observed high 7Be and mineral dust concentrations in ambient air on the Island of Tenerife". *Atmospheric Environment* 42, 4247–4256, 2008.

Levels and evolution of atmospheric nanoparticles in a suburban area with Atlantic influence

S. Iglesias-Samitier, V. Juncal-Bello, M. Piñeiro-Iglesias, P. López-Mahía, S. Muniategui-Lorenzo and D. Prada-Rodríguez

Abstract — Atmospheric nanoparticles are presented in atmosphere, both by primary and secondary formation processes, and they can affect human health and climate change. Secondary formation processes encompass both new particle formation and growth events, among other processes. The study of levels and evolution of atmospheric nanoparticles was carried out at the University Institute of Research in Environmental Studies of University of A Coruna, a suburban area during 2013. The Scanning Mobility Particle Sizer (SMPS) was used to measure the submicron particles, and meteorological parameters were also measured. The influence of sea breeze to take place nucleation events had studied and this demonstrated that nucleation mode was presented by new particle formation process with the presence of sea breeze and at midday hours and by direct emissions, like road traffic, during the rest hours, regardless the origin of air masses. Also, during 2013 lower nanoparticle concentrations were measure than during 2012 and 2011 and the three years presented one maximum in Aitken mode but 2012 had other maximum in nucleation mode too.

Keywords — Atmospheric nanoparticles, new particle formation process, Scanning Mobility Particle Sizer, sea breeze.

1 Introduction

The presence of nanoparticles in the atmosphere, both by primary and secondary formation processes, is important both for climate and epidemiology studies [1] so, recent researches indicate that the number of small particles (e.g. ultrafine particles) and the particle surface area exhibit stronger association with health effects than mass related metrics (e.g. PM10) [2], as well as, urban visibility and their influence on the chemistry of the atmosphere, through their chemical composition and reactivity opening novel chemical transformation pathways [3].

Secondary nanoparticle formation process involves gas to particle processes whereby homogenous or ion-induced nucleation of ion or neutral clusters occurs. H_2SO_4, formed from the oxidation of SO_2, is believed to be the most important nucleating agent in the atmosphere [1] which can nucleate with high solar radiation. Moreover, elevated solar radiation intensities not only provide enough energy for gaseous precursors to nucleate, but favour the dilution processes as a result of the growing of the mixing layer and the activation of mountain and sea breezes [4].

These processes had been studied in different areas around the world, from urban [5, 6] to rural sites [7, 8].

_____

Grupo Química Analítica Aplicada, Instituto Universitario de Medio Ambiente (IUMA), Departamento de Química Analítica, Facultade de Ciencias, Universidade da Coruña, Campus de A Coruña, 15071 A Coruña, Spain,
purificacion.lopez.mahia@udc.es

2 Methodology

2.1 Sampling point

The study of evolution and levels of atmospheric nanoparticles was carried out at the University Institute of Research in Environmental Studies of University of A Coruna, (in the northwest of Spain, 43°20'13.24''N-8°21'2.56''W, Figure 1). This area is a residential zone where the principal source of particulate matter is the traffic. However, there are industries close to the study area that can influence in the air quality, like industries of the energy sector, production and transformation of metals, chemical industry, waste management and wastewater, paper manufacturing and processing, food and beverage industry, as well as ports and airports, hospitals, funeral homes, printers, laundries, and other diverse activities.

Fig. 1. Sampling point, University Institute of Research in Environmental Studies of University of A Coruna.

The sampling period was during May, June, July, September and October 2013 and this area, with Atlantic influence, presented the meteorological conditions showed in Table 1 (no data during September). The predominant wind directions were SE-S and NW-N, being this northwest direction the cause of the presence of sea breeze (SB) in the sampling point, and on the other hand, the southeast direction is a land breeze (LB). The presence of sea breeze in the area was higher during spring and summer.

Table 1. Meteorological conditions during the sampling period

	May	June	July	October
Temperature (ºC)	14	17	23	17
Relative humidity (%)	76	79	76	84
Solar radiation (Wm^{-2})	326	290	382	176
Winds from S-SE sector (%)	20	44	42	60
Winds from N-NW sector (%)	77	45	48	23

2.2 Instrumentation

The system used to carry out the measurements of nanoparticles was the Scanning Mobility Particle Sizer (3936 Model, TSI), which consists in an Electrostatic Classifier (3080 Model, TSI) and a Differential Mobility Analyser (3081 Model, TSI) connected to a Water Condensation Particle Counter (3785 Model, TSI).

The SMPS was set to the sheath and polydisperse aerosol flow rates of 10 and 1 l/min, respectively, to scan the size range between 10 and 289 nm. A pre-impactor with nozzle 0,0514 cm was used and the system sampled periodically every 5 minutes with two scans per sample and 120 seconds scan up. Finally, the distributions were corrected for multiple charging and diffusion.

Moreover, several meteorological parameters were measured at the site of study by the meteorological station (Model 03002, R.M. Young Company, Michigan, EEUU): wind direction and velocity and solar radiation. Temperature and relative humidity were measured with a sensor (1.153 Model).

3 RESULTS

During all studied months in 2013, two peaks at morning and evening hours have been identified for nucleation, Aitken and accumulation modes, due to road traffic emissions. On the other hand, nucleation and Aitken mode presented another maximum around midday, coinciding with high solar radiation and the presence of sea breeze, which bring on the

photochemical nucleation and their further growth. Below, there are some examples of these situations during May (Figures 2-4).
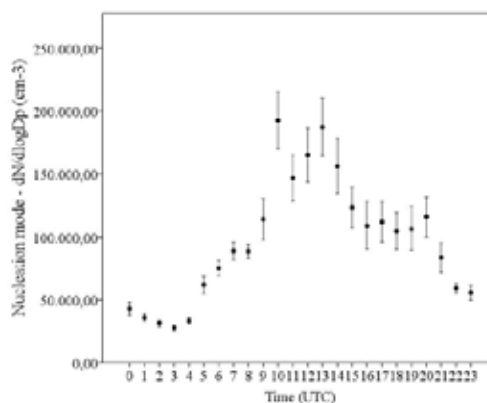
Fig. 2. Daily mean of nucleation mode during May.
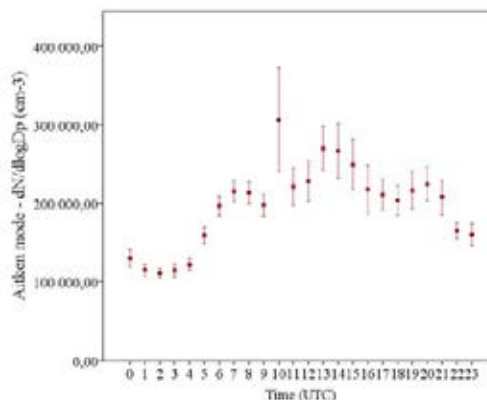
Fig. 3. Daily mean of Aitken mode during May.
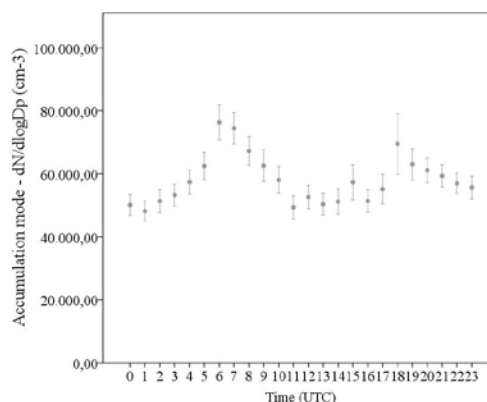
Fig. 4. Daily mean of accumulation mode during May.

The presence of sea breeze favoured the new particle formation process because this air mass is characterized by presenting low concentrations of atmospheric pollutants. Furthermore, growth events of nanoparticles have been identified too, coinciding in this case with the presence of preexisting particles in the atmosphere. So, all data during 2013 were classified into 4 clusters depending on the wind

direction: cluster SB1 which includes the nanoparticles from the NW sector, cluster SB2 from the N sector, cluster LB1 from the SE sector and finally cluster LB2 from the S sector. In this way, clusters SB1 and SB2 encompass the winds from the sea, and they determine the presence of the sea breeze in the sampling point and, on the other hand, LB1 and LB2 encompass winds from the land. Each month has been studied individually and the results are below (Figure 5). In May, there was a lower presence of air masses from S-SE sector but these contributed with higher nanoparticle concentrations than the rest of air masses which arrived at sampling point. On the other hand, the remaining months reached higher concentrations when air masses came from N-NW sector, standing out the bimodal distribution obtained during October.

To know better the sources of these nanoparticles and the influence of the presence of sea or land breeze at the sampling point, the results have been divided into 4 periods: 0-6 h, 7-11 h, 12-17 h and 18-23 h (UTC) (Figure 6; when SB1, SB2, LB1 or LB2 clusters were less than 10% of the total, these distributions have not been represented). In the evening, during all months Aitken mode is the one which presented higher concentrations in particle number concentration, regardless of the origin of air masses, due to road traffic or industrial activity.

Early hours of the morning (7-11 h UTC), wind direction was from S-SE sector, except May, and maximums have been reached both in nucleation and Aitken modes. The obtained maximum of nucleation mode in May coincided with the presence of sea and land breeze (SB1 and LB1, respectively), but the majority wind direction was SB2 and in this case the maximum was in Aitken mode. These maximums could be due to morning traffic in the area.

On the other hand, between 12-16 h (UTC) was when new particle formation processes were presented, during June and October specially, and when winds came from N-NW sector (sea breeze) during these events. However, the presence of sea breeze was lower in October than the other studied months but when it was presented the nucleation events were held and high nucleation particle concentrations had been reached. In June new particle formation processes coincided with high solar radiation, low relative humidity and wind velocity and presence of sea breeze (Figure 8).

Finally, during last hours of the day maximums corresponded with Aitken mode, around 30-50 nm, regardless of origin air masses. These maximums could be due to the influence of traffic in the area.
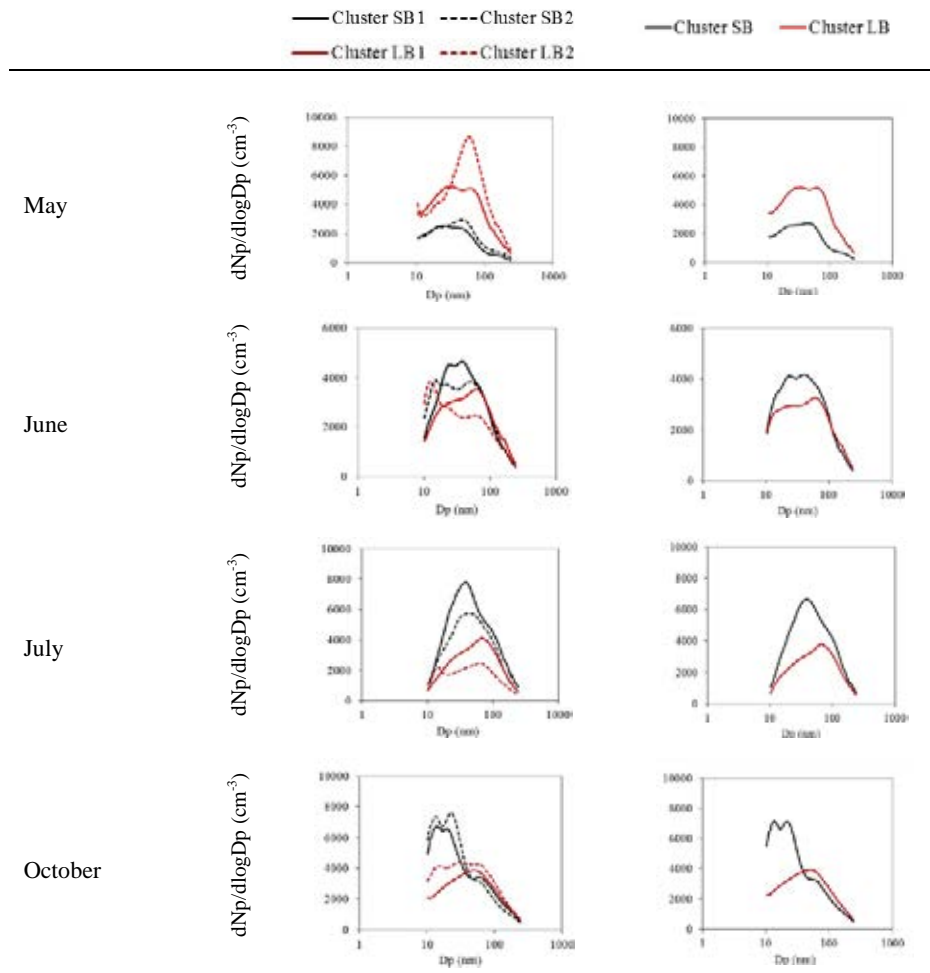
Fig. 5. Particle size distribution depending on wind direction for each studied month
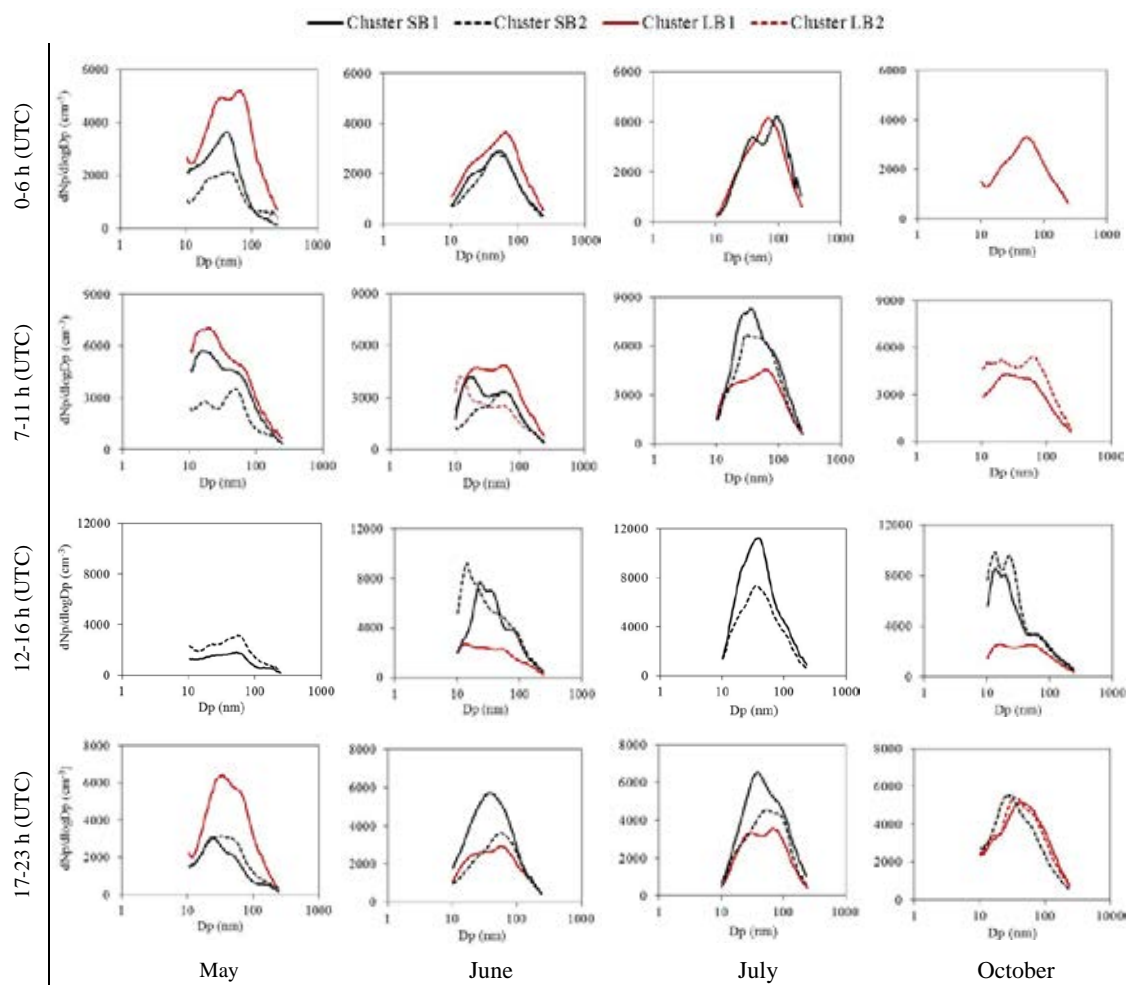
Fig. 6. Particle size distribution depending on wind direction and daily hour for each studied month
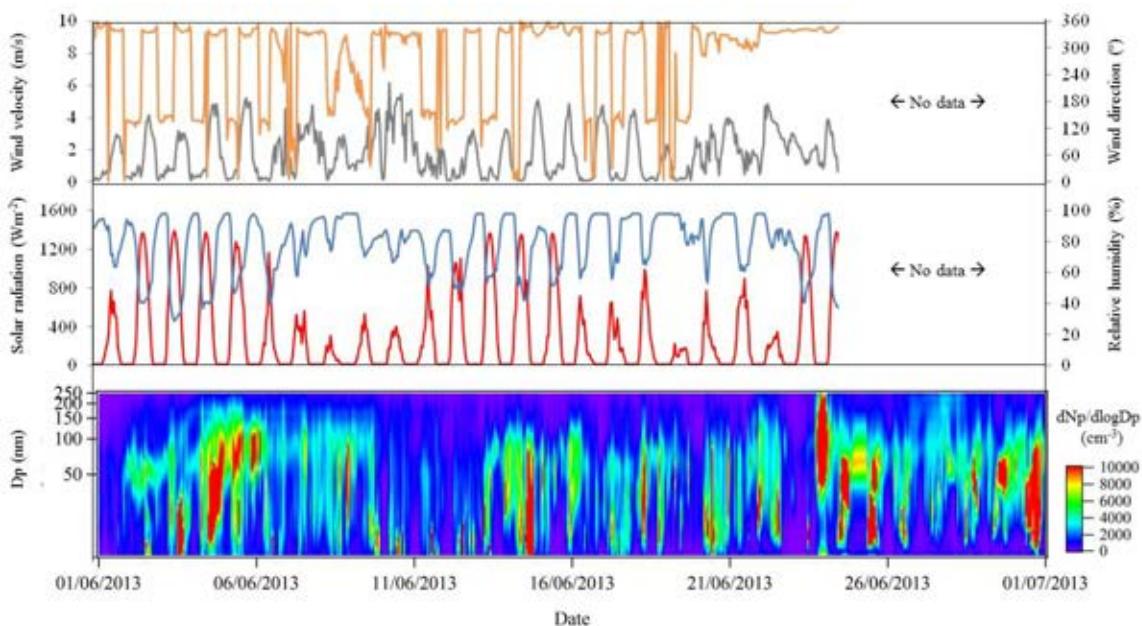
Fig. 7. Nanoparticle concentration and some meteorological conditions during June 2013.

82

Comparing results with previous years, when measurements were carried out in 2012 and 2011 too, the average number concentration during 2013 was 2605 cm^{-3} lower than during 2012 and 2011 when the average number concentrations were 3697 cm^{-3} and 3210 cm^{-3}, respectively. Generally, lower particle number concentrations were reached during summer months when atmospheric dispersion conditions were presented (e.g. sea breeze).

In 2012, a large number of nucleation events were identified, particularly during June, which was reflected in the particle size distribution (Figure 8). In fact, the results in 2012 followed a bimodal distribution with maximums in 17 and 43 nm, instead 2011 and 2013 results which showed one maximum around 40 nm both.
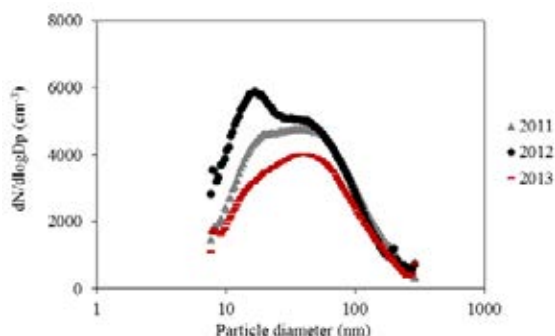
Fig. 8. Particle size distribution during 2011, 2012 and 2013.

However, during summer months, particularly in June, a large number of new particle formation events have been identified. June 2012 and 2013 presented more nucleation events than June 2011, and these processes were characterized by occur at midday, predominantly. Furthermore, the nucleation events were longer in June 2013 (2-4 h duration) than in June 2012 (1-2 h).

4   CONCLUSIONS

Evolution and levels of atmospheric nanoparticles during 2013 had been studied.

The influence of the presence of sea breeze to take place new particle formation processes had been studied, and this demonstrated that nucleation mode was presented by photochemical nucleation process with presence of sea breeze, high solar radiation, low wind velocity, low relatively humidity and at midday hours and by direct emissions, like traffic, during the rest hours, regardless the origin of air masses.

On the other hand, mean particle number during 2013 was lower than in 2012 and 2011, and particle size distribution had only one peak around 40 nm (Aitken mode).

REFERENCES

[1]   M., Cusack, A. Alastuey and X. Querol, "Case studies of new particle formation and evaporation processes in the western Mediterranean regional background," *Atmospheric Environment*, vol 81, pp. 651-659, 2013.

[2]   C. von Bismarck-Osten, W. Birmili, M. Ketzel, A. Massting, T. Petäjä and S. Weber, "Characterization of parameters influencing the spatio-temporal variability of urban particle number size distributions in four European cities," *Atmospheric Environment,* vol 77, pp. 415-429, 2013.

[3]   P. Kumar, A. Robins, S. Vardoulakis and R. Britter, "A review of the characteristics of nanoparticles in the urban atmosphere and the prospects for developing regulatory controls," *Atmospheric Environment*, vol 44, pp. 5035-5052, 2010.

[4]   C. Reche, X. Querol, A. Alastuey, M. Viana, J. Pey, T. Moreno, S. Rodríguez, Y. González, R. Fernández Camacho, A.M. Sánchez de la Campa, J. de la Rosa, M. Dall' Osto, A.S.H. Prévôt, C. Hueglin, R.M. Harrison and P. Quincey, "New considerations for PM, Black Carbon and particle number concentration for air quality monitoring across different European cities", *Atmospheric Chemistry and Physics*, vol 11, pp. 6207-6227, 2011.

[5]   I. Salma, T. Borsós, Z. Németh, T. Weidinger, P. Aalto and M. Kulmala, "Comparative study of ultrafine atmospheric aerosol within a city," *Atmospheric Environment*, vol 92, pp.154-161, 2014.

[6]   S. Rodríguez, E. Cuevas, Y. González, R. Ramos, P.M. Romero, N. Pérez, X. Querol and A. Alastuey, "Influence of the sea breeze circulation and road traffic emissions on the relationship between particle number, black carbon, PM1, PM2,5 and PM2,5-10 concentrations in a coastal city," *Atmospheric Environment*, vol 42, pp.6523-6534, 2008.

[7]   D.L. Yue, M. Hu, Z.B. Wang, M.T. Wen, S. Guo, L.J. Zhong, A. Wiedensohler and Y.H. Zhang, "Comparison of particle number size distributions and new particle formation between the urban and rural sites in the PRD region, China," *Atmospheric Environment*, vol 76, pp.181-188, 2013.

[8]   V.P. Kanawade, D.R. Benson, S.-H. Lee, "Statistical analysis of 4-year observations of aerosol sizes in a semi-rural continental environment," *Atmospheric Environment*, vol 59, pp.30-38, 2012.

Medida y caracterización de la concentración numérica (CPC) de partículas atmosféricas en la ciudad de Valladolid

A. Marcos[1], V. E. Cachorro[1], Y. Bennouna[1], M.A. Burgos[1], D. Mateos[1], J.F. López[1], S.Mogo[1,2,3], A. M. de Frutos[1]

Abstract — La importancia del estudio de los aerosoles atmosféricos radica en el impacto que estos tienen en la determinación de la calidad del aire así como en el clima. Las medidas de concentración de aerosoles "in situ" focalizan el primer aspecto, y medidas de tipo "remote sensing" son más indicadas para el segundo. En este trabajo se presenta el análisis de la concentración numérica de partículas atmosféricas a 4 km de la ciudad de Valladolid, desde junio de 2011 a junio del 2013, medidas con un CPC 3022A de la casa TSI.

El análisis de la base de datos (medidas directas y valores promedios), ha permitido observar la existencia de dos períodos anómalos y muy dispares entre sí. El período de valores más altos (junio 2011 a julio 2012), presenta un promedio diario de 9708 cm^{-3} y se ha visto afectado por la cercanía de las instalaciones a la construcción de la autovía Valladolid-Soria (800 m). El período de valores más bajos (octubre 2012 a junio 2013), con un promedio diario de 3165 cm^{-3}, puede ser representativo del fondo de la ciudad, pero ha sido peculiar por las elevadas precipitaciones en la primavera de 2013 (disminuyen la concentración). Con los valores diarios se evalúa el impacto de las obras de la autovía tomando como referencia la mediana del segundo período (2708 cm^{-3}). Es decir, se ha cuantificado la anomalía originada por dicha construcción, y aun suponiendo que en el segundo periodo la concentración media de partículas esté por debajo de un "valor más realista" debido a las precipitaciones, el aporte de la autovía ha supuesto doblar o triplicar el valor normal o habitual de la zona.

Keywords — CPC, in situ aerosols, number concentration.

1 INTRODUCCIÓN

Dada la importancia del estudio de los aerosoles por el impacto que éstos tienen, entre otros aspectos, en la calidad del aire y el clima, el Grupo de Óptica Atmosférica de la Universidad de Valladolid (GOA-UVA) dispone de un laboratorio de investigación de medida de aerosoles in-situ dotado de instrumentos de alta tecnología, cuyo objetivo es el de la caracterización y monitorización continua de las propiedades de los aerosoles representativos de un área determinada. Las propiedades que son objeto de estudio son, por una parte, las relativas a la microfísica de los aerosoles (un contador de partículas (CPC) que estudia la concentración total de partículas y un APS que estudia la distribución de tamaños micrométricas en el rango de 0.5-10 µm) y por otra, las medidas de las propiedades ópticas correspondientes a los coeficientes de "scattering" y absorción de las partículas. Todo este conjunto de medidas permiten obtener las características de los aerosoles troposféricos de la ciudad de Valladolid. Este objetivo se enmarca dentro de la temática de la "Calidad del Aire", que deben seguir las directivas comunitarias relativas a este tema [1],[2]. Aquí

presentamos, en concreto, la caracterización de la concentración numérica de partículas atmosféricas de "fondo" representativos de la ciudad de Valladolid desde junio de 2011 a junio del 2013, medidas con un CPC 3022A de la casa TSI. Específicamente realizaremos el análisis de la evolución temporal de la base de datos generada junto al estudio estadístico de estas series de datos, que enlazará con el estudio del impacto de la construcción de una autovía sobre los valores de fondo de la ciudad.

2 METODOLOGÍA

2.1 Área de estudio

La ciudad de Valladolid está situada en la meseta norte de España, (41º39'07''N, 4º43'43''O). Tiene una población entorno a los 315.000 habitantes.

El objetivo que se pretendía necesitaba una ubicación adecuada en los alrededores de la ciudad, y las instalaciones deportivas universitarias de Fuente de la Mora reunía los requisitos necesarios, ya que aunque se encuentren situadas en un entorno aparentemente rural, está cercana a la capital (3-4 km), a la autovía que rodea la ciudad (VA-20) y además está adyacente a la carretera del Valle del Esgueva, Fig. 1. Estas características son las adecuadas para el estudio representativo de los valores de "fondo" de la ciudad [3].

1. Grupo de Óptica Atmosférica, Facultad de Ciencias, Universidad de Valladolid, Paseo Belén 7, 47011, Valladolid, Spain. E-mail: amarcos@goa.uva.es

2. Departamento de Física, Universidad de Beira Interior, Covilha, Portugal. E-mail: smogo@ubi.pt

3. Instituto Dom Luiz, Portugal.

Fig. 1. Localización del laboratorio de medidas respecto al centro de la ciudad de Valladolid (zoom para localización).

2.2. Instrumento

El instrumento utilizado para la medida de la concentración numérica total (N_T) de partículas ha sido un contador de partículas condensadas (CPC) de TSI, Modelo 3022A [2],[4],[5]. Dicho instrumento forma parte del equipamiento del Laboratorio o estación de medida de aerosoles "in situ" que el Grupo de Óptica Atmosférica (GOA-UVA) dispone a las afueras de Valladolid. Este modelo posee una eficiencia de detección del 90% en partículas de 0.015 μm y del 50% para partículas de 0.007 μm. El corte superior a la entrada del sistema de muestras se fijó en 10 μm. Este laboratorio de aerosoles "in situ" dispone de los elementos necesarios así como de las comunicaciones (internet inalámbrico) para el control en tiempo real de la instrumentación y el acceso a las medidas.

2.3 Datos experimentales

La base de datos está compuesta por las muestras de la concentración de partículas registradas por el CPC con una resolución temporal de 5 minutos, 24 horas al día, desde el 16 de junio de 2011 hasta el 3 de junio de 2013. Este tipo de medidas son las primeras que se realizan en la provincia de Valladolid siendo 138569 el número total de datos registrados.
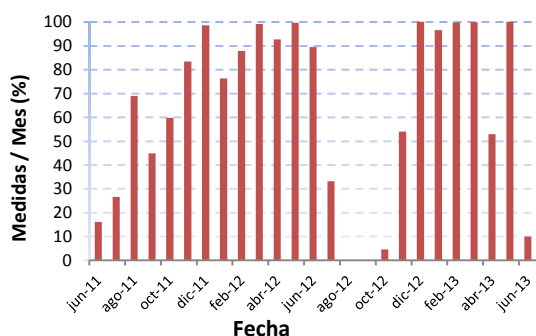
Fig. 2. Porcentaje de medidas cada mes por el CPC desde el 16 de junio de 2011 hasta el 3 de junio de 2013.

Para adquirir una visión general de la base de datos se comienza representando la proporción de los datos obtenidos sobre el máximo posible en cada mes, Fig. 2. Los intervalos temporales en los que ha habido menor número de mediciones corresponden en primer lugar con la fase de puesta a punto (junio y julio de 2011) y a diversas incidencias (cortes de luz, cierre de las instalaciones, etc...), como por ejemplo en el verano de 2012 donde no se realizaron medidas (desde el 17 de julio hasta el 30 de octubre). El resto de los meses tienen un número suficiente de medidas para alcanzar el objetivo pretendido.

3 RESULTADOS Y ANÁLISIS DE DATOS

Se va a realizar un análisis detallado de la serie de datos obtenida mediante la presentación del comportamiento temporal de la concentración numérica total de partículas (N_T) en base a un estudio estadístico convencional [6], [7], [8].

3.1 Medidas cinco-minutales
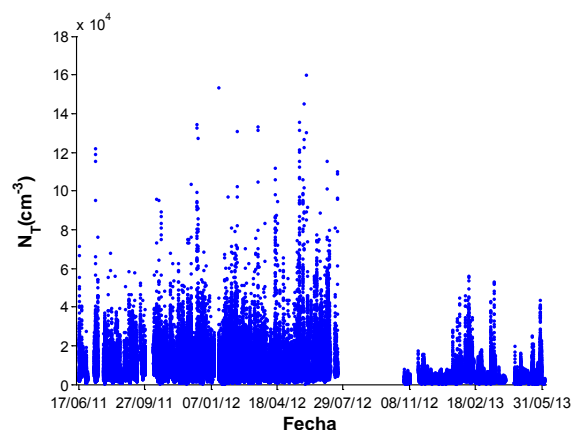
Fig. 3. Evolución de las medidas cinco-minutales durante los casi 2 años de medida.

La Fig. 3. presenta la evolución de los datos cinco-minutales durante el período de medida. En una visión inicial de esta figura se puede observar que hasta julio de 2012 se tienen los valores más altos en la concentración de partículas, que van acompañados de una gran dispersión. En el segundo período de medidas, a partir de octubre de 2012 y coincidiendo con la reanudación de la toma de datos, tanto los valores obtenidos como la dispersión disminuyen considerablemente. Es decir, los dos períodos son distintos y no tienen correlación alguna.

Ante esta diferencia entre períodos deben plantearse dos cuestiones. En primer lugar: ¿existen hechos externos a los que podamos atribuir ésta diferencia? Sí, ya que coincidiendo con el primer período de medidas se estaba construyendo a una distancia de apenas 1 km en dirección contraria al centro de la ciudad (Fig. 1) los primeros enlaces (rotonda, circunvalación, desvíos…) de la Autovía que une Valladolid y Soria. Estas obras provocaron mayor cantidad de partículas en el entorno, lo cual podía apreciarse a simple vista. Además, la carretera

del Valle Esgueva (en cuyo lateral están situadas las instalaciones deportivas universitarias donde está emplazado el laboratorio de medidas) era paso obligado para la maquinaria pesada que se usaba diariamente y sin descanso nocturno ni de fin de semana en las labores de construcción. La segunda pregunta que nos surge es: ¿de qué período son representativos los valores de la concentración de "fondo" de la ciudad de Valladolid? Si los valores del primer período han sido expuestos a agentes externos, la respuesta a esta pregunta es, por exclusión, que los valores de fondo de la ciudad de Valladolid serán los correspondientes al segundo período de medidas. Pero esto no se puede afirmar de forma rotunda y es preciso matizar que este segundo período ha sido muy peculiar debido a las condiciones meteorológicas existentes. Desde marzo hasta finales de mayo de 2013 la pluviosidad de toda la zona (al igual que la del resto de España) dio lugar a una primavera atípica. Los registros de lluvia en el mes de marzo de ese año son los mayores que se tienen en Valladolid desde que se comenzó a tener control de las precipitaciones en 1891; los de abril y mayo también fueron muy elevados. Éste hecho provocó que la concentración de partículas en este período fuera mucho menor respecto a las condiciones normales o standard.

Según lo expuesto, no se puede realizar un estudio de la serie temporal en conjunto, sino que cada período debe estudiarse por separado. En primer lugar los datos de la época de alta concentración (junio2011 - julio2012), período en el que estaba teniendo lugar la construcción de una autovía adyacente al laboratorio de medidas. Y en segundo lugar los de menor concentración (finales de octubre 2012 - junio 2013), que en principio parecen los valores de "fondo" de la ciudad de Valladolid, aunque hay que matizar la peculiaridad de la meteorología de este período (lluvias persistentes).

En la Tabla 1 se presentan los resultados de una estadística básica de cada uno de los períodos. Cabe destacar que estamos tratando datos cinco-minutales, y que éstos no son representativos de un estudio de estas características, ya que pueden aparecer eventos puntuales que modifiquen la situación habitual.

Tabla 1. Estadística de los valores cinco-minutales para cada período.

	Media (cm⁻³)	STD (cm⁻³)	P_{100} (cm⁻³)	P_0 (cm⁻³)	P_{50} (cm⁻³)	P_{10} (cm⁻³)	P_{90} (cm⁻³)
N_T Periodo1	9568	8503	160100	31	7113	2764	18983
N_T Periodo2	3118	3163	55950	337	2361	1062	5513

Se observa que, excepto el mínimo, todos los valores del primer período triplican a los del segundo, dando cuenta de la enorme disparidad existente entre ellos. El de valores más alto (junio 2011 a julio 2012), afectado por la construcción de la autovía, tiene un valor promedio de (9568 ± 8503) cm⁻³, mientras que el del segundo período, (octubre 2012 a junio 2013) es (3118 ± 3163) cm⁻³. Es decir, el valor promedio del primer período es tres veces superior al del segundo. La desviación estándar, que en el primer período representa el 88% del promedio y en el segundo más del 100%, da cuenta de la alta variabilidad (dispersión) de nuestras medidas. La mediana en cada período es menor que el valor promedio, por lo que la situación habitual de cada época ha sido la de tener valores más bajos que los proporcionados por la media. La diferencia de un orden de magnitud entre los valores máximos y el percentil 90 de cada período, (160100 vs. 18983) cm⁻³ para el primero y (55950 vs. 5513) cm⁻³ para el segundo, hace entender que esos valores son eventos puntuales con muy poca persistencia temporal. Idéntica situación se da con los mínimos.

3.2 Promedios horarios

En cuanto a la calidad de los datos, es evidente que los valores promediados son de mayor calidad que los cinco-minutales, y cuantitativamente el resultado inmediato de realizar promedios horarios ha sido el pasar de tener 138569 medidas cinco-minutales a 11683 medidas horarias distribuidas en 524 días. Estos 11683 promedios horarios representan un 74.8% de los datos horarios que teóricamente se deberían tener. De éstos, 7179 corresponden al primer período y 4504 corresponden al segundo.
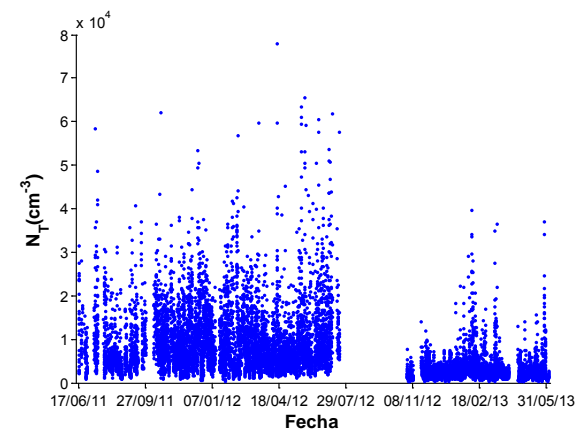
Fig. 4. Evolución de los promedios horarios.

En la Fig. 4. se observan los dos períodos diferenciados, aunque la realización de promedios da lugar a dos hechos que a primera vista son ya destacables: por una parte, el máximo de la escala ha disminuido un orden de magnitud, pasando de ser de $2 \cdot 10^5$ cm⁻³ a $8 \cdot 10^4$ cm⁻³, y por otra, se ha suavizado considerablemente la diferencia entre períodos.

Además son evidentes 3 episodios de alta concentración en el período 2, cuyo origen aún es desconocido y que se está analizando. En la Tabla 2 se presentan los parámetros estadísticos de los promedios horarios de cada uno de los períodos.

Tabla 2. Estadística de los promedios horarios para cada período

	Media (cm⁻³)	STD (cm⁻³)	P₁₀₀ (cm⁻³)	P₀ (cm⁻³)	P₅₀ (cm⁻³)	P₁₀ (cm⁻³)	P₉₀ (cm⁻³)
N_T Periodo1	9605	7417	78109	366	7597	3014	18837
N_T Periodo2	3122	3034	39795	356	2374	1084	5501

La diferencia entre períodos obtenida con los datos cincominutales (los valores del primero son 3 veces mayores que los del segundo) se mantiene tras la realización de promedios horarios, que además actúa como un primer método de filtrado de los datos cinco-minutales más abruptos, reduciendo considerablemente la diferencia entre los valores máximos, que pasan a estar en el mismo orden de magnitud (~78000 vs. ~39000) cm⁻³. Los mínimos se igualan (~360 cm⁻³), dándose en las horas habituales (noche). La gran diferencia entre los valores extremos y sus percentiles asociados (máximo-percentil90 y mínimo-percentil10) demuestra que tanto los eventos de alta como los de baja concentración han sido poco persistentes. Se mantiene la alta dispersión de los datos, existiendo un 77% de variación típica en el primer período y 97% en el segundo. Que la mediana en cada período sea menor que la media evidencia que la situación habitual de cada época ha sido la de tener valores más bajos que los proporcionados por ésta.

3.3 Promedios diarios

En total hay 524 días de medición sobre los cuales hay un porcentaje mayor del 90% en lo que se refieren a valores horarios, y de los que 332 corresponden al primer período y 192 al segundo.
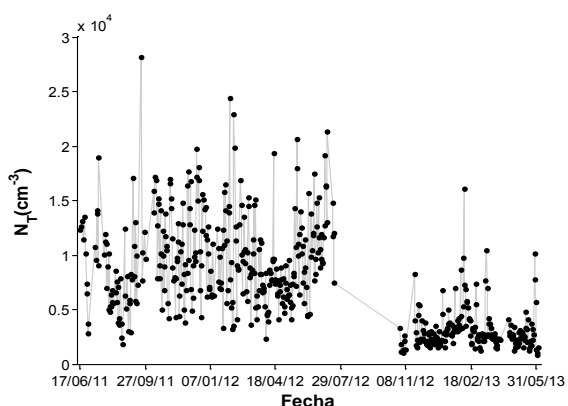
Fig. 5. Evolución de los promedios diarios.

En la Fig. 5. se observa que el límite superior del eje vertical pasa de ser de $8 \cdot 10^4$ cm⁻³ en los promedios horarios a $3 \cdot 10^4$ cm⁻³. En la Tabla 3 se presentan los parámetros estadísticos de cada uno de los períodos para estos datos diarios.

Tabla 3. Estadística de los promedios diarios para cada período

	Media (cm⁻³)	STD (cm⁻³)	P₁₀₀ (cm⁻³)	P₀ (cm⁻³)	P₅₀ (cm⁻³)	P₁₀ (cm⁻³)	P₉₀ (cm⁻³)
N_T Periodo1	9708	4188	28183	1806	9071	4898	15234
N_T Periodo2	3165	1948	16070	794	2708	1558	5398

Con la realización de los promedios se vuelve a constatar el efecto de acotamiento al que se ven sometidos los valores más abruptos cada vez que se promedia (valor máximo del primer período 28183 cm⁻³ y 16070 cm⁻³ del segundo). Los mínimos, antes iguales, ahora divergen, siendo el del primer período (1806 cm⁻³) mayor que el del segundo (794 cm⁻³), como era de esperar por el efecto que las obras de la autovía han tenido en él. Continúa la razón de diferencia 3 entre períodos, con valores promedio (9708 vs. 3165) cm⁻³, y disminuye la variabilidad de los datos (la desviación estándar del primero representa el 43% del promedio y la del segundo el 62%). La mediana en cada período es menor que el valor promedio, por lo que la situación habitual de cada época ha sido la de tener valores más bajos que los proporcionados por la media.

Realizados dos promedios (horarios y diarios) se observa que se refleja la realidad sin situaciones anómalas, la calidad de datos es más alta y la cantidad de valores es representativa (524) de tal modo que se pueden tomar estos valores diarios como referencia para ampliar información y profundizar en el análisis de los datos como veremos en el apartado 3.5.

3.4 Promedios mensuales

La imposibilidad de realizar un promedio interanual debido a la falta de una base de datos más amplia y a la no correlación entre meses de distinto período nos obliga a realizar un estudio idéntico al realizado hasta ahora, sin obtener nuevas conclusiones que las ya obtenidas previamente, como se observa en la Fig. 6. A destacar el mes de febrero de 2013, que por razones aún desconocidas aporta la tercera parte de variabilidad al total del periodo 2 rompiendo así la estabilidad de dicho período. A este respecto se comenzarán a estudiar las condiciones meteorológicas y posibles factores externos que hayan provocado esta ruptura en la estabilidad de este período.
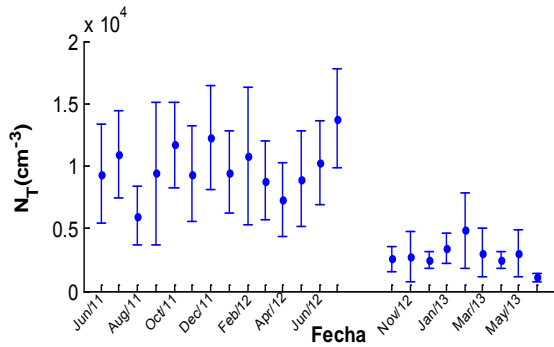
Fig. 6. Evolución de los promedios mensuales.

3.5 Cuantificación de la anomalía ocasionada por la construcción de la autovía

Con los *datos diarios* se va a cuantificar el impacto que la construcción de la autovía ha tenido en nuestra zona de medidas, y por consiguiente, en las afueras de Valladolid. Este tipo de construcción resulta de gran interés por su elevado aporte a la concentración de partículas [9].

La metodología a seguir para este fin es la siguiente:

1. Tomaremos el segundo período de medida, que es *más representativo* del "fondo" de la ciudad de Valladolid que el primero, en el que sabemos que la construcción de la autovía disparó los niveles de concentración durante el día, pero sobre todo, por la noche. Y se tiene que precisar *"más representativo"* porque no se puede afirmar que sea representativo del fondo de Valladolid ya que para hablar de "fondo" se necesita un período más largo y más estable que lo que las condiciones meteorológicas dieron (intensas lluvias).

2. Se va a tomar la mediana (2708 cm^{-3}) de los promedios diarios como valor más representativo de la situación habitual de este segundo período, y por ser, además, un valor más resistente ante datos anómalos que la media.

3. Este valor lo restamos a todos los valores diarios del primer período de medidas.

4. El resultado de recalcular los parámetros estadísticos de todos estos nuevos valores será la anomalía originada en nuestro emplazamiento por la construcción de la Autovía Valladolid-Soria.

En la Tabla 4 se presentan los valores asociados a dicha anomalía acompañados del valor que tenían sin restar el fondo (datos diarios del período 1).

Tabla 4. Estadística de los valores diarios del período 1 (azul) y de la anomalía (naranja).

	Media (cm^{-3})	STD (cm^{-3})	P$_{100}$ (cm^{-3})	P$_0$ (cm^{-3})	P$_{50}$ (cm^{-3})	P$_{10}$ (cm^{-3})	P$_{90}$ (cm^{-3})
N$_T$ Periodo1	9708	4188	28183	1806	9071	4898	15234
Anomalía	7000	4188	25475	-902	6363	2190	12526

Por tratarse de una resta, la desviación estándar no varía: la dispersión entre los valores es la misma, pero ahora éstos están desplazados una cantidad fija. Se observa que ante los valores tan elevados del primer período (afectado por la autovía), la resta de la mediana del segundo período no ejerce un gran descenso en éstos. Éste hecho es más evidente visualizando la Fig. 7, que representa la cuantificación del impacto de la autovía.
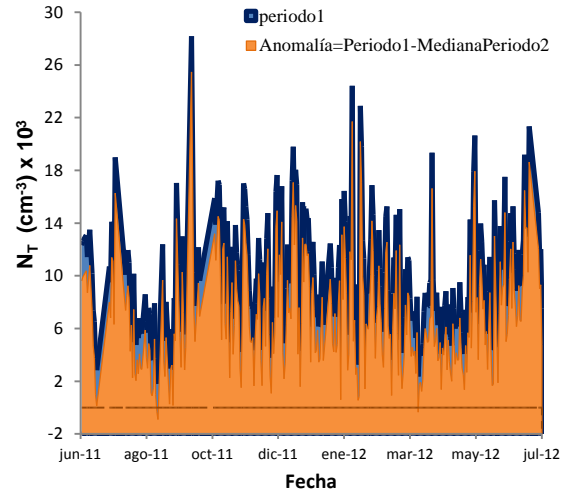
Fig. 7. Cuantificación del impacto de la autovía. El cero se representa con una línea punteada.

Hay que precisar que el eje vertical comienza en -2000 cm^{-3} y que se ha representado el cero con una línea punteada. Se observa que hay un número considerable de valores que llegan hasta cero e incluso que lo sobrepasan, lo que significa que ha habido bastantes días en este primer período que, en promedio, han tenido el mismo valor o similar al más habitual del segundo período (la mediana).

La falta de medidas durante más tiempo impide cerciorarse de si el segundo período es o no característico del fondo de Valladolid. Por esta razón no se puede extender mucho más éste resultado, pero éste hecho deja abierta una línea de investigación evidente: acumular datos de la concentración de Valladolid durante un tiempo suficiente que permita hablar de fondo.

Ahora bien, suponiendo que el fondo de Valladolid sea el dado por el segundo período y que las intensas lluvias no han afectado a la concentración numérica total de partículas (disminuyéndola), el impacto que se observa es muy elevado. Como vemos en la Tabla 4 su valor medio es de 7000 partículas por cm^3 y su mediana de 6363 cm^{-3}, valor este último que da cuenta de la cantidad de partículas que de manera habitual ha estado aportando la construcción de la autovía a los alrededores de la estación de medidas.

En resumen, aun suponiendo que en el segundo periodo la concentración media de partículas esté por debajo de un "valor más realista", el aporte de la

autovía ha supuesto doblar o triplicar el valor normal o habitual de la zona (2707 vs. 6363 cm^{-3}).

4 CONCLUSIONES

Se ha analizado la concentración numérica de partículas atmosféricas en la periferia de Valladolid durante un período aproximado de 2 años, obteniendo como principales resultados:

1. Se ha observado la existencia de dos períodos anómalos y muy dispares entre sí. El de valores más altos (junio de 2011 a julio de 12) se ha visto afectado por la construcción de la autovía Valladolid-Soria y el de valores menores (octubre de 2012 a junio de 2013), puede ser representativo del "fondo" de la ciudad, aunque ha sido peculiar por las elevadas precipitaciones en la primavera de 2013 (disminuyen la concentración).

2. Con los valores diarios se ha cuantificado el impacto de las obras de la autovía, tomando como referencia la mediana del segundo período, llegando a triplicar los valores de concentración que se asumieron como "fondo".

Este estudio preliminar [10] con los datos obtenidos entre los años 2011 y 2013 se sigue desarrollando en los siguientes aspectos:

1. En primer lugar el análisis actual que se está realizando del ciclo diurno parece indicar claramente que el comportamiento de la concentración numérica de partículas a lo largo del día para ambos períodos es el mismo. Un estudio comparativo entre ambos períodos demuestra que la razón de diferencia del valor promedio de la noche y del día es similar.

2. Con el fin de caracterizar por completo el fondo de la ciudad de Valladolid, se deben seguir acumulando datos de la concentración de partículas durante los próximos años.

3. Se deben interrelacionar estos datos con las variables meteorológicas más relevantes (temperatura, precipitación, velocidad y dirección del viento, humedad relativa, cobertura nubosa...) así como con los datos registrados en la localidad de concentración másica de partículas (PM1, PM2.5 y PM10).

4. Continuar el estudio del impacto de la construcción de la autovía con los datos suministrados por el espectrómetro APS, que da la distribución de tamaños en el rango (0.523-20) μm, así como los datos de medidas de "scattering", del que se disponen registros durante ese primer período.

REFERENCIAS

[1] Ziemba L.D., Griffin R.J. & Talbot R.W.2006. Observations of elevated particle number concentration events at a rural site in New England. Journal of Geophysical Research, 111, D23S34, doi: 10.1029/2006JD007607.

[2] Sorribas M. 2007. Medida y caracterización del aerosol atmosférico en un ambiente rural y costero del suroeste de Europa. La distribución numérica de tamaños en el rango sub-micrométrico. Dpto. de Física Teórica, Atómica y Óptica. Universidad de Valladolid. España.

[3] López, J.F. 2011. Medidas y análisis del coeficiente de scattering de aerosoles en un área de la costa Atlántica de Huelva. Dpto. de Física Teórica, Atómica y Óptica. Universidad de Valladolid. España.

[4] TSI. 2002b. Model 3022A Condensation Particle Counter. Instruction Manual.

[5] Aalto P, Hameri K, Paatero P, Kulmala M, Bellander T, Berglind N, Bouso L, CastañoVinyals G, Sunyer J, Cattani G, Marconi A, Cyrys J, von Klot S, Peters A, Zetzsche K, Lanki T, Pekkanen J, Nyberg F, Sjovall B, Forastiere F. Aerosol particle number concentration measurements in five European cities using TSI-3022 condensation particle counter over a three-year period during health effects of air pollution on susceptible subpopulations. Journal of the Air & Waste Management Association 2005; 55: 1064-1076

[6] Toledano C. 2005. Climatología de los aerosoles mediante la caracterización de propiedades ópticas y masas de aire en la estación 'El Arenosillo' de la red AERONET. Tesis Doctoral. Dpto. de Física Teórica, Atómica y Óptica. Universidad de Valladolid. España.

[7] Mogo S. 2006. Técnicas ópticas para la medida de la absorción por aerosoles atmosféricos, ejemplos de aplicación. Tesis doctoral. Dpto. de Física Teórica, Atómica y Óptica. Universidad de Valladolid. España.

[8] Rodríguez E. 2009. Caracterización de los aerosoles en la estación sub-ártica ALOMAR (69ºN, 16ºE) mediante el análisis de propiedades ópticas. Tesis Doctoral. Dpto. de Física Teórica, Atómica y Óptica. Universidad de Valladolid. España.

[9] Zhu Y., Hinds W.C, Kim S. & Sioutas C. 2002. Concentration and size distribution of ultrafine particles near a major highway. Journal of the Air & Waste Management Association, 52:9, 1032-1042

[10] Marcos A. 2013. Análisis de la concentración numérica (CPC) de partículas atmosféricas en la ciudad de Valladolid. Trabajo Fin de Máster. Dpto. de Física Teórica, Atómica y Óptica. Universidad de Valladolid. España.

Prediction of Black Carbon concentration in an urban site by means of different regression methods

C. Marcos[1], S. Segura[1], G. Camps-Valls[2], V. Estellés[1], R. Pedrós[1], P. Utrillas[1], J. A. Martínez-Lozano[1]

Abstract — Motor vehicle emissions are one of the major sources of Black Carbon (BC) in urban areas, where it contributes significantly to air pollution. However, quantifying the direct effect of traffic on BC concentration is not straightforward, since meteorological conditions may affect the distribution and transport of this pollutant. In this work we analyse the ability of four different regression methods to predict BC concentrations in the surroundings of a main highway, using traffic and meteorological data as predictors. We observe that, amongst the analysed methods, the best results are obtained with two non-linear models: Kernel Ridge Regression and Gaussian Process Regression. These results suggest that some processes affecting the BC concentration might not be properly described by linear models.

Keywords — black carbon, traffic, regression methods

1 INTRODUCTION

Black carbon (BC) aerosol is a type of carbonaceous material produced as a result of combustion processes which include motor vehicle emissions, biomass burning, and industrial activity [1]. In urban sites, BC contributes significantly to air pollution, which is one of the major environmental problems in developed countries as it has great impact on human health, visibility, and Earth's climate system [2]. BC concentrations are strongly related to local sources and affected by meteorological conditions. It has a short atmospheric lifetime (days to weeks) and it is quickly removed from the atmosphere by deposition [3].

In places close to main roads or streets where vehicles are the main source of BC, information about traffic volume together with meteorological data can be used to predict BC concentrations by means of regression methods. For example, in [4], a generalized linear model was used to relate BC concentration to traffic, temperature and wind during school dismissals. Other example is found in [5], where BC concentration was estimated by means of a linear method combined with time-series techniques, using vehicle counts and different meteorological parameters as predictors.

In this work we analyse the ability of four different regression methods to predict BC concentrations in an urban site close to a main

highway. In addition to a linear method, we also test three non-linear methods: Boosting Trees, Kernel Ridge Regression and Gaussian Process Regression.

2 DATA

The data used in this work has been obtained in the University Campus of Burjassot (39.507 N, 0.420 W), within the metropolitan area of Valencia (~1,500,000 inhabitants) in Eastern Spain. The area is mainly flat, and the measuring site is 60 m.a.s.l., less than 10km far from the Mediterranean Sea. We expect BC concentration in this site to be affected by traffic from the close-by CV-35 highway, one of the main access routes to the city (Fig. 1).

Fig. 1. Map of the measuring site showing the location of the Aethalometer (red), the meteorological station (yellow) and the CV-35 highway (pink). Copyright: 2014 Microsoft Corporation.

2.1 Black Carbon

BC concentration has been obtained using an Aethalometer AE-31, Magee Scientific. This instrument measures light attenuation at 7 different wavelengths, from 370 to 950 nm. At 880 nm, BC is the main absorber, while absorption from other aerosol compounds is negligible [6]. Therefore, this

_____

1. *Solar Radiation Group, Department of Earth Physics and Thermodynamics, University of Valencia. C/Doctor Moliner 50 Burjassot (Valencia), Spain, Carlos.Marcos@uv.es*
2. *Image Processing Laboratory (IPL) Parc Científic Universitat de València C/ Catedràtic José Beltran, 2 46980 Paterna (València). Spain*

wavelength is considered the standard channel for BC measurements.

The BC mass concentration is optically estimated by measuring the attenuation of light transmitted through a sample collected on a quartz fiber filter. Attenuation (ATN) is obtained by the variation in the transmission as the filter loads. Once the attenuation is measured, the conversion to BC mass concentration is performed using the specific attenuation cross section σ_λ (m^{2}g^{-1}). The BC concentration is obtained using the following equation:

$$BC(\lambda) = -\frac{\Delta ATN(\lambda,t)}{\Delta t} \cdot \frac{A}{V \cdot \sigma \lambda} \quad (1)$$

where A is the spot size (1.67 cm^2), V is the volume obtained as a product of the flow (4 litres/minute), and Δt is the measurement frequency (5 min). The value of σ_{880} is assumed to be 16.6 m^{2}g^{-1}, as recommended by the manufacturer [7]. No aerosol size cut-off has been used during the measurements.

2.2 Meteorological and traffic data

Four meteorological parameters that might affect BC concentration have been taken into account in this work: wind speed, wind direction, boundary layer height and boundary layer stability.

Wind speed and direction are measured by a meteorological station located in the University Campus of Burjassot and processed every 10 minutes. From the data obtained within each of these 10-minutes batches we obtain the maximum speed, mean speed, and mean direction of the wind. Boundary layer height and Pasquill Stability Classes are retrieved though the HYSPLIT model with a 3-hour resolution [8], [9], [10]. Vehicle counts in both directions of the CV-35 highway are provided by the City Council of Valencia with a 1-hour resolution. A summary of the data used in this study is shown in Table 1.

2.3 Time resolution

The time resolution of the different data sets is normalized to a 20-minute time grid. New-resolution traffic and boundary layer data are obtained by linearly interpolating the original sets. BC concentration, wind mean speed and wind mean direction data are averaged in order to reach the coarser new resolution. Finally, for the maximum wind speed we select the maximum value associated to each 20-minute interval. The new-resolution data availability is shown in Fig. 2.

3 METHODOLOGY

Four regression methods are used in this work [11], [12]: Regularized Linear Regression (RLR),

Boosting Trees (BT) [13], Kernel Ridge Regression (KRR) [11] and Gaussian Process Regression (GPR) [15], [16].

For the prediction of BC concentration at a time t_1, we use the measured BC concentration at a time t_1-Δt and the meteorological data obtained within the time interval Δt as predictors in our regression models. Results for four different time intervals have been obtained, corresponding to Δt = 60 minutes, Δt = 180 minutes, Δt = 360 minutes and Δt = 1440 minutes (24 hours). For each time interval, the models are trained with a randomly selected 25% of the available data and then tested against the remaining 75%. To avoid negative values and to reduce the effect of outliers, the logarithm of the BC concentration is used instead of the BC concentration actual value.

Table 1. List of the different parameters used in this work, with their corresponding units, source and original time-resolution. In italics: parameters obtained by means of models.

Parameter	Units	Source	Time resolution (min)
BC	nanograms/meter^3	Aethalometer	5
Wind max speed	meters/second		10
Wind mean speed	meters/second	Met. station	10
Wind direction	degrees		10
BL height	meters	HYSPLIT model	180
BL stability	Pasquill classes		180
Traffic	number of vehicles	City Council	60
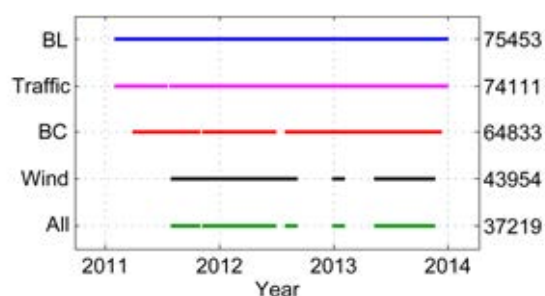
Fig. 2. Availability of the normalized-resolution data. Figures on the right stand for the number of 20-minutes data intervals available between February 2011 and January 2014.

4 RESULTS AND DISCUSSION

The comparison between the predicted and the measured BC can be seen in Fig. 3. Four statistical parameters have been retrieved from these comparisons: the linear correlation coefficient (R),

the root-mean-squared error (RMSE) and the linear fit slope (A) and intercept (B). The results of the statistical analysis are shown in Fig. 4.

Based on these parameters we can see that the best predictions of BC concentration are made by the KRR and GPR methods for all Δt considered, and that differences between these two methods are very small, always lower than the differences found between any other pair of methods. The results obtained by the BT model, although worse than those given by KRR and GPR, show better agreement with actual data than the RLR method.

If we analyse the results as a function of Δt, we can see that the best results are always obtained for the shortest interval considered (60 min). This can be explained by the high autocorrelation between BC concentrations for that time difference (Fig. 5). The biggest differences between predicted and actual data are obtained for Δt = 360min, corresponding to the lowest autocorrelation in BC concentration. However, two exceptions to this fact can be seen in the BT method, where the worst values of R and RMSE are found for the longest Δt considered (1440 min, 24h).

Fig. 3. Comparison between measured and predicted logarithm of BC concentration for all time intervals and regression methods. The linear fit results obtained for each comparison are shown with a dashed black line, while the 1:1 line is shown in red. Colours in the scatter plot represent the point density.
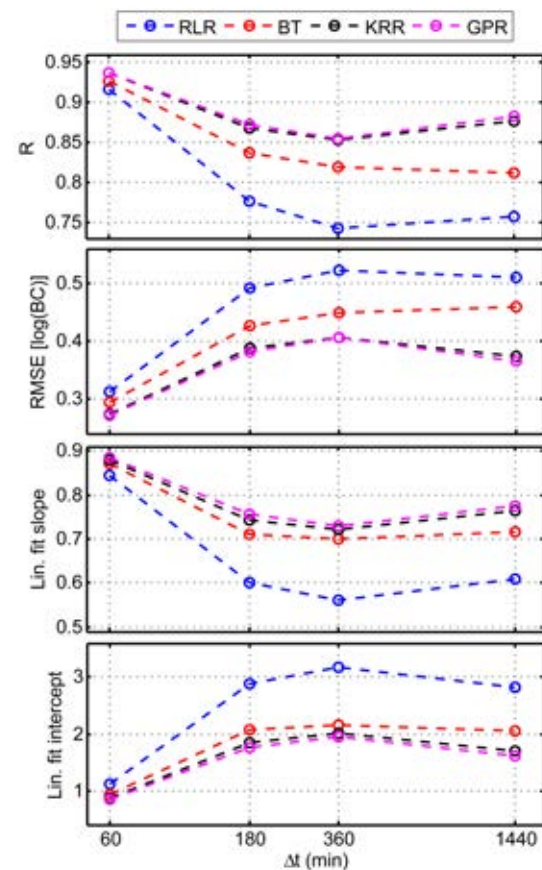
Fig. 4. Statistical parameters obtained from the comparison between the measured and predicted logarithm of BC concentration. From top to bottom: linear correlation coefficient (R), root-mean-square error (RMSE), linear fit slope and linear fit intercept. The x axis is represented in logarithmic scale.

The fact that the best results are obtained by the non-linear methods, especially by KRR and GPR, suggests the existence of some processes affecting the BC concentration that linear models are not able to completely describe.
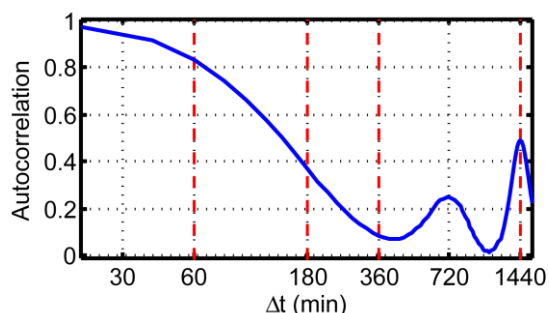
Fig. 5. Autocorrelation analysis of the BC concentration. Vertical red dashed lines show the time lags used in this study: 60, 180, 360 and 1440 min. The x axis is represented in logarithmic scale.

6   CONCLUSIONS AND FUTURE WORK

Four regression methods have been used for the prediction of black carbon (BC) concentration: Regularized Linear Regression (RLR), Boosting Trees (BT), Kernel Ridge Regression (KRR), and Gaussian Processes Regression (GPR). Traffic data, previous BC measurements and meteorological information have been used as predictors in the regression models.

The best results have been obtained by the GPR and KRR methods, while the lowest agreement with actual data has been found for the RLR model. This fact suggests that non-linear methods are able to describe some of the processes affecting the concentration of BC more accurately than linear ones.

In future works we intend to make use of these regression methods to study the effect of each individual parameter in the concentration of BC. This will allow us to estimate the effect of changes in traffic volume or meteorological conditions on this type of pollutant.

REFERENCES

[1] V. Ramanathan and G. Carmichael, "Global and regional climate changes due to black carbon", *Nature Geoscience*, vol. 1, pp. 221 – 227, March 2008

[2] M. Z. Jacobson, "Strong radiative heating due to the mixing state of black carbon in atmospheric aerosols", *Nature,* vol. 409, pp. 695 – 697, Feb 2001.

[3] T. C. Bond et al. "Bounding the role of black carbon in the climate system: A scientific assessment", *J. Geophys. Res. Atmos.*, vol. 118, pp. 5380 – 5552, Jun 2013

[4] J. Richmond-Bryant, C. Saganich, L. Bukiewicz, and R. Kalin, "Associations of PM2.5 and black carbon concentrations with traffic, idling, background pollution, and meteorology during school dismissals", *Sci Total Environ*, vol 407, issue 10, pp. 3357-3364, May 2009

[5] B. R. deCastro, L. Wang, J. N. Mihalic, P. N. Breysse, A. S. Geyh, T. J. Buckley, "The longitudinal dependence of black carbon concentration on traffic volume in an urban environment", *J. Air Waste Manag. Assoc*, vol 58, issue 7, pp. 928-939, July 2008

[6] B.A. Bodhaine, "Aerosol absorption measurements at Barrow, Mauna Loa and the south pole", *J. Geophys. Res*, vol 100, issue D5, pp 8967–8975, May 1995.

[7] A. D. A. Hansen, "The Aethalometer™" http://www.mageesci.com/images/stories/docs/Aethalometer _book_2005.07.03.pdf   Magee Scientific Company, Berkeley, California, USA, 2005. (URL link 2014)

[8] R. R. Draxler, and G.D. Hess, "Description of the HYSPLIT_4 modeling system", NOAA Tech. Memo. ERL ARL-224, NOAA Air Resources Laboratory, Silver Spring, MD, USA, Dec 1997.

[9] R. R. Draxler, and G.D. Hess, "An overview of the HYSPLIT_4 modeling system of trajectories, dispersion, and deposition", *Aust. Meteor. Mag*, vol 47, pp 295-308, Jan 1998.

[10] R. R. Draxler, and G.D. Rolph, "HYSPLIT (HYbrid Single-Particle Lagrangian Integrated Trajectory) Model access via NOAA ARL READY Website" http://ready.arl.noaa.gov/HYSPLIT.php , NOAA Air Resources Laboratory, Silver Spring, MD, USA, 2014. (URL link 2014)

[11] G. Camps-Valls, L. Gómez-Chova, J. Muñoz Marí, M. Lázaro-Gredilla and J. Verrelst, "A simple educational Matlab toolbox for statistical regression", http://www.uv.es/gcamps/code/simpleR.html , June 2013. (URL link 2014)

[12] M. Lazaro-Gredilla, M.K. Titsias, J. Verrelst and G. Camps-Valls, "Retrieval of Biophysical Parameters With Heteroscedastic Gaussian Processes", *Geoscience and Remote Sensing Letters*, IEEE , vol.11, no.4, pp.838,842, April 2014

[13] J. Elith1, J. R. Leathwick T. Hastie, "A working guide to boosted regression trees", *J Anim Ecol*, vol. 77, issue 4, pp 802-813, July 2008

[14] G. Camps-Valls, J. Muñoz-Marí, L. Gómez-Chova, L. Guanter and X. Calbet, "Nonlinear Statistical Retrieval of Atmospheric Profiles from MetOp-IASI and MTG-IRS Infrared Sounding Data", *IEEE Trans. Geosci. Remote Sensing*, vol. 50, issue 5, pp 1759 – 1769, April 2012.

[15] C. E. Rasmussen and C. K. I. Williams, "Gaussian Processes for Machine Learning", New York, NY, USA: MIT Press, 2006.

[16] J. Verrelst, L. Alonso, G. Camps-Valls, J. Delegido, and J. Moreno, "Retrieval of vegetation biophysical parameters using Gaussian process techniques," *IEEE Trans. Geosci. Remote Sens.*, vol. 50, no. 5, pp. 1832–1843, May 2012.

Relation between the cloud radiative forcing and the aerosol optical depth

M.D. FREILE-ARANDA[1], J.L. GÓMEZ-AMO [1,2], M.P. UTRILLAS[1], J.A. MARTÍNEZ-LOZANO[1]

Abstract — Clouds are one of the most important factors that regulate the Earth's climate. They interact scattering and absorbing solar and thermal radiation. Because of this interaction, clouds modify the quantity of radiation that reaches the Earth's surface. The cloud radiative forcing (CRF) accounts for the changes that clouds produce on net radiation and it is defined as the difference between the net radiation in all sky and clear sky conditions. Another important factor is the presence of aerosols, because they interact with the radiation too, but differently from clouds. They can directly scatter or absorb radiation, but also alter the microphysical properties of clouds, so the radiative effects of clouds will change.

In this work we analyse the influence of aerosols on the cloud radiative forcing at surface and the top of the atmosphere (TOA), using the aerosol optical depth (AOD) and considering the shortwave and longwave spectral regions. This way, we have studied how the AOD affects the radiative properties of clouds at the Iberian Peninsula from March of 2000 to December of 2012.

All the data employed in this work has been obtained from CERES. CERES (Clouds and Earths Radiant Energy System) is an instrument on board of the satellite Terra and Aqua which provides global estimations of the radiative fluxes of the atmosphere, clouds properties and other atmospheric characteristics. Some of these measurements are provided by the instrument MODIS (Moderate Resolution Imaging Spectrometer), located on Terra and Aqua too, as it happens with the aerosol information. To calculate the cloud radiative forcing we will use the shortwave and longwave fluxes given by CERES at surface, while the aerosol optical depth is provided by MODIS. The spatial resolution of the data used is of 1° longitude x 1° latitude, while the temporal resolution is daily.

Results show us that the CRF does not suffer large changes when the AOD at 470nm increases when we consider the longwave radiation. On the contrary in the case of the shortwave radiation, the AOD can produce an increase of 60W/m^2 on the CRF, what proves the impact of aerosols on the cloud radiative forcing.

Keywords — Aerosol optical depth, CERES, cloud radiative forcing.

1 INTRODUCTION

Clouds are one of the most important factors that modify the Earth-atmosphere radiative budget. Their interaction with the radiation is produced by scattering and absorbing solar and thermal radiation. The role of clouds for the climate system can be described by the radiative forcing, defined as the net change of radiative fluxes under all-sky and clear-sky conditions. Using this concept, clouds produce a cooling effect concerning shortwave radiation, while the opposite heating effect is observed for longwave radiation. Their resulting over-all effect for the Earth-atmosphere climate system is cooling [1].

Another important factor that intervenes in the Earth's radiation budget is the presence of aerosols. Aerosols are tiny particles in the atmosphere produced by both natural processes and anthropogenic activities [2]. As clouds, they interact with radiation when it crosses the atmosphere. Their effects on radiation can be differentiate as direct and indirect. Through the direct effect they scatter solar radiation back to space [3], altering the radiative balance of the Earth-atmosphere system [4]. Within the indirect effects, the aerosols alter clouds properties in two ways: a) the increase in "cloud albedo" when an increase in the aerosol load produces an increase of droplet concentration and a decrease of droplet size with no variation on liquid water content [5]; b) the impact on the precipitation efficiency, since a reduction of cloud droplets due to a great aerosol load may reduce the precipitation resulting in an increase of clouds lifetime [6].

The cloud radiative forcing is closely related with their properties. Therefore, as a consequence of modifying cloud properties, the aerosol impact the cloud radiative forcing too [7], [8].

_____

1. Departamento de Física de la Tierra y Termodinámica, Universidad de Valencia, Dr. Moliner 50 Burjassot (Valencia), E-mail: M.Dolores.Freile@uv.es .

2. Laboratory for Earth Observations and Analyses, ENEA, Rome.

A lot of studies have investigated the clouds-aerosols interaction and its origin. In Mauger and Norris [9], it is examined the influence of the meteorological history in the relationship between aerosol optical depth (AOD) and cloud fraction

On the other side, Li et al. [2] conclude that using a long period of data, the influence of meteorological variability on clouds is minimized and conversely the impact of aerosols becomes evident.

In this work, we use a 13-year database to quantify the aerosol impact on the cloud radiative forcing taking into account the shortwave and longwave spectral ranges. The analysis is carried out in terms of aerosol optical variations and it has been evaluated either at surface as at the top of the atmosphere (TOA).

2 DATA

The CERES level 3 data have been used for this study. The product CERES_SYN1deg_Day Ed3A provides the radiative fluxes at TOA and the surface. It is coincident with the MODIS-derived cloud properties and aerosol properties [10]. The parameters have been analysed on a daily basis and the spatial resolution is 1º longitude x 1º latitude. The study region is the Iberian Peninsula, so the CERES product is chosen covering a surface with latitudes varying between 44º and 35.5º and a longitudes from -9.70º to 4.40º. Data provided by Terra and Aqua platforms from March 2000 to December 2012 have been used. Therefore, 353679 daily data have been used in the statistical analysis.

Specifically, the parameters employed here are the TOA and surface fluxes for all-sky and clear sky and the aerosol optical depth (AOD) at 470nm.

3 METHODOLOGY

3.1 Cloud radiative forcing

The cloud radiative forcing (CRF) has been obtained as the difference between the net radiation in all-sky and clear-sky conditions. In this work we will study the longwave and shortwave cases separately. In addition, the total cloud radiative effect, defined as the sum of longwave and shortwave effects, has been studied.

To obtain the CRF at surface (SUR), it must be taken into account the upward ($F_{LW}^{\uparrow}$ and $F_{SW}^{\uparrow}$) and downward fluxes ($F_{LW}^{\downarrow}$ and $F_{SW}^{\downarrow}$). Equations (1), (2) and (3) describe this parameter for the longwave, shortwave and total spectral regions, where the superscripts all and clear mean all-sky and clear-sky situations, respectively.

$$CRF_{LW}^{SUR} = \left(F_{LW}^{\downarrow} - F_{LW}^{\uparrow}\right)^{all} - \left(F_{LW}^{\downarrow} - F_{LW}^{\uparrow}\right)^{clear} \text{ (1)}$$

$$CRF_{SW}^{SUR} = \left(F_{SW}^{\downarrow} - F_{SW}^{\uparrow}\right)^{all} - \left(F_{SW}^{\downarrow} - F_{SW}^{\uparrow}\right)^{clear} \text{ (2)}$$

$$CRF_{TOTAL}^{SUR} = CRF_{LW}^{SUR} + CRF_{SW}^{SUR} \text{ (3)}$$

On the other hand, to calculate CRF at the top of the atmosphere (TOA) we only consider the upward fluxes, since the downward fluxes are the same for the all-sky and clear-sky. We use the equations (4), (5) and (6).

$$CRF_{LW}^{TOA} = (F_{LW}^{\uparrow})^{clear} - \left(F_{LW}^{\uparrow}\right)^{all} \text{ (4)}$$

$$CRF_{SW}^{TOA} = (F_{SW}^{\uparrow})^{clear} - \left(F_{SW}^{\uparrow}\right)^{all} \text{ (5)}$$

$$CRF_{TOTAL}^{TOA} = CRF_{LW}^{TOA} + CRF_{SW}^{TOA} \text{ (6)}$$

Once we know the CRF, the upper and lower 5% extreme values of each situation (longwave, shortwave and total spectral regions at surface and TOA) are not taken into account in our study, so atypical values of CRF will be avoid.

3.2 Aerosol optical depth

The AOD data is provided by a CERES product. More than the 90% of AOD data are distributed from 0.025 to 0.5 (Fig.1). To analyse the CRF dependency on AOD, the CRF changes have been averaged every 0.005 units of AOD. The standard deviation has been also obtained.
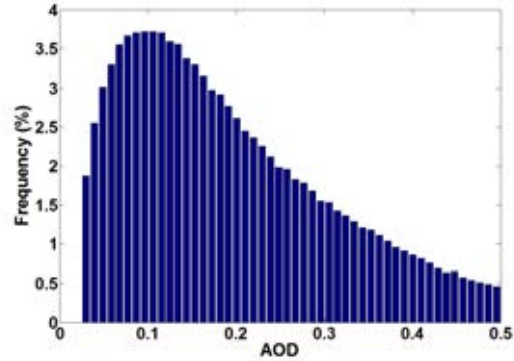
Fig 1. AOD values distribution at the Iberian Peninsula since year 2000 to 2012.

4 RESULTS

In table 1 mean values of CRF during the studied period for the entire Iberian Peninsula at surface and TOA are presented. Little differences are observed between CRF at surface and TOA, which are independent on the spectral range. The shortwave effect is larger than the longwave effect indicating that the cloud albedo is more important than the cloud absorption. Consequently, the clouds produce a net cooling effect of -12.7 and -14.5 W/m² at surface and TOA respectively. In addition, a net energy loss of -1.8 W/m², within the atmosphere, is obtained as CRF^{TOA} – CRF^{SUR}.

Table 1. Mean values of longwave, shortwave and total CRF at surface, TOA and atmosphere for the Iberian Peninsula along 13 years (2000-2012).

	CRF_{LW} (W/m^2)	CRF_{SW} (W/m^2)	CRF_{TOTAL} (W/m^2)
SURFACE	26.9	-39.6	-12.7
TOA	21.1	-35.6	-14.5
ATMOSPHERE	-5.8	4	-1.8

4.1 Longwave

The aerosol impact on the longwave range is only important when large particles or great aerosol load are involved. Therefore, a very limited effect on the CRF is observed in the longwave spectral region since in this work the AOD values are lower than 0.5. The CRF_{LW} show a little dependency on AOD at both surface and TOA (Fig. 2 and 3 respectively). A similar CRF_{LW} variation of around 15 W/m^2 is observed at surface and TOA from AOD 0.025 to 0.5.
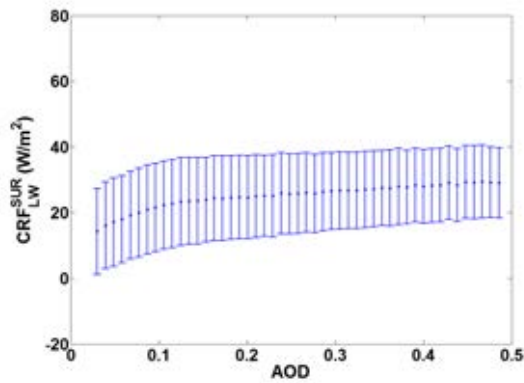
Fig. 2. Longwave cloud radiative forcing at surface as a function of the aerosol optical depth at 470nm.
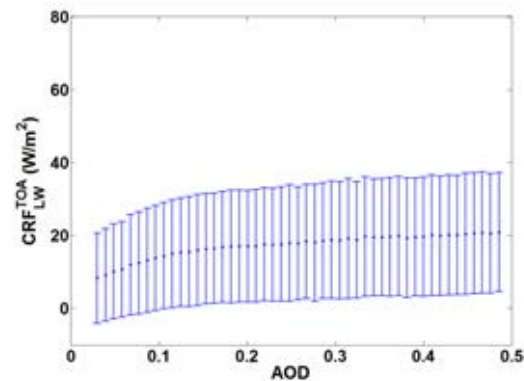
Fig. 3. Longwave cloud radiative forcing at the top of the atmosphere as a function of the aerosol optical depth at 470nm.

In Table 2 it can be found the mean and median values for the CRF_{LW}, their standard deviation and standard error. The large standard deviation in all

figures can be explained by the fact that all types of clouds are considered. Since their properties are different, this will be reflected on its radiative effects [11]. In contrast, the low standard error is a consequence of using a great data amount. Similar results will be found on the shortwave and total spectral range.

Table 2. Mean, median, standard deviation and standard error of the CRF_{LW} for different AOD intervals at surface and TOA at the Iberian Peninsula (2000-2013).

CRF_{LW} (W/m^2)	AOD	Mean	Median	Std Dev	Std Error
SUR	0-0.1	18.74	16.09	13.53	0.05
	0.1-0.2	23.67	22.65	13.11	0.04
	0.2-0.3	25.60	24.98	12.26	0.05
	0.3-0.4	27.27	26.85	11.55	0.06
	0.4-0.5	28.91	28.77	11.07	0.08
TOA	0-0.1	11.50	5.94	13.67	0.05
	0.1-0.2	15.95	11.62	15.08	0.05
	0.2-0.3	17.80	14.51	15.66	0.06
	0.3-0.4	19.35	16.93	16.17	0.09
	0.4-0.5	20.35	18.64	16.48	0.12

4.2 Shortwave

If we focus on the shortwave range, now the dependency of the CRF_{SW} on AOD is larger than in CRF_{LW}. In Fig. 4 it is represent how the CRF_{SW} value decreases from -10W/m^2 to -50W/m^2 at surface when the AOD increases from 0.025 to 0.5. Thus the change produced in the CRF_{SW} is close to the 40W/m^2. No significant differences are observed at surface and TOA in the shortwave ranges. A similar CRF decreases with AOD is obtained (Fig. 5) indicating that the large is aerosol load the more is the contribution of aerosol to CRF.
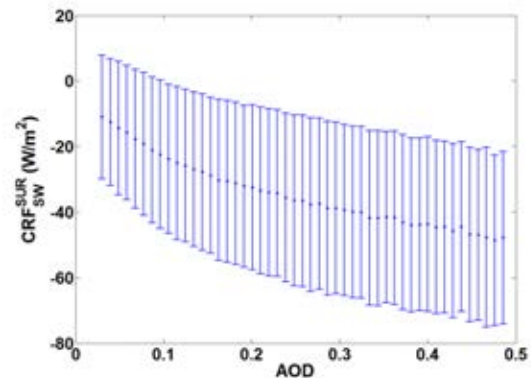
Fig. 4. Shortwave cloud radiative forcing at surface as a function of the aerosol optical depth at 470nm.
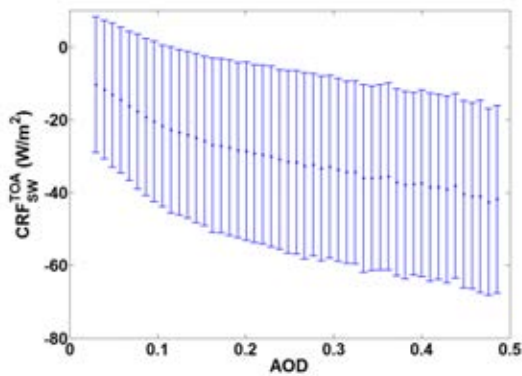
Fig. 5. Shortwave cloud radiative forcing at the top of the atmosphere as a function of the aerosol optical depth at 470nm.
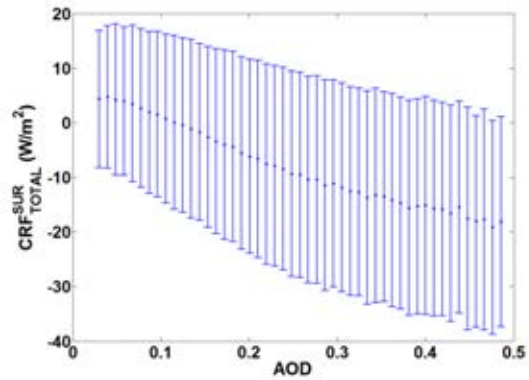
Table 3. Mean, median, standard deviation and standard error of the CRF_{SW} for different AOD intervals at surface and TOA at the Iberian Peninsula (2000-2013).

CRF_{SW} (W/m²)	AOD	Mean	Median	Std Dev	Std Error
	0-0.1	-17.28	-7.53	21.38	0.08
	0.1-0.2	-28.02	-20.22	24.06	0.08
SUR	0.2-0.3	-35.71	-29.15	25.94	0.11
	0.3-0.4	-41.41	-36.62	26.42	0.14
	0.4-0.5	-46.2	-43.1	26.4	0.2
	0-0.1	-15.96	-6.34	20.78	0.08
	0.1-0.2	-25.19	-17.53	23.37	0.08
TOA	0.2-0.3	-31.05	-25.05	24.96	0.10
	0.3-0.4	-35.68	-31.38	25.4	0.14
	0.4-0.5	-40.03	-37.27	25.73	0.19

4.3 Total wavelength range

Finally, the total CRF variation with the AOD at surface and TOA is shown in Fig. 6 and 7. A net shortwave effect is prevalent in the total range since the change in the CRF_{TOTAL} is about 20W/m², which is the net effect of AOD over clouds. Also in this case, the aerosol impact at surface and TOA is similar.

Fig. 6. Total cloud radiative forcing at surface as a function of the aerosol optical depth at 470nm.
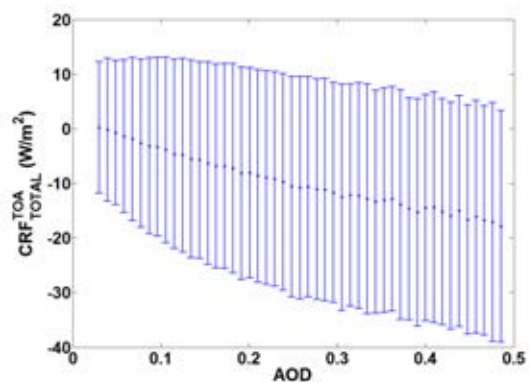
Fig. 7. Total cloud radiative forcing at the top of the atmosphere as a function of the aerosol optical depth at 470nm.

Table 4. Mean, median, standard deviation and standard error of the CRF_{TOTAL} for different AOD intervals at surface and TOA at the Iberian Peninsula (2000-2013).

CRF_{TOTAL} (W/m²)	AOD	Mean	Median	Std Dev	Std Error
	0-0.1	3.25	3.42	14.16	0.05
	0.1-0.2	-2.12	1.31	16.66	0.05
SUR	0.2-0.3	-8.8	-3.37	18.67	0.08
	0.3-0.4	-13.52	-9.16	19.38	0.1
	0.4-0.5	-17.01	-14.16	19.79	0.15
	0-0.1	-1.81	-0.43	14.72	0.06
	0.1-0.2	-5.9	-2.99	18.27	0.06
TOA	0.2-0.3	-9.95	-7.13	19.94	0.08
	0.3-0.4	-13.14	-11.12	20.68	0.11
	0.4-0.5	-15.97	-14.9	21.08	0.16

5 CONCLUSIONS

In this work we have studied the effect of AOD on the CRF at surface and TOA, and also considering shortwave or longwave spectral range in the Iberian Peninsula, using a 13-year satellite data base (2000-2012). The CRF increases in absolute value with the AOD. Therefore in general, aerosols enhance the cloud radiative effect either this being a cooling (shortwave) or heating (longwave) effect.

The aerosol impact in the longwave is almost negligible and changes in AOD produced a CRF variation of 10 W/m^2. On the contrary, the CRF variations due to aerosols in the shortwave range reach the 40 W/m^2.

Similar CRF dependency on AOD was observed at surface and TOA, which was independent of the considered spectral range.

In future studies, more accurate results can be obtained if different cloud types are distinguished, considering that their properties have an important influence on cloud radiative effects [11]. Thus try to minimize the large standard deviation presented on all our results.

ACKNOWLEDGMENT

REFERENCES

[1] T. Cori, T. Peter, "A simple model for cloud radiative forcing," Atmos. Chem. Phys. Discuss., vol. 9, pp. 5751-5758, 2009.

[2] Z. Li, F. Niu, J. Fan, Y. Liu, D. Rosenfeld, Y. Ding, "Long-term impacts of aerosol son the vertical development of clouds and precipitation," Nature Geoscience, vol. 4, pp. 888-894, 2011.

[3] A. Jones, D.L. Roberts and A. Slingo, "A climate model study of indirect radiative forcing by anthropogenic sulphate aerosols," Nature, vol. 370, pp. 450-453, Aug. 1994.

[4] J. Haywood, O. Boucher, "Estimates of the direct and indirect radiative forcing due to tropospheric aerosols: a review," Reviews of Geophysics, vol. 38, 4, pp. 513-543, 2000.

[5] S. Twomey, "Pollution and the planetary albedo," Atmospheric Enviroment, vol. 8, pp. 1251-1256, 1974.

[6] B.A. Albrecht, "Aerosols, Cloud Microphysics, and Fractional Cloudiness," Science, vol. 245, pp. 1227-1230, 1989.

[7] D. Mateos, M. Antón, A. Valenzuela, A. Cazorla, F.J. Olmo, L. Alados-Arboledas, "Short-wave radiative forcing at Surface for cloudy systems at a midlatitude site," Tellus B, vol. 65, 21069, 2013.

[8] D. Mateos, M. Antón, A. Valenzuela, A. Cazorla, F.J. Olmo, L. Alados-Arboledas, "Efficiency of clouds on shortwave radiation using experimental data," Applied Energy, vol. 113, pp. 1216-1219, 2014.

[9] G.S. Mauger, J.R. Norris, "Meteorological bias in satellite estimates of aerosol-cloud properties," Geophysical research letters, vol.34, L16824, 2007.

[10] B.A. Wielicki, B.R. Barkstrom, E.F. Harrison, R.B. Lee III, G.L. Smith and J.E. Cooper, "Clouds and the Earth's Radiant Energy System (CERES): An Earth Observing System Experiment," Bull. Amer. Meteor. Soc., vol. 77, pp.853-868.

[11] T. Cheng, W.B. Rossow, Y. Zhang, "Radiative Effects of Clouds-Type Variations," Journal of Climate, vol. 13, pp. 264-286.

[12] H. Yan, Z. Li, J. Huang, M. Cribb, J. Liu, "Long-term aerosol-mediated changes in cloud radiative forcing of deep clouds at the top and bottom of the atmosphere over the Southern Great Plains," Atmos. Chem. Phys. Discuss., vol. 14, 4599-4625, 2014.

Study Cases of Shrinkage Events of the Atmospheric Aerosol

E. Alonso-Blanco*, F.J. Gómez-Moreno, L. Núñez, M. Pujadas and B. Artíñano

Abstract — Two shrinkage events of particles identified in a urban background station of Madrid are discussed in this work. The first occurs during the growth phase of the newly formed particles and the second in the absence of a prior nucleation. These events have been identified in the summer period, towards the end of the day. An increase of the wind speed triggers the displacement of semivolatile species from the particle phase to gas phase producing a shrinkage. The estimated particle shrinkage rates were 6.7 and 4.7 nm·h^{-1} respectively, for each process identified.

Keywords — Meteorological Conditions, New Particle Formation (NPF), Shrinkage Events, SMPS

1 INTRODUCTION

The aerosol size is one of the most important properties in relation to the study of aerosols and their implications for air quality, human health and climate. This property is conditioned by the generating sources and the formation processes, as well as by the transformations that particles may suffer during their stay in the atmosphere [1].

Aerosol size determines many of the characteristics of the aerosol as its hygroscopicity or its optical properties [1] and consequently the processes involved, related to air quality, visibility, human health as the ability to enter the respiratory system [2] or to atmospheric processes such as activation of cloud condensation nuclei [3], [4].

Shrinkage events are analyzed in very few studies. These processes are identified mainly associated with new particle formation (NPF), during the growth phase of the newly nucleated particles [5], [6], [7] although we have identified in the literature only two studies on shrinkage processes in the absence of a previous process of particle growth [5], [8].

Shrinkage events have been documented in measurement areas with rather different characteristics. Young et al. [7] observed shrinkage processes in an urban site under a subtropical climate, [5] in a regional background station under a Mediterranean climate, [8] in an urban background site under a subtropical climate and [6] in a coastal suburban site under a subtropical climate.

These processes are attributed fundamentally to:
1) Displacement from the particle phase to gas phase as a result of the dilution of the chemical species involved in the growth of the newly formed particles [9].
2) Evaporation of water and/or semivolatile species associated to dilution processes and temperature changes, especially when the condensation process or the chemical reactions involved in the growth of particles are reversible [10].

Both physical and chemical mechanisms are associated with changes in meteorological conditions, mainly an increase of wind speed and temperature.

Particle shrinkage is usually accompanied by dilution of the particle concentration corresponding to the nucleation mode (D_p<30 nm) [5], [6], [7]. Changes in concentrations of aerosol due to dilution processes have been identified by several authors [11], [12] observing negative correlations between wind velocity and aerosol concentration.

The NPF and its causes have been already studied in Madrid [13]. However there is a certain amount of uncertainties concerning the transformations that the newly formed particles suffer in the atmosphere. Shrinkages have been identified during newly nucleated particle growth and also in the absence of NPF.

In this work it is presented a detailed study of two events of shrinkage: a NPF+shrinkage case and a shrinkage one. With this aim, the evolution of the particle concentration, the estimation of the condensation sink (CS), the sulfuric acid concentration in gas phase, the growth/evaporation rate and the impact of meteorological variables have been analyzed.

2 MEASUREMENT AREA

The measurements interpreted in this work have been carried out at an urban background station located in the CIEMAT facilities (40°27′23.2″N, 03°43′32.3″E). This zone is located northwest of the city of Madrid, surrounded by natural areas.

At a regional scale the city, located at an average altitude of 650-700 m asl, is within an airshed

―――――――――――――――

E. Alonso-Blanco, F.J. Gómez-Moreno, L. Núñez, M. Pujadas and B. Artíñano belong to Department of Environment, Research Center for Energy, Environment and Technology (CIEMAT), Avda. Complutense 40, 28040, Madrid, Spain. E-mail: elisabeth.alonso@ciemat; fj.gomez@ciemat.es; lourdes.nunez@ciemat.es; manuel.pujadas@ciemat.es; b.artinano@ciemat.es.*

bordered by the Central System, both in the North and the Northeast.

The low industrial activity taking place within the metropolitan area and the high population density, 5000 inhabitants/km^2, cause that the main sources of pollutants, both particulate and gaseous compounds, are motor vehicles and heating devices [14].

The Madrid climate is Continental Mediterranean influenced by the geographical surrounding of the city.

3 MATERIALS AND METHODS

3.1 Data Acquisition

3.1.1 Scanning Mobility Particle Size (SMPS)

An SMPS installed at CIEMAT facilities allowed us to measure atmospheric particle size distribution in the size range 15-660 nm during the summer of 2010.

This equipment is composed by a **D**ifferential **M**obility **A**nalyser (TSI-SMPS: **DMA** 3081), connected to Condensation Particle Counter (CPC; TSI Model 3775). The neutralizer used was a radioactive source: ^{85}Kr with an activity of 2 mCi.

Both the instrument control and the data acquisition software have been carried out by a software program **AIM** (**A**erosol **I**nstrument **M**anager) developed by **TSI** Company. The temporal resolution is 4.5 min.

The total number of particles (N_t) and particle concentrations for each of the three modes; nucleation ($N_{<30}$ nm), Aitken (N_{30-100} nm) and accumulation ($N_{>100}$ nm) have been obtained from aerosol size distributions.

3.1.2 Meteorological Data

Meteorological data have been provided by a meteorological station installed about 70 m distance from the sampling point.

This station measures wind speed, wind direction, temperature, precipitation, solar radiation, relative humidity (RH) and pressure. Data are recorded automatically every 10 min.

3.1.3 Further Measurements

A **D**ifferential **O**ptical **A**bsorption **S**pectrometer (**DOAS**: OPIS AR-500) was used to chemically characterize the gaseous pollutants (NO, NO$_2$ and O$_3$), in the air masses arriving at the sampling point.

The CIEMAT DOAS has a total atmospheric light-path of 228 m on average 10 m agl. The temporal resolution of the equipment for the whole species measured is about 7 min.

Furthermore, data provided by the air quality monitoring network of the city of Madrid have also been used in this work. The SO$_2$ concentration data were obtained in the suburban station of Casa de Campo (3º 44' 50.44" W, 40º 25' 09.68" N, 645 m asl). This station is located about 5 km CIEMAT. The choice of this air quality station was determined by the similarity found between the concentrations of SO$_2$ measured in Casa de Campo station and those obtained in various campaigns carried out in CIEMAT. The SO$_2$ concentration was supplied with an hourly temporal resolution.

The DOAS database has been completed with data of NO$_2$ and O$_3$ corresponding to the Casa de Campo station for those days with absence of data due to maintenance or equipment failure. This station does not provide data for NO.

3.2 Shrinkage Events Analysis

3.2.1 Identification of New Particle Formation and Shrinkage

The identification of NPF processes has been made based on the methodology developed by [15] and used by others authors as [5] and [13]. This methodology has also allowed the identification of shrinkage processes of particles, because it facilitates the observation of the trend of the particle size.

Furthermore, during these events both growth and evaporation rate as outlined [16] were calculated. The calculation was made from the mode/s of the size distributions averaged every 15 minutes, (D_{mode}). The aerosol size distributions were fitted to a lognormal function to estimate the mode.

3.2.2 Calculation of the Condensation Sink

The aerosol condensation sink (CS) determines how rapidly molecules will condense onto pre-exiting aerosols [17]. The particles formation by nucleation processes requires low CS values indicating the presence of a low concentration of preexisting particles. The CS has been calculated according to [18] and is defined by the following expression:

$$CS = 2\pi D \sum_i^0 \beta_{M.i} d_p N_i \quad (1)$$

Where CS is the "condensation sink" (unit s^{-1}), D is the diffusion coefficient; $\beta_{M.i}$ is the transitional correction factor, d_p is the particle diameter and N_i is the particle number concentration for each size discrete.

3.2.3 Estimation of H$_2$SO$_4$ Concentration

Many authors suggest that the gas-phase sulphuric acid is the main contributor to NPF [19], [20], [21]. During the NPF event analyzed, the sulfuric acid concentration has been estimated following the model developed by [22]:

$$[H_2SO_4] = 8.21 \times 10^{-13} * \kappa * Radiation * [SO_2]^{0.62} * (CS * RH)^{-0.13}$$
$$(2)$$

Where $[H_2SO_4]$ is the estimated concentration of sulfuric acid in the gas phase measured in molec·cm^{-3}, κ is the reaction rate constant, which is calculated according to Eq. (3) in [22], and is scaled by multiplying it with 10^{12} (m^{2}W^{-1}s^{-1}), *Radiation* is global radiation (W·m^{-2}), $[SO_2]$ is the measured SO$_2$ concentrations (molec·cm^{-3}), CS is the condensation sink (s^{-1}), and RH is the relative humidity (%).

4 RESULTS AND DISCUSSION

4.1 NPF+Shrinkage Event

A process of shrinkage preceded by NPF of type Ia according to the methodology developed by [15] was identified the 3rd August 2010. The event lasted a total of 14.5 h; distributed in 10 h of NPF and 4.6 h of shrinkage (Fig. 1).

The period in which the event took place corresponds to summer. It is in this season and in spring when NPF have been identified to mainly occur in this measurement area [13]. The environmental conditions during both periods were optimal for their development. On the one hand, chemical compounds which allowed the initiation of nucleation processes, such as sulphuric acid and ammonium in gas-phase, were available in the atmosphere. Most of authors who study these processes as [21], [23] and [24] identified the sulfuric acid in gas-phase as the main compound involved in the NPF. According to the methodology developed by [22] for the estimation of sulfuric acid in gas-phase, the availability of this species during NPF analyzed in this study is high because this compound followed the same pattern as the solar radiation. On the other hand, the environmental conditions of relative humidity and irradiance [1] were suitable for the development of nucleation processes.

Finally, the presence of a higher concentration of volatile organic compounds as a result of the enhanced vegetation activity during this season contributed to the growth of freshly nucleated particles [25], allowing its observation.

Temperature and relative humidity (RH) maintained typical daily values for summer in these latitudes, with daily mean values of 24.3±4.9 ℃ and 45±21 % respectively.

During this study day, significant transports of particulate matter from emissions traffic were not observed, neither during the first period of the morning, (between 06:00 and 08:00 UTC, approximately), nor during the last period of the afternoon (between 21:00 and 22:00 UTC, approximately). In this sense they did not followed the typical daily pattern in this area observed by [13].

Furthermore the concentration of NO, trace compound from primary anthropogenic emissions, kept low and roughly constant throughout the day, 4.8±2.1 µg·m^{-3}. The NO$_2$ concentration had a greater fluctuation throughout the study day associated with the photochemical activity, with an average daily value of 10.8±7.1 µg·m^{-3}. Average daily concentration for O$_3$ was 78.2±22.5 µg·m^{-3}. This pollutant followed the typical daily pattern as a result of its formation by photochemical activity, with high values during the period of increased solar radiation and low values during the period of less solar radiation. The average O$_3$ concentration during NPF was 101.0±13.2 µg·m^{-3} (period of increased solar activity, between 09:30 and 19:30 UTC on 3rd July 2010) and during shrinkage was 72.9±5.2 µg·m^{-3} (period of less solar activity between 19:30 on 3rd July 2010 and 00:00 UTC on 4th July 2010). These gaseous compounds, both NO$_2$ and O$_3$, are involved in the chemistry of NO [1].

A NPF started at 09:30 UTC and lasted until 19:30 UTC. When the nucleation began D$_{mode}$ was 19.6 nm and at the end reached 64.5 nm, with a growth rate of 4.6 nm·h^{-1}.

The wind speed and direction remained constant during NPF with a dominant component ENE-NE and an average wind speed of 2.2±0.7m/s, i.e. no atmospheric dilution conditions.

Nucleation began under conditions of high solar radiation, 676 W·m^{-2}, and low condensation sink, 4.9×10^{-3} s^{-1}. The latter had an increasing trend until shrinkage started at which time reaches a maximum value of 1.5×10^{-2} s^{-1}.

CS behavior observed in this work is in accordance with those shown by other studies focused on NPF, [5], [6], [7] and [26]. This is due to two factors: an increase in the concentration of particles and an increase of their size, thus facilitated the condensation of the gases present in the atmosphere on aerosols.

The total concentration of particles suffered a significant increase during the NPF. In the first hours, while the particles were nucleating, the nucleation mode was the main contributor to the total concentration of particles. At 09:30 UTC (time at which nucleation began) the concentration of particles corresponding to this mode was 1272 particles·cm^{-3}, observing the maximum concentration at 12:39 UTC, when it reached the value of 7586 particles·cm^{-3}.

The particles corresponding to Aitken mode also suffered a simultaneous increase but with a significant displacement with respect to observed increase for mode nucleation.

While at 09:30 UTC the particle concentration for Aitken mode was higher than that observed for nucleation mode, 1480 particles·cm^{-3}, when the nucleation mode reached maximum concentration, the particles concentration corresponding to Aitken mode was 3589 particles·cm^{-3} and it was not until 13:52 UTC when the particles concentration of both modes was similar, around 5400 particles·cm^{-3}. Such

situation was possibly associated with a process of growth of newly nucleated particles by coagulation

or condensation processes.
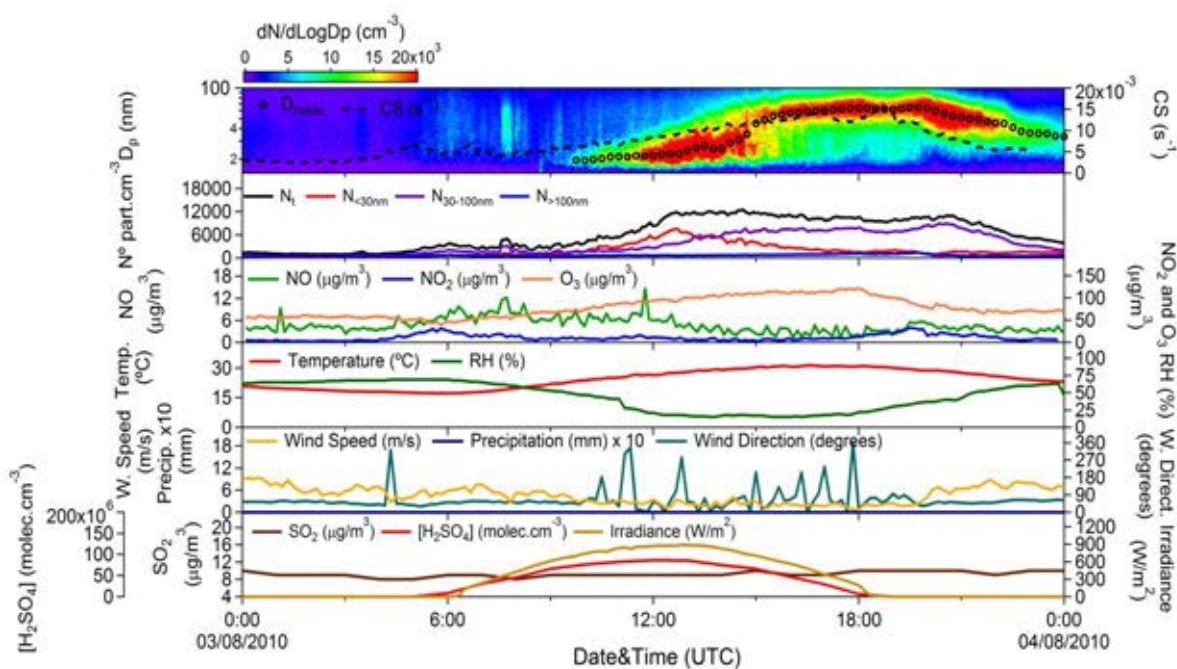
Fig. 1. Evolution of the aerosol size distributions, the total number of particles (N_t) and particle concentration for each of the three modes; nucleation ($N_{<30}$ nm), Aitken (N_{30-100} nm) and accumulation ($N_{>100}$ nm), CS, particle mode diameter (D_{mode}), NO, NO_2 and O_3 concentrations and estimation of [H_2SO_4] and the meteorological conditions (temperature (ºC), relative humidity (%), wind speed (m/s), wind direction (degrees), precipitation (mm) and irradiance (W/m^2) on 3rd August 2010.

The particles concentration corresponding to accumulation mode remained more or less constant throughout the event. The behavior of the total concentration of particles and corresponding to the different modes during the NPF is typical of these processes [27], [28], [29].

Numerous authors have identified NPF in different measurement sites under similar conditions to those described in this work [12], [26], [30], [31] coinciding its formation with the hours of higher photochemical activity.

Shrinkage was observed from 19:30 UTC and ended at 00:00 UTC on 4th August. The increase of wind speed since 19:30 UTC triggered the shrinking process.

The wind speed increased from 2.2±0.7m /s during NPF to 6.6±1.5 m/s during shrinkage, while the wind direction kept the same dominant component observed during NPF, i.e. ENE-NE.

Between 19:30 and 00:00 UTC, the D_{mode} and CS decreased from 64.5 to 33.3 nm (evaporation rate of 6.7 nm·h^{-1}) and 1.5×10^{-2} to 5.3×10^{-3} s^{-1}, respectively. The reversal of particle growth was due to loss of the semivolatile fraction of the aerosol as a result of a partial displacement of the particle phase to gas phase due to air dilution triggered by the significant increase of the wind speed. Young et al. [7] identified these processes associated with an increase in wind speed and temperature. Yao et al.

[6] made it with a decrease in the photochemical activity, the result of a reduction in the generation of atmospheric gases to form or grow new particles. In the current case the temperature did not appear to be a factor determining in the formation of shrinkage, as it occurred at the end of the day when solar radiation was low and consequently also the temperature.

During shrinkage there was a clear dominance of the Aitken mode, on the nucleation mode and the latter on the accumulation mode. This situation is usual in the study area [13]. The total concentration of particles was not affected by increasing wind speed. It was around 10000 particles cm^{-3} from the early hours of the shrinkage until 20:47 UTC.

At this time a significant reduction of the concentration of particles corresponding to the Aitken mode occurred and consequently a reduction in the concentration of total particles. This reduction of the particle concentration was not associated with changes in the meteorological conditions.

4.2 Shrinkage Event

A shrinking process was observed on the 5th July 2010 (Fig. 2) during the last hours of the day, between 18:00 on 5th July 2010 and 00:00 UTC on 6th July 2010. The event also occurred during summer.

The average temperature and RH between 18:00 and 00:00 UTC was 29.7±2.7 ºC and 58±0.7 % respectively. The average wind speed was 5.8±0.7 m/s and wind direction maintained the characteristic pattern of the study area, northeasterly flows were generated at the end of the day conditioned by the geography of the zone [32].

The physico-chemical characteristics of the air masses have been documented through data on NO_2 and O_3 provided by the air quality automatic station of Casa de Campo. The average concentration of O_3 and NO_2 between 18:00 and 00:00 UTC was 15.9±8.8 and 103.6±27.8 µg·m^{-3} respectively. A high concentration of NO_2, between 21:00 UTC and 00:00 UTC, were observed as a result of traffic emissions, reaching the NO_2 concentration 21.8±6.7 µg·m^{-3}.

At 18:30 UTC there is an increase in the total concentration of particles resulting from the transport of material from the city of Madrid to the study area associated with particle emissions from anthropogenic activity. At 19:15 the total concentration of particles exceeded 10000 particles·cm^{-3}. Between 19:15 and 21:45 D_{mode} was around 53 nm, approximately. The average wind speed during this period was 5.8±0.4 m/s with a NE dominant directional component.

At 21:45 UTC, while the wind direction kept the NE dominant component, a slight increase in wind speed with an average value for the period of 6.3±0.6 m/s triggers the shrinkage. This caused a D_{mode} reduction from 54.2 nm achieved at 21:45 UTC to 41.8 nm at 00:00 UTC on 6th July 2010. The evaporation rate during shrinkage was of 4.7 nm·h^{-1}. Cusack el at. [5] and Vehkamäki et al. [26] also identified shrinkages in the absence of a previous process of nucleation, mainly associated with an increased temperature.

The shrinkage was accompanied by a process of dilution of particle concentration. While between 19:15 and 21:15 UTC it was 12162±2044 particles·cm^{-3}, during the period of shrinkage was 9696±519 particles·cm^{-3}. This decrease in the particle concentration was also observed in the three modes.
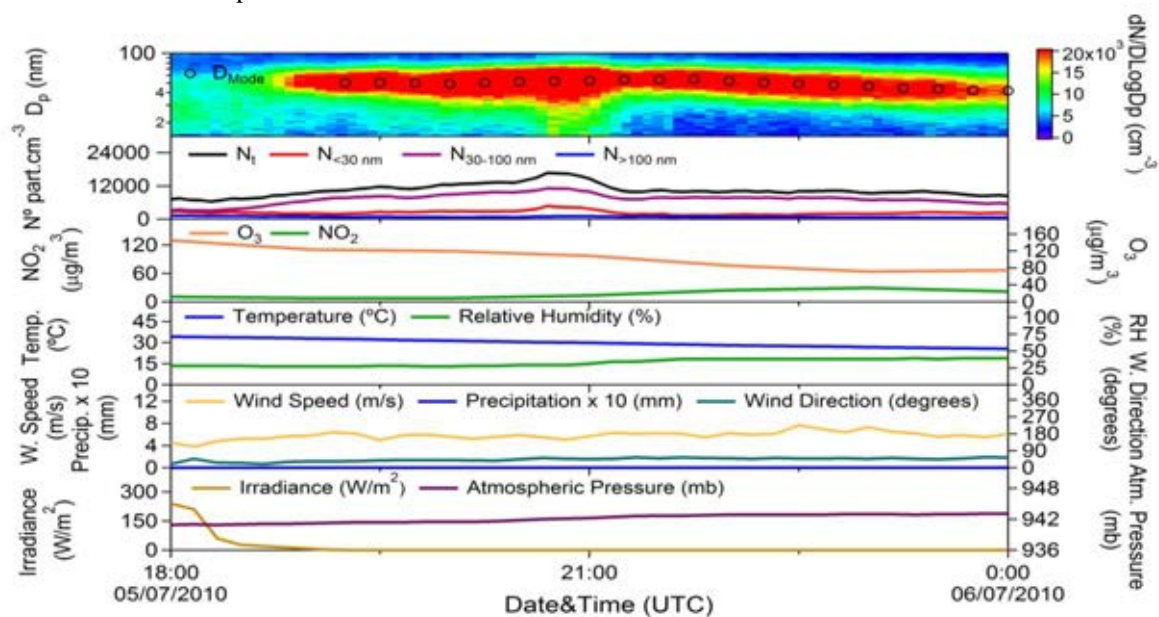
Fig. 2. Evolution of the aerosol size distributions, the total number of particles (N_t) and particle concentration for each of the three modes; nucleation ($N_{<30}$ nm), Aitken (N_{30-100} nm) and accumulation ($N_{>100}$ nm), particle mode diameter (D_{mode}), concentration of NO_2 and O_3 and the meteorological conditions (temperature (ºC), relative humidity (%), wind speed (m/s), wind direction (degrees), precipitation (mm), irradiance (W/m^2) and atmospheric pressure (mb) on 5th July 2010.

5 CONCLUSIONS

This study provides a detailed analysis of two shrinkage events: after a NPF and in absence of nucleation

In both events the shrinkage was associated with an increase in the wind speed which triggers the shift of condensed semivolatile species from particle phase to gas phase.

REFERENCES

[1] J.H. Seinfeld, S.N. Pandis, "Atmospheric chemistry and physics: from air pollution to climate change," John Wiley & Sons, 2012.

[2] G. Oberdärster, E. Oberdärster, J. Oberdärster, "Nanotoxicology: an emerging discipline evolving from studies of ultrafine particles," *Environ. Health Persp.*, vol. 113, 2005.

[3] U. Dusek, G.P. Frank, L. Hildebrandt, J. Curtius, J. Schneider, S. Walter, D. Chand, F. Drewnick, S. Hings, D. Jung, "Size matters more than chemistry for cloud-nucleating ability of aerosol particles," *Science*, vol. 312, pp. 1375-1378, 2006.

[4] H.W. Gaggeler, "Size dependent aerosol activation at the high-alpine site Jungfraujoch (3580 m ASL)," *Volume V General Energy*, vol. 115, 2001.

[5] M. Cusack, A. Alastuey, X. Querol, "Case studies of new particle formation and evaporation processes in the western Mediterranean regional background," *Atmos. Environ.*, vol. 81, pp. 651-659, 2013.

[6] X. Yao, M.Y. Choi, N.T. Lau, A.P.S. Lau, C.K. Chan, M. Fang, "Growth and shrinkage of new particles in the atmosphere in Hong Kong," *Aerosol Sci. Technol.*, vol. 44, pp. 639-650, 2010.

[7] L.H. Young, S.H. Lee, V. Kanawade, T.C. Hsiao, B.F. Hwang, Y.J. Liou, H.T. Hsu, P.J. Tsai, "New particle growth and shrinkage observed in subtropical environments," *Atmos. Chem. Phys.*, vol. 13, pp. 547-564, 2013.

[8] J. Backman, L.V. Rizzo, J. Hakala, T. Nieminen, H.E. Manninen, F. Morais, P.P. Aalto, E. Siivola, S. Carbone, R. Hillamo, "On the diurnal cycle of urban aerosols, black carbon and the occurrence of new particle formation events in springtime São Paulo, Brazil," *Atmos. Chem. Phys.*, vol. 12, pp. 11733-11751, 2012.

[9] K.M. Zhang, A.S. Wexler, Y.F. Zhu, W.C. Hinds, C. Sioutas, "Evolution of particle number distribution near roadways. Part II: the "Road-to-Ambient" process," *Atmos. Environ*, vol. 38, pp. 6655-6665, 2004.

[10] R. Zhang, A. Khalizov, L. Wang, M. Hu, W. Xu, "Nucleation and growth of nanoparticles in the atmosphere," *Chem. Rev. Columbus*, vol. 112, pp. 1957, 2012.

[11] E.L. Agus, D.T. Young, J.J.N. Lingard, R.J. Smalley, J.E. Tate, P.S. Goodman, A.S. Tomlin, "Factors influencing particle number concentrations, size distributions and modal parameters at a roof-level and roadside site in Leicester, UK," *Sci. Total Environ.*, vol. 386, pp. 65-82, 2007.

[12] Y. Zhu, T. Kuhn, P. Mayo, W.C. Hinds, "Comparison of daytime and nighttime concentration profiles and size distributions of ultrafine particles near a major highway," *Environ. Sci. Technol.*, vol. 40(8), pp. 2531-2536, 2006.

[13] F.J. Gómez-Moreno, M. Pujadas, J. Plaza, J.J. Rodríguez-Maroto, P. Martínez-Lozano, B. Artiñano, "Influence of seasonal factors on the atmospheric particle number concentration and size distribution in Madrid," *Atmos. Environ.*, vol. 45, pp. 3169-3180, 2011.

[14] P. Salvador, B. Artíñano, M. Viana, A. Alastuey, X. Querol, "Evaluation of the changes in the Madrid metropolitan area influencing air quality: Analysis of 1999-2008 temporal trend of particulate matter," *Atmos. Environ.*, vol. 57, pp. 175-185, 2012.

[15] M. Dal Maso, M. Kulmala, I. Riipinen, R. Wagner, T. Hussein, P.P. Aalto, K.E.J. Lehtinen, "Formation and growth of fresh atmospheric aerosols: eight years of aerosol size distribution data from SMEAR II, Hyytiala, Finland," *Boreal Env. Res.*, vol. 10, pp. 323, 2005.

[16] M. Kulmala, T. Petäjä, T. Nieminen, M. Sipilä, H.E. Manninen, K. Lehtipalo, M. Dal Maso, P.P. Aalto, H. Junninen, P. Paasonen, "Measurement of the nucleation of atmospheric aerosol particles," *Nature protocols*, vol. 7, pp. 1651-1667, 2012.

[17] L. Pirjola, M. Kulmala, M. Wilck, A. Bischoff, F. Stratmann, E. Otto, "Formation of Sulphuric Acid Aerosols and Cloud Condensation Nuclei: An Expression for Significant Nucleation and Model Comprarison," *J. Aerosol Sci.*, vol. 30, pp. 1079-1094, 1999.

[18] M. Kulmala, M. Maso, J.M. Mäkelä, L. Pirjola, M. Väkevä, P. Aalto, P. Miikkulainen, K. Hämeri, C.D. O'Dowd, "On the formation, growth and composition of nucleation mode particles," *Tellus B*, vol. 53, pp. 479-490, 2001.

[19] V. Fiedler, M.D. Maso, M. Boy, H. Aufmhoff, J. Hoffmann, T. Schuck, W. Birmili, M. Hanke, J. Uecker, F. Arnold, "The contribution of sulphuric acid to atmospheric particle formation and growth: a comparison between boundary layers in Northern and Central Europe," *Atmos. Chem. Phys.*, vol. 5, pp. 1773-1785, 2005.

[20] M. Kulmala, A. Laaksonen, "Binary nucleation of water-sulfuric acid system: Comparison of classical theories with different H2SO4 saturation vapor pressures," *J. Chem. Phys.*, vol. 93, pp. 696-701, 1990.

[21] I. Kusaka, Z.G. Wang, J.H. Seinfeld, "Binary nucleation of sulfuric acid-water: Monte Carlo simulation," *J. Chem. Phys.*, vol. 108, pp. 6829-6848, 1998.

[22] S. Mikkonen, S. Romakkaniemi, J.N. Smith, H. Korhonen, T. Petäjä, C. Plass-Duelmer, M. Boy, P.H. McMurry, K.E.J. Lehtinen, J. Joutsensaari, "A statistical proxy for sulphuric acid concentration," *Atmos. Chem. Phys.*, vol. 11, pp. 11319-11334, 2011.

[23] M. Kulmala, L. Pirjola, J.M. Mäkelä, "Stable sulphate clusters as a source of new atmospheric particles," *Nature*, vol. 404, pp. 66-69, 2000.

[24] P. Korhonen, M. Kulmala, A. Laaksonen, Y. Viisanen, R. McGraw, J.H. Seinfeld, "Ternary nucleation of H2SO4, NH3, and H2O in the atmosphere," *J. Geophys Res.: Atmospheres (1984-2012)*, vol. 104, pp. 26349-26353, 1999.

[25] R. Zhang, I. Suh, J. Zhao, D. Zhang, E.C. Fortner, X. Tie, L.T. Molina, M.J. Molina, "Atmospheric new particle formation enhanced by organic acids," *Science*, vol. 304, pp. 1487-1490, 2004.

[26] H. Vehkamäki, M.D. Maso, T. Hussein, R. Flanagan, A. Hyvärinen, J. Lauros, P. Merikanto, M. Mönkkönen, K. Pihlatie, K. Salminen, "Atmospheric particle formation events at Värriö measurement station in Finnish Lapland 1998-2002," *Atmos. Chem. Phys.*, vol. 4, pp. 2015-2023, 2004.

[27] H. Guo, D.W. Wang, K. Cheung, Z.H. Ling, C.K. Chan, X.H. Yao, "Observation of aerosol size distribution and new particle formation at a mountain site in subtropical Hong Kong," *Atmos. Chem. Phys.*, vol. 12, pp. 9923-9939, 2012.

[28] J. Du, T. Cheng, M. Zhang, J. Chen, Q. He, X. Wang, R. Zhang, J. Tao, G. Huang, X. Li, "Aerosol Size Spectra and Particle Formation Events at Urban Shanghai in Eastern China," *Aerosol Air Qual. Res.*, vol. 12, pp. 1362-1372, 2012.

[29] B. Zhu, H. Wang, L. Shen, H. Kang, X. Yu, "Aerosol spectra and new particle formation observed in various seasons in Nanjing," *Adv. Atmos. Sci.*, vol. 30, pp. 1632-1644, 2013.

[30] M.J. Dunn, J.L. Jiménez, D. Baumgardner, T. Castro, P.H. McMurry, J.N. Smith, "Measurements of Mexico City nanoparticle size distributions: Observations of new particle formation and growth," *Geophys Res Lett.*, vol. 31, 2004.

[31] H.C. Cheung, L. Morawska, Z.D. Ristovs, "Observation of new particle formation in subtropical urban environment," *Atmos. Chem. Phys.*, vol. 11, 2011.

[32] P. Salvador, "Characterization of air pollution produced by particles in suspension in Madrid". Doctoral Thesis. Faculty of Physics, University Complutense of Madrid, Madrid (Spain), 2004.

Study of the industrial emissions impact on air quality of the city of Cordoba

Y. González-Castanedo[1], M. Avilés[1], J. Contreras González[2], C. Fernández[2], J.D. de la Rosa[1]

Abstract — A regional study shows how the maximum Cu, Zn and Cd levels of Andalusia (South of Spain) were registered in Lepanto, an urban background site located in Cordoba city. These levels were higher than ones registered in historical industrial polluted areas such as Huelva or the strait of Gibraltar. In this study we carried out an intensive measurement campaign with the aim of investigating the relationship between several metallurgic airborne emissions and the geochemical anomalies observed at the city. The results show how geochemical anomalies (Cu, Zn, Pb and Cd, specially) observed in the ambient air samples collected in the city are closely related to the geochemical profile obtained in the stack and fugitive metallurgy emissions.

Keywords — metallurgy, stack emissions, fugitive emissions, urban pollution

1 INTRODUCTION

Cordoba is one of the main touristic destinations located in the South of Spain in Andalusia region. The city has a population around 300.000 inhabitants and road traffic may be considered its main source of air pollution [1],[2]. However, a regional study carried out by de la Rosa et al., [3] shows how the maximum Cu, Zn and Cd levels of Andalusia region were registered in Lepanto, an urban background site located in Cordoba city. These levels were higher than ones registered in historical industrial polluted areas such as Huelva [4] or the strait of Gibraltar [5].

In this study we carried out an intensive multi-sampling campaign (stack, fugitive emissions, and ambient air measurements) in October 2012 with the aim of investigating the relationship between several metallurgic airborne emissions and the geochemical anomalies observed at the city since 2007 to present.

2 METHODOLOGY

2.1 Study area

The industrial state is located to the west of the city of Cordoba. Several populated areas are situated relative close to the north and east of the metallurgy installations (Fig. 1). Nowadays, there are three active factories in the industrial involved in copper and brass metallurgy. The main final product is copper rod by electrolytic copper smelting and brass ingots or bars by brass and other materials (e.g. Cu, Zn, Pb) scrap and shavings smelting.

Fig. 1 also includes the wind rose inlet during sampling campaign. Cordoba city is located downwind of the industrial source with respect to the SW-SSW prevailing wind direction channelled through Guadalquivir river valley.
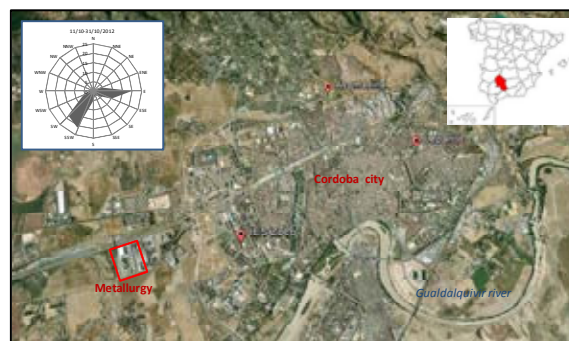
Fig. 1. Ambient air monitoring sites and metallurgy area in the city of Cordoba.

2.2 Sampling strategies

An aerosol sampling campaign using multidisciplinary techniques (stack and fugitive emissions and ambient air measurements) was performed between 11th and 31st October 2012 in Cordoba city:

a) Stack emissions sampling: Individual PM sample (1 hour) from the chimney stacks in the three metallurgical industries were isokinetically obtained using a Napp 31-200TC particulate sampling probe using the standard EPA Reference Method, with particles being retained in a heating filter. A total of 5 stack emissions samples from the three, brass and copper, metallurgical industries were collected. The main stages of the process such as smelting furnace and drying shavings emissions were tested. The effectiveness of this methodology to characterize refinery [6] or smelter [7] atmospheric stacks emissions has already been tried and tested.

b) Fugitive emissions sampling: These problematic emissions defined as not canalized gases that arise and escape via openings in the installation, spread near ground level and have an impact on the immediate environment. The characterization of fugitive emissions inside the installations were daily (24 hours) sampled was performed with a high volume sampler equipped with a Total Suspended Particle (TSP) inlet that was located close to the furnace melting. The characterization of the impact of fugitive emissions on the ground outside the industrial point source was performed using two high volume transportable air sampler (MCV) equipped with a PM10 and PM2.5 inlets which was placed at the public street in the industrial estate. Sampling periods were made with about 2 hours resolution, as long as the emissions were impacting on the ground. The main aim of the ground level impact measurement in and around the industry was to evaluate the metal and metalloid released from potential fugitive emissions.

c) Ambient air sampling: three sites were set up for measuring and sampling PM_{10} with a 24-hour resolution (Lepanto, Asomadilla and Zoco sites; Fig.1). Lepanto and Asomadilla sites belong to the Andalusia Autonomus Air Quality Network. "Lepanto" was selected as urban background reference station because it has a historical record of chemical composition of PM10 since 2007. "Asomadilla" is located in the big urban park of the same name and it is the farthest station from the metallurgical area. The third high volume sampler was located in the "Zoco" High School due to the proximity of this populated area to the industrial estate.

2.2 Sample preparation and chemical analysis

PM samples were collected on the microquartz fibre filters, during emissions and ambient air sampling. PM mass concentration was determined by standard gravimetric procedures.

The analytical methodology [8] comprises several techniques for determining the major and trace elements content. A fraction of each filter was acid digested (2.5 mL HNO3:5 mL HF: 2.5 mL HClO4) for the determination of trace elements by inductively coupled plasma-optical emission (ICP-OES) and spectrometry inductively coupled plasma atomic mass spectrometry (ICP-MS). The analytical error was controlled and estimated by repeated analysis of NBS-1633a (fly ash) certified reference material. The error range for most elements was 5-10%.

3 RESULTS AND DISCUSSION

3.1 Stack emission samples

The PM samples collected from the metallurgy chimney emissions are characterized by extremely high concentrations of metal and metalloids. The mean chemical composition of brass and copper metallurgy emissions sampled is shown in Fig. 2.
Overall, brass metallurgy emissions are more metal enrichment that copper ones. The main elements emitted in the whole brass smelter production in the industrial state are Cu (241 $\mu g/m^3$ maximun recorded in melting furnace), Zn (4249 $\mu g/m^3$, melting furnace), Pb (138 $\mu g/m^3$, shavings drying), Sc (54 $\mu g/m^3$, casting furnace) and Ba, Mo and Ni as minor elements (>10 $\mu g/m^3$) recorded specially in shavings drying emissions. Furthemore, copper metallurgy emissions are defined by the presence of the same tracer (Cu, Zn and Pb) but at much lower concentration: Cu, 0.98 $\mu g/m^3$; Zn, 20 $\mu g/m^3$ and Pb, 1.20 $\mu g/m^3$.
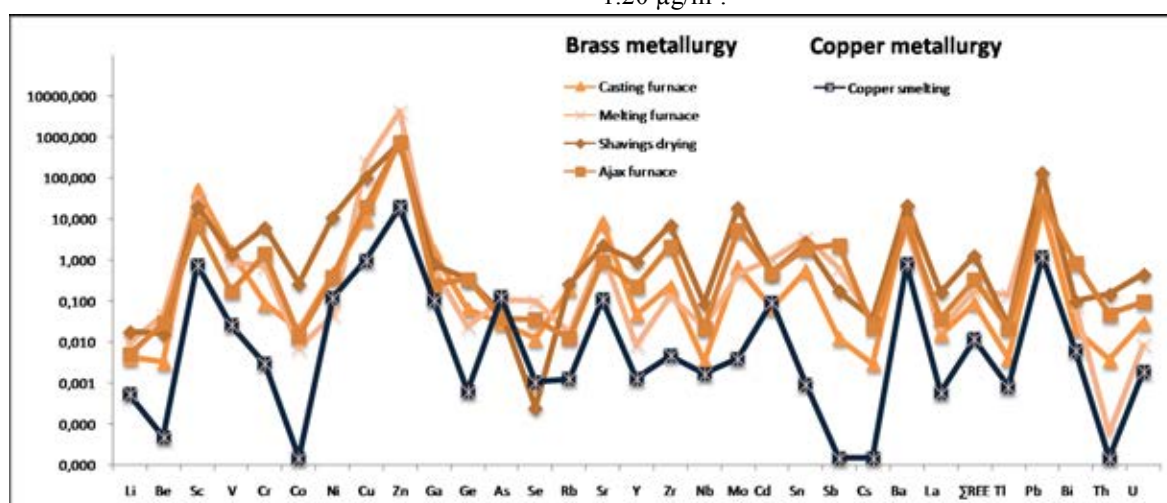
Fig. 2. Chemical composition from chimney stack emissions samples of brass and copper metallurgy.

The results show how as fugitive emissions inside the brass metallurgy factories represent a significant contribution of PM released with daily mean concentration up to 2048 µg/m3 (Table 1). These samples collected very close to the furnace are once again especially enriched in Cu, Zn and Pb with mean concentrations exceeding 1000 ng/m^3.

These no-stack emissions release outside the factories impacting in the immediate environment at ground level. High levels of PM10 and PM2.5 were measured around the industry during around 2 hour impact episodes (309 µgPM10/m^3 and 330 µgPM2.5/m^3). , PM impact samples collected at ground level tended to have lower metal and metalloids enrichments than the direct emission samples measured in the stacks and fugitive emissions inside the factory. However, high concentration of Cu, Zn, Pb and Cd were observed (Table 1).

Figure 3 shows the chemical composition of the ambient air samples (PM10) collected at the three sites located in the city of Cordoba during campaign. The highest average concentration of most elements analyzed is registered at Zoco site probably due to its proximity to the industrial area. The highest mean daily concentration of the main anomalies was observed at Zoco site on 25th October (122 ngCu/m^3, 5785 ngZn/m^3, 5,18 ngCd/m^3 y 96,3 ngPb/m^3), which corresponds to an episode when metallurgy emissions are carried by winds from SSE to the city. The mean Cu, Zn and Cd concentration observed in Zoco site, Zn and Mo at Lepanto site and and Zn at Asomadilla site, are higher than the reference range of urban background stations in Spain (Fig.3).

Table 1. Mean concentration and chemical composition of the fugitives emissions samples collected inside and outside of the metallurgy facilities

	Fugitive emissions					
	Outside		Inside			
	M1+M2		M1		M2	
	PM10	PM2.5	TSP		TSP	
PM (µg/m^3)	309	330	541	1104	1168	2048
n	2	2	17		20	
ng/m^3	Mean	Mean	Mean	Max	Mean	Max
Li	1.31	1.22	0.01	0.07	0.13	0.59
Be	1.20	0.86	2.41	6.97	1.31	3.85
Sc	0.34	0.34	0.01	0.05	0.00	0.01
Ti	198	248	SD	SD	SD	SD
V	3.82	3.44	0.36	2.07	1.07	2.28
Cr	24.8	11.0	11.2	38.1	7.17	23.0
Mn	32.3	22.3	SD	SD	SD	SD
Co	0.73	0.62	0.19	0.54	0.20	0.42
Ni	5.50	1.40	4.19	10.8	3.39	7.06
Cu	**1824**	**1467**	**2006**	**5590**	**4569**	**7404**
Zn	**48069**	**39609**	**16424**	**33328**	**41204**	**73418**
Ga	0.43	0.53	0.01	0.01	0.01	0.01
Ge	0.38	0.21	0.04	0.07	0.01	0.02
As	3.11	3.16	14.3	180	5.42	67.7
Se	5.77	2.95	0.79	1.32	1.34	2.27
Rb	2.92	3.82	0.14	0.61	0.17	0.35
Sr	12.3	17.7	0.09	1.33	0.58	2.33
Y	1.13	0.62	0.01	0.13	0.03	0.11
Zr	8.90	39.00	0.99	8.07	4.25	18.0
Nb	0.35	0.50	0.06	0.34	0.07	0.20
Mo	21.3	7.69	2.86	11.6	12.7	24.3
Ag	102	80.9	0.77	1.78	0.73	1.23
Cd	**35.6**	**34.6**	**16.2**	**37.2**	**7.44**	**16.5**
Sn	26.0	20.7	15.7	36.7	45.4	81.5
Sb	6.66	3.97	2.69	6.67	8.84	19.7
Cs	0.20	0.30	0.01	0.03	0.01	0.02
Ba	85.4	73.0	8.98	28.5	43.7	99.97
∑REE	4.57	5.21	0.11	1.02	0.30	1.19
W	0.78	0.54	11.4	148	3.03	5.38
Tl	1.72	1.65	0.68	1.30	0.91	1.91
Pb	**1107**	**995**	**479**	**918**	**522**	**1010**
Bi	0.61	0.56	0.29	0.51	0.45	2.39
Th	0.33	0.21	0.01	0.15	<0.01	0.01
U	0.28	0.08	0.01	0.01	0.01	0.03
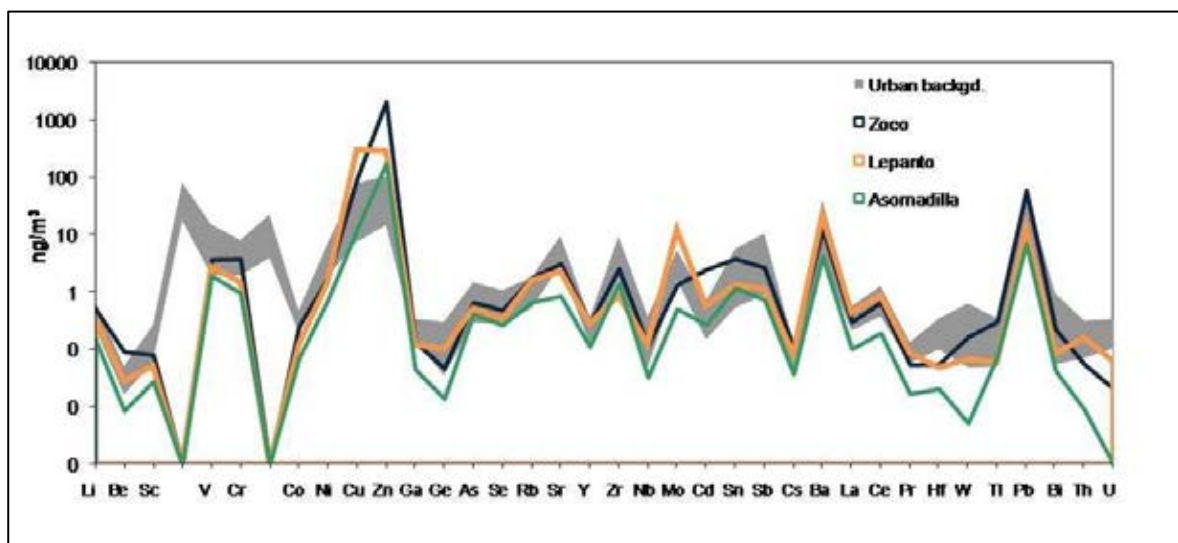
Fig. 3. PM10 chemical composition at Zoco, Lepanto and Asomadilla site during Cordoba sampling campaign in reference to urban background range in Spain from [9].

4 CONCLUSIONS

Results show metallurgy is an important source of metals and metalloids in the city of Cordoba, being much more polluting the brass metallurgy than the copper one. The fugitive emissions measurements, both inside and outside of the brass metallurgy facilities, demonstrate that there is an important part of the industrial emissions that are no stack and so no controlled. This metal released impact in the immediate environment. The geochemical anomalies (Cu, Zn, Pb and Cd, specially) observed in the ambient air samples collected in the city are closely related to the geochemical profile obtained in the stack and fugitive metallurgy emissions. These industrial emissions are carried by SW-SSE wind directly to the city. The neighbourhoods closest to the industrial estate, like "Zoco" residential area, are the most affected.

REFERENCES

[1] Lozano A., Usero J., Vanderlinden E., Raez J., Navarrete B., El Bakouri H., 2009. Design of air quality monitoring networks and its applications to NO_2 and O_3 in Cordova, Spain. Microchemical Journal 93, 211-219.

[2] Amato F., Alastuey A., de la Rosa J., González-Castanedo Y., Sánchez de la Campa A.M., Pandolfi M., Lozano A., Contreras González J., Querol X., 2013. Trends of road dust emissions contributions on ambient PM levels at rural, urban and industrial sites in Southern Spain. Atmospheric Chemistry and Physic Discussion, doi:10.5194/acpd-13-31933-2013.

[3] de la Rosa J.D., Sánchez de la Campa A.M., Alastuey A., Querol X., González-Castanedo Y., Fernández-Camacho R., Stein A.F., 2010.Using PM10 geochemical maps for defining the origin of atmospheric pollution in Andalusia (Southern Spain). *Atmospheric Environment*, 44, 4595-4605.

[4] Fernández-Camacho R., de la Rosa J., Sánchez de la Campa A.M., González-Castanedo Y., Alastuey A., Querol X., Rodríguez S., 2010. Geochemical characterization of Cu-smelter emission plumes with impact in an urban area of SW Spain. *Atmospheric Research* 96, 590-601.

[5] Pandolfi M., Gonzalez-Catanedo Y., Alastuey A., de la Rosa J.D., Mantilla E., Querol X., Pey J., Amato F., Moreno T. Source apportionment of PM10 and PM2.5 at multiple sites in the Strait of Gibraltar by PMF: impact of shipping emissions. *Environmental Science Pollution Research*, 18, 260-269.

[6] Sánchez de la Campa A.M., MorenoT., de la Rosa J.D., Alastuey A., Querol X., 2011. Size distribution and chemical composition of metalliferous stack emissions in the San Roque petroleum refinery complex, southern Spain. *Journal of Hazardous Materials*, 190, 713-722.

[7] González-Castanedo Y., Moreno T., Fernández-Camacho R., Sánchez de la Campa A.M., Alastuey A., Querol X., de la Rosa J., 2014. Size distribution and chemical composition of particulate matter stack emissions in and around a copper smelter. *Atmospheric Environment*, submitted for publication.

[8] Querol X., Alastuey A., Rodríguez S., Plana F., Ruiz C.R., Cots N., Massagué G., Puig O., 2001. PM10 and PM2.5 source apportionment in the Barcelona Metropolitan Area, Catalonia, Spain. *Atmospheric. Environment* 35, 6407–6419.Querol et al., 2006

Temporal and Spatial Evolution Study of Air Pollution in Portugal

José Manuel Fernández-Guisuraga[1], Amaya Castro[2], Célia Alves[3], Ana Calvo[4], Elisabeth Alonso-Blanco[5], Roberto Fraile[6]

Abstract — This study provides an analysis of the spatial distribution and temporal evolution of NO, NO_2 and O_3 seasonal and annual concentrations in Portugal during the period 1995-2010. The contribution of nitrogen oxides and several meteorological variables to the variation of O_3 concentration was evaluated with multiple regression analysis in Entrecampos and Douro Norte stations. The variation in NO concentration shows a marked seasonality and presents a significant decreasing annual trend in most of the urban type stations considered, especially those under the influence of road traffic. Despite the downward trend in the concentration of NO, a statistically significant trend in NO_2 concentration is not observed in most of the monitoring stations, except those less influenced by traffic, in which the emission of primary NO_2 is much lower and the reduction in NO emissions leads to less photochemical production of NO_2. The pattern of O_3 concentration is completely opposed to that observed in NO. Several stations showed a significant upward trend in O_3 concentration as a result of the decrease in NO/NO_2 ratio. The correlation between the pollutants and ozone was stronger in Entrecampos than in Douro Norte. In this rural background station, the ozone concentration showed a strong correlation with meteorological variables. In Entrecampos urban station, 68% of the variance in ozone concentration was explained by the variables introduced in the regression model, being the NO_2/NO_X ratio the variable that explained most of the variance. In Douro Norte rural background station, only 43.4% of the variance in ozone concentration was explained by such variables. Therefore, long-range transport, high biogenic volatile organic compounds (BVOCs) concentration and the local geography may play a key role at this station.

Keywords — Portugal, O_3, NO_X, trends

1 INTRODUCTION

Current EU Directive on air quality (2008/50/EC) sets out a number of targets framed within the Thematic Strategy on Air Pollution [COM(2005)446] to improve human health and environmental quality. Ground level ozone and particulate matter ($PM_{2.5}$ and PM_{10}) are the pollutants of most concern in Europe [1].

NO is a primary pollutant, while NO_2 and O_3 are of secondary origin (although a small part of NO_2 in the atmosphere has a primary origin). The main source of nitrogen oxide emissions is road traffic [2]. The implementation of catalytic filters in cars has led to a large reduction not only in the absolute NO

concentration, but also in NO/NO_2 ratio, particularly in regions with dense transport networks. However, it is known that the cars using these filters emit NO_2 as primary pollutant [3]. Also, the increased use of diesel cars has led to an increase in primary NO_2 emissions, since they emit a higher fraction of this contaminant than gasoline cars [4]. This results in an increase of NO_2/NO_X ratio.

Recent estimates indicated that stratospheric-tropospheric exchanges are only responsible for 20% of tropospheric ozone, because at present, it is mainly generated by complex photochemical reactions [5]. Ozone is formed by photochemical reactions that involve anthropogenic pollutants (CO, volatile organic compounds-VOCs) and solar radiation, in the presence of nitrogen oxides [6].

Previous studies showed the existence of a NO_X-sensitive regime and a VOC-sensitive regime. In the NO_X-sensitive regime (NO_X is relatively low and biogenic volatile organic compounds - BVOCs - are high, typical of rural regions), O_3 levels are getting higher with increasing NO_X and changes little with respect to VOC. The VOC-sensitive regime (typical of urban areas) exhibits the opposite behaviour [7, 8].

This paper provides an analysis of the spatial distribution of NO, NO_2 and O_3 seasonal concentrations in mainland Portugal during the period 1995-2010, using data obtained from the air quality monitoring network of *Agência Portuguesa do Ambiente*. The temporal evolution of these pollutants was also studied in order to determine the

────────────────────────

1. *José Manuel Fernández-Guisuraga is with Department of Physics (IMARENAB), University of León, León 24071, Spain. E-mail: jferng11@estudiantes.unileon.es*
2. *Amaya Castro is with Department of Physics (IMARENAB), University of León, León 24071, Spain. E-mail: amaya.castro@unileon.es*
3. *Célia Alves is with the Centre for Environment and Marine Studies, Department of Environment, University of Aveiro, 3810-193 Aveiro, Portugal. E-mail: celia.alves@ua.pt*
4. *Ana Calvo is with Department of Physics (IMARENAB), University of León, León 24071, Spain. E-mail: aicalg@unileon.es*
5. *Elisabeth Alonso-Blanco is with Centro de Investigaciones Energéticas, Tecnológicas y Ambientales (CIEMAT), 28040 Madrid, Spain. E-mail: elisabeth.alonso@ciemat.es*
6. *Roberto Fraile is with Department of Physics (IMARENAB), University of León, León 24071, Spain. E-mail: roberto.fraile@unileon.es*

statistically significant trend in their concentrations and the year in which new trends started. Furthermore, the contribution of NO, NO_2, NO_X, NO/NO_2 and NO_2/NO_X ratios, SO_2, PM_{10} and several meteorological variables (solar radiation, temperature, pressure and wind speed) to the variation of O_3 concentration was evaluated in a Lisbon urban traffic station and Vila Real background station, during the period 2004-2010.

2 METHODOLOGIES

2.1 Area of study

The field of this study corresponds to mainland Portugal (37-42 °N, 6.5-9.5 °W), with an area of 8,908,893 ha. Mainland Portugal is covered by a monitoring network for air quality assessment and management purposes. The monitoring network density is greatest in those areas where the protection of human health is critical, corresponding to the urban areas of Lisbon and Oporto, with a population of 2 million and 1.2 million, respectively [9].

At the end of 2010, the *Agência Portuguesa do Ambiente* monitoring network had 91 operational monitoring stations of different types (urban, suburban or rural). These stations reported NO and NO_2 hourly concentrations by chemiluminescence, while O_3 concentrations were obtained by ultra-violet absorption detection, also being reported on an hourly basis. In the first part of this study, data from all these stations that meet the minimum sampling frequency that is required by the air quality Directive 2008/50/EC were used.

Entrecampos station (code 3072) was chosen to assess the contribution of nitrogen oxides and other pollutants, together with several meteorological variables, in the concentration of O_3 on a severely polluted environment. It is an urban traffic station located in Lisbon, with coordinates -9.14889 ° W, 38.7486 ° N and 86 m altitude. Douro Norte station (code 1048) was chosen to assess such contribution in a less polluted environment. It is a rural background station with coordinates -7.7908 ° W, 41.3714 ° N, located at an altitude of 1086 m.

2.2 Data and methods

Annual averages were performed to assess the trend in the concentration of these pollutants by the Mann-Kendall sequential test (SQMK) (rank statistic test) [10] for those stations with continuous data for a minimum of ten years. The SQMK test is a non-parametric test that can be applied to non-normally distributed data with missing points. This test allows us to calculate the year when the trend or change starts. A monotonic trend of increase or decrease is evaluated along with the non-parametric Sens's

method for estimating the slope of a linear trend [11].

To analyse the spatial distribution of short term NO, NO_2 and O_3, a seasonal average of concentrations throughout the entire study period was conducted. Subsequently, the results were plotted through Surfer, a contouring and surface modelling package.

Stepwise multiple regression analysis (SMRA) was employed to assess the contribution of NO, NO_2, NO_X, NO/NO_2 NO_2/NO_X ratio, SO_2, PM_{10}, solar radiation, temperature, pressure and wind speed to O_3 levels recorded in Entrecampos and Douro Norte stations (urban traffic and rural background type, respectively) during the period 2004-2010, in order to identify the variables that best predict the variation in the concentration of ozone in each case. The possible existence of multicollinearity between the independent variables by Inflation Factor Variance (VIF) and Condition Index (CI) was previously checked, the latter being one of the most suitable methods for detecting multicollinearity [12]. The presence of multicollinearity in a regression model makes difficult to correctly identify important contributors to a physical process [13], so multicollinearity should be avoided.

3 RESULTS AND DISCUSSION

3.1 Spatial distribution of NO, NO_2 and O_3 concentrations

Seasonal patterns show that the highest NO concentrations are reached during autumn and winter (Fig. 1a), especially in most densely populated areas of Portugal, corresponding to Lisbon and Oporto metropolitan areas. Also, the high concentration registered in Coimbra during these seasons stands out, although it is not a town with a large population density, but it has a dense road network with high traffic. This spatial pattern suggests that the main cause of these high concentrations is road traffic. During these seasons, adverse dispersion conditions and car engine operation, in addition to increased activity in the populated areas, result in an increased emission and accumulation of primary pollutants such as NO [14].

NO_2 concentration pattern (Fig. 1b) shows no marked seasonality as in the case of NO, although concentrations in summer are slightly lower, especially in the more populated coastal areas. The decrease in NO_2 concentration in summer is not as pronounced as in NO. Because NO_2 is mainly a secondary pollutant, the higher solar radiation and temperature during this season accelerates its production, although the emission of their precursors is reduced.
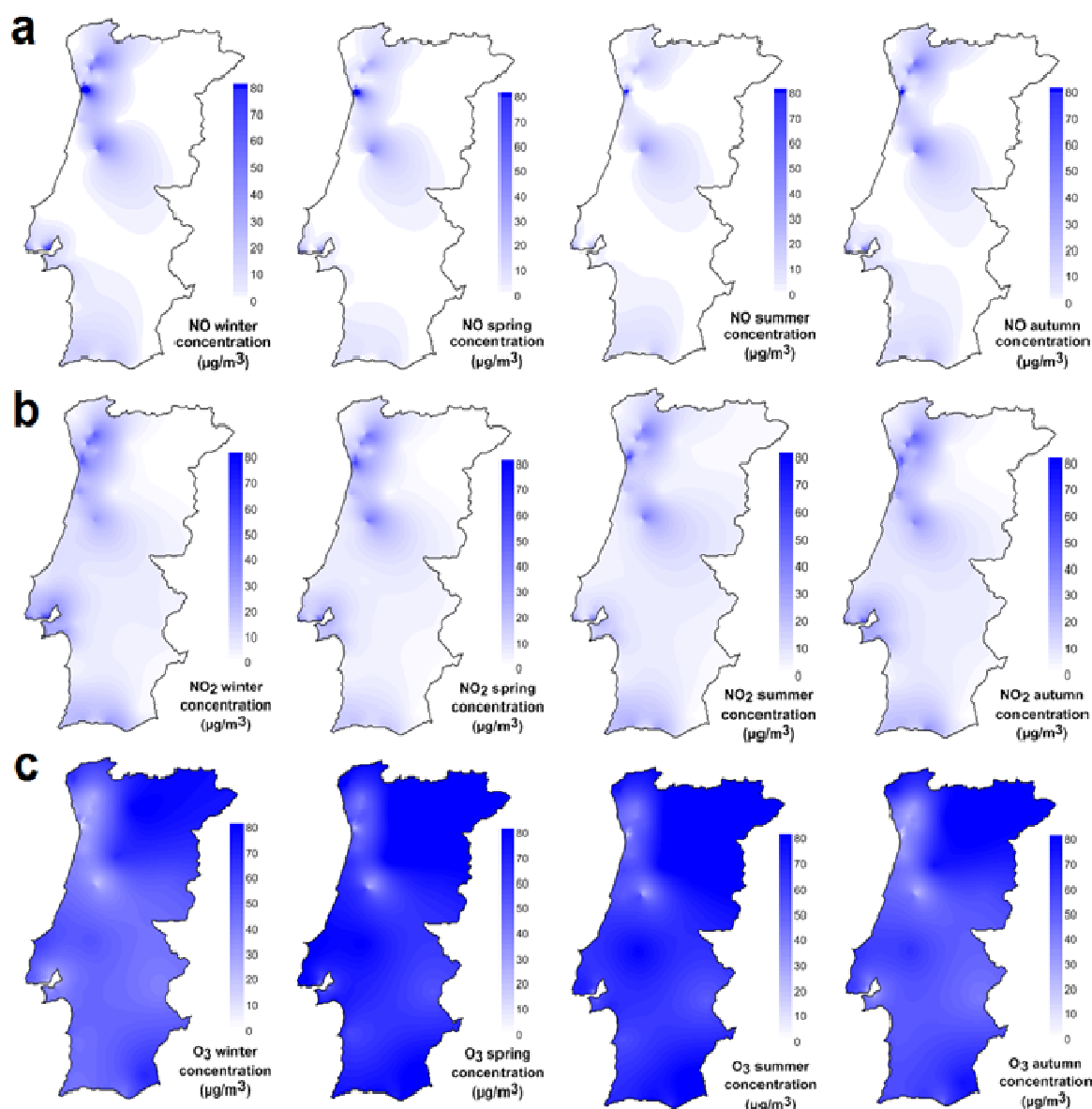
Fig. 1. Seasonally averaged (1995-2010) concentration maps of NO (a), NO_2 (b) and O_3 (c).

The highest O_3 concentrations are reached during the spring and summer (Fig. 1c), thus following a completely opposite pattern of NO. This is because the photochemical activity in these months is high because of the incident solar radiation and the temperature reach their annual maximum. Furthermore, reduction in the emission of primary pollutants (particularly NO) during these months results in an increased accumulation of ozone. Moreover, the high ozone concentration stands out throughout the entire year in Douro Norte monitoring station, located in a mountainous rural area NE of Portugal. This station showed the highest annual average (94.4 $\mu g/m^3$) of ozone hourly concentration recorded over the study period. Carvalho et al. [15] highlighted the importance of the long-range transport of atmospheric pollutants or its precursors due to atmospheric flow patterns, mainly from NW of Spain, to the high ozone levels registered in these areas.

3.2 Annual trend of NO, NO_2 and O_3 concentrations

The results obtained by the Mann-Kendall sequential test at 95% level of significance for 29 monitoring stations having a minimum of 10 years in the data series are shown in Table 1.

NO concentration presents a significant decreasing trend (U < -1.96) in most of urban and suburban stations. The high decreasing rate of NO concentration in Avenida da Liberdade (U = -3.33, -2.33 $\mu g\ m^{-3}\ year^{-1}$), Entrecampos (U = -3.60, -2.47 $\mu g\ m^{-3}\ year^{-1}$) and Mouzinho (U = -3.31, -3.40 $\mu g\ m^{-3}\ year^{-1}$) urban type stations stands out. These very steep declines of NO concentration in urban type stations can be attributed to the restrictions on the transport sector fuel requirements (Directive 98/70/EC) and the implementation of catalytic filters in vehicles. In contrast, the NO concentration does

not show any significant trend in any of the rural stations studied.

Despite the clear downward trend in NO concentration, a significant trend for the NO_2 is not observed in most cases. This absence of trend might be due to the fact that NO_2 is emitted as a primary pollutant because of the implementation of catalytic filters in cars [3]. This behaviour is not observed in Lavradio (U = -3.96, -2.01 µg m^{-3} year^{-1}) and Chelas (U = -2.52, -1.40 µg m^{-3} year^{-1}) monitoring stations, which show a decreasing trend in NO_2 concentration. The trend starting year is about the same as that pointed out for NO. This behaviour could result from considerably lower NO_2 primary emissions by less traffic. Therefore, a reduction in emissions of NO in the vicinity of this stations, leads to less formation of photochemical NO_2. Moreover, Alto Seixalinho station shows a significant upward trend in the concentration of NO_2 (U = 2.70, +0.82 µg m^{-3} year^{-1}) although its NO concentration trend is not significant, despite registering an increase rate of 0.32 µg m^{-3} year^{-1}. Again, primary NO_2 plays a fundamental role in this urban traffic station.

Several stations showed a significant upward trend in O_3 concentration, as in the case of Entrecampos (U = 4.86, +2.55 µg m^{-3} year^{-1}). This urban traffic station presented a strong downward trend in NO concentration, while NO_2 concentration did not exhibit a significant trend. This results in a decrease of NO/NO_2 ratio and therefore an increase in the availability of ozone. A similar behaviour can be observed in other stations. The rate of increase in O_3 concentration is higher in traffic stations than in industrial or background stations because the rate of decrease in NO concentration is higher at traffic-impacted sites.

3.3 Influence on ozone levels

The independent variables used for studying their contribution to ozone levels recorded during the period 2004-2010 in Entrecampos and Douro Norte monitoring stations were NO, NO_2, NO_X, NO/NO_2 and NO_2/NO_X, SO_2, PM_{10}, solar radiation (SR), temperature (Temp), pressure (P) and wind speed (WS). It was not possible to use relative humidity and wind direction as independent variables due to the lack of data.

Table 1. Sequential Mann-Kendall trend test results (U statistics and trend start year) for NO, NO_2 and O_3 concentration throughout the study period and slope estimation of the linear trend.

Monitoring station	Municipality	Type	NO			NO₂			O₃		
			U	Trend start	µg/m3·year	U	Trend start	µg/m3·year	U	Trend start	µg/m3·year
Laranjeiro	Almada	Urban background	-1.70		-0.5861	0.45		0.2523	3.85	2005	1.7382
Alfragide	Amadora	Urban background				0.14		-0.0759	-2.06	2005	-1.7451
Reboleira	Amadora	Urban background	-1.16		-0.1374						
Alto seixalinho	Barreiro	Urban traffic	1.44		0.3152	2.70	2006	0.8228	2.44	2009	1.8129
Escavadeira	Barreiro	Urban industrial	0.63		0.1457	0.09		0.0755			
Lavradio	Barreiro	Urban industrial	-3.33	2002	-1.5486	-3.96	2001	-2.0111			
Coimbra	Coimbra	Urban traffic				-1.32		-0.8186	0.86		0.6083
Av.24-Espinho	Espinho	Urban traffic	-2.77	2007	-0.8606	0.98		0.2905			
E. Avanca	Estarreja	Rural background				0.08		-0.1498			
E. Teixugueira	Estarreja	Suburban industrial	-2.52	2008	-0.6187	-0.86		0.1557	1.92		1.1197
Pe Joaquim Neves	Gondomar	Urban traffic							2.06	2009	0.9628
Av. da Liberdade	Lisboa	Urban traffic	-3.33	2005	-2.3316	1.08		-0.2622			
Beato	Lisboa	Urban background	-3.42	2004	-0.3846	1.71		0.3067	3.45	2001	1.6611
Chelas	Lisboa	Urban background	-4.14	2000	-1.0820	-2.52	1999	-1.4009			
Entrecampos	Lisboa	Urban traffic	-3.60	2001	-2.4701	0.63		0.4180	4.86	2000	2.5546
Olivais	Lisboa	Urban background	-0.63		-0.1148	1.35		0.4096			
St. Cruz de Benfica	Lisboa	Urban traffic	-2.43	2009	-1.6517	-0.99		-0.0646			
Loures Centro	Loures	Urban background	-0.63		-0.3557						
Don Manuel II	Maia	Urban traffic	-3.66	2004	-1.3649	-0.08		0.0254	1.95		1.2682
VN Telha-Maia	Maia	Suburban background	-2.74	2007	-0.3446	-1.37		-0.1883	0.14		0.1467
Custoias	Matosinhos	Suburban background	-2.74	2008	-1.3432	0.06		-0.3799	1.65		0.6820
Leça do Balio	Matosinhos	Suburban background	-1.70		-0.8023	1.52		0.9135	0.45		0.0609
Mouzinho	Porto	Urban traffic	-3.31	2003	-3.3975	-1.88		-1.5542			
Fco. Sá Carneiro	Porto	Urban traffic							1.52		1.3793
Monte Velho	S. do Cacém	Rural background	-1.34		-0.0790	-0.45		0.0047	0.54		0.0295
Sonega	S. do Cacém	Rural industrial	-1.44		-0.1389	-0.99		-0.0921	-0.86		0.1038
Paio Pires	Seixal	Suburban background	0.23		0.0330	1.32		1.0614	1.95		2.9147
Monte Chaos	Sines	Suburban industrial	-2.34	2008	-0.1037	-1.44		-0.2676	2.34	2009	1.4904
Ermesinde	Valongo	Urban background	-2.41	2008	-0.3487	0.86		0.2787	2.47	2005	0.8332

Pearson correlation test determined that O_3 concentration in Entrecampos station is negatively correlated with NO, NO_2 and NO_X concentration, NO/NO_2 ratio and SO_2 concentration, and positively correlated with NO_2/NO_X ratio and PM_{10} concentration. This is expected since NO and NO_2 are ozone precursors, and therefore a rise in ozone concentrations is associated with a reduction in NO and NO_2 levels [14]. NO and NO_2 enhance ozone's dissociation and production, respectively. Thus, if the NO/NO_2 ratio decreases, ozone concentrations increase [8], which explains the negative correlation between both parameters. For the same reason, if the NO_2/NO_X ratio increases, O_3 concentration also rises. Ozone has a strong positive correlation with solar radiation and temperature, since it is produced through photochemical processes.

In Douro Norte station, the correlation between ozone concentrations with those of most pollutants is significantly weaker than in Entrecampos station, although the direction of the correlations is the same. However, its correlation with solar radiation and temperature is stronger, at the suburban background station with less traffic influence, as previously observed [14].

When two or more explanatory variables in a model are highly correlated in the sample, as in the case of the different nitrogen oxides and their respective ratios, it is very difficult to separate the partial effect of each of these variables on the dependent variable in the regression model. For this reason, the independent variable in relation to nitrogen oxides introduced in the SMRA was NO_2/NO_X ratio, since in both stations it had the strongest correlation with ozone concentration regarding that group of variables. It should be expected that NO_2/NO_X ratio explained a greater proportion of the variance in the ozone concentration. Therefore, the independent variables included in the model were NO_2/NO_X ratio, SO_2, PM_{10}, solar radiation, temperature, pressure and wind speed. Independent variables left in the model were significant at 0.05 level. Those which failed to meet this level of significance were excluded from the model.

The variance inflation factor (VIF) in Table 2 is relatively low for all independent variables at both stations, not being in any case higher than 3. Kleinbaum et al. [16] suggests that there should not be problems with collinearity if the VIFs are less than 10 (tolerance < 0.1). However, other authors, such as O'Brien [17], argue that this rule should be taken with caution, since it may be collinearities not involving all independent variables and therefore not well detected by VIF, among many other reasons. For this reason, we also calculated condition indices (Table 2) for each variable in both stations. Condition indices ranging from 10-30 are associated with a weak collinearity, although they should not present problems, while indices higher 30 can cause a serious problem of collinearity and potential disaster in the regression model [18]. Condition indices did not exceed the value of 15 in both stations, so we can assume that the regression model may be appropriate to elucidate the contribution of the variables considered in the ozone concentration recorded at both stations.

SMRA results for Entrecampos and Douro Norte stations are shown in Table 3. In Entrecampos station, NO_2/NO_X ratio, solar radiation, wind speed, pressure, temperature and PM_{10} remained in the model with the required level of significance (0.05), while the variables that did not meet that requirement were excluded. The value of adjusted R^2 for this station was 0.680, which means that 68 % of the variance in the ozone concentration can be explained by the variables introduced in the model. It is a noticeably high value considering that relative humidity and wind direction were not introduced in the model as independent variables. The NO_2/NO_X ratio explained by itself 55.1 % of the variance in ozone concentration in Entrecampos station. He and Lu [13] also suggested that NO_2/NO_X ratio can be regarded as the dominant precursor of ozone concentration.

In Douro Norte rural station the variables that remained in the model were temperature, solar radiation, NO_2/NO_X, PM_{10} and wind speed. These variables only explained 43.4% of the variance in ozone concentration in this station (37.5 % of the variance was explained by temperature and solar

Table 2. Variance inflation factor and condition index of variables left in SMRA.

Entrecampos	Tolerance	VIF	Dimension	Eigenvalues	Condition index
NO_2/NO_X	0.413	2.419	1	4.551	1.000
SR	0.368	2.716	2	0.468	3.119
WS	0.558	1.792	3	0.298	3.908
P	0.887	1.127	4	0.101	6.715
PM_{10}	0.595	1.680	5	0.058	8.853
T	0.431	2.319	6	0.032	11.926
			7	0.021	14.729
Douro Norte	Tolerance	VIF	Dimension	Eigenvalues	Condition index
T	0.355	2.816	1	5.386	1.000
SR	0.383	2.613	2	0.381	3.759
NO_2/NO_X	0.878	1.139	3	0.267	4.488
PM_{10}	0.883	1.133	4	0.184	5.403
WS	0.921	1.085	5	0.124	6.604
			6	0.031	13.178

Table 3. Stepwise regression model for O_3 concentration in Entrecampos and Douro Norte stations with the variables NO_2/NO_X ratio, solar radiation, wind speed, pressure, PM_{10} and temperature.

Entrecampos	NO_2/NO_X	SR	WS	P	PM_{10}	T
Adjusted R^2	0.551	0.628	0.649	0.660	0.673	0.680
F change	462.402	78.395	23.823	13.077	15.857	8.923
Sig. F change	<0.0001	<0.0001	<0.0001	<0.0001	<0.0001	0.003
Douro Norte	T	SR	NO_2/NO_X	PM_{10}	WS	
Adjusted R^2	0.247	0.375	0.402	0.426	0.434	
F change	124.443	77.487	17.782	16.594	6.445	
Sig. F change	<0.0001	<0.0001	<0.0001	<0.0001	0.012	

radiation). It was noted in section 3.1 that high ozone concentrations recorded at this station may be due to long-range transport from the NW of Spain [15]. The low variance explained by the variables may suggest photochemical production of O_3 from its precursors during transport to this station. Moreover, taking into account that Douro Norte is located in a mountainous area, the amount of biogenic volatile organic compounds (BVOCs) would be significantly higher during the day and consequently contribute to the local photochemical ozone production from transported precursors. In addition, local geography would also play a key role in ozone concentrations recorded at this site. This hypothesis would explain the low correlation between the local ozone concentration and other pollutants, and the strong correlation with both temperature and solar radiation, which are the two factors that explain most of the variance in the regression model.

CONCLUSIONS

Together with meteorological variables, 16 years of NO, NO_2 and O_3 concentrations collected over the period 1995-2010 in several air quality stations of mainland Portugal were analysed. The variation in NO concentration showed a marked seasonal pattern, with the lowest levels occurring during the colder months, especially in the most densely populated areas. The seasonal fluctuations of NO_2 concentrations are not so marked. Despite an overall downward trend in the NO concentration, a statistically significant tendency towards a decrease of NO_2 levels was not observed in most of the monitoring stations. Ozone showed an opposite seasonal pattern to that of NO. Several stations showed a significant upward trend in O_3 level as a result of the decrease of the NO/NO_2 ratio. Long range transport of precursors to mountain sites in the northern region led to frequently high surface O_3 concentrations. A strong correlation between this photochemical pollutant and both solar radiation and temperature was obtained at a representative site of that region. For this rural site, the percentage of variance in O_3 concentrations explained by other pollutants is relatively low. At urban traffic sites, most of the variance is explained by the NO_2/NO_X ratio.

The ozone trends observed in this study in the northern region could be extrapolated to other rural areas of NW Iberian Peninsula, because this geographical area has homogeneous topographical and climatological characteristics. In addition, Galicia and the north of Portugal are affected by similar synoptic circulation patterns.

Taking into account that, in addition to meteorological variability, the O_3 trends are strongly affected by changes in the photochemical precursor emissions, the analysis of future concentration patterns should be very useful to confirm the influence of these factors. Despite the general drop on the NO levels, future long-term trend assessments will be desirable in order to evaluate the effectiveness of both air quality plans and emission control technologies.

REFERENCES

[1] A. Monteiro, R. Vautard, M. Lopes, A.I. Miranda, C. Borrego, "Air pollution forecast in Portugal: a demand from the new air quality framework directive," Int. J. Environ. Pollut., vol. 25, pp. 4-15, 2005.

[2] R.N. Colvile, E.J. Hutchinson, J.S. Mindell, R.F. Warren, "The transport sector as a source of air pollution," Atmos. Environ., vol. 35, pp. 1537-1565, 2001.

[3] K.A. Kourtidis, I. Ziomas, C. Zerefos, E. Kosmidis, P. Symeonidis, E. Christophilopoulos, S. Karathanassis, A. Mploutsos, "Benzene, toluene, ozone, NO_2 and SO_2 measurements in an urban street canyon in Thesalonniki, Greece," Atmos. Environ., vol. 36, pp. 5355-5364, 2002.

[4] D.C. Carslaw, S.D. Beevers, "Investigating the potential importance of primary NO_2 emissions in a street canyon," Atmos. Environ., vol. 38, pp. 3585-3594, 2004.

[5] A. Marenco, H. Gouget, P. Nédélec, J.-P. Pagés, "Evidence of a long-term increase in tropospheric ozone from Pic du Midi data series: Consequences: Positive radiative forcing," J. Geophys. Res., vol. 99, pp. 16617-16632, 1994.

[6] M.C.M. Alvim-Ferraz, S.I.V. Sousa, M.C. Pereira, F.G. Martins, "Contribution of anthropogenic pollutants to the increase of tropospheric ozone levels in the Oporto Metropolitan Area, Portugal since the 19th century," Environ. Pollut., vol. 140, pp. 516-524, 2006.

[7] S. Sillman, "The relation between ozone, NOx and hydrocarbons in urban and polluted rural environments," Atmos. Environ., vol. 33, pp. 1821-1845, 1999.

[8] A. Melkonyan, W. Kuttler, "Long-term analysis of NO, NO_2 and O_3 concentrations in North Rhine-Westphalia, Germany," Atmos. Environ., vol. 60, pp. 316-326, 2012.

[9] C. Borrego, E. Sá, J. Ferreira, A.I. Miranda, " Forecasting human exposure to atmospheric pollutants in Portugal - A modelling approach," Atmos. Environ., vol. 43, pp. 5796-5806, 2009.

[10] R. Sneyers, On the statistical analysis of series of observations. Geneva: WMO Tech. Note 143, pp. 10-15, 1990.

[11] P.K. Sen, "Estimates of the regression coefficient based on Kendall's tau," J. Am. Stat. Ass., vol. 63, pp. 1379-1389, 1968.

[12] O.G. Judge, W.E. Griffith, R.C. Hill, C.H. Lee, H. Lütkepohl, The theory and practice of econometrics. New York: Wiley, pp. 340-347, 1985.

[13] H. He, W.-Z. Lu, "Decomposition of pollution contributors to urban ozone levels concerning regional and local scales," Build. Environ., vol. 49, pp. 97-103, 2011.

[14] I. Mavroidis, M. Ilia, "Trends of NOx, NO_2 and O_3 concentrations at three different types of air quality monitoring stations in Athens, Greece," Atmos. Environ., vol. 63, pp. 135-147, 2012.

[15] A. Carvalho, A. Monteiro, I. Ribeiro, O. Tchepel, A.I. Miranda, C. Borrego, S. Saavedra, J.A. Souto, J.J. Casares, "High ozone levels in the northeast of Portugal: Analysis and characterization," Atmos. Environ., vol. 44, pp. 1020-1031, 2010.

[16] D.G. Kleinbaum, L.L. Kupper, K.E. Muller, Applied Regression Analysis and Other Multivariables Methods. Belmont, Calif.: Thomson, pp. 314-345, 1988.

[17] R.M. O'Brien, "A caution regarding rule of thumb for variance inflation factors," Qual. Quant., vol. 41, pp. 673-690, 2007.

[18] D.A.Belsley, Conditioning Diagnostics: Collinearity and Weak Data in Regression. New York: Wiley, 1991.

Temporal Characterization of Particulate Matter over the Iberian Peninsula to Support the Brightening Phenomena in the Last Decades

D. Mateos[1], V.E. Cachorro[1], A. Marcos[1], Y. Bennouna[1], C. Toledano[1], M.A. Burgos[1], A.M. de Frutos[1]

Abstract — The Iberian Peninsula has shown notable variations of the surface solar irradiance in the last decades. Particularly, an increase trend in its levels is reported since the 1990s (brightening period, BP). Aerosol particles are able to modulate solar radiation in the atmosphere. Hence, the main aim of this study is to evaluate the temporal trends of particulate matter (PM) over the Iberian Peninsula in order to analyze the role played by aerosol particles in the observed BP and, therefore, in the Earth's radiative budget. Six long-term sites belonging to EMEP (European Monitoring and Evaluation Programme) network are used in the periods 1988-2000 and 2001-2012. As a main result, a strong reduction of the PM concentration is found over the Iberian Peninsula in the 1988-2000 period, which is still observable between 2001-2012. Therefore, this reduction of the surface aerosols can contribute to the solar radiation increase in the last decades.

Keywords — Particulate matter, Iberian Peninsula, Temporal Trends, Climatology.

1 INTRODUCTION

Tropospheric aerosols have been deeply investigated due to their high relevance in terms of climate change and radiative budget, human health, visibility, impact on materials, among others [1].

The measurements of regional background aerosols since the 1980s have been a very useful tool to control the air quality degradation produced by different factors. To solve air pollution problems, the European Monitoring and Evaluation Programme (EMEP) was created as a scientifically based and policy driven program under the Convention on Long-range Transboundary Air Pollution (CLRTAP) for international co-operation. Before 2001, EMEP sites recorded total suspended particulate matter (SPM), and after that year started the measurements of particulate matter with diameters less than 10 μm (PM10) and 2.5 μm (PM2.5).

An average PM10 trend of -0.3 μg/m^3 per year is reported by the EMEP report of 2013 [2], which means a mean decrease of PM10 levels about 18% in Europe. This rate corresponds to a rather broad reduction in the primary PM emissions and secondary PM precursors in the period 2001-2011.

The Iberian Peninsula is of great interest due to the high PMx levels compared to Northern European regions. The source of the aerosols in Spain has been reported to be both natural and anthropogenic [3]. As Spain is placed closed to the Saharan desert, frequent African air masses go over the Spanish geography influencing its climate [4]. Other high pollution events can be observed by biomass burning due to the high occurrence of forest fires, particularly during the warm season, or by large pollution events in large cities (such as Madrid, Barcelona, Bilbao, Valencia, among others) or in suburban towns due to the traffic.

The main parameter to show the aerosol effect on the solar radiation is the aerosol optical depth (AOD). However, due to the short time series of measurements and poor sampling of AOD compared to PMx data, this latter variable is an alternative way to determine long-term aerosol trends.

In view of the foregoing, this study aims to provide a complete description of the evolution of SPM and PMx levels in the last quarter century. Six EMEP sites placed through the Spanish geography are analyzed in two different periods: 1988-2000 (SPM data) and 2001-2012 (PMx data). Temporal trends can be evaluated with stable long-term series, and the climatology of the surface aerosol particles can be analyzed.

---

1. *Grupo de Óptica Atmosférica, Facultad de Ciencias, Universidad de Valladolid, Paseo Belén 7, 47011, Valladolid, Spain. E-mail: mateos@goa.uva.es*

2 INSTRUMENTS AND METHODS

2.1 EMEP sites

Six ground-based sites belonging to EMEP network are used in this study. Fig. 1 shows their geographical position, the variable recorded in each site, and the time period of measurements. The description of the EMEP measurements in Spanish sites has been performed in detail by previous studies [4],[5]. The sites Logroño, Roquetas, and San Pablo Montes recorded SPM data between 1988 and 2000. The sites Peñausende, Campisabalos, and Barcarrota are selected since 2001 for the measurements of PM10 and PM2.5.
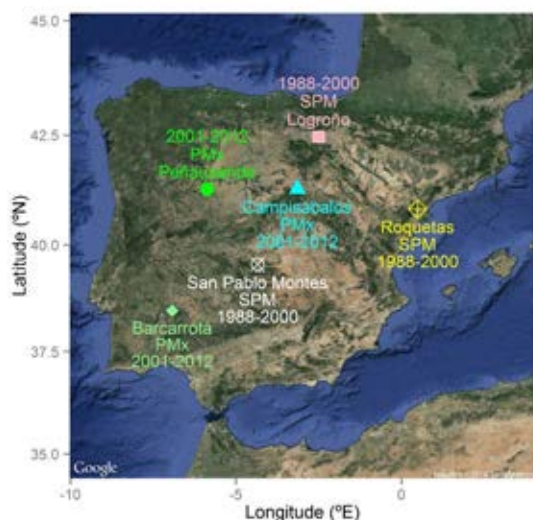
Fig. 1. Geographical position, variable and time period used of the six EMEP Spanish sites.

2.2 Methods

The temporal trend rates of SPM and PMx are evaluated following the Sen's slope method. The significance of the results is evaluated by the Mann-Kendall test. The monthly anomalies of the PM data are evaluated to cancel the seasonal dependence from the results. These anomalies are the difference between the monthly value and the corresponding climatic monthly mean (considering the whole period of measurement). Therefore, the temporal trend rates are obtained in $\mu g/m^3$ per year.
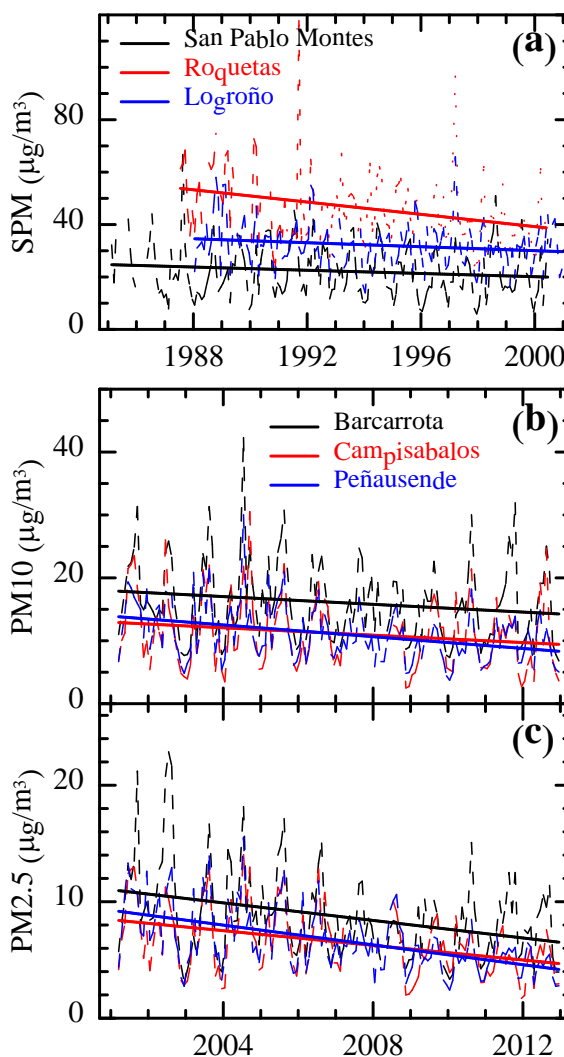
Fig. 2. Temporal evolution of monthly SPM (a), PM10 (b), and PM2.5 (c) at six Spanish sites. Dashed lines are the montly values and the solid lines are the Sen's estimates.

3 TEMPORAL EVOLUTION OF SPM AND PMx

Fig. 2 shows the temporal evolution of monthly means of SPM and PMx at the six stations mentioned above. An evident decrease trend in both variables can be observed. There is a clear south-north decreasing gradient in the concentration of PM in the troposphere. To quantify this reduction, Table 1 presents the results for the temporal trend rates for the six stations. With respect to SPM, the trend rates present low significance levels in Logroño and San Pablo Montes, while the significance reaches the 100% in Roquetas. This latter site exhibits the largest reduction of SPM in 13 years with a rate of -1.1 $\mu g/m^3$ per year. The three temporal trends are negative and a reduction of surface aerosol load is evident between 1988 and 2000.

Table 1. Temporal trends of SPM and PMx in the periods 1988-2000 (1) and 2001-2012 (2) expressed in $\mu g/m^3$ per year. The significance level is given in %.

	Variable	Trend	Significance	Period
Logroño	SPM	-0.3	87	1
Roquetas	SPM	-1.1	100	1
San Pablo Montes	SPM	-0.18	49	1
Peñausende	PM10	-0.47	100	2
Campisabalos	PM10	-0.36	100	2
Barcarrota	PM10	-0.33	100	2
Peñausende	PM2.5	-0.42	100	2
Campisabalos	PM2.5	-0.41	100	2
Barcarrota	PM2.5	-0.21	99	2

All the results for PM10 and PM2.5 are of high significance (>99%). In both cases, the trend rates are negative, and are in good agreement. The three stations, which can be interpreted as a large Central area in Spain, show decreases of PM10 levels between -0.33 and -0.47 $\mu g/m^3$ per year and PM2.5 levels between -0.21 and -0.42 $\mu g/m^3$ per year. These reductions can be attributed to various causes: a) the successful implementation of air pollution laws; b) the effect of the current economic crisis; c) the influence of meteorology observed during the winters of 2009 and 2010; and d) the decrease in the intensity of natural aerosol episodes coming from the Saharan desert [6],[7].

The results obtained in this study are in line with those published by previous studies in Spain or in the Western Mediterranean area. For instance, Barmpadimos et al. [8] analyzed the PM10 temporal trend at Peñausende site between 2001 and 2009 finding a rate of -0.6 $\mu g/m^3$ per year. At the same site, Bennouna et al. [9] have obtained a PM10 (PM2.5) trend of 0.42 (0.38) $\mu g/m^3$ per year in the period 2001-2012. All these values are similar to that shown in Table 2. The differences among them are only explained by the different time periods analyzed. Using yearly values between 2002 and 2010, Cusack et al. [6] have found a mean decrease around 4.4% per year in seven Spanish sites. Other studies in different Spanish stations have also shown a decrease in the SPM data [4].

This reduction in the surface aerosol concentration simultaneously occurs with a decrease trend in the aerosol optical depth since the early 2000s [9],[10].
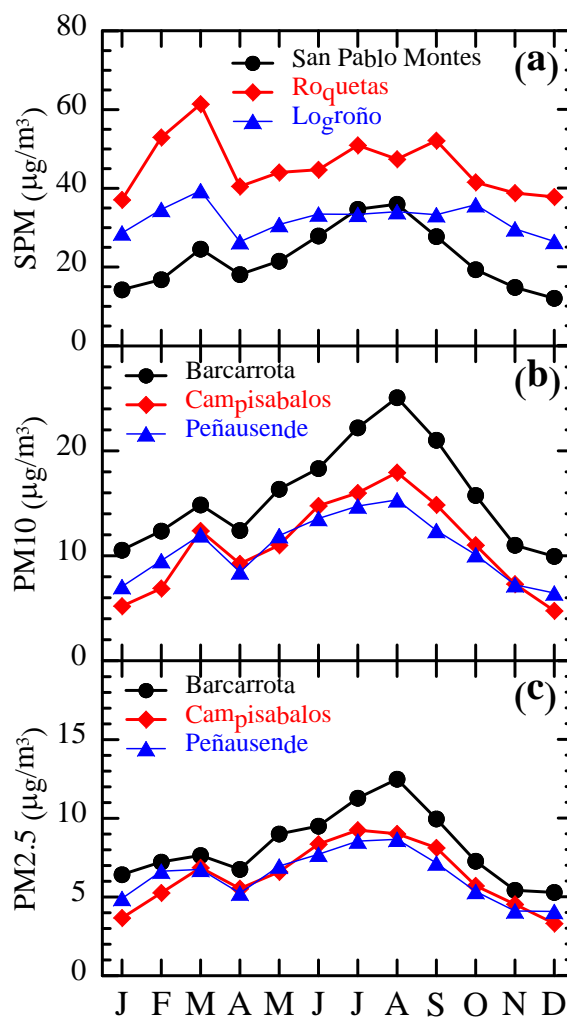
Fig. 3. Annual cycle of SPM (a), PM10 (b), and PM2.5 (c) at six Spanish sites.

4 ANNUAL CYCLE OF SPM AND PMx

To better show the monthly climatology of particulate matter levels over Spain, Fig. 3 shows the annual cycle of SPM and PMx at the 6 sites analyzed in this study. The three variables exhibit similar patterns. The low values during winter increase in the spring up to a summer maximum, and after that a progressive decline is observed. A pair of earlier maximum in March and minimum in April appears for all the sites and variables. In particular, the first maximum in the SPM values of Roquetas and Logroño is the largest monthly concentration. This bimodality was already reported by previous studies and it has been attributed to the impact of desert dust intrusions into the Iberian Peninsula climatology [9].

5 SUMMARY AND CONCLUSIONS

The measurements of the European Monitoring and Evaluation Programme (EMEP) were used to analyzed the evolution of suspended particulate matter (SPM), particulate matter under 10 μm (PM10) and 2.5 μm (PM2.5) in six Spanish sites: Logroño, Roquetas, Peñausende, Campisabalos, San Pablo Montes, and Barcarrota. The time periods for the analysis were: 1988-2000 (for the SPM) and 2001-2012 (for the PMx). The monthly climatology for the SPM, PM10, and PM2.5 exhibited similar features. For instance, a first maximum was observed in March, while a second one appeared during summer months. This effect of bi-modality was attributed to the influence of desert dust intrusions from African continent on the aerosol climatology of the Iberian Peninsula.

With respect SPM, an average temporal trend of -0.5 μg m^{-3} per year is evaluated. The maximum rate was obtained for Roquetas site with -1.1 μg/m^3 per year being statistically significant by the Mann-Kendall non parametric test. As regards PMx, the temporal trends (statistical significance level over 99%) for PM10 were -0.35 (Barcarrota and Campisabalos) and -0.47 (Peñausende) μg/m^3 per year. The rates for PM2.5 were similar to these values. Therefore, a clear and strong reduction of the particulate matter was found over the Iberian Peninsula in the 1988-2000 period, which is still observable between 2001-2012.

The PM results in the last decade are in line with the AOD trends observed in several stations of the Iberian Peninsula [9],[10]. Hence, there is a high agreement between PM (surface aerosols) and AOD (columnar aerosols) temporal trends. Since AOD measurements are only available beyond the early 2000s, the use of PM data offers the possibility to expand the knowledge of aerosol behaviour in the last quarter century in the Iberian Peninsula. Therefore, the decrease in the aerosol load can support (at least, partially) the increase trend in the surface solar irradiance between 1985 and 2010 observed in Spain [11],[12].

REFERENCES

[1] IPCC (2007), Climate Change 2007: The Physical Science Basis. Contribution of Working Group I to the Fourth Assessment Report of the Intergovernmental Panel on Climate Change [Solomon, S., D. Qin, M. Manning, Z. Chen, M. Marquis, K.B. Averyt, M. Tignor and H.L. Miller (eds.)]. Cambridge University Press, Cambridge, United Kingdom and New York, NY, USA, 996 pp.

[2] Aas, W., et al. (2013), Transboundary particulate matter in Europe Status report 2013, EMEP Report, 4/2013 (Ref. O-7726), ISSN: 1504-6109 (print), 1504-6192 (online).

[3] Toledano, C., V. E. Cachorro, A. M. de Frutos, B. Torres, A. Berjón, M. Sorribas, R. S. Stone, 2009: Airmass Classification and Analysis of Aerosol Types at El Arenosillo (Spain). *J. Appl. Meteor. Climatol.*, *48*, 962–981., doi: http://dx.doi.org/10.1175/2008JAMC2006.1

[4] Rua, A., L. Gimeno, E. Hernandez (1999), Trend, seasonal variation and sources of suspended particulated matter (SPM) in Spain. *Toxicol. Env. Chem., 70*, 181-193, doi:10.1080/02772249909358748

[5] Querol, X., et al. (2009), African dust contributions to mean ambient PM10 mass-levels across the Mediterranean Basin, *Atmos. Env.,* 43, 4266-4277, doi:10.1016/j.atmosenv.2009.06.013

[6] Cusack M., A. Alastuey, N. Perez, J. Pey, X. Querol (2012), Trends of particulate matter (PM2.5) and chemical composition at a regional background site in theWestern Mediterranean over the last nine years (2002–2010), *Atmos. Chem. Phys., 12*, 8341-8357, doi:10.5194/acp-12-8341-2012.

[7] Gkikas, A., N. Hatzianastassiou, M. Mihalopoulos, V. Katsoulis, S. Kazadzis, J. Pey, X. Querol, O. Torres (2013), The regime of intense desert dust episodes in the Mediterranean based on contemporary satellite observations and ground measurements, *Atmos. Chem. Phys., 13*, 12135-12154, doi:10.5196/acp-13-12315-2013

[8] Barmapadimos, I., J. Keller, D. Oderbolz, C. Hueglin, A.S.H. Prevot (2012), One decade of parallel fine (PM2.5) and coarse (PM10-PM2.5) particulate matter measurements in Europe: trends and variability, *Atmos. Chem. Phys. 12,* 3189-3203, doi:10.5194/acp-12-3189-2012

[9] Bennouna, Y.S., V. Cachorro, M.A. Burgos, C. Toledano, B. Torres, A. de Frutos (2014), Relationships between columnar aerosol optical properties and surface Particulate Matter observations in north-central Spain from long-term records (2003-2011), *Atmos. Meas. Tech. Discuss.,* In press.

[10] Mateos, D., M. Antón, C. Toledano, V.E. Cachorro, L. Alados-Arboledas, M. Sorribas, M.J. Costa, J.M. Baldasano (2014), Aerosol radiative effects in the ultraviolet, visible, and near-infrared spectral ranges using long-term aerosol data series over the Iberian Peninsula, *Atmos. Chem. Phys. Discuss., 14*, 1–39, doi:10.5194/acpd-14-1-2014.

[11] Sanchez-Lorenzo, A., J. Calbó, M. Wild (2013), Global and diffuse solar radiation in Spain: Building a homogeneous dataset and assessing trends, *Global Planet. Change, 100*, 343-352, http://dx.doi.org/10.1016/j.gloplacha.2012.11.010.

[12] Mateos, D., M. Antón, A. Sanchez-Lorenzo, J. Calbó, M. Wild (2013), Long-term changes in the radiative effects of aerosols and clouds in a mid-latitude region (1985–2010), *Global Planet. Change, 111*, 288-295, http://dx.doi.org/10.1016/j.gloplacha.2013.10.004.

The first desert dust event detected by Cimel photometer in Badajoz station (Spain)

M.A. Obregón[1], A. Serrano[2], M.L. Cancillo[3], M.J. Costa[4]

Abstract — This work focuses on the study of the first Saharan desert dust episode detected by the Cimel photometer in Badajoz station (Spain). This station works operatively since June 2012 as part of AERONET (AErosol RObotic NETwork) and RIMA (Red Ibérica de Medida fotométrica de Aerosoles) monitoring networks, and follows their calibration and measuring protocols.

Within the short period of measurements, several dust events have been detected. A particularly intense dust outbreak occurred between 8 and 12 August 2012, and was measured at our station. The transport of dust from the Sahara region towards the Iberian Peninsula is one regular phenomenon that notably influences the radiation balance as well as the atmospheric visibility at those sites overspread by these aerosols. This Saharan dust event has been analyzed in terms of the measurements of several optical and microphysical aerosol properties, such as aerosol optical depth, Ångström exponent α, single scattering albedo and size distributions, and the air mass back-trajectories computed by means of the Hybrid Single Particle Lagrangian Integrated Trajectory model (HYSPLIT4). The measurements show a significant increase in the atmospheric turbidity caused by the inflow of coarse particles, with daily averages of aerosol optical depth at 500nm of about 0.5, Ångström exponent α of about 0.2, and single scattering albedo values over 0.9. These values and their range of variation are typical for desert dust intrusions.

Keywords — AERONET, desert dust, Badajoz

1 INTRODUCTION

Solar radiation is the main source of energy for the Earth-atmosphere system. Any change in the atmospheric composition would significantly affect the radiative budget and, as a result, the global temperature of the Earth. One of these components is the atmospheric aerosol, with natural and anthropogenic origins.

It is known that atmospheric aerosols, in general, modify the energy balance of the Earth-atmosphere system, but there is still a large uncertainty concerning their climate effects. They directly interact with solar and terrestrial radiation through scattering and absorption as well as through emission processes. They also indirectly affect the radiation balance by influencing the cloud formation. According to the Intergovernmental

Panel on Climate Change (2013), the total aerosol radiative forcing is estimated to be -0.9 [-1.9 to -0.1] W m^{-2} [1]. A global cooling effect due to the aerosols is now relatively well established, despite some uncertainties still remain. Accurate and reliable measurements and analyses are demanded to reduce those uncertainties. Therefore, it is of great interest to continuously monitor aerosols all around the world. One way to characterize them focuses on measuring the optical properties of the atmospheric column. This is the aim of the AERONET network (AErosol RObotic NETwork), managed by NASA, and of the RIMA network (Red Ibérica de Medida Fotométrica de Aerosoles), whom the Badajoz station belongs to.

An important source of mineral aerosol in the Iberian Peninsula, and in general in the Northern Hemisphere [2] is the Saharan Desert, playing an important role in the radiation balance of the Climate System [3]. Moreover, due to the proximity of the Saharan Desert and the annual latitudinal displacement of the general atmospheric circulation, desert dust events in the Iberian Peninsula show a typical seasonal pattern [4, 5] associated to certain synoptic situations [6, 7, 8]. These intrusions have been widely studied by means of active and passive remote sensing techniques at different locations in the Iberian Peninsula [9, 10, 11, 12, 13, 14, 15, 16,

_____

1. M.A. Obregón is with the *Geophysics Centre of Évora, University of Évora. Rua Romao Ramalho, 59, 7000 Évora. Portugal* E-mail: nines@unex.es
2. A.Serrano is with the *Department of Physics, University of Extremadura. Avda. De Elvas, s/n, 06006 Badajoz. Spain. E-mail:* asp@unex.es
3. M.L. Cancillo is with the *Department of Physics, University of Extremadura. Avda. De Elvas, s/n, 06006 Badajoz. Spain. E-mail:* mcf@unex.es
4. M.J. Costa is with the *Geophysics Centre of Évora and Physics Dep., University of Évora. Rua Romao Ramalho, 59, 7000 Évora. Portugal. E-mail: mjcosta@uevora.pt*

17]. However, there is no study of desert dust in Badajoz in terms of the measurements of optical and microphysical aerosol properties performed with Cimel photometer.

Therefore, the aim of this study is to monitor an intense Saharan dust event in the atmospheric column over Badajoz, Spain. This work is organized as follows: a brief description of the study region and instrumentation is presented in Section 2; data set and methodology are provided in section 3; results are discussed in section 4. Finally, conclusions are given in section 5.

2 STUDY REGION AND INSTRUMENTATION

The location of Badajoz radiometric station is shown in Figure 1. It is installed on the terrace of the Physics Department building at the Campus of Badajoz of the University of Extremadura, with coordinates: 38.88ºN, 7.01ºW, 186 m a.s.l.. This location guarantees continuous maintenance and open horizon.
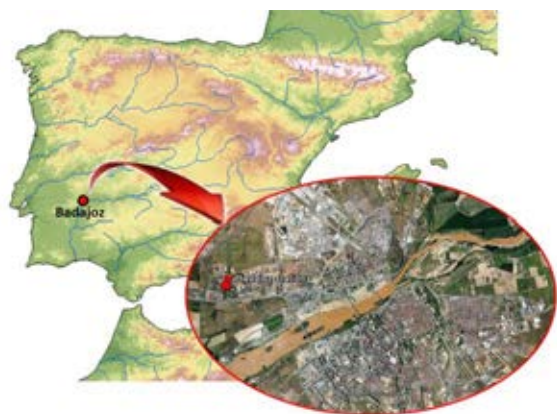
Figure 1. Iberian Peninsula showing the location of Badajoz station.

Badajoz station is managed by the AIRE (Atmósfera, clIma y Radiación en Extremadura) research group of the Physics Department, at the University of Extremadura (Spain). This station works operatively since June 2012 as part of AERONET (AErosol RObotic NETwork) and RIMA (Red Ibérica de Medida fotométrica de Aerosoles) monitoring networks, and follows their calibration and measuring protocols. This station is equipped with a CIMEL CE-318 sunphotometer, which makes direct sun measurements with a 1.2º full field of view at 340, 380, 440, 500, 675, 870, 940 and 1020 nm. In addition, the CIMEL measures sky radiances, both in almucantar and principal plane, at 440, 675, 870 and 1020 nm. More details

about this instrument are given by Holben et al. [18]. All radiance measurements are processed by AERONET protocol as described by Holben et al. [18], obtaining aerosol parameters at different quality levels (1.0, 1.5 and 2.0).

3 DATASET AND METHODOLOGY

In this work, a desert dust episode over Badajoz station, from 8 to 12 August 2012, has been identified and studied. For this purpose, we have analyzed four aerosol properties: the aerosol optical depth (τ), the Ångström α exponent (440-870) (α), the single scattering albedo (ω) and the aerosol volume size distributions (VSD). During this episode, level 2.0 data [18] are available, and have been used. However, since the conditions to reach level 2.0 are particularly restrictive for ω, there are very few values of this parameter and, therefore, level 1.5 was preferred.

The back trajectories of air masses arriving at Badajoz during this event have also been analyzed. For this analysis, 120-hour back trajectories ending at Badajoz were calculated using the HYSPILT (Hybrid Single-Particle Lagrangian Integrated Trajectory) version 4 [19, 20]. All trajectories have been calculated for 3000 m a.s.l. level (corresponding to approximately 700 hPa) arriving at 12:00 UTC. This height has been chosen because it is representative of the free troposphere, where there are hardly any aerosols except desert dust, which is transported at higher altitudes above the boundary layer. Back-trajectories were used to identify this episode, paying special attention to its origin over North Africa.

4 RESULTS

In this section, τ, α, ω, VSD and air mass back trajectories, during the period 7 – 12 August, are analyzed in order to verify the desert-dust nature of the episode. Figure 2 shows the time evolution of τ500 and α during the Saharan dust episode occurred between 7 and 12 August 2012. From 8 to 9 August there is an increase in τ from about 0.1 to 0.5 and a simultaneous significant decrease in α from about 1.2 to 0.5.
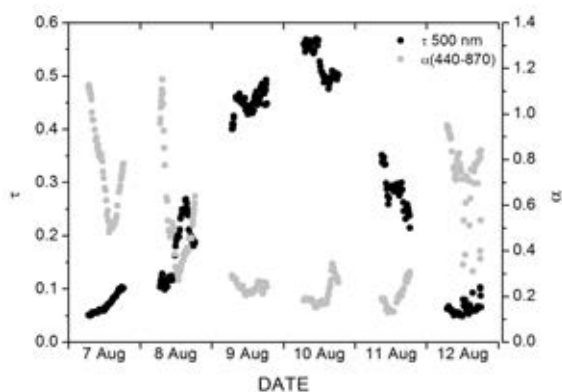
Figure 2. Evolution of τ500 nm and α during the time period 7-12/08/2012, which includes the desert dust event (9-11/08).

Daily average values, computed using all available data for each day, of aerosol optical depth τ at 500 nm, Ångström exponent α and single scattering albedo ω at 675 nm, during the days of dust influence, have been calculated (Table 1).

Table 1. Daily average values of aerosol optical depth at 500 nm, Ångström α exponent (440-870) and single scattering albedo ω at 675 nm during the time period 7-12/08/2012 at Badajoz.

Day	τ500	α	ω675
07-08-2012	0.07	0.78	0.84
07-08-2012	0.17	0.58	0.92
09-08-2012	0.45	0.24	0.96
10-08-2012	0.52	0.21	0.96
11-08-2012	0.28	0.21	0.96
12-08-2012	0.06	0.74	0.82

On 7 August τ was very low and significantly increased on 8 August as α decreased. As shown in Table 1, the highest daily average values of τ (0.45, 0.52 and 0.28) and the lowest daily average values of α (0.24, 0.21 and 0.210) were detected in Badajoz on the 9, 10 and 11 August. The data presented in Figure 2 and Table 1 agrees with the back trajectories shown in Figure 3. Figure 3a illustrates the atmospheric circulation from the North Atlantic area on 7 August. On 8 August (Figure 3b) trajectories passed near North Africa. On 9, 10 and 11 August (Figure 3c, 3d and 3e), all trajectories overpassed North Africa and surrounding areas transporting desert aerosol. On 12 August (Figure 3f) the back trajectories came again from the Atlantic area, similarly to the days before the dust event.
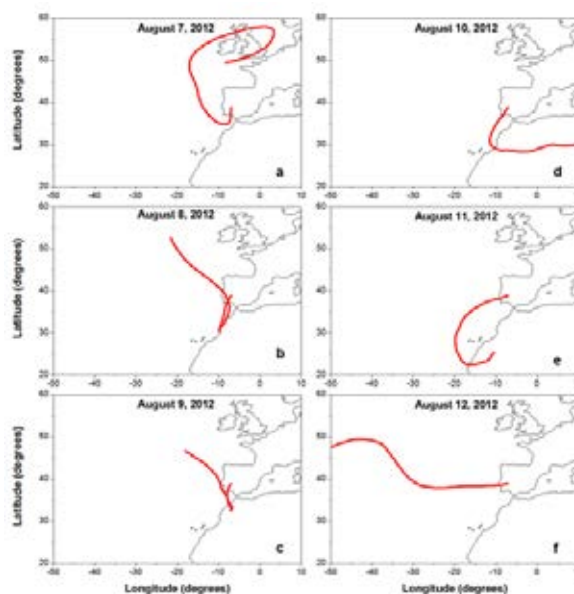
Figure 3. 120 h back trajectories at 3000 m a.s.l. arriving at Badajoz station from 7 to 12 August 2012.

Concerning ω (Table1 and Figure 4), its values were higher during the desert dust episode, increasing with the wavelength as it is expected for desert dust aerosols [21].
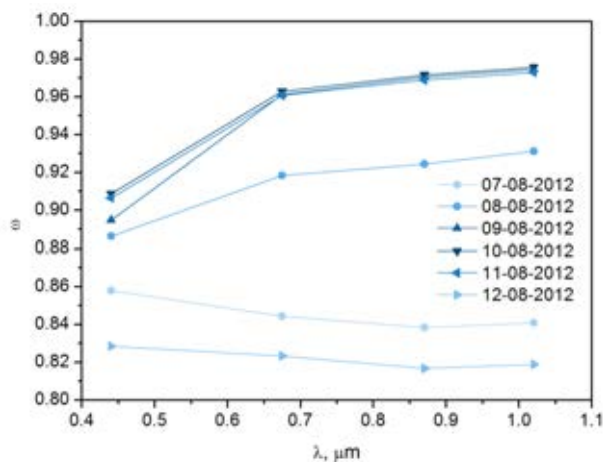
Figure 4. Relation between the average single scattering albedo values and the wavelengths during the time period 07-12/08/2012.

The behaviour of α during the desert dust episode is consistent with the measured aerosol volume size distributions (VSD) (Figure 5). On 9, 10 and 11 August, the proportion of coarse aerosols was clearly higher than before the beginning and after of the episode (7 and 12 August).
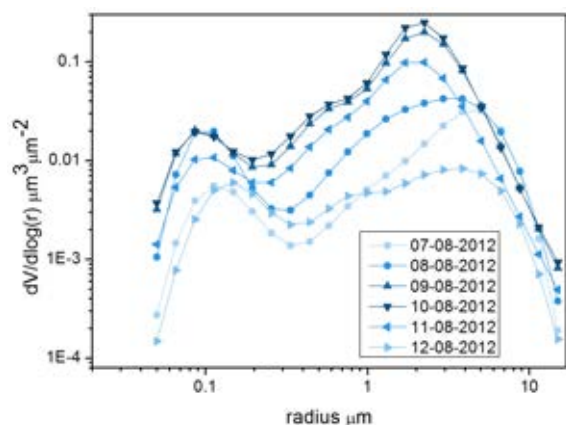
Figure 5. Daily average values of aerosol volume size distribution during the time period 07-12/08/2012.

5 CONCLUSIONS

This study contributes to the identification and analysis of a Saharan dust event over Badajoz (Spain). This event occurred between 7 and 12 August 2012. It has been detected from the analysis of different aerosol in-column radiometric properties, and from the back-trajectories of the air masses carrying the aerosols.

The measurements show a significant increase in the atmospheric turbidity caused by the inflow of coarse particles, with daily averages of aerosol optical depth at 500nm of about 0.5, Ångström exponent α of about 0.2, and single scattering albedo values over 0.9. These values and their range of variation are typical for desert dust intrusions.

REFERENCES

[1] Boucher, O., D. Randall, P. Artaxo, C. Bretherton, G. Feingold, P. Forster, V.-M. Kerminen, Y. Kondo, H. Liao, U. Lohmann, P. Rasch, S.K. Satheesh, S. Sherwood, B. Stevens and X.Y. Zhang, 2013: Clouds and Aerosols. In: Climate Change 2013: The Physical Science Basis. Contribution of Working Group I to the Fifth Assessment Report of the Intergovernmental Panel on Climate Change [Stocker, T.F., D. Qin, G.-K. Plattner, M. Tignor, S.K. Allen, J. Boschung, A. Nauels, Y. Xia, V. Bex and P.M. Midgley (eds.)]. Cambridge University Press, Cambridge, United Kingdom and New York, NY, USA.

[2] J. M. Prospero, P. Ginoux, O. Torres, S. E. Nicholson, and T. E. Gill, "Environmental characterization of global sources of atmospheric soil dust identified with the NIMBUS 7 Total Ozone Mapping Spectrometer (TOMS) absorbing aerosol products", Rev. Geophys., vol. 40, no, 1, 1002, doi:10.1029/2000RG000095, 2001.

[3] R. Arimoto, "Eolian dust and climate: relationship to sources, tropospheric chemistry, transport and deposition", Earth Sci. Rev., vol.54, pp.29-42, 2001.

[4] V.E. Cachorro, C. Toledano, A.M. de Frutos, M. Sorribas, J.M. Vilaplana, and B. de la Morena, "Aerosol characterization at El Arenosillo (Huelva, Spain) with an AERONET/PHOTONS CIMEL sunphotometer", Geophys. Res. Abstract, vol.7(08559), 2005.

[5] C. Toledano, "Climatología de los aerosoles mediante la caracterización de propiedades ópticas y masas de aire en la estación El Arenosillo de la red AERONET". PhD thesis, Universidad de Valladolid, Spain, 2005.

[6] S. Rodriguez, X. Querol, A. Alastuey, G. Kallos, and O. Kakaliagou, "Saharan dust contributions to PM10 and TSP levels in Southern and Eastern Spain", Atmos. Environ., vol.35, pp.2433–2447, 2001.

[7] X. Querol, S. Rodriguez, E. Cuevas, M.M. Viana, and A Alastuey, "Intrusiones de masas de aire africano sobre la Península Ibérica y Canarias: mecanismos de transporte y variación estacional", 3rd Asamblea Hispano portuguesa de Geodesia y Geofísica, Inst. Nac. de Meteorol. Esp., Valencia, 2002.

[8] M. Escudero, S. Castillo, X. Querol, A. Avila, M. Alarcón, M.M. Viana, A. Alastuey, E. Cuevas, and S. Rodríguez, "Wet and dry African dust episodes over eastern Spain", J. Geophys. Res., vol.110, D18S08, doi:1029/2004JD004731, 2005.

[9] L. Alados-Arboledas, H. Lyamani, and F.J. Olmo, "Aerosol size properties at Armilla, Granada (Spain)", Q. J. R. Meteorol. Soc., vol.129, pp.1395-1413, 2003.

[10] H. Lyamani, F.J. Olmo, and L. Alados-Arboledas, "Saharan dust outbreak over southeastern Spain as detected by Sun photometer", Atmos. Environ., vol.39, pp.7276-7284, 2005.

[11] Elias, T., A.M. Silva, N. Belo, S. Pereira, P. Formenti, G. Helas, and F. Wagner, "Aerosol extinction in a remote continental region of the Iberian Peninsula during summer", J. Geophys. Res. 111(D14204), 1–20, 2006.

[12] V.E, Cachorro, R. Vergaz, A.M. de Frutos, J.M. Vilaplana, D. Henriques, N. Laulainen, and C. Toledano, "Study of desert dust events over the southwestern Iberian Peninsula in year 2000: two cases studies", Ann,. Geophys., vol.24, pp.1-18, 2006.

[13] Toledano, C., V.E.Cachorro, A.M. de Frutos, M. Sorribas, N. Prats, and B. de la Morena, "Inventory of African desert dust events over the southwestern Iberian Peninsula in 2000-2005 with an AERONET CIMEL Sun photometer", *J. Geophys. Res*. 112 (D21201), 1–14, 2007.

[14] Cachorro, V.E., Toledano, C., Prats, N., Sorribas, M., Mogo, S., Berjón, A., Torres, B., Rodrigo, R., de la Rosa, J., De Frutos, A.M.." The strongest desert dust intrusion mixed with smoke over the Iberian Peninsula registered with Sun photometry". J. Geophys. Res. 113, D14S04, 2008, http://dx.doi.org/10.1029/2007JD009582.

[15] Guerrero-Rascado, J.L., Ruiz, B., Alados-Arboledas, L. "Multispectral lidar characterization of the vertical structure of Saharan dust aerosol over southern Spain". Atmos. Environ. 42, 2668–2681, 2008.

[16] Wagner, F., Bortoli, D., Pereira, S., Costa, M.J., Silva, A.M., Weinzierl, B., Esselborn, M., Petzold, A., Rasp, K., Heinol, B., Tegen, I. "Properties of dust aerosol particles transported to Portugal from the Sahara desert". Tellus B 61, 297–306, 2009.

[17] Valenzuela, A., Olmo, F.J., Lyamani, H., Antón, M., Quirantes, A., Alados-Arboledas, L., "Analysis of the desert dust radiative properties over Granada using principal plane sky radiances and spheroids retrieval procedure". Atmos. Res. 104–105, 292–301, 2012a, http://dx.doi.org/10.1016/j.atmosres.2011.11.005.

[18] B. Holben, T.F. Eck, I. Slutsker, D. Tanre, J. Buis, K. Setzer, E. Vermote, J. Reagan, Y. Kaufman, T. Nakajima, F. Lavenu, I. Jankowiak, and A. Smirnov, "AERONET-A Federated Instrument Network and Data Archive for Aerosol Characterization". Remote Sens. Environ.,vol. 66, pp.1–16,1998.

[19] R. Draxler, and G.D. Hess, "An overview of the HYSPLIT_4 modelling system for trajectories, dispersion and deposition", Aust. Met. Mag, vol.47, pp.295–308, 1998.

[20] R. Draxler, and G. Rolph, "HYSPLIT (HYbrid Single-Particle Langrangian Integrated Trajectory) Model access via NOAA ARL READY Website", (http://www.arl.noaa.gov/ready/hysplit4.html), NOAA Air Resources Laboratory Silver Spring, MD, 2003.

[21] O. Dubovik, B. Holben, T. Eck, A. Smirnov, Y. Kaufman, M. King, D.Tanré, and I. Slutsker, "Variability of absorption and optical properties of key aerosol types observed in worldwide locations. J.Atmos. Sci., vol.59, pp.590–608, 2002.

THE REDMAAS 2014 INTERCOMPARISON CAMPAIGN: CPC, SMPS, UFPM AND NEUTRALIZERS

F. J. Gómez-Moreno[1], E. Alonso[1], B. Artíñano[1], S. Iglesias Samitier[2], M. Piñeiro Iglesias[2],
P. López Mahía[2], N. Pérez[3], A. Alastuey[3], B. A. De La Morena[4], M. I. García[5], S. Rodríguez[5],
M. Sorribas[6,7], G. Titos[6,7], H. Lyamani[6,7], L. Alados-Arboledas[6,7], E. Filimundi[8] and
E. Latorre Tarrasa[9]

Abstract —The Spanish network on environmental DMAs (Red Española de DMAs Ambientales, REDMAAS), working since 2010, is currently formed by six groups involved in the measurement of atmospheric aerosol size distributions by means of Differential Mobility Analyzers (DMAs). One of its activities is an annual intercomparison of mobility size spectrometers (SMPS and UFPM). In this work we show the results obtained in the 2014 campaign: the verification of DMA calibrations with latex, the results of the CPC and SMPS + UFPM intercomparisons, and a comparison of the new TSI 3087 X-ray and the former TSI 3077 ^{85}Kr neutralizers. The concentrations measured by different types of CPC were within the range of 10% of the average value. CPCs working at higher flow rates measured slightly higher concentrations, probably related to the smaller losses in the lines. All the SMPS worked at the same sampling and sheath flow rates (1:10 lpm). Four of the SMPS gave very good results for particles larger than 20 nm. The UFPM measured particle number concentrations in the average +/-10% band measured by the SMPS. Instruments working with the X-ray neutralizer measured higher concentrations than with the ^{85}Kr neutralizers. This could mean that particle losses are smaller inside this neutralizer.

Keywords — Atmospheric aerosols, Particle size distribution, SMPS, UFPM, X-ray neutralizer

1 INTRODUCTION

Atmospheric particle size affects the particle behavior and provides information about its origin and history. Size distributions are a key parameter in those processes where the atmospheric aerosol is involved. For example, a critical point in health effect studies is to obtain the fraction of particles deposited in the lungs and the respiratory system in general, as well as those able to penetrate into the bloodstream. These effects are mainly dependent of the particle size distribution. Some studies have shown that the particle toxicity per mass unit increases as the particle size decreases [1, 2], and

————————————————

1. *Department of Environment, CIEMAT, Madrid, E-28040, Spain, First Author E-mail: FJ.Gomez@ciemat.es*
2. *Grupo Química Analítica Aplicada, Instituto Universitario de Medio Ambiente (IUMA), Departamento de Química Analítica, Facultade de Ciencias,Universidade da Coruña, Campus de A Coruña, 15071 A Coruña, Spain*
3. *Institute of Environmental Assessment and Water Research (IDAEA-CSIC), Barcelona, E-08034, Spain*
4. *Atmospheric Sounding Station 'El Arenosillo', INTA, Mazagón-Huelva, E-21130, Spain*
5. *Izaña Atmospheric Research Centre, (IARC/CIAI), AEMet, Santa Cruz de Tenerife, E-38001, Spain*
6. *Andalusian Institute for Earth System Research, IISTA-CEAMA, University of Granada, Granada, E-18071, Spain*
7. *Applied Physics Department, University of Granada, Granada, E-18071, Spain*
8. *TSI GmbH, Aachen, D-52068, Germany*
9. *Álava Ingenieros, Madrid, E-28037, Spain*

therefore, an important goal is to study the smaller particles or ultrafine particles.

The radiation-matter interaction processes known as scattering and absorption also depend on the particle size. Atmospheric particles play a key role in the Earth's radiative balance and thus influence climate change [3]. Some climate models indicate that aerosols are delaying the expected warming due to the greenhouse gases. Sulfate and organic particles have a particular influence on this delay and both kinds of particles are mainly found in the ultrafine range.

In addition to those works focused on particle formation by nucleation [4], the origin and distribution of ultrafine particles has been studied in different kinds of stations: rural [5], regional background [6, 7], arctic and coastal background [8], tropospheric background in Antarctica [9] ... but mainly in urban sites in some European and American cities, e.g. Birmingham [10], Helsinki [11], Pittsburgh [12], Barcelona [13].

The Spanish network on environmental DMAs (Red Española de DMAs Ambientales, REDMAAS) is currently formed by six groups involved in the measurement of atmospheric aerosol size distributions by means of Differential Mobility Analyzers (DMAs). These groups are: IUMA-UDC, IDÆA-CSIC, INTA, IARC-AEMET, University of Granada and CIEMAT. This network has been working since 2010. Its objective is to promote the exchange and transfer of knowledge between the

groups and to optimize the use of instrumentation such as the Scanning Mobility Particle Sizers (SMPS). This is reached through a series of activities to ensure the quality of the measurements and the cooperation between the groups. One of the activities of the REDMAAS is an annual campaign where DMA calibration checks, and Condensation Particle Counters (CPC), UltraFine Particle Monitor (UFPM) and SMPS intercomparisons are performed. In this paper we introduce the results obtained during the 2014 campaign.

2 CAMPAIGN LOCATION AND INSTRUMENTATION

2.1 Location

The intercomparison campaign was held in the Atmospheric Sounding Station El Arenosillo (37.10°N, 6.73°W, 40 m a.s.l.) belonging to Instituto Nacional de Técnica Aeroespacial (INTA) (www.inta.es/atmosfera) [14]. The observatory is located on the Atlantic coast of Andalusia, in the province of Huelva and within the Natural Area of the Doñana National Park. Around the observatory, from W to SE and clockwise over several tens of kilometers, it is possible to find a tree forest with predominance of pine. The Atlantic Ocean is in the SE-W clockwise area and less than 1 km from the observatory. The closest large population is the City of Huelva (160 000 inhabitants), 35 km to the northwest. This location allows the research of wide and different kinds of particle size distributions, covering several orders of magnitude for the particle concentration (from marine aerosols to secondary formation from industrial and natural precursors).

2.2 Instrumentation

In the 2014 intercomparison campaign, all the groups except AEMET participated. TSI and their Spanish representatives, Álava Ingenieros, were also involved with the new electrostatic classifier TSI 3082. During the campaign 7 CPCs (3x3772, 2x3776, 1x3785 and 1x3775), 5 SMPSs (4x3080 and 1x3082) and 1 UFPM (3031) were deployed, all of them manufactured by TSI. At the same time a new TSI 3087 X-ray and the former TSI 3077 [85]Kr neutralizers were used.

This campaign was performed from February 17th to 21th, 2014. The instrument deployment used during the campaign can be found in Fig. 1.

Fig. 1. In this figure it is possible to see the five SMPSs used during the instrument intercomparison.

3 RESULTS

3.1 DMA calibration checks

As in other REDMAAS campaigns, previously to the intercomparisons, a general routine maintenance was performed to ensure proper operation of the different instruments. A Gilian Gilibrator-2 just calibrated was used as primary standard for the calibration of air flows. The difference in the flow rates among the different CPCs was less than 5% and among the SMPS systems the sheath flow rate difference was less than 4%.

The high voltage sources were checked using a HV probe and all the instruments showed a deviation smaller than 0.3% in the calibration.

After these verifications, the DMAs calibrations were checked by using latex particles of 80 and 190 nm suspended in water and aerosolized using a Collinson atomizer [15].

During this campaign, the deviations obtained were higher than during the previous ones, reaching an average value of 6.3% for the 80 nm particles and 5.4% for the 190 nm ones. It is remarkable that the deviation among the instruments were very small, indicating that the problem could be in the generating system, not in the instruments.

3.2 CPC intercomparison

The second activity was the CPC intercomparison. All used butanol as condensation liquid, with the exception of one water-based CPC (TSI 3785). Ambient air was sampled from a common flow splitter, which was connected to an external probe. The results have been classified into two groups, depending on the CPC flow rates. The first group corresponds to the CPCs working at 1 lpm and the second one with those running at 0.3 or 1.5 lpm. During this intercomparison both flow rates were checked for this second group showing lower concentrations than the first group for 0.3 lpm and higher ones for 1.5 lpm. The reason for these differences is the diffusional losses in the lines,

smaller as the resident time is shorter (higher flow rates). The differences among the CPCs inside each group are smaller than 10% as can be seen in fig. 2.
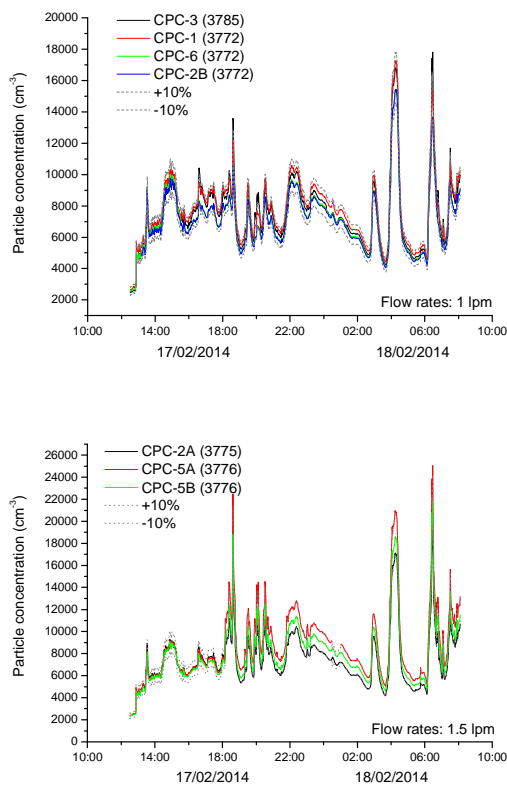
Fig. 2. CPC intercomparison during the campaign. They have been classified by their working flow rates.

3.3 SMPS and UFPM intercomparison

The SMPS intercomparison for a selected period is shown in Fig. 3. All SMPS systems worked at the same sampling and sheath flow rates (1:10 lpm).
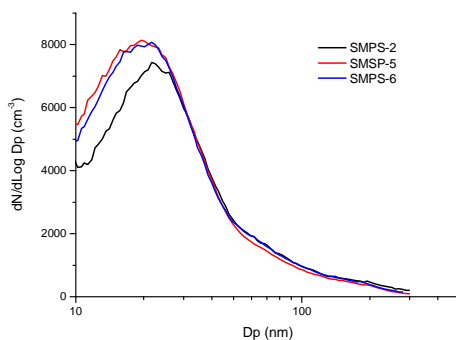
Fig. 3. SMPS measurement comparison for systems 2, 5 and 6. The results obtained are very good for particle sizes larger than 20nm. Below this size, it is very usual to find important differences among the

instruments.

In this figure, SMPS-1 is not included as it worked with the new TSI X-Ray neutralizer (see next section). SMPS-3 is also not included because of a leak observed during the measurements. The differences between the three systems shown in the graph are important below 20 nm, a size range where the differences among the instruments have shown to be very large [16]. Above this particle diameter, the differences are very small. SMPS-1 is compared with SMPS-6 in figure 5a, where, again, the differences are small for particles bigger than 10 nm. The four systems have shown to have a good behavior.
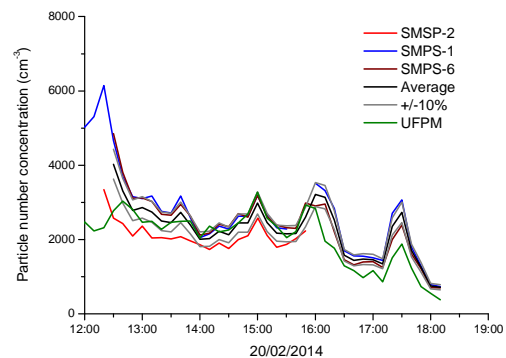
Fig. 4. Comparison of particle concentrations measured by the SMPSs and the UFPM.

The UFPM was also compared with the SMPSs. The period covered with these instruments can be found in figure 4. This figure shows the total particle number concentration measured by the 4 systems, the SMPS average values and the average +/- 10% band for these values. During the first period, before 16h, the UFPM measured properly the number concentration. SMPS-2 measured a lower concentration. This could be caused by a distribution with high concentrations of particles below 20 nm, where this SMPS measured smaller concentrations. After 16h, concentrations measured with SMPS-2 are within the average +/- 10% band, but the UFPM is below that band. The matrix selected in the UFPM was the factory calibration with ammonium sulfate.

3.4 Neutralizer intercomparison

In order to check the new TSI X-ray neutralizer model 3087 (< 9.5 keV), the Kr-85 source was removed from the SMPS-1 and the X-ray neutralizer was installed. This SMPS was previously compared with SMPS-6 proving to measure very similar distributions when using both instruments the Kr-85 neutralizer, as it can be observed in fig. 5a. Subsequently, both systems were working during 16 hours with the different neutralizers and the average distributions obtained are shown in fig. 5b and 5c. The first and second graphs reflect to periods with

low and high particle concentrations, respectively. It is possible that the new X-ray neutralizer has lower particle losses than the Kr-85 one. The differences between the neutralizers seem to depend on the particle concentration, as they were more evident as the number concentration increased. At the moment, in the TSI AIM software there is no option to indicate which neutralizer is in use, so when applying correction for diffusion losses it considers the same losses in both cases.
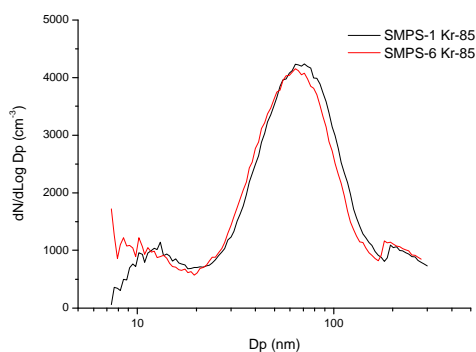
(a)
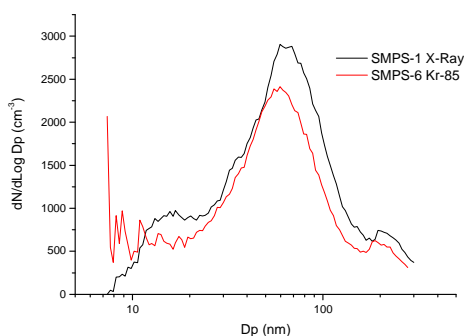
(b)
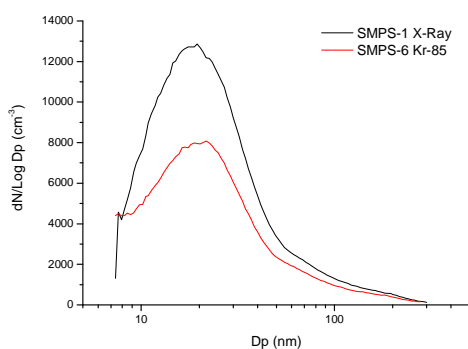
(c)

Fig. 5. Comparison of SMPS-1 and SMPS-6 measurements when: a) both had a Kr-85 neutralizer; b) SMPS-1 had an X-Ray neutralizer and the particle concentration was low; c) as b, with high particle concentration.

8 CONCLUSIONS

The instruments belonging to the Spanish network on environmental DMAs (REDMAAS) had shown similar behaviors during the 2014 campaign. CPCs working at higher flow rates measured slightly higher concentrations, probably related to the smaller losses in the lines. Taking this into account, particle concentrations measured by the different types of CPC were within the range of 10% of the average value. Four SMPSs have given good results for particle sizes above 20 nm. The X-ray neutralizer has shown to have smaller losses than the traditional Kr-85 source. The total number concentration measured with the UFPM was also within the average +/- 10% band measured by the SMPSs.

This kind of campaign is very useful as it allows detecting instrumental problems that are difficult to detect during routine operation of the instrumentation at the stations.

REFERENCES

[1] J.J.N Lingard, A.S. Tomlin, A.G. Clarke, K. Healey, A. Hay and C.P. Wild, "A study of trace metal concentration of urban airborne particulate matter and its role in free radical activity as measured by plasmidstrand break assay," Atmos. Environ., 39, pp. 2377-2384, 2005.

[2] G. Oberdorster, "Toxicology of ultrafine particles: in vivo studies," Phil. Trans. R. Soc. A, 358, 2719-2740, 2000.

[3] Climate change 2007: synthesis report. In: Contribution of Working Groups I, II and III to the Fourth Assessment Report of the Intergovernmental Panel on Climate Change, R.K Pachauri, A. Reisinger, eds. IPCC, Geneva, Switzerland, 2007.

[4] M. Kulmala, H. Vehkamäki, T. Petäjä, M. Dal Maso, A. Lauri, V.-M. Kerminen, W. Birmili and P.H. McMurry, "Formation and growth rates of ultrafine atmospheric particles: a review of observations," J. Aerosol Sci., 35, pp. 143–176, 2004.

[5] J.M. Mäkelä, P. Aalto, V. Jokinen, T. Pohja, A. Nissinen, S. Palmroth, T. Markkanen, K. Seitsonen, H. Lihavainen and

M. Kulmala, "Observations of ultrafine aerosol particle formation and growth in boreal forest," Geophys. Res. Lett., 24, pp. 1219-1222, 1997.

[6] M. Cusack, N. Pérez, J. Pey, A. Alastuey and X. Querol. "Source apportionment of fine PM and sub-micron particle number concentrations at a regional background site in the western Mediterranean: a 2.5 yr study," Atmos. Chem. Phys. Discuss. 13, pp. 3915-3955, 2013, submitted for publication in ACP.

[7] M. Cusack, N. Pérez, J. Pey, A. Wiedensohler, A.Alastuey and X. Querol, "Variability of sub-micrometer particle number size distributions and concentrations in the Western Mediterranean regional background," Tellus B, 65, pp. 19243, 2013.

[8] M. Sorribas, V.E. Cachorro, J.A. Adame, B. Wehner, W. Birmili, A. Wiedensohler, A.M. De Frutos and B.A. de la Morena, "Sub-micrometric aerosol size distributions in Southwestern Spain: Relation with meteorological parameter". ICNAA. Galway (Irlanda), 2007.

[9] J. L. Gras, "Condensation nucleus size distribution at Mawson, Antarctica: micro-physics and chemistry," Atmos. Environ., 27, Part A, pp. 1417-1425, 1993.

[10] R.M. Harrison, M. Jones and G. Collins, "Measurements of the physical properties of particles in the urban atmosphere", Atmos. Environ., 33, pp. 309-321, 1999.

[11] T. Hussein,, A. Puustinen, P.P. Aalto, J.M. Mäkelä, K. Hämeri and M.Kulmala, "Urban aerosol number size distributions," Atmos. Chem. Phys., 4, pp. 391-411, 2004.

[12] C.O. Stanier, A.Y. Khlystov and S.N. Pandis, "Ambient aerosol size distributions and number concentrations measured during the Pittsburgh Air Quality Study (PAQS)," Atmos. Environ., 38, pp. 3275-3284, 2004.

[13] J. Pey, S. Rodríguez, X. Querol, A. Alastuey, T. Moreno, J. P. Putaud and R. Van Dingenen, "Variations of urban aerosols in the western Mediterranean," Atmos. Environ., 42, pp. 9052-9062, 2008.

[14] M. Sorribas, B. A. de la Morena, B. Wehner, J. F. López, N. Prats, S. Mogo, A. Wiedensohler, and V. E. Cachorro, 2011. On the sub-micron aerosol size distribution in a coastal-rural site at El Arenosillo Station (SW – Spain). Atmospheric Chemistry and Physics, 11, 11185–11206.

[15] K.R. May, "The Collison Nebulizer. Description, Performance & Application," *J. Aerosol Sci.*, 4, pp. 235-243 1973.

[16] A. Wiedensohler, W. Birmili, A. Nowak, A. Sonntag, K. Weinhold, M. Merkel, B. Wehner, T. Tuch, S. Pfeifer, M. Fiebig, A. M. Fjäraa, E. Asmi, K. Sellegri, R. Depuy, H. Venzac, P. Villani, P. Laj, P. Aalto, J. A. Ogren, E. Swietlicki, P. Williams, P. Roldin, P. Quincey, C. Hüglin, R. Fierz-Schmidhauser, M. Gysel, E. Weingartner, F. Riccobono, S. Santos, C. Grüning, K. Faloon, D. Beddows, R. Harrison, C. Monahan, S. G. Jennings, C. D. O'Dowd, A. Marinoni, H.-G. Horn, L. Keck, J. Jiang, J. Scheckman, P. H. McMurry, Z. Deng, C. S. Zhao, M. Moerman, B. Henzing, G. de Leeuw, G. Löschau, and S. Bastian: Mobility particle size spectrometers: harmonization of technical standards and data structure to facilitate high quality long-term observations of atmospheric particle number size distributions, Atmos. Meas. Tech., 5, 657-685, 2012.

Trends in air pollution between 2000 and 2012 in the Western Mediterranean: a zoom over regional, suburban and urban environments in Mallorca (Balearic Islands)

J. C. Cerro[1], V. Cerdà[1], J. Pey[2,3]

Abstract — Particulate matter and gaseous pollutants concentrations (NO_x, SO_2 and O_3) have been measured on a regular basis in several European regions since the beginning of the 90's. Based on these long-term series of air pollutants, the study of trends over certain European regions has been reported.

In the context of the Balearic Islands, more than a decade of uninterrupted measurements at multiple locations has provided, for the first time at an insular location in the Western Mediterranean Basin, the opportunity to study the inter-annual tendencies and the variability of different air quality metrics. Hourly data of NO, NO_2, SO_2, O_3 and PM_{10} from 2000 to 2012 were compiled and validated. The monitoring sites were classified in urban, suburban, and rural (or regional) background. The selection of the monitoring sites considered in the trend analysis was done according to two essential criteria: 1) the annual data coverage should be over 75%; and 2) at least 8 of the last 10 years of data exists. Furthermore, the origin of air masses was daily computed, which is a useful way to account for long-range transport of pollutants or to address the occurrence of meso-scale atmospheric processes.

Daily, weekly, seasonal and inter-annual patterns of these pollutants have been studied at the different environments. The multi-year and multi-pollutant study, over three environments from the same region, together with the discrimination per air mass origins permitted us to follow those changes induced by the implementation of regional policies and those related to the enactment of continental strategies.

Up to now some clear results have been obtained. NO and NO_2 undergo clear decreasing trends in urban stations (-1.1 $\mu g/m^3$year), less evident in suburban and regional background stations (from no change to -0.3 $\mu g/m^3$year). The behaviour of O_3 is opposite to that of NO_x at urban stations (+1.0 $\mu g/m^3$year), almost parallel to the decrease in NO, one of its main depletion agents. At rural background sites O_3 shows a moderate increasing trend (+0.5 $\mu g/m^3$year), consistent with the observations in other European regions. Significant decreasing O_3 concentrations are patent at the suburban background (-0.4 $\mu g/m^3$year), probably caused by an increasing vehicular traffic over these areas.

Finally, a substantial decline in PM_{10} is obvious at urban and suburban (-0.7 $\mu g/m^3$year) areas, slightly lower over the regional background (-0.5 $\mu g/m^3$year).

Keywords — Air Pollution, Atmospheric Dust, Particulate Matter, pollutant gases, PM_{10}, NO_x, SO_2, O_3.

1 INTRODUCTION

Atmospheric pollution is one of the most important problems that countries have to face correlated with their economical growth. In Europe, a significant effort to abate air pollution from different sources has been done. Not only anthropogenic activities increase the concentrations of several pollutants in the atmosphere, but natural emissions also. Once in the atmosphere, these substances are diluted, transported and (photo)-chemically processed, and thus their impact is recorded both in nearby [1, 2] and distant areas [3, 4]. Airborne particles (coarse, fine and ultrafine with different chemical compositions) and gaseous compounds such as nitrogen oxides (NO_x), ozone (O_3) and sulphur dioxide (SO_2) are the traditionally parameters regulated in air quality.

Airborne particles are associated with different adverse impacts on human health. Similarly, nitrogen oxides (NO_x), ozone (O_3), sulphur dioxide (SO_2) can induce some cardiovascular and lung diseases, premature deaths and carcinogenic effects [5, 6]. In addition, these atmospheric pollutants also affect the ecosystems, the agriculture and the historical heritage [7].

National legislation has traditionally regulated airborne particles as Suspended Particulate Matter (PM) and atmospheric Deposition. In 2001, European Directives changed particulate matter standards to two parameters, PM_{10} and $PM_{2.5}$ (mass concentration under 10 and 2.5 µm of dynamic diameter, respectively).

Thus, PM and gaseous pollutants have been measured on a regular basis in several European countries since the 90 decade. This has allowed the research of trends at certain European regions [4, 8-11]. However, it is not always straightforward to discriminate the origin of the observed trends.

In Mallorca, the tourism became the main economy sector since the 60's. This has provided as main atmospheric anthropogenic emission sources vehicular traffic, power plants, construction sector, harbours and airports, strongly concentrated during the warm season. From a legislative point of view air quality in Mallorca could be currently considered as good nowadays, but PM

concentrations and specific gaseous pollutants exceed in different areas the WHO guidelines [5]. In fact, different abatement strategies have been implemented since 2000 in addition to the European mitigation strategies.

The Mallorca Isle can be regarded as representative of the background conditions in the Western Mediterranean. In the study area, a number of urban, suburban and regional background monitoring air quality sites are used. This work analyzes daily, weekly, seasonal and inter-annual patterns of diverse pollutants at different environments in this Isle.

2 METHODOLOGY

2.1 Database generation

The regional Government owns data of more than a decade of uninterrupted measurements. More than five million data have been stored in different types of database managers, like SQL and Database. It was essential to extract them and integrate in a unique table.

It is usual to find outliers in air quality values, and especially in such huge database. Therefore, a widespread review was necessary before starting to do any calculation. Finally, hourly data of NO, NO_2, SO_2, O_3 and PM_{10} from 2000 to 2012 were compiled.

According to the criteria included in the European Directive 2008/50/EC, the monitoring sites used in this work are classified in urban, suburban, and rural (or regional) background.

Additionally, it was compulsory to take into account two more criteria that are indicated in the guidelines of the European Environmental Agency [12] to choose monitoring sites for the analysis of trends: the annual data coverage should be over 75%; at least 8 of the last 10 years of data exists.

After discarding the air quality stations that didn't fit these criteria, a merged database for each pollutant (O_3, NO, NO_2, SO_2 and PM_{10}) was built-up for each type of environment.

2.2 Measurements and quality assurance

All the measurements performed in the air quality network of the Balearic Islands comply with the European directives in terms of reference methods (as EN standards), or equivalent ones after the demonstration of their equivalence with respect to those: EN 14212 for SO_2; EN 14211 for NO_2; EN 14626 for CO; and EN 14625 for O_3.

These standards normalize the measurement principle and the device performance, and also specify the minimum criteria for quality assurance in a week maintenance, two-week zero and span verification and quarter calibration. Laboratory of the Atmosphere from regional Government has take care of the compliance of these standards during the period in study.

The methods used for PM_{10} monitoring comprised real-time absorption of beta radiation and tapered oscillating microbalance. In both cases, routinely intercomparisons against the gravimetric reference method were performed to retrieve the correction factors, which were thereafter applied to correct the real-time measurements.

2.3 Statistical treatment

For daily and seasonal patterns only average concentrations have been calculated for all the period in study.

Patterns have been calculated using the software developed by the R project (http://www.R-project.org/). Specifically, we used the package Openair, which was specifically designed for air pollution data treatment.

Mann-Kendall test has been used to identify linear and non-linear trends.

3 RESULTS

3.1 Daily, weekly and seasonal

-Nitrogen Oxides (NO and NO_2)
NO concentrations display two daily peaks, coincident with vehicular traffic rush hours. This pattern is more pronounced in the urban background (Fig.1), less important in the suburban background (Fig. 2). In the regional background the second diurnal peak is almost absent (Fig.3). The afternoon peak is substantially reduced in magnitude with respect to the morning one, which can be related to the higher ozone concentrations (yielding to the fast oxidation of NO to NO_2), but also to the higher atmospheric ventilation.

NO_2, however, displays morning and evening peaks in all types of environment, with the vespertine augmentation only slightly lower than the morning one. These findings underline the rapidness of NO to NO_2 conversion in the presence of ozone in our region.

NO, similar to NO_2, SO_2 and PM_{10}, shows a slight accumulation during weekdays with an important drop during weekends. The differences between Monday and Friday evidence the lack of accumulation in all the environment in the island, depending and that air quality situation depend directly on the emission sources. In contrast, ozone concentrations tend to increase during the weekends in all type of environments, slight increase in regional and suburban areas and more important in urban.

NO and NO_2 show a clear seasonal behavior in urban (Fig.1) and suburban (Fig.2) areas, with higher winter concentrations and moderately or significantly reduced in summer, especially for NO_2. In regional background (Fig.3) this clear pattern is diluted.

-Sulfur Dioxide (SO_2)
The daily pattern of SO_2 indicates additional emission sources than land-traffic. The morning peak coincides with traffic rush hours, similar to NO_x and PM_{10}, but a midday peak is appreciable too, probably due to the affection of shipping and energy sector, two major emission sources of this pollutant.

In general, SO_2 concentrations increase in winter in all areas probably due to the contribution of the local sources

already commented.
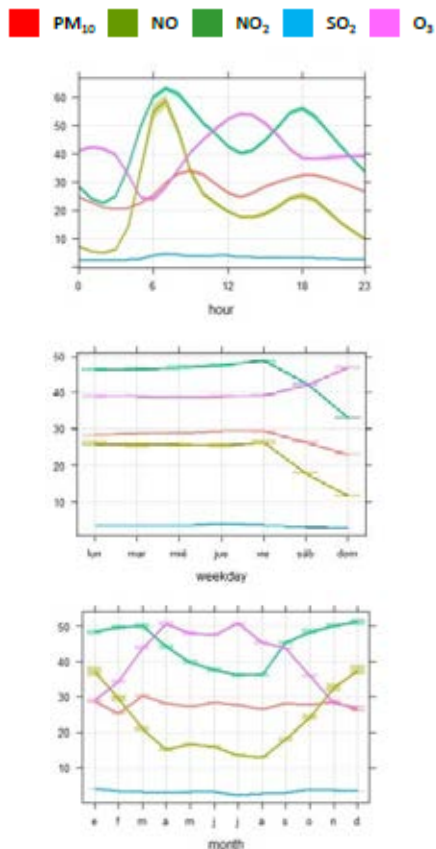
Fig. 1. Urban daily, weekly and monthly concentrations of NO, NO_2, O_3, SO_2 and PM_{10} (in µg m^{-3})

-Ozone (O_3)

Ozone shows a clear diurnal behavior at suburban and regional background environments, with maximal concentrations after midday and minimal early in the morning coinciding with the photochemical activity. The daily pattern of O_3 in the urban background is different, with two clear maxima and two obvious minima. Accordingly with rush hours, mainly by the reaction with NO. These urban patterns are valid for weekdays and they are interrupted during the weekends when all types of environment follow the typical regional background variability.

Seasonal variability of ozone is directly related with its photochemical production. Thus, a prominent maximum is observed in all types of environment during the warm season.

-Particulate Matter (PM_{10})

Daily variability of PM_{10} concentrations in the urban background is lined with NO_x and directly related to road traffic. This pattern is less important in the suburban and regional background.

Finally, a well-defined seasonality governs PM_{10}, with the highest concentrations in summer independently of the type of environment.
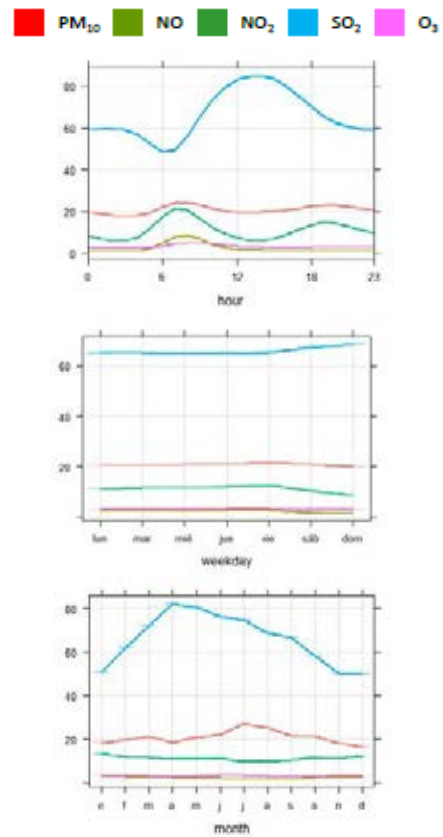
Fig. 2. Suburban daily, weekly and monthly concentrations of NO, NO_2, O_3, SO_2 and PM_{10} (in µg m^{-3})
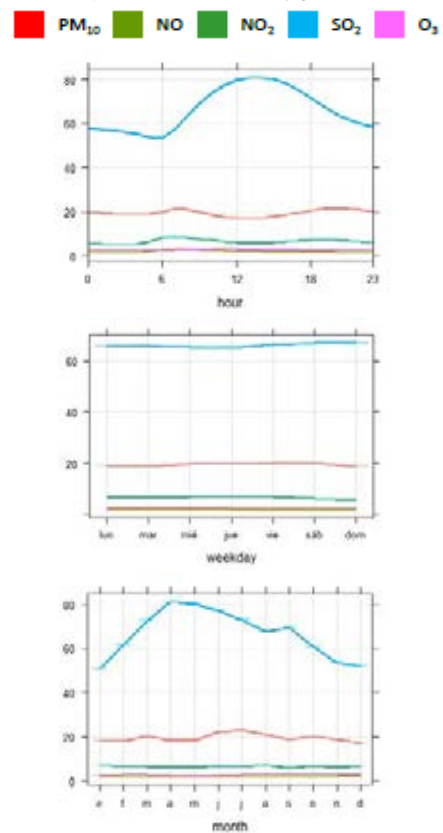
Fig. 3. Regional daily, weekly and monthly concentrations of NO, NO_2, O_3, SO_2 and PM_{10} (in µg m^{-3})

3.2 Trends

-Nitrogen Oxides (NO and NO₂)

A clear drop of NO have been detected at urban (-1.11 $\mu g m^{-3} year^{-1}$) and regional (-0.3 $\mu g m^{-3} year^{-1}$) background locations and no change has been observed at the suburban environments. Likewise, NO_2 concentrations have been reduced at all types of environments, and overall at urban areas (-1.02 $\mu g m^{-3} year^{-1}$).

-Sulfur Dioxide (SO₂)

No relevant changes have been observed for SO_2.

-Ozone (O₃)

The concentrations of ozone have experienced an increase during recent years. In particular, O_3 has risen significantly in the urban background (+1.04 $\mu g m^{-3} year^{-1}$) and moderately in the regional background (0.48 $\mu g m^{-3} year^{-1}$), showing a decreasing trend in the suburban background (-0.4 $\mu g m^{-3} year^{-1}$), probably due to the increasing traffic at the outskirts of the city.

The NO reduction observed in the urban background explains the rising trend in O_3. On the other hand, the regional background ozone augment is consistent with the observations at other European background areas [11, 13].

-Particulate Matter (PM₁₀)

PM_{10} concentrations show a clear diminution over all types of areas. The decrease is more important in urban (-0.73 $\mu g m^{-3} year^{-1}$) and suburban sites (-0.75 $\mu g m^{-3} year^{-1}$), but also significant over the regional (-0.54 $\mu g m^{-3} year^{-1}$). These results agree with other studies carried out across Europe [4, 10]. The regional background decrease have been attributed to the implementation of mitigation strategies across the continent [4, 14], to the impact of the financial crisis over southern Europe [4], and partially to the lower contribution of Saharan dust since 2006 [2].
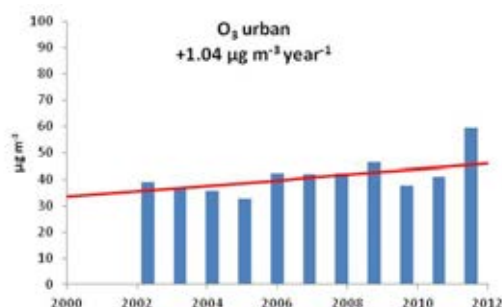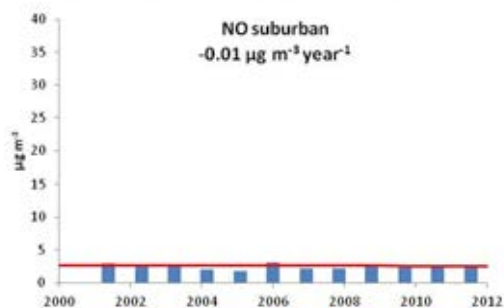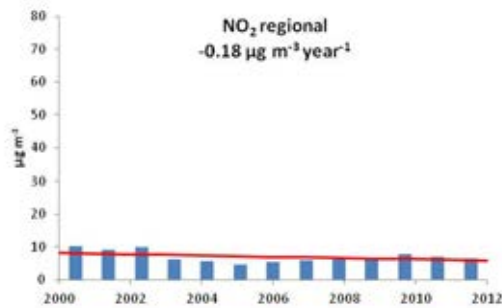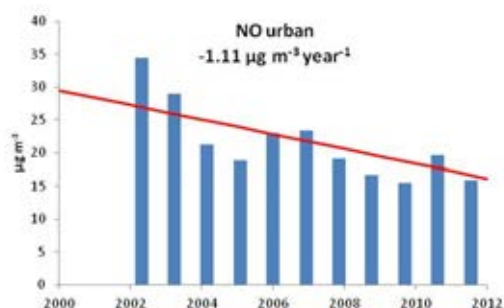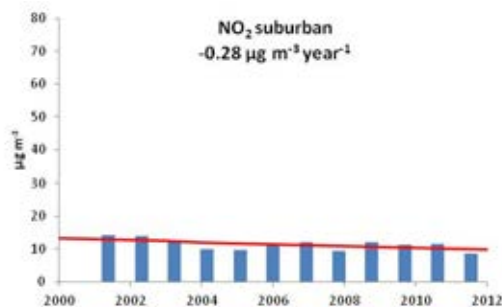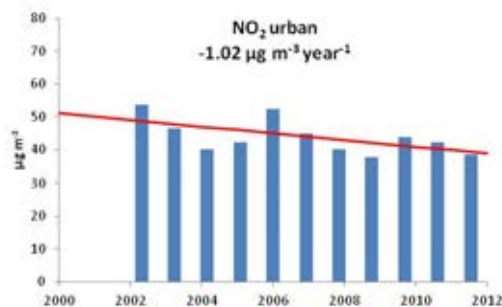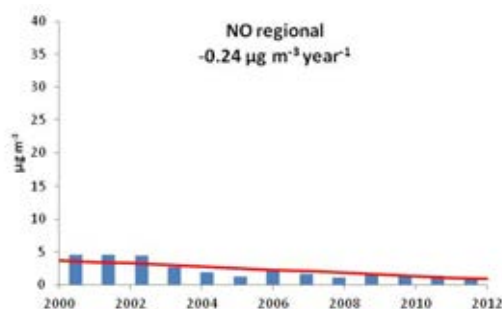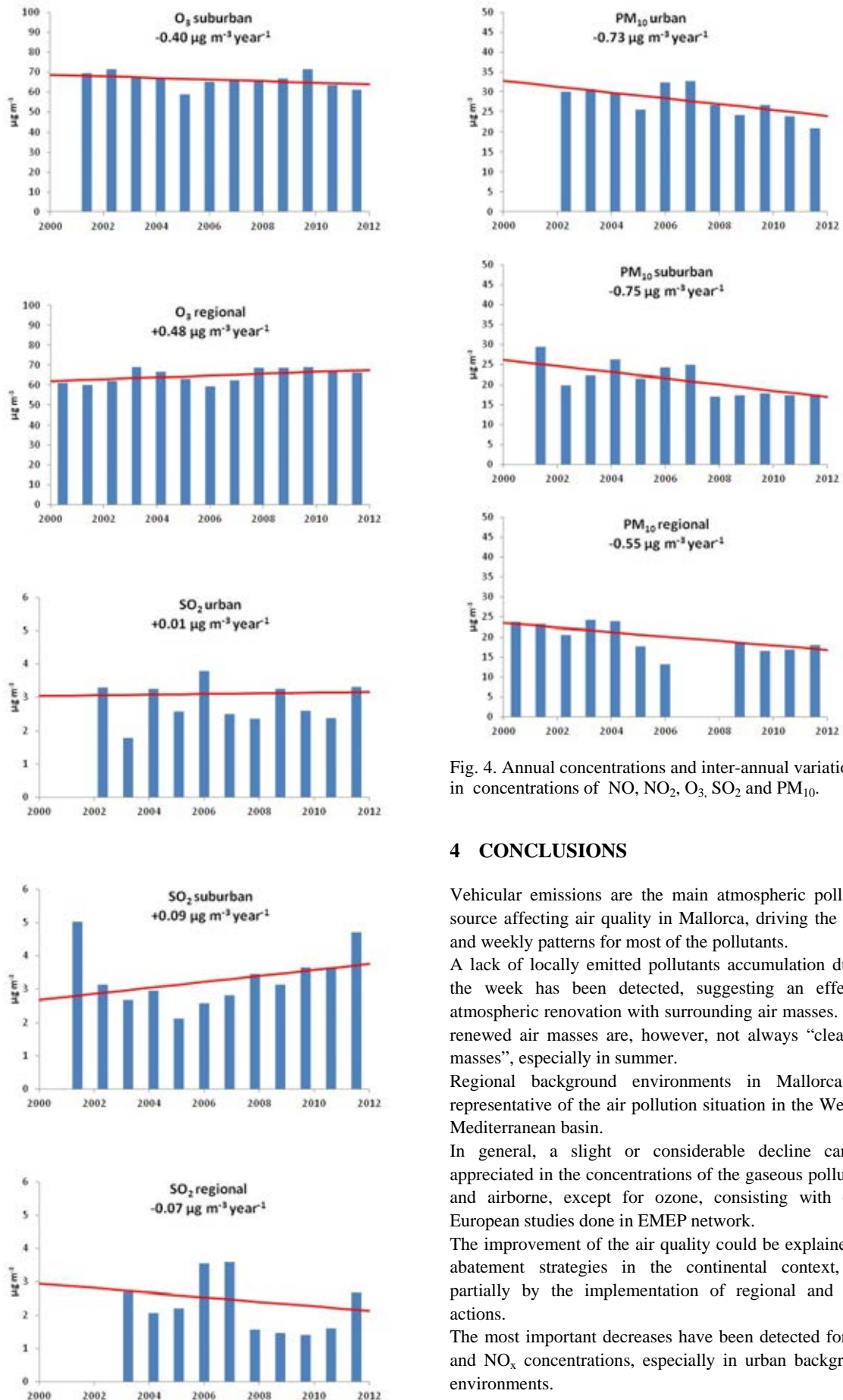
Fig. 4. Annual concentrations and inter-annual variations in concentrations of NO, NO_2, O_3, SO_2 and PM_{10}.

4 CONCLUSIONS

Vehicular emissions are the main atmospheric pollution source affecting air quality in Mallorca, driving the daily and weekly patterns for most of the pollutants.

A lack of locally emitted pollutants accumulation during the week has been detected, suggesting an effective atmospheric renovation with surrounding air masses. Such renewed air masses are, however, not always "clean air masses", especially in summer.

Regional background environments in Mallorca are representative of the air pollution situation in the Western Mediterranean basin.

In general, a slight or considerable decline can be appreciated in the concentrations of the gaseous pollutants and airborne, except for ozone, consisting with other European studies done in EMEP network.

The improvement of the air quality could be explained by abatement strategies in the continental context, and partially by the implementation of regional and local actions.

The most important decreases have been detected for PM and NO_x concentrations, especially in urban background environments.

REFERENCES

[1] Pey J., Querol X., Alastuey A. "Variations of levels and composition of PM10 and PM2.5 at an insular site in the Western Mediterranean" *Atmospheric Research*, 94, 285-299.

[2] Pey J., Querol X., Alastuey A., Forastiere F., Stafoggia M., "African dust outbreaks over the Mediterranean Basin during 2001–2011: PM10 concentrations, phenomenology and trends, and its relation with synoptic and mesoscale meteorology" *Atmospheric Chemistry and Physics*, 13, 1395-1410

[3] Pey J., Pérez N., Castillo S., Viana M., Moreno T., Pandolfi M., López-Sebastián J.M., Alastuey A., Querol X., "Geochemistry of regional background aerosols in the Western Mediterranean" *Atmospheric Research*, 94, 422-435.

[4] Cusack M., Alastuey A., Pérez N., Pey J., Querol X., "Trends of particulate matter (PM2.5) and chemical composition at a regional background site in the Western Mediterranean over the last nine years (2002–2010)" *Atmospheric Chemistry and Physics,* 12, 8341-8357

[5] WHO, *Air quality guidelines global update 2005. Report on a Working Group meeting*, Bonn, Germany, 18-20 October 2005.

[6] WHO, *Review of evidence on health aspects of air pollution-REVIHAAP Project. Technical Report*, Bonn, 2013

[7] Catalina Genestar, Carmen Pons, José Carlos Cerro, Víctor Cerdà, "Different decay patterns observed in a nineteenth-century building (Palma, Spain)" *Environmental Science and Pollution Research*, Apr. 2014.

[8] Hoogerbrugge, R., Denier van der Gon, H. A. C., van Zanten, M.C., and Matthijsen, J. "Trends in Particulate Matter Netherlands" *Research Program on Particulate Matter*, 2010

[9] Liu, Y.-J. and Harrison, R. M. "Properties of coarse particles in the atmosphere of the United Kingdom" *Atmospheric Environment.*, 45, 3267–3276, 2011

[10] Barmpadimos, J. Keller, D. Oderbolz, C. Hueglin, and A. S. H. Prévôt. "One decade of parallel fine ($PM_{2.5}$) and coarse (PM_{10}–$PM_{2.5}$) particulate matter measurements in Europe: trends and variability" *Atmospheric Chemistry and Physics*, 12, 3189–3203, 2012

[11] Environmental European Agency, *The contribution of transport to air quality. TERM 2012: transport indicators tracking progress towards environmental targets in Europe.* EEA Report No 10/2012. ISSN 1725-9177. Copenhagen, 2012

[12] Environmental European Agency, *Assessment of ground-level ozone in EEA member countries, with a focus on long-term trends*, Copenhagen, 56, 2009

[13] C. Ordóñez, H. Mathis, M. Furger, S. Henne, C. Hüglin, J. Staehelin, and A. S. H. Prévôt, "Changes of daily surface ozone maxima in Switzerland in all seasons from 1992 to 2002 and discussion of summer 2003" *Atmospheric Chemistry and Physics*, 5, 1187–1203, 2005

[14] Schembari C., Cavalli F., Cuccia E., Hjorth J., Calzolai G., Pérez N., Pey J., Prati P., Raes F.,"Impact of a European directive on ship emissions on air quality in Mediterranean harbours" *Atmospheric Environment,* 61, 661-669, 2012

Relative contribution and origin of Black Carbon during a high concentration winter episode in Madrid

M. Becerril[1], E. Coz[1], A. S. H. Prévôt[2], B. Artíñano[1]

Abstract — Black carbon (BC) is one of the most important of the atmospheric aerosol chemical components in urban environments. In Madrid, BC observations are rather limited on BC patterns under pollution episode scenarios. Therefore, BC monitoring has become a pending goal to be accomplished for this city.

The present study focuses on the evolution, significance, and source apportionment of the BC concentrations at an urban background station in Madrid measured by aerosol light absorption techniques. During the period of study presented in this work, the meteorological situation was characterized by three scenarios: a local episode and two long range transport events, one from North African origin and other from the North Atlantic.

PM$_{2.5}$ BC hourly average concentrations ranged from 0.10 ± 0.03 μg/m3 to 19 ± 4 μg/m^3, being the highest during the local episode and the lowest during the transport of Atlantic origin. The contribution of BC represented 36 ± 19 % of the total chemical species monitored at the site (BC, inorganic and organic compounds), being maximum during the local episode with 52 ± 15 %. This first BC apportionment study suggests that BC sources in Madrid are mostly of fossil fuel origin, especially during daytime.

Keywords — Black Carbon, Ångström exponent, fossil fuel, biomass

1 INTRODUCTION

Atmospheric aerosol particles influence the Earth's radiation budget and climate both directly, by scattering and/or absorbing solar and infrared radiation in the atmosphere and indirectly, by acting as cloud condensation nuclei or ice nuclei [1]. The radiative forcing of aerosols may be either positive or negative, determined by the optical properties, cloud properties and surface albedo [2, 3].

Black carbon (BC) is a distinct type of carbonaceous component of the atmospheric aerosols that absorbs all wavelengths of solar radiation, and is considered the most strongly light-absorbing component amongst all the aerosol types. It is formed during the incomplete combustion of fossil fuels, biofuels, and biomass burning, and it is always emitted with other particles and gases, such as sulfur dioxide (SO$_2$), nitrogen oxides (NO$_x$), and organic carbon (OC) [4, 5]. At urban and/or industrial areas the principal sources of BC are combustion of fossil fuels (diesel and coal) for the generation of energy industrial activities and heating, open biomass burning, and cooking with biofuels [6]. They are of anthropogenic origin. "Open biomass burning" also includes combustion of forests and grasslands, regardless of the natural or man-induced cause of the fire [5].

BC is unique in its physical properties, which makes it distinguishable from other forms of carbon and carbon compounds contained in atmospheric aerosols. It strongly absorbs visible light; it is refractory, i.e., it retains its basic form at very high temperatures, with a vaporization temperature near 4000 K; it is insoluble in water and common organic solvents; and it exists as an aggregate of small carbon spherules [5].

There are several mechanisms by which BC affects climate such as direct effect (contributing to warming of the atmosphere and dimming at the surface) and the effect on snow/ice albedo and clouds [4]. According to the latest report from the Intergovernmental Panel on Climate Change, BC is the only type of aerosol that increases global climate warming [7].

Thus, the quantification of atmospheric BC concentrations, as well as the characterization of physicochemical properties, sources, and transport pattern, is of particular interest for a better understanding of its associated direct and indirect effects.

Additionally, BC is a main chemical component of the particulate matter at urban and industrial areas, which accounts for a great part of ambient concentration levels, which sometimes exceeds the limit values set by the European regulation on air quality in such areas.

Madrid is the largest populated city in Spain with more than 3 million inhabitants. Opposite to most of the large European cities, it has no significant heavy industrial activities nearby. Thus, traffic exhaust, commercial and residential heating installations (natural gas, fuel-oil and some coal boilers and

---
1. *Department of Environment, CIEMAT. Avd. Complutense, 40, 28040 Madrid. Spain. E-mail: marta.becerril@ ciemat.es*
2. *Laboratory of Atmospheric Chemistry, Paul Scherrer Institute (PSI). 5232 Villigen-PSI, Switzerland.*

biomass burning stoves) and cooking activities are the major atmospheric pollution emitters in the whole metropolitan area (nearly 6 million inhabitants) during the winter period, characterized by strong anthropogenic pollution episodes that develop under atmospheric stagnation conditions.

There are some motivating reasons to quantify the black carbon in the city of Madrid, since BC is emitted primarily by traffic sources, becoming a major problem for the city in terms of pollution. BC is a main aerosol component of Diesel Particulate Matter (PM), which is regulated by several regulatory authorities. Diesel PM can seriously affect human health. For instance, it can cause respiratory and cardiovascular diseases in people who are exposed to this pollutant, even premature death [8].

2 METHODOLOGY

2.1 Experimental Site

Measurements have been carried out in the city of Madrid at the facilities of the Research Centre for Energy, Environment and Technology (CIEMAT) located in Ciudad Universitaria, a non-residential area (40°27′23″N 3°43′32″O, 669 m ASL) in the NW of the city outskirts. This site can be considered representative of the urban background and is located downwind of the centre of Madrid for the N to SW wind directions (clockwise), and downwind of a great-forested area with respect to the W and NW wind directions [9].

2.2 Meteorology

The procedure for the characterization of the winter episode in this study consisted of an analysis of the information provided by different sources and the analysis of meteorological charts at 500 hPa, air mass back-trajectories using the NOAA HYSPLIT4 model, and aerosol mass concentrations in the ambient air from rural and urban background and the measurement site stations.

Three-day (72 hours) air mass back-trajectories ending at 12:00 UTC for different arrival altitudes have been calculated for some selected days by means of the HYSPLIT4 model. The HYSPLIT (HYbrid Single-Particle Lagrangian Integrated Trajectory) model is a system for computing simple air parcel trajectories to complex dispersion and deposition simulations. Meteorological data correspond to GDAS (Global Data Assimilation System) global reanalysis provided by NCEP (National Center for Environmental Prediction).

Average PM concentrations from the Community of Madrid (regional government, http://gestiona.madrid.org/azul_internet/html/web/InformAnalizadoresAccion.icm?ESTADO_MENU=2_1_2) and Madrid City Council (local government,

http://www.mambiente.munimadrid.es/svca/index.php?lang=en) network stations were used to determine the evolution and impact of the episodes on a regional and local scale respectively.

Meteorological information was obtained from the meteorological tower of CIEMAT Wind direction and speed, precipitation and solar radiation, atmospheric temperature, humidity, and pressure are recorded every 10 minutes. It has four levels of measurement with several parameters and heights.

2.3 Instrumentation

Near infrared Black Carbon (nIR-BC) and Ultraviolet-absorbing Particulate Matter (UVPM) concentrations were recorded through aerosol light absorption using a 7-wavelength Aethalometer (Magee Sci. mod. AE33, Aerosol d.o.o., Slovenia) with cut-off size of 2.5 μm. The instrument was measuring at a flow rate of 5 Lmin^{-1}. Data were recorded with a time-resolution of 1 minute. Light attenuation by the aerosol particles (deposited on a filter) was measured at 7 wavelengths (λ=370, 470, 520, 590, 660, 880, and 950 nm). The nIR-BC or BC mass concentration was calculated using the measurement at 880 nm wavelength with a mass absorption cross-section, MAC, of 7.77 m^2/g. The Ultraviolet-absorbing Particulate Matter (UVPM) mass concentration was estimated at the 370 nm wavelength, with a mass absorption cross-section, MAC, of 18.47 m^2/g; which indicates the presence of organic compounds such as those found in wood smoke and biomass-burning smoke. The sampling air passed through a PM$_{2.5}$ inlet (BGI, MiniPM$^®$ Inlet) before entering into the Aethalometer.

The instrument is part of the ACTRIS (Aerosols, Clouds, and Trace gases Research InfraStructure Network), a European Infrastructure Project where ground-based stations equipped with advanced atmospheric probing instrumentation for aerosols, clouds, and short-lived gas-phase species are encompassed. It operates under the protocol of this network and participates in an intercoparison once a year.

The Aethalometer was first described by Hansen et al. (1984) [10]. It uses an optical technique to measure the concentration of the light-absorbing aerosol particles (mainly BC) in an air stream in real time. The operating principle of the Aethalometer is based on the measurement of the attenuation of a beam of light transmitted through a sample collected on a fibrous filter, while the filter is continuously collecting an aerosol sample. This measurement is made at successive regular intervals of a time base period, i.e., the flow rate is constant. The optical attenuation, ATN, is defined as

$$ATN = 100 \times \ln(I_0/I) \quad (1)$$

where the factor of 100 is for numerical convenience, I_0 is the intensity of light transmitted
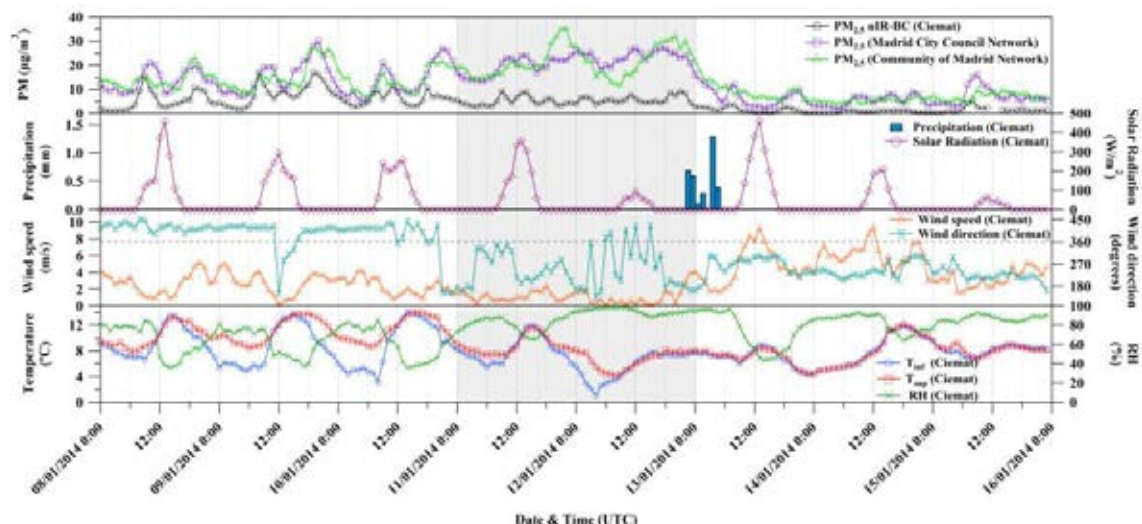
Fig. 1 Hourly average time series of the particulate matter at Ciemat, Madrid City Council and Community of Madrid Network, and the meteorological parameters recorded at Ciemat during the period of study.

through the original filter, or through a blank portion of the filter; and *I* the intensity of light transmitted through the portion of the filter on which the aerosol deposit is collected. The black carbon content of the aerosol deposit at each measurement time can be determined by applying the suitable value of the specific attenuation for that singular combination of filter and optical components. The increase in optical attenuation from one period to the next is due to the increment of aerosol black carbon collected from the air stream during the period. The mean BC concentration in the sampled air stream during the period is calculated by dividing that increment by the volume of air sample during that time [11]. The instrument has a dual light path, which means that only a small spot on the filter is exposed to aerosol [12].

The Aethalometer Model AE33 incorporates the patented DualSpot^{TM} method to compensate for the "spot loading effect"; and also to provide a real-time output of the "loading compensation" parameter, which may provide additional information about the physical and chemical properties of the aerosol [13].

From the absorption light coefficient, b_{abs}, for atmospheric aerosols, it can be studied the relation between aerosol composition and the wavelength dependence of b_{abs} by means of the following empirical power law fit:

$$b_{abs} \propto \lambda^{-\alpha} \quad (2)$$

where λ is the wavelength and α is the Ångström exponent of the absorption coefficient and is calculated by fitting an exponential curve [1].

The theoretical value of Ångström exponent of the absorption coefficient for black carbon is 1, with larger α values for biomass burning aerosols [14].

3 METEOROLOGICAL SCENARIOS

The period analyzed in this study (from the 8th to the 15th of January, 2014) was divided into three scenarios.

Scenario 1: Local Episode.

The first scenario (from the 8th to the 10th of January, 2014) corresponded to a small winter anticyclonic situation which was characterized by subsidence and hence temperature inversions in height. It was dominated by high pressures and low surface wind speeds (with an average wind speed of 2.6 ± 1.2 m/s) (Fig. 1). This situation gives rise to little or poor ventilation and high NO_x and PM concentrations in the surface layer of the atmosphere. The synoptic configuration during these days was characterized by the persistence of an anticyclone centred on the Iberian Peninsula. This situation caused subsidence, inhibiting the vertical motions in the lowest layer of the troposphere, favouring a high concentration of pollutants, causing a small pollution episode.

Scenario 2: North African Episode.

In the second scenario (from the 11th to the 12th of January, 2014) a Saharan dust intrusion took place together with a temperature inversion, which precisely coincided with the weekend.

The Saharan transport scenario corresponds to a typical late-winter episode characterized by the presence of the Azores pressure center slightly shifted to the east of its normal position; a ground level high is centered over Morocco, Algeria, Tunisia, or even the western Mediterranean, and the transport is confined to low altitudes [15].

In Fig. 2 can be seen the source origin in northern Africa and transport path through the Atlantic ending at 12:00 UTC on the 11th of January, 2014.
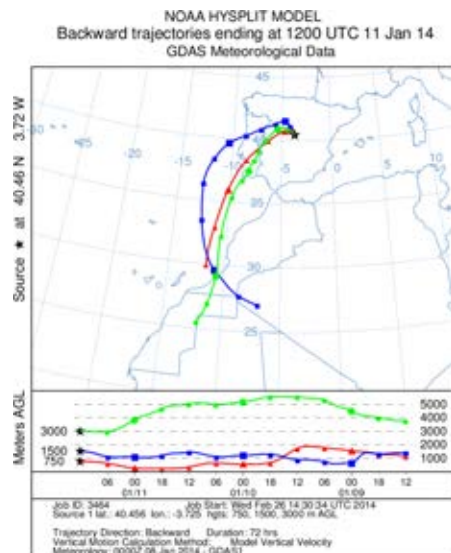
Fig. 2 HYSPLIT4 Backward trajectories ending at 1200 UTC on the 11th of January, 2014.

Scenario 3: North Atlantic Episode.

Finally, the third scenario (from the 13th to the 15th of January, 2014) was associated with an advection of Atlantic air characterized by a very low ambient particle concentration. The wind turned westerly due to an upper-level low pressure system and flew over the Iberian Peninsula from the Atlantic Ocean. It played a decisive role in cleaning up the air over the measurements site area.

Figure 3 shows the air mass transported from Atlantic Ocean ending at 12:00 UTC on the 13th of January, 2014.
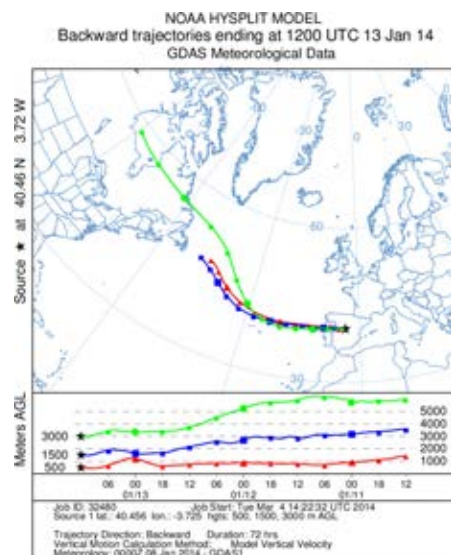
Fig. 3 HYSPLIT4 Backward trajectories ending at 1200 UTC on the 13th of January, 2014.

4   RESULTS AND DISCUSSION

4.1   Evolution and significance of the black carbon concentrations during the study

$PM_{2.5}$ mass concentration average from stations of the the Madrid air quality monitoring networks ranged from 2 $\mu g/m^3$ to 35 $\mu g/m^3$ during the period of study. The highest $PM_{2.5}$ concentrations corresponded to the North African scenario, whereas the lowest ones were recorded, as expected, during the North Atlantic one.

Results showed that the evolution of the $PM_{2.5}$ nIR-BC concentrations carried out at CIEMAT during the local period was in good agreement with the average $PM_{2.5}$ mass concentration levels of the average of all stations from the Madrid air quality monitoring networks (Fig. 1). BC/$PM_{2.5}$ ratios of 0.47 ± 0.24 and 0.47 ± 0.25 for the city Council and Community networks were recorded for this scenario respectively. By contrast, ratios of 0.26 ± 0.07 and 0.27 ± 0.11 for the North African scenario and of 0.18 ± 0.10 and 0.17 ± 0.16 for the North Atlantic one were found. For this reason, the site has been previously considered as representative of the atmospheric aerosol composition within the urban limits when this type of meteorological situations occurs.

The contribution of $PM_{2.5}$ nIR-BC to the total chemical species monitored at CIEMAT (nIR-BC, inorganic and organic compounds) represented 36 ± 19 %. Slightly lower percentages, of 31 ± 21 % and 31 ± 23 % were found when estimated the relative contribution of the BC recorded at CIEMAT with respect to the mean $PM_{2.5}$ mass concentration levels of the average of all stations from the Madrid City Council Network and the Community of Madrid Network, respectively. The contribution of $PM_{2.5}$ nIR-BC to the total chemical species monitored at CIEMAT were 52 ± 15 % during the local episode, 20 ± 5 % in the North African scenario, and 30 ± 14 % during the North Atlantic episode. The estimations of the relative contribution of the BC recorded at CIEMAT with respect to the mean $PM_{2.5}$ mass concentration levels of the average of all stations from the Madrid air quality monitoring networks were 47 ± 23 % during the local episode, 26 ± 8 % in the North African scenario, and 18 ± 12 % during the North Atlantic episode.

$PM_{2.5}$ nIR-BC hourly average concentrations ranged from 0.10 ± 0.03 $\mu g/m^3$ to 18.97 ± 4.19 $\mu g/m^3$ during the entire period of study (Fig. 1), with the highest values monitored during the local episode.

The diurnal cycles of the hourly average of $PM_{2.5}$ nIR-BC and the ratio of UVPM/nIR-BC are represented in Fig. 4 for each meteorological scenario.
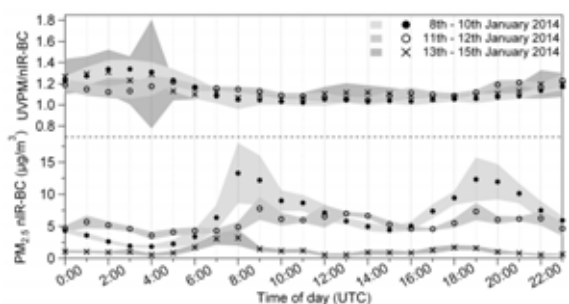
Fig. 4 Hourly average diurnal cycles for each episode data.

During the local episode, which coincided with working days, the PM$_{2.5}$ nIR-BC concentration was 6.73 ± 1.30 µg/m^3 in average. The diurnal evolution of the concentrations presented two peaks that corresponded to an increase in traffic activity of the city of Madrid. The first peak occurred between 8 and 9 UTC in the morning (13.30 ± 4.66 µg/m^3 and 12.19 ± 3.80 µg/m^3, respectively), while the second between 19 and 20 UTC in the evening (12.32 ± 3.38 µg/m^3 and 11.95 ± 2.72 µg/m^3, respectively). Both peaks were associated to traffic movements from home to the workplace and vice versa. The UVPM/nIR-BC ratios in the hours of maximum concentration during this episode confirmed the origin, since the values obtained were 1.05 ± 0.09 (8 UTC), 1.05 ± 0.04 (9 UTC), 1.06 ± 0.04 (19 UTC), 1.07 ± 0.03 (20 UTC), i.e., close to the unity.

During the North African episode, which corresponded to the weekend, the mean contribution of PM$_{2.5}$ nIR-BC was a bit lower (5.49 ± 0.67 µg/m^3) than in the local episode, and emission peaks were not clearly shown. The low standard deviation was an indication of a continuous contribution of BC along the whole scenario. This can be also observed in Fig. 1 and Fig. 4.

In the last scenario, the North Atlantic episode, it can be noted that the values of the PM$_{2.5}$ nIR-BC concentrations were very low (1.22 ± 0.32 µg/m^3) because of the air mass origin from the North Atlantic Ocean, which had a cleansing effect. For this same reason, no significant diurnal cycles were observed.

4.2 Source apportionment of black carbon during the study

Figure 5 shows the Ångström exponent of the absorption coefficient α estimated by fitting b$_{abs}$ for all available wavelengths. As it can be observed, not all seven points lie on the fitted curve. For example, for the local episode and the North African episode data, the b$_{abs}$ (590, 660, 880, and 940 nm) lie above the fitted curve. However, for the North Atlantic episode, the data lie better on the fitted curve than in the two previous scenarios. We calculated α for two different wavelength ranges (370 – 525 and 660 – 940 nm) for a better fit than obtained by an exponential curve fit over all seven wavelengths.

It can be noted that the values of α obtained in the North Atlantic episode were slightly higher than in the previous two episodes (Fig. 5). This result suggests the presence of more sources besides fossil fuel, such as biomass burning, or the existence of a higher degree of aging in the atmospheric plume during the transport of the air mass from the North Atlantic Ocean. Coefficients close to 1.5 during the local episode and Saharan scenarios indicate a major presence of fossil fuel sources in the BC origin. However, higher coefficients than 1.2 might be associated to the presence of some biomass burning activities. This is an interesting result that will need further investigation. Similar α values for the local and North African transport indicate either a local contribution of the BC due to the existence of a high pressure center at ground level and similar properties in the BC.potentially transported.
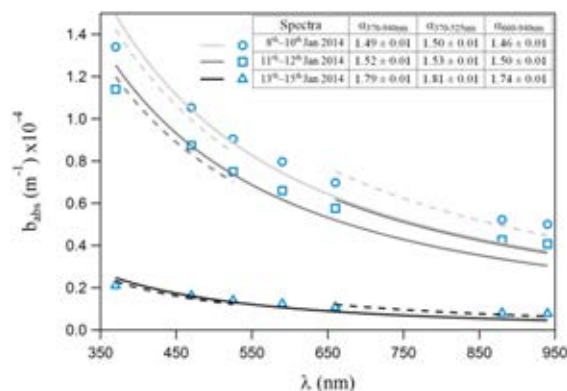
Fig. 5 Power law fits of data. The solid lines were generated by fitting the absorption coefficients b$_{abs}$ over all seven wavelengths. The dashed lines correspond to power law fits of b$_{abs}$ over 370–525 or 660–940 nm.

These results have been compared with previous studies. Kirchstetter et al. (2004) [16] reported α value of 2.2 for outdoor firewood burning, 1.8 for a savanna fire, and $0.8 - 1.1$ for traffic-dominated sites. Schnaiter et al. (2003, 2005) [17, 18] reported α value of 1.1 for uncoated diesel soot (measurements at 450, 550, and 700 nm wavelengths). Day et al. (2006) [19] measured fresh wood smoke from seven types of forest wood with an Aethalometer and they showed that the α value depends on the type of wood being burned, they obtained α values between 0.9 and 2.2. Sandradewi et al. (2008) [1] reported α values in the range of $2.1 - 3.6$ for wood smoke, $1.1 - 3.7$ for winter campaign, and $1.0 - 1.2$ for summer campaign, where there was no biomass influence, according to the specific wavelength range over which measurements were taken.

5 CONCLUSIONS

A multi-wavelength Aethalometer was used to study the aerosol light absorption at the CIEMAT-

Madrid site from the 8th to the 15th of January, 2014. Three different meteorological scenarios were identified during this period: local, North African and North Atlantic episodes.

PM$_{2.5}$ nIR-BC hourly concentrations varied from 18.97 ± 4.19 µg/m^3 to nearly cero (0.10 ± 0.03 µg/m^3). The highest concentration PM$_{2.5}$ nIR-BC was observed during the local episode, while the lowest was associated, as expected, to the North Atlantic transport. The highest relative contribution of BC to the total PM$_{2.5}$ was also found during the local episode, which represented, on average, nearly 50% of the total PM$_{2.5}$ mass recorded on the average of all stations from the Madrid air quality monitoring networks.

The diurnal cycles of the hourly average of PM$_{2.5}$ nIR-BC were clearly influenced by the meteorological situation. UVPM/nIR-BC ratios were close to the unity, indicating that there was no important contribution from biomass burning origin to the high BC concentrations during the entire period.

Based on the interpretation of the Ångström exponent of the absorption coefficient in the near-IR and UV wavelengths, it is shown that there was a predominance of fossil fuel combustion versus biomass burning during the period of study. Therefore, this result may be used as an indicator of the aerosol origin and composition.

REFERENCES

[1] J. Sandradewi, A.S.H. Prévôt, E. Weingartner, R. Schmidhauser, M. Gysel, and U. Baltensperger, A study of wood burning and traffic aerosols in an Alpine valley using a multi-wavelength Aethalometer, Atmos. Environ., 42, Issue 1, 101-112. doi: 10.1016/j.atmosenv.2007.09.034, 2008

[2] P. Chýlek and J. A. Coakley Jr., Aerosols and Climate. Science. 183 (4120), 75-77, doi: 10.1126/science.183.4120.75, 1974

[3] IPCC: Climate Change 2007: The Physical Science Basis. Contribution of Working Group I to the Fourth Assessment Report of the Intergovernmental Panel on Climate Change, edited by S. Solomon, D. Qin, M. Manning, Z. Chen, M. Marquis, K.B. Averyt, M.Tignor, and H.L. Miller. Cambridge University Press, Cambridge, United Kingdom and New York, NY, USA, 2007

[4] U.S. EPA., Report to Congress on Black Carbon, http://www.epa.gov/blackcarbon/, 2012

[5] T. C. Bond, et al., Bounding the role of black carbon in the climate system: A scientific assessment, J. Geophys. Res. Atmos., 118, 5380–5552, doi: 10.1002/jgrd.50171, 2013

[6] Ramanathan, V., and G. Carmichael, Global and regional climate changes due to black carbon, Nat. Geosci., 1, 221–227, doi: 10.1038/ngeo156, 2008

[7] IPCC: Climate Change 2013: The Physical Science Basis. Contribution of Working Group I to the Fifth Assessment Report of the Intergovernmental Panel on Climate Change, edited by T. F. Stocker, D. Qin, G. K. Plattner, M. Tignor, S. K. Allen, J. Boschung, A. Nauels, Y. Xia, V. Bex, and P. M. Midgley. Cambridge University Press, Cambridge, United Kingdom and New York, NY, USA, 2013

[8] WHO: Health effects of black carbon. Copenhagen: World Health Organization Regional Office for Europe, WHO. Report for the UNECE Convention on Long-range Transboundary Air Pollution, Task Force for Health, edited By Nicole AH Janssen, Miriam E Gerlofs-Nijland, Timo Lanki, Raimo O Salonen, Flemming Cassee, Gerard Hoek, Paul Fischer, Bert Brunekreef and Michal Krzyzanowski, (http://www.euro.who.int/__data/assets/pdf_file/0004/162535/e96541.pdf?ua=1), 2012

[9] J. Plaza, B. Artíñano, P. Salvador, F. J. Gómez-Moreno, M. Pujadas, and C. A. Pio, Short-term secondary organic carbon estimations with a modified OC/EC primary ratio method at a suburban site in Madrid (Spain), Atmos. Environ., 45, Issue 15, 2496-2506 doi: 10.1016/j.atmosenv.2011.02.037, 2011

[10] A.D.A. Hansen, H. Rosen, and T. Novakov, The aethalometer — An instrument for the real-time measurement of optical absorption by aerosol particles. Science of The Total Environment. 36, 191-196, doi: 10.1016/0048-9697(84)90265-1, 1984

[11] A.D.A. Hansen, The AethalometerTM. Magee Scientific Company, Berkley, California, USA. http://www.mageesci.com/images/stories/docs/Aethalometer_book_2005.07.03.pdf, 2005

[12] A. Gelencsér, Carbonaceous aerosol, Atmospheric and Oceanographic Sciences Library, 30, ISBN: 978-1-4020-2886-1 (Print), 978-1-4020-2887-8 (Online), 2004

[13] Aethalometer® Model AE33 User Manual. Magee Scientific, Aerosol d.o.o., Ljubljana, Slovenia, 2014

[14] P. B. Russell, R. W. Bergstrom, Y. Shinozuka, A. D. Clarke, P. F. DeCarlo, J. L. Jimenez, J. M. Livingston, J. Redemann, O. Dubovik, and A. Strawa, Absorption Angstrom Exponent in AERONET and related data as an indicator of aerosol composition, Atmos. Chem. Phys., 10, 1155-1169, doi: 10.5194/acp-10-1155-2010, 2010

[15] M. Escudero, S. Castillo, X. Querol, A. Avila, M. Alarcón, M. M. Viana, A. Alastuey, E. Cuevas, and S. Rodríguez, Wet and dry African dust episodes over eastern Spain, J. Geophys. Res., 110, D18S08, doi: 10.1029/2004JD004731, 2005

[16] T. W. Kirchstetter, T. Novakov, and P. V. Hobbs, Evidence that the spectral dependence of light absorption by aerosols is affected by organic carbon, J. Geophys. Res., 109, D21208, doi:10.1029/2004JD004999, 2004

[17] M. Schnaiter, H. Horvath, O. Möhler, K.-H. Naumann, H. Saathoff, and O.W. Schöck, UV–VIS–NIR spectral optical properties of soot and soot-containing aerosols, J. Aerosol Sci. 34, 1421–1444, doi: 10.1016/S0021-8502(03)00361-6, 2003

[18] M.Schnaiter, C. Linke, O. Möhler, K.-H. Naumann, H. Saathoff, R. Wagner, U. Schurath, and B. Wehner, Absorption amplification of black carbon internally mixed with secondary organic aerosols. J. Geophys. Res. Atmos. 110, D19204, doi:10.1029/2005JD006046, 2005

[19] D. E.Day, J. L. Hand, C. M. Carrico, G. Engling, and W. C. Malm, Humidification factors from laboratory studies of fresh smoke from biomass fuels, J. Geophys. Res. Atmos. 111, D22202, doi:10.1029/2006JD007221, 2006

Abstracts

CHARACTERIZATION OF CARBONACEOUS PARTICULATE MATTER AND FACTORS AFFECTING ITS VARATIONS IN THE VENETO REGION, ITALY

MD. BADIUZZAMAN KHAN[1], MAURO MASIOL[1,2], GIANNI FORMENTON[3], ALESSIA DI GIOLI[4], GIANLUIGI DE GENNARO[4], CLAUDIO AGOSTINELLI[1], BRUNO PAVONI[1]

[1]*Dipartimento di Scienze Ambientali, Informatica e Statistica, Università Cà Foscari Venezia, Dorsoduro 2157, 30123 Venice, Italy, md.khan@unive.it, claudio@unive.it, brown@unive.it*

[2]*Division of Environmental Health& Risk Management, School of Geography, Earth & Environmental Sciences, University of Birmingham, Edgbaston, Birmingham B15 2TT, United Kingdom, m.masiol@bham.ac.uk*

[3]*Dipartimento Provinciale di Padova, Agenzia Regionale per la Prevenzione e Protezione Ambientale del Veneto (ARPAV), Via Ospedale 22, 35121 Padova, Italy, g.formenton@arpa.veneto.it*

[4]*Dipartimento di Chimica, Università degli Studi di Bari, via Orabona 4, 70126 Bari, Italy, alessia.digioli@uniba.it, gianluigi.degennaro@uniba.it*

Abstract

Organic carbon (OC) and elemental carbon (EC) were determined in 360 $PM_{2.5}$ samples collected from April 2012 to February 2013 at six provinces in the Veneto region, in order to determine the factors affecting the carbonaceous aerosol variations. Sixty samples per province were collected for analysis in every alternate month (February, April, June, August, October and December): 10 samples per sampling site in 10 consecutive days of the months selected. EC and OC were analyzed using the NIOSH (National Institute of Occupational Safety and Health) 5040 thermal/optical transmittance method. OC concentration ranged from 0.98 µg m^{-3} to 22.34 µg m^{-3}, while the mean value was 5.48 µg m^{-3}, contributing 79% of the total carbon. EC concentrations fluctuated from 0.19 to 11.90 µg m^{-3} with a mean value of 1.31 µg m^{-3}, contributing 19% to the total carbon. The monthly OC concentration gradually increased from April to December. The EC did not vary in accordance with OC, but the highest values were recorded in winter, as well. Although there were concentration differences among the provinces, these were not statistically significant as confirmed by Kruskal-Wallis one-way analysis of variance test. The OC/EC ratios ranged from 0.71 to 15.38 with a mean value of 4.54, which is higher than the values observed in most of the other European cities. Statistically significant correlations between EC and OC were found in all the months except October and December. Statistically significant meteorological factors controlling OC and EC variations were investigated by fitting linear models using robust procedure based on weighted likelihood. Temperature and wind velocity turned out to be statistically significant, with a multiple R^2 value of 0.791. The secondary organic carbon (SOC) was calculated from the EC tracer method. The SOC contributed for 69% of the total organic carbon during the study period found both by OC/EC minimum ratio and regression approach.

Keywords: Organic carbon, Elemental carbon, OC-to-EC ratio, Meteorological factors, Secondary organic carbon

LIGAMENT CHARACTERIZATION IN MICRODIPPING DROPLET EMISSION MODE

A. J. HIJANO[1], S.E. IBÁÑEZ[2], F. HIGUERA[2], I.G. LOSCERTALES[1]

[1]*Departamento de Ingeniería Mecánica y Mecánica de Fluidos, Universidad de Málaga, Málaga, Spain,*
ajhijano@uma.es, loscertales@uma.es

[2]*Departamento de Motopropulsión y Termofluidodinámica, Universidad Politécnica de Madrid, Madrid,*
Spain, KIKE@aero.upm.es, fhiguera@aero.upm.es

When a meniscus of a highly conducting, low viscosity liquid hanging from a capillary tube is subjected to an intense electric field, it stretches in the direction of the field and the tip of the elongated meniscus develops a liquid ligament that eventually detaches to form a droplet (figure 1.a). After the droplet emission, the meniscus recedes to its original shape. If the meniscus is fed with liquid at a proper constant flow rate, this emission process may become periodic for a range of applied voltages between the meniscus and its surroundings. This emission regime is known as electric-microdripping (M. Cloupeau and B. Prunet-Foch, *Journal of Aerosol Science*, 25, 1021–1036, 1994).
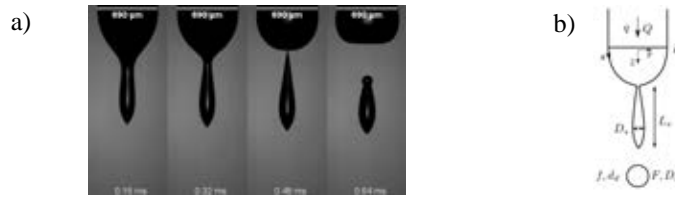
Figure 1. *a) Capillary outer diameter D = 690 μm, flow rate Q = 10 ml/h, Voltage ϕ = 3.05 kV. b) Ligament before droplet detachment. Droplet diameter D_d, oscillation frequency F, ligament length L_s, ligament width D_s.*

We have measured the dimensionless length and diameter of the liquid ligament right before its detachment, and have characterize the dependence of these parameters on the dimensionless liquid flow rate $q = \left(\frac{\rho Q^2}{\gamma D^3}\right)^{1/2}$ and the electric Bond number $B_E = \frac{\varepsilon_o \phi^2}{2\gamma D}$, where γ and ρ are the liquid surface tension an density, respectively, and ε_o is the permittivity of vacuum.
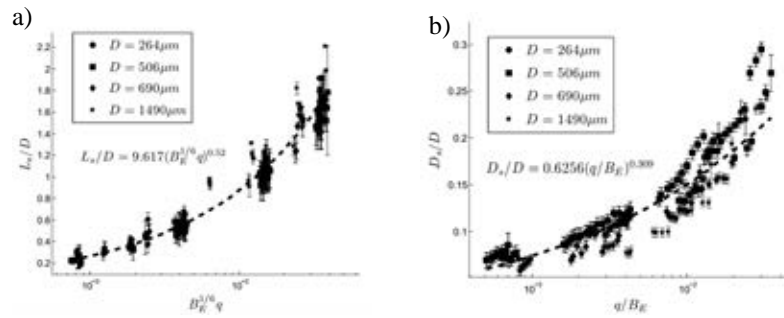
Figure 2. *Dimensionless ligament length a) and diameter b) as a function of B_E and q.*

The results, collected in figures 2.a and 2.b, show that $\frac{L_s}{D} \sim q^{1/2}$ and $\frac{D_s}{D} \sim q^{1/3}$, whereas the effect of B_E, which is always of order unity, seems to be much weaker. We rationalize qualitatively these trends in terms of asymptotic descriptions of the process.

SIMULACIÓN DE UN ELECTROSPRAY CERCA DEL CAUDAL MÍNIMO

SANTIAGO E. IBÁÑEZ[1], FRANCISCO J. HIGUERA[1]

[1]Departamento de Mecánica de Fluidos y Propulsión Aeroespacial, Universidad Politécnica de Madrid, ETSI Aeronáuticos. Pza. Cardenal Cisneros 3, Madrid, España.
santiagoenrique.ibanez@upm.es, fhiguera@aero.upm.es.

En el presente trabajo se estudia, mediante simulación numérica, la atomización electrohidrodinámica en el modo de cono-chorro. En la configuración mas común, un tubo capilar metálico se conecta a un voltaje elevado respecto a una placa metálica enfrentada al tubo. Por el tubo capilar se hace fluir un caudal constante de un líquido de conductividad eléctrica no nula que forma un menisco a la salida del tubo. El campo eléctrico debido al voltaje aplicado da lugar a una corriente eléctrica en el líquido que acumula carga eléctrica en su superficie y origina un esfuerzo eléctrico sobre la superficie que tiende a alargarla en la dirección del campo. Cuando el campo eléctrico es suficientemente intenso, el menisco adopta la forma de un cono (el cono de Taylor) de cuyo vértice sale un delgado chorro de líquido que a cierta distancia aguas abajo del cono se rompe en un spray de gotas prácticamente monodispersas cargadas eléctricamente. De esta forma, el chorro se lleva la carga que se acumula en la superficie del líquido. La intensidad de la corriente eléctrica generada depende del caudal y las propiedades físicas del líquido, pero no del voltaje aplicado entre los electrodos, puesto que el régimen descrito existe solo en un estrecho rango de valores del voltaje, y para caudales muy pequeños. Hay un caudal mínimo para el que el modo cono-chorro deja de existir y cerca del cual las gotas generadas son más pequeñas y monodispersas que a caudales mayores. A pesar de que los mecanismos responsables del caudal mínimo han sido muy estudiados, no existe aún una teoría completa del mismo.

Se formula un modelo simplificado del flujo, el campo eléctrico y el transporte de carga en el menisco y el chorro del electrospray. El movimiento del líquido se supone casiunidireccional y se describe usando la aproximación de Cosserat para un chorro esbelto. Esta aproximación, ampliamente usada en la literatura, permite simular con relativa facilidad múltiples casos y cubrir amplios rangos de valores de los parámetros reteniendo los efectos de la viscosidad y la inercia del líquido. Los campos eléctricos dentro y fuera del liquido están acoplados y se calculan sin simplificación alguna usando un método de elementos de contorno. La solución estacionaria del problema se calcula mediante un método iterativo. Para barrer el espacio de los parámetros, se fijan primero las propiedades del líquido y el voltaje aplicado y se va calculando la solución para caudales cada vez menores hasta que el método iterativo deja de converger.

Los resultados numéricos proporcionan una descripción del dominio de operación del electrospray en el modo cono-chorro, que es la región del plano voltaje-caudal donde existe solución estacionaria del problema anterior. El caudal mínimo, que delimita parte del contorno del dominio de operación, decrece primero y luego crece al ir aumentando el voltaje, en buen acuerdo con los datos experimentales. La corriente eléctrica transportada por el electrospray es la suma de la corriente debida a la conducción en el interior del líquido y la debida a la convección de la carga eléctrica acumulada en su superficie. La primera domina en el menisco y la segunda en el chorro lejano, mientras que las dos son comparables en una región intermedia de transferencia de corriente que, para valores grandes de la constante dieléctrica del líquido, está situada al comienzo del chorro pero aguas abajo de la región de transición en la que el menisco deja de ser un cono de Taylor. Los resultados numéricos muestran que el tiempo de residencia del líquido en esta última región disminuye al disminuir el caudal, llegando a hacerse comparable al tiempo de relajación dieléctrica del líquido, propiedad física del mismo. Cuando el caudal es cercano al mínimo, las fuerzas dominantes en la región de transferencia de corriente son las debidas al esfuerzo tangencial eléctrico y a la variación de presión generada por el esfuerzo normal eléctrico, mientras que la sobrepresión generada por la tensión superficial entra en juego al final de la región de transferencia de corriente, donde el radio del chorro disminuye rápidamente. La corriente eléctrica calculada en estas condiciones varía como la raíz cuadrada del caudal y es independiente del voltaje, en línea con los resultados experimentales y las estimaciones de Fernández de la Mora y Loscertales (J. Fluid Mech., 1994). Cuando el voltaje aplicado disminuye, la región de transición se aleja del tubo notablemente. Para ciertos valores de los parámetros, los resultados obtenidos muestran que la distancia a la que ocurre la transición cono-chorro puede ser mucho mayor que el radio del tubo. Para valores muy grandes del caudal, el radio del chorro es comparable al del tubo y decrece lentamente con la distancia al mismo, mientras que la corriente eléctrica se hace independiente del caudal y depende solo del voltaje aplicado y de las propiedades físicas del líquido.

ELECTROHYDRODYNAMIC ATOMIZATION OF LIQUID SUSPENSIONS FOR PREPARATION OF CATALYTIC MATERIALS

PEDRO L. GARCIA-YBARRA, SANTIAGO MARTIN, BEATRIZ MARTINEZ-VAZQUEZ, JOSE L. CASTILLO

Dept. Fisica Matematica y de Fluidos, Facultad de Ciencias, UNED, Paseo Senda del Rey 9, 28040 Madrid, Spain, pgybarra@ccia.uned.es

The electrohydrodynamic atomization of a liquid suspension is used as the feeding source to aerosolize nanoparticles which are driven by the external electrical field towards a collector where a deposit is formed. The electrospray works in a stable cone-jet mode in a large parameter space region [1] and the structure of the deposit can be controlled by adjusting the dynamics of particle arrival to the collector [2].

This method allows manufacturing very porous materials with a large active area which are suitable for catalytic processes. In this work, Pt on carbon nanoparticles dispersed in ethanol constitutes the blocks to build nanostructured catalytic layers which are tested as electrodes for PEM fuel cells.

The electrodes assembled in this way have shown a large performance which overcomes the maximum platinum utilization compared to catalytic layers prepared by other techniques. Moreover, the fuel cells may work in a stable regimen for long times [3]. These results encourage the application of this aerosol process for other purposes.

References:

[1] Martin, S., Perea, A., Garcia-Ybarra, P. L. & Castillo, J. L. (2012) *J. Aerosol Sci.*, **46**, 53-65.

[2] Castillo, J. L., Martin, S., Rodriguez-Perez, D., Perea, A. & Garcia-Ybarra, P. L. (2014) *KONA Powder and Particle J.*, **31**, 214-233.

[3] Martin, S., Martinez-Vazquez, B., Garcia-Ybarra, P. L. & Castillo. J. L. (2013) *J. Power Sources*, **229**, 179-184.

Airborne Phl p 5 in Different Fractions of Ambient Air and Grass Pollen Counts in 10 Countries across Europe

J.T.M. Buters[1], C. Antunes[2], R. Brandao[3] and the HIALINE working group[4]

[1] Division of Environmental Dermatology and Allergology, Helmholtz Zentrum München/TUM, ZAUM - Center for Allergy and Environment, Technische Universität München, Munich, Germany, buters@lrz.tu-muenchen.de

[2] CNC - Centre for Neurosciences and Cell Biology, University of Coimbra, Portugal, cmma@uevora.pt

[3] ICAAM-Inst. Ciencias Agrarias e Ambientais Mediterranicas, Universidade de Evora, Évora, Portugal, ruibrand@uevora.pt

[4] M. Thibaudon, France, M. Smith, Great Britain, C. Galan, Spain, R. Albertini, Italy, L. Grewling, Poland, G. Reese, Germany, A. Rantio-Lehtimäki, Finland, S. Jäger and U. Berger, Austria, M. Sofiev, Finland, I. Sauliene, Lithuania, L. Cecchi, Italy

Introduction Allergies to grass pollen are the number one cause of outdoor hay fever worldwide. The human immune system reacts with symptoms to allergens released from pollen. Because biological material varies in component content we investigated the biological variation in release of the major group 5 allergen from grass pollen across Europe.

The HIALINE consortium was a multidisciplinary group of experts from research groups in Europe. The main purpose of HIALINE was to assess factors that influence the allergen exposure of European citizens in order to improve forecasting both for the patient and for health care demands. It was intended to: i) Monitor pollen in ambient air; ii) Measure allergen load in ambient air; iii) Assess the pollen and allergen distribution and thus the allergen potency of airborne pollen across Europe; iv) Integrate multi-taxa modelling and forecasting system for pollen and allergens.

Methods Ambient air was collected daily simultaneously with a pollen trap and a high-volume cascade impactor for allergen determination across Europe for 3 consecutive years. Group 5 allergen was determined with a Phl p 5 specific ELISA in two fractions of ambient air: Particulate Matter (PM) >10µm and 10µm>PM>2.5µm. Mediator release by ambient air was determined in FcεR1-humanized basophils. Origin of pollen was modeled and condensed to pollen potency maps.

Results On average grass pollen released 2.0 pg Phl p 5/grain. However, pollen varied about 17-fold, $p<0.001$ in allergen release per pollen grain (potency). The main variation was locally day-to-day. Average potency maps across Europe were not stable and varied between years. Mediator release from basophilic granulocytes correlated better with allergen/m^3 ($r^2=0.80$, $p<0.001$) than with pollen/m^3 ($r^2=0.62$, $p<0.001$). Thus allergen monitoring to predict patient symptoms could have advantages. Indeed, pollen released different amounts of allergen in the non-pollen bearing fraction of ambient air depending on relative humidity.

Conclusion Across Europe, the same amount of pollen may release 17-fold different amounts of the major group 5 grass pollen allergen. This variation in allergen release is on top of variations in pollen counts. Molecular aerobiology, i.e. determining allergen in ambient air, correlated better with mediator release from immune cells than pollen concentrations, and may better represent allergen exposure. Moreover, within his project both geographical and temporal variations of allergen/pollen ratio were found. Pollen counts are not representative of the allergen load in the air, thus failing to be an accurate marker for allergen exposure.

Assessment of the human health risks and toxicity associated to particles (PM10, 2.5 and 1), organic pollutants and metals around cement plants

FRANCISCO SÁNCHEZ[1], NEUS ROIG[1], JORDI SIERRA[1,2,] MARTA SCHUHMACHER[1]

[1]*Departament d'Enginyeria Quimica, Universitat Rovira i Virgili, Av. Països Catalans 26
43007 Tarragona , Spain, marta.schuhmacher@urv.cat*

[2]*Laboratori d'Edafologia, Universitat de Barcelona, Av. Joan XXIII s/n,
08028 Barcelona, Spain, sierra@ub.edu*

Particulate matter (PM) is widely recorded as a source of diseases, being considered by some studies as the most harmful air pollutant. In fact, it is estimated that PM is responsible of 800.000 premature deaths annually. Among PM, the fine fraction (those smaller than 2.5μm of diameter) is identified as the most dangerous. PM is released in the environment as a consequence of different activities, being one of them the concrete production. Although some studies have been carried out relating fine PM emission from cement plants and health effects, we still don't have much info about the behavior this pollutant adopts inside the human body. Moreover, currently many plants are starting to use biomass/waste as fuel, and new efforts have to be made in order to identify if the use of this combustibles involves a greater health risk for the population. In order to clarify the effects of cement manufacturing fine PM over the population, our study will go over different milestones. Three cement plants (Montcada, Alcanar, Els Monjos) have been selected, and an evaluation of the affected area have been performed using atmospheric dispersion modeling (AERMOD). After the sampling of ambient PM, the morphology and the main composition of particles was determined by an Environmental Scanning Electron Microscope. Chemical characterization of the particles (through the analysis of metals, poliaromatic hydrocarbons, dioxins and furanes), and a subsequently ecotoxicity (microtox) and toxicity (lung cell cytotoxicity, genotoxicity, PM-Reactive Oxygen Species, lung macrophages, and endocrine disruptors) tests are performed to evaluate the potential adverse effects on health. Afterwards, the developing of a chronic exposure model will help to evaluate the effects and assess the risk to the population. Our preliminary results show that the 31-50 % of the samples exhibit citotoxicity, while the 18% express a positive response to the genotoxicity test. The microtoxicity seems to be higher in the coarse fraction (particles between 10 and 2.5 μm of diameter) than in the fine one. Further research is needed in order to keep on with the sampling and analysis stage, and to assess the possible health damage over the population. To reach this goal we propose to explore an integrated human respiratory tract (HRT) and physiologically based pharmacokinetic (PBPK) model in order to quantitatively estimate the relationship between exposure to PM and tissue dosimetry, while taking explicitly into account the physiological characteristics of the human biological system.

MICROBIAL INDICATORS OF BIOLOGICAL CONTAMINATION AT INDOOR WORKPLACES

MAŁGORZATA GOŁOFIT-SZYMCZAK, RAFAL L. GÓRNY,
ANNA ŁAWNICZEK-WAŁCZYK

Biohazard Laboratory, Department of Chemical, Aerosol, and Biological Hazards, Central Institute for Labour Protection – National Research Institute, Warsaw, POLAND, magol@ciop.pl

Keywords: Bioaerosol, Occupational exposure, Bacteria, Fungi

INTRODUCTION: In many occupational environments workers can be exposed to a wide spectrum of biological agents. In Europe, Directive 2000/54/EC on the protection of workers against health and safety risks related to exposure to biological agents lays down the principles for the management of biological risks and assigns to employers the duty of assessing the risks posed by biological agents in the occupational environment. The aim of this study was to determine the most common microorganisms present in the form of bioaerosol at different workplaces.

METHODS: The bioaerosol sampling was carried out at several industrial (recycling plants, automobile workshop, biomass-processing facilities, food production facilities, and printing house) and non-industrial (air-conditioning offices, archives, museums, libraries, schools, cosmetic and hairdresser salons, restaurants and bars) workplaces in Poland using MAS-100 *Eco* impactor. The flow rate and sampling time were 100 L/min and 1.5 min, respectively. Standard Petri dishes filled with blood trypticase soy agar and malt extract agar were used for bacterial and fungal sampling, respectively. The bioaerosol measurement was done at height of 1.4 m above the ground level to simulate the human breathing zone. All microorganisms isolated from the air samples were qualitatively analyzed to genus and/or species level.

RESULTS: Qualitative analysis revealed that the most prevalent and numerous microbial species in the air at industrial workplaces were filamentous fungi, mainly from genus *Aspergillus* and *Penicillium,* Gram-negative (*Escherichia, Proteus, Enterobacter, Pantoea, Pasteurella, Acinetobacter*, and *Pseudomonas*) and Gram-positive bacteria including species from genus *Bacillus* and mesophilic actinomycetes. Among the most common isolated species in non-industrial workplaces were Gram-positive bacteria, i.e. cocci (mainly from *Staphylococcus*, *Micrococcus*, and *Kocuria* genera) and endospore-forming rods (from genus *Bacillus*). All isolated species present in studied premises were classified to hazard groups I and II according to Directive 2000/54/EC.

CONCLUSIONS: Occupational exposure to biological agents depends on the source of biological contamination and the character of work activities. Based on bioaerosol sampling and analyzes, microbial indicators of biological pollution can be established to facilitate hygienic control of occupational environment.

MICROORGANISMS ON FIBERS AS INDOOR AIR POLLUTANTS

RAFAL L. GÓRNY[1], ANNA LAWNICZEK-WALCZYK[2]

[1]*Biohazard Laboratory, Department of Chemical, Aerosol, and Biological Hazards,
Central Institute for Labour Protection – National Research Institute, Czerniakowska 16 Street,
Warsaw, Poland, ragor@ciop.pl*

[2]*Biohazard Laboratory, Department of Chemical, Aerosol, and Biological Hazards,
Central Institute for Labour Protection – National Research Institute, Czerniakowska 16 Street,
Warsaw, Poland, anlaw@ciop.pl*

Introduction. Bacteria and fungi together with the structures and substances they produce may exert a harmful influence upon exposed individuals leading to numerous adverse health outcomes. They can be airborne as single cells or spores, their fragments and as aggregates of microbial only or mixed microbial and non-microbial constituents. As far as a transport of microbial agents on dust particles is relatively widely studied, a role of fibers as their carrier is not well recognized. The aim of this study was to check an ability of different natural and man-made fibers to carry microbial particles in the air in real indoor conditions.

Materials and Methods. The aerosol sampling was carried out at two industrial facilities producing and processing natural (cotton, silk, wool, flax, hemp) and synthetic (polyacrylonitrile, polyamide, polypropylene, polyester, viscose) fibrous materials, at four homes where dogs or cats were kept and one stable where horses were bred. At each of these premises, fibrous aerosol was sampled using 37-mm open-faced cassette on sterile teflon filter during "routine" activities, i.e. during final stages of fibrous material manufacturing cycle, dog or cat grooming and horse currying. Simultaneously with aerosol sampling, settled fibrous dust at industrial facilities and hair gathered during hygienic treatment of animals were collected. All man-made and animal fiber samples were weighed and laboratory analyzed for their microbiological purity.

Results. Both animal and plant fibers were microbiologically polluted; whereas all five tested synthetic fibers were free from such contamination. Both airborne and settled (or those derived straight from the animals) fibers were able to transport analogous microbial strains. Among animal fibers, the highest microbial load had horsehair (up to $9\times10^5/5.3\times10^3$ and 6.3×10^4 cfu/g for aerobic/anaerobic bacteria and fungi, respectively), then dog coat (up to $3.3\times10^5/9.1\times10^4$ and 4.3×10^3 cfu/g) and cat fur (up to $4.5\times10^3/1\times10^0$ and 2.5×10^3 cfu/g). From among the plants, the most contaminated were hemp (up to $7.7\times10^4/3.4\times10^4$ and 1.4×10^2 cfu/g), flax (up to $1.1\times10^3/4.8\times10^2$ and 5×10^1 cfu/g) and cotton fibers (up to $9.2\times10^2/3.1\times10^2$ and 1.4×10^2 cfu/g). The most frequently present on tested fibers were aerobic endospore-forming (hemp, cotton, wool) and non-sporing Gram-positive rods (wool, dog, horse), Gram-positive cocci (flax, horse) and Gram-negative rods (flax, cotton, wool, cat); however, from 0.8% (horse) to 43.3% (hemp) and from 0.1% (hemp) to 10.3% (cotton) of microbiota were constituted by anaerobic bacteria and fungi (mainly molds), respectively. From all tested fibers, pathogenic species classified by Directive 2000/54/EC to hazard group 2 were isolated.

Conclusions. Natural fibers are able to carry a substantial number of microbial particles, including those of pathogenic properties. Animal fibers should be thoroughly eliminated from indoor environment; whereas plant fiber products, if possible, should be replaced by synthetic ones to avoid unwanted dissemination and subsequent exposure to harmful microbial agents.

SENSITIVITY OF THE AIRBORNE POLLEN TO THE CLIMATE VARIABILITY IN THE NORTH EAST OF THE IBERIAN PENINSULA

MARTA ALARCÓN[1]; JORDINA BELMONTE[2,3]; HUSAM T. MAJEED[1]; CRISTINA PERIAGO[1]

[1] *Departament de Física i Enginyeria Nuclear, Universitat Politècnica de Catalunya, C/ Urgell 187, 08036 Barcelona, Spain. marta.alarcon@upc.edu*

[2] *Institut de Ciencia i Tecnología Ambientals (ICTA), Universitat Autònoma de Barcelona (UAB). Edifici C, 08193 Bellaterra, Spain. jordina.belmonte@uab.cat*

[3] *Departament de Biologia Animal, Biologia Vegetal i Ecologia, Universitat Autònoma de Barcelona (UAB). Edifici C, 08193 Bellaterra, Spain*

Here we present a study about the sensitivity to the climate variability showed by the biological component (pollen) of the atmospheric particulate matter in Catalonia, NE of the Iberian Peninsula. In this sense, the relationships between the phases of the North Atlantic Oscillation (NAO), Western Mediterranean Oscillation (WeMO) and the Arctic Oscillation (AO) and different parameters of the airborne pollen such as the Annual Pollen Index (API), the start, the end and the length of the pollination seasons have been analyzed. To this end, the Spearman and Kendall correlations between the three climatic indices (NAO, WeMO, and AO) and the main airborne pollen parameters of 22 taxa collected at 6 aerobiological stations in Catalonia during the 18 years-period 1994-2011, have been computed in order to determine their respective vulnerability to climate variability. Considering that the climatic indices show their most relevant dynamics during the cold months, both, the annual and the winter (December to March) indices have been used.

WeMO was the climatic index which showed more significant correlations with the pollen parameters. On the other hand, the API of most of the taxa exhibited negative correlations with the indices, indicating that in years of positive phase, the API values are lower than in years of negative one. This result is consistent with the wetter conditions associated to the negative mode of the climatic indices in western Iberian Peninsula. The only exception was *Corylus* which showed positive significant correlations. *Alnus*, *Betula*, *Fagus* and *Ambrosia* did not show significant correlations, which could be attributed to a major influence of the long range transport. Negative correlation of climatic indices with pollination start indicates that in years with positive phase of the indices (lower precipitation and intensification of the solar radiation) there is an advance in the pollination season and vice versa. Positive correlation with length indicated that in years with positive phase (lower precipitation and intensification of the solar radiation) there is an enlargement of the flowering period and vice versa.

ANNUAL BEHAVIOR OF BLACK CARBON AEROSOLS AT VARANASI, INDIA

MANOJ K. SRIVASTAVA[1], R. S. SINGH[2], B. P. SINGH[1], R. K. SINGH[1], B. N. RAI[2], S. TIWARI[3], A. K. SRIVASTAVA[3]

[1]*Department of Geophysics, Banaras Hindu University*
Varanasi, INDIA, mksriv@gmail.com

[2]*Department of Chemical Engineering and Technology, IIT-BHU*
Varanasi, INDIA

[3]*Indian Institute of Tropical Meteorology- Delhi Center*
New Delhi, INDIA

Black carbon mass concentration (BC) data is collected at Varanasi using a seven channel Aethalometer. Variations of BC at various temporal scales have been studied. Mean BC mass concentrations showed highest concentration during post-monsoon, followed by winter, summer and monsoon. On the diurnal cycle, gradual increase of BC mass concentration started at around 0700 local time (LT) to reach its primary peak at around 0900 LST, followed by an afternoon minima and a secondary peak between 2100 to mid-night. This diurnal behavior is, however, changed for pre-monsoon season, where it was found to be increasing at 0500 LT till 0800 LT, followed by a sudden drop of the concentration during afternoon till evening. The lower values start gradual increase after this drop period that continued till next morning. General behavior of gradual decrement of BC mass concentrations from 0900 LST to noon/afternoon is likely caused by extending depth of the local boundary layer that supports pumping of pollution to the free atmosphere. BC mass concentrations over Varanasi were approximately six times higher than the pristine background environment of Himalayas. The correlation between BC showed significant positive and negative correlations with various weather parameters, and indicate pronounced effect of atmospheric conditions on reduction and enhancement of BC mass concentration for this region. On the basis of spectral absorption characteristics, it is found that the source of BC over Varanasi is mostly related to the burning of fossil fuel, with some intermittent sources of biomass/ biofuels, etc.

APLICACIÓN DEL SISTEMA TANDEM DMA-MS AL ANÁLISIS ATMOSFÉRICO

ARTURO ÁLVARO CARBALLIDO[1,2], DAOIZ ZAMORA PÉREZ[1], GONZALO FERNANDEZ DE LA MORA[1]

[1]*Sociedad Europea de Análisis Diferencial de Movilidad,*
Parque Tecnológico de Boecillo. Parcela 205. 47151
Boecillo, España, arturo.alvaro@seadm.com

[2]*Universidad de Valladolid. Paseo del cauce, 59 47011*
Valladolid, España

El análisis atmosférico de nanopartículas y aerosoles finos puede ser de gran interés en ámbitos variados como estudios de nucleación, química atmosférica o de impacto en la salud. En particular existe un creciente interés en el estudio de aerosoles nanométricos a partir de precursores moleculares (tanto en la atmósfera como en fuentes de combustión o ablación por laser o descarga eléctrica).

Un instrumento combinado de Análisis de Movilidad- Espectrometría de masas (DMA-MS) en modo cuádruplo triple permite alcanzar niveles de sensibilidad y de resolución impensables hasta hace poco tiempo en este campo. Permite tanto la identificación de moléculas como sus agregados hasta formar nanopartículas de varios nm de diámetro con sensibilidades por debajo de 1pg/m3.

En esta aplicación en particular se describe la presencia en la atmósfera de contaminantes en concentraciones del orden de 10 pg/m3 en 4 "canales". Denominamos "canal" a una configuración específica de detección, que fija los diferentes parámetros que el instrumento permite controlar. Estos son: tiempo de muestreo, temperatura y tiempo de desorción, movilidad eléctrica, masa, y masa de sus fragmentos. Los canales seleccionados corresponden a algunos explosivos de utilización común. El estudio atmosférico se completa con un estudio de las emisiones de motores Diesel en dichos "canales". Dado que muchos explosivos de interés son nitratos de sustancias orgánicas, abundan los puntos de contacto con los estudios de la riquísima química atmosférica del ácido nítrico con los vapores orgánicos ambientales.

Se presentarán las concentraciones de contaminantes medidas en cada uno de los canales, tanto en la atmósfera, como en las emisiones de los motores Diesel. Así mismo, y para mostrar el efecto de la adición del DMA al equipo, se presentará un estudio de movilidad en el entorno del valor diana. Se pueden apreciar los isómeros (masas y fragmentos idénticos, movilidades distintas) detectados en cada canal, que en ocasiones están presentes en concentraciones muy superiores a la molécula objetivo, y que ocultarían totalmente la misma en un análisis puro de espectrometría de masas.

Los resultados obtenidos indican que cada canal permite la identificación y monitorización de un contaminante atmosférico, con concentraciones típicas que varían entre 20 pg/m^3 (masa 262/46) y 0.3 pg/m^3 (masa 257/46). Podemos concluir que, al nivel actual de resolución de la instrumentación utilizada, la atmósfera presenta una variedad de contaminantes extraordinaria, y que prácticamente cualquier "canal" elegido al azar en la atmósfera permite la detección de al menos un contaminante, presente a concentraciones superiores a 1 pg/m^3.

ATMOSPHERIC AIR QUALITY ASSESSMENT IN AN INDUSTRIAL AREA IN GIJÓN, NORTH OF SPAIN

J. LAGE[1], S.M. ALMEIDA[1], M.A. REIS[1], P.C. CHAVES[1], M.C. FREITAS[1], S. GARCIA[2], J.P. FARIA[3], B.G. FERNÁNDEZ[3], H.TH. WOLTERBEEK[4]

[1]*Centro de Ciências e Tecnologias Nucleares, Instituto Superior Técnico, Universidade de Lisboa, Estrada Nacional10, km 139,7, 2695-066 Bobadela LRS;*

[2]*Instituto de Soldadura e Qualidade, Portugal;*

[3]*Global R&D – ArcelorMittal, Spain;*

[4]*Delft University of Technology, The Netherlands;*

Air pollution is one of the most pressing environmental concerns facing the world's nations. Since preindustrial time, human activities resulted in large increases in air pollution. The greatest anthropogenic threats to air quality come from transport, industrial and domestic emissions. In order to perform efficient pollution control strategies a good source apportionment to identify specific air pollution sources should be realized in target areas.

The objective of this work was 1) to assess the air quality of an industrial area composed by a steelwork, a cement industry, a power plant and a harbor, and 2) to assess the impact of these industries to the local air.

The applied methodology consisted on the collection of PM samples in the industrial area in two sampling campaigns, performed in the winter and summer seasons, and in four sampling periods in order to identify specific sources. For that one low volume sampler and one high volume sampler, operating side by side, were used to collect coarse and fine particles. Afterwards filters were analyzed by Instrumental Neutron Activation Analysis (INAA) with the k_0 methodology, and by Particle Induced X-Ray Emission (PIXE) for the elemental determination and by ion chromatography, indophenol-blue spectrophotometry and atomic absorption spectroscopy for the determination of water-soluble inorganic ions.

Source apportionment with Positive Matrix Factorization (PMF) was applied and seven emission sources were identified. The first source reflected the sea-spray composition, having high shares of Cl and Na, and contributed on average to 22% of the PM_{10} mass. The second source, which contributed on average to 11% of the total PM_{10} mass, was mainly composed by As, Cr, Cu, Ni, Pb, Sb and Zn and was attributed to mixed combustion processes and traffic. The third source contained high percentages of NH_4^+ that derives from gas to particle conversion processes. The contribution of this factor to PM_{10} mass was on average 12%. The fourth factor was made of Br and contributed for 1.8% of the total PM_{10} mass. The fifth source was dominated by NO_3^- and SO_4^{2-} and contributed on average for 19% of the PM_{10} mass concentration. The sixth source carried high percentages of Al, Ca, La, Si, Ti and V and accounted for 14% of the PM_{10}. These are the major constituents of soil and point out the fingerprint of mineral dust. The seventh factor was associated with steel production as it is defined by Fe and Mn. This source accounted for 21% of PM_{10} mass concentration.

FIRST MOON PHOTOMETRIC AEROSOL MEASUREMENTS AT ARCTIC STATIONS

M.MAZZOLA[1], V. VITALE[1], A. LUPI[1], R.S. STONE[2,3], T.A. BERKOFF[4,5], T.C. STONE[6], J. WENDELL[3], D. LONGENECKER[2,3], C. WEHRLI[7], N. KOUREMETI[7], K. STEBEL[8]

[1]*Institute of Atmospheric Sciences and Climate, National Research Council, Via Gobetti 101, Bologna, Italy, m.mazzola@isac.cnr.it*

[2]*Cooperative Institute for Research in Environmental Sciences, University of Colorado, Boulder, Colorado, USA*

[3]*Earth System Research Laboratory, National Oceanic and Atmospheric Administration, Boulder, Colorado, USA*

[4]*University of Maryland, Maryland, USA,*

[5]*NASA-Goddard,Greenbelt, Maryland, USA*

[6]*United States Geological Survey (USGS), Flagstaff, Arizona, USA*

[7]*Physikalisch-Meteorologisches Observatorium Davos (PMOD), Davos, Switzerland*

[8]*Norsk institutt for luftforskning (NILU), Kjeller, Norway, Kerstin.Stebel@nilu.no*

Aerosol particles emitted at mid-latitudes can be transported in the Arctic . Their monitoring in these areas is important both to study transport process itself, and the effects they may have on the energy balance. Unfortunately, during the polar night their monitoring by remote sensing techniques from the ground is limited to the use of LIDAR and stellar photometry , two techniques expensive in terms of money and manpower. A new possibility is to use the technique of photometry where the radiation source is the moon . This is made possible by the knowledge of the lunar reflectivity in any geometric configuration of the Sun-Moon-Earth system and of the Moon phase . This problem was studied and solved by USGS with the ROLO model.

In this contribution we will show the results of the first measurements made at Arctic stations, i.e. Barrow (Alaska) and Ny-Ålesund (Svalbard). The measurements started in November 2012 using a Carter -Scott SP02 sun photometer at Barrow, while in Ny-Ålesund first tests were made in February 2014 using a PFR sun photometer. Both instruments were modified in order to be able to effectively measure the weak radiation signals reflected from the Moon. Tests carried out in periods of alternating day and night have shown that this technique allows to obtain results consistent with those obtained using the solar photometry.

Other research groups around the world are gearing up to perform this type of measurements, and then monitoring of the columnar aerosol optical properties will be possible during the night in different places on the planet , both polar and not.

GAS AND PARTICLE PHASE CHEMICAL COMPOSITION OF MARINE EMISSIONS FROM MEDITERRANEAN SEAWATERS: RESULTS FROM A MESOCOSM STUDY

PEY J.[1], DEWITT H.L.[1], TEMIME-ROUSSEL B.[1], MÊME A.[2], CHARRIERE B.[4,5], SEMPERE R.[4], DELMONT A.[4], MAS S.[6], PARIN D.[6], ROSE C.[3], SCHWIER A.[3], RMILI B.[2], SELLEGRI K.[3], D'ANNA B.[2], MARCHAND N.[1]

[1] Aix-Marseille Université, CNRS, LCE FRE 3416, 13331 Marseille, France

[2] Université Lyon 1, CNRS, UMR5256, IRCELYON, Institut de Recherches sur la Catalyse et l'Environnement de Lyon, 69626 Villeurbanne, France

[3] Laboratoire de Météorologie Physique, CNRS-Université Blaise Pascal, Observatoire de Physique du Globe, Aubière, France

[4] Aix-Marseille Université, Université du Sud Toulon-Var, CNRS/INSU, UMR7294, IRD, MIO, UM110, 13288, Marseille, Cedex 09, France

[5] University Perpignan Via Domitia, CEntre de Formation et de Recherche sur les Environnements Méditerranéens, UMR5110, 66860, Perpignan, France

[6] Université de Montpellier 2 CC 093, UMR 5119, CNRS-UM2-IRD-IFREMER-UM1 ECOSYM, 34095 Montpellier, France

Marine emissions are among the largest sources of secondary organic aerosols (SOA) globally. Whereas physical processes control the primary production of marine aerosols, biological activity is responsible for most of the organic components, both aerosol and gas-phase, released from marine sources and potentially transformed into SOA when exposed to atmospheric oxidants.

As part of the Source of marine Aerosol particles in the Mediterranean atmosphere (SAM) project, a mesocosm study was conducted at the Oceanographic and Marine Station STARESO (Corsica) in May 2013. During these experiments, 3 mesocosms were deployed, filled with 2260 L of bay water and covered with a transparent Teflon dome. To observe the effect of biological activity on volatile organic compounds (VOCs) and aerosol emissions, two of the mesocosms were enriched with different levels of nitrate and phosphate respecting Redfield ratio (N:P = 16) and one was left unchanged to be used as a control. Physical and chemical properties of mesocosms and ambient atmospheres were followed during 20 days by using a high resolution real-time instruments. Aerosol size and concentration were measured by a Scanning Mobility Particle Sizer; gas-phase composition of VOCs was determined by using Proton Transfer Reaction Time-of-Flight Mass Spectrometer; and aerosol chemical composition was obtained from High Resolution Time-of-Flight Aerosol Mass Spectrometer.

In parallel, numerous additional measurements were conducted to fully characterize the water within each of the enclosed mesocosms, including water temperature, pH, conductivity, chemical and biological analyses, fluorescence of chlorophyll-a, and dissolved oxygen concentration. Incident light within the mesocosms was also measured.

Preliminary results suggest new particle formation processes linked to iodine chemistry. Aerosol composition inside the mesocosms was slightly enriched in organic aerosols with respect to the outside atmosphere. Oxygenated organic compounds were the most important species in terms of mass concentration, but amine-related aerosol mass peaks varied the greatest in concentration between the mesoscosms. Finally, a clear enhancement of VOCs occurred in the enriched mesocosms.

GROUND-BASED ATMOSPHERIC MONITORING IN MALLORCA AND CORSICA IN SUMMER 2013 IN THE CONTEXT OF CHARMEX: RESULTS ON NUMBER-SIZE DISTRIBUTIONS, ON-LINE AND OFF-LINE AEROSOL CHEMISTRY, AND VOLATILE ORGANIC COMPOUNDS

PEY J.[1], CERRO J.C.[2,3], HELLEBUST S.[1], DEWITT H.L.[1], TEMIME-ROUSSEL B.[1], ELSER M.[4], PÉREZ N.[5], SYLVESTRE A.[1], SALAMEH D.[1], MOČNIK G.[6], PRÉVÔT A.S.H.[4], ZHANG Y.L.[7], SZIDAT S.[7], MARCHAND N.[1]

[1] *Aix-Marseille Université, CNRS, LCE FRE 3416, 13331 Marseille, France*
jorge.pey@univ-amu.fr
[2] *University of the Balearic Islands, 07122 Palma de Mallorca, Spain*
[3] *Department of Agriculture, Environment and Territory, Balearic Islands Government, 07009 Palma de Mallorca, Spain*
[4] *Laboratory of Atmospheric Chemistry, Paul Scherrer Institute, 5232 Villigen, Switzerland*
[5] *Institute of Environmental Assessment and Water Research CSIC, 08034 Barcelona, Spain*
[6] *Aerosol d.o.o., 100 Ljubljana, Slovenia*
[7] *Department of Chemistry and Biochemistry, University of Bern, 3012 Bern, Switzerland*

As part of the Chemistry-Aerosol Mediterranean Experiment (ChArMEx), simultaneous field campaigns were conducted in the summer of 2013 in several Mediterranean observatories. Among these observatories, the Ersa, Corsica site had the most complete set of instrumentation and was where most of the scientific effort was concentrated. In addition to participating in the Ersa supersite, the Laboratoire the Chimie de L'Environnement, in collaboration with the University of the Balearic Islands, installed a complementary observatory in Mallorca (Spain) in the Spanish Ministry of Defense facilities "Cap des Pinar". A number of European institutions were involved in the campaign. Overall, a complete instrumentation set-up to measure the aerosol and gas-phase chemical and physical properties and concentrations in Mallorca was deployed: a HR-ToF-AMS to measure the real-time non-refractory chemical composition and mass loading of aerosols with aerodynamic diameters between 50 and 1000 nm (e.g., sulfate, nitrate, ammonium, chloride and organic compounds); a PTR-ToF-MS to determine and quantify a wide spectral range of volatile organic compounds (VOCs), including primary species such as isoprene, monoterpenes, benzene, xylene and DMS, and secondary products such as methacrolein, glyoxal, methylvinylketone; a SMPS to obtain particle number and size distribution of aerosols in the range 10-700 nm; a LAAPTOF to characterize in real time individual particles in terms of size and chemical composition; a 7 length-wave aethalometer to monitor the absorption coefficients of < 1000nm aerosols; two high-volume samplers for subsequent chemical determinations, including off-line 14C analysis, of the PM_{10} and PM_1 fractions; a mobile van with air quality surveillance instruments (e.g., CO, CO_2, NO_x); and a meteorological tower.

During the campaign, wide-scale atmospheric episodes were observed at both Mallorca and Corsica, including Saharan dust outbreaks, new-particle formation events and regional accumulation of pollutants. Different air mass sources and meteorology were found to influence Mallorca and Corsica. In particular, more Saharan dust episodes and persistent accumulation processes were observed in Mallorca, while outflows from the Po valley were observed at times in Corsica. Thus, the general atmospheric characteristics of the Mediterranean basin as well as region-specific aerosol episodes were able to be differentiated and characterized by the comparison of these two sampling sites and conclusions about factors influencing anthropogenic aerosol concentrations in the Mediterranean can be drawn.

LONGWAVE RADIATIVE FORCING OF MINERAL DUST: IMPROVEMENT OF ITS ESTIMATION WITH TOOLS RECENTLY DEVELOPED BY THE EARLINET COMMUNITY

MICHAËL SICARD[1,2], SANTI BERTOLÍN[1], CONSTANTINO MUÑOZ[1], ADOLFO COMERÓN[1], ALEJANDRO RODRÍGUEZ[1]

[1] *RSLab, Universitat Politècnica de Catalunya, Barcelona, Spain;*
msicard@tsc.upc.edu, santiberto@gmail.com, constan@tsc.upc.edu, comeron@tsc.upc.edu,
alejandro@tsc.upc.edu

[2] *IEEC-CRAE, Universitat Politècnica de Catalunya, Barcelona, Spain*

Atmospheric aerosols have a remarkable effect on the Earth-atmosphere radiative budget. Indeed, aerosols and their interactions with clouds contribute to the largest uncertainties in the estimation of the Earth's changing energy budget. Nowadays many radiative transfer models have been developed to locally estimate the aerosol direct radiative forcing (RF). In the longwave (LW) spectral range, the aerosol radiative properties are usually estimated theoretically with a Mie code. The parameter that contains the absorption and scattering quantities, the extinction coefficient, is normalized to the extinction coefficient in the shortwave spectral range, most of the time in the visible spectral range, or to the number concentration. As measurements of the extinction coefficient or of its integral, the optical thickness, are available in the shortwave spectral range, the equivalent extinction coefficient or optical thickness in the LW spectral range can be deduced thanks to that normalized, theoretical extinction coefficient.

Since relatively little the EARLINET/ACTRIS community has developed codes that combine sun-photometer and lidar data to retrieve a set of parameters vertically-resolved related to the size distribution (fine and coarse mode extinction coefficients, fine and coarse mode volumetric concentrations, etc.). We concentrate on the case of mineral dust whose size distribution is often dominated by the coarse mode. This work demonstrates how the knowledge of the vertically-resolved fine and coarse mode aerosol optical thickness modify the LW RF as compared to the classical approach with a total aerosol optical thickness. The results show that when the coarse mode predominates the classical approach underestimates the dust LW RF by 4 to 20 %.

TRENDS IN AIR POLLUTION BETWEEN 2000 AND 2012 IN THE WESTERN MEDITERRANEAN: A ZOOM OVER REGIONAL, SUBURBAN AND URBAN ENVIRONMENTS IN MALLORCA (BALEARIC ISLANDS)

J. C. CERRO[1], V. CERDÀ[1], J. PEY[2,3]

[1] *Laboratory of Environmental Analytical Chemistry , Illes Balears University, Ctra. Palma-Valldemossa, Km 7.2, 07008, Palma de Mallorca, Spain, jccerro@dgqal.caib.es, victor.cerda@uib.es*

[2] *Institute of Environmental Assessment and Water Research, IDÆA-CSIC, C/ Jordi Girona 18-26, 08034, Barcelona, Spain*

[3]*Laboratory of Environmental Chemistry LCE-IRA, Aix Marseille University, 3 Place Victor Hugo,13001 Marseille, France, jorge.pey@univ-amu.fr*

Particulate matter and gaseous pollutants concentrations (NO_x, SO_2, CO and O_3) have been measured on a regular basis in several European regions since the beginning of the 90's. Based on these long-term series of air pollutants, the study of trends over certain European regions has been reported.

In the context of the Balearic Islands, more than a decade of uninterrupted measurements at multiple locations has provided, for the first time at an insular location in the Western Mediterranean Basin, the opportunity to study the inter-annual tendencies and the variability of different air quality metrics. Hourly data of NO, NO_2, SO_2, O_3 and PM10 from 2000 to 2012 were compiled and validated. The monitoring sites were classified in urban, suburban, and rural (or regional) background. The selection of the monitoring sites considered in the trend analysis was done according to two essential criteria: 1) the annual data coverage should be over 75%; and 2) at least 8 of the last 10 years of data exists. Furthermore, the origin of air masses was daily computed, which is a useful way to account for long-range transport of pollutants or to address the occurrence of meso-scale atmospheric processes.

Daily, weekly, seasonal and inter-annual patterns of these pollutants have been studied at the different environments. The multi-year and multi-pollutant study, over three environments from the same region, together with the discrimination per air mass origins permitted us to follow those changes induced by the implementation of regional policies and those related to the enactment of continental strategies.

Up to now some clear results have been obtained. NO and NO_2 undergo clear decreasing trends in urban stations (-1.1 $\mu g/m^3$year), less evident in suburban and regional background stations (from no change to -0.3 $\mu g/m^3$year). The behaviour of O_3 is opposite to that of NO_x at urban stations (+1.0 $\mu g/m^3$year), almost parallel to the decrease in NO, one of its main depletion agents. At rural background sites O_3 shows a moderate increasing trend (+0.5 $\mu g/m^3$year), consistent with the observations in other European regions. Significant decreasing O_3 concentrations are patent at the suburban background (-0.4 $\mu g/m^3$year), probably caused by an increasing vehicular traffic over these areas.

Finally, a substantial decline in PM10 is obvious at urban and suburban (-0.7 $\mu g/m^3$year) areas, slightly lower over the regional background (-0.5 $\mu g/m^3$year).

CHEMICAL COMPOSITION OF HOUSEHOLD DUST AS AIR QUALITY TRACER OF THE CITY OF HUELVA

RAQUEL TORRES[1], ANA Mª SÁNCHEZ DE LA CAMPA[1], MARÍA BELTRÁN MUNIZ[1], DANIEL SÁNCHEZ-RODAS[1], JESÚS D. DE LA ROSA[1]

[1]*Associate Unit CSIC-UHU "Atmospheric Pollution". Center for Research in Sustainable Chemistry (CIQSO), University of Huelva, Campus El Carmen E21007, Huelva, Spain, jesus@uhu.es*

Historically, the city of Huelva has been characterized by a poor air quality due mainly to the impact of emissions from industrial states (Punta del Sebo, New Pueto and Tartessos). Querol et al. (2002) first described the geochemical anomalies of atmospheric particulate matter (TSP), consisting of high concentrations of As + Se + Bi + Cu + Zn + Pb among others. A decade later, the joint results of the Associated Unit CSIC-UHU "Atmospheric Pollution" with the Air Quality Office of the Andalusian Government show the compliance with European Directives, although geochemical anomalies of the mentioned elements are still present compared to other monitoring stations of Andalucía (de la Rosa et al., 2010) and Spain (Querol et al., 2008).

In this work, we present the results of a geochemical characterization of major and trace elements of household dust in the city of Huelva. Dust samples were collected in 100 house distributed in the city in October 2013. Also, control-dust was sampled in small villages around Huelva. Analyses were performed by ICP-OES and ICP-MS at the Central Laboratories of the University of Huelva, after attack with HF + HNO3 + HClO4 according to Querol et al. (2004).

The results were normalized to Upper Continental Crust (Rudnick & Gao 2003), highlighting the positive anomalies in metals such as Cu + Zn + Sb. In the case of Sb, high concentrations have been observed in samples of homes close to heavy traffic. Samples with high residence time are enriched in metals compare to new dust. High concentrations of Cu and Zn can also be related to the anomalies described by Castillo et al. (2013) in deposition particles, related with polymetallic sulphide raw materials from the industrial area and polluted soils of Huelva.

References
Castillo S., et al. (2013) Atmospheric Environment 77: 509–517

De la Rosa J.D., et al. (2010) Atmospheric Environment 44: 4595–4605.

Querol X, et al. (2002) Atmospheric Environment 36: 3113-3125.

Querol X., et al. (2004) Journal of Aerosol Sciences 35: 1151–1172.

Querol X., et al. (2008) Atmospheric Environment 42: 3964-3979.

Rudnick R.L., Gao S. (2003) Composition of the continental crust. Treatise on Geochemistry 3: 1-64. Elsevier.

COMPUTER SIMULATION OF ELECTROSPRAYING OF VOLATILE LIQUIDS

AJITH K. ARUMUGHAM-ACHARI[1], JORDI GRIFOLL[1], JOAN ROSELL-LLOMPART[1,2]

[1]*Chemical Engineering Department, Universitat Rovira i Virgili, Av. Països Catalans 26, Tarragona, Spain, joan.rosell@urv.cat*

[2]*ICREA - Catalan Institution for Research and Advanced Studies, Passeig Lluís Companys 23 Barcelona, Spain*

A model has been developed and implemented in a numerical code to simulate electrosprays of volatile liquids. We have accounted for all the relevant phenomena that happen in such systems: (1) droplet dynamics (Grifoll and Rosell-Llompart, 2012), considering evaporation; (2) surrounding gas flow field (either induced externally or by the droplets' motion; Arumugham-Achari *et al.*, 2013); (3) vapor transport by convection and diffusion (Wilhelm *et al.*, 2003); (4) Coulomb explosions; and (5) transport of residual charge that results from evaporation and Coulomb explosions. For the case of a methanol electrospray, Figure 1(a) shows a snapshot of a simulated spray plume, with the streamlines of the air flow induced by the droplets' drag. Panel (b) shows the intensity map of the volumetric rate of charge production associated with droplets with diameter d below $d*$ (=1 μm). Since this charge is mostly due to Coulomb explosions, the different bands delimitate the regions of intense explosions.
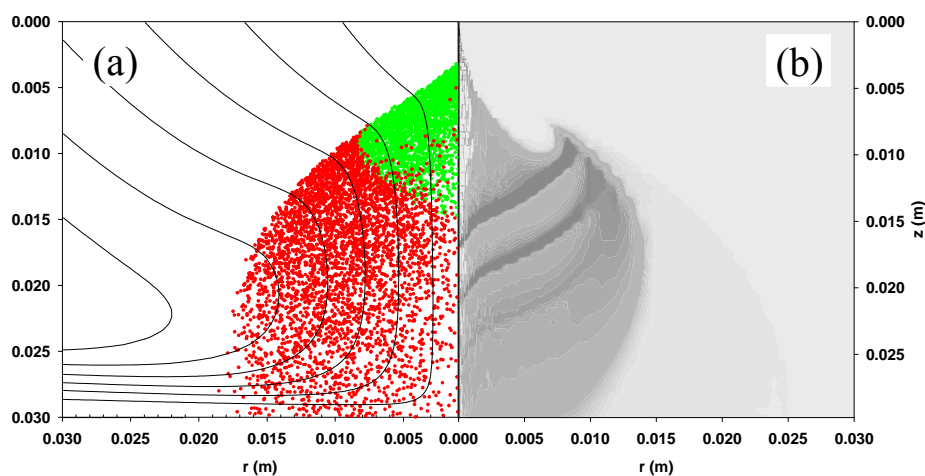
Figure 1. (a) Snapshot of evaporating methanol electrospray droplets (initial d_{10} = 8 μm; coefficient of variation = 10%) and induced air flow streamlines. (b) Mono-mobile charge source rate from droplets with $d < d* = 1$ μm.

References
Arumugham-Achari, A. K., Grifoll, J. and Rosell-Llompart, J. (2013). *J. Aerosol Sci.*, **65**, 121-133.
Grifoll, J. and Rosell-Llompart, J. (2012). *J. Aerosol Sci.*, **47**, 78-93.
Wilhelm, O., L. Madler and S. E. Pratsinis (2003). *J. Aerosol Sci.*, **34**, 815-836.

MATHEMATICAL MODEL OF THE GAS ANTI-SOLVENT PRECIPITATION (GASP) PROCESS

MANUEL ARIAS-ZUGASTI[1], DANIEL E. ROSNER[2]

[1]*Departamento de Física Matemática y de Fluidos, UNED, Apdo. 60141 Madrid, Spain,*
maz@dfmf.uned.es

[2]*Chemical and Environmental Engineering Dept., Yale University, 9 Hillhouse Avenue,   New Haven, CT 06511, USA, daniel.rosner@yale.edu*

Keywords: homogeneous nucleation kinetics, crystal growth kinetics, micronization of pharmaceutical powders

Gas Anti-Solvent Precipitation (GASP) is a well known micronization technique used to generate ultrafine powders of active pharmaceutical ingredients (APIs)---initially dissolved in a liquid solvent and often sprayed into compressed CO_2 antisolvent (AS). For industrial applications narrow distributions of ultrafine API particles are required. However, the complexity of the physical phenomena involved in this process have hampered its optimization. In this regard, a simple mathematical model has been developed (loc.cit.), enabling the calculation of expected precipitate size distribution function and process yield. This model exploits Classical Nucleation Theory with an environment-dependent surface energy, and a Peng-Robinson EOS formulation for the fluid phase equilibria. However, the current formulation is based on a tractable "well-mixed droplet" approx., neglecting intra-droplet CO_2 diffusion---an assumption that has been found to be too restrictive, and is being relaxed in current extensions of our model.

The present study focuses on evaluating the characteristic times governing the dynamics of the GASP process (homogeneous nucleation-, precipitate particle growth-, AS uptake-, particle coagulation- and intra-droplet AS diffusion-times). We show that during AS uptake particle nucleation is the dominant process, with negligible particle growth or aggregation. While this model neglects intra-droplet AS-diffusion, in the absence of gas-expanded liquid circulation and/or turbulence our estimation of characteristic times shows that CO_2 diffusion limitations will become non-negligible in many cases of practical interest. Nevertheless, because AS intra-droplet diffusion should produce higher local supersaturations, our results are expected to underestimate the amount of precipitated API. Besides revealing valuable trends, the present results provide useful approximations to droplet volume-averaged results, at least for cases leading to intense API nucleation.

The principal conclusion from our model is that, to obtain high yields of ultrafine, nearly-monodisperse precipitate, one needs to operate under high CO_2-pressures with solvent droplets large enough to allow for a high yield, but small enough to avoid increased values of the Sauter mean diameter (SMD) and population spread. We anticipate an optimal interval of initial droplet diameters, depending on the relative importance of the conflicting goals of high precipitate yield and small SMD and dimensionless spread.

References

Martin, A. and Cocero, M. J. (2008), Advanced Drug Delivery Reviews, 60, 339-350.

Rosner, D. E. and Arias-Zugasti, M. (2014). Ind. & Eng. Chem. Res., Surface Energy `Evolution' (SEE) in Pharmaceutical Powder `Micronization' Using Compressed Gas Anti-Solvent (Re-) Precipitation (GASP), in press.

Rosner, D. E. and Arias-Zugasti, M. (2014). J. Supercrit. Fluids, Theory of Pharmaceutical Powder `Micronization' Using Compressed Gas Anti-Solvent (Re-) Precipitation, submitted.

PARTICLE DEPOLARIZATION RATIO PROFILING OVER THE SOUTHWESTERN IBERIA PENINSULA DURING SAHARAN DUST OUTBREAKS.

S. PEREIRA[1,2], J. L. GUERRERO-RASCADO[2,3], D. BORTOLI[1], J. PREISSLER[4], A. M. SILVA[1], F. WAGNER[5]

[1] *Geophysics Centre of Évora, Rua Romão Ramalho nº59, Évora, 7000, Portugal*
sergiopereira@uevora.pt
[2] *Andalusian Institute for Earth System Research (IISTA - CEAMA), University of Granada, Spain*
[3] *Dpt. Applied Physics, University of Granada, Fuentenueva s/n, 18071, Granada, Spain*
[4] *now at: Centre for Climate and Air Pollution Studies (C-CAPS), National University of Ireland.*
[5] *now at: Deutscher Wetterdienst, Hohenpeißenberg Meteorological Observatory, Germany.*

The development of multi-wavelength Raman lidars with polarization capabilities was one important step for improving the vertically-resolved characterization of mineral dust particles, which are typically characterized by their irregular shape (i.e. non-spherical). Thus they can change significantly the polarization state of the emitted laser beam; in that case, a backscattered signal, which is no longer linearly polarized (rather elliptical), is detected. The particle linear depolarization ratio, δ_P, is the parameter which quantifies this change in the polarization state due to particles.

The Raman lidar PAOLI (Portable Aerosol and Cloud Lidar) is installed at the observatory of the Évora Geophysics Centre, Portugal. It includes three elastic channels in the UV-VIS-IR range (355 nm, 532 nm, 1064 nm), two inelastic (Raman) channels (387 nm, 607 nm) and a further (polarization) channel which detects the cross polarized component at 532 nm. Thus δ_P can be determined at 532 nm. For accurate depolarization measurements, the calibration of the channels involved (in this case the 532_{TOTAL} and 532_{CROSS} channels) is essential. The depolarization calibration of PAOLI depends on the determination of the transmission ratios of these two channels. The efficiency of the 532_{TOTAL} channel is polarization dependent because a beam splitter is sensitive to polarization of light incident upon it. This effect has to be corrected in case of detection of non-spherical particles. The errors introduced with the correction of the signal are smaller than 5% to 10% for the particle backscatter coefficient and the linear particle depolarization ratio. The overall uncertainty of the linear particle depolarization ratio, including the calibration, correction, statistical and systematic errors is 25%.

This work presents the first results on profiles of δ_P measured during nighttime at Évora, in 2011 and 2012, during Saharan dust outbreaks. Up to now more than 30 profiles are included, which were obtained during different episodes and during different days within the same episode, in order to gain a general overview on the average depolarizing properties of the Saharan dust which is regularly transported towards the Iberian Peninsula. These "average features" shown in the figure above indicate that: i) the dust particles are usually transported at altitudes up to about 5 km and ii) the dust particles are often found away from the lower atmospheric layers or they mix with the polluted aerosols produced near the surface.
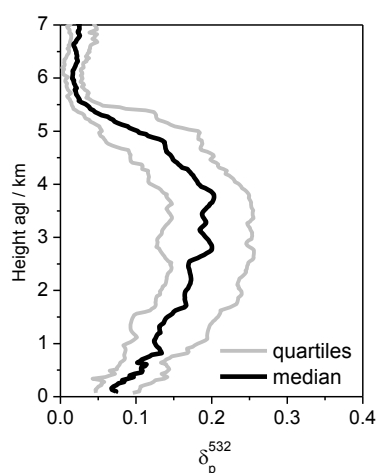
RETRIEVAL OF FINE AND COARSE MODE AEROSOL VOLUME CONCENTRATIONS FROM COMBINATION OF LIDAR AND SUN-PHOTOMETER MEASUREMENTS OVER THE ÉVORA AND GRANADA EARLINET/AERONET STATIONS

V.M.S.CARRASCO[1], M. MELGÃO[1], S.N. PEREIRA[1,2], J.L. GUERRERO- RASCADO[1,2,3], M.J. GRANADOS-MUÑOS[2,3], A.M. SILVA[1]

[1] *Évora Geophysics Center, Rua Romão Ramalho, 59, 7000 Évora, Portugal,*
victorm.sanzc@gmail.com

[2] *Andalusian Institute for Earth System Research (IISTA - CEAMA), University of Granada, Av. del Mediterráneo, s/n, 18006, Granada, Spain*

[3] *Dpt. Applied Physics, University of Granada, Fuentenueva s/n, 18071, Granada, Spain*

One of the recent approaches for improving the understanding of the aerosols effects on climate, based on ground-based observations, consists in the combination of active and passive remote sensing techniques, namely lidar and sun-photometer. The Lidar/Radiometer Inversion Code (LIRIC) combines the multiwavelength lidar with sun/sky photometry for the retrieval of particle microphysical properties separately for fine- and coarse-mode particles (Chaikovsky et al. 2008) and also particle optical properties. LIRIC uses profiles of backscattered lidar signals at 355, 532 and 1064 nm and AERONET photometer retrieval products (column-integrated particle size distribution, complex refractive index and other radiative properties). From them, a height-resolved dataset of microphysical and optical properties is created which is in agreement with the respective column-integrated sun-photometer observations. After an exhaustive evaluation (Wagner et al., 2013; Granados-Muñoz et al., accepted), a set of case studies with different aerosol types (namely anthropogenic pollution layers, forest fires smoke and desert dust) observed during 2011 and 2012 are presented which were observed over the EARLINET/AERONET southern Iberian stations of Évora (Portugal) and Granada (Spain).

References

Chaikovsky, A., Dubovik, O., Goloub, P., Balashevich, N., Lopatsin, A., Karol, Y., Denisov, S. and Lapyonok, T.: Software package for the retrieval of aerosol microphysical properties in the vertical column using combined lidar/photometer data (test version), Tech. rep., Institute of Physics, National Academy of Sciences of Belarus, Minsk, Belarus, 2008.

Granados-Muñoz, M. J., Guerrero-Rascado, J. L., Bravo-Aranda, J. A., Navas-Guzmán, F., Valenzuela , A., Lyamani, H., Chaikovsky, A., Wandinger, U., Ansmann, A., Dubovik, O., Grudo, J. and Alados-Arboledas, L.: Retrieving aerosol microphysical properties by LIdar-Radiometer Inversion Code (LIRIC) for different aerosol types, J. Geophys. Res., accepted.

Wagner, J., Ansmann, A., Wandinger, U., Seifert, P., Tesche, M., Chaikovsky, A. and Dubovik, O.: Evaluation of the Lidar/Radiometer Inversion Code (LIRIC) to determine microphysical properties of volcanic and desert dust. Atmos. Meas. Tech., 6, 1707-1724, 2013.

Acknowledgements

ON THE INSTRUMENTAL CHARACTERIZATION OF LIDAR SYSTEMS IN THE FRAMEWORK OF LALINET: SÃO PAULO LIDAR STATION

J. L. GUERRERO-RASCADO[1,2], F. J. S. LOPES[3,4], R. F. DA COSTA[4], M. J. GRANADOS-MUÑOZ[1,2], A. E. BEDOYA[5], E. LANDULFO[4]

[1]*Andalusian Institute for Earth System Research (IISTA-CEAMA), Av. del Mediterráneo, 18006, Granada, Spain, rascado@ugr.es*

[2]*Dpt. Applied Physics, University of Granada, Fuentenueva s/n, 18071, Granada, Spain*

[3]*Universidade de São Paulo, Instituto de Astronomia, Geofísica e Ciências Atmosféricas, Rua do Matão, 1226, Cidade Universitária, CEP 05508-000, São Paulo, Brazil*

[4]*Centro de Lasers e Aplicações, Instituto de Pesquisas Energéticas e Nucleares (IPEN), Avd. Prof. Lineu Prestes 2242, 05508-000, São Paulo, Brazil*

[5] *Dpt.de Físca , Universidad Nacional de Colombia- Sede Medellín, Calle 59ª Nº 63-20, Medellín, Colombia*

The Latin America Lidar Network (LALINET, http://lalinet.org) is a Latin American coordinated lidar network, established in 2001, focused on the measurement particle backscatter and extinction profiles for climatological studies of the particle distribution over Latin America, as well as other atmospheric species such as ozone and water vapor. This federative lidar network aims to establish, on voluntary basis, a consistent and statistically relevant database to enhance the understanding of the particle distribution over the continent and its direct and indirect influence on climate. The network presently consists of 9 stations with 11 lidars distributed over South America (from Cuba to Argentina and from Chile to Brazil). The construction of an un-biased spatiotemporal database of vertical profiles of particle optical properties on continental scale requires the use of a throughout characterization, as much as possible, of their non-standardized instruments to perform high quality research. Therefore, the instrumental quality of the lidar systems in LALINET must be tested. For this aim, the present work aims to be illustrative for the evaluation of the technical quality of LALINET through the analysis and characterization of the optical subsystem (optics, filters, and sensors) for the multichannel lidars at the São Paulo LALINET station. This task has been accomplished by means of several tools. On one hand, the telecover test compares lidar signals by using different parts of the receiver telescope, and allows the characterization of the lidar performance in the near height range. On the other hand, the Rayleigh fit (molecular fit) is a test to estimate the quality of lidar signals in the far height range, by comparing the experimentally measured lidar signal with the expected molecular signal at this height range. In addition, dark current test characterizes electronic noise and zero-bin calibration detects delays between the laser shots and real detection of signals. By means of this study, it is expected to increase the technical knowledge of the LALINET community and to go a step further in its consolidation as an operative lidar network.

ESTIMATING FINE PM CONCENTRATIONS AT URBAN SCALE BY IMAGE ANALYSIS BASED ON EFFECTIVE BANDWIDTH MEASURE

YAEL ETZION[1], BARAK FISHBAIN[1], DAVID BRODAY[1]

[1]*The Division of Environmental Water and Agricultural Engineering, Technion- IIT,*
Technion City 32000
Haifa, Israel, eyael@tx.technion.ac.il

Size and concentration of airborne particulate matter (PM) are important indicators of air pollution events and public health risks. However, the important efforts of monitoring size resolved PM concentrations in ambient air are hindered by the highly dynamic spatiotemporal variations of the PM concentrations. Satellite remote sensing is a common approach for gathering spatiotemporal data regarding aerosol events but its current spatial resolution is limited to a large grid that does not fit high varying urban areas. Moreover, satellite-borne remote sensing has limited revisit periods and it measures along vertical atmospheric columns. Thus, linking satellite-borne aerosol products to ground PM measurements is extremely challenging. In the last two decades visibility analysis is used by the US Environmental Protection Agency (US-EPA) to obtain quantitative representation of air quality in rural areas by horizontal imaging. However, significantly fewer efforts have been given to utilize the acquired scene characteristics (color, contrast, etc.) for quantitative parametric modeling of PM concentrations. We suggest utilizing quantitative measures of image characteristics, mainly related to contrast, for predicting PM concentrations. In particular, we examined an innovative measure, called image effective bandwidth (IEB) that tallies the image blurriness. The method was validated by assembling and analyzing a large dataset of time-series imaging of a selected urban scene, as well as PM concentrations and meteorological data (wind direction and velocity, relative humidity, etc.) that were simultaneously measured from air quality monitoring stations located in the imaged scene and its neighborhood, i.e., the study area. Quantitative and qualitative statistical evaluation of the suggested method shows that dynamic changes of PM concentrations can be inferred from the acquired images.

CAPTURE OF CHARGED AEROSOLS BY A REPELLING PLATE IN A BIPOLAR ELECTROSPRAY CONFIGURATION

JOSE L. CASTILLO, SANTIAGO MARTIN, BEATRIZ MARTINEZ-VAZQUEZ, PEDRO L. GARCIA-YBARRA

Dept. Fisica Matematica y de Fluidos, Facultad de Ciencias, UNED, Paseo Senda del Rey 9, 28040 Madrid, Spain, jcastillo@ccia.uned.es

The bipolar electrospray configuration consists of an electrically conducting liquid pumped at a constant flow rate through a needle maintained at a constant voltage with a collecting plate located perpendicular to the needle and kept at a different voltage. A proper choice of needle voltage and plate voltage allows extending the domain of liquid flow rates leading to the electrospray working in the stable cone-jet configuration [1].

The cone-jet mode is achieved even when an adverse voltage drop is imposed between the needle and the plate (with the surroundings kept grounded). Then, the charged aerosols emitted by the electrospray encounter a repelling electrical field near the plate. But still under these circumstances, some charges are collected by diffusion on the plate. In this experimental work the ratio of charges arriving to the collector with respect to the charges emitted at the needle is measured as a function of the experimental controlling parameters (voltages and flow rate).

This diffusion leakage of charged particles against a repelling mean field is compared with previous theoretical predictions [2, 3].

References:

[1] Martin, S., Perea, A., Garcia-Ybarra, P. L. & Castillo, J. L. (2012) *J. Aerosol Sci.*, **46**, 53-65.

[2] Garcia-Ybarra, P.L. & Castillo, J.L. (1997) *J. Fluid Mechanics*, **336**, 379-409

[3] Castillo J.L.; Rodríguez-Pérez, D.; Martín, S.; Perea, A. & García-Ybarra, P.L (2010), in *Mathematics in Industry*, vol **15**: *Progress in Industrial Mathematics at ECMI 2008*. Fitt, A.D.; Norbury, J.; Ockendon, H.; Wilson, E. (Editors). Springer-Verlag (Berlin).

EVALUATION OF LOW-COST FINE PM SENSORS FOR USE IN A DENSE MONITORING GRID

YAEL ETZION[1], ILAN LEVY[1], BARAK FISHBAIN[1], DAVID BRODAY[1]

[1]The Division of Environmental Water and Agricultural Engineering, Technion- IIT,
Technion City 32000
Haifa, Israel, eyael@tx.technion.ac.il

Exposure to particulate matter (PM), especially its fine fraction, was found to be associated with adverse health effects in humans, such as respiratory and cardiovascular diseases, and therefore it is an important measure of both air quality and health risks. To date, measurements of PM levels in urban areas are conducted at air quality monitoring stations by bench-mark instrumentation that is too expensive and bulky to deploy at high density. As a result, urban areas are typically monitored only at sparse locations. Yet, multiple and dynamic sources of urban emissions result in spatio-temporal variability of PM concentrations and large uncertainties, even in a neighborhood scale.

Here we evaluated a complementary approach that is based on low-cost sensors, which are less accurate but can be deployed in large numbers over relatively small areas. Two brands of such particle counters (Dylos DC 1700 and MetOne 804) were applied to measure number concentrations of fine particles in the 0.5-2.5 µm size range. Initial evaluation of these units found inter-unit consistency, and a good fit to particle counts by a high-end aerosol spectrometer (DMT's PCASP-X2). Setting the low-cost units at different locations within a residential neighborhood demonstrated their ability to detect local anthropogenic emissions, including traffic related PM (Figure 1), in a neighborhood scale.
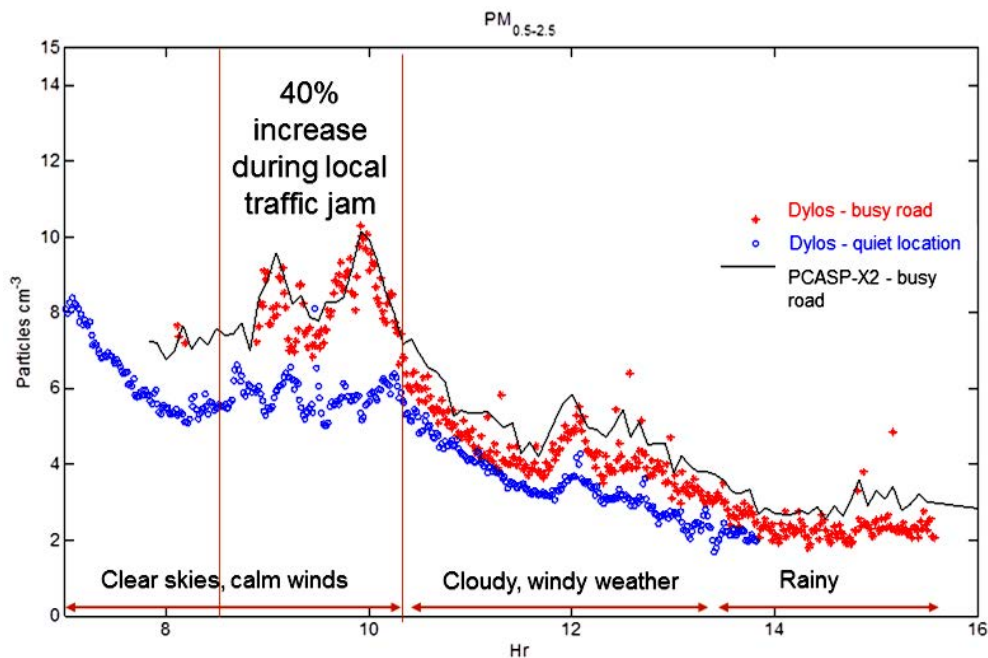

Figure 1 - Sensitivity to local traffic. When placed near a busy road at the center of the neighborhood, the low cost unit (red + marks) showed good agreement with a benchmark aerosol spectrometer (PCASP-X2, solid line) in responding to local traffic, and increased concentrations in comparison to a second low-cost unit, set at a quiet place, less than 1 km away.

SCALING OF LINEARLY ALIGNED ELECTROSPRAYS

NIKOLAS SOCHORAKIS[1], ESZTER BODNAR[1], JORDI GRIFOLL[1],
JOAN ROSELL-LLOMPART[1,2]

[1]*Chemical Engineering Department, Universitat Rovira i Virgili, Av. Països Catalans 26,
Tarragona, Spain, joan.rosell@urv.cat*
[2]*ICREA - Catalan Institution for Research and Advanced Studies, Passeig Lluís Companys 23
Barcelona, Spain*

We aim to develop robust geometries based on the stacking of one dimensional (1D) linear electrospray arrays. In 1D geometries the electric field lines easily focus onto the end of the electrospray injectors ("needles"), allowing electrospraying at moderate electric potentials without assistance from extractor electrodes. In addition, solvent vapor is easily removed from the spray area, a requirement for making particles by droplet drying.

Our contribution is a comprehensive study of how the spray plumes geometry and the stability of the Taylor cones scale as a function of the array geometry parameters. We investigate also system configurations that consider end electrodes and their effect on the expansion of the deposition spots. The use of end electrodes was suggested by Rulison and Flagan (1993) for 1D - arrays, and by Deng *et al.* (2006) for 2D arrays.

Figure 1(a-b) show example collections ('spots') of polymeric particles from 3- and 5-needle linear arrays with an inter-needle pitch of 5 mm. In going to 5 needles, the deposition spots compress strongly along the array direction, but not in the traverse direction. The spots also are smaller because of the 8 % higher electric potential needed for sustaining Taylor cone stability. In the 5-needle case, the separation between the central 3 spots is already close to the inter-needle pitch, namely the theoretical minimum spacing. A general view of the system with 3 sprays and 2 end electrodes is depicted in Figure 1(c). Figure 2 shows the effect of the number of needles and the number of end electrodes on the geometry of the spots.
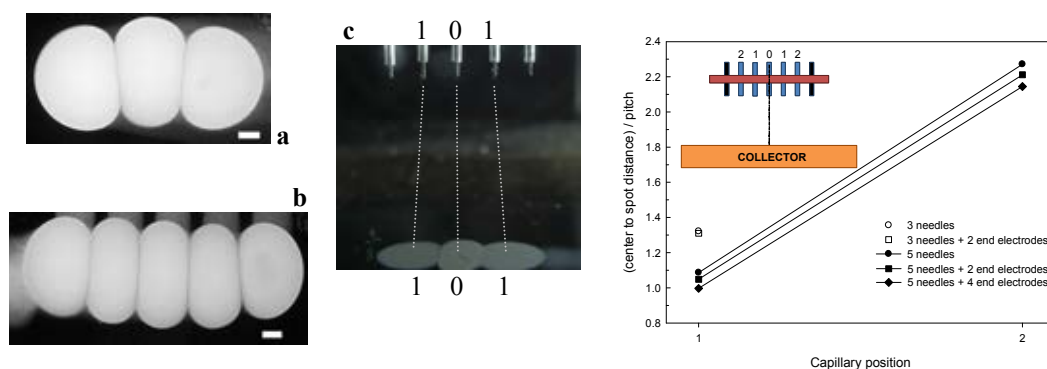
Figure 1. (a)-(b) Collected 'Spots' of ethyl cellulose particles from 3 and 5 needle arrays after a 3 min. collection. Scale bars are 2 mm long. (c) Spots produced by 3 functional needles + 2 end electrodes (in this case, non-spraying needles) and spot numbering.

Figure 2. Distance from the center-of-area of each collected spot to the center, normalized by inter-needle pitch, as a function of capillary position (inset), for different configurations of the linear array.

References

Deng, W., J. F. Klemic, X. Li, M. A. Reed and A. Gomez (2006). *J. Aerosol Sci.*, **37**, 696-714,
Rulison, A. J. and Flagan, R. C. (1993). *Rev. Sci. Instr.*, **64**, 683-686.

Airborne olive pollen Measurements are not representative of exposure to the major olive allergen Ole e 1

C. M. Antunes[1,4], C Gálan[2], R Ferro[3], C Torres[2], E Caeiro[1,3], H Garcia-Mozo[2], R Brandão[1], JMT Buters[5] & On behalf of the HIALINE working Group[6]

[1] ICAAM-Inst. Ciencias Agrarias e Ambientais Mediterranicas, Universidade de Evora, Évora, Portugal, ruibrand@uevora.pt

[2] Department of Botany,Ecology and Plant Physiology, University of Cordoba, Cordoba, Spain, bv1gasoc@uco.es

[3] Portuguese Society for Allergology Clinical Immunology, Lisbon, Portugal, aerobiologia@uevora.pt

[4] CNC - Centre for Neurosciences and Cell Biology, University of Coimbra, Portugal, cmma@uevora.pt

[5] Division of Environmental Dermatology and Allergology, Helmholtz Zentrum München/TUM, ZAUM - Center for Allergy and Environment, Technische Universität München, Munich, Germany, buters@lrz.tu-muenchen.de

[6] M. Thibaudon, France, M. Smith, Great Britain, C. Galan, Spain, R. Albertini, Italy, L. Grewling, Poland, G. Reese, Germany, A. Rantio-Lehtimäki, Finland, S. Jäger and U. Berger, Austria, M. Sofiev, Finland, I. Sauliene, Lithuania, L. Cecchi, Italy

Introduction Ole e 1 is the major allergen of olive pollen (*Olea europaea* L.), the second largest cause of pollinosis in some areas of the Mediterranean Region. Although it has been assumed that airborne pollen is a representative parameter for allergen exposure, variability of allergen content and/or release from pollen has been demonstrated for other taxa. The aim of this study was to: i) estimate the correlation between daily airborne olive pollen and Ole e 1 in ambient air; ii) evaluate the annual and geographical variation of pollen and allergenic loads in southwest Iberian Peninsula; iii) evaluate the contribution of meteorological parameters to ambient Ole e 1 loads variations.

Methods Airborne Ole e 1 and olive pollen were assessed simultaneously in Cordoba, Spain and Evora, Portugal. Aeroallergens were collected in 2009-2011 using prewashed polyurethane foam as impacting substrate (Rupprecht& PatashnickChemVol®2400 high-volume cascade impactor, Albany, NY, USA). Flow was adjusted to 800 L/min with a rotameter controlled high-volume pump (DigitelDHM-60, Ludesch, Austria). After extraction, Ole e 1 was quantified by ELISA. Airborne Olea pollen was monitored with a Burkard Hirst-type Seven-Day Recording Volumetric SporeTrap®. Both samplers were placed side-by-side with the air input at the same level.

Results Pollen and allergen profiles: In all the cases allergen followed the pollen profile but pollen counts were not representative for allergen loads; the same pollen counts yielded different amounts of allergen. Allergen and Pollen loads**:** The allergen and pollen loads presented geographical and annual variation, with considerably higher levels in Spain. Pollen potency (allergen/pollen): The mean allergen release per pollen grain presented geographical and annual variation; the latter was particularly important in Portugal. Rain and annual pollen potency: **c**ummulative precipitation (P, mm) previously to the pollen season are correlated with higher pollen potency, particularly in March or April.

Conclusion These results have shown that Ole e 1 is mostly associated with olive pollen grains but aeroallergen load was not always directly proportional to airborne pollen counts. This suggests that Ole e 1 quantification is a better marker for olive allergen exposure. In conclusion, aeroallergen monitoring may contribute to a better understanding of the Ole e 1 exposure from airborne pollen.

ASSESSMENT OF MICROBIOLOGICAL AIR QUALITY IN OFFICE ROOM AFTER WATER DAMAGE – A CASE STUDY

AGATA STOBNICKA, MARCIN CYPROWSKI, MAŁGORZATA GOŁOFIT-SZYMCZAK, ANNA ŁAWNICZEK-WAŁCZYK, RAFAŁ GÓRNY

Biohazard Laboratory, Department of Chemical, Aerosol, and Biological Hazards, Central Institute for Labour Protection – National Research Institute, Warsaw, POLAND, agsto@ciop.pl

INTRODUCTION: One of the most frequent causes of water damage in offices is malfunction of air conditioning units. In old office buildings, wet wooden floor, often covered with carpet lining, relatively quick creates excellent conditions for growth of microorganisms. The aim of the study was to assess the level of microbial contamination in indoor air due to a massive leakage of the air conditioning unit and some corrective measures taken after such water damage.

MATERIALS AND METHODS: The measurements were carried out in multi-storey office building before and after replacement of flooded floor surface material (wood to concrete, both with carpet lining). The bioaerosol sampling was carried out using MAS-100 NT impactor. The flow rate and sampling time were 100 L/min and 1 min, respectively. Standard Petri dishes filled with blood trypticase soy agar and malt extract agar were used for bacterial and fungal sampling, respectively. The bioaerosol measurements were done at height of 1.5 m above the ground level to simulate aspiration from the human breathing zone. All microorganisms isolated from the air were qualitatively analyzed to genus and/or species level.

RESULTS: The average concentrations of bacterial and fungal aerosols after failure of air conditioning unit were 70 and 715 CFU/m^3, respectively. Qualitative analysis revealed that the most prevalent microbial species in the air microbiota were filamentous fungi (91%; represented by four genera *Aspergillus fumigatus*, *Aspergillus terreus*, *Penicillium crustosum* and *Trichoderma viride*) followed by Gram-positive bacteria (9%; mainly *Staphylococcus epidermidis*, *Micrococcus* spp. and *Bacillus* spp.). The mean concentrations of bacteria and fungi in the air after introduction of corrective measures (floor surface material replacement) were equal to 50 and 80 CFU/m^3, respectively. Qualitative evaluation of air samples revealed that the percentage of filamentous fungi in total identified microbiota significantly decreased (up to 62%) and a growth of the most toxigenic fungi was suppressed.

CONCLUSIONS: The results of this study confirmed that a full elimination of microbial contamination source (such as floor surface material replacement) can effectively protect health of office workers.

ASSESSMENT OF RELEASE FROM NEW MATERIALS WITH NANOSTRUCTURED ADDITIONS IN THE CASE OF ACCIDENTAL FIRE IN THE BUILDING SECTOR

CELINA VAQUERO[1], NEKANE GALARZA[1], AITOR BARRIO[1], SARA VILLANUEVA[1], JESÚS M. LÓPEZ DE IPIÑA[1], GAIZKA ARAGÓN[2], IÑAKI MUGICA[2], MIREN LARRION[2], CRISTINA GUTIERREZ-CAÑAS[2], BEN HARGREAVES[3], GARY POYNTON[3].

[1]TECNALIA. PTA- Miñano (Álava), Spain(01510). celina.vaquero@tecnalia.com

[2]Department of Chemical and Environmental Engineering, University of the Basque Country (UPV/EHU), Alameda Urquijo s/n, 48013, Bilbao, Spain

[3]NetComposites Ltd. 4A Broom Business Park Bridge Way Chesterfield S41 9QG (United Kingdom)

New products based on nanotechnology are currently being incorporated in the construction sector to achieve materials with improved performance as de-pollutants, fire retardants or insulations. However concerns about potential effects on health still remain that should be investigated to assure the acceptance of manufactured nano-materials (MNM's) in the sector. This work focuses on the analysis of aerosols released from the combustion of these new materials. It has been done in the frame of SCAFFOLD project (nº 280535), which aims to manage the potential risks arising from the use of MNM's in the construction sector.

The experimental method consists of the comparison of aerosols released from glass fibre reinforced polyester composites filled and not filled with nano-clay. The set-up was developed to on-line measure the number concentration and size distribution of aerosols produced in a cone calorimeter that works according to ISO-5660-1 (2002) standard, similar to the work of Mortzkus (2012). A CPC and ELPI are coupled in the system to analyze the particles released from the samples. Figure 1 shows preliminary results achieved during the combustion of a control sample and one filled with nano-clay. Data suggest that the release of particles is different for both materials attributable to different combustion mechanisms. However, SEM analysis of samples showed no evidence of nano-clays in the released aerosols.

Work is currently ongoing and it is expected that the results may give new insights related to the composition of smoke produced by the combustion of new MNM's, which may have implications for potential effects on health in case of accidental fires.

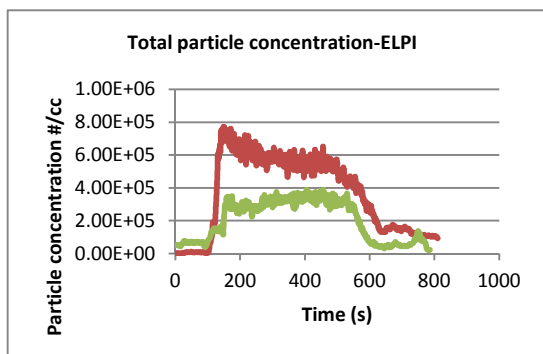Figure 1. Total particle concentration during the combustion of composite control (green) and composite filled with organoclay (red).

ISO-5660-1 (2002) Reaction-to-fire tests -- Heat release, smoke production and mass loss rate -- Part 1: Heat release rate (cone calorimeter method)

Motzkus et al (2012).Aerosols emitted by the combustion of polymers containing nanoparticles. J Nanopart Res (2012) 14:687

CHARACTERISTICS OF INDOOR AEROSOL SIZE DISTRIBUTION IN A GYMNASIUM

AMAYA CASTRO[1], ANA CALVO[1], CÉLIA ALVES[2], LILIANA MARQUES[2],
TERESA NUNES[2], ELISABETH ALONSO-BLANCO[3], ROBERTO FRAILE[1],

[1]*Department of Physics, IMARENAB University of León, 24071 León, Spain, acasi@unileon.es*

[2]*Centre of Environmental and Marine Studies, Department* of Environment,
University of Aveiro, *3810-193 Aveiro, Portugal,*

[3]*Centro de Investigaciones Energéticas, Tecnológicas y Ambientales (CIEMAT), 28040 Madrid, Spain*

The significance of indoor air quality (IAQ) has been recognised in recent years due to its impact on public health. In modern societies people spend about 90% of their time indoors. IAQ in recreation facilities is of special interest as the amounts of pollutants drawn into the lungs increase proportionally with increasing ventilation rates. Furthermore, the air is inhaled through the mouth, bypassing the normal nasal mechanisms for filtration of particles.

In this study, an indoor/outdoor monitoring programme was carried out in a gymnasium belonging to the University of Leon (Spain). The 0.1-10 μm latex particle size spectra were measured in 31 discrete channels (size ranges) using a laser spectrometer probe (Passive Cavity Aerosol Spectrometer Probe, PMS Model PCASP-X). The air quality of the gymnasium was strongly influenced by the use of magnesia alba ($MgCO_3$). For this reason, aerosol size distributions under several conditions were studied: i) without sports activity, ii) activity without using magnesia alba, iii) activity using magnesia alba, iv) cleaning activities and v) outdoors. Using the aerosol size composition, the aerosol refractive index and density, outdoors and indoors, were estimated. The values obtained were: 1.549- 0.025i and 1.577-0.003i, and 1.940 and 2.055 g/cm^3 for outdoors and indoors, respectively. Using the estimated density, the mass concentration was calculated, and the evolution of PM_1, $PM_{2.5}$ and PM_{10} was assessed.

As particle size determines its deposition site and fraction in human lungs and its potential translocation to other target organs, a study was conducted according to the Spanish standard UNE 77213, equivalent to the ISO 7708:1995, about aerosol size fractions associated with health problems. First, it was assessed the inhalable and thoracic fractions and, then, the tracheobronchial and respirable fractions for healthy adults and high risk people (children, frail or elderly people).

FLY-ASH EMISSIONS CONTROL EFFICIENCY AND HEAVY METALS PARTICLE SIZE DISTRIBUTION IN AN APPLICATION OF A HYBRID FILTER TO BIOMASS-WASTE CO-FIRING FLUE GAS

GAIZKA ARAGON[2], DAVID SANZ[1], ENRIQUE ROJAS[1], JESUS RODRIGUEZ-MAROTO[1], RAQUEL RAMOS[3], RICARDO ESCALADA[3], ELENA BORJABAD[3], MIREN LARRION[2], IÑAKI MUJICA[2], CRISTINA GUTIERREZ-CAÑAS[2]

[1]*Grupo de Emisiones Industriales Contaminantes, CIEMAT, Avda. Complutense 40 28040 Madrid, España, david.sanz@ciemat.es*

[2]*Dpto. De Ing. Quim. y del Medio Ambiente, Universidad del País Vasco, Alda. de Urquijo s/n 48013 Bilbao, España, garagon001@ikasle.ehu.es*

[3]*Unidad de Procesos de Conversión Térmica, CEDER-CIEMAT, Autovía A-15, salida 56 42290 Cubo de la Solana, España, raquel.ramos@ciemat.es*

Control of emissions of heavy metals is a necessary requirement for waste-to-energy applications through combustion either with or without co-firing. Even in pure biomass combustion, emissions of certain heavy metals may pose a so far unnoticed or underestimated risk. It is important to consider that agricultural waste from crops such as olives or vines, that may contain high concentrations of copper from phytosanitary treatments, are among the most important sources of biomass in Spain.

Hybrid filters (HF) (combination of electrostatic precipitator and fabric filter) applied to the control of emissions of particulate matter (PM) present more robust performance under varying operating conditions, and increased efficiency in the control of PM emissions in the particle size range where a greater enrichment in heavy metals is expected.

This paper investigates the fractional penetration of different metals of interest, under different operating conditions, through a semi-industrial scale HF applied to the control of emissions from co-combustion of biomass and wastes. Heavy metals size distribution in fly-ash was determined. Results regarding the overall effectiveness for the control of PM and heavy metals enrichment in different fractions of fly-ash collected in the HF are also presented.

Depending on operating conditions, an average efficiency of 96.85 to 99.41% in terms of total mass concentration of PM was found. Some of the corresponding values for heavy metals were 79.17-98.57%, in the case of Pb, and 93.63-99.27% , in the case of Cu, in the solid phase; note that some elements may be also present in vapor phase depending on volatility.

A preferential enrichment in Cl, Na, K, Cd, and Pb was found in the fly-ash collected in the fabric filter module, showing Pb and Cd even higher enrichment than Na. Copper was found preferably in the submicron fraction of the raw fly-ash, being able the HF to produce a depurated emission without preferential size enrichment in Cu.

The HF ability to efficiently control emissions of both overall PM, and heavy metals fraction in particular has been demonstrated within a wide range of load and different fuels. The preferential occurrence of some heavy metals in the ultrafine fraction of fly-ash has been detected, which makes clear the need of effective control systems for PM in that size range.

Health Impact of Airborne aLlergen Information NEtwork (HIALINE PROJECT): Ambient loads of pollen and the major allergens from birch, grass and olive in Europe

J.T.M. Buters[1], R. Brandao[2], C. Antunes[3] and the HIALINE working group[4]

[1] Division of Environmental Dermatology and Allergology, Helmholtz Zentrum München/TUM, ZAUM - Center for Allergy and Environment, Technische Universität München, Munich, Germany, buters@lrz.tu-muenchen.de

[2] ICAAM-Inst. Ciencias Agrarias e Ambientais Mediterranicas, Universidade de Evora, Évora, Portugal, ruibrand@uevora.pt

[3] CNC - Centre for Neurosciences and Cell Biology, University of Coimbra, Portugal, cmma@uevora.pt

[4] M. Thibaudon, France, M. Smith, Great Britain, C. Galan, Spain, R. Albertini, Italy, L. Grewling, Poland, G. Reese, Germany, A. Rantio-Lehtimäki, Finland, S. Jäger and U. Berger, Austria, M. Sofiev, Finland, I. Sauliene, Lithuania, L. Cecchi, Italy

Introduction Aeroallergen triggered allergic diseases are among the most prevalent chronic diseases in Europe and its prevalence have been steadily increasing during past decades. Exposure to allergens is one of several factors determining sensitization and allergic symptoms. A difference in aeroallergen exposure in a changing environment, due to climate diversity and/or climate changes, may certainly be one factor contributing to this increase in prevalence. However, allergen loads in the air have for long remained elusive.

The HIALINE consortium was a multidisciplinary group of experts from research groups in Europe. The main purpose of HIALINE was to assess factors that influence the allergen exposure of European citizens in order to improve forecasting both for the patient and for health care demands. It was intended to: i) Monitor pollen in ambient air; ii) Measure allergen load in ambient air; iii) Assess the pollen and allergen distribution and thus the allergen potency of airborne pollen across Europe; iv) Integrate multi-taxa modelling and forecasting system for pollen and allergens.

Methods Ambient air was sampled at 800L/min with a Chemvol high-volume cascade impactor equipped with stages PM>10µm, 10 µm>PM>2.5µm. The allergens Bet v 1 from birch, grass group 5 and Ole e 1 from olive were determined with allergen specific ELISA´s. Pollen loads were assessed with a Burkard pollen traps. The System for Integrated modeLling of Atmospheric coMposition (SILAM) was used to compute the origin of the collected airborne particles, including pollen.

Results During the three studied years the allergen and pollen profiles overlapped for birch, grasses and olive, although the loads were variable. The allergens were distributed among the PM>10 µm (≈90%) and the 10 µm>PM>2.5µm (≈10%) fractions. The allergen/pollen varied annually up to 3 fold and between sites in the intervals 2-3 pg/grain, <2-4 pg/grain and <1-4 pg/grain for birch, grasses and olive, respectively. Thus, pollen counts do not represent allergen loads in the air.

Conclusion HIALINE achieved the implementation and standardization of allergen monitoring methodology across Europe. In addition, a forecast has been successfully achieved for birch, olive and grass pollen.

Moreover, within his project both geographical and temporal variations of allergen/pollen ratio were found. Pollen counts are not representative of the allergen load in the air, thus failing to be an accurate marker for allergen exposure.

VOLATILE AND NON-VOLATILE PM CHARACTERIZATION FROM THE TURBOFAN ENGINE EXHAUST

VÍCTOR ARCHILLA-PRAT[1*], JESÚS RODRIGUEZ-MAROTO[2], ENRIQUE ROJAS[2], DAVID SANZ[2], MIGUEL IZQUIERDO[1], MANUEL PUJADAS[2] , RICARDO DIAZ[3]

[1]*Turbojet Engine Test Centre, INTA, Ctra. Torrejón-Ajalvir
Torrejón de Ardoz, Spain, e-mail address: archillapv@inta.es*

[2]*Department of Environment, Industrial Emission Group, CIEMAT, Avda. Complutense 40
Madrid, Spain, e-mail: jesus.maroto@ciemat.es*

[3]*Higher Polytechnic School, University San Pablo CEU, Madrid*

The global effects of aircraft Particulate Matter (PM) emissions are a major concern for human health and climate change. Controls on aircraft emissions and maintaining compliance for local air quality standards on European airports is expected to be an issue). It is demanded a nvPM emissions database for aircraft turbine engines which include mass and number-based emission indices, size distribution and chemical speciation data. It is also requested to relate the PM emissions to key engine parameters, LTO cycle operation and fuel characteristics. The majority of the available data set coming from commercial aircraft engines do not include a full characterization of volatile or non-volatile components resulting from atmospheric cooling and dilution effects

INTA Turbojet Engine Test Cell in collaboration with CIEMAT have designed a system's configuration combining an Electrical Low Pressure Impactor ELPI+ (Dekati), CPC (TSI) and a SMPS (TSI) to measure the emission of PM to atmosphere during aircraft engine testing cycles. Particle concentration in mass and number, aerodynamic and mobility size distributions have been measure in real time. The particle emissions have been sampled through a heated probe located in the stack at 40 meters far from the jet engine exhaust. Therefore the methodology used applies both to volatiles and non-volatiles compounds.

Nowadays not only mass distribution measurement is important, but number size distribution as well. Ultra-fine aerosol particles are potential hazard to human health, as their small sizes allow them to reach any part of the human lungs. A detailed study of the aerosol has been done according to the particle's aerodynamic size. The method proposed in this paper allows the control of the aircraft aerosol emissions not only like a result of a total number concentration but according to number concentration for a particular aerodynamic size.

AEROSOL DEPOSITION IN BALEARIC ISLANDS AS OVERLOOK OF THE DEPOSITION IN THE WESTERN MEDITERRANEAN

J. C. CERRO[1], S. CABALLERO[2], C. BUJOSA[3], A. ALASTUEY[4], X. QUEROL[4], J. PEY[4,5]

[1]*Laboratory of Environmental Analytical Chemistry , Illes Balears University, Ctra. Palma-Valldemossa, Km 7.2, 07008, Palma de Mallorca, Spain, jccerro@dgqal.caib.es*

[2]*Atmospheric Pollution Laboratory, Miguel Hernández University, Av.de la Universidad s/n, 03202 Elche, Spain, san.cab@umh.es*

[3]*ENDESA c/ Sant Joan de Déu 1, 07007, Palma de Mallorca, Spain, carles.bujosa@endesa.es*

[4]*Institute of Environmental Assessment and Water Research, IDÆA-CSIC, C/ Jordi Girona 18-26, 08034, Barcelona, Spain, andres.alastuey@idaea.csic.es , xavier.querol@idaea.csic.es*

[5]*Laboratory of Environmental Chemistry LCE-IRA, Aix Marseille University, 3 Place Victor Hugo,13001 Marseille, France, jorge.pey@univ-amu.fr*

Atmospheric deposition, as the last stage of the aerosol cycle, brings nutrients and pollutants to earth and sea surfaces. The quantification of deposition fluxes, their chemical characterization and the knowledge about the sources becomes necessary when analyzing different ecosystem responses.

In the context of the ChArMEx (The Chemistry-Aerosol Mediterranean Experiment, https://charmex.lsce.ipsl.fr) initiative, a 2-year study on wet and dry deposition of atmospheric aerosols has been conducted at a regional background environment in Mallorca (Balearic Islands, western Mediterranean). From September 2010 to August 2012 weekly dry and wet deposition samples were collected. In addition, atmospheric particulate matter was regularly sampled in both PM10 and PM1 fractions, as well as gaseous pollutants and meteorological parameters were continuously registered.

Deposition samples were subjected to different analytical procedures including quantification of deposition volumes and subsequent filtration on quartz fibre filters, determination of pH, and complete acidic digestion of filters. Solutions obtained were analysed by a number of techniques determining the concentrations of soluble and insoluble fractions of a number of species including typical mineral elements (Al, Ba, Ca, Mg, Mn, Sr, Ti), major marine components (Cl, Na, Mg), anthropogenic tracers (Cu, K, Mn, Ni, NO_3^-, NH_4^+, Pb, V, Zn), and some multiple-origin components such as SO_4^{2-}.

Episodic and seasonal patterns were assessed, and differences between wet and dry deposition, and their relation with specific scenarios were established.

Special attention has been paid to the deposition of phosphorous, nitrogen (as NH_4^+ and NO_3^-) and iron and their possible influence on the the sea Chlorophyll concentration, detected by different satellites (www.globcolour.info).

A preliminary source exploration by means of Principal Component Analysis has been done. Wet deposition samples exhibit three sources: crustal, marine and mixed-anthropogenic, whereas dry deposition samples split the anthropogenic source in three different components: a Cu-Zn-Fe, a K-Ni-Pb and a NO_3^--NH_4^+.

AMMONIA LEVELS IN DIFFERENT KINDS OF SAMPLING SITES IN THE CENTRAL IBERIAN PENINSULA

M.A. REVUELTA[1,2]*, B. ARTÍÑANO[1], F. J. GÓMEZ-MORENO[1], M. VIANA[3], C. RECHE[3], X. QUEROL[3], A.J. FERNÁNDEZ[1], J.L. MOSQUERA[1], L. NÚÑEZ[1], M. PUJADAS[1], A. HERRANZ[1], B. LÓPEZ[1], F. MOLERO[1], J.C. BEZARES[1], E. COZ[1], M. PALACIOS[1], M. SASTRE[1], J. M. FERNÁNDEZ[1], P. SALVADOR[1], B. ACEÑA[1]

[1]*Department of Environment, CIEMAT, Avda. Complutense 40, 28040, Madrid, Spain.*
*arevueltame@cofis.es

[2]*Currently at AEMET,C/Leonardo Prieto Castro 8, 28071 Madrid, Spain*

[3]*Institute for Environmental Assessment and Water Research (IDÆA-CSIC), Barcelona, Spain*

Ammonia (NH_3) is the secondary inorganic aerosol (SIA) gaseous precursor studied to a lesser extent in the Madrid Metropolitan Area up to date. Its main role in the formation of secondary particles raises the interest in its study. In the global scale, the main source of ambient ammonia is livestock waste, followed by vegetation and agriculture. However, the source contribution to ammonia in urban areas is not yet fully characterised.

A study conducted in the city of Madrid with the aim of characterizing levels of ammonia took place in 2011. A 10-11 days sampling was performed in two periods - winter and summer, and allowed to make a first estimation of the main contributing sources. Passive samplers were used, obtaining a measurement integrated over the exposure time period. Madrid campaigns formed part of a larger study conducted in 6 Spanish cities: Barcelona, A Coruña, Valencia, Huelva and Santa Cruz de Tenerife. The results obtained in Barcelona were presented by Reche et al (2012).

In the winter period, 64 samplers were deployed all over the Metropolitan Area of Madrid with the objective of identifying ammonia sources and also obtaining the highest possible spatial coverage. 29 samplers were placed in traffic sites, 28 in urban background sites, 6 close to sewage treatment plants and 1 close to a solid waste treatment plant. Some of the samplers had a duplicate separated around 10m to study the reproducibility of the procedure, taking into account shielding effects and the proximity to point sources (sewers). In the summer campaign the number of available passive samplers was smaller.

Ancillary data were used to complement the results obtained. A time series of weekly integrated ammonia measurements is available at a rural site in the Central Iberian Peninsula (Campisábalos). PM and gases data are routinely measured at 25 sites belonging to the Madrid Townhall Air Quality Network.

Sites close to sewage and solid waste treatment plants registered the highest concentrations. The traffic sites showed significant higher values than the urban background sites in both seasons. Traffic emissions could be related to catalytic converters, which have been proved to lead to outstanding reductions in NOx emissions, but also to generate gaseous ammonia, raising controversy on the use of these devices. No significant differences between winter and summer were registered for any kind of sampling site in the Madrid Township, in contrast with the summer maxima observed at the rural EMEP site most of the years. In winter the mean concentrations registered at the urban background sites were consistent with the monthly mean in March 2011 at Campisábalos, but in summer 2011 the mean NH_3 registered at the rural site was extremely low.

ANALYSIS OF AEROSOL AND CLOUD QUANTITIES OBTAINED FROM DIFFERENT PLATFORMS

M. J. COSTA[1,2], V. SALGUEIRO[1], D. SANTOS[1], A. M. SILVA[1] AND D. BORTOLI[1]

[1]*Évora Geophysics Centre, University of Évora, R. Romão Ramalho, 59, 7000 Évora, Portugal.*
mjcosta@uevora.pt

[2]*Department of Physics, University of Évora, R. Romão Ramalho, 59, 7000 Évora, Portugal.*
mjcosta@uevora.pt

Aerosols influence the global climate system through direct and indirect effects. Along with clouds, aerosols continue to be the main contributors to the large uncertainty of the Earth's energy budget, mainly due to the great variability of their amounts and properties in space and time. It is fundamental to monitor these amounts and properties in order to develop and improve conceptual and predictive global climate models.

Monitoring of aerosol and cloud quantities is nowadays attained from different instruments onboard satellites or installed at the surface. While ground-based measurements constitute an accurate way to monitor atmospheric parameters, global coverage with adequate spatial resolution may only be accomplished with satellite data.

A comparison between aerosol and cloud optical thickness obtained from satellite imagery and ground-based retrievals is presented for two Iberian AERONET sites, in order to check the accuracy of the satellite derived parameters in this area. Subsequently, a detailed analysis of their spatial and temporal variability is presented for Iberia, using some of the currently available satellite retrieval datasets (MODIS, MISR, OMI, etc), corresponding in some cases to more than twelve years of measurements. Other aerosol and cloud parameters (Ångström exponent, cloud effective radius, etc) are also discussed whenever available, in terms of space-time distribution over the same area.

.

ANALYSIS OF THE AEROSOL OPTICAL PROPERTIES AT A CONTINENTAL BACKGROUND SITE IN THE SOUTHERN PYRENEES (EL MONTSEC, 1574 M A.S.L.)

YOLANDA SOLA, ALBA LORENTE, JERÓNIMO LORENTE

[1]Departament d'Astronomia i Meteorologia,Universitat de Barcelona, Martí i Franquès 1
08028 Barcelona, Spain, ysola@am.ub.es

The aerosol optical properties derived from AERONET Cimel CE-318 sunphotometer in El Montsec (42° 3' N, 0° 43' E, 1574 m a.s.l.) have been analyzed. The instrument is measuring from 2011 but we have analyzed the quality-assured AERONET level 2.0 data with pre and post field calibration applied (May 2012-April 2013) in the framework of the Red Ibérica de Medida de Aerosoles (RIMA). The photometer has filters centered at 8 wavelengths (340, 380, 440, 500, 675, 870, 940, 1020 nm). Besides the Cimel photometer, the station includes measurements of mass particulate matter, black carbon and particle number concentrations from instruments of the Institute of Environmental Assessment and Water Research (IDAEA-CSIC). This high altitude station is located in a mountain range, distant from anthropogenic aerosol sources, both urban and industrial ones and most of the days out of the boundary layer. Previous studies from in-situ monitoring data have shown the importance of Saharan dust transport and new particle formation (Ripoll et al., 2013).
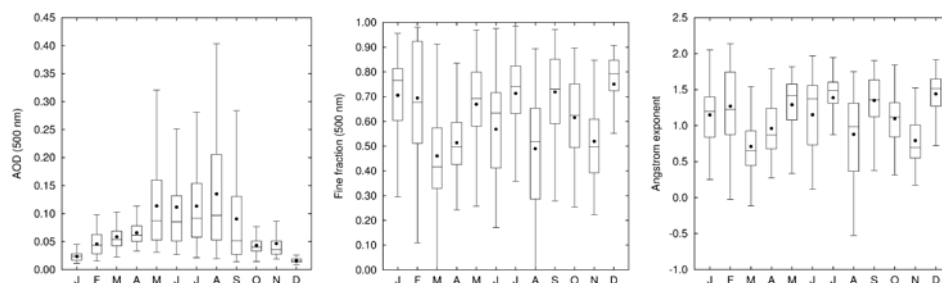

Figure 1: Monthly boxplots of the AOD at 500 nm (left panel), fine mode fraction (middle panel) and Angstrom exponent (right panel).

The lowest aerosol optical depth (AOD) are observed during winter months since the station is in the free troposphere most of the days, on the other hand larger variation range and values are detected in summer months (Figure 1). The fine-mode fraction dominates in winter due to the prevalence of Atlantic advections and its location in the free troposphere (Ripoll et al., 2013) but in summer months, the occurrence of Saharan dust outbreaks, the presence of regional aerosol and lower precipitations result in a reduction in the fine-mode fraction and an increase of the AOD. Even though it is not observed in the AOD, a decrease in the fine fraction and the Angstrom exponent is also observed in spring. Pey et al. (2013) related it with a peak in the occurrence of Saharan dust episodes.

Pey, J., Querol, X., Alastuey, A., Forastiere, F., and Stafoggia, M., Atmos. Chem. Phys., 13, 1395-1410, doi:10.5194/acp-13-1395-2013.

Ripoll, A., Pey, J., Minguillón, M.C., Pérez, N., Pandolfi, M., Querol, X., Alastuey, A., Atmos. Chem. Phys. Discuss., 13, 27201-27241, doi:10.5194/acpd-13-27201-2013.

ANALYSIS OF THE REPRESENTATIVENESS OF THE STATIONS OF A NETWORK. THE CASE OF THE XARXA AEROBIOLÒGICA DE CATALUNYA

JORDINA BELMONTE[1,2], JAVIER MATEOS[3], CONCEPCIÓN DE LINARES[1,2], ROSARIO DELGADO[3]

[1]*Institut de Ciència i Tecnologia Ambientals (ICTA), Universitat Autònoma de Barcelona, Edifici Z, 08193 Bellaterra, Spain, jordina.belmonte@uab.cat, concepcion.delinares@uab.cat*

[2]*Dept. de Biologia Animal, Biologia Vegetal i Ecologia, Universitat Autònoma de Barcelona, Edifici C, 08193 Bellaterra, Spain, jordina.belmonte@uab.cat, concepcion.delinares@uab.cat*

[3]*Dept. de Matemàtiques, Universitat Autònoma de Barcelona, Edifici C, 08193 Bellaterra, Spain, delgado@mat.uab.cat*

The aerobiological network of Catalonia (Xarxa Aerobiològica de Catalunya, XAC), operating since 1983, adopted the standardized sampling methods accorded at an international level in 1994. At present, the XAC comprises nine stations (Barcelona, Bellaterra, Girona, Tarragona, Lleida, Manresa, Planes de Son, Roquetes-Tortosa and Vielha) distributed throughout the territory. The criteria applied for the selection of the XAC sampling sites were to cover as much territory as possible taking into consideration the population concentrations, the different landscapes and environments with different urbanization degree.

After several years of monitoring, our database provides the possibility to statistically compare the pollen spectra and analyse the representativeness of the stations. The aim is to have scientific evidence for the best distribution of the sampling stations and to optimize the allocation of resources.

The annual pollen index of the 21 most representative pollen taxa of the six stations (Barcelona, Bellaterra, Girona, Tarragona, Lleida, Manresa) with data for the period 1996-2012 have been analysed. The methodology we use is based on the comparison between each of the stations and a fictitious one that aggregates all the stations but itself, on the basis of the *Annual Ratio Matrix* (ARM), which represents the percentage of each taxon with respect to the total given by the 21 taxa.

With the assistance of the R software (R Development Core Team 2007), we perform Spearman's Rho tests to measure API correlations of each taxon between each pair of stations. We also introduce the Malahanobis distance as a measure of the dissimilarity between stations, and conduct the Pearson's chisquared goodness of fit test by considering the 10 most common taxa and grouping the rest under the category "leftover". Finally, we confirm the results by using the Friedman test and the corresponding post-hoc multiple comparison tests.

Bellaterra resulted to be the more representative station both, when considering the whole set of 21 taxa and when considering the reduced set of the 10 most common taxa plus the leftover category grouping the rest. In contrast, Barcelona is the station that has resulted to be the more representative if we just consider the 11 taxa gathered in the leftover category.

ASSESSMENT OF BSC-DREAM8B MODEL USING LIRIC (LIDAR AND RADIOMETER INVERSION CODE)

J. L. GUERRERO-RASCADO[1,2], M. J. GRANADOS-MUÑOZ[1,2], J. A. BRAVO-ARANDA[1,2], S. BASART[3], J. M. BALDASANO[3], L. ALADOS-ARBOLEDAS[1,2]

[1]*Andalusian Institute for Earth System Research (IISTA-CEAMA), Av. del Mediterráneo, 18006, Granada, Spain, rascado@ugr.es*

[2]*Dpt. Applied Physics, University of Granada, Fuentenueva s/n, 18071, Granada, Spain*

[3]*Earth Sciences Department, Barcelona Supercomputing Center-Centro Nacional de Supercomputación, Barcelona, Spain*

Every year a large amount of mineral dust is transported from arid regions and injected into the atmosphere under specific weather conditions. The fact that mineral dust can produce a variety of problems to inhabitants both in and around desert areas (deaths and damage caused by traffic accidents, road disruption, aviation operations and impacts on human health, such us allergies, respiratory diseases and eye infections, among others) inspired the development of different dust forecast models as BSC-DREAM8b. Several approaches have been used to assess the columnar [Basart et al., 2012] and vertically-resolved [e.g. Guerrero-Rascado et al., 2009] performance of BSC-DREAM8b model using sunphotometric and lidar data, respectively. However, the available lidar data used (i.e. particle backscatter coefficient profiles) did not allow a quantitative evaluation up to now. Recently, the LIRIC software (lidar and radiometer inversion code) have been developed [Chaikovsky et al., 2008] and disseminated in the EARLINET community. After its exhaustive evaluation [Granados-Muñoz et al., 2014], a comparison with BSC-DREAM8b skills in terms of dust vertical distribution have been performed at Granada using LIRIC retrievals during an intensive period from June to August 2012 (246 profiles). The LIRIC vs. BSC-DREAM8b comparison has been done in terms of direct profiles (concentrations) and normalized profiles (shape), considering statistical parameters for the whole profile and each level. After a preliminary evaluation, it is found that the direct comparison mainly shows underestimations in the range 25-125 $\mu g/m^3$, slopes between 0 and 0.6, and only 55% cases with R>0.6. It is also found that BSC-DREAM8b better reproduces the vertical layering. After normalization, 48% of profiles show mean relative deviation $\pm$ 20% and slopes are closer to unity. BSC-DREAM8b better reproduces the profile shape between 2 and 4 km, and shows some limitations below 2 and very large differences > 4 km.

References:
Basart et al., Tellus B (2012)

Chaikovsky et al., Technical report, Institute of Physics, National Academy of Sciences of Belarus, Minsk, Belarus (2008)

Guerrero-Rascado et al., Atmos. Chem. Phys., doi:10.5194/acp-9-8453-2009 (2009)

Granados-Muñoz et al., J. Geophys. Res. (2014)

BUILDING, TUNE-UP AND FIRST MEASUREMENTS OF AEROSOL HYGROSCOPICITY WITH AN HTDMA

E. ALONSO-BLANCO[1*], F.J. GÓMEZ-MORENO[1], S. SJOGREN[2] AND B. ARTÍÑANO[1]

[1]*Department of Environment, Research Center for Energy, Environment and Technology (CIEMAT), Avda.Complutense 40, 28040, Madrid, Spain, *elisabeth.alonso@ciemat.es.*

[2]*University of Applied Sciences Northwestern Switzerland, Brugg-Windisch, Switzerland*

Changes of water absorption by atmospheric aerosols can lead to variations of both the direct (scattering and absorption of radiation that reaches and leaves the Earth´s atmosphere) and the indirect effect (associated with the modification of clouds' properties and coverage). Hygroscopicity therefore influences climate. Furthermore, for human health, the capacity of water absorption of the aerosol determines the modification of their deposition pattern within the respiratory tract. This defines how deep into the respiratory tract the aerosol enters.

Aiming at measuring hygroscopicity, a Hygroscopic Tandem Differential Mobility Analyzer (HTDMA) has been built and tuned up to allow us to know the size changes of the submicrometer aerosol in relation to the relative humidity (RH). This instrument consists of two custom-made Vienna-type Differential Mobility Analyzers (DMAs) connected in tandem with a humidification system in between (*Nilsson et al., 2009*). It allows measuring the growth factor between 10-98% RH. In the first DMA, a single aerosol size is selected, while the second DMA, connected to a Condensation Particle Counter (CPC) works as a traditional Scanning Mobility Particle Size (SMPS). In this way the growth factor distribution can be measured once the monodisperse aerosol has passed through the humidifier. This instrument has a temporal resolution of about 3 min for each measure. Both the instrument regulation and the data acquisition software were developed in LabVIEW code.

In this work, the tune-up and quality assurance procedures used are shown. To ensure the accuracy of the measurements, the different components of the H-TDMA have been calibrated, the pressure and flow mass sensors, on the one hand, and the high voltage sources, on the other. Next, the DMAs have also been calibrated with PSL spheres of two different sizes and furthermore the humidity/temperature sensors were validated with saline suspensions saturated to known RH.

The quality of the whole measurements has been validated through laboratory tests made with a polydisperse aerosol of pure ammonium sulphate. With its known efflorescence-deliquescence hysteresis cycle it allows us to ensure the reliability of the measured hygroscopicity.

The first measurements of the ambient atmospheric aerosol hygroscopicity with HTDMA in a suburban area in Madrid have been carried out during a short campaign. It allowed us to study the variation of the growth factor of atmospheric aerosol for aerosol sizes between 50 to 265 nm, at 90% RH, under different meteorological conditions.

References: Nilsson, E., Swietlicki, E., Sjogren, S., Löndahl, J., Nyman, M., Svenningsson, B., 2009. Development of an H-TDMA for long-term unattended measurement of the hygroscopic properties of atmospheric aerosol particles. Atmospheric Measurement Techniques 2, 313-318.

CHARACTERIZATION OF AFRICAN DUST SOURCE AREAS CONTRIBUTING TO AMBIENT AEROSOL LEVELS ACROSS THE WESTERN MEDITERRANEAN BASIN

P. SALVADOR[1], B. ARTÍÑANO[1], F.J. GÓMEZ-MORENO[1], S. ALONSO[2,3], J. PEY[2,4], A. ALASTUEY[2], X. QUEROL[2]

[1]Environmental Department, CIEMAT - Unidad Asociada en Contaminación Atmosférica CSIC-CIEMAT, Avenida Complutense 40, 28040 Madrid, Spain,
pedro.salvador@ciemat.es

[2]Institute of Environmental Assessment and Water Research, CSIC, Jordi Girona 18, 08034 Barcelona, Spain

[3]Centro de Investigación Atmosférica de Izaña, AEMET, C)La Marina 20,38071 Santa Cruz de Tenerife, Spain

[4]Aix-Marseille Université, CNRS, LCE FRE 3416, Marseille, 13331, France

The occurrence of African dust outbreaks over the western Mediterranean basin were identified on an 11-year period (2001-2011). PM10 daily data from nine regional background air quality monitoring sites across the study area were compiled and the net dust load transported during each event was estimated. Then, the potential source areas of mineral dust were identified by trajectory statistical methods (Stohl, 1998) for any year of the period of study. Our results indicate that the sources areas of African mineral dust strongly depended on the atmospheric circulation patterns prevailing during each of the years, which condition the intensity of the dust outbreaks and the areas affected by the transport and deposition of the mineral dust.

Stohl, A.: Computation, accuracy and applications of trajectories – a review and bibliography, Atmos. Environ., 32: 947-966, 1998

CHARACTERIZATION OF PMₓ DATA BELONGING TO THE DESERT-DUST-INVENTORY BASED ON AOD-ALPHA RIMA-AERONET DATA AT PALENCIA-AUTILLA STATIONS

V.E. CACHORRO[1], M.A. BURGOS[1], Y. BENNOUNA[1], C. TOLEDANO[1], B. TORRES[1], D. MATEOS[1], A. MARCOS[1], A.M. DE FRUTOS[1]

[1] *Grupo de Óptica Atmosférica (GOA-UVa), Departamento de Física Teórica, Atómica y Óptica, Universidad de Valladolid, Paseo de Belén,7, 47011, Valladolid, España, chiqui@goa.uva.es*

The study and characterization of the main features of PMx data recorded in the inventory of desert dust intrusions over northern-central Spain during the period 2003–2012 was carried out. The inventory was developed by taking the AOD-alpha data from sun-photometers measurements at the stations of Palencia and Autilla del Pino (province of Palencia) belonging to the RIMA-AERONET network. The detection and characterization of the desert dust episodes was based on a manual inspection of AOD-Alpha instantaneous data, although complementary information such as air masses back trajectories, MODIS images and synoptic weather maps was used.

Two types of desert dust intrusions were distinguished. One named pure desert (D) and another named continental-desert (CD), the latter is composed of a mix of continental and pure desert dust aerosols. Both are given by instantaneous values of AOD ≥ 0.2 but pure desert aerosols D are characterized by alpha values lower than 1 and CD mixed aerosols are given by values of alpha between 1 and 1.5.

With the aim of characterizing PMx values for the days composing the inventory, these values were taken from the database of Peñausende station belonging to the EMEP network. Despite the distance between Peñausende and Palencia stations, about 140 km, both areas present an identical sensitivity to detect desert dust intrusions. The monthly climatology, interannual variability and trends for PM10, PM2.5 and the ratio (PM2.5/PM10) have been established for both D and DC, and for the subsets of D and DC separately. The study is complemented with the evaluation of frequency histograms of all these parameters.

The monthly climatology was first calculated in terms of daily values and in terms of monthly means afterwards in order to look for the differences introduced by these two calculation approaches.

The most relevant aspect of this study is the evaluation of desert dust contribution of PMx data to the monthly climatology and mean annual values for the whole period 2003-2012. The results show the bimodal contribution, peaked in March and August. The evaluation of the tendency also shows the decreasing contribution along the decade 2003-2012 with a pronounced minimum in 2009 and new increases in 2011-2012 reversing the decreasing earlier trend. Finally, scatter plots relating PM10 with AOD (440 nm) and PM10 with PM2.5 or PMcoarse for the values belonging to the days of the desert-dust inventory are presented.

CIRRUS CLOUDS PROFILING AT SUBTROPICAL AND POLAR LATITUDES: OPTICAL/MACROPHYSICAL PROPERTIES DERIVED FROM ACTIVE REMOTE SENSING OBSERVATIONS

CARMEN CÓRDOBA-JABONERO[1]*, ELIANE G. LARROZA[2], EDUARDO LANDULFO[2], WALTER M. NAKAEMA[2], EMILIO CUEVAS[3], HÉCTOR OCHOA[4], MANUEL GIL-OJEDA[1]

[1]*Instituto Nacional de Técnica Aeroespacial (INTA), Atmospheric Research and Instrumentation Branch, Ctra. Ajalvir km.4, Torrejón de Ardoz-28850, Madrid, Spain, *cordobajc@inta.es*

[2]*Instituto de Pesquisas Energéticas e Nucleares (IPEN), Centro de Lasers e Aplicações, Sao Paulo, Brazil*

[3]*Agencia Estatal de Meteorología (AEMET), Atmospheric Research Centre of Izaña, Sta. Cruz de Tenerife, Spain*

[4]*Dirección Nacional del Antártico/Instituto Antártico Argentino (DNA/IAA), Buenos Aires, Argentina*

Clouds, and mainly high-altitude cirrus clouds, have a significant role in the radiation balance of the Earth–atmosphere system, since they can act as modulators of the net radiative forcing either by heating or by cooling effects at both regional and global scales (Liou, 1986). Additionally, the reaction of cirrus clouds to factors resulting from human-induced climate changes (i.e, greenhouse effect and contamination of the upper troposphere from increasing aircraft traffic) is still poorly investigated. Indeed, the climate-related changes in cirrus cloud properties could alter (i.e., enhancing, opposing or even negating) the widely assumed global warming effect related to the aerosols. In particular, in a changing climate, cirrus induced by aircraft contrails would increase the upper tropospheric albedo and counteract the greenhouse gases warming effect. The predominance of infrared greenhouse warming versus solar albedo cooling depends sensitively on both the altitudes and microphysical compositions of the cirrus clouds. Indeed, cloud height has an evident impact. Hence, high tropical cirrus (derived from deep convection above warm moist layers, for example) can be particularly effective greenhouse modulators. Conversely, lower cirrus over cold extended areas could be more efficient for albedo effects. Thus, mid-latitude cirrus clouds are assumed to reveal radiative implications varying with the season. Moreover, it should be noticed that cirrus clouds are product of weather processes, and then their occurrence and macrophysical/optical properties can vary significantly over different regions of the globe.

In this sense, this work presents a few case studies of cirrus clouds observed at both subtropical and polar latitudes. Observations were carried out in three locations: Sao Paulo (Brazil, 23.6°S 46.8°W) and Sta. Cruz de Tenerife (Spain, 28.5°N 16.3°W), both are subtropical stations, and the Belgrano II base (Argentina, 78°S 35ºW) in the Antarctic continent. Active remote sensing (LIDAR) was used for profiling measurements and cirrus clouds features were retrieved by using a recently proposed methodology (Larroza et al., 2013). Optical and macrophysical properties (COD-cloud optical depth, top/base heights, thickness and Lidar Ratio, mainly) of both the subtropical and polar cirrus clouds are reported. Similarities/discrepancies found between them and radiative forcing implications are also discussed.

References

Larroza, E. G., Nakaema, W. M., Bourayou, R., Hoareau, C., Landulfo, E., and Keckhut, P.: Towards an automatic lidar cirrus cloud retrieval for climate studies, *Atmos. Meas. Tech.,* 6, 3197-3210, doi:10.5194/amt-6-3197-2013, 2013.
Liou, K.-N.: Influence of cirrus clouds on weather and climate processes: A global perspective, *Mon. Weather Rev.,* 114, 1167–1200, 1986.

COMPARISON BETWEEN SIMULATED AND MEASURED SOLAR IRRADIANCE DURING A DESERT DUST EPISODE

M.A. OBREGÓN[1], V. SALGUEIRO[1], M.J. COSTA[1], S. PEREIRA[1], A. SERRANO[2,1], A.M. SILVA[1]

[1]Geophysics Centre of Évora,, Rua Romão Ramalho, 59, 7000, Évora ,Portugal
[2]University of Extremadura, Avda de Elvas, S/N, 06006, Badajoz, Spain

The aim of this study is to analyze the reliability of the libRadtran model (Mayer and Kylling, 2005) in the estimation of irradiance in the shortwave spectral range (280-2800 nm) during a desert dust episode. The transport of dust from the Sahara region towards the Iberian Peninsula is a regular phenomenon that notably influences the radiation balance. For that purpose, downward irradiance measurements at the surface and corresponding model simulations have been compared during the three days of a desert dust event (9-11 August 2012) in Évora (38.6º N, 7.9º W, 293.0 m a.s.l), Portugal.

Version 1.7 of the libRadtran is used in this study with inputs of aerosol, total ozone column, precipitable water vapor column and surface albedo data. Level 1.5 AERONET (Aerosol Robotic NETwork) aerosol optical properties have been used in the simulations. Total ozone column was provided by the Ozone Monitoring Instrument (OMI). Surface albedo values were obtained from the Surface and Atmospheric Radiation Budget (SARB) working group (http://snowdog.larc.nasa.gov/surf/index.html). Radiation was measured by an Eppley pyranometer installed at Évora Geophysics Center Observatory in Évora. Only cloud-free measurements corresponding to solar zenith angle lower than 80º have been considered in this study.

The comparison between measured and simulated values shows a highly significant correlation, with a correlation coefficient of 0.999 and a slope very close to unity (0.995±0.006) was found, supporting the validity of the model in the estimation of irradiance in the shortwave spectral range. Relative differences between the simulated and measured irradiances with respect to the measured values have also been calculated and indicate that the libRadtran model slightly underestimates the experimental global irradiance, being most of the differences around 1 % (mean relative difference equal to 1.2 %). These small differences could be associated with experimental errors in the measurements as well as uncertainties in the input values given to the model, particularly related with the actual aerosol properties. The notably good agreement between simulated and measured irradiances indicates that the libRadtran model can be used to estimate irradiance when no radiation measurements are available. In order to obtain accurate estimations of the irradiance, the model must be fed with reliable values of the aerosol properties.

Acknowledgments

References

Mayer, B., and A. Kylling (2005), Technical note: The libRadtran software package for radiative transfer calculations – description and examples of use, Atmos. Chem.Phys., 5, 1855–1877.

COMPARISON OF CALIBRATION METHODS FOR DETERMINING WATER VAPOR MIXING RATIO BY RAMAN LIDAR

M. J. GRANADOS-MUÑOZ[1,2], R. F. DA COSTA[3], F. NAVAS-GUZMÁN[1,2,4], P. FERRINI[3], J. L. GUERRERO-RASCADO[1,2], F. LOPES[3], E. LANDULFO[3], L. ALADOS-ARBOLEDAS[1,2]

1 Dpt. Applied Physics, Faculty of Sciences, University of Granada, Fuentenueva s/n, 18071, Granada, Spain

2 Andalusian Institute for Earth System Research (IISTA-CEAMA), Avda. del Mediterráneo s/n, 18006, Granada, Spain

3Centro de Lasers e Aplicaçoes, Instituto de Pesquisas Energéticas e Nucleares (IPEN), Avd. Prof. Lineu Prestes 2242,

05508-000, São Paulo, Brazil

4 Institute of Applied Physics (IAP), University of Bern, Bern, Schwitzerland

5Instituto de Astronomia, Geofísica e Ciências Atmosféricas, Universidade de São Paulo (USP),Rua do Matão,

1226, 05588-000, São Paulo, Brazil

This study focuses on the comparison of different methods to determine the water vapor mixing ratio calibration factor for Raman lidar. The lamp mapping technique applied to a Raman lidar system [Venable et al., 2013] is compared to the iterative calibration with radiosounding data, described in Navas-Guzmán et al., [2013]. The retrieved calibration factors are applied to data measured with a Raman lidar system located at the Center for Laser and Applications at IPEN (São Paulo, Brasil, 23º33' S, 46º44'W) during the summer of 2014 to obtain tropospheric water vapor mixing ratio profiles. The lamp mapping technique has been previously applied to the Raman Lidar at IPEN obtaining successful results [Landulfo et al., 2009], whereas the iterative procedure based on calibration with radiosounding is implemented here for the first time. The combination of the lidar retrieved water vapor mixing ratio profiles and aerosol optical properties vertical profiles allows the analysis of aerosol hygroscopic properties based on active remote sensing [Granados-Muñoz et al., 2014].

References:
Granados-Muñoz, M. J., (2014). Ph. D. Dissertation.
Landulfo, E., et al., (2009). Proceedings of SPIE Europe Remote Sensing, pp. 74790J-74790J
Navas-Guzmán, F., et al., (2013). Atm. Measur. Tech. Discuss., 6(6).
Venable, D. D. et al., (2011). Appl. Opt., 50(23), 4622-4632.

DETERMINATION OF ATMOSPHERIC BROWN CARBON IN AERSOLS COLLECTED OVER BAY OF BENGAL: IMPACT OF INDO-GANGETIC PLAI

AMANI GUPTA[1], M.M. SARIN[2], SRINIVAS BIKKINA[3]

[1]*Department of Natural Resources, TERI University, Delhi, India,*
amani262626@gmail.com

[2] *Physical Research Laboratory, Ahmedabad, India,*
sarin@prl.res.in

[3]*Institute of Low Temperature Science, Hokkaido University, Sapporo, Japan*
srinivas.prl@gmail.com

The light absorbing organic aerosol, so called Brown Carbon, has been recently brought to the attention of scientific community owing to its prominent UV-absorption, therefore, could have impact on radiative forcing estimates. In this study, aerosol samples collected from the Bay of Bengal during a national field programme, Integrated Campaign of Aerosols and trace gases Radiation Budget (ICARB-W, January'09) were investigated for assessing the spectral absorption properties of atmospheric "Brown Carbon", a light absorbing organics. Aqueous extracts of aerosol filters have been used to assess the brown carbon absorption. In all aerosol samples analyzed from the Bay of Bengal, a significant near UV-absorption is evident. The absorbance measured at 365 nm relative to 700 nm is used for assessing the mass absorption coefficient (MAC). It is noteworthy that MAC shows a linear relationship ($R^2 = 0.89$; P-value < 0.05) with concentration of water-soluble organic carbon (WSOC); suggest their common source. The slope of the regression ($m = 0.5$ m^2 g^{-1}) provides a better estimate of mass absorption efficiency (MAE) of brown carbon (C_{brown}). This estimate is comparable with that reported for vegetation burning emissions (Hecobian et al., 2010; Cheng et al., 2011). These results have implications for estimating the radiative forcing of brown carbon over the Bay of Bengal.

Keywords: Brown carbon, Mass absorption efficiency, Indo-Gangetic Plain, Combustion sources, Bay of Bengal.

References:

Cheng Y, He K B, Zheng M, Duan F K, Du Z Y, Ma Y L, Tan J H, Yang F M, Liu J M, Zhang X L, Weber R J, Bergin M H and Russell A G 2011 Mass absorption efficiency of elemental carbon and water-soluble organic carbon in Beijing, China *Atmos. Chem. Phys.* **11** 11497-510

Hecobian A, Zhang X, Zheng M, Frank N, Edgerton E S and Weber R J, 2010 Water-Soluble Organic Aerosol material and the light-absorption characteristics of aqueous extracts measured over the Southeastern United States *Atmos. Chem. Phys.* **10** 5965-77

DISCRIMINATION BETWEEN AEROSOL AND CLOUD CONTRIBUTIONS TO GLOBAL SOLAR RADIATION TRENDS BETWEEN 2003 AND 2010 IN NORTH-CENTRAL SPAIN

D. MATEOS[1], A. SANCHEZ-LORENZO[2], V.E. CACHORRO[1], M. ANTÓN[3], C. TOLEDANO[1], J. CALBO[2]

[1]*Grupo de Óptica Atmosférica, University of Valladolid, Valladolid, Spain, e-mail: mateos@goa.uva.es*
[2]*Group of Environmental Physics, University of Girona, Girona, Spain*
[3]*Department of Physics, University of Extremadura, Badajoz, Spain*

Aerosols and clouds are the main factors involved in the determination of the energy balance of the planetary system. Surface solar radiation trends observed during the last decades have evidenced a progressive increase, i.e., a substantial reduction in the radiative effects at the surface of the cloud-aerosol system. This effect is known as 'brightening' phenomenon and started around the 1990s and it is a worldwide phenomenon which is more noticeable at developed countries. However the separate contributions of aerosols and clouds to these trends are not well analyzed yet. Hence, the main aim of this study is to evaluate the radiative effects of three systems: cloud and aerosols (CARE), clouds (CRE), and aerosols (ARE). Specifically, the temporal trends are determined by using monthly measurements of global solar radiation at Valladolid (Spain) site (belonging to the Spanish Meteorological Agency) together with simulations performed with the libRadtran model. Simulations are fed with 8-year monthly measurements of: aerosol properties at Palencia site (40 km apart, belonging to the Aerosol Robotic Network); total ozone and water vapor data obtained from ERA-Interim reanalysis; and surface albedo data from MERRA Monthly History Data Collection. The trend for the monthly global solar radiation data is +11 W m^{-2} per decade (period 2003-2010), although it presents a very low significance level according to the Mann-Kendall non-parametric test. The anomalies of the monthly CARE, CRE, and ARE are evaluated to minimize the impact of the annual cycle on the evolution of these variables. The temporal trends for the analyzed time period are the following (with a significance level over 95%): +10.6, +6.0, and +3.9 W m^{-2} per decade, respectively. Overall, clouds and aerosols have contributed around 2/3 and 1/3 to the solar radiation increase at the study site between 2003 and 2010, respectively.

DUST EVENTS OF SYNOPTIC SCALE ASSOCIATED TO FRONTAL PASSAGES FROM THE ATLANTIC

R. FERRER, J.A.G. ORZA

SCOLAb & Aeolian Erosion Group, Department of Physics, Universidad Miguel Hernández
Avda. de la Universidad, s/n. Edif. Alcudia
Elche, Spain, ja.garcia@umh.es

Periods of significant winds associated with frontal passages from the Atlantic have a strong impact on air quality. These situations are known to facilitate dispersion of local air pollutants, which are replaced in most situations by fresh air masses. Furthermore, they are frequently accompanied by rain in most of western Europe.

In drier areas less impacted by frontal precipitation, such as southeastern Spain, we find that these episodes lead to the simultaneous decrease in NOx and *increase* in PM10 concentrations. Resuspension is far more dominant than dilution and daily limit values are commonly surpassed in the area. The passage of trains of fronts, lead to decreasing PM10 levels after the first ones.

We have analyzed meteorological and air quality data from stations located near the coast in southeastern Spain (provinces of Alicante, Murcia and Almería) for the period 2006-2008. A number of this kind of dust events can be observed directly in MODIS satellite imagery as dust plumes blown off the coast. Additionally, a few selected cases were studied with data of a broader area covering the southern Iberian Peninsula. These ones further highlight the synoptic scale of the episodes with the generalized presence of dust plumes blown from the land all over the southern coast of the Iberian Peninsula.

We present a phenomenological description of different episodes and an overall assessment of the impact on air quality. Variations in surface level pressure together with the characteristic opposing behavior of PM10 and NOx during these dust events was used to identify episodes without imposing wind speed thresholds. Instead, wind gust thresholds were obtained from the analysis.

DUST EXPORT FROM EPHEMERAL LAKES IN THE WESTERN MEDITERRANEAN

J. A. G. ORZA, M. CABELLO, E. DOMENECH

SCOLAb & Aeolian Erosion Group, Department of Physics, Universidad Miguel Hernández
Avda. de la Universidad, s/n, Edif. Alcudia
Elche, Spain, ja.garcia@umh.es

The role of dry lakebeds as sources for aeolian export of soil particulates is studied in relation to their inundation extent, soil and meteorological conditions. Two areas in the western Mediterranean were investigated for the period 2005-2012: (1) El Hondo Nature Park in southeastern Spain (2400 ha), and (2) the region of the Chotts in southern Tunisia, including el-Djerid and el-Gharsa (vast saline lakes of 495000 and 42000 ha, respectively).

Field campaigns conducted at El Hondo during the period 2009-2012 measured size distribution of suspended particles, PM10 concentration and chemical composition; saltation profiles, composition and granulometry; and meteorological and soil parameters. The Chotts area was studied by making use of the `present weather´ observations of local dust reported at Tozeur, as well as from meteorological and visibility data in the area. Variations in water sheet and salt crusted surface in bothe areas were estimated from the 7-2-1 spectral bands of MODIS. AOT data from MODIS was also used to complement ground observations.

Surface changes were driven primarily by the precipitation regime. In El Hondo, conditions may change dramatically due to additional anthropic intervention, as inflow and outflow are ultimately managed by humans.

The majority of the dust storms registered at El Hondo were associated to the passage of Atlantic frontal systems with no rainfall. W/NW/SW winds > 9 m/s (at 2 m above the ground) and average friction velocity of 0.46 m/s triggered these erosion events.

Local dust events in the Chotts were associated (80% of the cases) to windspeed $\geq$ 8 m/s (at 10 m above the ground), mostly of E component (55%) and then W (28%), relative humidity < 75% and lead to horizontal visibility < 5 km. The episodes were primarily of synoptic origin, registered from March to May, although local dust was mostly registered in the afternoon. The larger inundation extent in the Chotts in spring 2009 resulted in a reduced frequency of erosion events with respect to other years. However dust events occurred also with moderately large dried areas located upwind of the measurement sites. In fact, our measurements at El Hondo showed that dry eroding areas of around 1000 ha are enough to sustain for several hours dust storms which can be observed in MODIS images.

EVALUATION OF LIRIC WITH TWO SUN PHOTOMETERS AT DIFFERENT HEIGHT LEVELS: STATISTICAL ANALYSIS

M. J. GRANADOS-MUÑOZ[1,2], J. L. GUERRERO-RASCADO[1,2], J. A. BRAVO-ARANDA[1,2], F. NAVAS-GUZMÁN[1,2,3], H. LYAMANI[1,2], A. VALENZUELA[1,2], F. J. OLMO[1,2], L. ALADOS-ARBOLEDAS[1,2]

1 Dpt. Applied Physics, Faculty of Sciences, University of Granada, Fuentenueva s/n, 18071, Granada, Spain

2 Andalusian Institute for Earth System Research (IISTA-CEAMA), Avda. del Mediterráneo s/n, 18006, Granada, Spain

3 Institute of Applied Physics (IAP), University of Bern, Bern, Schwitzerland

The availability of a unique experimental setup based on the use of a lidar system together with a sun photometer located in Granada (EARLINET+AERONET station) and a second sun photometer in Cerro Poyos (AERONET station), allows us to perform a comparison between LIRIC retrievals from two different heights. The statistical analysis performed during the summer of 2012, based on 112 retrievals, indicates very good agreement between the retrievals from both stations, with discrepancies below 5 $\mu m^3/cm^3$ for almost 90% of the data (Figure 1). Slopes and correlation coefficients R corresponding to linear fits indicate also very good agreement, with most of the values close to one (60 and 80% of the data for the slope and R, respectively). In spite of the good agreement, in general larger values of the total volume concentration are obtained in the retrieval from Cerro Poyos than in the retrieval from Granada. Besides, it is observed that the largest discrepancies are obtained in those cases with (i) very low aerosol load, (ii) different aerosol types above and below Cerro Poyos station, and (iii) very low aerosol load above Cerro Poyos station. Therefore, according to the results of the analysis, LIRIC is a very robust and self-consistent tool, but it is inferred that assumptions such as the height independency of the size distribution or the refractive index and the incomplete overlap effect in the lowermost region of the profiles need to be carefully reviewed in some cases.
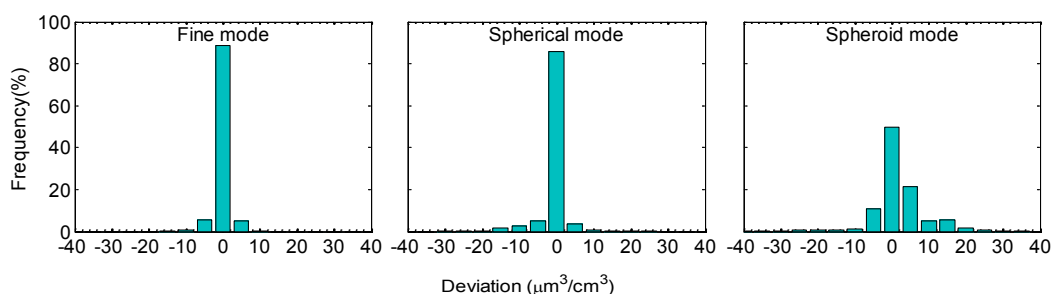

Figure 1. Histogram of the frequency distribution of the deviations for the whole dataset corresponding to summer 2012. Deviations were obtained by substcracting the profiles from Granada above 1820 m a.s.l. to the profiles retrieved from Cerro Poyos at every height level (15 m vertical resolution).

HETEROGENEOUS REACTIVITY OF INTERNALLY MIXED ORGANIC/INORGANIC AEROSOLS WITH OZONE

LORENA MIÑAMBRES, ESTÍBALIZ MÉNDEZ, MARÍA N. SÁNCHEZ, FRANCISCO J. BASTERRETXEA

Department of Physical Chemistry, University of the Basque Country (UPV/EHU), Barrio Sarriena s/n, 48940, Leioa, Spain

Keywords: Ozonolysis, dicarboxylic acid, sodium halides, infrared spectroscopy

Atmospheric aerosols generally consist of inorganic species mixed with a wide variety of organic compounds and elemental carbon. On the one hand, sea salt aerosols constitute one of the most abundant types of naturally suspended particulate matter in the troposphere, and are the dominant aerosol species by mass above the oceans. On the other hand, field measurements have shown that a significant mass fraction of atmospheric aerosol consists of organic compounds (Jacobson et al., 2000), that can alter the physical properties of the particles and are extremely susceptible to atmospheric oxidation. Although general ozonolysis reactions have been studied in depth for some time, reactions of sea salt internally mixed with unsaturated organic species on aerosol particles are likely to show important differences because of the presence of water or the influence of the mixture of components. Our aim is to understand the influence of the salt in the reactive properties of the organic compound. Moreover, the reactive behavior can change with relative humidity, as manifested by the different ozonolysis mechanisms in dry and aqueous particles (Nájera et al., 2009, Nájera et al., 2010).

In the present work we study the ozonolysis of submicrometric sodium halide aerosols (NaCl, NaBr and NaI) internally mixed with maleic acid. Fourier-transform absorption infrared spectroscopy has been used to characterize particle composition, phase and water content, as well as gas-phase composition. The morphology of the internally mixed aerosol particles has been imaged by Scanning Electron Microscopy (SEM) before and after the ozonolysis in order to study the structural changes in the reaction. The characterization of the ozonolysis reaction products has been supplemented with Electrospray Ionization Mass Spectrometry (ESI-MS) off-line analysis.

The ozonolysis of internally mixed maleic acid particles has been spectroscopically monitored at different relative humidities (RH): low (RH~0%), intermediate (RH~50%) and high (RH~100%). Preliminary results indicate that formic acid is generated as a product in the gas phase, and that it is produced at higher rate under high RH conditions, thus suggesting that a different mechanism operates in dry and aqueous particles. These results are in agreement with previous results in pure maleic acid (Nájera et al., 2009, Nájera et al., 2010). Also SEM pictures show that the internally mixed particles are not spherical and have complex

forms. The obtained kinetic data are used to test the validity of the proposed general reaction mechanism for this system by applying the kinetic model framework for aerosol surface chemistry and gas-particle interactions, proposed by Pöschl et al. (Pöschl et al., 2007). Further results will be presented at the meeting.
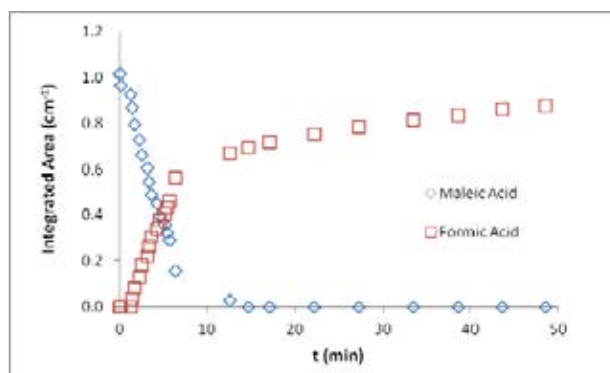
Figure 1. Time evolution of maleic acid (reactive) and formic acid (product) after ozonolysis of pure maleic acid particles in an aerosol flow cell.

Jacobson, M. C, Hansson H. C., Noone K. J. and Charlson R. J., *Reviews of Geophysics*, 2000, 38, 267-294.

Nájera J. J., Percival C. J. and Horn A. B., 2010. *Physical Chemistry Chemical Physics*, 11, 11417-11427.

Pöschl U., Rudich Y. and Ammann M., 2007. Atmospheric Chemistry and Physics, 7, 5989-6023.

INFERING BLACK CARBON FRACTION IN THE ATMOSPHERIC COLUMN FROM AERONET DATA OVER GRANADA (SPAIN)

VALENZUELA, A.[1, 2], OLMO, F. J.[1, 2], AROLA, A.[3], LYAMANI, H.[1, 2], ANTÓN, M.[4], GRANADOS-MUÑOZ, M. J.[1, 2], AND L. ALADOS-ARBOLEDAS [1,2]

[1]*Department Applied Physics, University of Granada, Fuentenueva s/n, 18071, Granada*

[2]*Andalusian Institute for Earth System Research (IISTA-CEAMA), Avda. del Mediterráneo s/n, 18006, Granada, Spain*

[3]*Finnish Meteorological Institute (FMI), Kuopio, Finland*

[4]*Departament of Physics, University of Extremadura, Badajoz, Spain*

Column-integrated aerosol black carbon fraction ($BC_{fraction}$) has been retrieved over Granada for the period 2005-2012. $BC_{fraction}$ has been derived from AERONET-retrieved size distribution using Maxwell-Garnett mixing rules in a mixture of BC, organic carbon (OC) and $(NH_4)_2(SO_4)$ embedded in water host. The volume fraction of each component is retrieved by matching the mixture refractive index (real, $n(\lambda)$ and imaginary, $k(\lambda)$) with AERONET retrieved refractive index (Arola et al., 2011). Figure 1 shows the seasonal variation of $BC_{fraction}$ with higher values during winter and autumn than during warm seasons. Furthermore, this plot also shows the annual variation of the slope of the single scattering albedo, $\omega(440-1020nm)$, as function of wavelength calculated in the wavelength range 440-1020 nm. As can be seen, the slope of $\omega(440-1020nm)$ exhibits an anti-correlation with the annual evolution of $BC_{fraction}$. Negative values of the slope of $\omega(440-1020nm)$ indicate the absorption at 440 nm wavelengths is lower than at 1020 nm wavelengths, behavior typical of the BC. A more comprehensive study will be necessary in order to look for a direct method to get one of these variables if another one is known.
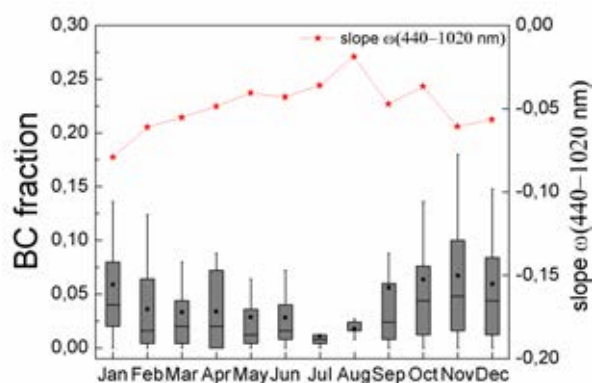
Figure 1. Monthly statistics of $BC_{fraction}$ over Granada from 2005 to 2012 represented as box diagrams. In these box diagrams, the mean is represented by a blank dot and the median by a middle line. The top/bottom box limits represent the percentiles 25% and 75%. In addition, the error bars of the box are the percentiles 5% and 95%.The red line and stars represent the slope of $\omega(440-1020nm)$.

References

A. Arola, G. Schuster, G. Myhre, S. Kazadzis, S. Dey, and S. N, Tripathi. Inferring absorbing organic carbon content from AERONET data, Atmos. Chem. Phys., 11, 215–225, 2011.

INFLUENCE OF AIR MASSES ORIGING ON RADIOACTIVITY IN AEROSOLS

FRANCISCO PIÑERO-GARCÍA, Mª ÁNGELES FERRO-GARCÍA

Radiochemistry and Environmental Radiology Laboratory (LABRADIQ), Department of Inorganic Chemistry, University of Granada, Granada, 18071, franciscopigar@ugr.es

The aim of this research is to study influence of the air masses origin on radioactivity in aerosols at surface air, (Gross α, Gross β and ^{7}Be activity concentration). A total of 148 samples were weekly collected from January 4th, 2011 to December 31st, 2013. The specific activity (Bq/m^3) of gross alpha and gross beta was measured by α/β Low-Level counter, whereas ^{7}Be was detected by gamma spectrometry (Eγ = 477.6 KeV, Yield = 10.42 %). In all samples, the activity concentration of ^{7}Be, Gross α and Gross β were higher than the Minimum Detectable Activity (MDA). Evolution of Gross α and Gross β show a Log-Normal distribution, while ^{7}Be fits better a Normal distribution according to Kolmogorov Simirnov test.

k-means clustering of daily 72-h kinematic 3D backward trajectories was used to set an air mass classification of different synoptic circulation patterns at altitudes of: mean altitude of Spain (500 m; 950 hPa), planetary boundary layer (1500 m; 850 hPa) and free atmosphere (3000 m; 700 hPa). Figure 1 shows the average cluster (centroid) at the studied altitudes. The classification of the air masses origins over Granada were: a) West (W, Wf); tropical and warm polar maritime air masses generate over Atlantic Ocean. In addition, fast west air masses were identified as Wf. b) North West (Nw, Nwf); polar maritime air masses. Furthermore, fast northwest backward trajectories were classified as Nwf. c) North (N); this group collect continental air masses generated over Europe as well as maritime arctic air masses crossing British Isles and Northwest Europe. These air masses transport maritime and also urban aerosols. d) Mediterranean (Med); warm polar continental air masses over Mediterranean Sea. They transport mineral dust since they are influenced by slow tropical continental air masses from African desserts. e) Saharan (Sh); tropical maritime and continental air masses that cross the northern of Africa and enter in Spain through the Straits of Gibraltar. These air masses are related to entrance of high concentration of mineral dust and dessert aerosols
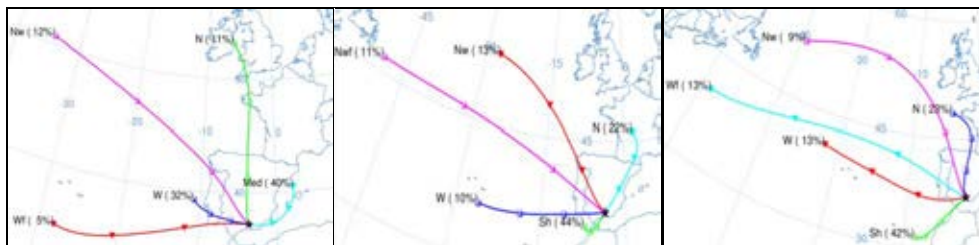
Figure 1 Centroids of the 5 clusters at (left) 500 m, (centre) 1500 m and (left) 3000 m for the 3 year 2011 – 2013

Multiple Regression Analysis (MRA) was applied to determine the influence of the air mass origin (Backward trajectory), wind direction, temperature and rainfall on Gross α, Gross β and ^{7}Be activity concentration. In brief, the MRA results show that the re-suspended continental particles from northern Africa and the southern part of western and central Europe transported by Mediterranean air masses at low altitude (Med-500) and African air masses as high altitude (Sh-3000) increase the radioactivity concentration in aerosols at surface atmosphere.

LEVELS AND EVOLUTION OF ATMOSPHERIC NANOPARTICLES IN A SUBURBAN AREA WITH ATLANTIC INFLUENCE

S. IGLESIAS-SAMITIER, V. JUNCAL-BELLO, M. PIÑEIRO-IGLESIAS, P. LÓPEZ-MAHÍA,
S. MUNIATEGUI-LORENZO, D. PRADA-RODRÍGUEZ

*Grupo Química Analítica Aplicada, Instituto Universitario de Medio Ambiente (IUMA),
Departamento de Química Analítica, Facultade de Ciencias, Universidade da Coruña, Campus de
A Coruña, 15071 A Coruña, Spain, silvia.iglesias.samitier@udc.es*

The presence of nanoparticles in the atmosphere, both by primary and secondary formation processes, is important both for climate and epidemiology studies [1] so, recent researches indicate that the number of small particles (e.g. ultrafine particles) and the particle surface area exhibit stronger association with health effects than mass related metrics (e.g. PM_{10}) [2].

The study of evolution and levels of atmospheric nanoparticles was carried out in the *University Institute of Research in Environmental Studies* of *University of A Coruna*, (in the northwest of Spain). The sampling period was during May, June, July, September and October 2013 and this area, with Atlantic influence, presented an average temperature and relatively humidity of 18ºC and 79%, respectively. The predominant wind directions were SE and NW-N, being this northwest direction the cause of the presence of sea breeze in the sampling point. The system used to carry out the measurements of nanoparticles was the Scanning Mobility Particle Sizer (3936 Model, TSI), and the meteorological parameters were measured using a meteorological station (03002 Model, R.M. Young Company).

The average number concentration during 2013 was 2605 cm^{-3}, lower than during 2012 and 2011, when the average number concentrations were 3697 cm^{-3} and 3210 cm^{-3}, respectively. Generally, lower particle number concentrations were reached during summer months when atmospheric dispersion conditions were presented (e.g. sea breeze). However, during summer months, particularly in June, a large number of new particle formation events have been identified. June 2012 and 2013 presented more nucleation events than June 2011, and these processes were characterized by occur at midday, predominantly. Furthermore, the nucleation events were longer in June 2013 (2-4 h duration) than in June 2012 (1-2 h).

During all studied months in 2013, two peaks at morning and evening hours have been identified for nucleation, Aitken and accumulation modes, due to traffic emissions. On the other hand, nucleation mode presented another maximum around midday, coinciding with high solar radiation and the presence of sea breeze. Sea breeze favored the new particle formation process because this air mass was characterized by presenting low concentrations of atmospheric pollutants. Furthermore, growth events of nanoparticles have been identified too, coinciding in this case with the presence of preexisting particles in the atmosphere.

[1] Cusack, M., Alastuey, A. and Querol, X. *Atmospheric Environment* 81(2013)651-659.
[2] von Bismarck-Osten, C., Birmili, W., Ketzel, M., Massting, A., Petäjä, T. and Weber, S. *Atmospheric Environment* 77(2013)415-429.

LIDAR DEPOLARIZATION UNCERTAINTIES ANALYSIS USING THE LIDAR POLARIZING SENSITIVITY SIMULATOR (LPSS)

J.A.BRAVO-ARANDA[1,2], J.L. GUERRERO-RASCADO[1,2], M.J. GRANADOS-MUÑOZ[1,2], F.J. OLMO[1,2], L. ALADOS-ARBOLEDAS[1,2]

[1]*Andalusian Institute for Earth System Research (IISTA-CEAMA), Av. del Mediterráneo, 18006, Granada, Spain, jabravo@ugr.es*

[2]*Dpt. Applied Physics, University of Granada, Fuentenueva s/n, 18071, Granada, Spain*

Lidar depolarization measurements are becoming a very important tool for typing the atmospheric aerosol [Gross et al., 2011] and improving the retrieval of aerosol microphysical properties [Granados-Muñoz et al., 2014]. The most relevant properties derived from the lidar depolarization measurements are the volume (δ') and particle linear depolarization ratios (δ^p). In terms of uncertainties, both properties are different as the δ' is retrieved directly from the lidar measurements whereas the δ^p is a secondary product. In the case of δ', random errors are determined by means of the Monte Carlo technique whereas uncertainty range of δ' ($U_{\delta'}$) due to the systematic errors can be estimated using the Stokes-Müller formulism to model the polarizing response of lidar systems. To this aim, the setup of a lidar system is subdivided in functional blocks: laser, laser emitting optics, receiving optics, the polarizing beam splitter including the detectors and the depolarization calibrator.

For the first time, $U_{\delta'}$ due to the lidar polarizing response is quantified in detail using a simulator, the so-called Lidar Polarizing Sensitivity Simulator (LPSS). This software is based on the work given by Freudenthaler [2014]. In order to obtain general results, LPSS was used to simulate $U_{\delta'}$ of a synthetic lidar system. The properties and uncertainties of the synthetic lidar were derived or assumed from different technical specifications of commercial optical devices.

A total $U_{\delta'}$ of [-0.082, 0.243] was found. As typical δ' values at 532 nm are in the range 0.01-0.03, it can be concluded that the hardware polarization sensitivity can affect the depolarization results causing relative errors even larger than 100%. The most critical properties are the purity polarization parameter of the laser and the effective diattenuation of the receiving optics with a contribution to the total $U_{\delta'}$ larger than 0.05. Next, the phase shift of the emitting and receiving optics and the rotational misalignment between the polarizing plane of the laser respect the incident plane of the polarizing beam splitter are relevant lidar properties as well, contributing with 0.03 to the total $U_{\delta'}$. It is worthy to note that the uncertainty range is asymmetric being greater the positive deviation, and thus, it can be concluded that the lidar polarizing sensitivity usually overestimates δ'. This study is crucial as it allows improvements on the depolarization calibration and it demonstrates the relevance of the polarizing response of lidar systems.

References:

Freudenthaler, V. (2014, in preparation), Atmopheric Measurements and Techniques (Earlinet Special Issue).

Granados-Muñoz, M. J., et al. (2014, accepted), Journal of Geophysical Research D: Atmospheres.

Gross, S., M. Tesche, V. Freudenthaler, C. Toledano, M. Wiegner, A. Ansmann, D. Althausen, and M. Seefeldner (2011), Tellus B, 63(4), 706-724.

MEDIDA Y CARACTERIZACIÓN DE LA CONCENTRACIÓN NUMÉRICA (CPC) DE PARTÍCULAS ATMOSFÉRICAS EN LA CIUDAD DE VALLADOLID

A. MARCOS, V.E. CACHORRO, Y. BENNOUNA, M.A. BURGOS, D. MATEOS, J.F. LOPEZ, S. MOGO[2,3], A.M. DE FRUTOS

[1]*Grupo de Óptica Atmosférica, Universidad de Valladolid, Valladolid, España, email:amarcos@@goa.uva.es*

[2]*Universidad de Beira Interior, Portugal*

[3] *Instituto Don Luis, Portugal*

La importancia del estudio de los aerosoles atmosféricos radica en el impacto que estos tienen en la determinación de la calidad del aire así como en el clima. Las medidas de concentración de aerosoles "in situ" focalizan el primer aspecto, y medidas de tipo "remote sensing" son más indicadas para el segundo. El Grupo de Óptica Atmosférica (GOA-UVA) dispone de una estación de medida de aerosoles "in situ" a las afueras de la ciudad de Valladolid con el objetivo de la caracterización, entre otros, de los valores de concentración numérica de partículas, distribución de tamaños en el rango micrométrico, coeficientes de absorción y scattering. En este trabajo se presenta el análisis de la concentración numérica de partículas atmosféricas desde junio de 2011 a junio del 2013 medidas con un CPC 3022A de la casa TSI.

El análisis de la base de datos (medidas directas y valores promedios) y del ciclo diurno, ha permitido observar la existencia de dos períodos anómalos y muy dispares entre sí. El período de valores más altos (jun11- jul12), presenta un promedio diario de 9708.8 cm^{-3} y se ha visto afectado por la cercanía de las instalaciones a la construcción de la autovía Valladolid-Soria (3 km). El período de valores más bajos (oct12-jun13), con un promedio diario de 3164.6 cm^{-3}, puede ser representativo del fondo de la ciudad, pero ha sido peculiar por las elevadas precipitaciones en la primavera de 2013 (disminuyen la concentración). Con los valores diarios se evalúa el impacto de las obras de la autovía tomando como referencia la mediana del segundo período (2707.8 cm^{-3}). Es decir, se ha cuantificado la anomalía originada por dicha construcción, y aun suponiendo que en el segundo periodo la concentración media de partículas esté por debajo de un "valor más realista" debido a las precipitaciones, el aporte de la autovía ha supuesto doblar o triplicar el valor normal o habitual de la zona.

Por otra parte, el estudio del ciclo diurno de cada período ha revelado que el comportamiento de la concentración numérica de partículas a lo largo del día para ambos períodos es el mismo. Presenta valores mínimos entre las 4h y 6h, aumenta con el inicio de la actividad laboral (entre las 7h y 10h), y se mantiene constante hasta las 21h cuando comienza a decrecer. Un estudio comparativo demuestra que la razón de diferencia del valor promedio de la noche y del día es similar (1.33 en el primer período vs. 1.39 en el segundo). Que se encuentren coincidencias en el comportamiento a lo largo del día y además en la razón de diferencia entre las franjas horarias de mayor y menor concentración, permite afirmar que se ha conseguido caracterizar el fondo de los niveles de concentración de partículas en la ciudad de Valladolid y su comportamiento diario.

PREDICTION OF BLACK CARBON CONCENTRATION IN AN URBAN SITE BY MEANS OF DIFFERENT REGRESSION METHODS

CARLOS MARCOS[1], SARA SEGURA[1], GUSTAVO CAMPS-VALLS[2], VÍCTOR ESTELLÉS[1], ROBERTO PEDRÓS[1], PILAR UTRILLAS[1], J. ANTONIO MARTÍNEZ-LOZANO[1]

[1]*Solar Radiation Group, Department of Earth Physics and Thermodynamics, University of Valencia. C/Doctor Moliner 50*
Burjassot (Valencia), Spain, Carlos.Marcos@uv.es

[2] *Image Processing Laboratory (IPL) Parc Científic Universitat de València C/ Catedràtic José Beltran, 2 46980 Paterna (València). Spain*

Black carbon (BC) aerosol is a type of carbonaceous material produced as a result of combustion processes which include motor vehicle emissions, biomass burning, and industry. In urban sites, BC contributes significantly to the air pollution which is one of the major environmental problems in developed countries as it has great impact on human health, visibility, and Earth's climate system. BC concentrations are strongly related to local sources and affected by meteorological conditions. It has a short atmospheric lifetime (days to weeks) and it is quickly removed from the atmosphere by deposition.

The aim of this work is to analyze the performance of different regression methods in the prediction of BC concentration from meteorological and traffic data. The measuring station is located in the University Campus of Burjassot, within the metropolitan area of Valencia (~1,800,000 inhabitants) in Eastern Spain. BC concentrations are measured by a 7-wavelength Aethalometer, while wind speed and wind direction data are collected by a meteorological station. Traffic data, consisting on vehicle counts of the close by CV-35 highway, are provided by Valencia city council, and boundary layer data, height and stability, are obtained by means of the HYSPLIT model. Data are averaged (BC and wind) or interpolated (traffic and boundary layer) to a 20 minutes resolution. A total of 22 months of measurements are available, corresponding to more than 35000 cases.

The regression methods are used to relate the BC measured at a time t_1 with the BC measured in $t_1 - \Delta t$ and the meteorological parameters and traffic volume measured during Δt. Four different methods are used: Regularized Linear Regression (RLR), Boosting Trees (BT), Kernel Ridge Regression (KRR) and Gaussian Process Regression (GPR).

According to the correlation factor (R), and the root-mean-squared difference (RMSD) obtained in the comparison of the logarithm of the measured and the predicted BC concentration, we find that the best results are obtained by KRR and GPR for all Δt considered. For example, if we take $\Delta t = 360$ min, we get for the correlation: $R_{RLR} = 0.74$, $R_{BT} = 0.82$, $R_{KRR} = 0.86$, $R_{GPR} = 0.86$; and for the RMSD: $RMSD_{RLR} = 0.522$, $RMSD_{BT} = 0.447$, $RMSD_{KRR} = 0.405$, $RMSD_{GPR} = 0.403$.

PRELIMINARY STUDY ON ULTRAFINE PARTICLES AND OC-EC OF ATMOSPHERIC PARTICULATE MATTER IN OLIVE AREAS OF ANDALUCIA

ANA Mª SÁNCHEZ DE LA CAMPA[1], ROCÍO FERNÁNDEZ CAMACHO[1], PEDRO SALVADOR[2], ESTHER COZ[2], BEGOÑA ARTIÑANO[2], JESÚS D. DE LA ROSA[1]

[1] *Associate Unit CSIC-UHU "Atmospheric Pollution". Center for Research in Sustainable Chemistry (CIQSO), University of Huelva, Campus El Carmen E21007, Huelva, Spain,* ana.sanchez@pi.uhu.es

[2] *Environment Department, CIEMAT, Avda. Complutense 40, Madrid E28040, Spain*

Andalucía is the region with the largest area of olive groves of Spain, estimated at about 1.5 million hectares, 30% of the cultivated area (Junta de Andalucía, 2002). The main olive groves areas are Jaén (0,57 MHa), Córdoba (0,34 MHa) and Sevilla (0,22 MHa). Although the production of olives and olive oil is the main commercial interest, in recent years it is using different agricultural wastes in power generation. The olive oil production generates large amounts of solid waste ("alperujo"). The treatment of this solid waste with high relative humidity (up 80%RH) in olive oil refineries produces a dry residue ("orujillo"), which is used as fuel in the biomass boilers and energy production plants of 25 MW. 270.000 annual Tn of biomass are submitted to combustion, generating atmospheric emission of pollutant gases and particulate matter, which could negatively affect the air quality in rural areas of Andalucía.

In this work, monitoring of the air quality in the olive groves area of Baena (Córdoba, South of Spain) was performed between November 2013-March 2014. We present preliminary data of ultrafine particles (UFP) and black carbon (BC) using CPC, MAAP and Aethalometer. Chemical composition of atmospheric particulate matter (PM10) was obtained on filters collected with a MCV high volume captor in order to know the source contribution of PM. A portion of 1.5 cm^2 of each filter was used for the elemental analysis of organic and elemental carbon (OC and EC) by a Thermal-Optical transmission technique, using a Sunset Laboratory OC-EC Analyser with the EUSAAR_2 temperature protocol.

The main constituents of biomass combustion emissions in waste treatment plants olive are volatile organic compounds and fatty acids. In addition, maximum concentrations were observed in OC and K. Mean concentrations of PM10 are low compared to the annual EU limit value of 40 µg m^{-3} (2008/50/CE European Directive; EU, 2008). However, exceedances of the daily 50 µg m^{-3} limit can occur. Peaks of UFP levels and OC-EC concentrations during the late afternoon have been related with local domestic combustion sources. Ctotal concentration represents 30-50% of PM10, being OC the dominant specie (85% of Ctotal). Olive wood burning is considers as an important source in PM during winter in this region.

References
EU, 2008. 2008/30/CE Council Directive on Ambient Air Quality and Cleaner Air for Europe. The Council of the European Union.

Junta de Andalucía (2013) Aforo de Olivar Campaña 2013-2014. Web link http://bit.ly/1plCVBQ

RELATION BETWEEN THE CLOUD RADIATIVE FORCING AT SURFACE AND THE AEROSOL OPTICAL DEPTH

M.D. FREILE-ARANDA[1], J.L. GÓMEZ-AMO[1, 2],M.P. UTRILLAS[1],
J.A. MARTÍNEZ-LOZANO[1]

[1]*Departamento de Física de la Tierra y Termodinámica, Universidad de Valencia, Dr. Moliner 50 Burjassot (Valencia), M.Dolores.Freile@uv.es*

[2]*Laboratory for Earth Observations and Analyses, ENEA, Rome*

Clouds are one of the most important factors that regulate the Earth's climate. They interact scattering and absorbing solar and thermal radiation. Because of this interaction, clouds modify the quantity of radiation that reaches the Earth'ssurface.The cloud radiative forcing (CRF) shows us the changes that clouds produce on net radiation and it is defined as the difference between the net radiation in all sky and clear sky conditions. Another important factor is the presence of aerosols, because they interact with the radiation too, but differently from clouds. They can directly scatter or absorb radiation, but also alter the microphysical properties of clouds, so the radiative effects of clouds will change.

In this work we will analyse the influence of aerosols on the cloud radiative forcing at surface, using the aerosol optical depth (AOD) and considering the shortwave and longwave spectral regions. This way, we will see how the AOD affects the radiative properties of clouds at the Iberian Peninsula from March of 2000 to December of 2012.

All the data employed in this work has been obtained from CERES. CERES (Clouds and Earths Radiant Energy System) is an instrument on board of the satellite Terra which provides global estimations of the radiative fluxes of the atmosphere, clouds properties and other atmospheric characteristics. Some of these come from the instrument MODIS (Moderate Resolution Imaging Spectrometer), located on Terra too, as it happens with the aerosol information. To calculate the cloud radiative forcing we will use the shortwave and longwave fluxes given by CERES at surface, while the aerosol optical depth is registered by MODIS. The spatial resolution of the data used is of 1° longitude x 1° latitude, while the temporal resolution is daily.

Results show us that if we consider the longwave radiation, the CRF does not suffer large changes when the AOD at 470nm increases. But, in the case of the shortwave radiation, the AOD can produce an increase of 60W/m^2 on the CRF, what proves the influence of aerosols on the cloud radiative forcing.

RELATIVE CONTRIBUTION AND ORIGIN OF BLACK CARBON DURING A HIGH CONCENTRATION WINTER EPISODE IN MADRID

M. BECERRIL[1], E. COZ[1], A.S.H PRÉVÔT[2], B. ARTÍÑANO[1]

[1]*Department of Environment, CIEMAT, Avd. Complutense 40, Madrid, ES-28040, Spain, marta.becerril@ciemat.es*

[2]*Laboratory of Atmospheric Chemistry, Paul Scherrer Institut. Villigen-PSI, CH-5232, Switzerland*

Black carbon (BC) is considered the most strongly light-absorbing component of particulate matter (PM), and is a product of the incomplete combustion of fossil fuels, biofuels, and biomass burning (EPA, 2012). In a very populated urban metropolitan area, such as Madrid, where there is no industry nearby and the principal sources are traffic and domestic activities, BC can be considered as one of the most important components within the aerosol chemical atmospheric field. Therefore, BC monitoring has become a goal to accomplish for the city.

The main objective of this work was to study the aerosol light absorption coefficient at Ciemat station in Madrid by means of two 7-wavelength Aethalometers (Magee Sci. mod. AE33, Aerosol d.o.o., Slovenia) during a weekly winter thermal inversion period in January 2014. The two Aethalometers were measuring in parallel with $PM_{2.5}$ and PM_1 cut-off size, at a flow rate of 5 L/min. Data were recorded with a time-resolution of 1 minute. The meteorological situation was characterized by subsidence and hence temperature inversions with altitude, it was dominated by high pressures and low wind speeds (with an average wind speed of 2.02 ± 1.31 m/s). BC was calculated using the measurement at 880 nm wavelength (mass absorption cross-section, MAC = 7.77 m^2/g), while the Ultraviolet-absorbing Particulate Matter (UVPM) was estimated at the 370 nm wavelength (mass absorption cross-section, MAC = 18.47 m^2/g), which indicates the presence of organic compounds such as are found in wood smoke and biomass-burning smoke.

$PM_{2.5}$ BC hourly average concentrations ranged from 0.21 ± 0.03 μg/m^3 to 17 ± 5 μg/m^3 during the period of study. Results showed that the evolution of the $PM_{2.5}$ BC concentrations carried out at Ciemat during the small anticyclonic situation were in concordance with the averaged $PM_{2.5}$ mass concentration levels of the average of all stations from the Madrid city Council air quality monitoring network, which ranged from 2 μg/m^3 to 56 μg/m^3. The contribution of BC represented 39 ± 19 % of the total chemical species monitored at Ciemat (BC, inorganic and organic compounds) and 33 ± 19 % of the averaged $PM_{2.5}$ mass concentration levels of the average of all stations from the Madrid Network. A linear regression analysis of the data from the $PM_{2.5}$ BC and PM_1 BC cut-off sizes suggested that 98.2 ± 0.6 % of BC was present in the submicrometric fraction of the atmospheric aerosol particles. The measurements at ultraviolet (UVPM, 370 nm) and near infrared (nIR-BC, 880 nm) wavelength channels were evaluated (Sandradewi et al., 2008) and ratios close to the unity suggest that there was no important contribution from biomass burning origin to the high BC concentrations during the event.

References

[1] U.S. EPA., 2012. Report to Congress on Black Carbon, http://www.epa.gov/blackcarbon/
[2] Sandradewi et al., 2008. Atmos. Environ. 42, 101-112. DOI: 10.1016/j.atmosenv.2007.09.034

ROLE OF THE SPHEROIDS PARTICLES ON THE CLOSURE STUDIES FOR MICROPHYSICAL-OPTICAL PROPERTIES

M. SORRIBAS[1,2], F. J. OLMO[1,2], A. QUIRANTES[1], J.A. OGREN[3], M. GIL-OJEDA[4] AND L. ALADOS-ARBOLEDAS[1,2]

[1]*Department of Applied Physics, University of Granada, Granada, 18071, Spain*
[2]*Andalusian Institute for Earth System Research (IISTA), University of Granada, 18006, Spain*
[3]*Earth System Research Laboratory, NOAA, Boulder, 80305, USA*
[4]*Atmospheric Research and Instrumentation Branch, INTA, Madrid, 28850, Spain*

The natural and anthropogenic atmospheric particles alter the Earth's energy budget and they are drivers of climate change. To evaluate the influence of aerosols on the solar radiation a rigorous knowledge of the absorption and scattering processes is needed. For the sake of simplicity it is common to use spherical geometry when studying atmospheric aerosols. However, they rarely exhibit a spherical shape, being its geometry significantly more complex. Some examples of non-spherical particles are volcanic ash, desert dust and the sea salt particles. The knowledge of non-spherical particles is poor and the limitation in climate models is known, making necessary more achievements in this direction.

In order to carry out studies about the scattering properties, theoretical calculations are computed using the Mie or the T-matrix Theory (i.e. Mishchenko and Travis, 1998), assuming homogeneous and spherical particles or non-spherical particles, respectively.

The Mie model and T-matrix code can be also used to clarify the uncertainties associated with the instrumentation for measuring microphysical and optical aerosol properties. One example of this application is the study of the uncertainty of an integrated nephelometer, instrument widely used to measure the aerosol scattering and backscattering properties. It integrates the scattered light by the particles from a volume of air ideally over a full range of angles from 0º to 180º. All these directions are required for an accurate study of the aerosol scattering properties. However, a systematic uncertainty of the integrating nephelometry technique is that the light scattered is truncated near-forward and near-backward direction below 7º. This limitation is commonly known as the angular truncation error. Taking into account that the nephelometer was included as reference instrumentation for aerosol scattering monitoring of the World Meteorological Organization (WMO), an effort to improve the accurate measurement was carried out over the last few decades. One of the most popular corrections was presented in Anderson and Ogren (1998), where a parameterization of the truncation correction is determined by the ratio between full and truncated scattering computed by Mie Theory for spherical particles. The effect to the particle size was also taken into account in terms of the experimentally determined Ångström exponent (å) which is related directly to the particle size. However, this popular correction has some limitations related to the particle shape and size range (i.e., Quirantes et al., 2008).

In this study we present the results of a field campaign performed to examine instrumental closure in aerosol optical and microphysical properties with the aim: (1) to compare the observed and the computed optical properties, using the spherical and spheroids approximations; and (2) to analyse the angular truncation correction in terms of sub- and super-micron particles size ranges.

Anderson, T.L. and Ogren, J.A. 1998. Determining aerosol radiative properties using the TSI 3563 integrating nephelometer. Aerosol Sci Technol, 29:57–69.

Mishchenko, M. I. and Travis, L. D. 1998. Capabilities and limitations of a current Fortran implementation of the T-matrix method for randomly oriented rotationally symmetric scatterers. JQSRT, 60, 309–324.

Quirantes, A., Olmo, F.J., Lyamani, H. and Alados-Arboleda, L. 2008. Correction factors for a total scatter/backscatter nephelometer. JQSRT, 109, 1496-1503.

SAHARAN DUST PROFILING DURING AMISOC 2013 CAMPAIGN: OPTICAL AND MICROPHYSICAL PROPERTIES DERIVED FROM MULTI-PLATFORM IN-SITU AND REMOTE SENSING TECHNIQUES

CARMEN CÓRDOBA-JABONERO[1]*, JAVIER ANDREY[1], LAURA GÓMEZ[1], M.C. PARRONDO[1], JOSÉ ANTONIO ADAME[1], OLGA PUENTEDURA[1], EMILIO CUEVAS[2], MANUEL GIL-OJEDA[1]

[1]*Instituto Nacional de Técnica Aeroespacial (INTA), Atmospheric Research and Instrumentation Branch, Ctra. Ajalvir km.4, Torrejón de Ardoz-28850, Madrid, Spain, *cordobajc@inta.es*

[2]*Agencia Estatal de Meteorología (AEMET), Atmospheric Research Centre of Izaña, Sta. Cruz de Tenerife, Spain*

The vertical distribution of dust is a key parameter for atmospheric radiative forcing assessment (IPCC 2013). In addition, height-resolved information of the dust properties is also required for aerosol forecast modeling and satellite data validation. Canary Islands offer a suitable site as located downwind of the Saharan sources for dust monitoring. The arrival of dust plumes to that area is a regular feature, more frequently observed in summertime and extended up to high altitudes. The vertical characterization of individual dust events is relevant for the determination of the so-called Saharan Air Layer (SAL), defined as a mass of warm and dusty air, in order to evaluate the climate impact of such phenomena, even at local scales.

AMISOC-Tenerife (AMISOC-TNF) is a multi-instrumented campaign devoted to study the behavior of minor traces gases under clean skies and heavy aerosol loading, and in particular focused on dust impact in climate-related studies. Simultaneous aerosol observations were carried out extending from 01 July 2013 to 05 August 2013 (36 days), by using different platforms and techniques: airborne (aboard INTA aircraft C-212) in-situ measurements together with ground-based remote sensing observations by aerosol LIDAR and columnar-integrated sun-photometry, and MAX-DOAS instruments were deployed as well. Attempts of aerosol profile inversion (using O_4 signature retrievals) have also been performed. Both backtrajectories of air masses and meteorological analysis complete this study. Table 1 summarizes the main instrumentation and techniques used for aerosol profiling observations.

Table 1. Instrumentation/techniques used for aerosol profiling observations in AMISOC-TNF (*).

Instrument / technique	Platform	Measurements	Particle parameter
PCASP (OPC)	Airborne	In-situ, vertical profiles	SD (acc. mode: < 3 μm)
CAPS (OPC)	Airborne	In-situ, vertical profiles	SD (acc. + coarse: 0.5-50 μm)
LIDAR (MPL)	Ground-level	Remote sensing, vertical profiles	EX, BS, LR
Sun-photometer (CIMEL)	Ground-level	Remote sensing, columnar-integrated	AOD, AEx, SD
MAX-DOAS	Ground-level	Remote sensing, vertical retrieval	O_4 signature

(*) AEx – Angstrom Exponent, AOD – Aerosol Optical Depth, BS – BackScattering coefficient, EX – EXtinction coefficient, LR – Lidar Ratio, MAX-DOAS - Multi AXis Differential Optical Absorption Spectroscopy, MPL – Micro Pulse Lidar, OPC - Optical Particle Counter, and SD – Size Distribution.

In this work we present preliminary results obtained for SAL characterization in AMISOC-TNF campaign, reporting dusty conditions during 50% of the overall time (18 out of 36 days). This study focuses on the optical and microphysical properties of the Saharan dust layer including vertical aspects (single/multi-layered structure, top height, ...) of the dusty episodes, in addition to other dust features (Free-Troposphere dust contribution to the total AOD, LR frequency, particle SD mode predominance, ...).

SEASONAL VARIATION OF AEROSOL PROPERTIES IN SOUTHERN SPAIN

I. FOYO-MORENO[1,2], I. ALADOS[3], H. LYAMANI[1,2], F.J. OLMO[1,2], L. ALADOS-ARBOLEDAS[1,2]

[1]*Departamento de Física Aplicada, Universidad de Granada, Granada, Spain*

[2]*Andalusian Institute for Earth System Research (IISTA-CEAMA), Granada, Spain*

[3]*Departamento de Física Aplicada II, Universidad de Málaga, Málaga, Spain*

In this work we have compared aerosol properties at two locations in South of Spain (Granada and Málaga), an urban site and a coastal site, respectively. In this analysis we used columnar aerosol proprieties measured during three years (2010, 2011 and 2012). Columnar aerosol properties were measured by a CIMEL sun/sky photometer, which is the standard sun/sky photometer used in the AERONET network (Holben et al., 1998). This instrument is within RIMA (http://www.rima.uva.es/RIMA/) Iberian network of sun-photometers included in AERONET.

The aerosol optical depth (AOD) shows a very clear annual cycle at both sites, with maximum in summer (0.22 ± 0.14 at Málaga and 0.20 ± 0.13 at Granada, at 440 nm) and minimum in winter at Granada (0.14 ± 0.08) and in autumn at Málaga (0.11 ± 0.08). The fine mode fraction (FMF) also showed a clear seasonal pattern but opposite to that of AOD, with maximum in winter and minimum in summer at both sites (0.71 ± 0.18 and 0.42 ± 0.14 at Granada; 0.61 ± 0.17 and 0.46 ± 0.13 at Málaga), suggesting predominance of fine particles in winter and coarse particles in summer at both sites and the presence of more fine particles in the aerosol population over Granada in comparison to Málaga. We have also found significant differences in the single scattering albedo obtained in both sites(ω_o), with lower values over Granada. The minimum ω_o value (0.75 ± 0.22) was obtained in autumn over Granada and (0.87 ± 0.11) in winter over Málaga. The ω_o maximum values (0.90) were found in summer for both locations. The coarse mode radius shows value close to 5.1 µm at Málaga and 2.2 µm at Granada. This difference may be related to the difference in the relative humidity. This preliminary analysis reveals substantial differences in the aerosol properties observed at both sites.

SEASONAL VARIATION OF PM$_1$ MAIN COMPONENTS AT A TRAFFIC SITE IN SOUTHEASTERN SPAIN

NURIA GALINDO[1], EDUARDO YUBERO[1], JOSE FRANCISCO NICOLÁS[1], SILVIA NAVA[2], GIULIA CALZOLAI[2], MASSIMO CHIARI[2], FRANCO LUCARELLI[2], JAVIER CRESPO[1]

[1]*Department of Physics, Miguel Hernández University, Avda. Universidad, 03202, Elche, Spain, ngalindo@umh.es*

[2]*Department of Physics, University of Florence and INFN, via Sansone 1, I-50019, Sesto Fiorentino, Italy*

In the present work the major ionic (SO$_4^{2-}$, NO$_3^-$, NH$_4^+$) and carbonaceous components (OC and EC) of PM$_1$ were measured from March 2011 to September 2012 in a street canyon in Elche (southeastern Spain). Daily samples were collected using a low volume sampler (2.3 m^3 h^{-1}) and analyses of ions and carbonaceous species were carried out by ion chromatography and a themal-optical method, respectively.

The average PM$_1$ concentration for the whole study period was 13.3 µg m^{-3}. As expected, OC was the main component, accounting for almost 30% of the total concentration, followed by sulfate (16%) and EC (11%). Ammonium represented 6% of the average PM$_1$ concentration, while the contribution of nitrate was only 3%.

PM$_1$ levels showed little seasonal variations, although concentrations were slightly higher in winter and summer (14.8 and 13.6 µg m^{-3}, respectively) than in autumn and spring (12.5 µg m^{-3}). This was probably due to the different seasonal cycles of PM$_1$ major components (Fig. 1).
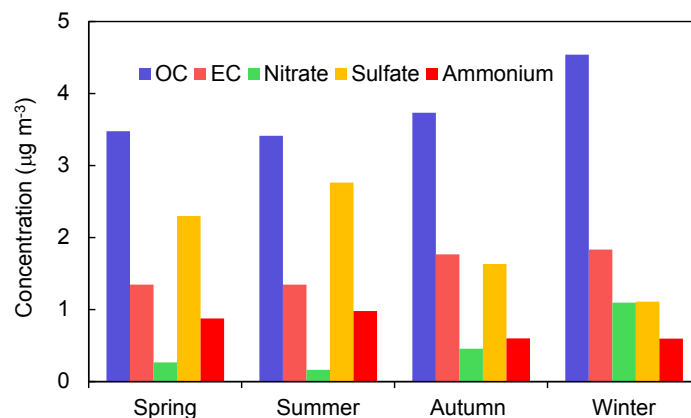

Figure 1. Seasonal average concentrations of PM$_1$ main components at a traffic site in Elche

OC levels were highest in winter due to the lower temperatures that favor the condensation of organic compounds and the higher frequency of stagnant conditions, which promote the accumulation of pollutants. For EC, the greatest average concentrations were observed in winter and autumn. Since traffic, the dominant source of EC in Elche, was quite constant at the sampling site, the increase in EC levels in the cold months was most likely due to the higher occurrence of stagnant conditions. Sulfate and ammonium maximum concentrations were measured in summer as a result of the higher photochemical oxidation rate of SO$_2$ to NH$_4$SO$_4$. As regards nitrate, it exhibited much greater seasonal variation than the other PM$_1$ components, since the winter average concentration was about a factor of 7 higher than the summer one. This is due to the lower winter temperatures that prevent the evaporation of semi-volatile ammonium nitrate and the higher occurrence of stagnant conditions that favor the formation of this compound.

SHORTWAVE AND LONGWAVE AEROSOL RADIATIVE EFFECTS DURING A STRONG DESERT DUST EVENT AT GRANADA (SPAIN)

M. ANTÓN[1], A. VALENZUELA[2,3], D. MATEOS[4], I. ALADOS[5], I. FOYO-MORENO[2,3], F.J. OLMO[2,3], L. ALADOS-ARBOLEDAS[2,3],

[1]*Departamento de Física, Universidad de Extremadura, Badajoz, Spain, mananton@unex.es*

[2]*Departamento de Física Aplicada, Universidad de Granada, Granada, Spain*

[3]*Andalusian Institute for Earth System Research (IISTA-CEAMA), Granada, Spain*

[4]*Grupo de Óptica Atmosférica, Universidad de Valladolid, Valladolid, Spain*

[5]*Departamento de Física Aplicada II, Universidad de Málaga, Málaga, Spain*

Dust aerosol particles interact with both solar and terrestrial radiation, affecting directly Earth's radiative budget and hence the climate system. This work studies the influence of a very intense Saharan dust event on shortwave (SW) and longwave (LW) downwelling irradiance recorded at Granada (Spain) during 6 September 2007. This episode has been identified as one of the strongest dust events recorded in Southern Spain in the last ten years. The contribution of coarse mineral dust particles to the aerosol load was evidenced from the large aerosol optical depth (between 0.8 and 1.5) and the small Ångström exponent (between 0.1 and 0.25) values derived from sun-photometer measurements. This high-aerosol load case allows to obtain a reasonably accurate estimate of the LW aerosol radiative effect since in most cases this effect is small and is within the uncertainties associated with the LW measurements.

The SW and LW instantaneous aerosol radiative effects are determined as the difference between downwelling irradiances measured every minute during the dust event day (6 September) and the equivalent experimental data recorded during a nearby dust-free day (3 September). SW data (0.305 to 2.800 μm) and LW measurements (4 to 100 μm) were simultaneously measured by a CM-11 pyranometer (Kipp & Zonnen) and an Eppley pyrgeometer model PIR, respectively. When the highest AOD values were measured (around solar noon), the SW instantaneous aerosol effect reached values between -180 and -190 W/m^2, while the LW effect exhibited values between +40 and +45 W/m^2 (about 23% of the SW effect). This result shows that LW irradiance may compensate a non-negligible part of the strong SW decrease observed at surface during desert dust episodes. Furthermore, daily (24 h) average of the instantaneous effects is calculated due to its great interest from a climatic point of view. The aerosol radiative perturbation in the LW spectral range acts continuously over the 24 h, differently from the effects in the SW spectral range. In this sense, the daily averages of the SW and LW aerosol radiative effects showed values of -57 W/m^2 and +22 W/m^2, respectively. Overall, on daily average, the LW radiative effect is large and contributed significantly (around 40%) to offset the SW effect detected during the studied strong dust event.

Solar global radiation and its relationship with aerosol characteristics over Varanasi (25° 20' N, 83° 00' E)

B. P. Singh[1*], P. Agarwal[2], S. Tiwari[3], A. K. Srivastava[3], R. K. Singh[1], and Manoj K. Srivastava[1]

1. Department of Geophysics, Banaras Hindu University, Varanasi- 221005, India, E-mail: bpsrathaur@gmail.com

2. Department of Physics, Indian Institute of Technology-BHU, Varanasi - 221005

3. Indian Institute of Tropical Meteorology ó Delhi Centre, New Delhi ó 110060, India

We first time calculated solar global radiation (G,W/m^2) using SMARTS (Simple Model of the Atmospheric Radiative Transfer of Sunshine) model over Varanasi (25° 20' N, 83° 00' E), India located in the eastern part of Indo Gangetic Plain and result are validated with satellite and ground based measurement data. Its variation with aerosol characteristic is studied for this region. Results are found to be similar in trend, however, some bias is noticed during specific seasons. Results encourage to use the SMARTS model results for computation of solar radiation for places where direct measurements are not available.

SOURCES OF ULTRAFINE AND BLACK CARBON PARTICLES IN SEVILLE URBAN CITY

R. FERNÁNDEZ-CAMACHO[1], S. RODRÍGUEZ[2], J.D. DE LA ROSA[1]

[1] Associate Unit CSIC-University of Huelva "Atmospheric Pollution", Center for Research in Sustainable Chemistry (CIQSO), University of Huelva, 21071, Huelva, Spain

[2] Izaña Atmospheric Research Centre, AEMET Joint Research Unit to CSIC "Studies on Atmospheric Pollution", La Marina 20, planta 6, Santa Cruz de Tenerife, E38071, Canary Islands, Spain.

Urban air quality impairment by ultrafine particles (diameter < 0.1 μm) has become in matter of concern due to adverse effects on human health (Araujo and Nel, 2009). Most of studies on ultrafine particles in urban air quality have focused on vehicle exhaust emissions (Kumar et al., 2014). Thus, ultrafine particle emissions in vehicle exhaust has recently been subject to limit values in a recent stage of the EURO standards. In addition, black carbon concentrations, mainly present in the ultrafine fraction, is currently being discussed in science and environmental policy areas due to the effects on the human health (Class 1 carcinogen; WHO, 2012) and climate change (IPCC, 2013).

We present a study based on the assessment of particle number concentration, black carbon, gaseous pollutants, meteorological parameters, road traffic intensity and composition of $PM_{2.5}$ with daily resolution in Seville urban city. This research is based on experimental data collected between March 2012 and June 2013.

The increase in road traffic intensity / wind speed in the rush hours correlated with PN, BC and NO_x concentrations pointing that fresh vehicle exhaust emissions and dilution/ventilation conditions modulate the behaviour of these pollutants. The vehicle exhaust emissions are the main source of ultrafine particles in Seville. However, other sources can contribute at midday with the breeze circulation according to Guadalquivir Valley orography. The high linearity observed between PN and BC with road traffic intensity allows concluding that the BC concentration increases in 1 μg / m^3 per 250 vehicles in circulating. This conclusion could be used by a manager of air quality to reduce ultrafine particles pollution by limiting the number of vehicles at a given point.

In Seville, like others European cities (Reche et al., 2011), ultrafine particles concentrations show a maximum during the morning rush hours due to the vehicle exhaust emissions. BC concentrations are similar to those recorded in Barcelona and slightly lower than those observed in London and Lugano.

Araujo, J.A., Nel, A.E., 2009. Particle and Fibre Toxicology 6, 24.

Kumar et al., 2014. Environmental International 66,1-10.

Reche et al., 2011. Atmos. Chem. Phys., 11, 6207–6227, 2011.

STUDY CASES OF SHRINKAGE EVENTS OF THE ATMOSPHERIC AEROSOL

E. ALONSO-BLANCO[*], F.J. GÓMEZ-MORENO, L. NÚÑEZ, M. PUJADAS AND B. ARTÍÑANO

*Department of Environment, Research Center for Energy, Environment and Technology (CIEMAT), Avda. Complutense 40, 28040, Madrid, Spain, *elisabeth.alonso@ciemat.es.*

While the mechanisms of formation and growth of new atmospheric particles have been widely studied, changes related to the decrease of the size of already formed particles, *a.k.a.* shrinkage, have been understudied, partly due to the complex characteristics of these processes.

Shrinkage phenomena, which can occur after the aerosol's nucleation/growth process, are associated mainly to the evaporation of condensed semivolatile species, especially when the condensation process or the chemical reactions involved in the growth of particles are reversible.

The implication of meteorological variables in the shrinkages is decisive. The ocurrence of these processes is determined by changes in the atmospheric conditions, being especially crucial the wind speed and temperature increases (*Cusack et al.,* 2013; *Young et al., 2013*).

In order to study this phenomena, aerosol and gases measurements carried out in the urban background station located at the CIEMAT facilities in Madrid (Spain) during the period 2009-2012 have been analysed. A Scanning Mobility Particle Size (TSI-SMPS; DMA 3081 with CPC 3775) provided the aerosol size distribution in the range 15-600 nm. To document the physic-chemical characteristics of the air masses a Differential Optical Absorption Spectrometer (DOAS: OPSIS AR-500) provided the ambient concentrations of NO, NO_2 and O_3, and the meteorological parameters were obtained by a permanent tower at the site.

In this urban background station some shrinkage processes have been identified during the summer period. Mostly, these shrinkages took place after nucleation processes formation (NPF) and, to a lesser degree, after aerosol growth processes.

The objective of this work is to accomplish a detailed study of various NPF+shrinkage and growth process+shrinkage events of the atmospheric aerosol. With this aim, the evolution of the particle concentration, the estimation of the condensation sink (CS), the sulfuric acid concentration in gas phase, the growth/evaporation rate and the impact of meteorological variables have been analyzed.

References

Cusack, M., Alastuey, A., & Querol, X., 2013. *Case studies of new particle formation and evaporation processes in the western Mediterranean regional background. Atmospheric Environment, 81, 651-659.*

Young, L. H., Lee, S. H., Kanawade, V. P., Hsiao, T. C., Lee, Y. L., Hwang, B. F., Hsu, H. T., & Tsai, P. J., 2013. *New particle growth and shrinkage observed in subtropical environments. Atmospheric Chemistry & Physics, 13(2).*

STUDY OF THE INDUSTRIAL EMISSIONS IMPACT ON AIR QUALITY OF THE CITY OF CORDOBA

Y. GONZÁLEZ-CASTANEDO[1], M. AVILÉS[1], J. CONTRERAS GONZÁLEZ[2], C. FERNÁNDEZ[2], J.D. DE LA ROSA[1]

[1]*Associate Unit CSIC-University of Huelva "Atmospheric Pollution", Center for Research in Sustainable Chemistry (CIQSO), Campus El Carmen s/n, University of Huelva, 21071, Spain*
[2]*Consejería de Agricultura, Pesca y Medio Ambiente, Manuel Siurot 50, 41071, Sevilla, Spain*

Cordoba is one of the main touristic destinations located in the South of Spain in Andalusia region. The city has a population around 300.000 inhabitants and road traffic may be considered its main source of air pollution (Lozano et al., 2009, Amato et al., 2013). However, a regional study carried out by de la Rosa et al., (2010) shows how the maximum Cu, Zn and Cd levels of Andalusia region were registered in Lepanto, an urban background site located in Cordoba city. These levels were higher than ones registered in historical metallurgy polluted areas such as Huelva. In this study we carried out an intensive measurement campaign in October 2012 with the aim of investigating the relationship between several metallurgic airborne emissions and the geochemical anomalies observed at the city since 2007. The campaign consisted on different particulate matter (PM) measurements and subsequent detailed chemical characterization by ICP-MS: a) stack emissions samples from the three metallurgy industries (copper and brass) located at SW of the city which are currently active b) TSP fugitive emissions and bulk deposition samples inside the metallurgy installations c) ground levels impact in the immediate environment outside the industry and d) daily PM immision samples in three sites located in the city. The monitoring stations were a high school located near of the industrial area (IES Zoco) and two monitoring sites (Lepanto and Asomadilla) belongs to Andalusia

Figure 1. A) Monitoring sites and metallurgy area in the city of Cordoba B) Immision (ng m^{-3}) and emissions (µg m^{-3}) trace metals content.

Autonomus Air Quality Network (Figure 1-A). In addition, a geochemical database of PM10 samples collected during 2007-2012 in Lepanto site has been interpreted according to meteorological and gas pollutants parameters. Results show high concentrations of toxic elements (Cu, Zn, Cd, Pb, Cr and Sn specially) due to the impact from industrial activity on the city of Córdoba. Figure 1-B shows the high trace metal concentration observed at the three monitoring sites. All of these metals were identified in the cocktail of pollutants emanating from different stacks and fugitive emissions from the metallurgy industry.
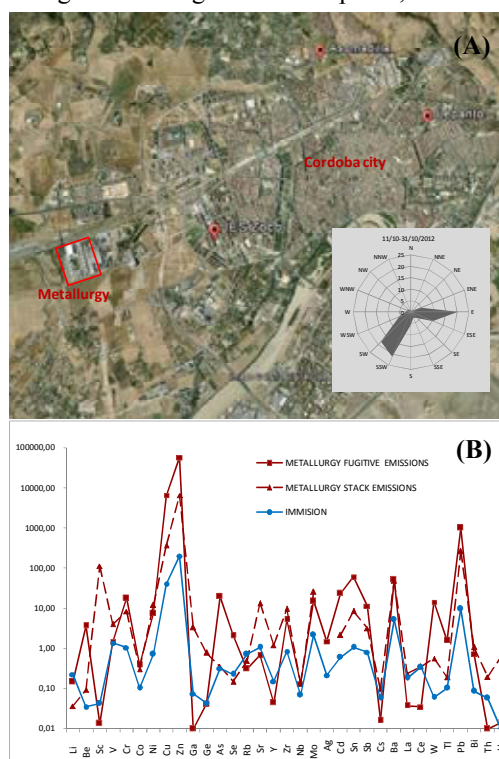
Lozano A. et al., (2009) Microchemical Journal 93, 211-219.
de la Rosa, J.D. et al., (2010) Atmospheric Environment 44, 4595-4605.
Amato F. et al., (2013) Atmos. Chem. Phys. Discuss., doi:10.5194/acpd-13-31933-2013.

STUDY OF THE OPTICAL AND HYGROSCOPIC PROPERTIES OF ATMOSPHERIC AEROSOLS DURING A HIGH CONCENTRATION WINTER EPISODE IN MADRID

M. BECERRIL[1], E. COZ[1], M. LABORDE[2,3], S.N. PANDIS[2,3,4], B. ARTÍÑANO[1]

[1]*Department of Environment, CIEMAT, Avd. Complutense 40, Madrid, ES-28040, Spain, marta.becerril@ciemat.es*

[2]*Department of Chemical Engineering, University of Patras, Caratheodory 1, University Campus, Patras, GR-265 04, Greece*

[3]*AerosolConsultingML GmbH, Ennetbaden, Switzerland*

[4]*Ecotech Pty Ltd, Knoxfield, Australia*

[5]*Institute of Chemical Engineering Science, Foundation for Research and Technology Hellas (ICEHT/FORTH), Leoforos Plastira 100, Iraklio, GR-700 13, Greece*

[6]*Department of Chemical Engineering, Carnegie Mellon University, Pittsburgh, PA-15213, USA*

Atmospheric aerosol particles undergo hygroscopic growth at high relative humidity (RH). As a consequence, their microphysical and optical properties – particularly the aerosol light scattering – are strongly conditioned by RH.

The main purpose of this work was to study the aerosol scattering enhancement due to water uptake and its relation with the aerosol chemical composition in Madrid during a small winter thermal inversion period, dominated by high pressures and low wind speeds.

The aerosol scattering enhancement at 525 nm of wavelength was estimated using the data obtained at very dry conditions (RH $\leq$ 15%) and ambient RH by means of two Nephelometers (Aurora 1000 and Aurora 3000 respectively, Ecotech Pty Ltd., Australia). The aerosol chemical composition was monitored with an ACSM (Aerosol Chemical Speciation Monitor, Aerodyne Research Inc., MA) and black carbon (BC) was estimated using the measurement at 880 nm of a 7-wavelength Aethalometer (mass absorption cross-section, MAC = 7.77 m^2/g) (Magee Sci. mod. AE33, Aerosol d.o.o., Slovenia).

The hygroscopic growth factor of aerosol scattering coefficient (f(RH)), defined as the ratio of the aerosol scattering coefficient at wet over dry conditions, is one of the key parameters needed for evaluating short-wave aerosol radiative climate forcing (McInnes et al., 1998). This parameter has been proven to be closely related to the aerosol volume growth factor (VGF) derived from the DAASS (Dry Ambient Aerosol Size Spectrometer) measurements, commonly used to estimate aerosol hygroscopicity (Pilinis et al., 2014).

Preliminary results from this event in Madrid confirmed previous measurements of the aerosol hygroscopic growth during polluted influenced episodes. As expected, the hygroscopic growth was related to inorganic species, and inorganic-organic mixtures, and inversely related to the concentrations of BC. The highest hygroscopic growth was observed in early morning hours, when RH was the highest.

References

[1] McInnes, L., et al., 1998. Geophys. Res. Lett., 25, 513-516. DOI: 10.1029/98GL00127.
[2] Pilinis C., et al., 2014. Atmos. Environ., 82, 144-153. DOI: 10.1016/j.atmosenv.2013.10.024.

TEMPORAL AND SPATIAL EVOLUTION STUDY OF AIR POLLUTION IN PORTUGAL

JOSE MANUEL FERNÁNDEZ-GUISURAGA[1], AMAYA CASTRO[1], CÉLIA ALVES[2],
ANA I. CALVO[1], ELISABETH ALONSO-BLANCO[3], ROBERTO FRAILE[1]

[1]*Department of Physics, IMARENAB University of León, 24071 León, Spain,*
jferng11@estudiantes.unileon.es

[2]*Centre of Environmental and Marine Studies, Department of Environment, University of Aveiro, 3810-193 Aveiro, Portugal*

[3]*Centro de Investigaciones Energéticas, Tecnológicas y Ambientales (CIEMAT), 28040 Madrid, Spain*

The current EU Directive on air quality (2008/50/EC) sets out a number of targets to improve environmental quality and human health. Ground level ozone and particulate matter ($PM_{2.5}$ and PM_{10}) are the pollutants of most concern in Europe.

During the study period (1995-2010) we analyzed the temporal evolution of several air pollutant concentrations (C_6H_6, CO, NO, NO_2, O_3, SO_2, $PM_{2.5}$ and PM_{10}) in mainland Portugal, especially in the most populated areas. Based on validated data collected from the "Agência Portuguesa do Ambiente" in air quality monitoring stations, we determined the annual and seasonal concentration trend by the Mann-Kendall trend test. We also evaluated monthly, seasonal and annual spatial distributions of these pollutants. Furthermore, we assessed the total annual emissions obtained from the revised EMEP/MSC-E models for mainland Portugal during the study period.

A significant decrease in the emission of most contaminants reported in national inventories was observed. However, the annual mean concentrations of photochemical species such as ozone is on a clear upward trend around the most densely populated areas, as can be seen in an urban background station located in the vicinity of Lisbon (Fig. 1). In mountainous rural areas within the NE of Portugal, the ozone concentration trend is stable or downward despite the fact that concentrations remain higher than in the more industrialized and populated coastline.
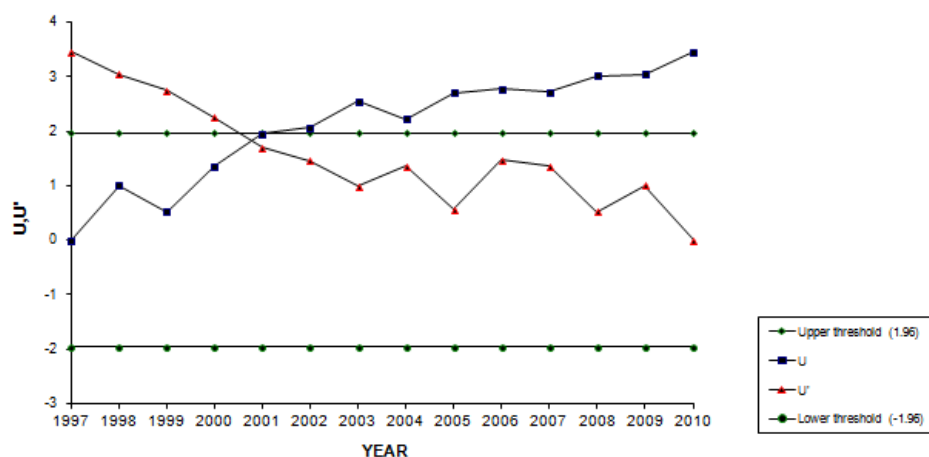

Fig. 1. Annual trend test (Mann-Kendall) for an urban background station in the vicinity of Lisbon.

TEMPORAL CHARACTERIZATION OF PARTICULATE MATTER OVER THE IBERIAN PENINSULA TO SUPPORT THE BRIGHTENING PHENOMENA IN THE LAST DECADES

D. MATEOS, V.E. CACHORRO, A. MARCOS, Y. BENNOUNA, C. TOLEDANO, M.A. BURGOS, A.M. DE FRUTOS

Grupo de Óptica Atmosférica, Universidad de Valladolid, Paseo Belén 7, 47011, Valladolid, Spain. e-mail: mateos@goa.uva.es

Surface solar irradiance (SSI) measurements from various regions around the globe exhibit an increase trend in the 1990s which continues after the 2000s. The Iberian Peninsula also shows this behavior, known as brightening phenomenon (BF). As BF affects the levels of SSI, it can have substantial impacts on Earth's radiative budget and global warming. BF has been attributed to changes in clouds and aerosols and their interactions. Aerosol particles are able to absorb and scatter part of the solar radiation in the atmosphere; hence, they can modify the radiative budget. Therefore, the main aim of this study is to evaluate the temporal trends of particulate matter (PM) over the whole Iberian Peninsula in order to translate the observed BF as a consequence of a reduction in the atmospheric aerosol load. The main parameter to show the change of aerosol load in the atmosphere is the columnar aerosol optical depth (AOD). However, due to the short series of measurements and poor sampling of AOD compared to PMx data, the latter was selected for this purpose in a comparative exercise. The measurements of the European Monitoring and Evaluation Programme (EMEP) were used to analyzed the evolution of suspended particulate matter (SPM), particulate matter under 10 μm (PM_{10}) and 2.5 μm ($PM_{2.5}$) in all the available Spanish stations. The time periods for this analysis were: 1988-2000 (for the SPM) and 2001-2012 (for the PM_X). With respect SPM, an average trend of -0.5 μg m^{-3} per year was observed using data from three sites (San Pablo de los Montes, Roquetas, and Logroño). The maximum rate was obtained for Roquetas site with -1.1 μg m^{-3} per year being statistically significant by the Mann-Kendall non parametric test. As regards PM_X, only the results for Peñausende, Barcarrota, and Campisabalos are discussed in this abstract. For these stations, the temporal trends (statistical significance level >95%) for PM_{10} were -0.3 (Barcarrota and Campisabalos) and -0.45 (Peñausende) μg m^{-3} per year. The rates for $PM_{2.5}$ were similar to these values. Therefore, a clear and strong reduction of the particulate matter was found over the Iberian Peninsula in the 1988-2000 period, which is still observable between 2001-2012. The monthly climatology for the three variables showed similar features. For instance, a first minimum in the particulate matter was observed in April for most of the stations, while a second one appeared during summer months (particularly in July). This effect of bi-modality was attributed to the influence of desert dust intrusions from African continent on the aerosol climatology of the Iberian Peninsula.

TEMPORAL VARIATION OF [7]BE AIR CONCENTRATION DURING THE 23RD SOLAR CYCLE AT MÁLAGA (SOUTH SPAIN)

C. DUEÑAS, M.C. FERNÁNDEZ, M. CABELLO, E. GORDO, E. LIGER, S. CAÑETE, M. PÉREZ
Department of Applied Physics I, Universidad de Málaga, 29071 Málaga (Spain)
E-mail: mcabello@uma.es

[7]Be is a natural radionuclide produced by galactic cosmic ray impact on atmospheric nitrogen and oxygen atoms in the stratosphere (Lal and Peters, 1967). Anticorrelation between the solar activity and galactic cosmic ray flux on the Earth has been observed (Alegría et al., 2010).
In the present work, we study the impact of different factor (i.e. cosmic ray, sunspot and flux of energetic protons) on the [7]Be concentration in surface air.

Atmospheric concentrations of [7]Be were measured at the Faculty of Sciences of the University of Málaga during 1997-2007. Aerosol samples were collected weekly in cellulose membrane filters of 0.8 μm pore size and 47 mm diameter with an air sampler (Radeco, mod AVS-28A) at a flow rate of approximately 40 l/min. Measurement of [7]Be was carried out by a high-resolution gamma-ray spectrometer. The peak analysis of [7]Be (I= 10.52 %, 477.7 KeV) was done using SPECTRAN AT peak analysis software. The counting time was 172800 s. The sunspot number as an index of solar activity and the cosmic ray were registered by the Solar Influences Data analysis Center (SIDC) and the University of Oulu respectively. Flux of energetic protons (1, 10 and 100 MeV) was recorded by the Geosynchronous Operational Environmental Satellite (GOES) operated by the National Oceanic and Atmospheric Administration (NOAA).

The annual [7]Be activity concentration and sunspot number for the study period are displayed in Fig.1. Surface level air specific activity of [7]Be is inversely correlated to the sunspot number and the proton fluence (>100 MeV) with a coefficient of determination of -0.45 and -0.4 respectively. The correlation coefficient for the flux of energetic protons increases for the higher energetic particles, as protons with an energy of 100 MeV can invade the lower stratosphere more than protons with lower energy. On the other hand, a positive correlation between the [7]Be activity concentrations and the cosmic ray is found (r^2= 0.33).
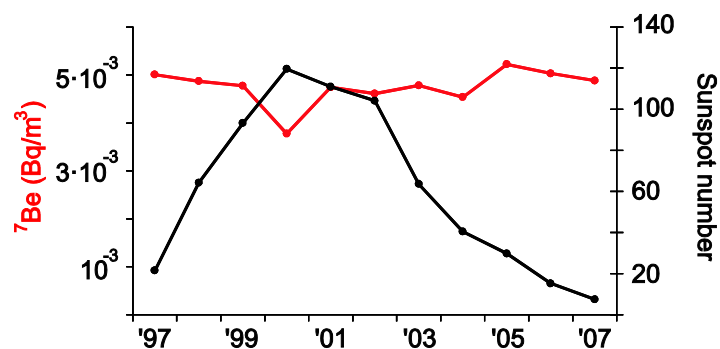

Fig.1: Yearly variations in the [7]Be concentration (red line) and sunspot number (black line) for the period 1997–2007.

References:
Alegría et al., J. Radioanal. Nucl. Chem, 286, 347-351 (2010).
Lal, D. and Peters, B., Sitte, K. (Ed), Enciclopedia of Phsics, Springer-Verlg, NY, pp. 551-612, (1967).

THE FIRST DESERT DUST EVENT DETECTED BY CIMEL PHOTOMETER IN BADAJOZ STATION (SPAIN)

M.A. OBREGÓN[1], A. SERRANO[2,1], M.L. CANCILLO[2], M.J. COSTA[1]

[1]Geophysics Centre of Évora, Rua Romão Ramalho, 59, 7000, Évora ,Portugal
[2]University of Extremadura, Avda de Elvas, S/N, 06006, Badajoz, Spain

It is well known the interest to accurately quantify the effects of aerosols on the Earth's radiation balance. Additionally, aerosols act upon cloud formation and modification, affecting the radiation balance also by this indirect effect. Regarding the human health, high concentration of aerosols at low levels can be very harmful, favoring allergies and respiratory diseases. Therefore, it is of great interest to continuously monitoring aerosols at a global and regional scales. According to this demand, a CIMEL-314 photometer has been installed at the radiometric station of the AIRE research group in Badajoz (Spain). This station is located at western Spain in a very plain region, being representative for a wide area of the Iberian Peninsula. This station is installed on the terrace of the Physic Department building at the Campus of Badajoz of the University of Extremadura, with coordinates: 38.88ºN, 7.01ºW, 186 m a.s.l.. This location guarantees continuous maintenance and open horizon. This station works operatively since June 2012 as part of AERONET (AErosol RObotic NETwork) and RIMA (Red Ibérica de Medida fotométrica de Aerosoles) monitoring networks, and follows their calibration and measuring protocols.

Within the short period of measurements, several dust events have been detected. A particularly intense dust outbreak occurred between 8 and 12 August 2012, and was measured at our station. The transport of dust from the Sahara region towards the Iberian Peninsula is one regular phenomenon that notably influences the radiation balance as well as the atmospheric visibility at those sites overspread by these aerosols. In this study, the 8-12 August 2012 Saharan dust event is analyzed in terms of the measurements of several optical and microphysical aerosol properties, such as aerosol optical depth, Ångström exponent α, single scattering albedo and size distributions, and the air mass back-trajectories computed by means of the Hybrid Single Particle Lagrangian Integrated Trajectory model (HYSPLIT4). The measurements show a significant increase in the atmospheric turbidity caused by the inflow of coarse particles, with daily averages of aerosol optical depth at 500nm of about 0.5, Ångström exponent α of about 0.2, and single scattering albedo values over 0.9. These values and their range of variation are typical for desert dust intrusions.

Acknowledgments

THE REDMAAS 2014 INTERCOMPARISON CAMPAIGN: CPC, SMPS, UFP AND NEUTRALIZERS

F. J. GÓMEZ-MORENO[1], E. ALONSO[1], B. ARTÍÑANO[1], S. IGLESIAS SAMITIER[2], M. PIÑEIRO IGLESIAS[2], P. LÓPEZ MAHÍA[2], N. PÉREZ[3], A. ALASTUEY[3], B. A. DE LA MORENA[4], M. I. GARCÍA[5], S. RODRÍGUEZ[5], M. SORRIBAS[6,7], G. TITOS[6,7], H. LYAMANI[6,7], L. ALADOS-ARBOLEDAS[6,7], E. FILIMUNDI[8] AND E. LATORRE TARRASA[9]

[1]*Department of Environment, CIEMAT, Madrid, E-28040, Spain*
[2]*Grupo Química Analítica Aplicada, Instituto Universitario de Medio Ambiente (IUMA), Departamento de Química Analítica, Facultade de Ciencias,Universidade da Coruña, Campus de A Coruña, 15071 A Coruña, Spain*
[3]*Institute of Environmental Assessment and Water Research (IDAEA-CSIC), Barcelona, E-08034, Spain*
[4]*Atmospheric Sounding Station 'El Arenosillo', INTA, Mazagón-Huelva, E-21130, Spain*
[5]*Izaña Atmospheric Research Centre, (IARC/CIAI), AEMet, Santa Cruz de Tenerife, E-38001, Spain*
[6]*Andalusian Institute for Earth System Research, IISTA-CEAMA, University of Granada, Granada, E-18071, Spain*
[7]*Applied Physics Department, University of Granada, Granada, E-18071, Spain*
[8]*TSI GmbH, Aachen, D-52068, Germany*
[9]*Álava Ingenieros, Madrid, E-28037, Spain*

The Spanish network on environmental DMAs (Red Española de DMAs Ambientales, REDMAAS) is currently formed by six groups involved in the measurement of atmospheric aerosol size distributions by means of Differential Mobility Analyzers (DMAs). These groups are: IUMA-UDC, IDÆA-CSIC, INTA, IARC-AEMET, University of Granada and CIEMAT. The network has been working since 2010. One of the main activities developed in the network is an annual intercomparison of mobility size spectrometers (SMPS and UFP). In the 2014 intercomparison campaign, all the groups except AEMET have participated. TSI and their Spanish representatives, Álava Ingenieros, were also involved with the new electrostatic classifier TSI 3082. In this work we show the results obtained in this campaign: the verification of DMA calibrations with latex, the results of the CPC and SMPS + UFP intercomparisons, and a comparison of the new TSI 3087 X-ray and the former TSI 3077 [85]Kr neutralizers.

Comparing different types of CPC (e.g. CPC3772 and WCPC3785 with a flow rate of 1 lpm, and CPC3775/76, with 1.5 or 0.3 lpm) the concentrations measured during the intercomparison were within the range of 10% of the average value. CPCs working at higher flow rates measured slightly higher concentrations, probably related to the smaller losses in the lines. To avoid this, all the SMPS worked at the same sampling and sheath flow rates (1:10 lpm). Two clear groups were observed: two SMPS systems measured higher concentrations, and the other three gave smaller concentrations. The UFP measured concentrations oscillating between both groups. An evaluation of instrument behavior along the years has been done using data collected during previous campaigns.

The tests performed with the two different neutralizers show that the instrument operating with the X-ray neutralizer measured higher concentrations. This could mean that particle losses are smaller inside this neutralizer. To take this into account, a correction for the losses of different types of neutralizer could be included as an option in the next TSI AIM software

TRENDS OF PM10 CONCENTRATIONS IN WESTERN EUROPEAN ATLANTIC AREAS

BARRERO M.A.[1], ORZA J.A.G.[2], CANTÓN L.[1]

[1]*Department of Applied Chemistry, University of the Basque Country, P. Manuel de Lardizabal, 3
20018 San Sebastián, Spain, miguelangel.barrero@ehu.es*

[2] *SCOLAb, Department of Physics, Universidad Miguel Hernández,
Av. de la Universidad, s/n, edificio Alcudia
03202 Elche, Spain*

The atmospheric levels of PM_{10} can be used as an indicator of both local and regional pollution. The primary aim of this work is to assess the existence of temporal trends of PM_{10} concentrations in rural, urban background, industrial and traffic stations in the Basque Country. In addition, we want to evaluate whether the observed behavior is a local phenomenon or whether it can be related to larger scale variations. Therefore, we compare the temporal trends of PM_{10} concentrations observed in the Basque Country with other European regions with Atlantic climate influence. The air quality monitoring networks of Portugal and United Kingdom were selected based on the number of stations, data coverage and accessibility. Hourly PM_{10} data from a total of 104 stations in the period from 2005 to 2012 were collected and processed in order to remove anomalous data, calculate daily PM_{10} concentrations and obtain monthly averages. Trends in the monthly data were evaluated with the Mann-Kendall and seasonal Kendall tests and the Theil-Sen estimator, for the individual stations and by groups based on station type and country.

A general downward trend is observed, with an average slope of -1.4 μg m^{-3} yr^{-1}. This downward trend is higher in industrial stations (-1.7 μg m^{-3} yr^{-1}) and is less evident in rural background stations (-0.79 μg m^{-3} yr^{-1}) (Figure 1). Overall, the stations in Portugal present the stronger trends. Three main factors can be related to this generalized downward trend: (i) economic crisis, (ii) the implementation of pollution abatement strategies in the EU and (iii) year-to-year variations in meteorology. The analysis of the behavior of major pollutants and climatic series allowed evaluating the relative contribution of natural and anthropogenic factors to this decreasing trend.
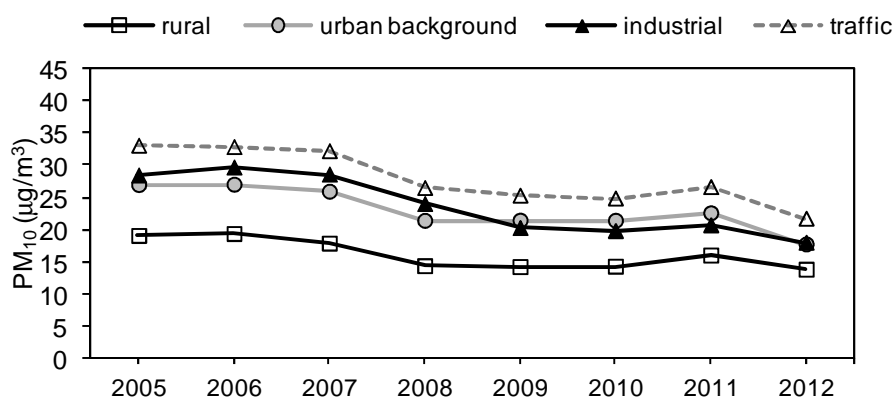

Figure 1. Evolution of annual average PM_{10} concentrations by station type.

VALIDACIÓN DE PRODUCTOS MODIS (NIVEL 3) SOBRE DIFERENTES ESTACIONES DE LA COSTA MEDITERRÁNEA SEPTENTRIONAL

MANUEL A. PESANTEZ[1], SARA SEGURA[1], VÍCTOR ESTELLES[1], M. DOLORES FREILE-ARANDA[1], Mª PILAR UTRILLAS[1], JOSÉ ANTONIO MARTÍNEZ-LOZANO[1]

[1]*Departament de Física de la Tierra i Termodinàmica. Facultad de Física. Universitat de València, Avda. Dr. Moliner, 50 Burjassot (Valencia), maupegon@alumni.uv.es*

Resumen

El estudio de los aerosoles es de gran importancia ya que, debido a su alta variabilidad temporal y espacial, constituyen una de las mayores fuentes de incertidumbre en diferentes procesos que ocurren en la atmósfera y que afectan tanto al clima como a la visibilidad, la calidad del aire y la salud humana. El estudio de sus propiedades puede realizarse empleando diferentes técnicas de medida, todas ellas complementarias. Por un lado, existen métodos de medida in-situ con gran resolución temporal en la obtención de las propiedades de los aerosoles, aunque con escasa o nula representatividad en columna. Por otro lado, existen técnicas de teledetección que permiten medir desde el espacio las propiedades de los aerosoles en columna. La fotometría solar, la técnica del LÍDAR o los sensores a bordo de satélites, son algunos ejemplos.

En la última década se han puesto en marcha diferentes misiones enfocadas a la medida de aerosoles mediante técnicas de Teledetección, en las que se emplean sensores como por ejemplo MODIS (Espectroradiómetro de Imágenes de Resolución Media). MODIS es un sensor a bordo de los satélites Aqua y Terra que forman parte de EOS (Earth Observation System) cuya misión es monitorizar, entre otros, las propiedades de los aerosoles. MODIS ofrece productos en varios niveles debidamente procesados de propiedades concretas, entre ellas los aerosoles. Los diferentes niveles se diferencian, entre otras cosas, por la resolución espacial de los datos. El producto de nivel 3 es un producto de valor agregado que se deriva de las variables geofísicas de niveles inferiores, especialmente del nivel 2. Contiene diferentes parámetros atmosféricos entre ellos el espesor óptico de aerosoles (AOD) a una resolución espacial de 1º x 1º. Los valores de este parámetro se obtienen a partir de las medidas de la radiancia, obtenidas directamente por el sensor MODIS, y sobre las que se aplican diferentes algoritmos en función del tipo de superficie subyacente: océano (Remer et al., 2005) y tierra (Levy et al., 2007).

En este trabajo se realiza una validación del espesor óptico de aerosoles proporcionado por el sensor MODIS sobre diferentes estaciones de la costa mediterránea, empleando para ello medidas del espesor óptico obtenido con fotómetros solares CIMEL CE318 pertenecientes a la red internacional AERONET. Para llevar a cabo la validación de MODIS empleamos el producto MOD08/MYD08 de nivel 3 de la colección 5.1. La validación de las medidas de una celda se realiza considerando el enfoque espacio temporal propuesto por Ichoku et al. (2002), que consiste en comparar las estadísticas espaciales de MODIS con las estadísticas temporales del CIMEL.

Palabras claves: Terra, Aqua, aerosoles, MODIS, CIMEL, AERONET

Preferencia para la presentación: Póster

VERTICAL DISTRIBUTION OF THE MINERAL DUST RADIATIVE FORCING IN TENERIFE

R.D. GARCÍA[1-2], V.E. CACHORRO[2], O.E. GARCÍA[1], E. CUEVAS[1], C. GUIRADO[2,1], Y. HERNÁNDEZ[1] and A. BERJÓN[1]

[1]*Izaña Atmospheric Research Center, Meteorological State Agency of Spain, AEMET Spain, rgarciac@aemet.es*

[2]*Atmospheric Optics Group. Valladolid University (GOA-UVA), Spain*

This work examines the vertical distribution of the Saharan mineral dust radiative forcing (ΔF) and radiative forcing efficiency (ΔF^{eff}) from sea level to about 3.5 km in Tenerife Island (Canary Islands, Spain). To do so, we combine global shortwave downward radiation (SDR) and aerosol optical properties measured at three stations, managed by the Izaña Atmospheric Research Center (IARC, AEMET): Santa Cruz Atmospheric Observatory (SCO) at 52 m a.s.l., Izaña Atmospheric Observatory (IZO) at 2.367 m a.s.l. and Pico del Teide Observatory (PTO) at 3.555 m a.s.l.. These stations are located only 37 km far away in the horizontal and usually under different aerosol conditions. While SCO is located in an urban environment in the Maritime Boundary Layer, IZO and PTO are located at the free troposphere and, then, not affected by local pollution.

The instantaneous SDR ΔF and ΔF^{eff} have been evaluated under cloud-free conditions, around the solar noon (12-14 UTC), and when Saharan mineral dust events simultaneously may affect the three stations (July-September 2013). The Saharan episodes were selected taking the SCO station as reference, i.e., aerosol optical depth (AOD) at 500 nm is higher than 0.1 and Ångström parameter (α) smaller than 0.75, which assures mineral dust conditions. Furthermore, these events were confirmed by using LIDAR measurements simultaneously taken at SCO station.

The mean ΔF values are -27±6, -11±5 and -10±3 Wm^{-2} for SCO, IZO and PTO, respectively (mean AOD at 500 nm of 0.28±0.05, 0.16±0.04 and 0.10±0.02), whereas the mean ΔF^{eff} values are -123±4, -126±3 and -103±7 Wm^{-2} per unit of AOD at 500 nm for SCO, IZO and PTO, respectively. The ΔF^{eff} values are rather consistent in the vertical and, then, well representative of Saharan mineral dust. These results show the significant potential of mineral dust particles to cool the Earth-atmosphere system.

Sponsors